Analysing the role of Pten in the murine small intestine

Victoria Marsh

Cardiff University

Ph.D.

2004-2008

ProQuest LLC
789 East Eisenhower Parkway
P.O. Box 1346
Ann Arbor, MI 48106-1346

Acknowledgements

First and foremost, I must thank my supervisor, Professor Alan Clarke, for his advice, guidance and scientific wisdom upon which this project is largely based. He has provided much inspiration and encouragement, and taught me to strive for perfection in my research. Huge thanks are also due to my advisor, Dr Owen Sansom, who first initiated this project before moving to the Beatson Institute, Glasgow. Without his influence, I would not have had such an insightful and entertaining start to my scientific career.

In terms of data analysis, Prof Geraint T. Williams (Department of Pathology, University Hospital of Wales, Cardiff University) has been an invaluable source of expert histopathology advice, as has Dr Marnix Jansen (Hubrecht Institute, The Netherlands). Dr Richard Kemp and Dr Doug Winton (both Cambridge Research Institute, U.K.) were instrumental to this work by providing Cre-expressing lines, assistance with induction procedures and also helping to solve problems with my epithelial isolation protocol. I would also like to thank Dr Nicole Dubois (McEwen Centre for Regenerative Medicine, UHN, Canada) and Prof Andreas Trumpp (ISREC, Switzerland) for kindly sharing their intestinal Pten data. Finally, I wish to thank our numerous collaborators, who have not been mentioned here, for their interest in my research and for providing new and interesting perspectives on my data.

Much of the work presented in this thesis would not have been possible without the technical assistance of a number of skilled individuals within Cardiff University. In particular, Derek Scarborough and Marc Isaacs provide an excellent histology service, and have saved me from many laborious hours of tissue sectioning. Also, credit is due to Mark Bishop, Lucie Pietzka and Luke Piggott; who together make up the PCR genotyping team. I am totally indebted to them for providing genotypes of my many, genetically complex animals. Additional thanks to Lucie for performing tail biopsies, and also for educating me in the skills of mouse husbandry.

I must also thank Emma J. Davies, a first year PhD student in the laboratory who will be continuing the work described here for her own doctoral project. She has been of great assistance to me, taking over the running and maintenance of mouse colonies during my 'writing-up' time. She assisted me in collecting the data described in Chapter 7 (See footnotes within the chapter for details). Thanks also to Dr Kirsty Greenow and Dr Lee Parry, for providing caffeine, the odd scientific debate and plenty of advice. Finally, I would like to thank all the members of the 4th and 5th floors of BIOSI3 who I have not mentioned in person, but who have all contributed in some way to the enjoyable, educational and productive experience I have had during my PhD.

On a more personal note, I am indebted my parents for their unconditional support, both financially and otherwise. Also to the rest of my family and friends, both near and far, who, each in their own ways have helped to keep me sane over the last 4 years. Finally, I would like to thank Dewi, for providing me with a quiet place in which to write without distraction, for encouraging me to work hard, and for de-stressing me when I've felt the pressures of work. Without him, I would probably still be thinking of good excuses not to start writing up!

The work presented in this thesis was funded by a studentship provided by Cancer Research UK.

Contents

Declarations ..... *ii*

Acknowledgements ..... *iii*

List of Figures ..... *ix*

List of Tables ..... *xii*

Abbreviations and Definitions ..... *xiii*

Abstract ..... *xvi*

Chapter 1: General Introduction **1**

1.1 Intestinal Tumourigenesis ***1***

1.1.1 Intestinal Cancer in Humans 1

1.1.2 The mammalian small intestine 2

1.1.3 The intestinal stem cell 14

1.1.4 Multi-step carcinogenesis of the intestine 25

1.2 PTEN: A tumour suppressor ***32***

1.2.1 Discovery, structure and function of Pten 32

1.2.2 The PI3K/Akt pathway 36

1.2.3 Pten and carcinogenesis 41

1.3 Modelling colorectal cancer in the mouse using conditional transgenesis ***43***

1.3.1 Mouse models of intestinal tumourigenesis 43

1.3.2 Constitutive versus conditional transgenesis 44

1.3.3 Conditional transgenic approaches 45

1.3.4 The Cre-LoxP approach 45

1.3.5 Regulation of Cre activity in the intestine 46

1.4 Project Aims ***50***

Chapter 2: Materials and Methods **51**

2.1 Experimental Animals ***51***

2.1.2 Animal Husbandry 51

2.1.3 Experimental Procedures 51

2.1.4 PCR Genotyping 52

2.2 Tissue sampling and processing ***57***

2.2.1 Removal of tissues 57

2.2.2 Tissue fixation for histology 57

2.2.3 Tissue processing and sectioning 58
2.2.4 Cryosectioning of tissues 58
2.2.5 Preservation of whole tissues for future protein, RNA or DNA extraction 58
2.2.6 Analysis of beta-galactosidase activity 59
2.2.7 Isolation of intestinal epithelium 60
2.3 Histological Analysis 61
2.3.1 Haematoxylin and Eosin (H&E) staining of tissue sections 61
2.3.2 Quantification of H&E-stained tissue sections 62
2.3.3 Use of special stains to identify specific cell types 63
2.4 Immunohistochemistry (IHC) 64
2.4.1 Generic Immunohistochemistry protocol 64
2.4.2 Specific Immunohistochemistry protocols 66
2.5 Protein Analysis 70
2.5.1 Protein extraction from tissue samples 70
2.5.2 Quantification of proteins 70
2.5.3 Western Analysis 71
2.6 Gene Expression analysis 75
2.6.1 Isolation of RNA 75
2.6.2 Preparation of cDNA for quantitative PCR analysis 76
2.6.3 Quantitative, Real-time (qRT) PCR analysis 76
2.6.4 PCR analysis of genomic recombination 78
2.7 Statistical Analyses 82
2.7.1 Kaplan-Meier survival analysis 82
2.7.2 Mann-Whitney-U Test 82
2.7.3 Kolmogorov-Smirnov Analysis 82

Chapter 3: Analysing the short-term effects of AhCre-driven Pten deficiency in the intestinal epithelium 83

3.1 Introduction 83

3.2 Results 85
3.2.1 AhCre drives recombination in the intestine with high efficiency 85
3.2.2 Recombination results in loss of Pten transcript and protein from the intestinal epithelium 87
3.2.3 Recombination outside the intestine recapitulates previously observed phenotypes 91
3.2.4 Pten deficiency does not perturb gross structure or histology of the intestinal epithelium 93
3.2.5 Pten-deficient cells show a normal apoptotic response to DNA damage 98
3.2.6 Epithelial cells differentiate normally in the absence of Pten 100
3.2.7 Pten-deficient cells exhibit no block in migratory ability 103
3.2.8 Akt is activated following epithelial Pten deletion 107
3.2.9 Downstream targets of Akt are not activated following Pten loss 110

3.2.10 Pten loss has no effect on multiplicity of intestinal stem cells 114

3.2.11 Pten is not required for normal embryonic development of the intestinal epithelium 118

3.3 Discussion ***120***

3.3.1 Epithelial Pten is not required for normal intestinal homeostasis 121

3.3.2 Pten loss in the epithelium does not alter stem cell number or result in immediate tumourigenesis 122

3.3.3 Pten is not required for *in utero* development of the intestinal epithelium 126

3.3.4 Summary and Future Directions 126

Chapter 4: Analysing the long-term effects of Pten deficiency in the intestine using AhCreER^{T} 129

4.1 Introduction ***129***

4.2 Results ***131***

4.2.1 Low-level recombination in the intestinal epithelium following induction of AhCreER^{T} 131

4.2.2 Pten$^{f/f}$ animals show a reduced lifespan compared to controls 133

4.2.3 Multiple tissue phenotypes associated with Pten deficiency 135

4.2.4 Delayed onset of intestinal tumourigenesis following deletion of Pten 139

4.2.5 Intestinal tumours show varied histology, and are partly comprised of Ki67-positive cells 141

4.3 Discussion ***144***

4.3.1 Multiple tissue phenotypes associated with deletion of Pten 144

4.3.2 Delayed onset of intestinal tumourigenesis in Pten$^{f/f}$ animals 145

4.3.3 Summary and future directions 146

Chapter 5: Investigating the effects of epithelial Pten loss in the context of activated Wnt signalling 148

5.1 Introduction ***148***

5.2 Results ***150***

5.2.1 Activation and relocalisation of Akt in Pten-deficient, Wnt activated intestinal epithelial cells 150

5.2.2 Dramatically reduced lifespan of Pten-deficient mice in the context of Apc heterozygosity 154

5.2.3 Increased multiplicity of small intestinal tumours, but not large intestinal tumours, following Pten loss 156

5.2.4 Small intestinal tumours arising in Pten-deficient Apc heterozygotes are more advanced compared to controls 159

5.2.5 Moderate activation of Akt in Pten-proficient tumours arising in Apc heterozygotes.. 163

5.2.6 Consistent strong activation and relocalisation of Akt in Pten- and Apc-deficient small intestinal tumours 165

5.3 Discussion ***170***

5.3.1 Synergistic effect of Pten and Apc loss upon activation and subcellular localisation of Akt 170

5.3.2 Rapid progression of Wnt-initiated tumourigenesis in the context of Pten deficiency 172

5.3.3 Summary and future work 174

Chapter 6: Multiple tissue phenotypes associated with AhCreER^{T}-driven deletion of Pten and activation of k-Ras 177

6.1 Introduction 177

6.2 Results 179

6.2.1 Mice with induced deficiency of Pten and activation of k-Ras show a dramatic reduction in survival time 179

6.2.2 Highly penetrant phenotypes of gall bladder and bile duct lesions, and forestomach squamous hyperplasia in Pten$^{f/f}$;kRas$^{+/T}$ animals 181

6.2.3 AhCreER^{T} drives recombination in the gall bladder epithelium and forestomach squamous epithelium 183

6.2.4 Co-ordinate loss of Pten and activation of k-Ras results in hyperplasia and papilloma of both gall bladder epithelium and bile duct epithelium 185

6.2.5 Papillomatous lesions of the gall bladder are characterised by activation and membrane localisation of Akt 191

6.2.6 The mitogen-activated protein kinases, MEK and ERK, are activated in gall bladder papillomata 193

6.2.7 Akt is moderately activated, but not membrane localised in bile duct hyperplasia 195

6.2.8 Activation of MEK and ERK in bile duct lesions 197

6.2.9 Pten$^{f/f}$;kRas$^{+/T}$ animals develop hyperplasia of the forestomach squamous epithelium199

6.2.10 Activated Akt is present, but its levels are not increased in hyperplastic forestomach epithelium 201

6.2.11 Limited increase in expression of MEK and ERK in forestomach hyperplasia 203

6.3 Discussion 205

6.3.1 Activation of PI3K/Akt signalling and the Raf-MEK-ERK pathway drives papillomatous hyperplasia of the biliary epithelium 206

6.3.2 Hyperplasia of the forestomach squamous epithelium is not characterised by increased activation of PI3K/Akt signalling, and shows only limited increase in activation of the Raf-MEK-ERK pathway 207

6.3.3 Summary and future directions 208

Chapter 7: Analysis of the short- and long-term consequences of Vil-CreER^{T}-mediated activation of k-Ras and loss of Pten in the intestine 210

7.1 Introduction 210

7.2 Results 212

7.2.1 Induction of Vil-CreER^{T} causes recombination in epithelial cells at the LoxP-targeted Pten locus and the k-Ras^{V12} transgene 212

7.2.2 No change in gross intestinal structure associated with Pten loss and k-Ras activation at day 14 PI 214

7.2.3 Increase in mitosis, but not apoptosis, in Pten-deficient k-Ras-activated intestinal epithelium 216

7.2.4 Increase in size of crypts and villi in Pten$^{f/f}$;kRas$^{+/T}$ intestines compared to controls ... 218

7.2.5 No change in number or location of Ki67-positive proliferative cells in Pten$^{f/f}$;kRas$^{+/T}$ tissue ... 220

7.2.6 No impairment in differentiation of epithelial cells associated with combined Pten loss and activation of k-Ras ... 222

7.2.7 Increase in activation of Akt at day 14 following induction of Pten deficiency and activation of k-Ras ... 225

7.2.8 Preliminary data indicates a reduction in survival time in double-mutant animals ... 227

7.2.9 Decrease in survival of Pten$^{f/f}$;kRas$^{+/T}$ animals is caused by intestinal pathologies ... 229

7.3 Discussion ... ***231***

7.3.1 Combined loss of Pten and activation of k-Ras results in an increase in proliferation and expansion in crypt and villus size in the intestinal epithelium at day 14 PI ... 232

7.3.2 Increase in activation of Akt following co-ordinate loss of Pten and activation of k-Ras ... 233

7.3.3 Hyperplasia of the intestinal epithelium following prolonged loss of Pten and activation of k-Ras ... 234

7.3.4 Summary and future directions ... 235

Chapter 8: General Discussion ... **237**

8.1 Pten, the intestinal stem cell and epithelial-stromal interactions ... ***238***

8.2 Pten suppresses tumour progression ... ***240***

8.2.1 In the context of activated Wnt signalling ... 240

8.2.2 In the context of k-Ras activation ... 241

8.3 Potential significance of membrane-localised activated Akt ... ***242***

8.4 Developing a faithful mouse model of step-wise colorectal cancer progression ... ***243***

Reference List ... **245**

Appendix 1: Publication List ... **260**

List of Figures

	Page
Figure 1.1: Structure and organisation of the mammalian small intestinal epithelium	**5**
Figure 1.2: Major regulatory signalling pathways influencing homeostasis of the intestinal epithelium	**13**
Figure 1.3: Candidate locations of the intestinal stem cell and components of the stem cell niche	**24**
Figure 1.4: Multi-step tumourigenesis of the intestinal epithelium	**31**
Figure 1.5: Structure and function of Pten	**35**
Figure 1.6: Activation of PI3K and Akt	**39**
Figure 1.7: Downstream targets of Akt	**40**
Figure 1.8: Strategies for regulation of Cre activity in the intestine	**49**
Figure 2.1: Blotting apparatus set-up for Western Analysis	**72**
Figure 2.2: Schematic representation of primer positions and product sizes for recombined allele-specific PCR	**81**
Figure 3.1: Use of the ROSA26R LacZ reporter to indicate recombination in the intestine	**86**
Figure 3.2: Epithelial enrichment of intestinal tissue samples, and use of epithelial extracts to confirm loss of Pten transcript after induction	**89**
Figure 3.3: Confirmation of loss of Pten protein from the intestinal epithelium after induction	**90**
Figure 3.4: Pathologies outside the intestine observed following Pten deletion	**92**
Figure 3.5: No changes in histology or location of TA zone following epithelial Pten loss	**95**
Figure 3.6: Quantification of crypt and villus size following Pten deletion	**96**
Figure 3.7: Quantification of levels of apoptotic and mitotic cells within the crypt	**97**
Figure 3.8: No impairment of apoptotic response to DNA damage following Pten loss	**99**
Figure 3.9: Identification of differentiated epithelial cell types following Pten loss	**101**
Figure 3.10: Quantification of Goblet cells and enteroendocrine cells following Pten loss	**102**
Figure 3.11: BrdU labelling of cells reveals no deficiency in cell migration following Pten loss	**105**
Figure 3.12: Quantification of epithelial BrdU-labelled cell migration	**106**
Figure 3.13: Deletion of Pten results in activation of Akt	**109**
Figure 3.14: Downstream targets of Akt are not activated following Pten deletion	**112**
Figure 3.15: Q-PCR analysis of PI3K/Akt pathway components and Wnt signalling components in Pten-deficient intestinal epithelium	**113**
Figure 3.16: Clonogenic survival assay reveals no difference in epithelial repopulation following gamma-irradiation in the context of Pten deficiency	**116**
Figure 3.17: No difference in expression of putative stem cell markers following Pten loss	**117**
Figure 3.18: Loss of Pten during development of the intestine does not perturb epithelial structure	**119**
Figure 3.19: Epithelial versus stromal deletion of Pten in the intestine	**125**

Figure 4.1: Analysis of recombination in the intestine driven by AhCreER^{T} **132**

Figure 4.2: Reduced survival of Pten$^{f/f}$ animals compared to controls **134**

Figure 4.3: Aged Pten$^{f/f}$ mice are susceptible to prostate neoplasia, hepatic steatosis and cholangiocarcinoma of varying histology **136**

Figure 4.4: Pten$^{f/f}$ animals are predisposed to intestinal lesions, prostate neoplasia, liver steatosis and lymphoma **138**

Figure 4.5: Probability of Pten$^{f/f}$ and control animals bearing intestinal tumours increases with time **140**

Figure 4.6: Intestinal lesions in aged Pten$^{f/f}$ animals show varied histopathology **142**

Figure 4.7: Anti-Ki67-positive cells are present within intestinal lesions of Pten$^{f/f}$ mice **143**

Figure 5.1: Increase in activation of Akt within crypts following acute loss of Pten and Apc **151**

Figure 5.2: Increase in activation and relocalisation of Akt in villus epithelium following acute loss of Pten and Apc **153**

Figure 5.3: Pten loss in the context of Apc heterozygosity reduced longevity **155**

Figure 5.4: Gross appearance and histology of tumours arising in Apc$^{f/+}$;Pten$^{f/f}$ mice **157**

Figure 5.5: Increase in small intestinal tumour burden in Apc$^{f/+}$;Pten$^{f/f}$ animals **158**

Figure 5.6: Histological categorisation of varying grades of tumour severity seen in Apc$^{f/+}$;Pten$^{f/f}$ intestines and Apc$^{f/+}$ controls **161**

Figure 5.7: Increased severity of small intestinal tumours in Apc$^{f/+}$;Pten$^{f/f}$ animals compared to controls **162**

Figure 5.8: IHC on tumours arising in Apc$^{f/+}$ control animals confirms loss of Apc and retention of Pten, and indicates a moderate increase in Akt activation **164**

Figure 5.9: IHC on tumours arising in Apc$^{f/+}$;Pten$^{f/f}$ animals indicates loss of Pten and Apc in epithelial cells **166**

Figure 5.10: Recombined-specific PCR indicates recombination at Pten and Apc alleles in tumours **167**

Figure 5.11: Activation and cell-surface localisation of Akt in intestinal tumours arising in Apc$^{f/+}$;Pten$^{f/f}$ animals **169**

Figure 5.12: The potential of Apc- and Pten-deficient mice to generate an animal model of step-wise progression of colorectal cancer **176**

Figure 6.1: Kaplan-Meier survival analysis of Pten$^{f/f}$;kRas$^{+/T}$ mice compared to controls **180**

Figure 6.2: Scoring of pathologies found in Pten$^{f/f}$;Ras$^{+/T}$ and control animals **182**

Figure 6.3: Low-level recombination in the forestomach and gall bladder epithelium driven by AhCreER^{T} **184**

Figure 6.4: Pten$^{f/f}$;kRas$^{+/T}$ mice are susceptible to hyperproliferative papilloma of the gall bladder epithelium **187**

Figure 6.5: Pten$^{f/f}$;kRas$^{+/T}$ mice show susceptibility to papilloma of the bile duct **188**

Figure 6.6: Anti-cytokeratin 19 IHC reveals ductal origins of gall bladder and bile duct papillomatous lesions **189**

Figure 6.7: Biliary papillomatous lesions arising in Pten$^{f/f}$;kRas$^{+/T}$ mice are Ki67 antigen-positive **190**

Figure 6.8: Upregulation and cell surface localisation of pAkt^{Ser473} in gall bladder lesions of **192**

$Pten^{f/f}$;$kRas^{+/T}$ mice

Figure 6.9: Upregulation of $pMEK^{Ser221}$ and $pERK^{Thr202/Tyr204}$ in gall bladder lesions of $Pten^{f/f}$;$kRas^{+/T}$ mice **194**

Figure 6.10: Upregulation of $pAkt^{Ser473}$ in bile duct lesions of $Pten^{f/f}$;$kRas^{+/T}$ mice **196**

Figure 6.11: Upregulation of pERK in bile duct lesions of $Pten^{f/f}$;$kRas^{+/T}$ mice **198**

Figure 6.12: Susceptibility of $Pten^{f/f}$;$kRas^{+/T}$ mice to papillomatous hyperplasia of the forestomach squamous epithelium **200**

Figure 6.13: Hyperplastic cells of forestomach squamous epithelium in $Pten^{f/f}$;$kRas^{+/T}$ mice express normal levels of $pAkt^{Ser473}$ **202**

Figure 6.14: Hyperplastic forestomach squamous epithelial cells of $Pten^{f/f}$;$kRas^{+/T}$ mice show a limited increase in expression of pMEK and pERK **204**

Figure 7.1: Recombined-specific PCT confirms recombination at the Pten locus and the $kRas^{V12}$ transgene in the intestinal epithelium of experimental animals **213**

Figure 7.2: No perturbation of gross intestinal histology at 14 days following intestine-specific loss of Pten and activation of k-Ras **215**

Figure 7.3: Increase in mitosis with no change in apoptosis following loss of Pten and activation of k-Ras **217**

Figure 7.4: Significant increase in size of crypts and villi in $Pten^{f/f}$;$kRas^{+/T}$ intestines at day 14 PI **219**

Figure 7.5: No significant alteration in number of Ki67-positive cells in $Pten^{f/f}$;$kRas^{+/T}$ intestines at day 14 PI **221**

Figure 7.6: No alteration in presence or localisation of Paneth cells and Goblet cells in $Pten^{f/f}$;$kRas^{+/T}$ intestines at day 14 PI **223**

Figure 7.7: No alteration in differentiation or localisation of Enterocytes and Enteroendocrine cells in $Pten^{f/f}$;$kRas^{+/T}$ intestines at day 14 PI **224**

Figure 7.8: IHC analysis of Akt activation in $Pten^{f/f}$;$kRas^{+/T}$ intestines **226**

Figure 7.9: Survival analysis of Villin-Cre;$Pten^{f/f}$;$kRas^{+/T}$ mice compared to Villin-Cre;$kRas^{+/T}$ controls **228**

Figure 7.10: Intestinal histology of aged Ptenf/f;kRas+/T mice reveals hyperproliferation of epithelial cells, abnormal villus structure and adenocarcinoma **230**

List of Tables

	Page
Table 2.1: PCR genotyping reaction conditions	**55**
Table 2.2: Primer sequences used for PCR genotyping	**56**
Table 2.3: Summary of IHC protocols	**68, 69**
Table 2.4: Western blotting gel and buffer compositions	**73**
Table 2.5: Summary of antibodies and protocols used for Western analysis	**74**
Table 2.6: Primer sequences used for Q-PCR analysis	**77**
Table 2.7: Recombined PCR conditions and primer sequences	**80**
Table 3.1: Scoring of Apoptosis and mitosis in control and $Pten^{f/f}$ intestines reveals no significant difference compared to controls	**94**

Abbreviations and Definitions

°C	degrees Celsius
µg	micrograms
µl	microlitres
µM	micromolar (micromoles per litre)
5-FU	5-Fluorouracil
Ab	antibody
ABC	Avidin-Biotin complex
ACF	Aberrant crypt foci
Ad	Adenoma
Ah	Aryl hydrocarbon
Ahr	Aryl hydrocarbon receptor
AIA	Advanced invasive adenocarcinoma
Apc	Adenomatous polyposis coli
Apc^{MIN}	Multiple intestinal neoplasia (MIN) mutation of the Adenomatous polyposis coli gene
Bad	B-cell leukaemia/lymphoma 2-associated death promoter
Bcl2	B-cell leukaemia/lymphoma 2
beta-Gal	beta-Galactosidase
Bmi-1	B-lymphoma Mo-MLV insertion region 1 polycomb ring-finger oncoprotein
BMP	Bone morphogenic protein
BMPRI	Bone morphogenic protein receptor, type I
BMPRII	Bone morphogenic protein receptor, type II
bNF	beta-Naphthoflavone
bp	base pairs
BrdU	5-Bromo-2-deoxyuridine
BSA	Bovine serum albumin
CBC	Crypt base columnar cell
Cdc25a	Cell division cycle 25a
cDNA	complimentary deoxyribonucleic acid
Chk1	Checkpoint kinase 1
CK	Casein kinase
cm	centimetres
c-Myc	cellular-Myelocytomatosis oncogene
CoA	Co-activators
CoR	Co-repressors
Cos-2	Costal-2
CRC	Colorectal cancer
Cre	Causes recombination
$CreER^{T}$	Causes recombination-Estrogen receptor fusion protein
C_T	Cycle time
DAB	3,3'-diaminobenzidine
dATP	deoxyadenosine triphosphate
DCAMKL-1	Doublecortin and calmodulin kinase-like 1
DCC	Deleted in colorectal carcinoma
dCTP	deoxycytidine triphosphate
ddH2O	ultrapure water
DEPC	Diethyl pyrocarbonate
dGTP	deoxyguanosine triphosphate
dH2O	distilled water
Dhh	Desert hedgehog
Dkk-1	Dickkopf-1
DNA	deoxyribonucleic acid
DNase	deoxyribonuclease
DTT	Dithiothreitol
dTTP	deoxythymidine triphosphate
ECL	Electrochemiluminescence
ECM	Extracellular Matrix
EDTA	Ethylenediamine tetra-acetic acid
EGFP	Enhanced green fluorescent protein
EGFR	Epidermal growth factor receptor
EIA	Early invasive adenocarcinoma
eIF4E	Eukaryotic translation initiation factor 4E
eIF4E-BP1	Eukaryotic translation initiation factor 4E binding protein 1
EMT	Epithelial-Mesenchymal transition
eNOS	Endothelial nitric oxide synthase
ER	Estrogen Receptor
ERK	Extracellular signal-regulated kinase
EtOH	Ethanol
FAP	Familial Adenomaous Polyposis
FOXO	Forkhead box O transcription factor
Frt	Flp recognition target
Fu	Fused
GAP	guanosine triphosphatase-activating protein
GDP	guanosine diphosphate
GEF	Guanine nucleotide exchange factor

Gli	Glioma-associated oncogene homolog
Gpr49	G-protein coupled receptor 49
GSK3-beta	Glycogen synthase kinase 3-beta
GTP	guanosine triphosphate
GTPase	guanosine triphosphatase
Gy	Gray (Absorption of 1 Joule of radiation energy by 1 kilogram of matter)
H&E	Haematoxylin and Eosin
HBSS	Hanks's balanced salt solution
Hh	Hedgehog
Hhip	Hedgehog interacting protein
HNPCC	Hereditary non-polyposis colorectal cancer
HPRT	hypoxanthine-guanosine phosphoribosyl transferase
hr	Hour
HRP	Horseradish peroxidase
IHC	Immunohistochemistry
Ihh	Indian hedgehog
IKKα	Inhibitor of kappa-B kinase
ip	Intraperitoneal
IRES	Internal ribosomal entry site
IRS1/2	Insulin receptor substrate1/2
ISC	Intestinal stem cell
IκB	Inhibitor of kappa-B
JPS	Juvenile Polyposis Syndrome
kg	kilograms
k-Ras	Kirsten-Ras
KS	Kolmogorov-Smirnov
L	Litre
LEF	Lymphoid enhancer factor
Lgr5	Leucine rich repeat-containing G-protein coupled receptor 5
LN2	Liquid nitrogen
LOH	Loss of heterozygosity
LoxP	Locus of crossover of bacteriophage P1
LRC	Label-retaining cell
LRP	Low density lipoprotein receptor related protein
M	Molar (moles per litre)
mAb	Monoclonal antibody
mAd	Microadenoma
MAPK	Mitogen-activated protein kinase
Mdm2	Transformed mouse 3T3 cell double minute 2
MEK	Mitogen-activated protein kinase (MAPK), Extracellular signal-regulated kinase (ERK) kinase
mg	milligrams
mins	minutes
ml	millilitres
mM	millimolar
MMP	Matrix Metalloproteinase
MMR	Mis-match repair
MMTV	Murine mammary tumour virus
MOPS	3-(N-morpholino)propanesulfonic acid
MSI	Microsatellite instability
MT	Microtubules
mTOR	Mammalian target of rapamycin
NFκB	Nuclear Factor of kappa light polypeptide gene enhancer in B-cells
NGS	Normal goat serum
NICD	Notch intracellular domain
NO	Nitric oxide
NOD/SCID	Non-obese diabetics/severe combined immunodeficient
NRS	Normal rabbit serum
O/N	overnight
pAb	Polyclonal antibody
PAGE	polyacrylamide gel electrophoresis
PAS	Periodic acid-Schiff's reagent
PBS	Phosphate buffered saline
PBS/T	0.1% TWEEN-20 in Phosphate buffered saline
PCR	Polymerase chain reaction
PDK	Phosphoinositide-dependent kinase
PH	Pleckstrin homology domain
PHTS	Pten hamartoma tumour syndrome
PI	Post-induction
PI3K	Phosphatidylinositol 3-kinase
PIP2	Phosphatidylinositol-4,5-bisphosphate
PIP3	Phosphatidylinositol-3,4,5-trisphosphate
PJS	Peutz-Jeghers syndrome
PLL	Poly-L-Lysine
Ptch	Patched
Pten	Phospatase and Tensin homolog mutated on chromosome 10
PVDF	Polyvinylidene difluoride
qRT	Quantitative real-time
Ras	Rat sarcoma viral oncogene homolog
Rheb	Ras homolog enriched in brain
RNA	Ribonucleic acid
RNase	Ribonuclease

RPM	Revolutions per minute
RT	Room temperature
RTK	Receptor tyrosine kinase
S6	Ribosomal protein S6
S6K	Ribosomal protein S6 kinase
SD	Standard deviation
SDS	Sodium dodecyl sulphate
secs	seconds
Shh	Sonic hedgehog
SHIP	SH2 domain-containing inositol phosphatase
SMAD	Mothers against decapentaplegic homolog
Smo	Smoothened
STK36	Serine-threonine kinase 36
SuFu	Suppressor of fused
TACE	Tumour necrosis factor alpha converting enzyme
Tam	Tamoxifen
Taq	DNA polymerase isolated from *Thermus aquaticus*
TBE	Tris-Borate-EDTA buffer
TBRI	TGF-beta receptor, type I
TBRII	TGF-beta receptor, type II
TBS	Tris buffered saline
TBS/T	0.1% TWEEN-20 in Tris buffered saline
TCF	T-cell factor
TCF-4	Transcription factor 4
TEMED	N,N,N',N'-Tetramethylethylenediamine
Tet	Tetracycline
TGF-beta	Transforming growth factor-beta
TNF-alpha	Tumour necrosis factor alpha
TSC	Tuberous sclerosis
TSC2	Tuberous sclerosis gene 2
TTM	Non-fat milk powder in Tris buffered saline containing 0.1% TWEEN-20
UV	Ultraviolet
V	Volts
v/v	Volume per volume
W	Watts
w/v	Weight per volume
w/w	Weight per weight
Wnt	Wingless-type murine mammary tumour virus integration site family
x g	times gravity
X-Gal	5-bromo-4-chloro-3-indolyl beta-D-galactopyranoside
YFP	Yellow fluorescent protein

Abstract

Colorectal cancer is a significant cause of mortality in the UK, being the third most common cancer type. Activating mutations within the Phosphoinositide 3-Kinase/Akt pathway have previously been reported in a significant proportion of sporadic colorectal cancers. Phosphatase and tensin homolog mutated on chromosome 10 (PTEN) is an antagonist of the PI3K/Akt pathway, and as such is a well characterised tumour suppressor. In this thesis I aimed to characterise the role of Pten within the murine intestine, with respect to homeostasis of otherwise normal epithelium, and also in the context of activated Wnt signalling and activation of the oncogene k-Ras. This has been achieved using a Cre-LoxP-based approach to conditionally delete Pten specifically from the adult murine intestinal epithelium.

Deletion of Pten alone is reported here to have little immediate effect on normal homeostasis of the intestinal epithelium or the intestinal stem cell. At extended timepoints after Pten loss, delayed formation of hamartomas and adenomas within the intestine is reported. In the context of activated Wnt signalling, additional loss of Pten is found to accelerate tumourigenesis, resulting in adenocarcinoma formation. These lesions are characterised by strong activation and membrane localisation of Akt.

Co-ordinate deletion of Pten and activation of k-Ras is reported here to show strong synergy in promoting the formation of both papillomatous lesions of biliary epithelia and widespread hyperplasia of the forestomach squamous epithelium. Lesions within the biliary epithelium are characterised by strong activation of Akt, with gall bladder lesions again showing membrane localisation of Akt. In the intestine, preliminary data reported here also indicates synergy between Pten loss and k-Ras activation in promoting hyperproliferation of the epithelium.

Together, these data therefore indicate that, in normal intestinal epithelium, PTEN is a weak tumour suppressor, but is critical for suppressing neoplasia in the context of other mutations.

Chapter 1: General Introduction

1.1 Intestinal Tumourigenesis

1.1.1 Intestinal Cancer in Humans

1.1.1.1 Incidence

It is now estimated that one in three people will suffer from a form of cancer at some point in their lives. Colorectal cancer (CRC) is one of the most prevalent forms of cancer, with recent statistics placing it as the third most common cancer type across both genders, after lung and breast cancer (excluding non-melanoma skin cancer). Over 36000 new cases are diagnosed per year in the UK, and the incidence of colorectal cancer is increasing (Cancer Research UK, 2007). Despite this fact, mortality rates for colorectal cancer are actually steadily decreasing within the UK (Cancer Research UK, 2007). This is probably largely attributed to enhanced awareness and detection of disease, and improved treatment methods.

1.1.1.2 Environmental risk factors

The observed increase in colorectal cancer incidence in the western world is often attributed to modern lifestyles (Cancer Research UK, 2007). The 'westernised' diet, typically comprising high consumption of red meats and processed foods coupled with low consumption of fresh vegetables and dietary fibre, is thought to be one of the biggest risk factors for colorectal cancers (Norat et al., 2005). Decreased physical activity is also known to contribute towards an increased risk of CRC (Slattery et al., 2003). Associated with these two factors, obesity is also known to be an important risk factor (Murphy et al., 2000), and it is estimated that up to 11% of cases within Europe are obesity-related (Bergstrom et al., 2001). Finally, smoking (Giovannucci et al., 1994, Chao et al., 2000) and high alcohol consumption (Bardou et al., 2002) have also been linked to increased risk of colorectal malignancy.

1.1.1.3 Genetic risk factors and predisposition

Recognised hereditary CRC predisposition syndromes are known to contribute significantly to the overall incidence of CRC. Two such syndromes are the most common and are well-characterised; Familial Adenomatous Polyposis (FAP), which is associated with mutations in the Adenomatous polyposis coli gene (Apc), and Hereditary Non-Polyposis Colorectal Cancer (HNPCC; also known as Lynch Syndrome) which is associated with mutations in a number of

mismatch repair (MMR) genes (OMIM, 2008, de la Chapelle, 2004). However, many cases of colorectal cancers show familial tendency, even without identification of an underlying inherited mutation. It has previously been shown that individuals who have a family history of CRC in first degree relatives show more than double the risk of developing CRC, compared to an individual with no family history of the disease (Johns and Houlston, 2001).

1.1.1.4 Treatment

As with any cancer, the course of treatment a patient undergoes is largely dependent upon the severity of disease at diagnosis. The vast majority of cases (approximately 80%) will undergo invasive surgical resection of the intestine to remove malignant tissue, which may involve a temporary or permanent stoma (NICE Guidelines, 2004). Pre-operative radiotherapy is given in a small number of cases, and has been shown to reduce rates of local recurrence of disease after surgery, though long-term toxicity of radiotherapy is a significant problem. Many patients with more advanced disease will also receive chemotherapy after surgery, providing they remain healthy enough to tolerate it. Traditionally, therapies involve the use of 5-Fluorouracil (5-FU)/Folinic acid (FUFA) as standard, which also carries a number of problems caused by off-target effects (NICE Guidelines, 2004). For therapies to improve, they need to become more specifically targeted towards cancer cells, both to reduce toxicity problems elsewhere in the body and to increase efficacy. In order to achieve this, modern therapeutic agents are becoming much more sophisticated, and the development of these has been largely facilitated by basic research into intestinal tumourigenesis. Generic examples of more recently developed chemotherapeutics include: therapeutic monoclonal antibodies targeting particular signalling pathways (such as Cetuximab, an epidermal growth factor receptor (EGFR) antagonist) (Rivera et al., 2008), Topoisomerase inhibitors (such as Irinotecan, a Topoisomerase II inhibitor) and small molecule tyrosine kinase inhibitors (such as Gefitinib, an EGFR inhibitor) (Van Cutsem and Geboes, 2007).

1.1.2 The mammalian small intestine

1.1.2.1 Gross structure and function of the small intestine

The mammalian small intestine is a highly specialised organ, adapted for the maximal absorption of nutrients from food. The intestine is comprised of three tissue layers; the external smooth muscle layer, the submucosal stroma and the inner mucosal surface (Crane, 1968)(See Figure 1.1). The main function of the smooth muscle layer is to facilitate the movement of food along the intestine by peristalsis. The submucosa functions largely as a supportive structure for the mucosal layer, and is comprised of blood vessels, enteric neurons, infiltrating immune cells and supportive stromal and mesenchymal cells. At regular intervals, the normal structure of the

submucosa is interrupted by the presence of lymphoid follicles, known as Peyer's patches (MacDonald, 2003). The inner, mucosal surface of the intestine is in direct contact with food within the lumen, and consists of a continuous layer of epithelial cells. The mucosa is responsible both for the secretion of a number of agents to facilitate digestion and digestive transit, and for the selective transfer of nutrients from the lumen of the intestine into the blood supply.

1.1.2.2 Organisation of the epithelium

The mucosal lining of the intestine consists of a simple columnar epithelium. The epithelium is organised into finger-like projections into the lumen of the intestine, called villi, which are surrounded by invaginations of the epithelium known as the crypts of Lieberkühn ('crypts') (See Figure 1.1). These structures serve to greatly increase the absorptive surface area of the epithelium, and also compartmentalise the epithelium into regions of immature cells (the crypt) and mature cells (the villus) (Sancho et al., 2003).

The intestinal epithelium is constantly being renewed. Cells originate from stem cells, thought to be located towards the bottom of the crypt (see below). The stem cell divides slowly; approximately once every 24 hours in mice (Potten et al., 1990), though this is thought to be up to eight times slower in humans (Potten et al., 1992). The slowly dividing stem cell gives rise to a population of immature epithelial progenitor cells, known as transit amplifying (TA) cells. These cells proliferate extremely rapidly in order to generate the large numbers of cells needed to repopulate the epithelium. This region of highly proliferative cells within the crypt is known as the transit amplifying zone (Sancho et al., 2003). As TA cells move up the crypt-villus axis they become progressively more differentiated, which is coupled with loss of their proliferative capacity. By the time cells exit the TA zone, they have terminally differentiated into one of the mature epithelial cell types of the intestine. All mature cells reside on the villus, with the exception of Paneth cells, which reside at the very base of the crypt. Paneth cells secrete antimicrobial agents into the lumen of the intestine, which act to regulate the composition of the intestinal flora (Cheng, 1974b). Of the mature cell types on the villus, the most predominant are enterocytes. The primary function of these cells is the absorption of nutrients (Cheng and Leblond, 1974a), and together they form the brush border (Crane, 1968). Enterocytes also secrete hydrolases, to aid the digestion of food within the lumen. At numerous points within the villus, the brush border is interrupted by the presence of Goblet cells. These are mucin-secreting cells, providing lubrication and protection for the epithelium (Cheng, 1974a). Also present are hormone-secreting enteroendocrine cells, which function to allow paracrine control of secretions within the intestine (Cheng and Leblond, 1974b). Rarely, a fifth mature epithelial cell type is found; the microfold or 'M' cell (Owen and Jones, 1974). These cells are found exclusively in epithelium over-lying Peyer's

patches (Rosner and Keren, 1984), and function as antigen-presenting cells, transferring antigens by transcytosis from the intestinal lumen to the underlying lymphoid tissue.

Once on the villus, all differentiated cell types continue to migrate up the crypt-villus axis. As cells approach the end of the villus, they either undergo apoptosis or are shed into the intestinal lumen and undergo anoikis, with the entire migratory process taking just a few days (Heath, 1996) (See Figure 1.1).

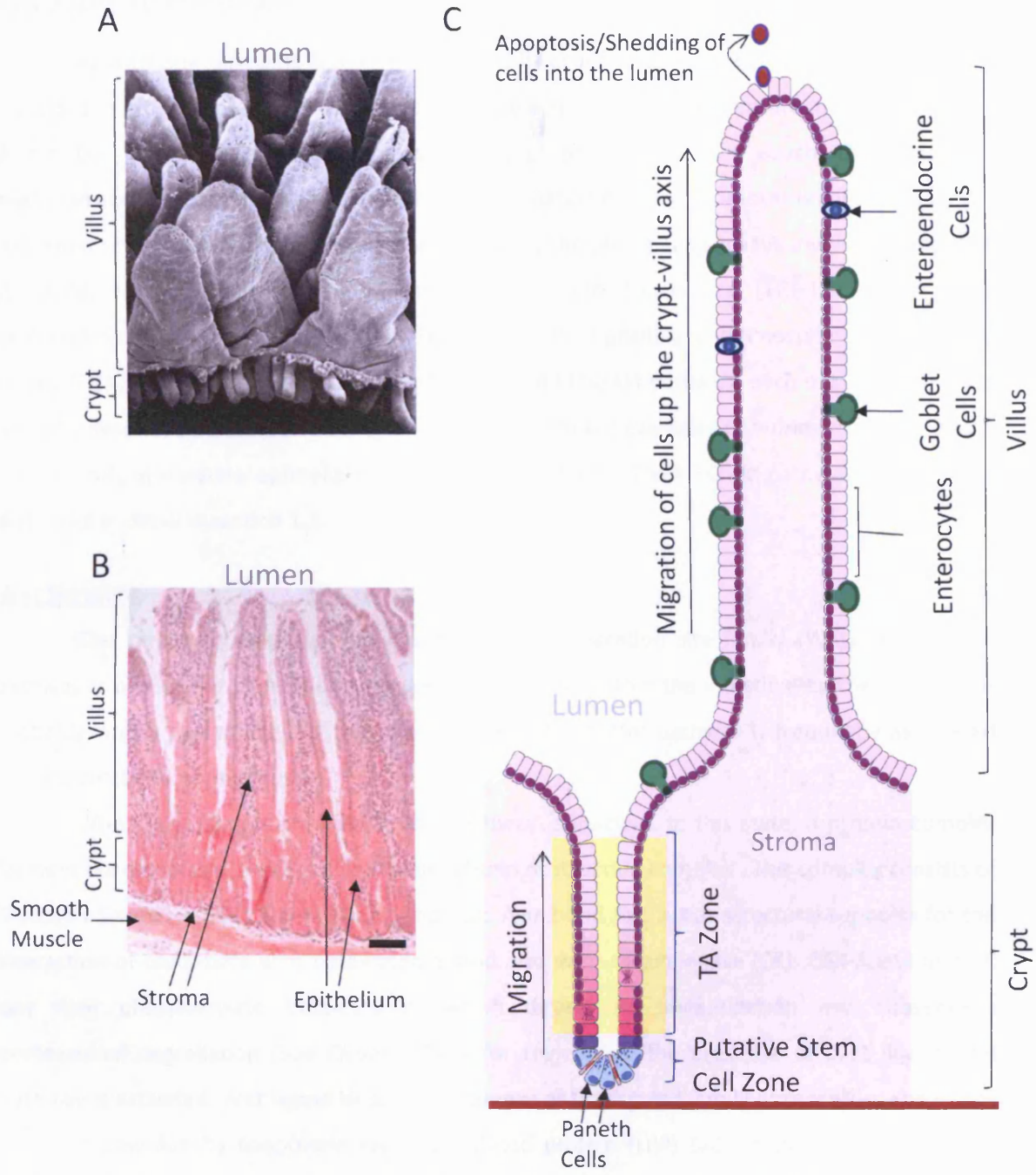

Figure 1.1: ***Structure and Organisation of the mammalian small intestinal epithelium.***
Scanning Electron Microscopy of the mouse small intestine (A) reveals organisation of the epithelium into invaginations into the mucosa, known as crypts of Lieberkuhn ('crypts') and projections into the lumen of the intestine, known as villi. Image courtesy of Alastair Watson, University of Liverpool.
Histological appearance of normal small intestinal epithelium (B) reveals distinct layers of the intestine, including the epithelium, the underlying stroma, and the smooth muscle layer. Scale bar indicates 100μm.
Cartoon representation of a single crypt-villus unit (C). Epithelial cells are born in the stem cell zone, and proliferate rapidly and become progressively more differentiated as they move up the crypt-villus axis through the TA zone (Yellow). Mature, differentiated cells reside on the villus, with the exception of Paneth cells (Pale blue), which are found at the base of the crypt. The villus is supplied by cells from many crypts, and is comprised of differentiated enterocytes (Pale pink), Goblet cells (Green) and Enteroendocrine cells (Dark blue). Cells continue to migrate up the crypt-villus axis until they reach the villus tip, where they undergo apoptosis and/or are shed into the lumen of the intestine.

1.1.2.3 Epithelial homeostasis

As with any renewing tissue, the balance of proliferation and cell loss must be closely regulated in order to prevent either ablation of the epithelium or aberrant accumulation of cells. Within the intestinal epithelium, the processes of proliferation, cell death, differentiation, migration and cell positioning are closely linked. Regulation of these processes is controlled by the combined action of a number of signalling pathways, the principal pathways involved being Wnt signalling, Notch/Delta signalling, Transforming growth factor-beta (TGF-beta) and bone morphogenic protein (BMP) signalling, Hedgehog (Hh) signalling and Phosphatidylinositiol 3-kinase (PI3K)/Akt signalling. With the exception of the PI3K/Akt pathway, each of these pathways is briefly described below (See also Figure 1.2), and pertinent examples of murine *in vivo* evidence for their role in intestinal epithelial homeostasis are outlined. The PI3K/Akt pathway and Pten are discussed in detail in section 1.2.

Wnt Signalling

The canonical Wingless-type murine MMTV integration site family (Wnt)/beta-catenin pathway is one of the best studied regulatory pathways within the intestinal epithelium. This is probably largely due to the fact that dysregulation of the Wnt pathway is frequently associated with colorectal tumourigenesis.

When Wnt ligands are absent, the pathway is inactive. In this state, a protein complex forms in the cytoplasm, known as the 'beta-catenin destruction complex'. This complex consists of Glycogen Synthase (GSK) 3-beta, Axin2 and Apc. Axin2 and Apc act as structural supports for the interaction of GSK3-beta with beta-catenin, and also with casein kinase (CK). GSK-3beta and CK can then phosphorylate beta-catenin, which directs its ubiquitination and subsequent proteasomal degradation (See *Clevers, 2006* for review). In the presence of Wnt ligand, the pathway is activated. Wnt ligand binds to a member of the frizzled family of receptors and its co-receptor, Low-density lipoprotein receptor related protein (LRP) 5/6, at the cell surface. This results in activation of dishevelled within the cytoplasm, and also in phosphorylation of the LRP co-receptor, which can recruit and bind axin. Although the exact mechanism remains unclear, it is known that these events ultimately result in the disassembly of the beta-catenin destruction complex. Beta-catenin is therefore stabilised, it can accumulate within the cytoplasm and translocate to the nucleus. Once in the nucleus, beta-catenin can interact directly with members of the T-cell factor (TCF)/Lymphoid enhancer factor (LEF) family of transcription factors to stimulate transcription of a variety of Wnt target genes (For review see Clevers, 2006, Sancho et al., 2004).

A gradient of Wnt activity is known to exist within the intestine, with active Wnt signalling being at its highest at the base of the crypt and gradually decreasing up the crypt-villus axis

(Gregorieff et al., 2005). This gradient of signalling is arguably one of the major influential factors on epithelial homeostasis.

A number of studies, using a variety of approaches, have demonstrated that Wnt activity in the crypt is essential for maintenance of the proliferative compartment. Early studies indicated that constitutive deletion of the Wnt effector TCF-4 causes complete loss of the proliferative compartment of the embryonic epithelium, but has no effect either on the development of epithelium from primitive gut endoderm, or on differentiated enterocytes and goblet cells on the villus (Korinek et al., 1998). More recently, *Pinto et al.* (2003) and *Kuhnert et al.* (2004) have demonstrated that inhibition of Wnt signalling (by ectopic expression of the Wnt antagonist Dickkopf-1 [Dkk-1]) in the adult mouse small intestine results in loss of epithelial proliferation and rapid degeneration of the crypt-villus architecture. Additionally, loss of the proliferative zone and ablation of the epithelium is also observed following conditional deletion of the critical Wnt transducer and effector, beta-catenin (Ireland et al., 2004). Interestingly, these phenotypes are replicated following deletion of the well-characterised Wnt target gene cellular-Myelocytomatosis oncogene (c-Myc) (Muncan et al., 2006), suggesting that stimulation of proliferation by wnt signals is entirely dependent upon c-Myc. In a similar but opposite approach, both *Sansom et al.* (2004) and *Andreu et al.* (2005) find that activation of Wnt signalling by deletion of Apc results in a 'crypt progenitor' phenotype, with a dramatic increase in proliferative cells within the crypt. This is also coupled with a complete block in cell migration and impaired apoptotic response, which probably also contribute to the proliferative phenotype. Associated with its role in controlling proliferation in the crypt, Wnt activity is also postulated to be essential for maintenance of the intestinal stem cell; this role is described in more detail in section 1.1.3.

There is also evidence to suggest that Wnt signals are important for the differentiation of cell types within the epithelium. As described above, *Korinek et al.* (1998) find that inhibition of Wnt signalling by deletion of TCF-4 causes loss of proliferation in embryonic gut. Interestingly, this study also notes that, while goblet cells remained present in the epithelium, enteroendocrine cells were entirely absent. It has also been demonstrated that, not only is Wnt signalling required for correct localisation of paneth cells, but also for their full maturation (van Es et al., 2005a). Concurrent with these observations, it has also recently been shown that abrogation of wnt signalling by deletion of beta-catenin results in a skew in differentiation pattern towards the enterocytic cell lineage (Fevr et al., 2007).

Wnt signalling is also known to be important for cell positioning within the crypt, particularly for the paneth cell. Activation of Wnt signalling by deletion of Apc has been shown to cause loss of paneth cell location at the very base of the crypt, with diffuse distribution of cells throughout the crypt observed instead (Sansom et al., 2004, Andreu et al., 2005). A similar phenotype is observed following inactivation of Wnt signalling by deletion of the Frizzled 5

receptor (van Es et al., 2005a), suggesting that paneth cell localisation is dose-dependent, with both too much and too little Wnt activity resulting in aberrant cell positioning. Further to this, work has indicated that a particular group of Wnt target genes are particularly influential with regard to cell positioning within the intestine; the B-type Eph receptors, EphB2 and EphB3. EphB receptors and their cognate ligands, the cell surface proteins of the ephrinB family, are expressed in a reciprocal fashion along the length of the crypt-villus. EphB receptor expression is strongest in the lower regions of the crypt, concurrent with the fact that the receptors are targets of Wnt signalling, whereas ephrinB ligand expression is observed only on the villus (Batlle et al., 2002). Following deletion of both EphB2 and EphB3 genes in the mouse, cell positioning was found to be greatly perturbed in the crypt, with observation of defects similar to those occurring following deletion of Apc. That is, Paneth cells were found to be distributed throughout the crypt rather than restricted to the crypt base, and the proliferative zone was found to be poorly organised, with intermingling of proliferative progenitor cells with other more differentiated cell types within the crypt and lower villus. Additionally, loss of migratory direction up the crypt-villus axis was also observed (Batlle et al., 2002). Consequently, the conclusion of this study was that Wnt signalling exerts its regulatory effect on cell positioning within the epithelium principally through modulation of expression of EphB receptors (See also *Clevers and Batlle, 2006* for review).

Notch/Delta Signalling

Notch signalling is known to play a number of important roles in the homeostasis of self-renewing tissues, including regulation of proliferation, differentiation and cell fate specification (Wilson and Radtke, 2006).

Notch pathway activation is achieved by binding of the Notch cell surface receptor to one of the Delta-like or Jagged family of membrane-bound ligands on an adjacent cell. This stimulates cleavage of the Notch receptor, both extracellularly, by Tumour necrosis factor (TNF)-alpha converting enzyme (TACE), and intracellularly, by gamma-secretase. The intracellular portion of the notch receptor, which is released following cleavage by gamma-secretase, is known as the Notch intracellular domain (NICD). The NICD is then able to translocate to the nucleus where, together with the essential transcription factor CSL, it activates transcription of its target genes (Wilson and Radtke, 2006).

In the intestine, a number of elegant experiments have demonstrated the importance of Notch signalling for the differentiation of epithelial secretory cell lineages and for maintenance of the undifferentiated state of TA cells.

One of the first direct studies investigating the role of notch signalling in vivo in the intestine was that of *van Es* and colleagues (van Es et al., 2005b). Upon deletion of the essential notch transcription factor CSL/RBP-J, transit amplifying cells were found to be replaced with

mature, differentiated goblet cells. Closer analysis revealed almost complete loss of all replicative cells within the crypt, and their replacement with post-mitotic cells. The impact of this was that repopulation of the crypt-villus axis was absolutely inhibited. The presence of enteroendocrine cells and paneth cells was found to be unaffected. An identical phenotype was obtained following treatment of mice with a specific inhibitor of gamma-secretase. The authors conclude that notch signalling is essential for preventing differentiation of immature proliferative cells, and also for specifying cell fate.

At the same time as this study, a reverse approach was being pursued by *Fre et al.* (2005), who overexpressed a constitutively active form of the Notch-1 receptor in the mouse intestine. This study essentially observed an exact reciprocal phenotype to that described above, in that activation of notch signalling resulted in severe deficiency of secretory cell types in the intestine. Paneth cells, enteroendocrine cells and goblet cells were totally undetectable following notch activation. Absorptive enterocytes were found to be present; however they exhibited some abnormalities, particularly of the apical brush border. In addition to this, expansion of the proliferative compartment was observed.

One further study has added an additional layer of complexity to the role of notch signalling in the intestine. In a similar approach to *Fre et al.* (2005), a constitutively active form of Notch-1 receptor has been expressed in the intestine by *Zecchini and colleagues* (2005). However, in this case the experimental approach employed results in much stronger expression of the mutant receptor. *Zecchini et al.* observed a phenotype much more similar to that of *van Es et al.* (van Es et al., 2005b), with a dramatic increase in the numbers of goblet cells observed, however in this case they were found to be predominantly on the villus rather than within the crypt. Interestingly, this study also reports no effects on the proliferative zone of the crypt. Taken together, these data therefore suggest that whilst the presence of notch signalling is essential for maintenance of the transit amplifying zone, dose-dependency of signalling operates with respect to control of cell differentiation. It appears that a fine balance of notch signalling must be present within the intestine to adequately maintain differentiation down secretory cell lineages. Indeed, such sensitivity to levels of notch signalling has also been implied from work performed in intestinal cells of *Drosophila* (Ohlstein and Spradling, 2007).

TGF-beta and BMP Signalling

Transforming growth factor (TGF)-beta signalling is known to modulate proliferation and differentiation of cells in a number of tissue types. In the intestine, the observation that disruption of TGF-beta signalling is linked to the progression of colorectal cancers suggests that this pathway may play a role in homeostasis of the epithelium (Sancho et al., 2004).

Bone morphogenic proteins (BMPs) are part of the Transforming growth factor-beta (TGF-beta) superfamily. BMP signalling is required both for development and maintenance of the intestinal epithelium, and plays a particularly interesting role in regulating the interaction between epithelial cells and the underlying mesenchyme (Ishizuya-Oka, 2005). Mutations in BMP pathway components are also known to be the cause of Juvenile polyposis syndrome (JPS) in humans, a condition characterised by the development of multiple intestinal lesions at a young age (OMIM, 2008). Loss of BMP signalling has also been reported in a large proportion of sporadic colorectal tumours (Kodach et al., 2008b).

Both TGF-beta proteins and BMPs are soluble, extracellular signalling proteins. TGF-beta proteins bind preferentially to TGF-beta type II receptors (TBRII), which then associate with the type I receptor (TBRI). Conversely, BMPs bind preferentially to their type I receptors (BMPRI), which then dimerise with the BMP type II receptor (BMPRII) (Shi and Massague, 2003). In both cases, the type I receptor can then be phosphorylated and activated by the type II receptor. These events activate an intracellular signalling cascade involving the activation of members of the Mothers Against Decapentaplegic homolog (SMAD) family of signal transducers. Receptor-associated SMADS (R-SMADS), including SMADs 1, 2, 3, 5 and 8, are phosphorylated and activated by type I receptors. SMAD2 and 3 are preferentially phosphorylated by the TGF-beta type I receptor, whereas BMP type I receptor signalling is usually transduced by SMAD1, 5 or 8. Activated R-SMADs then associate with SMAD4 (also known as common or co-SMAD), and translocate to the nucleus. Once in the nucleus, the active SMAD complex can then modulate gene expression in combination with transcriptional coactivators or corepressors, the presence of which is largely determined by cell type (For review see *Shi and Massague, 2003*).

Abrogation of BMP signalling in the intestine has previously been shown to disrupt intestinal homeostasis (He et al., 2004). Deletion of the BMP type I receptor (BMPRI) was found to result in an increase in proliferation within the epithelium, and the development of intestinal polyps similar to that seen in human JPS. This study also proposes a role for BMP signalling in maintenance of the intestinal stem cell, which is discussed below (Section 1.1.3.4). A further study investigating the effect of attenuating BMP signalling employed the use of an inhibitor of BMP signalling, Noggin (Haramis et al., 2004). *Haramis and colleagues* found that transgenic expression of Noggin resulted in mildly abnormal villus structure, and the development of ectopic crypt structures. The crypts which formed appeared normal in structure and composition, but were mis-localised. This led the authors to conclude that BMP signalling is important for interactions between epithelial cells and underlying mesenchymal cells to coordinate the development of epithelial structures in the correct context. Like *He et al.* (He et al., 2004), this study also reports the development of intestinal tumours reminiscent of human JPS. The results of this study have also been corroborated by a very similar independent study (Batts et al., 2006).

To further investigate the role of BMP signalling in interaction between intestinal epithelial cells and their surrounding cell types, *Kim et al.* (2006) (Kim et al., 2006) have deleted SMAD4 in both intestinal epithelial cells and in T-cells. This study found that deletion of SMAD4 in intestinal epithelial cells results in a surprising lack of phenotype. However, deletion of SMAD4 from T-cells was found to result in a number of alterations in the intestinal epithelium, including aberrant growth of crypt structures similar to that seen by *Haramis et al.* (Haramis et al., 2004). This study also reports the development of intestinal polyps and invasive carcinomas of the intestine following T-cell specific deletion of SMAD4, which raises the hypothesis that human JPS may, in some cases at least, arise due to loss of BMP signalling in T-cells rather than within the epithelium itself.

The role of epithelial TGF-beta signalling in the maintenance of intestinal homeostasis appears to be less well understood. Studies employing the expression of a dominant negative TGF-beta type II receptor to abrogate TGF-beta signalling have indicated that TGF-beta signalling is dispensable in normal mouse epithelium (Beck et al., 2003). However, TGF-beta signalling appears to be essential for re-establishing homeostasis of the epithelium following injury. Again, the dominant negative TGF-beta type II receptor model has been used to demonstrate that mice deficient for TGF-beta signalling activity show increased susceptibility to both colitis (Beck et al., 2003) and to tumourigenesis (Hahm et al., 2002) following treatment with chemical inducing agents. Several other models employing different strategies to diminish TGF-beta signalling have also confirmed the finding that pre-existing intestinal lesions are predisposed to progression in the context of reduced TGF-beta signalling (Sancho et al., 2004).

Hedgehog Signalling

Hedgehog (Hh) signalling in the intestine plays its most important role during embryonic development of the gastrointestinal tract, where hedgehog proteins act as morphogens which are critically important for establishment of crypt-villus architecture of the gut (For extensive review, see van den Brink, 2007). Although mutations of the hedgehog pathway are only very rarely reported to be associated with colorectal cancers, study has suggested that hedgehog signalling plays a role in maintaining intestinal homeostasis in the adult organ.

The hedgehog family of proteins consists of Sonic hedgehog (Shh), Indian hedgehog (Ihh) and Desert hedgehog (Dhh). In the absence of Hedgehog proteins, the signalling pathway is inactive. Unbound cell surface receptors of the Patched family (Ptch1 and Ptch2) elicit an inhibitory effect upon the transmembrane signal transducer, Smoothened (Smo). Inactive Smo permits the intracellular formation of a protein complex consisting of Costal-2 (Cos-2) and Fused (Fu), which assemble together with microtubules. This complex is able to bind the Hh effector and transcription factor, Glioma-associated oncogene homolog (Gli), which serves to both sequester

Gli away from the nucleus, as well as to target its proteolytic cleavage and inactivation. Hedgehogs are able to bind to Ptch receptors, and in doing so allow release of the repressive activity of the unbound Ptch receptor on Smo. This in turn allows activation of the serine-threonine kinase (STK) 36, which both inhibits formation of the Cos-2/Fu-containing protein complex as well as activating Suppressor of Fused (SuFu). These events allow accumulation of full-length Gli, which can then translocate to the nucleus and activate transcription of its target genes (For review see *Lees et al., 2005, Katoh and Katoh, 2006*).

Much of the study into the role of hedgehog signalling in the small intestine has focused on its role during development. However, such studies have provided some clues as to how hedgehog signals may be involved in homeostasis in the fully mature adult. Nullizygosity for either Shh or Ihh has been shown to cause serious malformation of the entire gastrointestinal tract, resulting in lethality (Ramalho-Santos et al., 2000). Closer analysis of the embryonic small intestine of $Ihh^{-/-}$ mice revealed a marked reduction of cell proliferation resulting in villus atrophy. The authors suggest that this implies a role for hedgehog signalling in maintaining proliferation of the intestinal stem cell. A dramatic reduction in enteroendocrine cells is also observed, suggesting a further role for hedgehog signalling in cell fate determination in the epithelium (Ramalho-Santos et al., 2000). In contrast to this study, complete abrogation of hedgehog signalling in the intestine by expression of the inhibitory hedgehog interacting protein (Hhip) has been shown to result in hyperproliferation of the epithelium. Hhip was expressed in the intestinal epithelium throughout development from the *Villin* gene promoter, and animals were analysed at very early stages of life (up to postnatal day P5). The crypt-villus architecture of the epithelium was found to be perturbed, caused by hyperproliferation of epithelial cells, along with ectopic crypt development and abnormal branching of villi (Madison et al., 2005). This study also reports abnormalities in differentiation of epithelial cells following Hh inhibition, but in this case defects in absorptive enterocytes are reported, resulting in the generation of an incomplete and ineffective brush border (Madison et al., 2005). The discrepancy in phenotype observed between these studies could be due to a number of reasons, for instance the latter study examines the effect of abrogation of all Hh signals, whereas *Ramalho-Santos and colleagues* have examined the specific effects of blocking signalling only through Ihh. This suggests that the outcomes of hedgehog signalling initiated by different hedgehog proteins may not be equivalent in the intestine.

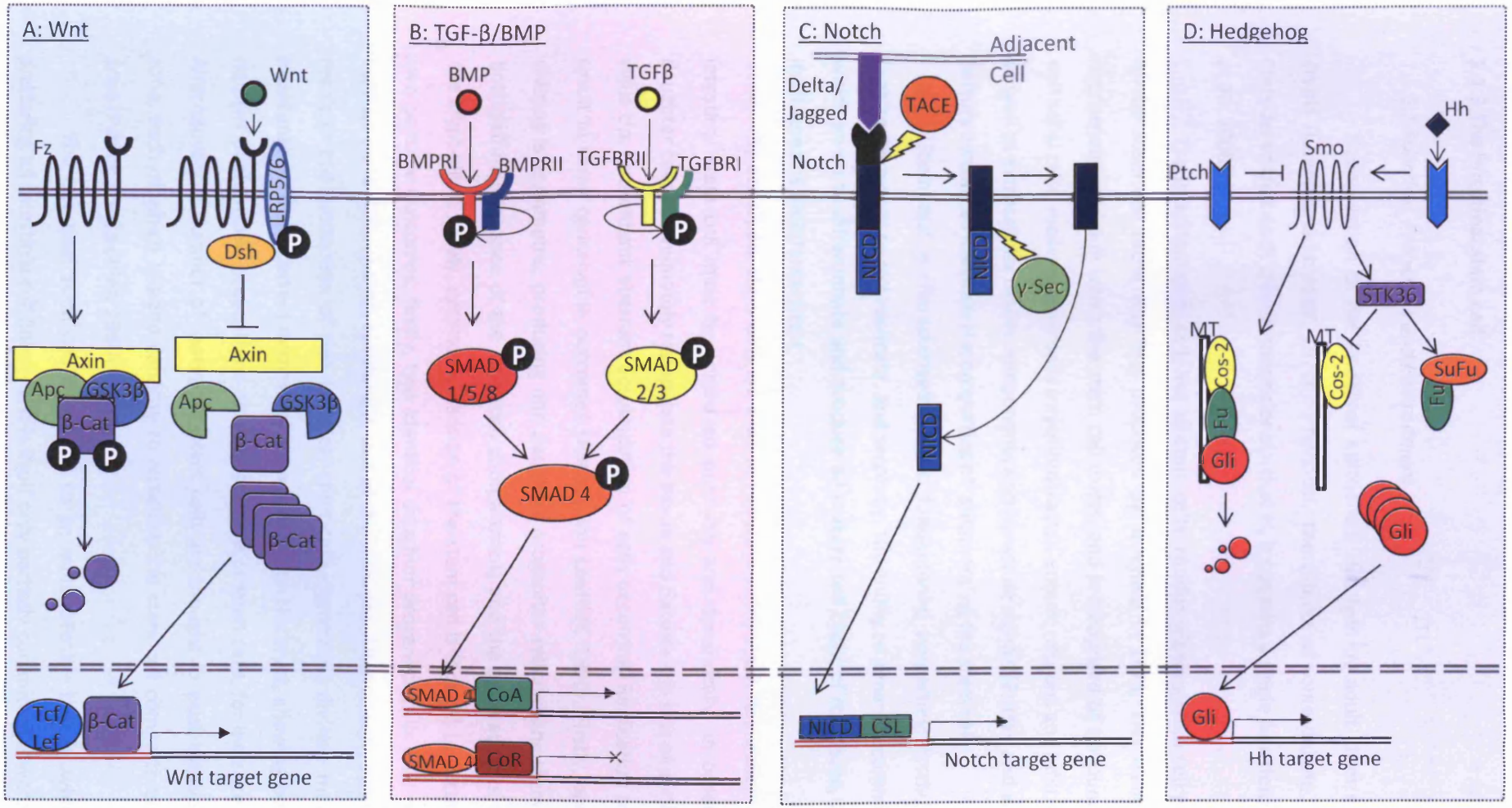

Figure 1.2: ***Major regulatory signalling pathways influencing homeostasis of the intestinal epithelium.***

A: Wnt Signalling. Absence of Wnt ligand permits formation of the 'β-catenin destruction complex', comprised of Axin, Apc and GSK3β, which binds β-catenin and mediates its phosphorylation and proteasomal degradation. Binding of Wnt ligand to Frizzled (Fz) receptor and LRP5/6 co-receptor results in activation of Dishevelled (Dsh) and phosphorylation of LRP5/6, which together inhibit the β-catenin destruction complex, allowing accumulation and translocation of β-catenin to the nucleus where, genes with Tcf/Lef factors, it activates transcription of Wnt target.

B: TGF-β/BMP Signalling. BMPs or TGFβs bind to their cognate type I/II receptors, resulting in phosphorylation of the type I receptor. BMP signals are transduced through SMAD1/5/8, TGFβ signals through SMAD2/3. Both result in activation of SMAD4, which translocates to the nucleus and acts with co-activators (CoA) or co-repressors (CoR) to modulate target gene expression.

C: Notch Signalling. Binding of notch receptor by cell-surface ligands of the Delta/Jagged family stimulates cleavage of the Notch receptor by TACE and γ-secretase (γ-Sec). Cleavage by γ-secretase releases the notch intracellular domain (NICD), which translocates to the nucleus and acts with the transcription factor CSL to activate expression of target genes.

D: Hedgehog Signalling. Unbound Patched (Ptch) receptors inhibit the smoothened (Smo) signal transducer, allowing formation of Cos-2/Fu complex with microtubules (MT), which binds the Gli transcription factor, sequestering it away from the nucleus and targeting its cleavage. Binding of Hedgehogs (Hh) to Ptch, releases repression of Smo, which in turn activates STK36. Suppressor of Fused (SuFu) is activated, and the Cos-2/Fu-containing complex can not form. Full-length Gli accumulates, and translocates to the nucleus, where it activates target genes.

1.1.3 The intestinal stem cell

1.1.3.1 Function, Properties and Environment

Repopulation of the intestinal epithelium is driven by adult stem cells residing within crypts (Cheng and Leblond, 1974c). Previously the subject of some debate, it is now generally considered that each crypt is monoclonal - that is, it contains a single functional stem cell (Scoville et al., 2008).

The intestinal stem cell, like all stem cells, resides within a stem cell niche. The existence of the stem cell niche was first proposed by *Schofield* in 1978. This niche is defined as the microenvironment in which the stem cell exists, and is comprised of surrounding cells, including epithelial cells, mesenchymal cells (myofibroblasts), enteric neurons and infiltrating immune cells, as well as extracellular matrix components and paracrine signals (Brittan and Wright, 2002). These factors interact to maintain the properties of 'stemness' of the stem cell.

'Stemness' is characterised by two fundamental properties; firstly, the possession of limitless potential to self-replicate, and secondly, the ability to generate committed daughter cells which go on to differentiate and produce all mature cell types of the tissue, whilst the stem cell itself remains undifferentiated.

By definition, stem cells are able to replicate indefinitely. Replication and renewal of the intestinal stem cell must be controlled precisely and dynamically, in order generate enough daughter cells to adequately repopulate the tissue and balance the loss of epithelial cells from the villus tip, but without aberrant accumulation of cells occurring. Replication of the stem cell can result in three conceivable outcomes (Potten and Loeffler, 1990). Firstly, and most commonly, division is asymmetric, producing one daughter progenitor cell and one stem cell, thus allowing both self-maintenance of the stem cell compartment and the generation of cells to repopulate the crypt-villus. Rarely, symmetric division of the stem cell is thought to occur. This can result in two possible outcomes; firstly, two identical daughter progenitor cells may be produced, which both go on to differentiate, resulting in loss of the stem cell. Alternatively, symmetric division may result in the production of two identical stem cells. Symmetric division may operate to allow maintenance of the correct number of stem cells within the crypt, allowing both reduction in the number of stem cells present and also replacement of stem cells, for instance following damage. Alternatively, a number of 'potential' stem cells are thought to exist transiently within the TA zone, each of which has the capacity to replenish the stem cell compartment should the need arise (Potten and Loeffler, 1990).

The intestinal stem cell is thought to be multipotent – that is, whilst it is capable of producing all intestinal cell lineages, it is itself only partially committed towards an intestinal fate (and can therefore not produce cells of other tissues). In order to achieve homeostasis of the

intestinal epithelium, this partially undifferentiated state must be maintained. A number of signalling pathways are known to contribute to this, and are discussed below (see section 1.1.3.3).

1.1.3.2 Location and Markers of the intestinal stem cell

The exact location of the intestinal stem cell within the crypt has been the subject of much debate, and this debate has recently been revived with vigour. Undoubtedly, one of the major factors hampering the definitive identification of the location of the stem cell is the lack of a good marker of the ISC. Conversely, many of the candidate markers of the stem cell currently known have been identified based on their restricted expression within a small number of cells within candidate stem cell regions. It is therefore apparent that identification of the location of the stem cell and of a good marker of it, are closely linked.

The stem cell zone is widely thought to be located at around positions +4 to +6 (i.e. 4 to 6 cell positions from the base of the crypt) (See Figure 1.3), directly above the paneth cell compartment. Evidence for this was based largely on long-term label-retention studies (See *Potten, 1998* for review). The rationale behind such studies lies in the differential kinetics of cell replication and migration occurring within the crypt. Labelling of replicating cells can be achieved by exposing cells to short pulses of labelled bases, such as tritiated (H^3-) thymidine or Bromodeoxyuridine, which are incorporated into DNA during replication. This approach will label both stem cells and TA cells within the crypt. However, TA cells rapidly proliferate and migrate out of the crypt. Thus, delayed 'chasing' and detection of labelled cells can allow differentiation between rapidly migrating and immotile cells, and hence visualisation of the presumptive population of stem cells, or 'label-retaining cells' (LRCs). Such experiments, as performed in a series of studies by *Christopher Potten and colleagues*, revealed that the LRC is normally found in the lower region of the crypt, with the most common position being between 4 and 9 cells from the crypt base (Potten, 1998).

An alternative position for the stem cell was originally proposed by Cheng and Leblond (Cheng and Leblond, 1974c, Also reviewed in Bjerknes and Cheng, 2005a). This alternative position is within the slender cells which are found intercalated between Paneth cells at the very bottom of the crypt, and are known as crypt base columnar cells (CBCs). This model proposes that cells below position 4 in the crypt are slowly dividing, and are able to maintain an undifferentiated state, whereas cells in positions 5 and above are more rapidly cycling and are committed to differentiation.

Following much investigation, a number of putative markers of the ISC have recently been proposed. However, these markers do not necessarily label the same populations of cells, and apparently show only limited overlap in labelling patterns.

One of the first proposed molecular markers of the intestinal stem cell was the RNA-binding protein, Musashi-1 (Potten et al., 2003). Originally identified in *Drosophila* as regulator of asymmetric division in neural precursor cells (Nakamura et al., 1994), Musashi-1 has also been shown to be a negative regulator of the Notch pathway in neuronal stem cells (Okano et al., 2005). Expression of Musashi-1 has been shown to be high in murine neonatal small intestinal crypts, which at this stage, are thought to be rich in stem cells. In adult murine tissue, Mushashi-1 expression is seen to be restricted to the lower region of the crypt, with labelling most frequent at approximately position +5 (Potten et al., 2003). Interestingly, this study also observes staining of CBC cells, between paneth cells at the very base of the crypt. Following radiation injury, the regenerative clonogenic response of the intestine is seen to coincide with a rise in expression of Musashi-1, as well as a more widespread expression pattern within the repopulating crypt structure. It was, however, noted that not all proliferating cells participating in crypt repopulation were positive for Musashi-1 staining. Finally, this study shows that Musashi-1 is found to be highly expressed in adenomas of Apc^{MIN} mice. The authors therefore propose that Musashi-1 is a marker of both the intestinal stem cell, and of very early intestinal cell lineages, but does not mark all proliferative cells within the crypt.

More recently, three markers have been proposed which may more specifically mark the stem cell; Doublecortin and Calmodulin-kinase like-1 (DCAMKL-1), Leucine-rich repeat containing G-protein coupled receptor 5 (Lgr5) and B-lymphoma Mo-MLV insertion region 1 polycomb ring-finger oncogene (Bmi1).

DCAMKL-1 is a microtubule-associated kinase expressed throughout the central nervous system, specifically in post-mitotic neurons (Ohmae et al., 2006). Recent work has identified that DCAMKL-1 is expressed within progenitor cells of the crypt (May et al., 2008). Further investigation into this revealed that only a very limited number of cells within the crypt express DCAMKL-1, and these are generally located in approximately the +4 position, though cells within the CBC cell population were also occasionally labelled. Additionally, positively-stained cells were observed in only one in six crypts in tissue sections, which is approximately consistent with the notion that crypts are monoclonal. Further investigation into the properties of DCAMKL-1-positive cells revealed them to be very slowly cycling, suggesting that the ISC is quiescent, but mitoses expressing DCAMKL-1 were found to be present following irradiation, suggesting that the quiescent stem cell had become activated. These data appear to provide good evidence for DCAMKL-1 being a specific marker of the ISC. However, it should be noted that occasional staining of cells on the villus was also reported. This may suggest that DCAMKL-1 actually labels a mature cell type and its precursors, and from the frequency of staining and the morphology of the stained cells presented, it seems possible that the cell type identified may in fact be of an

enteroendocrine lineage. Furthermore, this study lacks functional evidence to suggest that DCAMKL-1 positive cells are indeed ISCs, and without this validation the study lacks conviction.

Lgr5 (also known as G-protein coupled receptor 49, Gpr49) was identified as a candidate marker of the ISC based on a screen of Wnt-target genes (Barker et al., 2007). Localisation of Lgr5 revealed positively-stained cells to be within the CBC cell population at the very base of the crypt, and these cells were shown to be distinct from both the paneth cell population and from the cells of the transit amplifying zone. Additionally, Lgr5-positive cells were observed within adenomas arising in Apc^{MIN} mice. In contrast to the quiescent DCAMKL-1 labelled cells described above, Lgr5-expressing CBC cells were found to be rapidly cycling, with cells incorporating BrdU following a short pulse-chase, and increasing in numbers over 24 hours. The authors go on to describe generation of knock-in mice bearing combined EGFP reporter and inducible cre-expressing construct under the control of the endogenous Lgr5 promoter. These mice confirmed that Lgr5 expression is specific to CBC cells between paneth cells. These mice were also crossed to mice bearing the Rosa26-LacZ allele, and then used to trace cell lineages within the intestine. Upon activation of Cre, the entire crypt-villus was populated with LacZ-expressing cells. The significance of this finding is that it elegantly proves that all epithelial lineages within the intestine are derived from cells which, at some point, have expressed Lgr5. This provides convincing functional evidence that Lgr5-positive cells are indeed intestinal stem cells. However, these results are controversial in that they appear to go against the previously proposed concepts of the stem cell residing at position +4, and the stem cell being quiescent in normal tissue.

Very recently, the oncogene Bmi1 has also been proposed as a marker of the ISC (Sangiorgi and Capecchi, 2008). Bmi-1 is a polycomb group protein, which is known to play a role in renewal of stem cells of both haematopoietic (Park et al., 2003) and neuronal systems (Molofsky et al., 2003), and more recently of the breast epithelium (Pietersen et al., 2008). In their study, *Sangiorgi and Capecchi* have generated mice expressing an inducible form of Cre under the control of the Bmi1 promoter, which were then crossed to reporter mice bearing either the Rosa26-LacZ transgene or a Rosa26-YFP transgene. Using this approach, the authors observe that reporter-expressing cells are most commonly located at positions +4 and +5 in the crypt, directly above paneth cells. Rarely, Bmi1-expressing cells were also observed between paneth cells, within the CBC population. However, it is also noted that a large number of crypts contain more than one labelled cell, which is not consistent with the notion that crypts are monoclonal. The authors propose that these cells may be the early mitotic progeny of Bmi1 positive cells. In a similar lineage-tracing experiment to that performed by *Barker et al.* (2007), LacZ-positive cells were found to completely populate the majority of whole crypts at day 17 after Cre induction, and stable LacZ expression was observed on the crypt-villus axis up to 9 months after induction. Again, this indicates that cells expressing Bmi1 populate the crypt-villus epithelium. Further to this, it

was demonstrated that Bmi1-positive cells give rise to all differentiated cell types of the epithelium, but do not themselves express any markers of the differentiated cell types. Unlike *Barker et al.*, who report that Lgr5-positive cells are rapidly cycling, *Sangiorgi and Capecchi* note that Bmi1-positive cells are slowly cycling. Finally, the effects of activating Wnt signalling or completely deleting Bmi1-positive cells were investigated. Activation of Wnt signalling was achieved by conditional expression of a constitutively activated form of beta-catenin, driven by the Bmi1-CreER construct. Following Cre induction, animals were rapidly found to develop epithelial hyperplasia along with the formation of numerous adenomas, indicating that Wnt activation in Bmi1-expressing cells is sufficient to generate much of the phenotype associated with more widespread Wnt activation. Ablation of the presumptive stem cell population was achieved by expression of diphtheria toxin from the Rosa26 allele which was driven by the Bmi1-CreER construct. Cre induction was found to result in rapid lethality, caused by extensive death of cells within the intestine, and complete loss of crypt structures from large areas of the mucosa. These studies therefore provide convincing evidence that Bmi1-expressing cells play a key role in the repopulation of the crypt-villus.

These data are compelling, providing thorough evidence that Bmi1 labels the intestinal stem cell. However, much of this data is clearly at odds with that proposed by *Barker et al.*, and it appears that Bmi1 and Lgr5 may label distinct populations of cells. However, the overlap between Bmi1-expressing cells and Lgr5-expressing cells has, as yet, not been fully investigated. Based on the observed difference in cell cycle kinetics between Bmi1-positive and Lgr5-positive cells, *Sangiorgi and Capecchi* propose that these markers may in fact label different populations of stem cells, with Bmi1 being a marker of quiescent cells and Lgr5 labelling more active stem cells, with the possibility of cells migrating between the two observed stem cell niches (Also discussed by *Batlle*, 2008).

One final proposed marker of the stem cell is also particularly noteworthy; inactive phosphorylated Pten. *He et al.* (2004) have observed that long-term BrdU-retaining cells within the crypt, which are located approximately at positions +4 and +5, co-stain for phosphorylated (inactivated) Pten. Due to inactivation of Pten, these LRCs also exhibit activation (by phosphorylation) of Akt, which lies downstream of Pten in the PI3K/Akt pathway. In addition, LRCs (referred to as 'stem cells' by the authors) which are phospho-Pten-positive also show nuclear accumulation of beta-catenin and activation of Wnt signalling. Actively dividing phospho-Pten-positive LRCs are also shown to retain nuclear localisation of beta-catenin. Quiescent, phospho-Pten-negative LRCs were shown not to exhibit nuclear accumulation of beta-catenin. This observation led the authors to conclude that inactive Pten may influence Wnt signalling within the ISC to promote stem cell division, but is not necessarily sufficient to initiate division.

However, these conclusions have been the subject of some debate. *Bjerknes and Cheng* (2005b) argue that, based on their morphology, the phospho-Pten labelled cells identified by *He et al.* within the crypt are in fact early enteroendocrine cells. Furthermore, in the hands of *Bjerknes and Cheng*, the antibody used by *He et al.* to detect phospho-Pten was also found to label a number of cells throughout the crypt-villus. All phospho-Pten-positive cells were also found to co-stain with Chromogranin A, a marker of enteroendocrine lineages, though not all Chromogranin A-positive cells were found to be phospho-Pten-positive, suggesting that Pten is inactivated in only a subset of enteroendocrine cells. Furthermore, *Bjerknes and Cheng* point out that it has not currently been proven that BrdU label-retaining cells and intestinal stem cells are equivalent. These observations therefore cast significant doubt over the fact that inactivated Pten may be a reliable marker of the ISC.

1.1.3.3 Maintenance and regulation of the intestinal stem cell

The lack of a definitive marker of the intestinal stem cell has clearly held back direct studies investigating the roles of various signals in maintaining the characteristics of stemness. However, indirect evidence has implicated a number of signals in maintenance and homeostasis of the ISC. These signals are both intrinsic to the stem cell, including signalling pathways such as Wnt, BMP, Notch and PI3K/Akt, as well as extrinsic to the stem cell, including signals from surrounding cellular components comprising the stem cell niche.

As described above, Wnt signals are known to be critical for maintenance of the proliferative capacity of the crypt and repopulation of the crypt-villus axis. Ablation of Wnt signals results in loss of the proliferative compartment and inhibition of repopulation of the crypt-villus axis. Conversely, aberrant activation of Wnt signalling results in expansion of the proliferative zone and induction of a 'crypt progenitor' phenotype, along with loss of compartmentalisation of cells within the crypt. The aberrant progenitor cells which arise following activation of Wnt signalling have not directly been identified as stem cells, however they are found to express the putative stem cell marker, Musashi-1 (Sansom et al., *Unpublished data*). The consequence of modulating Wnt signalling on the whole intestinal epithelium is relatively well characterised, however attempts to characterise the effects of Wnt modulation specifically within the stem cell population are less common. Recently, one study has attempted to characterise the effects of deletion of beta-catenin more specifically in the ISC. *Fevr et al.*, have used conditional transgenesis to delete beta-catenin from the adult intestinal epithelium (Fevr et al., 2007). Essentially, this study recapitulates the phenotype seen previously by *Ireland et al.* (2004) in a similar study, with loss of the proliferative compartment and progressive ablation of the epithelium. However, the authors go on to examine the effects of beta-catenin loss more specifically in the stem cell population, or at least within label-retaining cells. Proliferating cells

were labelled using tritiated (^{3}H-) thymidine by treating animals over a course of four days. Following an interval of three weeks, loss of beta-catenin was induced. Crypts of wild-type mice were observed to contain LRCs at the crypt base, between paneth cells, as expected. However, four days following loss of beta-catenin, LRCs were found scattered throughout the crypt and villus. These LRCs were found to co-stain for fatty-acid binding protein (FABP), a marker of differentiated enterocytes. Thus, it was concluded that active Wnt signalling is needed to maintain the undifferentiated state of label-retaining stem cells, with loss of signalling resulting in differentiation of LRCs and entry into the normal migratory program of differentiated enterocytes.

PI3K/Akt signalling has previously been reported to be essential for cell proliferation within the intestine, and particularly for regeneration of the crypt-villus axis following injury (Sheng et al., 2003). This therefore suggests that PI3K/Akt signalling may be essential for activating stem cell replication within the intestine. As described above, *He et al.* (2004) have proposed that inactive phosphorylated Pten is a key feature of ISCs, allowing activation of Akt and modulation of Wnt activity within the stem cell to promote division. Further to this, the same group have investigated the effects of Pten deletion from the intestine (He et al., 2007). Following Pten deletion, putative stem cells were identified in the crypt based on both long-term retention of label and on positive staining for Musashi-1. It was noted that Musashi-1-positive LRCs, which were also deficient for Pten, were much more rapidly cycling compared to Mushashi-1-positive LRCs which remained proficient for Pten. This excess of stem cells was seen to result in crypt fission within the intestine, and subsequent development of hamartomatous polyps. The authors therefore conclude that inactivation of Pten (and hence activation of the PI3K/Akt pathway) influences the kinetics of stem cell division. However, it remains unclear whether this study is truly examining Pten deficiency within the intestinal stem cell, rather than in a population of progenitor cells.

As previously described, BMP signalling is known to play a role in regulating proliferation within the intestine, and also in defining the location of the proliferative zone (see section 1.1.2.3). In their study identifying phospho-Pten as a putative marker of the intestinal stem cell, *He and colleagues* (2004) went on to analyse the effect of inactivating BMP signalling on the intestinal stem cell. They found that inactivation of BMP signalling by conditional deletion of the BMP type I receptor resulted in an increase in phospho-Pten-positive 'stem cells', and also in an increase in crypt number within the intestine. The authors therefore propose that BMP signals inhibit renewal of the stem cell by regulating Pten activity.

Although poorly characterised in the intestine, evidence from other organisms and other tissue systems indicates that signals from the stem cell niche are critical for homeostasis of the stem cell itself (Reviewed extensively, including Jones and Wagers, 2008). Indeed, the fact that

intestinal epithelium and its stem cells have not yet been established in cell culture points to the fact that signals from the microenvironment of the stem cell may be critical for its maintenance. Other cell types within the niche which may interact with the stem cell include epithelial progenitor cells (daughter cells of the stem cell), mesenchymal cells (including myofibroblasts) and infiltrating immune cells (See Figure 1.3).

Again, the lack of a robust marker of the intestinal stem cell has hampered efforts to study the interaction of the stem cell with its niche, however a small number of studies have pointed to the importance of cells adjacent to the epithelium in maintaining intestinal homeostasis. One example of this is the study of the mesenchymally-expressed transcription factor, Fkh6 (now known as FoxL1) (Kaestner et al., 1997). *Kaestner et al.* generated mice null for the Fkh6 gene. Despite the fact that Fkh6 is not normally expressed in epithelial cells, they noted marked epithelial abnormalities in the intestines of $Fkh6^{-/-}$ mice. During embryogenesis, Fkh6-null intestines were found to show delayed development of the intestinal epithelium, with abnormally small and sparse villus structures. Embryonic intestinal epithelium was also found to be poorly organised, with loss of definition of the proliferating zone. Examination of intestines from adult $Fkh6^{-/-}$ mice revealed expansion of crypt size and elongation of villi. This was coupled with increased proliferation and also perturbation of the normal differentiation program, with an excess of goblet cells present within mutant crypts. These data therefore hint at the fact that expression of factors within the mesenchyme may influence the behaviour of the stem cell, with relation to both proliferation and maintenance of the undifferentiated state. Although the stem cell itself is not explicitly studied, these data highlight the importance of signals originating in mesenchymal cells for normal homeostasis of the intestine.

One further elegant example illustrating the importance of non-epithelial cell types on intestinal homeostasis is described by the work of *Kim et al.* (2006). This study examines the role of TGF-beta/BMP signalling both in the intestinal epithelium itself, and in circulating T-cells, by conditional deletion of SMAD4. Following conditional inactivation of SMAD4 specifically in the intestinal epithelium, the authors surprisingly observed no significant effect on intestinal function or homeostasis, and did not observe tumourigenesis of the intestine. However, following T-cell-specific deletion of SMAD4, a marked intestinal phenotype was observed, despite the fact that TGF-beta signalling remains intact in the epithelial cells themselves. The intestinal phenotype observed included marked thickening of the mucosa, with evidence of stromal and immune cell infiltration. Rapid development of intestinal polyps, adenomas and invasive carcinomas was observed, described as being reminiscent of that seen in human juvenile polyposis syndrome (JPS). Again, although this study does not attempt to directly examine the intestinal stem cell, the rapid epithelial hyperplasia and subsequent tumourigenesis observed implies that the ISC may be dysregulated following TGF-beta signalling abrogation in T-cells.

1.1.3.4 An intestinal cancer stem cell?

The 'cancer stem cell' hypothesis was originally described by *Schofield* in 1978 (Schofield, 1978). This hypothesis proposes that tumour growth is maintained by one or a small number of replicative cells, which bear similarities to normal tissue stem cells. For many cancers, the idea that a 'cancer stem cell' population is responsible for the growth of a tumour is becoming increasingly popular. Indeed, if such a population of cells exists, it would provide a very attractive therapeutic target to facilitate effective destruction of a tumour by removing the very source of tumour growth.

Evidence for the existence of the cancer stem cell has been derived mainly from xenotransplantation studies. These studies are exemplified by the early work of *Bonnet and Dick* (1997), who showed that transplantation of a small subset of sorted cells (those which were CD34++/CD38-) derived from human acute myeloid leukaemia was sufficient to induce leukaemic transformation in immune-compromised (Non-obese diabetic/severe combined immunodeficient; NOD/SCID) mice. The fact that not all subsets of cells are able to initiate transformation suggests that some groups of cells contain cancer stem cells, which drive cancer initiation and development.

A small number of similar studies have been performed involving transplantation of sorted cells derived from human colorectal cancers (Dalerba et al., 2007, Ricci-Vitiani et al., 2007, O'Brien et al., 2007). In each of these studies, samples were removed from human colorectal tumours and sorted based on the expression of cell surface markers before being transferred into NOD/SCID mice. Success of the transfer was assessed on the basis of the ability of the sorted tumour cells to colonise the site of implantation, and to generate a tumour which was morphologically comparable to the original tumour from which the cell samples were derived. Successful transplantation was considered to be indicative of the presence of the cancer stem cell population within the cell fraction isolated. *Dalerba et al.* found that the cell fractions which were most successful at initiating tumourigenesis upon transplantation were characterised by high expression of epithelial cell adhesion molecule (EpCAM) and cell surface expression of CD44 and CD166 ($EpCAM^{High}/CD44^{+}/CD166^{+}$). Both *Ricci-Vitiani et al.* and *O'Brien et al.* found that subsets of cells expressing the surface marker CD133 were particularly tumourigenic following transplantation, and propose that $CD133^{+}$ cells include the colorectal cancer stem cell. It has also been mooted that CD133 may be a marker for the normal intestinal stem cell. However, contrary to this data, a recent similar study has indicated that $CD133^{-}$ colorectal cancer cells are also capable of initiating tumourigenesis upon xenotransplantation, and are in fact equally if not more tumourigenic than $CD133^{+}$ cells. Furthermore, expression of CD133 has been detected throughout the crypt-villus axis of the epithelium, with no indication of specific expression within the stem or progenitor cell compartments (Shmelkov et al., 2008). It is therefore clear that the search for a

specific marker of the intestinal cancer stem cell is likely to be as challenging as for that of the normal intestinal stem cell.

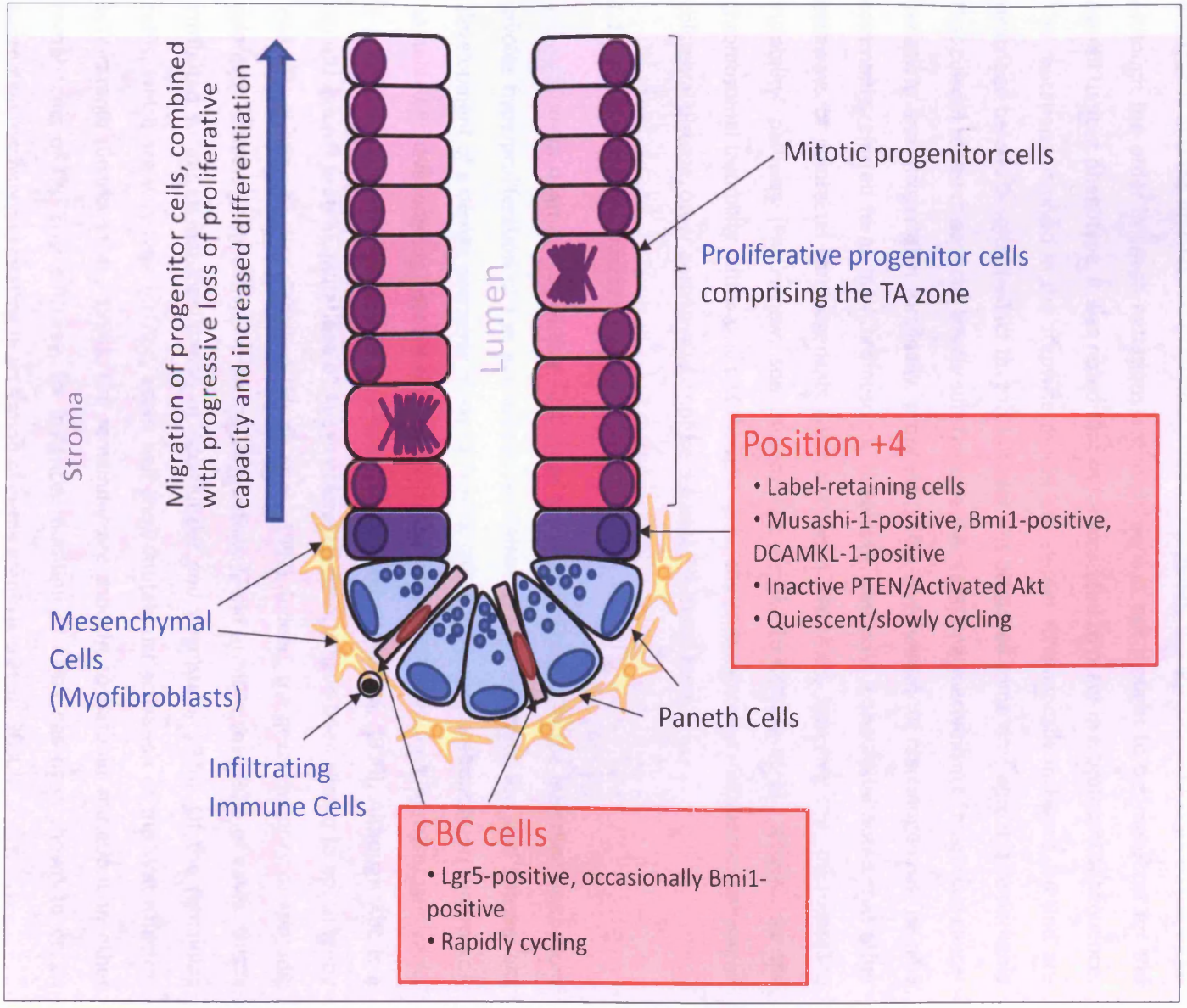

Figure 1.3: ***Candidate locations of the intestinal stem cell and components of the stem cell niche.***

The crypts of the small intestine house the intestinal stem cell.

Candidate locations of the ISC include within the crypt base columnar (CBC) cell population (Brown) and within the label-retaining cell population at approximately position +4 (Purple). Putative markers of the ISC have been identified for both candidate locations., and different properties of the stem cell are associated with each location (Red boxes).

The stem cell resides within a stem cell niche, which is critical for maintaining the properties of 'stemness', including limitless replication and maintenance of a relatively undifferentiated state. Components of the intestinal stem cell niche (Blue text) include proliferative precursor cells, mesenchymal cells, stromal components and infiltrating immune cells.

1.1.4 Multi-step carcinogenesis of the intestine

1.1.4.1 Step-wise development of disease

The widely accepted model of acquisition of multiple genetic mutations in a step-wise fashion leading to CRC was initially proposed almost 20 years ago (Fearon and Vogelstein, 1990). In this study, *Fearon and Vogelstein* examined data from mutational profiles of colorectal cancers at various stages of disease. From their observations, they proposed that 4 to 5 mutational 'steps' are necessary to result in colorectal malignancy. These steps involve both the activation of oncogenes and the inactivation of tumour suppressor genes, though the latter is more common. Although the order in which mutations are acquired was not thought to be important for the overall tumour phenotype, it was noted that mutations tend to occur in a preferential sequence. The mutations involved in the stepwise model are shown schematically in Figure 1.4 and are described below. Despite the fact that this model was proposed some time ago, it is remarkable that current research data still largely substantiate the mutational mechanism of colorectal cancer initiation and progression originally proposed. This mechanism of carcinogenesis is now commonly referred to as the 'Chromosomal instability' pathway. It should be noted that other pathways of colorectal carcinogenesis have also been identified, including the 'microsatellite instability' pathway (For review, see Laurent-Puig et al., 1999, Jass et al., 2002b). As the chromosomal instability pathway is still thought to be the most common mutational pathway of colorectal disease, other pathways will not be discussed in detail here.

1.1.4.2 Initiation of colorectal neoplasia

Current dogma dictates that first steps towards malignancy in the intestinal epithelium involve hyperproliferation of the epithelium, formation of aberrant crypt foci and subsequent development of a benign adenoma. Study of familial colorectal cancer predisposition syndromes, namely FAP, have long suggested that mutation of the 'gatekeeper' tumour suppressor gene, Apc, is a key initiating event in colorectal cancer (Kinzler and Vogelstein, 1996). Although Apc is a multifunctional protein, mutations of Apc in colorectal cancers have been shown to consistently lead to activation of Wnt signalling (Morin et al., 1997). Indeed, the great majority of sporadic colorectal cancers show activation of the Wnt pathway, and in more than 80% of cases, this is attributed to mutational inactivation of Apc (Kinzler and Vogelstein, 1996). Of the remaining cases, which are wild-type for Apc, about half show mutational activation of the Wnt effector, beta-catenin (Sparks et al., 1998). The remainder are thought to harbour mutations in other components of the Wnt pathway, for instance, mutation of Axin2 has been shown to be an alternative mechanism resulting in activation of beta-catenin (Liu et al., 2000).

Although Wnt activation is generally accepted as the crucial initiating step of colorectal neoplasia, it should also be noted that other, alternative mechanisms of initiation have been proposed. The major alternative pathway proposed involves loss of genes involved in DNA mismatch repair, either by mutation or epigenetic silencing. This mechanism of initiation seems to parallel that seen in the human hereditary disease HNPCC, whereas initiation of colorectal cancers by activation of Wnt signalling (as described above) is thought to parallel that seen in FAP. In particular, it is postulated that loss of mismatch repair proteins is the underlying mechanism for initiation of colorectal lesions which exhibit high levels of microsatellite instability (MSI). In such lesions, lack of DNA repair activity is thought to provide a genetically unstable environment, paving the way for mutation acquisition within other genes (Jass et al., 2002a).

1.1.4.3 Progression of disease

Progression of disease, and the eventual adenoma-to-carcinoma transition of a tumour, represents the switch from a benign to a malignant tumour phenotype. Disease advancement is characterised by sustained abnormal proliferation of cells resulting in an increase in mass of the tumour, and by progressive loss of normal structure and anatomy of the intestine. Proliferative cells are often found to be poorly or incompletely differentiated. Further advancement of disease eventually results in the ability of tumour cells to invade the submucosa. This change in phenotype resulting in invasive behaviour is complex, and is thought to involve a number of different mechanisms for modulating gene expression, including mutation and epigenetic modification.

A large array of gene and protein expression changes have been identified which are associated with progression of disease. However, for many of these changes, what remains unclear is whether these changes are causative, and therefore result in the advanced phenotype, of whether they are simply an epiphenomenon of disease progression.

According to the multistep model proposed by *Fearon and Vogelstein*, the events absolutely required for progression of disease following initiation of disease by activation of Wnt signalling include activation of the oncogene Kirsten-Ras, loss of chromosome 18q, and loss of expression of the tumour suppressor p53 (Fearon and Vogelstein, 1990). This pathway is commonly known as the 'chromosomal instability' (CIN) pathway, and is responsible for progression of the majority of sporadic colorectal cancers (For review, see Ilyas et al., 1999).

<u>Kirsten-Ras</u>

The Rat sarcoma viral oncogene homology (Ras) family is comprised of Harvey (H or Ha)-Ras, Kirsten (K or Ki)-Ras and Neuroblastoma (N)-Ras. This group of small G-proteins are commonly found to be activated in cancers of various origins (Bos, 1989). Ras proteins become

activated upon binding to GTP, which is stimulated by a number of Guanine nucleotide exchange factors (GEFs). GEFs themselves are activated in response to a number of cellular signals, including activation of growth factor receptor tyrosine kinases (RTKs) and the production of second messenger molecules such as calcium and diacylglycerol. Once bound to GTP, active Ras can then trigger numerous downstream pathways. Of these, the best characterised is the Raf-MEK-ERK mitogen-activated protein kinase (MAPK) cascade. Also of note, it has been shown that Ras-GTP can directly activate the catalytic subunit of PI3K, and thus directly stimulate PI3K/Akt signalling (Kodaki et al., 1994). Ras activity is antagonised by GTPase-activating proteins (GAPs), which catalyse hydrolysis of GTP to GDP, which remains bound to Ras and renders it inactive (See *Malumbres and Barbacid,* 2003 for review).

Oncogenic mutations of Ras generally result in its constitutive activation. Mutations in different members of the oncogenic Ras family are generally associated with certain types of tumours. In intestinal cancers, mutation of Kirsten (K)-Ras is much more common than mutations in the other family members, however the reason for this remains unclear (Malumbres and Barbacid, 2003).

In humans, several studies have examined biopsies of histologically normal intestinal tissue taken from patients bearing k-Ras mutant colorectal tumours, and surprisingly found that k-Ras mutations exist within this normal tissue (Zhu et al., 1997, Minamoto et al., 1995, Yamada et al., 2005). This clearly suggests that activation of k-Ras alone is not sufficient to perturb intestinal homeostasis. As proposed by *Fearon and Vogelstein*, activation of Ras signalling appears to occur after tumour initiation, but still at a relatively early stage of tumourigenesis; during adenoma growth (Fearon and Vogelstein, 1990). In sporadic colorectal cancers in humans, studies have placed k-Ras mutation frequency at between 38% and 50% of all tumours (van Engeland et al., 2002, Sancho et al., 2004). When very early stage colorectal cancers are specifically selected for examination, the incidence of k-Ras mutation is still found to be high at 26% (Andreyev et al., 1997). This supports the notion that k-Ras mutation is an early event following tumour initiation. However, this study also noted that in early stage tumours, there was no correlation between k-Ras mutation and prognosis. In contrast to this, a number of other reports, including one large, multi-centre study, have revealed a strong link between k-Ras mutation, particularly at codon 12, and poor prognosis (Andreyev et al., 2001, Conlin et al., 2005), again suggesting that k-Ras mutation drives tumourigenesis.

Animal models of intestinal-specific k-Ras activation have reported somewhat discrepant results. One study has expressed a Codon 12 glycine-to-valine point mutant form of activated k-Ras (k-Ras^{V12}) from a strongly expressed intestinal-specific promoter (that of the *Villin* gene) (Janssen et al., 2002). This study reports that k-Ras mutation alone is sufficient for development of intestinal lesions of varying severity, from aberrant crypt foci (ACF) to invasive

adenocarinomas, with high penetrance. This is in direct contrast to data obtained from humans, as described above, where k-Ras mutations are detected in histologically normal mucosa (Zhu et al., 1997, Minamoto et al., 1995, Yamada et al., 2005). Arguably, one of the problems with the experimental model presented by *Janssen et al.* is that the k-Ras oncogene has been both mutated *and* over-expressed in the intestinal epithelium. It is therefore conceivable that this may result in a phenotypic difference compared to mutation alone. To address this, a similar mutant form of k-Ras^{V12} has more recently been developed which is expressed from its endogenous promoter (Guerra et al., 2003). Indeed, expression of this mutant form of k-Ras in the mouse intestine recapitulates the observations seen in humans much more closely. Activation of k-Ras alone was found to have no significant impact on the homeostasis of otherwise normal intestinal epithelium. However, following loss of Apc and activation of the Wnt cascade, k-Ras activation was found to result in both an increase in tumour incidence, and a phenotype of tumour invasiveness into the submucosa and muscularis (Sansom et al., 2006). As such, this study supports a role for k-Ras activation in the progression, rather than initiation, of disease. Another form of k-Ras mutant transgene has more recently been developed by Tuveson et al. (2004), which is a different codon 12 point mutant form of k-Ras, but is again driven from its endogenous promoter. Intestinal-specific expression of this glycine-to-aspartate (G12D) form of k-Ras was found to result in widespread hyperplasia of the epithelium. This study therefore adds a further layer of complexity to the consequences of k-Ras mutation in the intestine, indicating that certain mutant forms of the oncogene may indeed be able to initiate intestinal neoplasia.

Loss of 18q

Following activation of k-Ras, the next 'step' toward malignancy, as proposed by *Fearon and Vogelstein*, is loss of the long arm of chromosome 18. Indeed, loss of 18q has been observed in around 70% of colorectal cancers (Fearon et al., 1990). One candidate for involvement in colorectal cancer progression found at this locus is the *Deleted in Colorectal Carcinoma* (DCC) tumour suppressor gene. Of the 70% of colorectal carcinomas which exhibit loss of 18q, the deleted region has been shown to include the *DCC* gene in 9 out of 10 cases (Fearon et al., 1990).

The product of the *DCC* gene is a transmembrane protein (Hedrick et al., 1994), the major cellular role of which is as a component of a receptor complex which binds the Netrin family of proteins (Keino-Masu et al., 1996). The role of Netrin signalling has been most thoroughly described in neural tissue, where it is known to provide cues for axon guidance and cellular migration (Mehlen and Furne, 2005). As such, the role of DCC in cancers was initially puzzling. However, more recent data has suggested that DCC may function as a 'dependence' receptor, acting as a pro-apoptotic factor when not bound to netrin (Mehlen and Fearon, 2004). Clearly, loss of DCC may then result in evasion of apoptosis. This notion is supported by the observation

that in the intestine, netrin expression is high at the base of the crypt, where apoptosis is relatively rare, and decreases along the crypt-villus axis. At the top of the villus, netrin expression is low and DCC therefore exists in its unbound state. It is therefore postulated that apoptosis of old cells, before they are shed into the intestinal lumen, is initiated by the presence of unbound DCC (Mehlen and Fearon, 2004). Indeed, it has been shown in mice that forced expression of netrin results in hyperplasia and neoplasia in the intestine, suggesting that DCC may indeed mediate cell survival (Mazelin et al., 2004). Despite this evidence, some uncertainty regarding the role of DCC as a tumour suppressor does remain. Perhaps the most confounding evidence has been obtained from the study of mice constitutively deleted for DCC (Fazeli et al., 1997). Whilst $Dcc^{-/-}$ mice exhibited marked neuronal abnormalities consistent with the previously proposed role for DCC in axon guidance, aged $Dcc^{+/-}$ mice were found to have no increased susceptibility to tumourigenesis of any tissue. Furthermore, *Fazeli et al.* unexpectedly found that deletion of Dcc in the context of the Apc Multiple Intestinal Neoplasia (Apc^{MIN}) mutation had no effect on tumour multiplicity, size or histology. Surprisingly, these data therefore suggest that DCC may not play a role either in initiation or in progression of intestinal disease.

Another factor which may discredit the role of DCC in colorectal cancer progression is that the SMAD4-encoding gene is present in very close proximity (at 18q21.1) to the DCC-encoding gene (at 18q21.3) on chromosome 18, and is present within the region most commonly deleted in colorectal cancers (Thiagalingam et al., 1996). As described above, SMAD4 is an essential component of both the TGF-beta and BMP signalling pathways (See section 1.1.2.3). The evidence for the role of SMAD4 as a tumour suppressor in colorectal cancers is somewhat more compelling than that for DCC. First and foremost, germline mutation of SMAD4 is known to be a causative factor of human Juvenile polyposis syndrome (JPS). Reports attribute SMAD4 mutation to approximately 20-25% of JPS cases (Friedl et al., 2002, Howe et al., 2004). In sporadic colorectal cancers, loss of the BMP signalling pathway has recently been reported as a frequent event (in 70% of specimens examined in this study), which is caused by loss of expression of either BMPRII, SMAD4 or both (Kodach et al., 2008b). Furthermore, a parallel study by the same group has shown that loss of BMP signalling is characteristic of adenocarcinomas but not of colonic adenomas (Kodach et al., 2008a). This clearly supports the hypothesis of BMP pathway inactivation (through loss of SMAD4) being a late event in the adenoma-carcinoma sequence. Further supporting this, murine studies have also placed a role for SMAD4 deletion in carcinogenic progression. *Takaku et al.* (1999) have deleted Smad4 (which, at the time of this study, was also known as Dpc4), both alone and in the context of an Apc mutation which is intestinal tumour-predisposing. Homozygous deletion of Smad4 was found to result in embryonic lethality, whereas Smad4 heterozygous mice exhibited no phenotypic differences compared to wild-type littermates. However, in $Apc^{+/-}$;$Smad4^{+/-}$ mice, intestinal lesions were found to show increased

malignancy compared to $Apc^{+/-}$ control mice. Tumours were found to be larger in mass, showed an increased desmoplastic response and were more invasive, consistent with a role for Smad4 loss resulting in progression of disease.

p53

According to *Fearon and Vogelstein*, the final transformation required for full-blown malignant disease is loss of the short arm of chromosome 17, which harbours the *TP53* gene, encoding the tumour suppressor p53. As the first tumour suppressor gene identified, p53 is probably the most extensively studied and best-characterised gene involved in malignancy. Germline mutations of p53 are known to cause the cancer-prone Li-Fraumeni syndrome (Li et al., 1988). The p53 pathway is found to be inactivated in many cancers of a huge variety of origins, either through loss of p53 itself, or of one of its isoforms (p63 and p73) (For review, see *Bourdon,* 2007). The predominant normal cellular function of p53 is as a sensor of cell stress and DNA damage; in normal cells it is rendered inactive by Mdm2, which binds to p53 and mediates its ubiquitination. Following cellular stress or damage to DNA, p53 is released from Mdm2-dependent suppression, and acts to coordinate the relevant response to trauma by selective transcription of target genes. This may result in cell cycle arrest, stimulation of DNA repair, senescence or cell death by apoptosis (Reviewed extensively, including Vogelstein et al., 2000, Vousden and Lane, 2007, Helton and Chen, 2007).

Loss of p53 is seen in approximately 50% of colorectal cancers (Iacopetta, 2003). As observed with other tumour suppressor genes involved in disease progression, loss of p53 is normally associated with late-stage carcinomas rather than early adenomas in humans (Purdie et al., 1991). Despite these observations in human samples, animal models examining the effect of p53 nullizygosity in a tumour-prone context have produced conflicting results. The work of *Halberg et al.* (2000) produced the expected results; deletion of p53 in mice bearing the Apc^{MIN} mutation was found to cause an increase in the number of tumours observed, and an increase in their invasiveness. However, a very similar study previous to this, by *Clarke et al.* (1995) showed that whilst p53 mutation in the Apc^{MIN} mouse causes acceleration of tumourigenesis in the pancreas, no changes in tumour progression were observed within the intestine. In support of this, very recent work has shown that conditional loss of p53 has very little effect on the acute phenotype observed following conditional loss of both alleles of Apc in the intestine (Reed et al., 2008). These data therefore suggest that the tumourigenic effects of p53 loss may only be manifest following the accumulation of more mutations than that of Apc alone, which is again consistent with the proposal that p53 mutation is a very late stage event in the intestinal adenoma-carcinoma sequence.

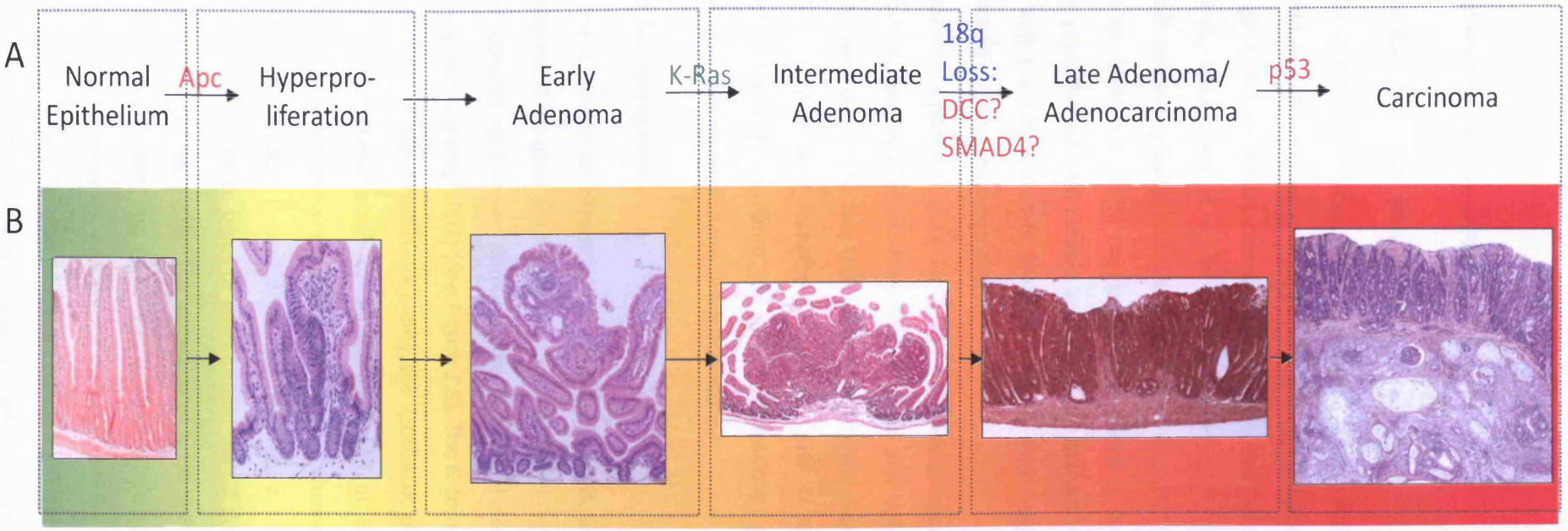

Figure 1.4: ***Multi-step tumourigenesis of the intestinal epithelium***

Step-wise accumulation of mutations leading to intestinal cancer formation and proposed by Fearon and Vogelstein (1990) (A). Inactivation of tumour suppressor genes (Red) and activation of oncogenes (Green) are proposed to cause step-wise progression of disease.

Histological appearance of multi-step tumour progression in the mouse (B). Images of hyperproliferation and early adenoma taken from the Mouse Tumour Biology Database (Naf et al., 2002), images of intermediate adenoma and carcinoma taken from *Boivin, 2003*.

1.2 PTEN: A tumour suppressor

1.2.1 Discovery, structure and function of Pten

1.2.1.1 A candidate tumour suppressor gene at 10q23.3

Abnormalities at the 10q23 locus have long been associated with sporadic cancers of a number of tissues, and also cancer-predisposing genetic diseases in humans. In 1997, a candidate tumour suppressor gene was identified, cloned and characterised by three separate groups (Li and Sun, 1997, Li et al., 1997, Steck et al., 1997), and was found to have phosphatase activity directed towards both protein tyrosine residues and lipids. This was the first potential tumour suppressor gene to be identified which has phosphatase activity, even though it had been recognised for many years that protein kinases are commonly oncogenic (Dahia, 2000). All three groups also found that the novel protein identified had a large degree of homology to the cytoskeleton-associated proteins tensin and auxilin.

The novel tumour suppressor gene identified by these groups is now most commonly known by the acronym coined by *Li et al.*; Pten (Phosphatase and tensin homolog, mutated on chromosome 10). However, due to the fact that *Steck et al.* initially designated this novel protein as MMAC1 (Mutated in Multiple Advanced Cancers 1), and *Li and Sun* named it TEP1 (Transforming growth factor [TGF]-regulated and epithelium-enriched phosphatase), Pten is still occasionally referred to by these pseudonyms in the literature.

1.2.1.2 Structure and function of Pten

The PTEN gene is located on chromosome 10q23 in humans, and on chromosome 19 in the mouse. Coding regions of the gene are highly conserved between the two species.

PTEN protein consists of 2 major domains; the N-terminal domain and the C-terminal domain (Reviewed by Waite and Eng, 2002) (See Figure 1.5). The N-terminal domain contains the phosphatase catalytic core of the protein, including the CKAGKGR phosphatase motif, which corresponds to the general phosphatase consensus sequence of HCXXGXXR (Simpson and Parsons, 2001, review). Solution of the crystal structure of PTEN showed the phosphatase motif forms a loop, known as the 'P-Loop' (Lee et al., 1999) (See Figure 1.5). The more complex C-terminal domain is comprised of three types of sub-domain; the C2 domain, two PEST domains and a PDZ domain (Waite and Eng, 2002). The presence of a C2 domain is characteristic of a protein involved in membrane-binding and signal transduction. C2 domains are also known to be involved in the binding of phospholipids, and the C2 domain of PTEN has been shown to have affinity for phospholipid membranes *in vitro* (Lee et al., 1999). PEST domains are known to play a role in the targeting of proteins for proteasomal degradation (Chu and Tarnawski, 2004). Finally,

PDZ motifs are regions associated with protein-protein interactions. The PDZ domain of PTEN is also thought to aid both recruitment of PTEN to the plasma membrane as well as assisting in orientation of the active site of the phosphatase domain so that it comes into optimal contact with its substrate (Lee et al., 1999).

PTEN functions predominantly as a lipid phosphatase *in vivo* (Maehama and Dixon, 1998). *Maehama and Dixon* found that overexpression of PTEN in cell lines resulted in decreased levels of the cellular phospholipid second-messenger, phosphatidylinositol-3,4,5-trisphosphate (PIP3). The same effect was not seen in a catalytically-dead mutant of PTEN. Further investigation showed that PIP3 was specifically dephosphorylated at the D3 position of the inositol ring structure to generate phosphatidylinositol-4,5-trisphosphate (PIP2). It was therefore concluded by *Maehama and Dixon* that PTEN directly antagonises Phosphatodylinositol-3 kinase (PI3K) by dephosphorylation of PIP3 to give PIP2, and generates a product which can be recycled as a substrate for PI3K (See below, and Figure 1.5).

PTEN also has limited activity towards phosphoprotein substrates. *In vitro*, PTEN has been shown to directly associate with and dephosphorylate Focal Adhesion Kinase (FAK), and is also implicated in the dephosphorylation of Shc which, in turn was shown to result in downregulation of the Mitogen-activated protein (MAP) kinase pathway (Gu et al., 1999). However, the protein phosphatase activity of PTEN has not been demonstrated *in vivo*.

1.2.1.4 Regulation of PTEN

Control of the activity of PTEN is complex, involving activation and repression at both the transcriptional level and the post-translational level, and regulation of the subcellular localisation of the protein (For review, see Tamguney and Stokoe, 2007). As such, the detailed mechanisms of PTEN regulation will not be discussed here.

However, several aspects of PTEN regulation are particularly notable with respect to intestinal homeostasis.

Firstly, as described above, inactive phosphorylated PTEN has been proposed as a feature of the intestinal stem cell (He et al., 2004). Phosphorylation of PTEN in the region of residues 380-385 in the C-terminal tail is known to attenuate PTEN activity. The mechanism proposed for this is that the phosphorylated tail region acts as a pseudo-substrate, blocking the active site of PTEN, and hence resulting in self-inhibition (Odriozola et al., 2007). Casein Kinase 2 (CK2) has previously been shown to phosphorylate PTEN at residues Ser380, Thr382, Thr383 and Ser385 both *in vitro* and in intact cells (Torres and Pulido, 2001). *Torres and Pulido* also observed that phosphorylation at these residues renders PTEN resistant to proteasomal degradation, thus it would appear that C-terminal tail phosphorylation both stabilises and inactivates PTEN. This may therefore represent a mechanism which allows very dynamic and rapid control over PTEN activity.

Secondly, PTEN has been shown to be regulated through interaction with other proteins present within the cell. Interestingly with respect to the intestine, beta-catenin and other components of the adherens junction have been shown to play a role in maintaining PTEN levels. One such component, vinculin, has been shown to be critical for interaction of PTEN with the adherens junction proteins beta-catenin and membrane-associated guanylate-kinase inverted 2 (MAGI-2). Maintenance of this interaction was shown to be critical for preservation of cellular PTEN protein levels, whilst not affecting levels of Pten mRNA (Subauste et al., 2005). Thus, modulation of other adherens junction components, such as beta-catenin, may play a critical role in regulating the normal activity of PTEN.

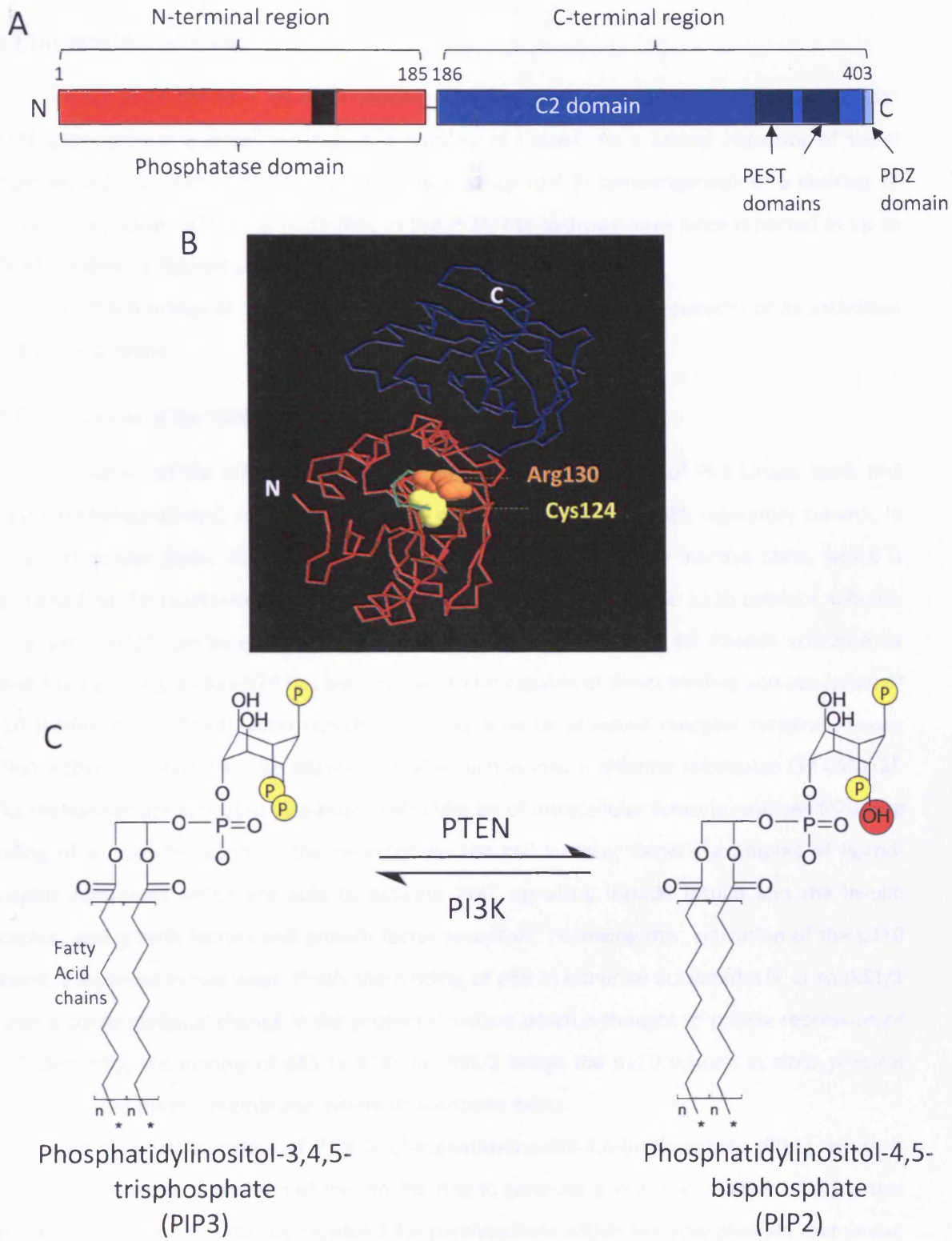

Figure 1.5: ***Structure and function of PTEN***

A: Schematic diagram of PTEN protein, which is divided into two regions; the N-terminal region (Red) and the C-terminal region (Blue). The N-terminal region contains the catalytic core of the protein (Black). The C-terminal region is comprised of the C2 domain, two PEST domains and a PDZ domain.

B: Crystal structure of PTEN protein as solved by *Lee et al.*, with the N-terminal region shown in Red and the C-terminal region in Blue. Critical active site residues, Arg130 and Cys124, which are situated within the P-loop (Green), are labelled.

C: PTEN functions principally as a lipid phosphatase, and acts to remove the Phosphate group (yellow) from position 3 of the inositol ring of phosphatidylinositol-3.4.5-trisphopshate, generating phosphatidylinositol-4,5-bisphosphate. PTEN directly reverses the reaction catalysed by PI3K. Adapted from *Vivanco and Sawyers*, 2002.

1.2.2 The PI3K/Akt pathway

Phosphatidylinositol-3 kinase (PI3K)/Akt signalling plays a crucial role in mediating cellular proliferation, growth and cell survival in a number of tissues. As a critical regulator of these processes, PI3K/Akt signalling is known to play a major role in tumourigenesis of a number of tissues. In particular, activating mutations in the PI3K/Akt pathway have been reported in up to 40% of all sporadic colorectal cancers in humans (Parsons et al., 2005).

Normal function of the PI3K/Akt pathway and the cellular consequences of its activation are discussed below.

1.2.2.1 Activation of the PI3K/Akt pathway

Activation of the PI3K/Akt pathway is dependent on activation of PI-3 kinase itself. PI-3 kinases are heterodimeric, composed of a p110 catalytic subunit and a p85 regulatory subunit. In its normal cellular state, PI3K exists in the cytoplasm in a catalytically inactive state, which is maintained by the repressive effect of the p85 regulatory subunit on the p110 catalytic subunit. Activation of p110 can be achieved in several ways. Firstly, p110 may be directly activated by active Ras signalling, as Ras-GTP has been shown to be capable of direct binding and activation of p110 (Kodaki et al., 1994). Alternatively, p85 may bind to activated receptor tyrosine kinases (RTKs), either directly or through adapter proteins such as insulin receptor substrates 1/2 (IRS1/2). RTKs themselves are activated by autophosphorylation of intracellular tyrosine residues following binding of a cognate ligand to the receptor on the cell surface. Generic examples of ligand-receptor complexes which are able to activate PI3K signalling include insulin and the insulin receptor, and growth factors and growth factor receptors. Following this, activation of the p110 subunit is achieved in two ways. Firstly the binding of p85 to either an activated RTK or to IRS1/2 causes a conformational change in the protein structure which is thought to relieve repression of p110. Secondly, the binding of p85 to RTKs or IRS1/2 brings the p110 subunit in close physical proximity to the plasma membrane, where its substrate exists.

The principal substrate of PI3K is phosphatidylinositol-4,5-bisphosphate (PIP2), which it phosphorylates at the 3 position of the inositol ring to generate a local rise in levels of the active signalling molecule, phosphatidylinositol-3,4,5-trisphosphate within the phospholipid membrane (Extensively reviewed, including Vivanco and Sawyers, 2002, Cully et al., 2006) (See also Figure 1.6).

1.2.2.2 Activation of Akt

The principal effect of PIP3 production is the activation of the serine-threonine kinase, Akt. Akt is recruited to the membrane through its PIP3-binding pleckstrin homology (PH) domain. Two other PH-domain-containing proteins, phosphoinositide-dependent kinases 1 and2 (PDK1

and 2) are also recruited to the membrane following PIP3 production. The close physical proximity of PDK1 and 2 to Akt allow them to phosphorylate Akt at residues Thr308 and Ser473 respectively. Phosphorylation of Akt at Thr308 is necessary for its activation, whilst phosphorylation at Ser473 results in its maximal activation (See Figure 1.6) (See Vivanco and Sawyers, 2002, Cully et al., 2006 for review).

1.2.2.3 Downstream targets of Akt

The downstream targets of Akt are extremely numerous and varied. A number of targets of Akt pertinent to tumourigenesis are outlined in Figure 1.7. One well-characterised downstream effect of Akt which is of particular note is modulation of the mammalian target of rapamycin (mTOR) pathway. The cellular role of the mTOR pathway is to integrate signals generated by both growth factor signalling (via the PI3K/Akt pathway) and nutrient stress (via LKB-1 and AMPK), and coordinate an appropriate response of translational modulation by acting on ribosomal S6 kinase (S6K), or on the translation initiation factor 4E binding protein (eIF4E-BP1) (Fingar et al., 2004, See also Tee and Blenis, 2005 for review). Dysregulation of the mTOR pathway itself is associated with human polyposis syndromes, such as Tuberous sclerosis (TSC) and Peutz-Jeghers syndrome (PJS) (Reviewed by Inoki et al., 2005).

Akt acts to directly phosphorylate the Tuberous sclerosis 2 (TSC2) gene product, Tuberin (Manning et al., 2002). This prevents formation of the TSC complex, allowing GTP-binding and activation of a Ras homolog, Rheb. Active Rheb in turn can directly phosphorylate and activate mTOR at serine residue 2448. Active mTOR then phosphorylates and activates S6K, and inactivates eIF4E-BP1 by phosphorylation. Both of these effects result in promotion of translation within the cell, facilitating cell growth and division (Hay and Sonenberg, 2004).

1.2.2.4 PI3K/Akt signalling and intestinal homeostasis

Although not classically thought of as a major regulatory pathway within the intestine, some evidence has suggested that PI3K/Akt signalling plays a role in intestinal homeostasis. In particular, the work of *Sheng et al.* (2003), mentioned above, has suggested a role for PI3K signalling in proliferation and regeneration of the intestine following injury. Having noted that PI3K inhibition (using the specific inhibitors, Wortmannin or LY-294002) resulted in at least an 80% reduction in proliferation of intestinal epithelial cell lines, *Sheng and colleagues* pursued these observations in a mouse model. The number of proliferating cells in the intestine was reduced by subjecting mice to a liquid diet for 72 hours, followed by reinstatement of solid diet. This resulted in rapid regeneration of proliferative cells, as assessed by expression of proliferating cell nuclear antigen (PCNA). PCNA-expressing cells were also found to be characterised by increased levels of phospho-Akt^{Ser473}. Treatment of mice with LY-294002 at the time of solid food

reinstatement was found to completely block the generation of PCNA-expressing cells, indicating that this process is entirely dependent upon PI3K/Akt signalling.

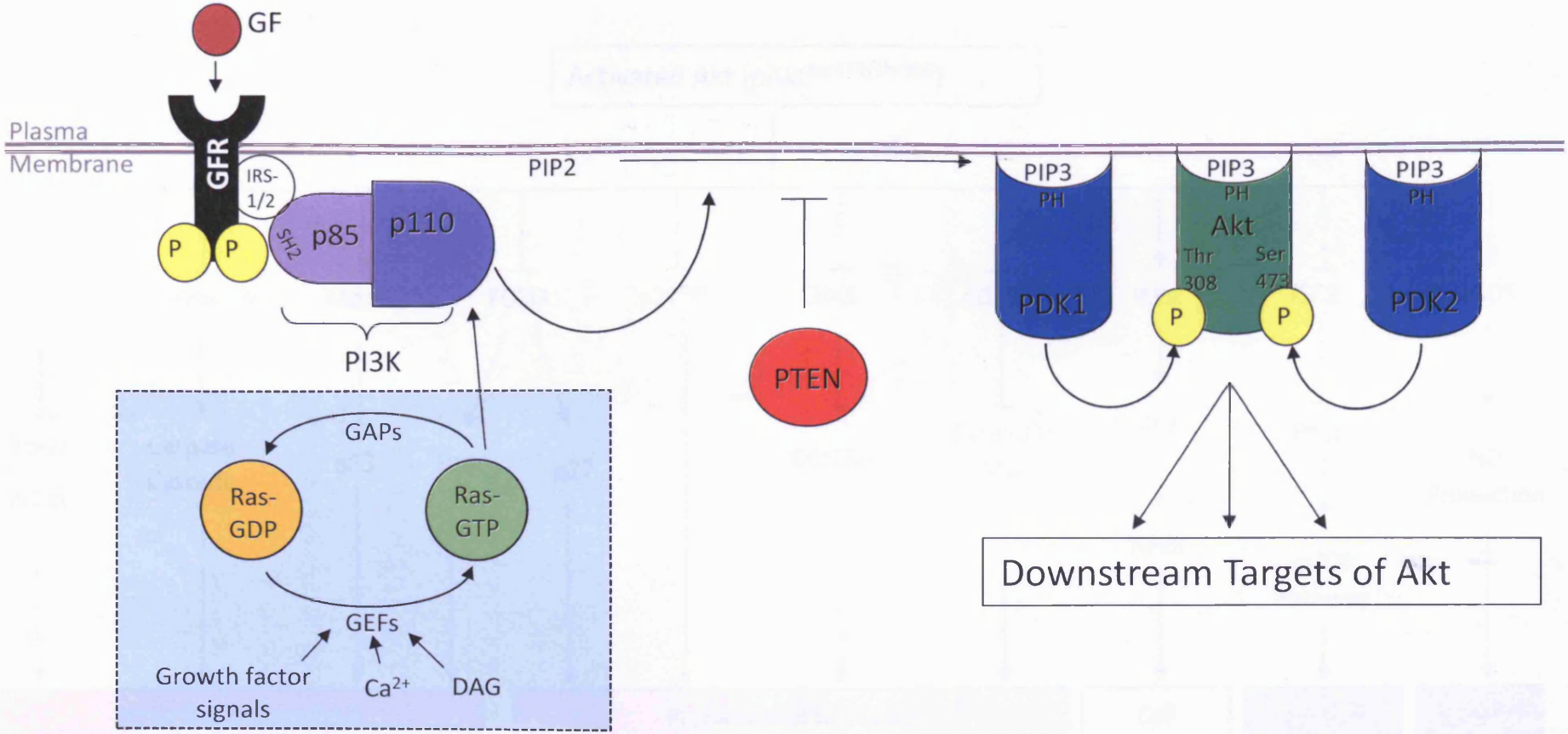

Figure 1.6: ***Activation of PI3K and Akt***

Binding of growth factors (GFs) to growth factor receptors (GFRs) (which are also receptor tyrosine kinases [RTKs]) causes receptor activation by autophosphorylation of tyrosine residues. This allows the binding of PI-3 kinase through the SH2 domain of the p85 subunit and IRS1/2. Binding of the p85 regulatory subunit causes allosteric activation of the p110 catalytic subunit. Alternatively, the catalytic p110 subunit can be directly activated by Ras. Ras is activated when bound to GTP, which is stimulated by guanine nucleotide exchange factors (GEFs). GEFs are activated in response to a range of signals, including growth factors, calcium (Ca^{2+}) and diacylglycerol (DAG). Stimulation of the GTPase activity of Ras by GTPase-activating proteins (GAPs) attenuates Ras activity.

Once activated, the catalytic p110 subunit of PI3K then locally produces PI-3,4,5-P3 from PI-4,5-P2 in the plasma membrane. This reaction is antagonised by the catalytic activity of PTEN. The PH-domain containing proteins PDK1, PDK2 and Akt are then recruited to the plasma membrane, and bind PIP3 through their PH domains. Here, due to the close physical location of the proteins, PDK1 and 2 are able to phosphorylate Akt at residues Thr308 and Ser473 respectively. Phosphorylation of Akt at these sites leads to its complete activation, and it can then act on its cellular substrates.

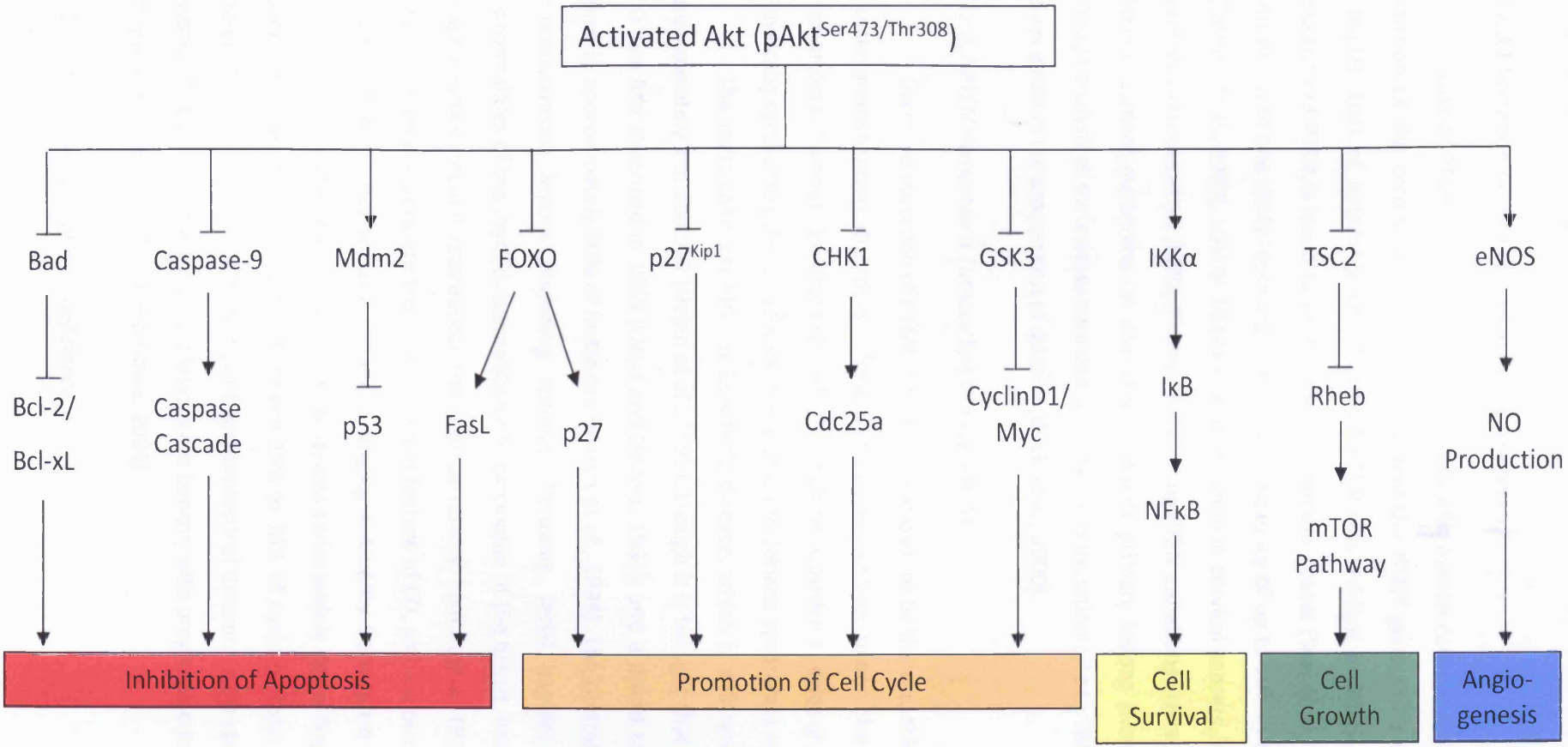

Figure 1.7: ***Downstream Targets of Akt***

The cellular targets of Akt kinase are numerous and varied. Here, the action of Akt on a number of its targets is shown, grouped according to the resultant cellular effect of Akt activation. In general, the effects of Akt activation promote processes associated with acquired tumourigenic properties of cancer cells, as described by *Hanahan and Weinberg, 2000*.

1.2.3 Pten and carcinogenesis

1.2.3.1 Somatic mutation of Pten in human cancers

Loss of PTEN is a frequent event in sporadic human cancers. *Cairns et al.* (1997) report deletion of the chromosome region containing the *PTEN* gene in 23 of 80 prostate tumour samples. Loss of heterozygosity (LOH) of *PTEN* was evident in 10 of these cases. Similarly, mutation of PTEN is found to be common in sporadic breast (Saal et al., 2008) and endometrial cancers, with one study reporting a mutation frequency of up to 50% in endometrial carcinomas (Tashiro et al., 1997). LOH of 10q23 is also common in cervical cancers, with a *PTEN* loss rate of over 35% (Kurose et al., 2000). Finally, inactivating *PTEN* mutations are reported in samples taken from malignant melanoma. In one study, 38% of primary lesions showed mutation of *PTEN*, though analysis of metastases revealed an increase in mutation rate to 58%, suggesting that PTEN plays a role in the progression of disease (Birck et al., 2000).

1.2.3.2 PTEN Hamartoma Tumour Syndromes (PHTS)

Germline mutation of *PTEN* in humans is known to be the causative factor in a number of cancer-predisposition disorders. These syndromes, known under the umbrella term 'PTEN Hamartoma Tumour Syndromes' (PHTS), include Cowden's disease (CD), Bannayan-Riley-Ruvalcaba syndrome (BRRS; also known as Bannayan-Zonana syndrome) and Proteus syndrome.

The most common PHTS is Cowden's disease, which is still rare, with an incidence of approximately 1 in 200,000 (Nelen et al., 1999), though it is thought that CD is under-diagnosed. CD was first described in 1963 (Lloyd and Dennis, 1963), and is linked to mutation of the *PTEN* gene in approximately 80% of instances (Marsh et al., 1998). The clinical features of CD include mucocutaneous lesions (including lipomas, fibromas, facial papules and oral papilloma), abnormalities of the thyroid, susceptibility to carcinoma of the breast, endometrium and thyroid, macrocephaly, mental retardation and gastrointestinal hamartomas (Reviewed by Eng, 2003). Mucocutaneous lesions are the most common feature of CD, and are present in almost all cases. Thyroid abnormalities are also common, ranging in severity from goitre to follicular carcinoma. The reported incidence of gastrointestinal lesions varies widely depending on the study, and has been estimated to be present in between 35% to 75% of cases (Carlson et al., 1984, Merg and Howe, 2004). The observed histology of gastrointestinal tumours in CD cases also appears to vary widely, though it is clear that most lesions are benign, with progression to carcinoma reported in only a handful of cases (Merg and Howe, 2004).

1.2.3.3 Mouse models of Pten deficiency

A null mutation for the mouse *Pten* gene was generated simultaneously by three independent groups (Podsypanina et al., 1999, Di Cristofano et al., 1998, Suzuki et al., 1998). All three groups report embryonic lethality in the homozygous mutant at between embryonic (E) days E6.5 and E9.5. Analysis of mice heterozygous for Pten has revealed predisposition to a number of neoplasias. *Suzuki et al.* (1998) report spontaneous tumourigenesis in 14% of mutant mice before the age of 28 weeks. Mutant mice were found to be predisposed to lymphoma, leukaemia, liver hyperplasia, teratocarcinoma and prostate neoplasia. In addition to this, many of the animals examined were found to have microscopic lesions of the intestinal mucosa, described as being hamartomatous. Similarly, *Di Cristofano et al.* (1998) report multiple system tumourigenesis at a young age. By the age of 14 weeks, heterozygotes were commonly found to have prostate hyperplasia and skin hyperkeratosis. Like *Suzuki et al.,* this study also reports a high incidence of gastrointestinal hyperplasia, and additionally the occurrence of colonic carcinoma is reported in 3 out of 18 mice studied. Finally, *Podsypanina et al.* show a similar phenotype of cancer predisposition, however the tumour spectrum reported included neoplastic changes of the thyroid and endometrial hyperplasia. Adenoma of the colon is also reported, most of which were found to be lymphoid-associated.

In order to circumvent the problem of embryonic lethality, a number of studies have employed the use of conditional transgenesis to examine the effect of homozygous *Pten* mutation in the adult and within specified tissues. *Lu et al.* (2007) have employed a strategy to globally delete both copies of Pten in the adult mouse, driven by the ROSA26 ubiquitously-expressed promoter. Following a latency period of 11 weeks and 21 weeks for females and males respectively, tumourigenesis was found to ensue. Lymphoma was the most common malignancy reported across both sexes, and epidermal squamous cell carcinoma was also found to occur in both males and females. Additionally, female mutants were found to develop endometrial carcinoma, and males were found to be susceptible to both prostate and intestinal cancers. The intestinal lesions reported in males were described as colorectal carcinomas, and were found to be one of the latest-developing malignancies in experimental animals.

Tissue-specific deletion of *Pten* has revealed a clear role for Pten in carcinogenesis of the liver (Stiles et al., 2004, Horie et al., 2004), breast (Li et al., 2002), prostate and skin (Backman et al., 2004). Further, deletion of *Pten* specifically within the intestine has been shown to lead to rapid polyposis (He et al., 2007). Within one month after induction of *Pten* loss, intestinal lesions were observed, which were found histologically to be hamartomatous. Thus, this study established a role for *Pten* in suppression of tumourigenesis in the intestine.

1.3 Modelling colorectal cancer in the mouse using conditional transgenesis

1.3.1 Mouse models of intestinal tumourigenesis

Murine models of human cancers are invaluable both for furthering knowledge into the basic biology of disease, and for providing a platform in which to test novel and potential therapeutic agents.

However, for the maximum possible benefit to be gleaned from such models, they need to accurately and faithfully recapitulate the disease situation as it would occur in humans.

For intestinal tumourigenesis, the classic example of a mouse model of disease is the Apc^{MIN} mouse. This model was generated using a random mutagenesis approach, involving exposure of mice to the mutagen ethylnitrosourea (ENU). This led to the isolation of a line which was found to spontaneously develop intestinal tumours within both the large and small intestine with very high penetrance (Moser et al., 1990). Following the establishment of this pedigree, the mutant line was sequenced and found to bear a mutation in the gene encoding *Apc*, at codon 850 (Su et al., 1992). This mutation is analogous to that commonly found in human FAP, and the Apc^{MIN} mouse has since been established as a good murine model of this disease, and also of sporadic tumour formation.

As such, the Apc^{MIN} mouse has been valuable both to allow study of tumour initiation and neoplastic development in an *in vivo* setting (Shoemaker et al., 1997), and has also allowed exploration of the potential efficacy of a number of therapeutic agents. For instance, the use of non-steroidal anti-inflammatory drugs (NSAIDs) including aspirin (Sansom et al., 2001) and Sulindac (Boolbol et al., 1996), have been explored in the Apc^{MIN} mouse, both for prophylaxis and for treatment of pre-existing intestinal tumours. *Boolbol et al.* reported dramatic suppression of tumourigenesis following treatment of mice with Sulindac, and these data have also been recapitulated in human FAP patients treated with the same agent (Giardiello et al., 2002), providing very convincing evidence validating the use of the Apc^{MIN} mouse model.

However, it should be noted that the Apc^{MIN} mouse has limitations with respect to modelling human disease. The distribution of tumours observed in Apc^{MIN} mice is considerably different to that observed in humans. In humans, small intestinal lesions are rare (Cancer Research UK, 2007), either in FAP or in sporadic disease. In contrast, the Apc^{MIN} mouse commonly develops tumours within the small intestine as well as in the colon (Moser et al., 1990). Furthermore, whilst Apc^{MIN} mice tend to bear a large tumour burden in terms of the number of lesions which develop, the severity of these lesions is rarely seen to advance past the stage of adenoma. In contrast, lesions in human FAP patients often progress to full-blown carcinoma, and indeed this is often the case in sporadic disease also.

Thus, although models such as the Apc^{MIN} mouse have been important for allowing research into intestinal tumourigenesis *in vivo*, it is clear that more sophisticated models of disease must be developed in order to model the finer aspects of tumour development and progression which occurs in humans.

1.3.2 Constitutive versus conditional transgenesis

The advent of directed transgenic technology in the mouse came in 1987 with the development of the first targeted knockout, bearing deletion of the hypoxanthine-guanosine phosphoribosyl transferase (HPRT) gene (Kuehn et al., 1987). Since then, numerous murine constitutive knockout models have been generated, with varying degrees of success. Although such studies have provided valuable insights into the *in vivo* function of a number of genes, it is becoming clear that constitutive models are beginning to fall short in their ability to assess more subtle aspects of gene function.

One of the most obvious flaws of constitutive models is that the expression of many genes is absolutely required during embryonic development. Thus, the generation of an adult mouse deleted for these genes is impossible. This rules out the use of constitutive transgenesis to study of a large number of genes, and it could be argued that these may be among some of the most interesting genes to study in vivo, particularly in the field of cancer biology. Indeed, many known tumour suppressor genes and oncogenes are absolutely required for embryonic development.

A second problem with constitutive knockout mice is that all the cells within the organism are deleted for the particular gene of interest. This poses several issues with regard to the study of gene function. Firstly, the study of a gene within a particular tissue may be precluded by more severe phenotypes occurring within other tissues of the organism. Secondly, the interaction between different cell types within a tissue may be altered, as all cell types within that tissue will be deficient for the gene of interest. This is particularly pertinent with regards to the study of neoplasia, as tumours generally arise due to the mutation of a single cell, without effect on any of its neighbouring cells or other components of its microenvironment.

Finally, constitutive gene deletion provides a large opportunity for developmental compensation within the organism. This may potentially mask the true cellular role of a gene.

In order to circumvent many of these problems, approaches employing the use of conditional transgenesis have been developed, and their use is becoming increasingly popular.

1.3.3 Conditional transgenic approaches

The basic principle of conditional transgenesis is that modification of gene expression will occur only once defined conditions have been met. This allows much finer control of gene deletion or activation, both spatially and temporally.

In its very simplest form, conditional transgenesis involves the use of a tissue-specific promoter to drive expression of a gene of interest. Clearly, this approach is generally applied to the study of overexpression rather than deletion of genes of interest. For example, the *Villin* gene promoter has been used to drive gene expression specifically in the small and large intestine (Pinto et al., 1999). This approach often successfully avoids problems of embryonic lethality and of over-riding phenotypes in other tissues. However, the fact that gene expression within the tissue is still constitutive means that the problem of developmental adaptation is not addressed. In order to do this, an element of control over the exact time in development in which is gene is lost needs to be introduced.

Early attempts to generate a temporally 'switchable' transgene involved the use of exogenous agents such as steroids, heat shock or heavy metals (Schweinfest et al., 1988, Hu and Davidson, 1990). However, such approaches were plagued with problems, such as toxicity of inducing agents and poor levels of recombination being achieved.

Recently, more sophisticated approaches have been used to develop truly switchable strategies. Such approaches are generally bipartite in mechanism, consisting of both an 'effector' transgene and a 'target' transgene. Examples of these approaches, which have been used in the mouse, include Causes recombination (Cre)-Locus of crossover of bacteriophage P1 (LoxP), Flp-Flp recognition target (Frt) and Tetracycline (Tet-) regulated techniques. The Cre-LoxP approach has proven particularly popular, and is described in detail below.

1.3.4 The Cre-LoxP approach

1.3.4.1 Mechanism of action

The Cre-LoxP system operates as a binary mechanism. Cre recombinase, the 'effector' component of the Cre-LoxP system, was originally isolated from Bacteriophage P1 (Abremski and Hoess, 1984). It is a site-specific DNA recombinase, which recognises sequences termed LoxP sites (Hoess et al., 1982, Sternberg and Hamilton, 1981). Upon recognition of a pair of LoxP sequences, cre recombines between these sites, excising the material in between. This can be utilised experimentally by engineering a gene of interest such that LoxP sites are inserted either surrounding the entire gene, or surrounding an essential coding region of the gene. Thus the gene has been 'targeted' for recombination. When the gene is then exposed to Cre recombinase, the region between LoxP sites is excised, or 'floxed' out, resulting in complete inactivation of the

gene. Activation of transgenes can also be achieved using the Cre-LoxP system; in this case the target transgene contains a 'STOP' cassette flanked by LoxP sites. Upon exposure to cre, the STOP cassette is excised and expression of the transgene is permitted.

Spatial and temporal control over this system can be readily attained through modulation of expression and activity of cre recombinase. Strategies which have been employed to achieve this in the intestine are discussed below (Section 1.3.3).

1.3.4.2 Benefits and disadvantages of the Cre-LoxP system

Undoubtedly, one of the major benefits of the Cre-LoxP system is its popularity; numerous murine genes have been targeted by insertion of LoxP sites, and Cre recombinase constructs have been generated to allow controlled expression of Cre in many different situations (Nagy, 2008). The variety of different promoters to drive Cre expression also means that modulation of gene expression can be controlled both temporally as well as spatially. Finally, different experimental approaches can allow either activation or deletion of a selected gene (as described above).

However, some drawbacks to the system also exist. One of the main problems of the system is that once activated and the target region excised, this can not be reversed, and the system can not be restored to its original state. Although less commonly used in the mouse, Tet-regulable systems do allow the switching on and off of transgenes at will (Gossen and Bujard, 1992).

Another common problem with many cre-expressing transgenes is that they allow a certain level of aberrant cre expression, or 'leakiness'. In some instances however, this cre leakiness has been exploited, and it has been argued to be one of the benefits of the system.

Finally, it has been proposed that expression of cre recombinase in mammalian cells may promote genomic instability. This point has been reinforced by the discovery of pseudo-LoxP sequences in mammalian genomes (Thyagarajan et al., 2000), upon which Cre recombinase may be able to act to cause double-stranded DNA breaks.

1.3.5 Regulation of Cre activity in the intestine

The requirement for tightly-restricted Cre activity within given cell types has led to the development of a number of ingenious strategies allowing transcriptional and post-translational regulation of Cre. The major approaches used within the intestine are described below, and are also summarised schematically in Figure 1.8.

1.3.5.1 Use of tissue-specific promoters

Tissue-specific promoters have been used to drive the expression of Cre in much the same way as they are used to drive the expression of other genes of interest, as described above (Section 1.3.2). However, in this case the system can be devised such that either the expression or deletion of a gene can be driven by recombination.

Within the intestine, both the Villin (el Marjou et al., 2004, Madison et al., 2002) and the Fatty acid binding protein (Fabp) (Saam and Gordon, 1999) gene promoters have been used to drive cre expression within all epithelial cell types .

As with tissue-specific promoter driven transgenes, this approach does not circumvent the problem of developmental compensation within the tissue in response to gene loss or activation. However, the use of tissue-specific promoters to drive cre expression can be used in combination with other methods of cre regulation to achieve finer control of recombination patterns (see below).

1.3.5.2 Use of inducible promoters

Inducible promoters require the administration of a xenobiotic agent in order to become active and allow the transcription of the cre transgene. Inducible promoters are commonly used to drive recombination in the intestine. The promoter of Cytochrome P450 1A (CYP1A1) is used to drive expression of cre in the AhCre construct specifically in the intestinal epithelium in response to administration of aryl hydrocarbons such as beta-naphthoflavone (Campbell et al., 1996, Ireland et al., 2004). Another example of the use of an inducible promoter to drive recombination in the intestine is Mx1Cre, which drives recombination in both the epithelium and in underlying stromal cells (Schneider et al., 2003). Induction by treatment using either interferon or polyinosinic-polycytidylic acid (which stimulates interferon production in the host) is required to activate transcription of Mx1Cre (Kuhn et al., 1995).

Such promoters have the advantage that as well as exhibiting spatially controlled expression, they also allow temporal control of cre activity. However, inducible promoters often exhibit some level of leakiness, depending on the promoter used.

1.3.5.3 Post-translational regulation of Cre activity

Approaches to regulate cre activity much more tightly have also been developed, employing the use of post-translational regulation through dependence on ligand binding. Several different studies have reported the generation of a fusion protein of cre and a modified estrogen receptor (ER) (el Marjou et al., 2004, Feil et al., 1996, Feil et al., 1997, Metzger et al., 1995). After transcription and translation of the fusion protein, the estrogen receptor (ER) domain of the fusion protein sequesters cre recombinase in the cytoplasm, preventing it from acting upon its target sequences which are contained within the nucleus. The estrogen receptor domain bears a

point mutation so that it is unresponsive to the binding of endogenous estrogens present in the host animal. However, upon binding of the ER to the estrogen analog, Tamoxifen, the nuclear localisation signal of the receptor is exposed, allowing the translocation of the CreER fusion protein to the nucleus, where cre can then act on its targets.

1.3.5.4 Combinatorial approaches

The most sophisticated forms of cre regulation employ the use of a combination of either a tissue specific promoter or an inducible promoter with a post-translationally regulated form of cre. For example, in the intestine, the Villin promoter has been coupled to a CreER fusion protein to allow temporal control over Cre expression within the epithelium (el Marjou et al., 2004). Also in the intestine, the inducible Ah promoter has been used to drive expression of a CreER fusion protein. Thus, cre activity requires induction both with an aryl hydrocarbon, to stimulate transcription of the transgene, and with Tamoxifen, to post-translationally activate cre (Kemp et al., 2004).

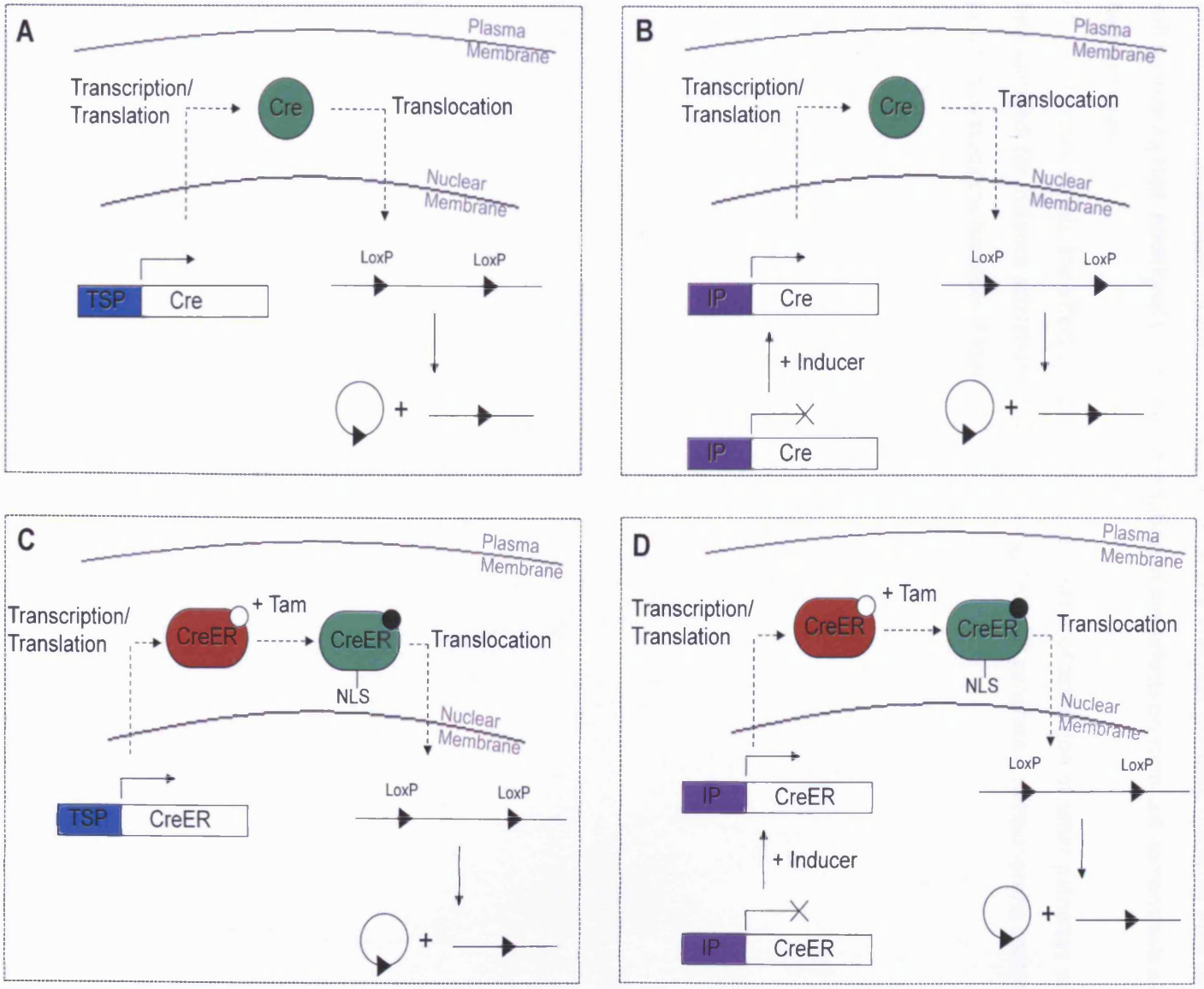

Figure 1.8: ***Strategies for regulation of Cre activity in the intestine.***
A: Regulation of Cre activity by use of a tissue-specific promoter (TSP). The Cre transgene is under the control of a promoter which is expressed only in certain tissues, for instance, the *Villin* or *Fabp* gene promoters are commonly used within the intestine. When the promoter is active, the cre transgene is expressed, and transcribed and translated in the cytoplasm. Cre can then freely enter the nucleus, and act on genes targeted with LoxP sites.
B: Use of an inducible promoter (IP) to allow temporal control of Cre activity. Expression of the cre transgene is restricted by use of an inducible promoter, such as the *Cyp1A1* promoter which is used to drive Cre expression in the intestine. The IP is only activated following administration of an exogenous inducing agent, for example beta-naphthoflavone efficiently induced *Cyp1A1* promoter expression. The Cre transgene is then expressed, transcribed and translated as described above (A).
C: Tissue-specific expression of a Cre-Estrogen receptor (CreER) fusion protein to allow post-translational control of Cre activity. The CreER fusion protein is expressed in a tissue specific manner from a TSP as descibed in A. However, following transcription and translation of CreER, the protein requires binding to tamoxifen (which is added exogeneously) in order to access the nucleus and act on its target sequences.
D: Combined use of an inducible promoter and a CreER fusion protein. Expression of CreER requires induction of the promoter, as described in B. Following promoter induction, the CreER fusion protein is transcribed and translated, but must bind tamoxifen in order to access the nucleus, as described in C. In the intestine, the Cyp1A1 promoter may be used to drive expression of the CreER fusion protein, thus induction with both beta-naphthoflavone and tamoxifen is required for cre-mediated recombination to occur.

1.4 Project Aims

PTEN is well recognised as a tumour suppressor, and is known to play an important role in both sporadic cancers and heritable cancer predisposition disorders in humans. In addition to this, there is evidence that PTEN plays a role in suppressing tumourigenesis specifically in the intestine, and may also play an important role in regulation of the intestinal stem cell.

The principal aim of this project is to characterise the effects of homozygous Pten deletion exclusively in the adult murine small intestinal epithelium. Both the short term effects of Pten deletion on intestinal homeostasis and the longer term implications of Pten loss on tumour formation will be assessed. In particular, activation of the PI3K/Akt pathway following Pten loss will be investigated. Additionally, the characterisation of any effects on stem cell homeostasis will be attempted.

Further to this, the effect of Pten loss in the context of activation of other pathways will be examined, for instance activation of Wnt signalling. This will generate a tumour-prone context in which to study the function of Pten.

Chapter 2: Materials and Methods

2.1 Experimental Animals

All experiments involving animals were conducted according to UK Home Office regulations, under valid personal and project licenses. Where experiments were conducted outside the UK by collaborators, appropriate local and national regulations were adhered to.

2.1.2 Animal Husbandry

2.1.2.1 Colony maintenance

Mice were maintained on an outbred background and housed in a standard facility. Animals had access to diet (Special Diets Service UK, RM3(E) expanded diet) and fresh drinking water *ad libitum* unless specified.

2.1.2.2 Breeding

Adult animals of known genotype were generally bred in trios (one male, two females). After birth, pups remained with their mothers until large enough to be weaned, usually at four weeks of age.

2.1.2.3 Identification and Tail Biopsy

At weaning age, mice were marked by ear clipping for identification purposes. Surgical biopsy of 5mm of the tail tip was also taken under local anaesthetic to allow PCR genotyping of all animals (see below).

2.1.3 Experimental Procedures

2.1.3.1 Injection of beta-Naphthoflavone

Expression of Cre recombinase from the AhCre transgene was induced using beta-naphthoflavone (bNF; Sigma) delivered in corn oil. Corn oil (Sigma) was heated in an amber bottle (to protect bNF from light) to 99°C and powdered bNF added to give a concentration of 10mg bNF per 1ml Corn oil. The solution was further heated and stirred vigorously to ensure complete dissolution of bNF. Aliquots were frozen in smaller amber bottles at -20°C until needed. Before injection, aliquots of bNF were defrosted, reheated to approximately 80°C to re-dissolve the bNF and kept at this temperature until just prior to injection to prevent precipitation. Animals were

then injected intraperitoneally (ip) at a dose of 80mg bNF per kg body weight. To achieve maximal Cre expression, this dose was repeated once a day for a further 3 days (four treatments in total) unless otherwise stated.

To induce recombination *in utero*, timed matings were generated, and pregnant females were injected intraperitoneally with a single 80mg/kg dose of beta-naphthoflavone as described above at day 12.5 after the appearance of a copulatory plug.

2.1.3.2 Injection of Tamoxifen

Animals expressing the Cre recombinase-Estrogen Receptor ($CreER^T$) fusion protein were induced by treatment with Tamoxifen (Tam; Sigma), delivered in corn oil. Corn oil was heated to 80°C and powdered Tamoxifen added to give a concentration of 10mg/ml. The solution was further heated and shaken until the Tamoxifen had completely dissolved, and was kept at this temperature until just prior to injection. Animals then received a single 80mg/kg dose ip once a day for 4 days unless otherwise stated.

2.1.3.3 Injection of beta-Naphthoflavone and Tamoxifen

Animals bearing the $AhCreER^T$ transgene required treatment with both bNF and Tam to induce Cre transcription and activity. bNF was dissolved in corn oil as described in 2.1.3.1. Upon reheating, Tamoxifen was added to a concentration of 10mg/ml as described in 2.1.3.2. Animals then received 4 daily doses of 80mg/kg of both bNF and Tam in a single ip injection unless otherwise stated.

2.1.3.4 Injection of 5-Bromo-2-deoxyuridine

Where indicated, certain experimental animals received an excess of 5-Bromo-2-deoxyuridine (BrdU; Amersham Biosciences) in order to label cells in S-phase. Animals were injected ip with 0.2ml BrdU reagent either 2 hours or 24 hours prior to harvesting.

2.1.3.5 Whole-body gamma-irradiation

Where indicated for clonogenic assays, animals were subjected to whole-body gamma-irradiation. Animals were restrained by placing in a small, well-ventilated Perspex chamber. Gamma irradiation of different doses (10Gy, 12.5Gy and 15Gy) was achieved by exposure to a Caesium-137 source delivering 2.2Gy per minute (IBL437C Irradiator, RPS Services).

2.1.4 PCR Genotyping

Genotyping was performed on all transgenic animals prior to experimental use using a PCR-based approach.

2.1.4.1 Digestion of tail biopsy samples

Tail biopsy samples were temporarily stored at -20°C to prevent degradation. To each biopsy, 500µl cell lysis solution (Puregene) containing 0.4mg/ml Proteinase K (from a 20mg/ml stock, Roche) was added. Samples were then digested overnight at 37°C with vigorous agitation.

2.1.4.2 Crude extraction of DNA

Digested samples were cooled to room temperature and 200µl protein precipitation solution (Puregene) added. Tubes were inverted to mix and centrifuged at 12000 x g for 5min to pellet all protein and insoluble material. The supernatant was removed into a clean tube containing 500µl isopropanol, and the pellet discarded. After mixing well by inverting, the mixture was centrifuged again at 12000 x g for 15 mins in order to pellet the precipitated DNA. The supernatant was then removed and the DNA pellet allowed to air-dry at room temperature for 1 hour. The dried pellet was then dissolved in 500µl sterile, PCR-grade water (Sigma) at 37°C with agitation.

2.1.4.3 Generic protocol for PCR genotyping

All PCR genotyping primers were designed using the Primer3 web-based program (http://frodo.wi.mit.edu/cgi-bin/primer3/primer3_www.cgi) unless previously published sequences were available. Sequences were verified using Blast (http://www.ncbi.nlm.nih.gov/blast) or Ensembl (http://www.ensembl.org) databases to check for mis-priming. Primers were then synthesised by Sigma-Genosys.

All PCR reactions were performed either in thin-wall 96-well PCR plates or in thin-wall 0.2ml strip tubes (both Greiner Bio-One) and run on a PTC-100 Peltier thermal cycler (MJ Research). Pipetting of all samples was performed using filtered pipette tips to prevent aerosol contamination of samples. Appropriate volumes of crude DNA extract (See Table 2.1) and a PCR-Grade water (Sigma) control (2.5µl) were loaded into wells using a multi-channel pipette. A master mix for all samples was then prepared containing all other reaction components (GOTaq DNA Polymerase [Promega] or DreamTaq DNA polymerase [Fermentas], GOTaq 5X PCR buffer [Promega], PCR-grade water [Sigma], Magnesium chloride [Sigma], dNTPs [Bioline], Primers [Sigma-Genosys]) according to Table 2.1. Master mix was added to each well to make the reaction volume up to 50µl, with gentle pipetting to ensure thorough mixing of master mix with crude DNA extract. Samples were gently tapped on the bench to remove air bubbles and ensure the reaction mixture was at the bottom of the well. 96-well plates were sealed with aluminium foil tape and strip tubes with appropriate caps (both Greiner Bio-One). Reactions were then run according to the cycle conditions detailed in Table 2.1.

2.1.4.4 Multiplex detection of Cre and LacZ transgenes

Detection of both the Cre and LacZ transgenes was performed in a single reaction. The reaction was set up and run as described above in section 2.1.4.3 and in Table 2.1. Presence of the Cre transgene yielded a PCR product of 1000 base pairs (bp) in size. Presence of the LacZ transgene yielded a PCR product of 512bp in size.

2.1.4.5 Confirmation of Responder status

Genotyping for the aryl hydrocarbon (Ah) receptor polymorphism was performed as described in section 2.1.4.3 and Table 2.1. The responder polymorphism generated a PCR product of 196bp in size. The non-responder polymorphism generated a PCR product of 178bp in size.

2.1.4.6 Genotyping for the LoxP-targeted Pten allele

Genotyping for presence of the LoxP-targeted Pten allele was performed as described in section 2.1.4.3 and Table 2.1. Homozygotes for the LoxP-targeted allele produced a PCR product of 335bp in size. Homozygotes for the wild-type Pten allele generated a PCR product of 228bp in size. Heterozygotes for the targeted Pten allele generated products of both sizes.

2.1.4.7 Genotyping for the LoxP-targeted Apc allele

Genotyping for presence of the LoxP-targeted Apc allele was performed as described in section 2.1.4.3 and Table 2.1. The targeted Apc allele generated a PCR product of 315bp in size, and the wild-type Apc allele a product of 226bp in size.

2.1.4.8 Genotyping for the LoxP-targeted p53 allele

Genotyping for presence of the LoxP-targeted p53 allele was performed as described in section 2.1.4.3 and Table 2.1. Homozygotes for the LoxP-targeted allele produced a single PCR product of 370bp in size. Homozygotes for the wild-type p53 allele generated a single PCR product of 288bp in size.

2.1.4.9 Detection of the k-Ras transgene

Genotyping for presence of the k-Ras transgene was performed as described in section 2.1.4.3 and Table 2.1. Presence of the transgene resulted in a PCR product of 621bp in size. The wild-type k-Ras allele generated a PCR product of 403bp in size.

2.1.4.10 Visualisation of PCR products

Following PCR reactions, products were visualised by gel electrophoresis. To each sample, 5µl DNA loading dye (50% Glycerol [Sigma], 50% distilled (d)H_2O, 0.1% [w/v] Bromophenol blue

	Cre/LacZ	Responder	PtenLoxP	ApcLoxP	p53LoxP	k-Ras
PCR Reaction components:						
Crude DNA Extract (See Section 2.1.4.2)	2.5µl	2.5µl	2.5µl	2.5µl	2.5µl	2.5µl
Master Mix:						
PCR-grade Water (Sigma)	31.5µl	31.7µl	31.7µl	31.7µl	31.7µl	31.7µl
GO Taq PCR Buffer (5X; Promega)	10µl	10µl	10µl	10µl	10µl	10µl
Magnesium Chloride (25mM)	5µl	5µl	5µl	5µl	5µl	5µl
dNTPs (25mM; dATP, dCTP, dGTP, dTTP)	0.4µl	0.4µl	0.4µl	0.4µl	0.4µl	0.4µl
Primer 1 (Sigma Genosys, 100mM)	0.1µl	0.1µl	0.1µl	0.1µl	0.1µl	0.1µl
Primer 2 (Sigma Genosys, 100mM)	0.1µl	0.1µl	0.1µl	0.1µl	0.1µl	0.1µl
Primer 3 (Sigma Genosys, 100mM)	0.1µl	N/A	N/A	N/A	N/A	N/A
Primer 4 (Sigma Genosys, 100mM)	0.1µl	N/A	N/A	N/A	N/A	N/A
Taq DNA polymerase	0.2µl	0.2µl	0.2µl	0.2µl	0.2µl	0.2µl
Brand of Taq DNA polymerase	GO Taq	Dream Taq	Dream Taq	Dream Taq	Dream Taq	Dream Taq
Total Reaction Volume:	50µl	50µl	50µl	50µl	50µl	50µl
Cycling conditions:						
Initial denaturation step (Time; Temperature)	3min; 94°C	5min; 94°C	2min 30sec; 95°C	3min; 95°C	3min; 94°C	5min; 94°C
Step 1: Denaturation (Time; Temperature)	30sec; 95°C	20sec; 94°C	1min; 94°C	30sec; 95°C	30sec; 94°C	1min; 94°C
Step 2: Annealing (Time; Temperature)	30sec; 55°C	20sec; 57°C	1min; 58°C	30sec; 60°C	20sec; 58°C	1min; 60°C
Step 3: Extension (Time; Temperature)	1min; 72°C	30sec; 72°C	1min; 72°C	1min; 72°C	1min; 72°C	1min; 72°C
Number of Cycles	30	30	35	30	30	30
Final Extension (Time; Temperature)	5min; 72°C	5min; 72°C	5min; 72°C	5min; 72°C	5min; 72°C	5min; 72°C
Hold (Time; Temperature)	∞; 15°C	∞; 15°C	∞; 15°C	∞; 15°C	∞; 15°C	∞; 15°C

Table 2.1: ***PCR Genotyping reaction conditions***

[Sigma]) was added. All samples were then loaded (along with an appropriate marker if necessary, such as 100bp ladder [Promega]) onto a 2% agarose (Eurogentech) gel (made in 1 X Tris-Borate-EDTA [TBE] Buffer [Sigma]) containing 0.007% [v/v] Ethidium bromide (Sigma) with the exception of products of the Responder status PCR reaction, which were loaded onto a 4% agarose (Eurogentech) gel (made in 1 X TBE) containing 0.007% [v/v] Ethidium bromide (Sigma). Gels were run in TBE buffer at 120V for approximately 30 minutes. Products were then visualised under UV light on a GelDoc (BioRad).

Target	**Forward Primer Sequence (5' to 3')**	**Reverse Primer Sequence (5' to 3')**
Cre	TGA CCG TAC ACC AAA ATT TG	ATT GCC CCT GTT TCA CTA TC
LacZ	CTG GCG TTA CCC AAC TTA AT	ATA ACT GCC GTC ACT CCA AC
Responder	TCA CCA AAC CCT CCA TCA GT	AGG TTC CCT GGG ACT TGT TT
PtenLoxP	CTC CTC TAC TCC ATT CTT CCC	ACT CCC ACC AAT GAA CAA AC
ApcLoxP	GTT CTG TAT CAT GGA AAG ATA GGT GGT C	CAC TCA AAA CGC TTT TGA GGG TTG ATT C
p53LoxP	CAC AAA AAC AGG TTA AAC CCA G	AGC ACA TAG GAG GCA GAG AC
k-Ras	AGG GTA GGT GTT GGG ATA GC	CTG AGT CAT TTT CAG CAG GC

Table 2.2: ***Primer Sequences used for PCR Genotyping***

2.2 Tissue sampling and processing

2.2.1 Removal of tissues

Upon dissection, tissue samples were removed and placed in appropriate fixatives as quickly as possible. In general, samples of the following tissues were taken routinely for analysis: Small and large intestine, liver, spleen, pancreas, kidney, stomach and genitourinary tract. Prior to fixation, small and large intestines were flushed well with water to remove debris from the intestinal lumen.

2.2.2 Tissue fixation for histology

Tissues were preserved for subsequent histological examination and immunohistochemical analysis by fixing either in Methacarn or Formalin.

2.1.2.1 Methacarn fixing

Small and large intestines (either whole or defined sections) were removed and flushed as described above. The intestine was then placed on a sheet of 3MM filter paper (Whatman) and opened longitudinally along the proximal-distal axis. Intestines were then completely immersed in a bath of freshly-prepared Methacarn (a 4:2:1 ratio of Methanol:Chloroform:Acetic acid, e.g. 300ml methanol, 150ml chloroform, 75ml glacial Acetic acid) and fixed overnight. The following day, intestines were rolled in swiss-roll fashion from stomach to caecum or from caecum to anus, secured with a needle and placed in 96% Ethanol for subsequent processing.

2.1.2.2 'Quick' fixing in formalin

Selected intestines or regions of intestine were chosen to be fixed in formalin (4% neutral buffered formaldehyde in saline, Sigma) rather than Methacarn. Intestinal samples were flushed with water and were either bundled using surgical tape (Micropore) or were opened longitudinally, rolled from end-to-end (without fixing) and secured with a needle as described above (section 2.1.2.1). Intestinal samples and samples of other tissues were then immersed in ice cold (4°C) formalin for between 12 and 24 hours. After this time, samples were either immediately processed as described below (section 2.2.3) or were transferred to ice cold (4°C) 70% Ethanol (in distilled H_2O) and stored at 4°C until processed.

2.2.3 Tissue processing and sectioning

2.2.3.1 Dehydration of tissue

Tissue was processed using an automatic processor (Leica TP1050). Tissue was dehydrated in increasing concentrations of alcohols, xylene and paraffin (70% ethanol for 1 hour, 95% ethanol for 1 hour, 2 x 100% ethanol for 1 hour 30 mins, 100% ethanol for 2 hours, 2 x Xylene for 1 hour, paraffin for 1hour, 2 x paraffin for 2 hours). After processing, tissue was embedded in paraffin wax.

2.2.3.2 Tissue sections

Paraffin blocks were sectioned on a microtome (Leica RM2135) at a thickness of 5µm. Sections were then floated onto poly-L-lysine (PLL) coated slides (Polysine, Thermo Fisher) and baked for 24 hours at 58°C before use.

2.2.4 Cryosectioning of tissues

2.2.4.1 Preservation of fresh tissues for cryosectioning

A number of tissues were preserved without fixing for cryosectioning. Small samples of tissue were removed and frozen on dry ice completely surrounded by OCT cryoprotectant medium (R. A. Lamb). Samples were frozen either on tin foil, on cork discs (R. A. Lamb) or directly onto aluminium chucks. Frozen samples were stored at -80°C until sectioned.

2.2.4.2 Sectioning of frozen tissues

Frozen tissue samples in OCT medium at -80°C were warmed up to -30°C for 30 mins just prior to sectioning, and were then adhered to aluminium chucks using OCT (if not already on a chuck). Sections were then cut on a cryostat at 15µm. Sections were removed onto Histobond slides (R. A. Lamb) and allowed to air-dry for approximately 20 mins. Sections were stored, wrapped in tin foil, at -80°C until needed.

2.2.5 Preservation of whole tissues for future protein, RNA or DNA extraction

2.2.5.1 For protein extraction

Tissue samples intended for future protein extraction were removed as quickly as possible to prevent protein degradation. Tissue was then places in an eppendorf tube fitted with a locking lid. Samples were then quickly immersed in liquid nitrogen (LN_2) to snap freeze tissue. When convenient, tissue was removed from LN_2 and stored at -80°C until needed.

2.2.5.2 For RNA extraction

Whole tissues intended for RNA extraction were removed quickly and immersed in RNA*later* (Sigma). Samples were then either stored at 4°C (for several weeks) or -20°C (for several months).

2.2.5.3 For DNA extraction

Tissue samples intended for DNA extraction were removed and placed into a clean eppendorf tube. Samples were then kept on ice until transferred to a freezer at -20°C for storage. DNA extraction was then usually performed within 2 weeks.

2.2.6 Analysis of beta-galactosidase activity

Mice bearing the Rosa26/LacZ reporter transgene were used to assess levels of recombination in various tissues. For intestinal tissue, either whole intestines or defined regions of the intestine were removed, prepared as wholemounts and stained for beta-galactosidase activity. For other tissues, small samples of tissue were removed, frozen and sectioned as described in section 2.2.4.

2.2.6.1 Intestinal wholemounts

Whole intestines or defined sections of intestine were removed and flushed well, once with ice cold (4°C) Phosphate-buffered Saline (PBS; Gibco) and once with ice cold (4°C) X-Gal fixative solution (2% formaldehyde [Sigma], 0.1% Glutaraldehyde [Sigma] in PBS). Intestines were then laid out and opened longitudinally. Opened intestines were pinned luminal side up onto wax plates (hot paraffin wax [Sigma] with 10% mineral oil [Sigma] added, poured into a 15cm petri dish and allowed to cool) using insect pins (Watkins & Doncaster).

2.2.6.2 Fixation and demucification of intestinal wholemounts for beta-galactosidase analysis

Intestinal wholemounts were fixed for no longer than 1 hour in X-Gal fixative solution. Plates were then washed with PBS before adding demucifying solution (10% Glycerol [Sigma], 20% Ethanol [Fisher scientific], 0.01M Tris [pH8.2], 0.003% [w/v] Dithiothreitol [DTT, Sigma] in Normal Saline [0.9% Sodium Chloride]). Intestines were incubated with demucifying solution with agitation for 30-60 mins. Demucifying solution was then poured off, and plates washed with PBS. Mucins were removed by pipetting PBS with force onto the intestine using a Pasteur pipette, and examined under a dissection microscope to ensure complete removal of mucins. This process was repeated using fresh PBS until intestines were clean.

2.2.6.3 Fixation and preparation of cryosections for beta-galactosidase analysis

Cryosections were prepared and stored as described in section 2.2.4. Section were removed from the -80°C freezer and allowed to acclimatise to room temperature for approximately 10 mins. Sections were then fixed in X-Gal section fixative solution (2% Formaldehyde [Sigma], 0.2% Glutaraldehyde [Sigma], 0.02% NP-40 in PBS) for 10 mins. After fixing, sections were washed twice for 10 mins each time in PBS.

2.2.6.4 Staining with X-Gal substrate

X-Gal buffer (1mM Magnesium chloride, 3mM potassium ferricyanide, 3mM potassium ferrocyanide in PBS) was prepared in advance and stored in the dark at 4°C. Just prior to use, X-Gal substrate was added (from a 5% stock in DMF [Promega]). For staining of intestinal wholemounts, X-Gal was added to a concentration of 0.02% and for staining of cryosections, X-Gal was added to a concentration of 0.04%. Wholemounts or sections were then stained overnight in the dark with agitation. Wholemounts were stained at room temperature and sections were stained at 37°C.

X-gal staining solution was then removed, and plates/sections washed once with PBS. Wholemounts were then fixed in formalin for 1 hour, before being stored in PBS. Sections were counterstained for 2 mins using nuclear fast red (0.1% [w/v] nuclear fast red [Sigma], 70mM Aluminium sulphate [Sigma] in dH_2O) before being dehydrated, cleared and coverslipped as described in section 2.4.1.9.

2.2.7 Isolation of intestinal epithelium

2.2.7.1 Isolation of epithelial cells

A method for enrichment of intestinal epithelial cells was developed based on that of Bjerknes and Cheng (Bjerknes and Cheng, 1981).

Intestines were removed and flushed well with water. A 10cm stretch of intestine from a defined location was used for epithelial cell extraction. The intestine was tied off at one end using non-soluble suture (Mersilk, Ethicon) and the intestine carefully inverted over a spiral-shaped glass rod. The intestine was then placed into a 50ml Falcon tube containing approximately 30ml epithelial extraction buffer (10mM EDTA pH8.0 [Sigma] in Hanks' balanced salt solution [HBSS, Gibco]) which had been pre-warmed to at 37°C. The tube was then shaken at the lowest setting on a vortex mixer for 15 mins, generating the first 'fraction' of epithelial cell extract. After this time, the intestine was removed to a clean, pre-warmed tube of epithelial extraction buffer. The tube was then shaken in the same fashion for a further 15 mins, generating the second 'fraction' of epithelial cell extract.

2.2.7.2 Processing of crude epithelial cell suspensions

Epithelial cell suspensions in epithelial cell extract buffer were centrifuged immediately at 3000 x g at 4°C for 15 mins to yield a pellet containing crudely purified epithelial cells. The supernatant was aspirated and the pellet processed either for future protein extraction (section 2.2.7.3) or RNA extraction (2.2.7.4).

2.2.7.3 Preservation of extracted epithelium for protein extraction

Epithelial cell extracts from the second fraction were used for protein extraction as these fractions were generally less mucinous than the first fraction. Epithelial cell pellets were washed by re-suspending in 5ml ice cold PBS, and then re-pelleted by centrifugation at 3000 x g at 4°C for 15 mins. The PBS was carefully aspirated, and the pellets snap frozen in LN_2 and stored at -80°C until used.

2.2.7.4 Preservation of extracted epithelium for RNA extraction

For RNA extraction, the first fractions of epithelial cell extracts were used. Pellets were re-suspended in 1ml Trizol (Invitrogen), transferred to a 1.5ml eppendorf tube, and stored at -20°C until needed.

2.2.7.5 Epithelial cell isolation by gut scraping

In some cases, epithelial cells were obtained by scraping of the gut rather than by the epithelial cell isolation protocol described above (section 2.2.7.1). To do this, defined regions of small intestine were selected and flushed well with water. The intestine was the opened longitudinally and laid out on a piece of 3MM filter paper (Whatman). The surface of the intestine was then gently scraped using a rounded blade disposable scalpel (Swann-Morton) to remove the surface epithelium. The scraped material was then transferred to an eppendorf tube, and was either frozen at -20°C for future DNA analysis, or was snap frozen in liquid nitrogen for future protein extraction, or was suspended in 1ml Trizol reagent (Invitrogen) for future RNA extraction.

2.3 Histological Analysis

2.3.1 Haematoxylin and Eosin (H&E) staining of tissue sections

Tissue sections were de-waxed and rehydrated as described in section 2.4.1.1. Sections were then stained in Mayer's Haemalum (R. A. Lamb) for 5 mins followed by washing in running tap water for 5 mins. Sections were then stained in 1% aqueous Eosin (R. A. Lamb) for 5 mins

followed by two 15 second washes in water. Sections were then dehydrated, cleared and mounted as described in section 2.4.1.9.

2.3.2 Quantification of H&E-stained tissue sections

Quantification of histological sections was performed on an Olympus BX41 light microscope fitted with a Colorview III (5 megapixel, Soft Imaging Systems) camera and with the aid of AnalySIS (Version 3.2, Build 831, Soft Imaging Systems) software. Areas of section were chosen which were not cross-cut and were free from any other sectioning artefacts. For all comparisons, sections from at least 3 animals of each genotype were scored to allow statistical analysis. A running mean was also calculated, to ensure convergence towards the overall mean.

2.3.2.1 Crypt size

Crypt size was scored by counting the total number of epithelial cells from the base to the top of the crypt. This was performed for 50 whole crypts per section.

2.3.2.1 Villus length

Villus length was scored by counting the number of epithelial cells from the base of the villus to the villus tip. This was performed for 50 half villi per section. Care was taken to ensure that comparable regions of the longitudinal axis of the intestine were selected for scoring, as villus length is known to vary along the length of the intestine.

2.3.2.2 Mitotic index

Mitotic cells were identified on H&E stained sections based on their morphological appearance. Number of mitotic figures was scored per crypt for at least 25 crypts per section. The average (mean) number of mitoses per crypt for each section was then calculated, and then the mean across all sections of the same genotype calculated. This generated an overall mean value. Standard deviation of the mean was calculated according to standard methods. Significance of any differences observed was confirmed using the Mann-Whitney-U test (see section 2.7.2 for details).

2.3.2.3 Apoptotic index

Apoptotic cells were identified on H&E stained sections based on their distinctive morphological appearance. Scoring was conducted in exactly the same way as for scoring for mitotic cells (Section 2.3.2.2).

Scoring of Apoptotic cells from Caspase-3 stained sections was also conducted to confirm morphology-based scoring results. Numbers of positively stained cells per crypt were scored per crypt in 25 full crypts per section. Mean values, standard deviations and significance analysis was conducted as described above (section 2.3.2.2).

2.3.3 Use of special stains to identify specific cell types

2.3.3.1 Grimelius method

The Grimelius staining method was used to stain for argyrophilic enteroendocrine cells. Methacarn-fixed tissue was selected, and sections de-waxed and rehydrated as described (section 2.4.1.1). All Glassware was rinsed with ultrapure (dd) H_2O before use. 1% [w/v] Silver nitrate (Sigma) was dissolved in Acetate buffer (0.02M Acetic acid (Fisher scientific), 0.02M Sodium acetate (Sigma) in ddH_2O) and preheated to 65°C in a slide jar in a hot water bath. Slides were then immersed in this solution (and kept at 65°C) for 3 hours. Meanwhile, reducing solution (0.04M Sodium sulphite [Fisher scientific], 0.1M hydroquinone [Sigma] in ddH_2O) was freshly prepared and preheated to 45°C. Slides were then transferred from silver solution into reducing solution, where they remained for approximately 5 minutes, or until tissue appeared yellow in colour. Sections were then dehydrated, cleared and mounted as described in section 2.4.1.9.

2.3.3.2 Staining with Alcian blue

Alcian blue staining for mucins was used to identify mucin-secreting Goblet cells. Tissue sections were de-waxed and rehydrated as described (section 2.4.1.1). Slides were then immersed in Alcian blue staining solution (1% [w/v] Alcian blue [Sigma] in 3% [v/v] Acetic acid [Fisher scientific]) for 5 mins Slides were then washed well in running tap water for 5 mins. Tissue sections were then counterstained in 0.1% Nuclear fast red (0.1% [w/v] nuclear fast red [Sigma], 0.07M Aluminium sulphate [Sigma] in dH_2O) for 5 mins. Sections were washed well in running tap water for 5 mins before being dehydrated, cleared and mounted as described in section 2.4.1.9.

2.3.3.3 Staining with Periodic acid/Schiff's solution (PAS)

Periodic Acid/Schiff's solution staining was used as an alternative to Alcian blue staining for Goblet cells. Sections were de-waxed and rehydrated as described in section 2.4.1.1. Sections were then treated with 1% [w/v] Periodic acid (Sigma) in dH_2O for 5 minutes. Slides were then rinsed in running tap water for 5 mins before being treated with Schiff's reagent (Sigma). Slides were rinsed again in running tap water for 10 mins. Sections were then counterstained in Mayer's haematoxylin, dehydrated, cleared and mounted as described in section 2.4.1.9.

2.3.3.4 Alkaline phosphatase staining

Alkaline phosphatase activity was detected as a marker of enterocytes. Slides were de-waxed and rehydrated as described in section 2.4.1.1. Fast Red substrate (DAKO), prepared as described in the manufacturer's instructions, was applied to slides for 20 mins at RT. Sections were then rinsed in dH2O, and counterstained in Mayer's haematoxylin as described in section 2.4.1.9. As Fast Red staining is not stable in solvents, slides were cover-slipped using aqueous mounting medium (DAKO).

2.4 Immunohistochemistry (IHC)

2.4.1 Generic Immunohistochemistry protocol

All immunohistochemistry was performed following the generic protocol described below with specific conditions/modifications to the protocol for each target described in Table 2.3. All incubations were performed at room temperature (approximately 18-22°C) in a humidified chamber where necessary to prevent tissue sections drying out. The protocol for anti-beta-catenin IHC differed more significantly from the generic protocol, and this is described in section 2.4.2.

2.4.1.1 De-waxing and rehydration of tissue sections

Tissue sections were de-waxed by washing for 2 x 5 mins in Xylene (Fisher scientific). Sections were rehydrated by sequential washes in decreasing concentrations of alcohols; 2 x 2 mins in 100% ethanol (Fisher Scientific), 1 x 2 mins in 95% ethanol, 1 x 2 mins in 70% ethanol. Sections were then washed in dH_2O before continuing.

2.4.1.2 Retrieval of antigens

Antigens were retrieved by heat treatment in a boiling water bath or microwave in either citrate buffer (Labvision) or a custom made buffer (See section 2.4.2), as described in Table 2.3. For retrieval in a boiling water bath, adequate buffer was preheated to 99.9°C in a glass slide jar (e.g. Coplin jar [R. A. Lamb]) before slides were immersed in the solution. For microwave antigen retrieval, adequate buffer was preheated in a plastic container for 5 mins in a domestic microwave at high power (850W). Slides were then immersed in the hot solution in a plastic slide rack, and further heated at high power for 3 x 5 mins. Care was taken to ensure the slides did not boil dry, with additional buffer added as necessary.

Following heat treatment, slides were allowed to cool (in antigen retrieval buffer) at room temperature for at least 30 mins before continuing. Slides were then rinsed once in dH_2O and

once in wash buffer. Wash buffers used were either PBS (Gibco) or TBS/T (Tris buffered saline [Gibco] plus 0.1% TWEEN-20 [Sigma]) as detailed in Table 2.3.

2.4.1.3 Blocking of endogenous tissue peroxidase activity

Endogenous peroxidase activity of tissue sections was blocked by treatment with hydrogen peroxide. Hydrogen peroxide (30% aqueous solution, Sigma) was diluted in dH_2O just prior to use (appropriate concentrations detailed in Table 2.3), or Peroxidase block solution provided with the Envision+ Kit (Dako) was used. Slides were immersed in the solution for an appropriate amount of time, before being removed and washed once in dH_2O and once in wash buffer.

2.4.1.4 Serum blocking

Non-specific binding of antibodies was blocked by incubation with normal serum from the species in which the secondary antibody was raised (e.g. if the secondary antibody was goat anti-rabbit, goat normal serum was used). Normal serum was diluted in wash buffer as described in Table 2.3. Slides were dried around the tissue sections using tissue paper, and the tissue circled using a water-resistant wax pen (Dako). Normal serum was applied and slides incubated for the times indicated in Table 2.3. Following incubation, normal serum was removed from the slide, and primary antibody applied without washing of slides.

2.4.1.5 Primary antibody

Primary antibodies were used either at a concentration recommended by the manufacturer, or the optimal concentration of primary antibody was determined. Primary antibody was appropriately diluted before use (Table 2.3) in serum block solution. Antibody was added to slides, and incubated under appropriate conditions (Table 2.3).

After incubation, primary antibody was removed from the section, and sections washed 3 x 5 mins in wash buffer.

2.4.1.6 Secondary antibody

Secondary antibodies (Dako) were either diluted 1/200 in serum block, or Horseradish perosidase (HRP)-conjugated secondary antibody polymer from the Envision+ kit (Dako) was used undiluted. Secondary antibody was applied to the slides, which were then incubated for an appropriate amount of time (Table 2.3). Slides were then washed 3 x 5 mins in wash buffer.

2.4.1.7 Signal amplification

Where Envision+ kits (Dako) were not used, a signal amplification step was incorporated into the protocol. This was provided by formation of an Avidin-Biotin Complex (ABC) using the 'Vectastain' ABC kit (Vector Labs). ABC reagent was prepared 30 mins before use as described by the manufacturer, and was then kept at room temperature until needed. ABC reagent was then applied to slides for 30 mins, then slides were washed 3 x 5 mins in wash buffer.

2.4.1.8 Signal detection using 3,3'-diaminobenzidine (DAB)

The 3,3'-diaminobenzidine (DAB) method was used for colourimetric detection of signal. DAB substrate buffer and DAB chromogen from the DAB+ kit (Dako) were mixed in the ratio 1ml:1 drop before use. DAB solution was then applied to slides at room temperature, and sections were monitored for development of the colourimetric signal. In general, this took between 2 mins and 10 mins. Slides were then washed 2 x 5 mins in wash buffer and 2 x 5 mins in dH_2O.

2.4.1.9 Counterstaining, dehydration, clearing and coverslipping of sections

Sections were counterstained for 45 secs with Mayer's Haemalum (R. A. Lamb) followed by thorough washing in running tap water for 5 mins.

Sections were then dehydrated by washing in increasing concentrations of alcohols (1 x 1 min in 70% ethanol, 1 x 1 min in 95% ethanol 2 x 1 min in 100% ethanol) and cleared by washing in xylene (2 x 5 mins). Sections were then mounted and coverslipped in DPX mounting medium (R.A. Lamb).

2.4.2 Specific Immunohistochemistry protocols

2.4.2.1 Anti-beta-Catenin IHC

Slides were de-waxed and rehydrated as described in 2.4.1.1. Endogenous peroxidase activity was quenched by immersing slides in 1.5% hydrogen peroxide (Sigma) in peroxidase buffer (0.02M citric acid [Sigma], 0.06M disodium hydrogen phosphate-2-hydrate [Sigma], plus 0.1% [w/v] sodium azide [Sigma] in dH_2O). Slides were rinsed briefly in dH_2O before antigen retrieval which was achieved by immersing slides in a large volume (1.5L) of boiling custom Tris/Ethylenediamine-tetraacetic acid (EDTA) buffer (0.04M Tris [Sigma], 1mM EDTA [Sigma] in dH_2O, pH8.0) for 50 mins. Slides were then allowed to cool in the antigen retrieval buffer on the bench for 1 hour. After briefly rinsing in dH_2O and then in PBS, sections were circled with water repellent pen (as described in section 2.4.1.4) and 1% [w/v] Bovine Serum Albumin (BSA, fraction V, lyophilised [Sigma]) in PBS applied to each section. Slides were incubated at room temperature for 30 mins, after which the serum block was removed and replaced with anti-beta-catenin antibody diluted in serum block as described in Table 2.3. Slides were then washed 3 x 5 mins in

PBS. Secondary antibody was HRP-conjugated anti-mouse secondary from the mouse Envision+ kit (Dako) which was applied for 1 hour at room temperature. Slides were then washed 3 x 5 mins in PBS, before signal detection, counterstaining and mounting as described in sections 2.4.1.8 and 2.4.1.9.

Target	**Pten**	**beta-Catenin**	**Villin**	**Lysozyme**	**BrdU**	**Ki67**	**Caspase-3**	**pAkt (Ser473)**
Commercial source of primary Ab	Cell Signalling	Transduction Labs	Santa Cruz	Neomarkers	Becton Dickinson	Vector Labs	R&D Systems	Cell Signalling
Catalog/Clone Number	9559, Clone 138G6	610154	SC 7672	RB 372	N357580	VP K452	AF835	3787, clone 736L11
Primary Ab raised in	Rabbit (pAb)	Mouse (mAb)	Goat (pAb)	Rabbit (pAb)	Mouse (mAb)	Mouse (mAb)	Rabbit (pAb)	Rabbit (pAb)
Antigen retrieval	Boiling water bath, Citrate buffer (Labvision)	Boiling water bath, custom buffer	Boiling water bath, Citrate buffer (Labvision)	Boiling water bath, Citrate buffer (Labvision)	Boiling water bath, Citrate buffer (Labvision)	Boiling water bath, Citrate buffer (Labvision)	Boiling water bath, Citrate buffer (Labvision)	Boiling water bath, Citrate buffer (Labvision)
Peroxidase block	3% H2O2, 20mins	1.5% H2O2, 30mins	3% H2O2, 20mins	1.5% H2O2, 30mins	Envision+ Kit peroxidase block, 20mins	0.5% H2O2, 20mins	2% H2O2, 45secs	3% H2O2, 20mins
Serum block	5% NGS, 45mins	1% BSA, 30mins	10% NRS, 30mins	10% NGS, 30mins	1% BSA, 30mins	20% NRS, 20mins	10% NGS, 45mins	5% NGS, 45mins
Wash buffer	TBS/T	PBS	TBS/T	TBS/T	PBS	TBS/T	PBS	TBS/T
Conditions for primary Ab	1/100, o/n at 4°C	1/300, 2 hours at RT	1/500, 1 hr at RT	1/100, 1hr at RT	1/150, 1hr at RT	1/50, 1hr at RT	1/750, o/n at 4°C	1/50, o/n at 4°C
Secondary Ab	Biotinylated Goat anti-Rabbit (Dako)	HRP-conjugated anti-mouse (Envision+ Kit, Dako)	Biotinylated Rabbit anti-Goat (Dako)	HRP-conjugated anti-rabbit (Envision+ Kit, Dako)	HRP-conjugated anti-mouse (Envision+ Kit, Dako)	Biotinylated Rabbit anti-Mouse (Dako)	Biotinylated Goat anti-Rabbit (Dako)	Biotinylated Goat anti-Rabbit (Dako)
Conditions for secondary Ab	1/200, 30mins at RT	1hr at RT	1/200, 30mins at RT	30min at RT	1hr at RT	1/200, 30mins at RT	1/200, 30mins at RT	1/200, 30mins at RT
Signal amplification	ABC kit (Vector Labs)	N/A	ABC kit (Vector Labs)	N/A	N/A	ABC kit (Vector Labs)	ABC kit (Vector Labs)	ABC kit (Vector Labs)
Signal detection	DAB+ (Dako)	DAB+ (Dako)	DAB+ (Dako)	DAB+ (Dako)	DAB+ (Dako)	DAB+ (Dako)	DAB+ (Dako)	DAB+ (Dako)

Table 2.3, Part I: *Summary of IHC protocols*

Target	**pmTOR (Ser2448)**	**pMEK1/2 (Ser221)**	**pErk1/2 (Thr202/Tyr204)**	**pS6K (Thr421/Ser424)**	**E-Cadherin**	**pGSK3beta (Ser9)**	**Cytokeratin 19**	**DCAMKL-1**
Commercial source of primary Ab	Cell Signalling	Cell Signalling	Cell Signalling	Cell Signalling	Transduction Labs	Cell Signalling	Abcam	Abcam
Catalog/Clone Number	2971	2338	4376	9204	C20820	9336	ab15463	ab37994
Primary Ab raised in	Rabbit (pAb)	Rabbit (pAb)	Rabbit (pAb)	Rabbit (pAb)	Mouse (mAb)	Rabbit (pAb)	Rabbit (pAb)	Rabbit pAb
Antigen retrieval	Microwave, Citrate Buffer (Labvision)	Microwave, Citrate Buffer (Labvision)	Microwave, Citrate Buffer (Labvision)	Microwave, Citrate Buffer (Labvision)	Microwave, Citrate Buffer (Labvision)	Microwave, Citrate Buffer (Labvision)	Microwave, Citrate Buffer (Labvision)	Microwave, Citrate Buffer (Labvision)
Peroxidase block	3% H2O2, 20mins	1.5% H2O2, 15mins	1.5% H2O2, 15mins	3% H2O2, 20mins	0.5% H2O2, 20mins	1.5% H2O2, 30mins	0.3% H2O2, 20mins	0.3% H2O2, 20mins
Serum block	10% NGS, 45mins	10% NGS, 45mins	10% NGS, 45mins	10% NGS, 45mins	20% NRS, 20mins	10% NGS, 45mins	5% NGS, 10mins	10% NGS, 45mins
Wash buffer	TBS/T	TBS/T	TBS/T	TBS/T	TBS/T	TBS/T	PBS/T	TBS/T
Conditions for primary Ab	1/100, o/n at 4°C	1/100, o/n at 4°C	1/75, o/n at 4°C	1/100, 2hrs at RT	1/100, o/n at 4°C	1/50, o/n at 4°C	1/100, o/n at 4°C	1/100, o/n at 4°C
Secondary Ab	Biotinylated Goat anti-Rabbit (Dako)	Biotinylated Goat anti-Rabbit (Dako)	Biotinylated Goat anti-Rabbit (Dako)	Biotinylated Goat anti-Rabbit (Dako)	Biotinylated Rabbit anti-Mouse (Dako)	Biotinylated Goat anti-Rabbit (Dako)	Biotinylated Goat anti-Rabbit (Dako)	Biotinylated Goat anti-Rabbit (Dako)
Conditions for secondary Ab	1/200, 30mins at RT	1/200, 30mins at RT	1/200, 30mins at RT	1/200, 30mins at RT	1/200, 30mins at RT	1/200, 30mins at RT	1/200, 30mins at RT	1/200, 30mins at RT
Signal amplification	ABC kit (Vector Labs)	ABC kit (Vector Labs)	ABC kit (Vector Labs)	ABC kit (Vector Labs)	ABC kit (Vector Labs)	ABC kit (Vector Labs)	ABC kit (Vector Labs)	ABC kit (Vector Labs)
Signal detection	DAB+ (Dako)	DAB+ (Dako)	DAB+ (Dako)	DAB+ (Dako)	DAB+ (Dako)	DAB+ (Dako)	DAB+ (Dako)	DAB+ (Dako)

Table 2.3, Part II: *Summary of IHC protocols*

2.5 Protein Analysis

2.5.1 Protein extraction from tissue samples

2.5.1.1 Preparation of whole tissues

Whole tissue samples in eppendorf tubes (see section 2.2.5.1) were removed from storage at -80°C and placed on dry ice. A pestle and mortar were then pre-cooled using LN_2. Tissue samples were removed one at a time, placed in the mortar and immersed in LN_2. Before the LN_2 completely evaporated, the tissue was crushed using the pestle, and more LN_2 added. This process was repeated until a fine powder was produced. Before the tissue defrosted, 200µl cell lysis buffer (20mM Tris-HCl pH 8.0, 2mM EDTA pH8.0, 0.5% [v/v] NP-40 [Sigma]) containing protease inhibitors (Complete mini protease inhibitor tablets [Roche]) and phosphatase inhibitors (25mM sodium beta-glycerophosphate [Calbiochem], 100mM sodium fluoride [Sigma], 20nM Calyculin A from *Discodermia calyx* [Sigma], 10mM sodium pyrophosphate [Sigma]) was added. The sample was allowed to warm up sufficiently for the tissue and lysis buffer to defrost, and this mixture was then removed to a clean eppendorf tube and kept on ice until proteins were extracted as described below (section 2.5.1.3). This process was repeated for all samples.

2.5.1.2 Preparation of epithelial cell extracts

Epithelial cell extract samples (prepared as described in section 2.2.7.3 and section 2.2.7.5) were removed from storage at -80°C and placed on ice. To each pellet, 200µl cell lysis buffer containing protease and phosphatase inhibitors (described in section 2.5.1.1) was added immediately, and pellets allowed to slowly defrost in the buffer with occasional pipetting to mix. Samples were then removed into clean eppendorf tubes and kept on ice until protein extraction (Section 2.5.1.3).

2.5.1.3 Extraction of proteins

In order to shear cells, samples were passed through a 23 gauge needle using a syringe at least 20 times. Tubes were then centrifuged at 9500 x g for 10 mins at 4°C to remove insoluble material. The supernatant (protein extract) was then removed to a clean tube, divided into aliquots and snap frozen in LN_2.

2.5.2 Quantification of proteins

2.5.2.1 Bradford Assay

Relative amounts of protein in each protein extract were assayed using the Bradford method (Bradford, 1976). Bradford reagent (Sigma) was diluted 1/5 in ultrapure water (ddH_2O) before use and 1ml of diluted Bradford reagent was used per assay. To each 1ml of diluted Bradford reagent, 1µl of protein extract was added, or 1µl cell lysis buffer was added to use as a blank. A standard curve was also generated by adding standard 2mg/ml BSA (Pierce) in varying volumes to 1ml diluted Bradford reagent to generate standards containing known concentrations (20, 10, 5, 2.5 and 1.25µg/ml) of protein. Samples were mixed well and the blue colour allowed to develop by incubating for at least 5 mins on the bench. Colour intensity of each sample was then read at 595nm on a colourimeter. The standard curve was then used to extrapolate the relative concentration of protein in each experimental sample.

2.5.3 Western Analysis

2.5.3.1 Preparation of protein samples for western analysis

Samples were removed from storage at -80°C, defrosted on ice and appropriate volumes removed to a clean eppendorf tube. For intestinal protein extracts, 30µg of total protein was prepared for loading. Samples were made up to 25µl using Laemmli buffer (0.125M Tris-HCl pH6.8, 4% [w/v] sodium dodecyl sulphate [SDS, Sigma], 40% [v/v] Glycerol [Sigma], 0.1% [w/v] Bromophenol blue [Sigma], 6% [v/v] beta-mercaptoethanol [Sigma] in ddH_2O). Just before loading, samples were heated to 95°C for 5-10 mins to denature proteins, and then quenched on ice.

2.5.3.2 Casting of polyacrylamide gels

Mini-Protean III (Bio-Rad) gel casting apparatus was used to prepare thick (1.5mm) polyacrylamide gels. Mixtures for 5% stacking and 10% resolving acrylamide gels were prepared in advance according to Table 2.4, but without addition of TEMED. Casting plates were cleaned thoroughly in water and 70% ethanol before being assembled. TEMED was then added to the 10% resolving gel mix, and the gel poured to a level of approximately 1.5cm from the top of the gel. This was then overlaid with 500µl ultrapure water. Once the gel had set (approximately 30 mins), the water overlay was poured off onto tissue paper. TEMED was then added to the 5% stacking gel mix and this was poured over the 10% gel and a 10-well comb inserted into the apparatus. Once set, the gels were removed from the casting apparatus, combs removed and the wells rinsed with ddH_2O.

2.5.3.3 Protein separation by SDS-PAGE

Gels were assembled in the Mini-Protean III (Bio-Rad) electrophoresis tank and adequate 1X tris-glycine SDS-PAGE running buffer (See Table 2.4) added. Prepared protein samples were then loaded into wells, along with two molecular weight markers – full-range Rainbow molecular weight marker (Amersham) and broad-range pre-stained molecular weight marker (New England Biolabs) according to the manufacturer's instructions. Gels were then run at 120-200V until the dye front was seen to reach the end of the gel.

2.5.3.4 Transfer of proteins to PVDF membrane

Gels were taken from the electrophoresis tank, separated from the glass plates and placed into Tris-glycine transfer buffer (See Table 2.4). Hybond-P polyvinylidene difluoride (PVDF) membrane (Amersham) was prepared before use by soaking in methanol for 30secs then dH_2O for 1min before being equilibrated in Tris-glycine running buffer. Blots were then assembled layer-by-layer in a wet electroblotting system (Flowgen biosciences) as shown in Figure 2.1, with careful rolling out of air bubbles after the addition of each layer. The blotting tank was then packed in ice and run at 100V for 1 hour. Blotting apparatus was then dismantled, and blots washed briefly in TBS/T wash buffer before being blocked for non-specific binding of antibodies (See section 2.5.3.5).

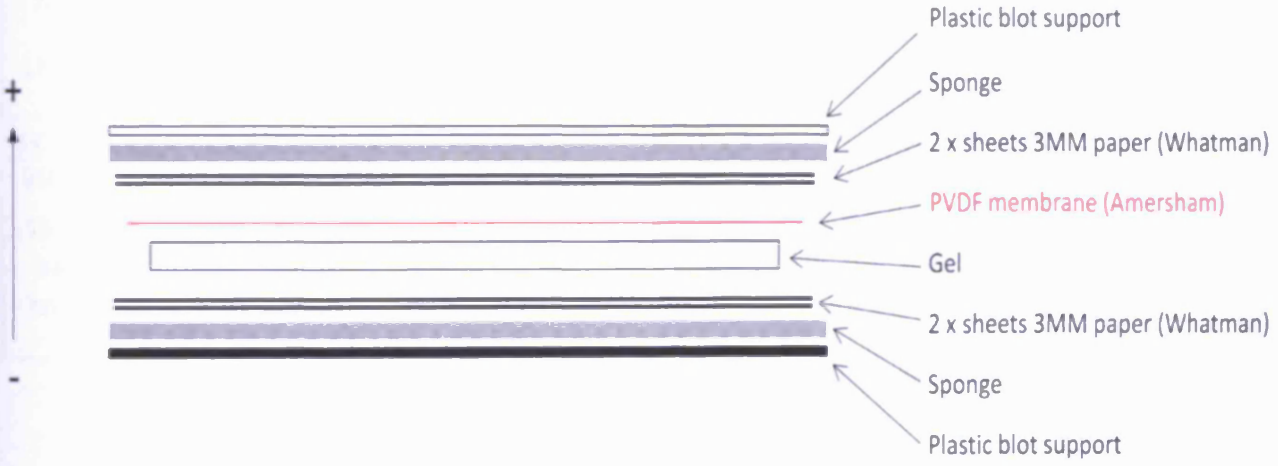

Figure 2.1: ***Blotting apparatus set-up for Western Analysis***

2.5.3.5 Generic protocol for probing of membranes

To block non-specific binding, blots were incubated in a large excess of blocking agent (either 5% BSA or 5% non-fat milk powder, see table 2.5 for details) diluted in TBS/T with agitation under the conditions described in Table 2.5. Primary antibody was diluted and applied to membranes with agitation as described in Table 2.5. Blots were then washed 3 x 10 mins in TBS/T. Secondary antibody was diluted in blocking solution and applied to membranes with agitation as described in Table 2.5. Blots were then washed again for 3 x 10 mins in TBS/T. Blots were then

developed using appropriate ECL reagent kit (Amersham) according to manufacturer's instructions and as described in Table 2.5. Blots were then wrapped in cling film before immediate signal detection.

2.5.3.5 Detection of signal

Chemifluorescent signal was detected by autoradiograph exposure. Under safelight conditions, X-ray film (FujiFilm Super RX blue background) was exposed to the blot for varying amounts of time in order to generate clear images. Film was then processed on an automatic film processor (Xograph Compact X4 automatic X-ray film processor). Processed films were then aligned with the original blot to identify the position of molecular weight markers and allow identification of the target protein.

10% Polyacrylamide Gel mix (2 gels)		**5% Polyacrylamide Gel mix (2 gels)**	
6.8ml	Ultrapure (dd) H_2O	6.9ml	Ultrapure (dd) H_2O
8.4ml	30% Acrylamide/bisacrylamide (Sigma)	1.7ml	30% Acrylamide/bisacrylamide (Sigma)
9.4ml	1M Tris-HCl pH8.8	1.3ml	1M Tris-HCl pH6.8
250µl	10% [w/v] Sodium dodecyl sulphate (SDS, Sigma)	100µl	10% [w/v] Sodium dodecyl sulphate (SDS, Sigma)
72µl	25% [w/v] Ammonium persulphate (Sigma)	66µl	25% [w/v] Ammonium persulphate (Sigma)
13.2µl	N,N,N',N'-Tetramethylethylenediamine (TEMED, Sigma)	13.2µl	N,N,N',N'-Tetramethylethylenediamine (TEMED, Sigma)
5X Tris-Glycine SDS-PAGE Running Buffer (1L)		**1X Tris-Glycine Transfer Buffer (1L)**	
950ml	dH_2O	800ml	dH_2O
15.1g	Tris base (Sigma)	200ml	Methanol (Fisher scientific)
94g	Glycine (Sigma)	2.9g	Tris base (Sigma)
50ml	10% [w/v] Sodium dodecyl sulphate (SDS, Sigma)	14.5g	Glycine (Sigma)

Table 2.4: *Western blotting gel and buffer compositions*

Target	Pten	Pten	Akt (Total)	pAkt (Thr308)	pAkt (Ser473)	beta-Actin
Commercial source of Primary Antibody	Labvision/Neomarkers	Cell Signaling	Cell Signaling	Cell Signaling	Cell Signaling	Sigma
Raised in	Rabbit	Rabbit	Rabbit	Rabbit	Rabbit	Mouse
Catalog Number	RB-072; Ab-2	9559	9272	9271	9275	A5316; Clone AC-74
Blocking Solution/conditions	10% TTM o/n at 4°C	5% TTM for 2 hrs at RT	5% TTM for 2 hrs at RT	5% TTM for 2 hrs at RT	5% TTM for 2 hrs at RT	5% TTM for 2 hrs at RT
Primary Antibody conditions	1/500 in 10% TTM, 1 hr at RT	1/1000 in 5% BSA/TBST, O/N at 4°C	1/1000 in 5% BSA/TBST, O/N at 4°C	1/1000 in 5% BSA/TBST, O/N at 4°C	1/1000 in 5% BSA/TBST, O/N at 4°C	1/5000 in 5% TTM, 1 hr at RT
Secondary Antibody	HRP-conjugated anti-Rabbit	HRP-conjugated anti-Rabbit	HRP-conjugated anti-Rabbit	HRP-conjugated anti-Rabbit	HRP-conjugated anti-Rabbit	HRP-conjugated anti-Mouse
Secondary Antibody Conditions	1/2000 in 10% TTM, 1hr at RT	1/2000 in 5% TTM, 1hr at RT	1/2000 in 5% TTM, 1hr at RT	1/2000 in 5% TTM, 1hr at RT	1/2000 in 5% TTM, 1hr at RT	1/5000 in 5% TTM, 1 hr at RT
Commercial source of Secondary Antibody	GE Healthcare	GE Healthcare	GE Healthcare	GE Healthcare	GE Healthcare	GE Healthcare
Detection reagents	ECL	ECL plus	ECL plus	ECL advance	ECL advance	ECL

Table 2.5: Summary of *Antibodies and Protocols used for Western analysis*

2.6 Gene Expression analysis

2.6.1 Isolation of RNA

Care was taken during RNA isolation to ensure that all glass and plastic-ware used was RNase-free. All solutions used were made using Diethyl pyrocarbonate (DEPC, Sigma)-treated water, RNase-free water (Sigma) or other solutions known to be RNase-free. Bench tops and pipettes were treated with RNaseZAP (Sigma) before use. Sterile, filtered pipette tips were used throughout.

2.6.1.1 Homogenisation of whole tissues and epithelial cell extracts

Whole tissues were removed from storage in RNA*later* (Sigma) and placed in 1ml Trizol reagent (Invitrogen). Epithelial cell extracts previously resuspended and frozen in 1ml Trizol (Invitrogen) were defrosted. Samples in Trizol were then transferred into screw-cap tubes containing 1.4mm ceramic beads (Lysing Matrix D tubes, MP Biomedical). Tissue samples were then homogenised by agitating the tubes in the Precellys 24 homogeniser (Bertin Technologies) at 6000RPM for 2 cycles of 25 seconds. Tubes were then centrifuged at 9500 x g for 10 mins at 4°C to pellet cell debris and the ceramic beads.

2.6.1.2 Crude extraction of total RNA

Supernatants were removed into clean 1.5ml eppendorf tubes, 200µl ice cold chloroform (Fisher scientific) added to each and tubes shaken well. Tubes were then centrifuged at 9500 x g at 4°C for 15 mins. Supernatants were removed into clean 2ml eppendorf tubes and 600µl ice cold isopropanol (Sigma) added to each. Tubes were shaken well and incubated at 4°C overnight to precipitate RNA. Tubes were then centrifuged at 9500 x g at 4°C for 15 mins to pellet RNA. The supernatant was carefully aspirated from the pellet. Pellets were washed once by adding 500µl ice cold 75% ethanol, and were then centrifuged again (9500 x g at 4°C for 15 mins), ethanol carefully aspirated and pellets left to air dry at room temperature for 5-10 mins. Pellets were then re-dissolved in 100µl RNase-free water (Sigma) with gentle heating (65°C) if necessary. Concentration and quality of RNA was quantified on the NanoDrop 1000 (Thermo Scientific).

2.6.1.3 Purification of RNA

Purification of RNA was achieved using the RNeasy mini kit (Qiagen). 100µg RNA was used for purification, and the kit was used according to the manufacturer's instructions. RNA was eluted in two 30µl aliquots of RNase-free water (Qiagen), and concentration and quality of RNA re-checked on the NanoDrop 1000 (Thermo Scientific).

2.6.1.4 Visual assessment of RNA quality

Quality of RNA was checked visually using a denaturing agarose gel (1.5% [w/v] Agarose (Eurogentech), 0.02M 3-(N-Morpholino)propanesulfonic acid [MOPS, Sigma], 5mM Sodium acetate [Sigma] 1mM EDTA [Sigma] 1% [v/v] Formaldehyde [Sigma], 0.003% [v/v] Ethidium bromide [Sigma] in DEPC-treated dH_2O). 1µl 4X RNA loading buffer (0.1% [w/v] Bromophenol blue [Sigma], 20% [v/v] Glycerol [Sigma], 30% [v/v] Formamide [Sigma], 3% [v/v] Formaldehyde [Sigma], 0.08M MOPS [Sigma], 0.02M Sodium acetate, 8mM EDTA [Sigma] in DEPC-treated dH_2O) was added to 3µl aliquots of each sample, and samples were heated to 60°C for 10 mins and then quenched on ice before being loaded onto the gel. The gel was then run in MOPS buffer (0.02M MOPS [Sigma], 5mM Sodium acetate [Sigma], 1mM EDTA [Sigma] in DEPC-treated dH_2O) at 120V for 30 mins.

2.6.2 Preparation of cDNA for quantitative PCR analysis

2.6.2.1 DNase treatment of RNA samples

Purified RNA samples were treated with DNase to remove any remaining contaminating DNA. 5µg samples of RNA were treated with RQ1 DNase (Promega) according to the manufacturer's instructions.

2.6.2.2 Reverse transcription

cDNA was synthesised from 1µg samples of purified, DNase-treated RNA. Reverse transcription was performed using the Superscript II RNase-H reverse transcriptase kit according to the manufacturer's instructions. Additional reagents used but not provided in the kit were dNTP mix (1mM dATP, dCTP, dGTP, dTTP per reaction [Bioline]) and Random Hexamers (20ng/µl per reaction [Invitrogen]). Controls were also prepared in exactly the same way but excluding the reverse transcriptase enzyme, to give control samples devoid of cDNA.

2.6.3 Quantitative, Real-time (qRT) PCR analysis

2.6.3.1 Design of qRT PCR primer sets

Primer sets for qRT-PCR reactions were designed such that the resulting product was in the 100-120bp size range, and where possible, primers were designed across exon boundaries. Primers were designed using the Primer3 web-based program (http://frodo.wi.mit.edu/cgi-bin/primer3/primer3_www.cgi) and primer sequences checked for mis-priming by performing *in silico* PCR (http://genome.cse.ucsc.edu/cgi-bin/hgPcr?command=start). Primers were then synthesised by Sigma-Genosys. Primer sequences used can be found in Table 2.6.

Target	Forward Primer Sequence (5' to 3')	Reverse Primer Sequence (5' to 3')
Pten	AGA CCA TAA CCC ACC ACA GC	CGT CCC TTT CCA GCT TTA CA
SHIP	TTG GAA CAT GGG TAA TGC AC	ATG GGG GAT GTA GTC AGC AG
Akt1	CTG AGG AGC GGG AAG AAT G	TGA GTT GTC ACT GGG TGA GC
Akt2	TCC ACA AAC GTG GTG AAT ACA TC	GGG GTA AGG TCT GGT CAG G
Akt3	TTC AGA AGA GGG GAG AAT ATA TAA AA	TCC ACA TCT TGA GGT TTC TCC T
TSC1	AAG AAA CCA GGC CAT GTG AC	CGC AGG AAG GAG ACG AAG T
TSC2	TGG AGG ACA GAT CCT ACA TGG	TTG AGA GAG TAG AGC CGG TGA
mTOR	GCA CAT TGA CTT TGG GGA CT	GAC CCG TAA CCT CCA TAG CA
eIF4E-BP1	CCG GGA GGA ACC AGG ATT AT	CAG GAA TGG CTG GCA GGT
Axin-2	GCT CCA GAA GAT CAC AAA GAG C	AGC TTT GAG CCT TCA GCA TC
CyclinD2	GGG ATC CCT GTA CAC TCG AA	TTG CAG GTA CGC ACA CTC TC
c-Myc	TGA GCC CCT AGT GCT GCA T	AGC CCG ACT CCG ACC TCT T
CD44	GGC AGA AGA AAA AGC TGG TG	TCT GGG GTC TCT GAT GGT TC
Musashi-1	GAT GCC TTC ATG CTG GGT AT	TAG GTG TAA CCA GGG GCA AG
Bmi1	CCC CAC TTA ATG TGT GTC CTG	TTG CTG GTC TCC AAG TAA CG
Lgr5	CCT TGG CCC TGA ACA AAA TA	ATT TCT TTC CCA GGG AGT GG
Beta-Actin	ACA GCT TCT TTG CAG CTC CTT	TGG TAA CAA TGC CAT GTT CAA T

Table 2.6: Primer sequences used for Q-PCR analysis

2.6.3.2 Running of qRT PCR reactions

All qRT PCR reactions were calibrated and run on the PTC-200 Peltier thermal cycler fitted with a Chromo4 continuous fluorescence detector (both MJ Research), in conjunction with Opticon Monitor (Version 2.03, MJ Research) software. Each reaction was performed in duplicate, and a minimum of biological triplicate (i.e. 3 mice of each genotype were compared). In addition to this, control samples devoid of cDNA (described in section 2.6.2.2) were run to ensure no contaminants were present in cDNA samples. On each plate, a reaction targeting at least one housekeeping gene (usually beta-actin) was run as a reference.

Master mixes were prepared containing DyNAmo Hot-Start (HS) SYBR green supermix (Finnzymes, supplied by GRI) as described by the manufacturer and 0.1µg cDNA (see section 2.6.2.2). All reactions were made up to a final reaction volume of 25µl using PCR-grade sterile water (Sigma).

Forward and reverse primers were mixed in equal quantities, and loaded onto a white, thin-wall, 96-well PCR plate (Abgene) such that the final concentration of primers in each reaction was 1µM. Master mix was then loaded onto the plate, and the plate sealed with optically clear sealing tape (GRI).

All reactions were run under the same cycling conditions (Initial denaturation at 95°C for 15 mins followed by 40 cycles of [95°C for 30 secs; 57°C for 30 secs; 72°C for 30 secs] with the

plate read after each cycle), a melting curve was constructed at the end of the reaction, and data collected automatically by the Opticon monitor package (MJ Research).

2.6.3.3 Analysis of qRT PCR data

Data was initially visually examined using Opticon monitor software (MJ Research). It was confirmed that all reactions devoid of cDNA were free of any product. Melting curves were also briefly examined, to confirm that each reaction yielded only one product, that this product was of the expected melting temperature, and that the formation of primer dimers was minimal.

Data was then analysed using the $2^{-\Delta\Delta C}{}_T$ method (Livak and Schmittgen, 2001). Cycle time (C_T) for each reaction was recorded, and duplicates averaged. The difference in Ct (ΔC_T) between samples amplified for a target gene of interest and corresponding samples amplifying a reference gene was then calculated. The average ΔC_T across all biological replicates (i.e. samples of the same genotype) was then taken, and $\Delta\Delta C_T$ calculated as the difference in ΔC_T average between genotypes. Fold change was then calculated according to the formula $2^{-\Delta\Delta C}{}_T$.

2.6.4 PCR analysis of genomic recombination

2.6.4.1 Preparation of DNA from tissue samples

DNA isolation from whole tissue samples, epithelial cell extracts or gut scrapes was performed exactly as described for tail tip biopsies in sections 2.1.4.1 and 2.1.4.2.

2.6.4.2 Pten recombined PCR

Primer sequences for Pten recombined-specific PCR were provided by Akira Suzuki, Akita University, Japan. Reactions were set up as described for PCR genotyping reactions (Section 2.1.4.3). Composition of the reaction mixture, cycling conditions and primer sequences are described in Table 2.7. Product sizes and approximate locations are shown schematically in Figure 2.2.

2.6.4.3 Apc recombined PCR

Primers used for detection of recombination of the Apc allele have been previously published (Shibata et al., 1997). Reactions were set up as described for PCR genotyping reactions (Section 2.1.4.3). Composition of the reaction mixture, cycling conditions and primer sequences are described in Table 2.7. Product sizes and approximate locations are shown schematically in Figure 2.2.

2.6.4.4 k-Ras recombined PCR

Primers used to detect recombination in the mutant k-Ras transgene were previously published (Guerra et al., 2003). Reactions were set up as described for PCR genotyping reactions (Section 2.1.4.3). Composition of the reaction mixture, cycling conditions and primer sequences are described in Table 2.7. Product sizes and approximate locations are shown schematically in Figure 2.2.

	Pten Recombined	Apc Recombined	k-Ras Recombined
PCR Reaction components:			
Crude DNA Extract	3µl	2.5µl	3µl
Master Mix:			
PCR-grade Water (Sigma)	31.1µl	31.4µl	31.1µl
GO Taq PCR Buffer (5X; Promega)	10µl	10µl	10µl
Magnesium Chloride (25mM)	5µl	5µl	5µl
dNTPs (25mM; dATP, dCTP, dGTP, dTTP)	0.4µl	0.4µl	0.4µl
Primer 1 (Sigma Genosys, 100mM)	0.1µl	0.1µl	0.1µl
Primer 2 (Sigma Genosys, 100mM)	0.1µl	0.1µl	0.1µl
Primer 3 (Sigma Genosys, 100mM)	0.1µl	N/A	0.1µl
Taq DNA polymerase	0.2µl, Go taq	0.2µl, Go Taq	0.2µl, Go Taq
Total Reaction Volume:	50µl	50µl	50µl
Cycling conditions:			
Initial denaturation step (Time; Temp)	2min 30sec; 94°C	3min; 95°C	5 min; 94°C
Step 1: Denaturation (Time; Temp)	30 secs; 94°C	30sec; 95°C	1 min; 94°C
Step 2: Annealing (Time; Temp)	30 secs; 63°C	30sec; 60°C	1 min; 60°C
Step 3: Extension (Time; Temp)	1min; 72°C	1min; 72°C	1 min; 72°C
Number of Cycles	30	30	30
Final Extension (Time; Temp)	10 min; 72°C	5min; 72°C	10 min; 72°C
Hold (Time; Temp)	∞; 15°C	∞; 15°C	∞; 15°C
Primer Sequences	1F 5'-GGCCTAGGACTCACTAGATAGC-3'	P3 5'-GTTCTGTATCATGGAAAGATAGGTGGTC-3'	5I0 5'-AGGGTAGGTGTTGGGATAGC-3'
	2R 5'-CTCCCACCAATGAACAAACAGT-3'	P4 5'-CACTCAAAACGCTTTTGAGGGTTGATTC-3'	3Ex1 5'-CTCAGTCATTTTCAGCAGGC-3'
	3F 5'-GTGAAAGTGCCCCAACATAAGG-3'	P5 5'-GAGTACGGGGTCTCTCTGTCTCAGTGAA-3'	103rev 5'-CTGCTCTTTACTGAAGGCTC-3'

Table2.7: *Recombined PCR conditions and primer sequences*

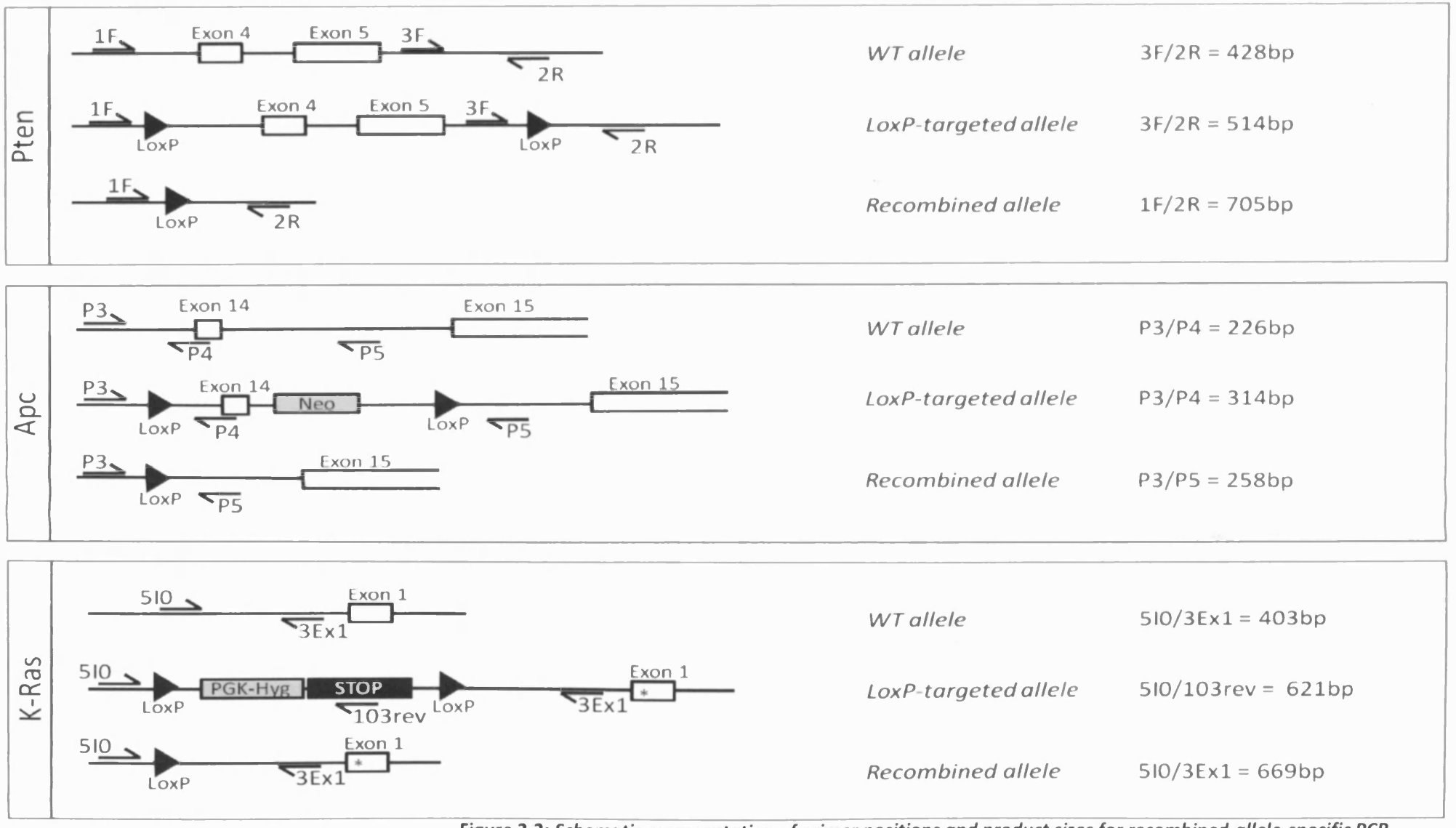

Figure 2.2: ***Schematic representation of primer positions and product sizes for recombined-allele-specific PCR***

2.7 Statistical Analyses

2.7.1 Kaplan-Meier survival analysis

Survival curves and statistical analysis of survival times was performed using the Kaplan-Meier method. All analyses were performed with the aid of MedCalc statistical analysis software (Version 9.3.0.0, Available from http://www.medcalc.be).

2.7.2 Mann-Whitney-U Test

The Mann-Whitney-U Test was used to show statistical differences between non-parametric data sets. Mann-Whitney-U analysis was performed using the Minitab statistics package (Version 14.20). A significant difference between data sets was accepted if p values were less than 0.01.

2.7.3 Kolmogorov-Smirnov Analysis

Differences in distribution of data within a non-parametric data set were tested for using the Kolmogorov-Smirnov approach. This was performed exactly as described in *Biometry: The Principles and Practise of Statistics in Biological Research* (Sokal, 1981).

Chapter 3: Analysing the short-term effects of AhCre-driven Pten deficiency in the intestinal epithelium

3.1 Introduction

PTEN is a potent tumour suppressor, identified based on the fact that it is found to be inactivated in human sporadic cancers of varying origins (Steck et al., 1997, Li and Sun, 1997, Li et al., 1997). Germline mutation of *PTEN* results in a number of cancer-predisposition disorders, known as the PTEN hamartoma tumour syndromes (PHTS), a feature of which is the development of intestinal lesions (Carlson et al., 1984, Merg and Howe, 2004).

PTEN functions as a negative regulator of the PI3K/Akt pathway (Maehama and Dixon, 1998), which normally functions to promote proliferation and cell survival. Activating mutations within PI3K/Akt pathway components are common in cancers, and have been shown to be present in up to 40% of all human colorectal malignancies (Parsons et al., 2005).

Given its close link with human disease, *in vivo* study of Pten function has been the subject of much attention. Murine studies of constitutive *Pten* deficiency have indicated that complete deletion of *Pten* is incompatible with life (Di Cristofano et al., 1998, Podsypanina et al., 1999, Suzuki et al., 1998), whilst heterozygous loss of *Pten* models some of the features associated with PHTS in humans, including predisposition to hamartoma of the gastrointestinal tract. Notably, *Di Cristofano and colleagues* report the development of invasive adenocarcinoma in the colon of Pten heterozygous animals.

Previous work has indicated that inactivation of Pten by phosphorylation is a feature of the elusive intestinal stem cell (ISC) (He et al., 2004). *He et al.* propose that, in the ISC, Pten may function to arbitrate the interaction between the BMP and Wnt pathways by mediating levels of activated (phosphorylated) Akt. Inactivation of Pten specifically in the stem cell is therefore proposed to promote Wnt signalling activity, which in turn enhances stem cell replication. However, this notion has been the subject of some debate (Bjerknes and Cheng, 2005b).

In a further study, *He et al.* have examined the effect of conditional Pten deletion in the adult intestine (He et al., 2007). By using the *Mx1* inducible promoter to drive Cre expression, *He et al.* have achieved deletion of Pten from both the epithelial and stromal cell compartments in the intestine. Following loss of Pten, they report proliferation of Pten-deficient ISCs, which leads to crypt fission and the rapid development of hamartomatous polyps within the intestine.

Thus, from studies published in the literature it would appear that Pten functions as a potent tumour suppressor within the intestine, though the specific role of Pten exclusively in the epithelial cell layer has not been thoroughly examined.

In this chapter, I aimed to characterise the effects of Pten deletion specifically from the epithelial cell compartment in the adult mouse small intestine. The experimental approach employed to achieve this was that of conditional transgenesis, involving LoxP-targeted *Pten* alleles (Suzuki et al., 2001) together with the inducible AhCre transgene. The Cre-expressing AhCre transgene has previously been used to drive Cre expression specifically and efficiently within epithelial cells of the intestine (Ireland et al., 2004). The effects of epithelial-specific *Pten* deletion both on epithelial homeostasis and on the intestinal stem cell will be characterised.

3.2 Results

3.2.1 AhCre drives recombination in the intestine with high efficiency

In order to examine the role of Pten specifically in the intestinal epithelium, animals bearing the AhCre transgene were crossed to animals bearing LoxP-targeted Pten alleles. This generated animals of an experimental genotype (AhCre^{+};Pten$^{fl/fl}$, referred to throughout this chapter as 'Pten$^{-/-}$') and appropriate controls (AhCre^{+};Pten$^{+/+}$, AhCre^{+};Pten$^{fl/+}$, AhCre^{-};Pten$^{fl/fl}$, AhCre^{-};Pten$^{+/+}$, referred to here as 'controls').

Previous reports have indicated that AhCre drives recombination efficiently in the murine small intestinal epithelium following a treatment regime of 4 consecutive daily intraperitoneal injections of beta-naphthoflavone at a dose of 80mg/kg (Ireland et al., 2004). In order to confirm this was the case in the strain of mice I was using, mice were bred onto a background bearing the ROSA26R LacZ reporter transgene (Soriano, 1999). This reporter construct consists of the LacZ (beta-galactosidase) transgene, containing a LoxP-flanked STOP cassette. In unrecombined cells, the STOP cassette prevents expression of the LacZ transgene. Upon expression of Cre in the cell, the STOP cassette is excised from the transgene, allowing expression of LacZ. Exposure of cells expressing LacZ to X-Gal substrate results in a colourimetric change from colourless to blue, thus allowing identification of cells expressing Cre recombinase (See Figure 3.1A).

Control and Pten$^{-/-}$ animals bearing the LacZ reporter construct (LacZ^{+}), and those lacking the reporter construct (LacZ^{-}) were induced as described above. At day 5 post-induction (PI), animals were culled, intestines prepared as wholemounts, and exposed to X-Gal substrate. As expected, intestines from AhCre^{+}LacZ^{+} animals stained blue, showing a near-100% recombination frequency as previously reported (Ireland et al., 2004). No difference was observed between animals wild-type for Pten and those bearing the LoxP-flanked Pten alleles (Figure 3.1B, i and ii respectively), indicating that Pten status does not affect recombination levels. Intestines from animals not bearing the LacZ transgene were found to be completely negative for any blue staining (Figure 3.1B, iii), confirming that beta-galactosidase activity is not endogenous to the murine intestine. In order to confirm that the intestinal epithelium is repopulated from recombined cells (and thus indicating that recombination occurs within the stem cell population), intestines from AhCre^{+};LacZ^{+};Pten$^{fl/fl}$ animals at over 100 days PI were stained with X-gal substrate. These intestines were found to stain equally as well as those at day 5 PI (Figure 3.1B, iv), indicating that Pten deficiency is tolerated in the epithelium, and that the epithelium is not repopulated from unrecombined cells.

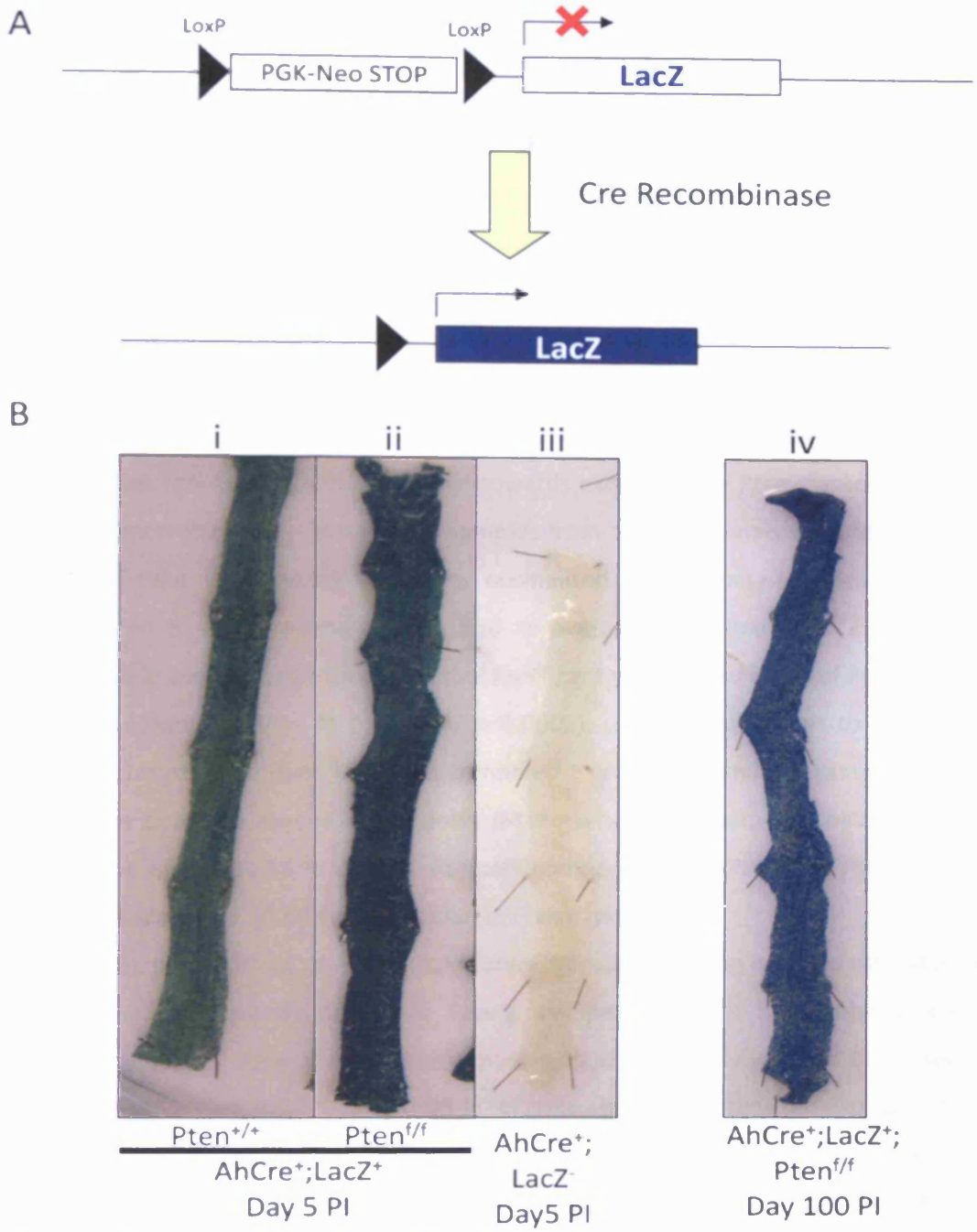

Figure 3.1: ***Use of the ROSA26R LacZ reporter to indicate recombination in the intestine***
The ROSA26R transgene was used to report recombination within the intestine (A). LoxP sites flank a PGK-Neo-STOP cassette inserted in the LacZ transgene. Following exposure to Cre recombinase, the PGK-Neo-STOP cassette is excised, allowing expression of beta-galactosidase from the LacZ transgene. Cells expressing beta-galactosidase can be detected by exposure to X-Gal substrate , which results in a colourimetric change from colourless to blue. Treatment of mice with 4 consecutive daily doses of 80mg/kg beta-naphthoflavone results in near-100% recombination of the intestinal epithelium, as indicated by X-Gal staining of wholemount intestines (B). Recombination levels are independent of Pten status, as AhCre$^+$;LacZ$^+$;Pten$^{+/+}$ intestines (i) stain identically to AhCre$^+$;LacZ$^+$;Pten$^{f/f}$ intestines (ii) at day 5 PI. Absence of the LacZ transgene results in no staining (iii). LacZ staining persists at over 100 days pi (iv), indicating that Pten deficiency is tolerated and that the epithelium is repopulated from recombined cells.

3.2.2 Recombination results in loss of Pten transcript and protein from the intestinal epithelium

Having confirmed that induction of Cre activity results in efficient recombination within the intestinal epithelium, I next examined the resulting effect upon levels of *Pten* transcript and of Pten protein within the epithelium of $Pten^{f/f}$ animals.

As recombination occurs only within the epithelial cell layer of the intestine, this first involved developing a protocol to generate samples enriched for epithelial cells, which could be used for both gene expression analysis and protein analysis. A protocol based on that of *Bjerknes and Cheng* (1981) was developed[1] (see Section 2.2.7). This allowed removal of the epithelial layer into suspension, whilst remaining intestinal tissue, including stromal cells and smooth muscle, could be discarded (Figure 3.2A i and ii).

cDNA produced from RNA extracted from epithelial-enriched samples was used to perform quantitative real-time (Q-) PCR directed towards exon 5 of the Pten transcript, which is excised following recombination. At day 5 PI, samples from control animals were found to have an average cycle time (± standard deviation, normalised against beta-actin expression) of 6.60±1.24 compared to $Pten^{f/f}$ animals which had an average cycle time of 9.72±0.77 (Figure 3.2B). This increase in average cycle time indicates significantly decreased levels of Pten transcript in $Pten^{f/f}$ animals (Mann-Whitney U test, n=3, $p<0.0001$), which is equivalent to an 8.68-fold reduction of *Pten* transcript in $Pten^{f/f}$ samples compared to controls. Similarly, samples obtained at day 50 PI were found to have a significantly (Mann-Whitney U test, n=3, $p<0.0001$) lower average cycle time of 6.17±1.65 in control samples compared to 9.57±0.94 in $Pten^{f/f}$ samples (Figure 3.2C), equivalent to a 10.62-fold reduction in *Pten* expression.

Loss of Pten protein from the epithelium following recombination was also assessed, both qualitatively (using IHC) and quantitatively (using western analysis). Immunohistochemistry revealed strong staining for Pten in the epithelium, stroma and smooth muscle of tissue sections from control animals at both day 5 and day 50 PI. In contrast, staining for Pten was absent from the epithelium of intestines from $Pten^{f/f}$ animals at both timepoints, whilst staining of the stroma and smooth muscle was retained (Figure 3.3A). Supporting the observation that recombination occurs within the intestine at just lower than 100% efficiency using this system, occasional crypts from $Pten^{f/f}$ animals at day 50 PI were found to retain positivity for Pten in the epithelium, surrounded by Pten-deficient tissue (Figure 3.3B).

Western analysis on protein extracted from epithelial-enriched samples was used to examine loss of Pten protein in a quantitative manner. This revealed a dramatic reduction in Pten protein levels in $Pten^{f/f}$ animals compared to controls at day 5 PI, and Pten was virtually undetectable in $Pten^{f/f}$ samples at day 30 PI and day 50 PI compared to controls. Level of Pten

[1] This protocol was developed with the assistance of Dr Richard Kemp, University of Cambridge, UK.

protein level was also assessed in a Cre Pten$^{-/-}$ animal at day 50 PI, which was not found to be different to Pten$^{+/+}$ controls. This indicates that LoxP-targeting of the Pten allele does not result in a hypomorphic effect upon expression of Pten protein compared to wild type Pten alleles (Figure 3.3C).

Thus, these data indicate that induction of AhCre according to the published protocol (Ireland et al., 2004) results in recombination within the intestine. *Pten* is efficiently and specifically deleted from the small intestinal epithelium, resulting in significant loss of both *Pten* transcript and Pten protein from day 5 after induction.

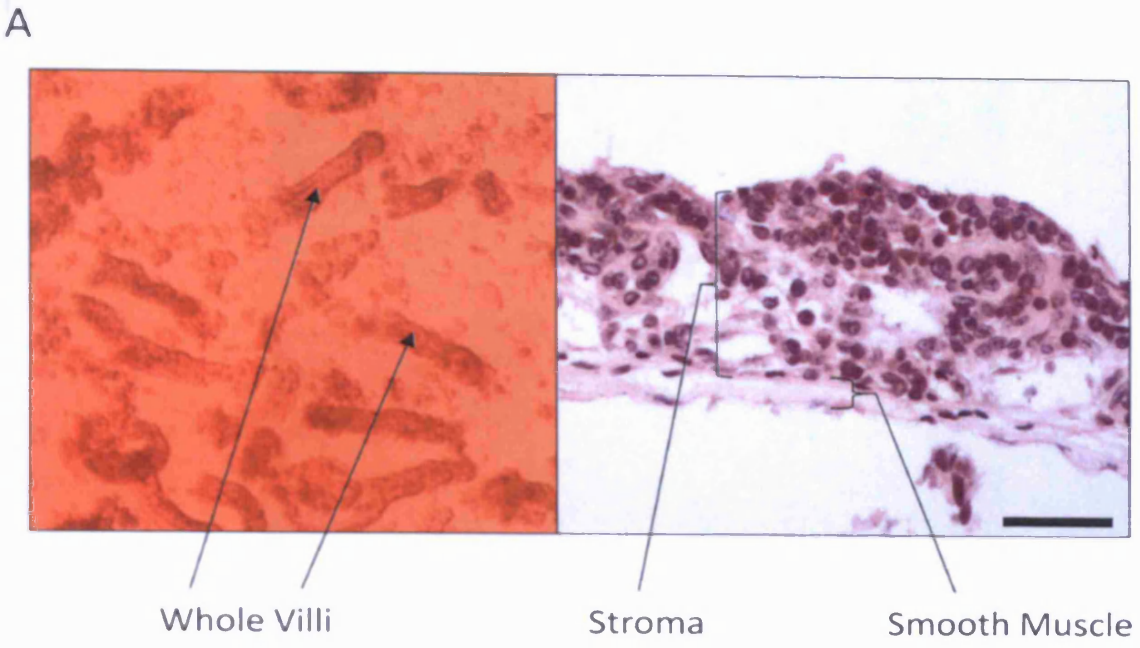

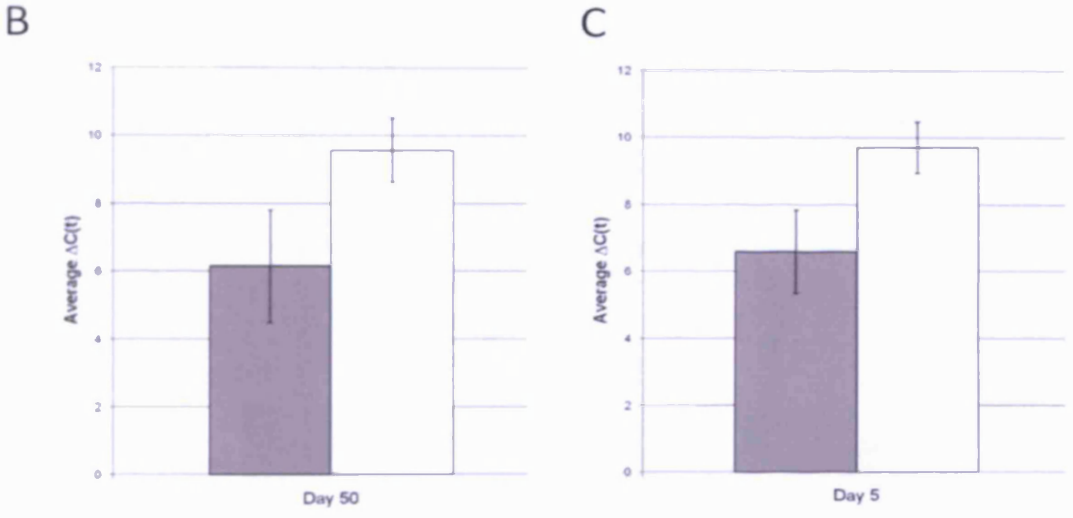

Figure 3.2: ***Epithelial enrichment of intestinal tissue samples, and use of epithelial extracts to confirm loss of Pten transcript after induction***

A protocol for enrichment of epithelium from fresh whole intestinal samples was developed (A), yielding samples containing predominantly epithelial cells (left) with whole villi clearly identifiable (indicated), whilst remaining intestinal tissue (right), composed of stroma and smooth muscle (indicated), was discarded. Scale bar indicates 100μm.

Quantitative real-time PCR analysis of Pten expression in epithelial-enriched samples derived from controls (grey bars) and $Pten^{f/f}$ (white bars) animals reveals an increase in average cycle time (C[t]) needed for product amplification following induction at both day 5 (B) and day 50 (C) PI. This indicates a significant reduction (Mann-Whitney U test, $p<0.001$) of Pten transcript levels in $Pten^{f/f}$ animals following recombination. Error bars indicate ±Standard deviation.

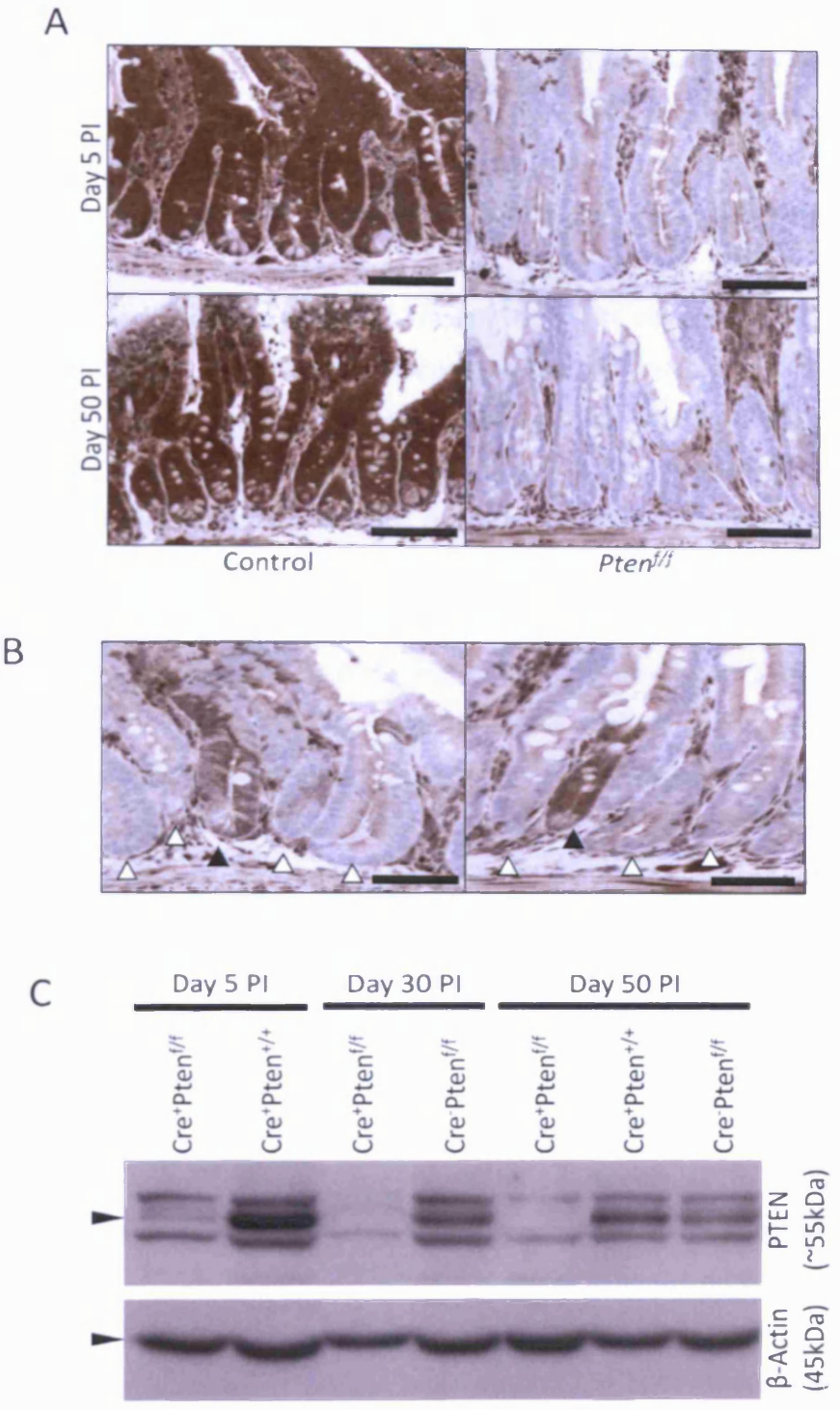

Figure 3.3: ***Confirmation of loss of Pten protein from the intestinal epithelium after induction***
IHC against Pten reveals loss of Pten protein from the epithelium of $Pten^{f/f}$ intestines compared to controls, which retain epithelial staining against Pten, at both day 5 and day 50 after induction (A). IHC against Pten at day 50 PI reveals occasional crypts which retain positivity for Pten (B, filled arrows) surrounded by crypts deficient for Pten (open arrows), reflective of the recombination frequency of just under 100%. Scale bars indicate 100μm. Western analysis (C) of epithelial-enriched samples from control and $Pten^{f/f}$ animals confirms reduction of Pten protein (detected at a size of approximately 55kDa) at day 5 PI, and levels of Pten protein are virtually undetectable at days 30 and 50 PI. Pten protein is detected in all controls. Beta-actin (45kDa) is shown as a loading control.

3.2.3 Recombination outside the intestine recapitulates previously observed phenotypes

Although the AhCre transgene drives recombination efficiently within the small intestinal epithelium, it is also known to drive recombination in other tissues with relatively high efficiency, such as the liver, forestomach, oesophagus and gall bladder (Ireland et al., 2004).

As such, deletion of Pten was observed to result in phenotypes outside the intestine, many of which have previously been reported in the literature.

In the liver, Pten loss was found to rapidly result in abnormal tissue pathology, reminiscent of steatosis of the liver. Hepatic steatosis was not observed in tissues from control animals (Figure 3.4A). Liver steatosis was also found to be accompanied by significant hepatomegaly in $Pten^{-/-}$ animals compared to controls. At day 5 PI, average weight of the whole liver of control animals was 1.32g (± standard deviation of 0.13, n=5) compared to 2.2g (± standard deviation of 0.29, n=4) in $Pten^{-/-}$ animals. This trend was also maintained at day 14 PI, where the average liver weight of control animals was 1.3g (± standard deviation of 0.15, n=3) compared to 2.2g (± standard deviation of 0.36, n=4) in $Pten^{f/f}$ animals (Figure 3.4B). The increase in liver weight in $Pten^{-/-}$ animals is significant in both instances (Mann-Whitney U test, $p<0.02$). In one case, a $Pten^{-/-}$ animal was found to develop hepatocellular carcinoma (HCC) (Figure 3.4C). The phenotypes observed in the liver following Pten loss are consistent with those observed in two previous studies, where Pten was deleted specifically from adult hepatocytes (Horie et al., 2004, Stiles et al., 2004).

$Pten^{-/-}$ animals were also noted to be predisposed to lymphoma formation (Figure 3.4D), which was rarely observed in controls. Again, this observation is consistent with previous reports in a number of Pten-deficient mouse models which report common incidence of lymphoma (Lu et al., 2007, Suzuki et al., 1998, Di Cristofano et al., 1998, Podsypanina et al., 1999).

Induced female $Pten^{f/f}$ animals were found to be susceptible to complex atypical hyperplasia of the endometrium (Figure 3.4E), which was not observed in control genotypes. Again, the development of endometrial hyperplasia and cancer in mouse models of Pten loss has previously been reported (Lu et al., 2007, Podsypanina et al., 1999).

Finally, significant behavioural defects were observed in both induced and uninduced $Pten^{-/-}$ animals, including ataxia, which was not observed in controls. This phenotype has previously been reported following specific deletion of Pten from the brain during development (Backman et al., 2001). As this phenotype is observed in uninduced $Pten^{f/f}$ animals, it is clear that AhCre must be spontaneously activated in the brain at some point during development or early life. In many instances, this phenotype forced the premature culling of $Pten^{f/f}$ animals, which has precluded the characterisation of very long term Pten loss from the intestine in this study.

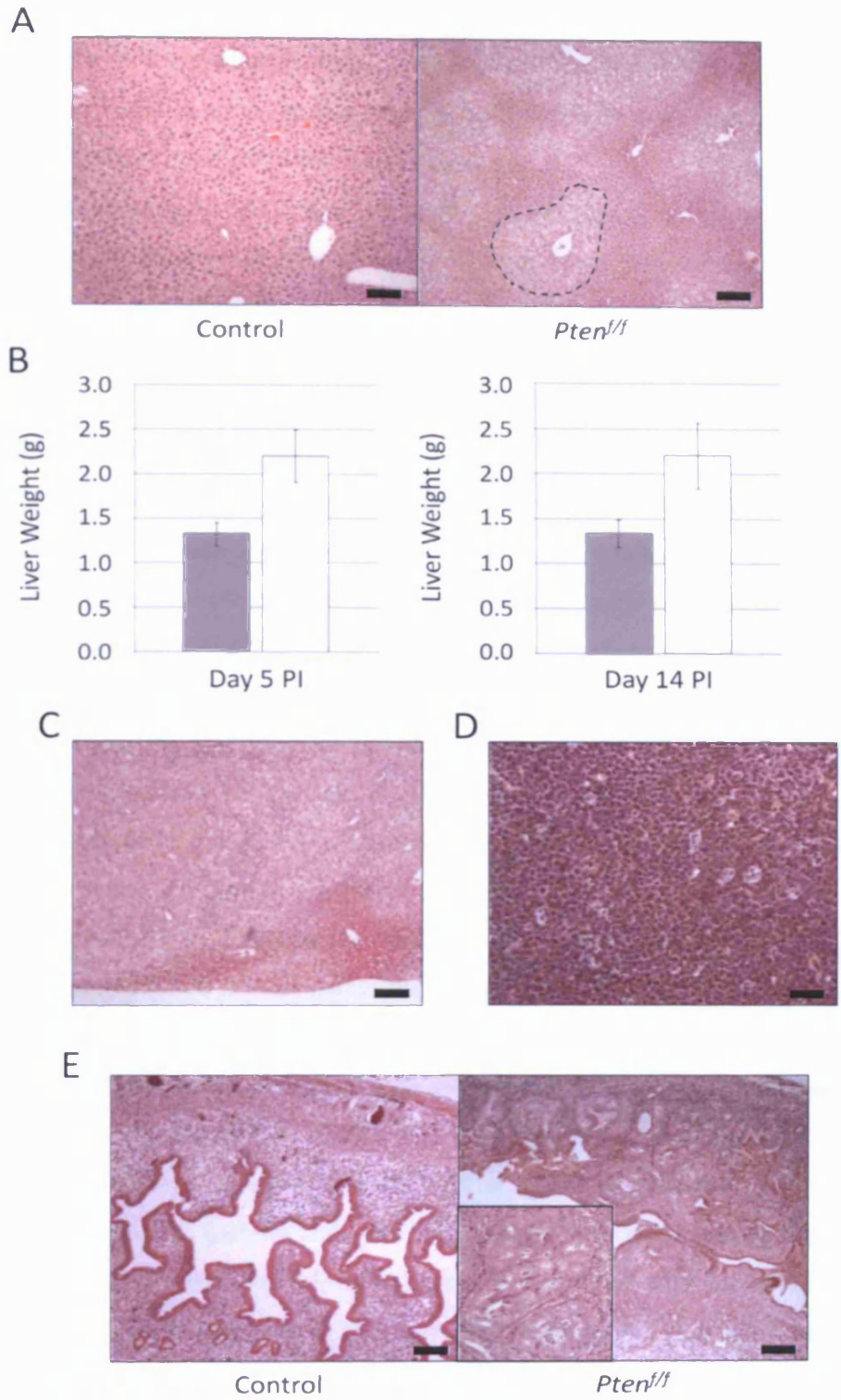

Figure 3.4: ***Pathologies outside the intestine observed following Pten deletion***
Induction of AhCre drives phenotypes associated with Pten loss in other tissues, which have previously been reported in other studies. Pten$^{f/f}$ animals were found to be susceptible to steatosis of the liver (B, outlined area shows example of steatosis) compared to controls (A). This was accompanied by a significant increase in liver weight (B) of Pten$^{f/f}$ animals (white bars) compared to controls (grey bars), evident from day 5 PI (left) and also at day 14 PI (right) (Mann-Whitney U test, $p<0.02$). Error bars indicate standard deviation. In once case, HCC developed in a Pten$^{f/f}$ animal (C). A high incidence of lymphoma (D) was also observed in Pten$^{f/f}$ mice, but not in controls. Female induced Pten$^{f/f}$ animals were found to commonly develop complex atypical hyperplasia of the endometrium (E, right, inset shows digital magnification of the area indicated), which was not seen in controls (left). Scale bars indicate 100µm.

3.2.4 Pten deficiency does not perturb gross structure or histology of the intestinal epithelium

Having validated this model of Pten deficiency, and confirmed loss of Pten from the intestinal epithelium, I next went on to characterise both the immediate and more protracted effects of Pten deletion specifically on intestinal homeostasis.

Upon dissection of control and $Pten^{+/+}$ animals at all timepoints, intestines were removed and examined closely for any gross changes in intestinal structure or for macroscopic appearance of any abnormal lesions. No differences between control and $Pten^{-/-}$ animals were observed, and no tumours were detected at any timepoint (Numbers of control and $Pten^{-/-}$ animals respectively examined were; at Day 5 PI: n=38 and n=22; at Day 14 PI: n=21 and n=9; at Day 30 PI: n=3 and n=5; at Day 50 PI: n=33 and n=35).

H&E-stained intestinal tissue sections of controls and $Pten^{-/-}$ animals at day 5 and 50 PI were examined microscopically, and intestines from $Pten^{-/-}$ animals were found to be histologically indistinguishable from controls at both timepoints (Figure 3.5A). No perturbations in crypt or villus structure were observed, and no dramatic difference in levels of apoptosis or mitosis within the epithelium was noted. IHC against the maker of proliferative cells, Ki67, was used to examine the location and numbers of proliferating cells in the crypt. This showed that again, control and $Pten^{-/-}$ tissue samples at day 50 PI were indistinguishable. The proliferative compartment was correctly located and approximate numbers of replicating cells were unchanged in the context of Pten deficiency (Figure 3.5B).

In order to reveal any subtle changes in structure or homeostasis of the epithelium, crypt and villus size and apoptosis and mitosis within the crypt were quantified. Crypt size was scored as the average number of epithelial cells within whole crypts. Numbers of cells (± standard deviation) per crypt were found to be unchanged in control versus $Pten^{-/-}$ tissue at either day 5 PI (44.30±0.87, n=5 Vs. 44.36±1.35, n=3) or day 50 PI (44.67±2.33, n=4 Vs. 44.34±1.28, n=5) (Figure 3.6A). Similarly, villus size was scored as the number of epithelial cells from the crypt-villus junction to the top of the villus. Care was taken to select comparable regions along the proximal-distal axis of the intestine, as villus length decreases along the proximal-distal axis of the intestine. Numbers of cells (± standard deviation) along the length of the villus was again found to be unchanged in control versus $Pten^{-/-}$ tissue respectively at either day 5 PI (157.01±8.48 n=3, Vs. 157.13±5.95, n=3) or day 50 PI (139.67±9.51, n=3 Vs. 143.31±9.76, n=3) (Figure 3.6B).

Levels of apoptosis and mitosis within the crypt were scored from H&E-stained sections and quantified as average apoptoses or mitoses as a percentage of the total number of cells per crypt. Percentage of apoptosis per crypt was not significantly changed (Mann-Whitney U test, $n \geq 3$, all p-values > 0.38) in $Pten^{-/-}$ compared to control samples across all four timepoints (Days 5, 14, 30 and 50 PI) (Table 3.1, Figure 3.7A). Similarly, scoring for mitosis revealed no significant

change (Mann-Whitney U test, n≥3, all p-values > 0.38) in mitotic index between $Pten^{f/f}$ and control genotypes across all timepoints (Table 3.1, Figure 3.7B).

Timepoint PI	Genotype	Average Percentage Apoptosis (%)	± Standard Deviation	Average Percentage Mitosis (%)	± Standard Deviation
Day 5	Control	1.34	0.67	6.55	4.37
	$Pten^{f/f}$	0.91	0.07	5.03	4.10
Day 14	Control	0.86	0.06	7.74	3.79
	$Pten^{f/f}$	0.56	0.29	10.88	1.76
Day 30	Control	0.60	0.19	6.00	2.93
	$Pten^{f/f}$	0.54	0.18	5.67	0.56
Day 50	Control	0.99	0.47	5.77	0.97
	$Pten^{f/f}$	0.92	0.39	5.20	1.44

Table 3.1: *Scoring of Apoptosis and mitosis in control and $Pten^{f/f}$ intestines reveals no significant difference compared to controls*

These data therefore indicate that, up to 50 days after induction, Pten loss is tolerated within the intestine, and does not perturb the normal architecture of the intestine or basic homeostasis of the epithelium.

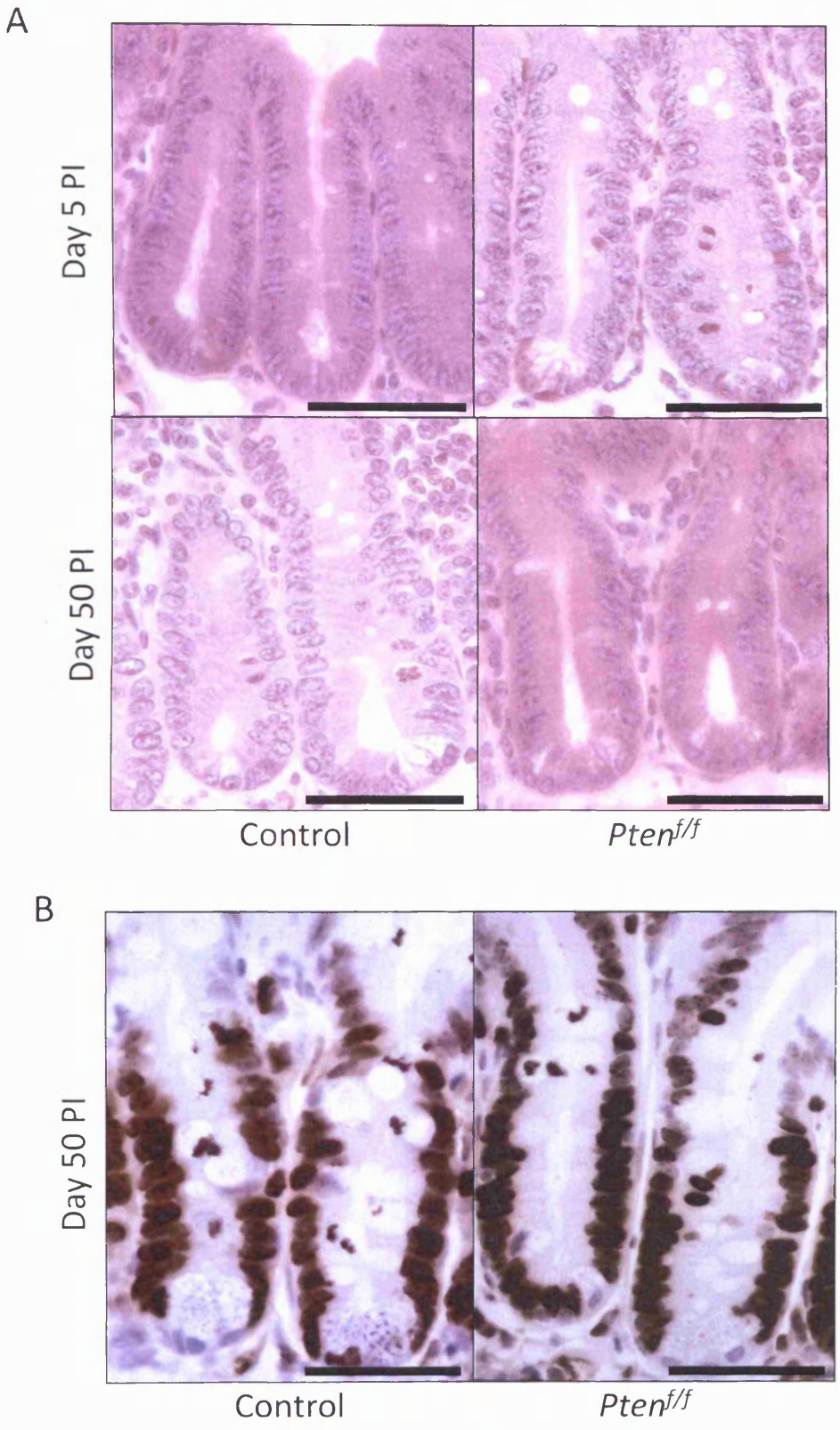

Figure 3.5: ***No changes in histology or location of TA zone following epithelial Pten loss***
H&E-stained sections of intestinal tissue from control and Pten$^{f/f}$ animals at days 5 and 50 PI revealed no gross changes in histological appearance. IHC against the proliferation marker Ki67 (B) revealed no change in the location of the transit amplifying (TA) at day 50 after Pten loss.

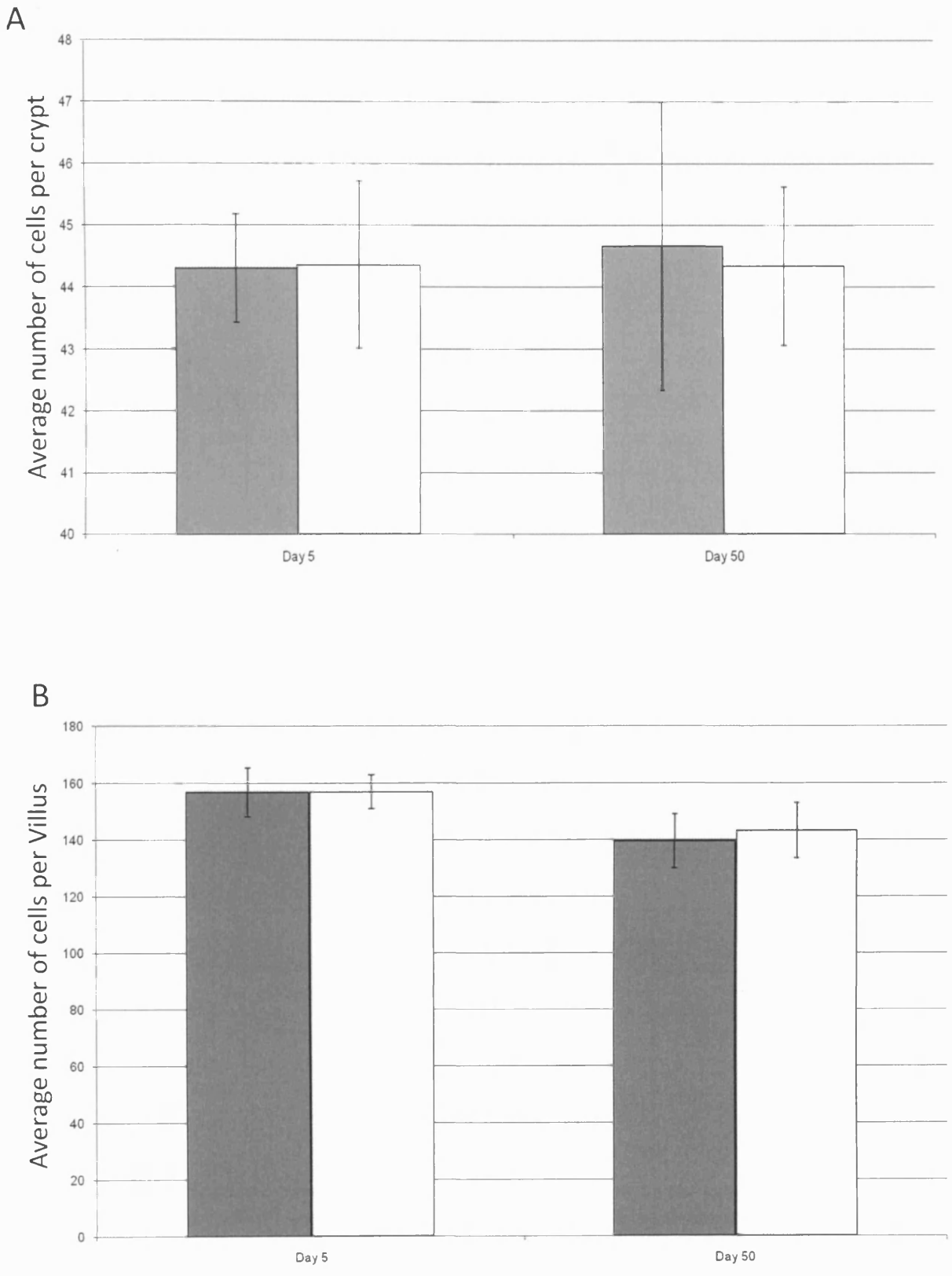

Figure 3.6: ***Quantification of crypt and villus size following Pten deletion***
Scoring of the number of cells present per full crypt (A) or per half villus (B) revealed no difference between control (grey bars) and $Pten^{f/f}$ (white bars) intestines at either day 5 or day 50 PI (Mann-Whitney U test, $p > 0.66$).

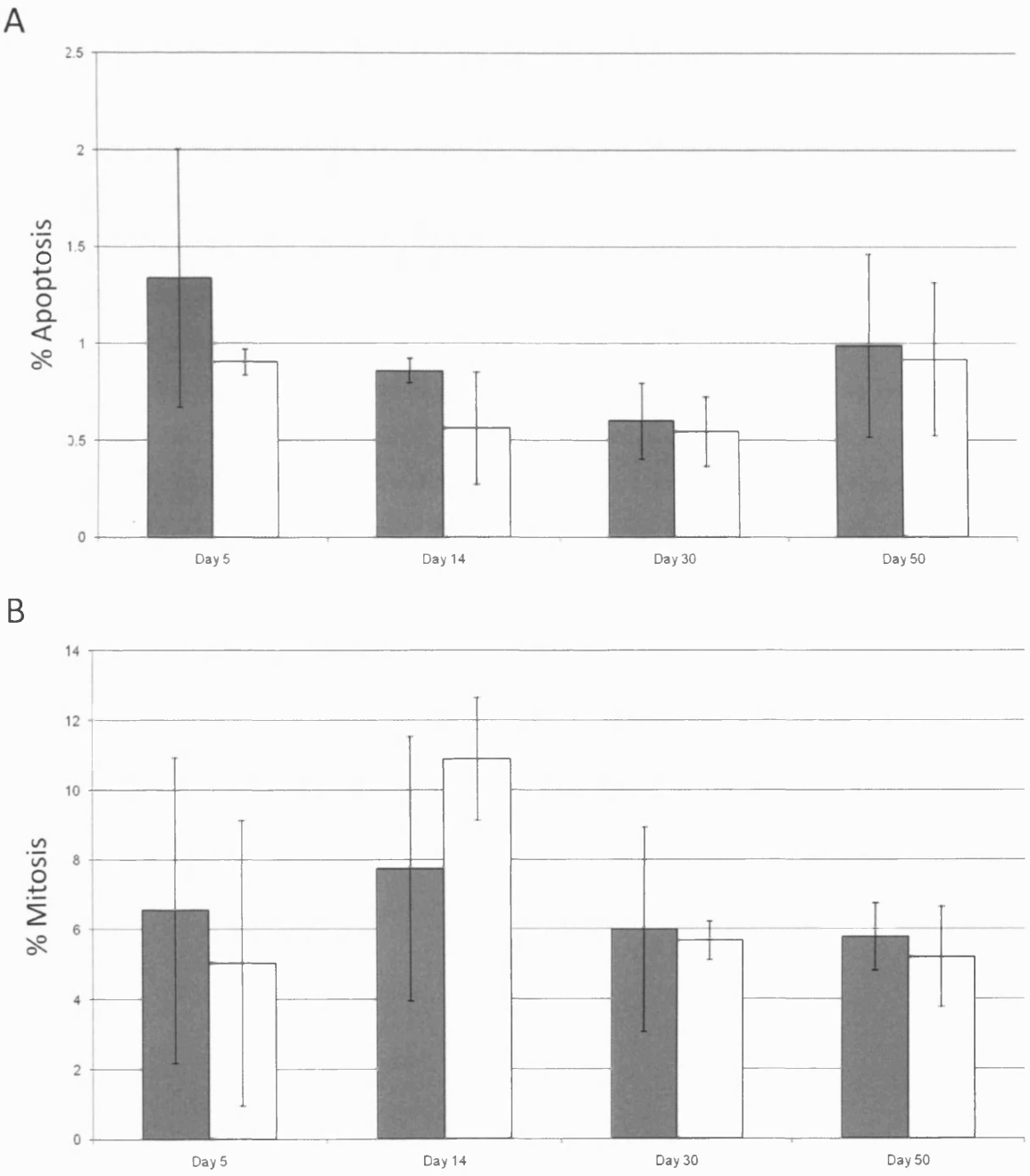

Figure 3.7: ***Quantification of levels of apoptotic and mitotic cells within the crypt***
Apoptosis (A) and mitosis (B) was scored from intestinal tissue sections of control (grey bars) and $Pten^{f/f}$(white bars) mice at days 5, 14, 30 and 50 PI. No significant difference (Mann-Whitney U test, $p>0.38$ for all comparisons) in either apoptosis or mitosis was observed between control and $Pten^{f/f}$ genotypes across all timepoints.

3.2.5 Pten-deficient cells show a normal apoptotic response to DNA damage

Previous work has indicated that Pten physically interacts with the pro-apoptotic factor, p53, and plays a role in promoting its stabilisation (Freeman et al., 2003). Within the intestine, the apoptotic response to gamma irradiation is known to be critically dependent upon p53-dependent mechanisms (Merritt et al., 1997). As such, I decided to test whether Pten-deficient intestines show any impairment in apoptotic response to DNA damage induced by irradiation. This will allow any reduction in levels or activity of p53 to be inferred.

Control and $Pten^{f/f}$ animals at day 50 PI were irradiated with a dose of 5Gy of gamma-irradiation from a caesium source. After three hours, animals were culled and intestines harvested. H&E-stained sections of intestine from control and $Pten^{f/f}$ animals were examined for the presence of apoptotic figures. Brief examination of sections revealed that apoptotic bodies were present in both control and Pten-deficient intestines, and were present in approximately equal numbers in each genotype (Figure 3.8A). Quantification of the percentages of apoptoses and mitoses present in the crypt following irradiation (Figure 3.8B) revealed that the percentage of apoptotic cells (± standard deviation) in control versus Pten-deficient intestines respectively (16.47±1.30 Vs. 16.77±1.30) was not significantly different (Mann-Whitney U test, n=3, p=0.7), nor was the percentage of mitotic cells (5.38±2.46 Vs. 5.62±2.01, Mann-Whitney U test; n=3, p=0.7).

Thus, it appears that p53-dependent apoptosis is not impaired in the context of Pten deficiency, implying that, in the intestine, Pten does not influence the stability or activity of p53.

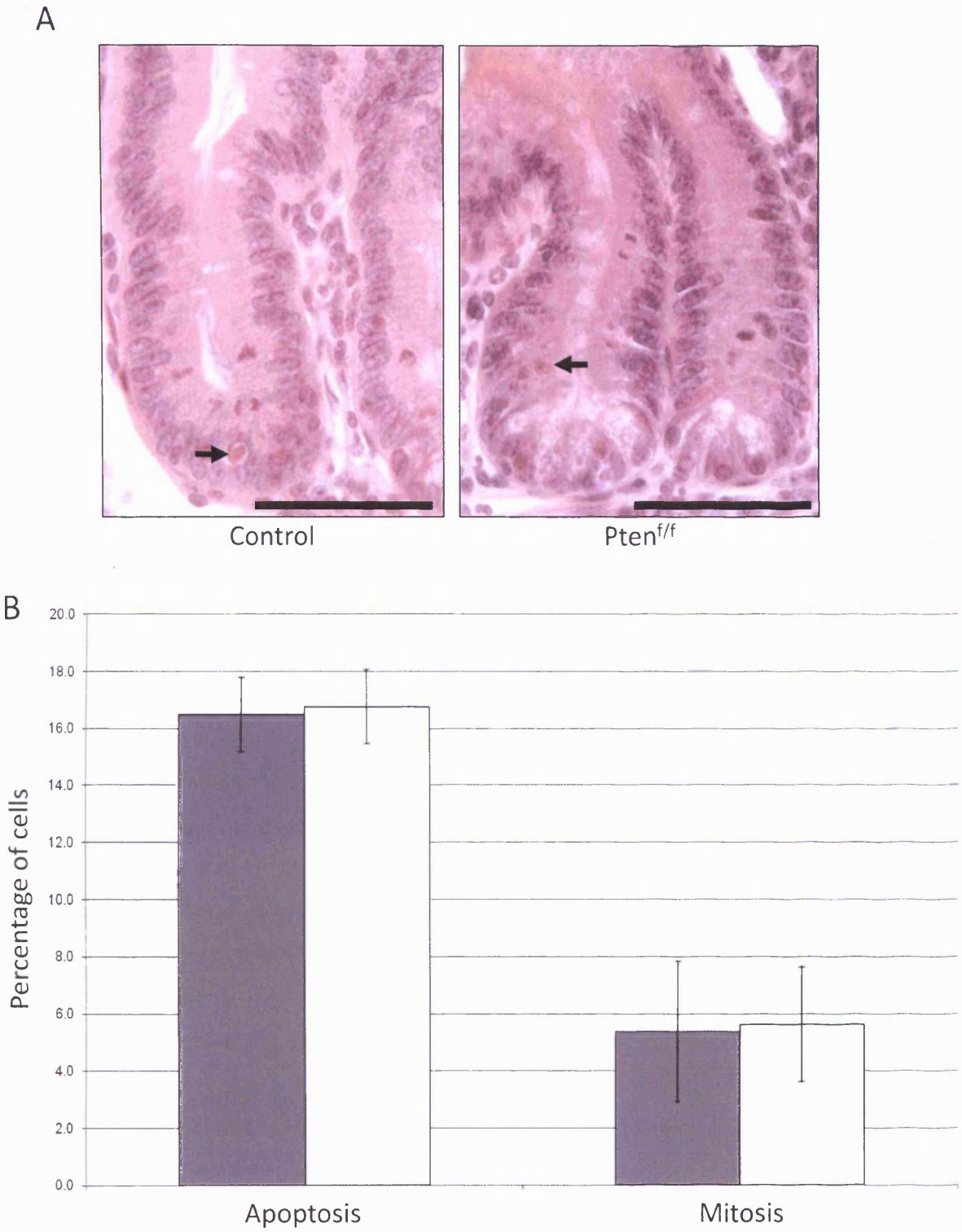

Figure 3.8: ***No impairment of apoptotic response to DNA damage following Pten loss***
In order to assess the apoptotic response to DNA damage in the context of Pten deficiency, mice were irradiated with 5Gy gamma-irradiation. This induces an apoptotic response in the intestine (A), and apoptotic figures (arrows) were found to be present in both controls and $Pten^{f/f}$ animals. Scale bars indicate 100μm. Quantification of levels of apoptosis and mitosis following irradiation (B) showed no difference in levels of either apoptosis or mitosis in controls (grey bars) compared to $Pten^{f/f}$ (white bars) animals (Mann-Whitney U test, p=0.7 for both comparisons). Error bars show standard deviation.

3.2.6 Epithelial cells differentiate normally in the absence of Pten

In order to examine the presence and localisation of the mature, differentiated cell types of the intestinal epithelium, IHC or specific stains were used to allow visualisation of cell types.

Tissue from control and $Pten^{f/f}$ animals at day 50 PI was stained immunohistochemically against lysozyme, a marker of Paneth cells. Positively-stained cells were present in both control and $Pten^{f/f}$ tissue samples, and were found to be located at the very base of the crypt, regardless of Pten status (Figure 3.9A).

Similar tissue samples were used for IHC against villin, a marker of mature enterocytes. Staining patterns indicated no alteration in the location of the brush border or differentiation of enterocytes in the context of Pten deficiency (Figure 3.9B).

The Periodic Acid-Schiff's reagent (PAS) stain and the Grimelius method were used to detect Goblet cells and enteroendocrine cells respectively. PAS stains mucins released by goblet cells, allowing their identification. This revealed that Goblet cells are present in Pten-deficient tissue compared to controls, and are correctly localised. The Grimelius method allows identification of enteroendocrine cells by the presence of silver deposits in the cells, which stain cells black. Again, this revealed no difference in the presence or localisation of enteroendocrine cells in the context of Pten loss.

Using these stained sections, the numbers of Goblet cells and enteroendocrine cells present in the crypt and on the villus was quantified in both control and $Pten^{f/f}$ tissue samples at day 50 PI. The average number of goblet cells (± standard deviation) present in the crypt of control (4.95±0.55) and $Pten^{f/f}$ (5.73±0.36) tissues and on the villus of control (13.87±3.24) and $Pten^{f/f}$ (13.87±1.51) tissue samples was not significantly different (Mann-Whitney U test, n=3, $p>0.19$) (Figure 3.10A). Similarly, the numbers of enteroendocrine cells (± standard deviation) observed in control versus $Pten^{f/f}$ tissue sections in the crypt (0.76±0.17 Vs. 0.67±0.02) or on the villus (1.55±0.14 Vs. 1.95±0.35) was not significantly different (Mann-Whitney U test, n=3, $p>0.27$) (Figure 3.10B).

Thus, it is clear that epithelial cells are able to differentiate normally in the absence of Pten, with all mature cell types being present, correctly localised and at the expected frequency compared to control tissue.

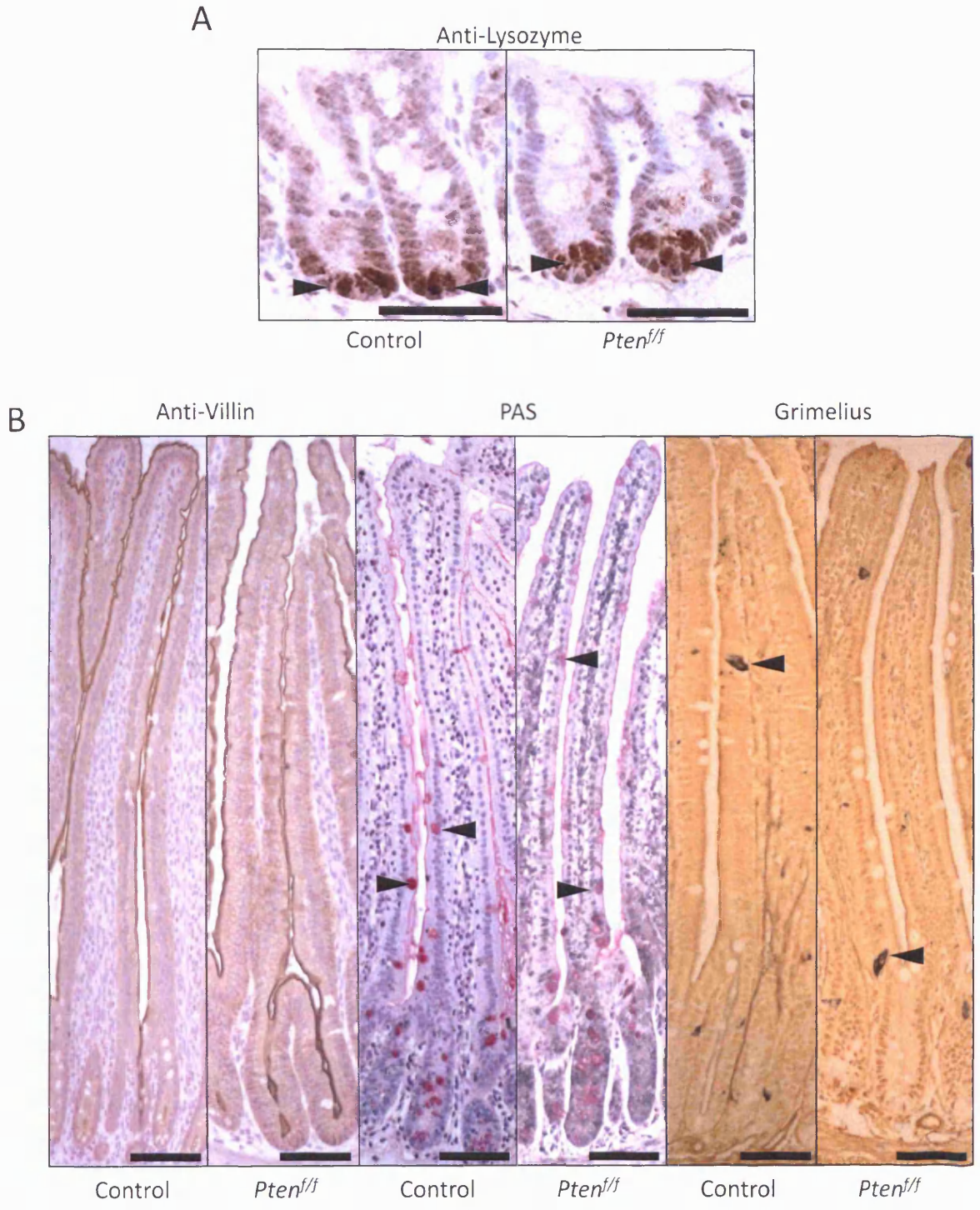

Figure 3.9: ***Identification of differentiated epithelial cell types following Pten loss***
Anti-lysozyme IHC was used to label paneth cells (A, arrows) at the base of the crypt, which were found to be correctly localised in Pten-deficient tissue at day 50 PI. Anti-villin IHC, Periodic acid-Schiff's stain (PAS) and the Grimelius method were used (B) to identify the brush border, goblet cells (arrows) and enteroendocrine cells (arrows) respectively, in tissue from control and $Pten^{f/f}$ animals at day 50 PI. In no case was the presence or localisation of differentiated cell types affected by Pten loss. Scale bars indicate 100μm.

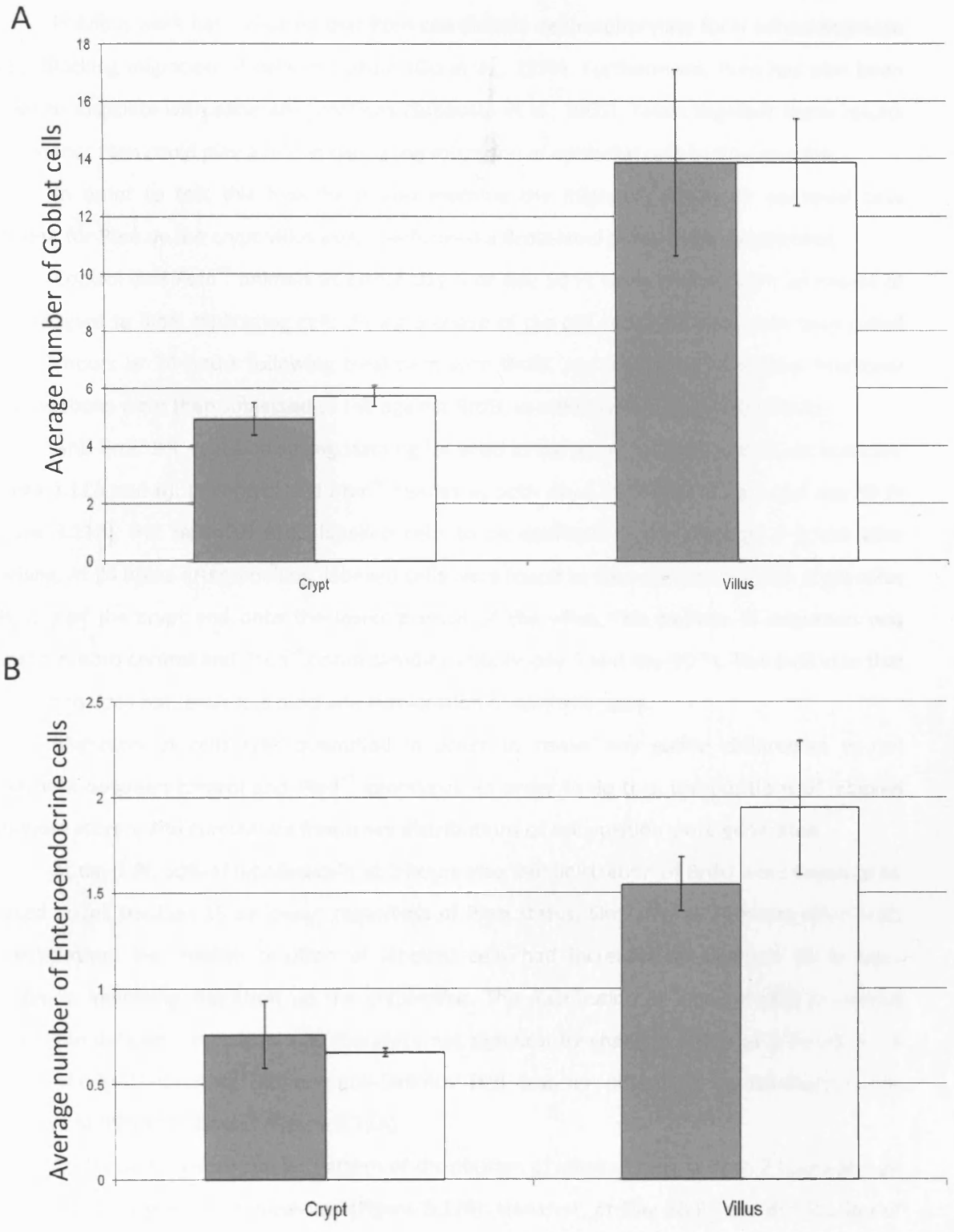

Figure 3.10: ***Quantification of Goblet cells and enteroendocrine cells following Pten loss***
Numbers of Goblet cells (A) and enteroendocrine cells (B) present in the crypt and villus of control (grey bars) and $Pten^{f/f}$ (white bars) animals at day 50 PI were quantified. No difference was observed in the numbers or location of these differentiated cell types in Pten-deficient tissue compared to controls (Mann-Whitney U test, $p>0.19$ for all comparisons). Error bars indicate ± Standard deviation.

3.2.7 Pten-deficient cells exhibit no block in migratory ability

Previous work has indicated that Pten can directly dephosphorylate focal adhesion kinase (FAK), blocking migration of cells in culture (Gu et al., 1999). Furthermore, Pten has also been shown to associate with adherens junctions (Subauste et al., 2005). Taken together these results suggest that Pten could play a role in regulating migration of epithelial cells in the intestine.

In order to test this hypothesis and examine the migratory ability of epithelial cells deficient for Pten up the crypt-villus axis, I performed a BrdU-label pulse-chase experiment.

Control and $Pten^{f/f}$ animals at either day 5 or day 50 PI were treated with an excess of BrdU reagent to label replicating cells during S-phase of the cell cycle. Animals were then culled either 2 hours or 24 hours following treatment with BrdU, and intestines harvested. Intestinal tissue sections were then subjected to IHC against BrdU, in order to visualise labelled cells.

Anti-BrdU IHC revealed strong staining for BrdU in the nuclei of labelled cells, as expected (Figure 3.11A and B). In control and $Pten^{f/f}$ tissues at both day 5 PI (Figure 3.11A) and day 50 PI (Figure 3.11B), IHC revealed BrdU-labelled cells to be confined to the crypt at 2 hours after labelling. At 24 hours after labelling, labelled cells were found to have migrated up the crypt-villus axis, out of the crypt and onto the lower portion of the villus. This pattern of migration was evident in both control and $Pten^{f/f}$ tissue samples at both day 5 and day 50 PI. This indicates that loss of Pten does not result in a blockade in migration of epithelial cells.

Migration of cells was quantified in order to reveal any subtle differences in cell movement between control and $Pten^{f/f}$ genotypes. In order to do this, the positions of labelled cells were scored, and cumulative frequency distributions of cell position were generated.

At day 5 PI, 50% of labelled cells at 2 hours after administration of BrdU were found to be located at cell position 15 or lower, regardless of Pten status. Similarly, at 24 hours after BrdU administration, the median position of labelled cells had increased to position 35 in both genotypes, indicating migration up the crypt-villus. The distribution of labelled cells in control versus Pten-deficient intestines was therefore not significantly changed either at 2 hours or 24 hours after BrdU labelling (Kolmogorov-Smirnov [KS] test for difference in distribution, not significant at 99% confidence) (Figure 3.12A).

At day 50 PI, a very similar pattern of distribution of labelled cells at both 2 hours and 24 hours after BrdU labelling is observed (Figure 3.12B). However, at Day 50 PI, the distribution of labelled cells in control and $Pten^{f/f}$ tissue is significantly different (KS test for difference in distribution; distributions are significantly different with a confidence level of 99%). Surprisingly, Pten-deficient cells are found to migrate more quickly than control cells, as indicated by a shift to the right of the cumulative frequency curve.

This pattern supports the predicted observation based on the published data described above, which would be that Pten deficiency would enahnce migration. Indeed, it appears that loss

of Pten does not result in any insufficiency in migratory ability, and may in fact enhance migration rates within the epithelium.

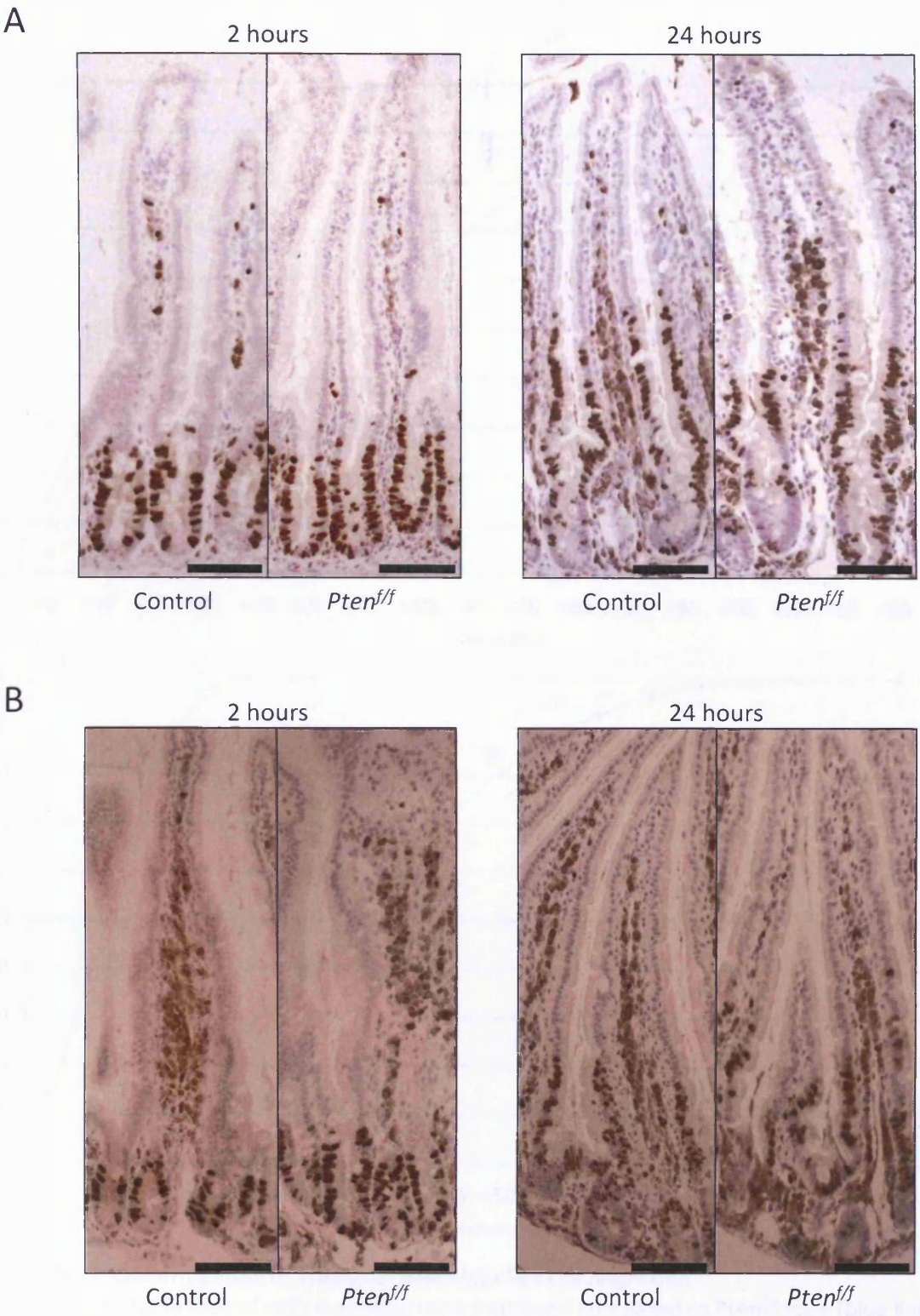

Figure 3.11: ***BrdU labelling of cells reveals no deficiency in cell migration following Pten loss***
BrdU was administered to Pten$^{f/f}$ and control animals at day 5 (A) or day 50 (B) PI. Intestines were harvested either 2 hours or 24 hours after BrdU labelling, and IHC used to detect labelled cells. This revealed no block in the migratory ability of Pten-deficient cells compared to controls, either at day 5 or day 50 PI. Scale bars indicate 100μm.

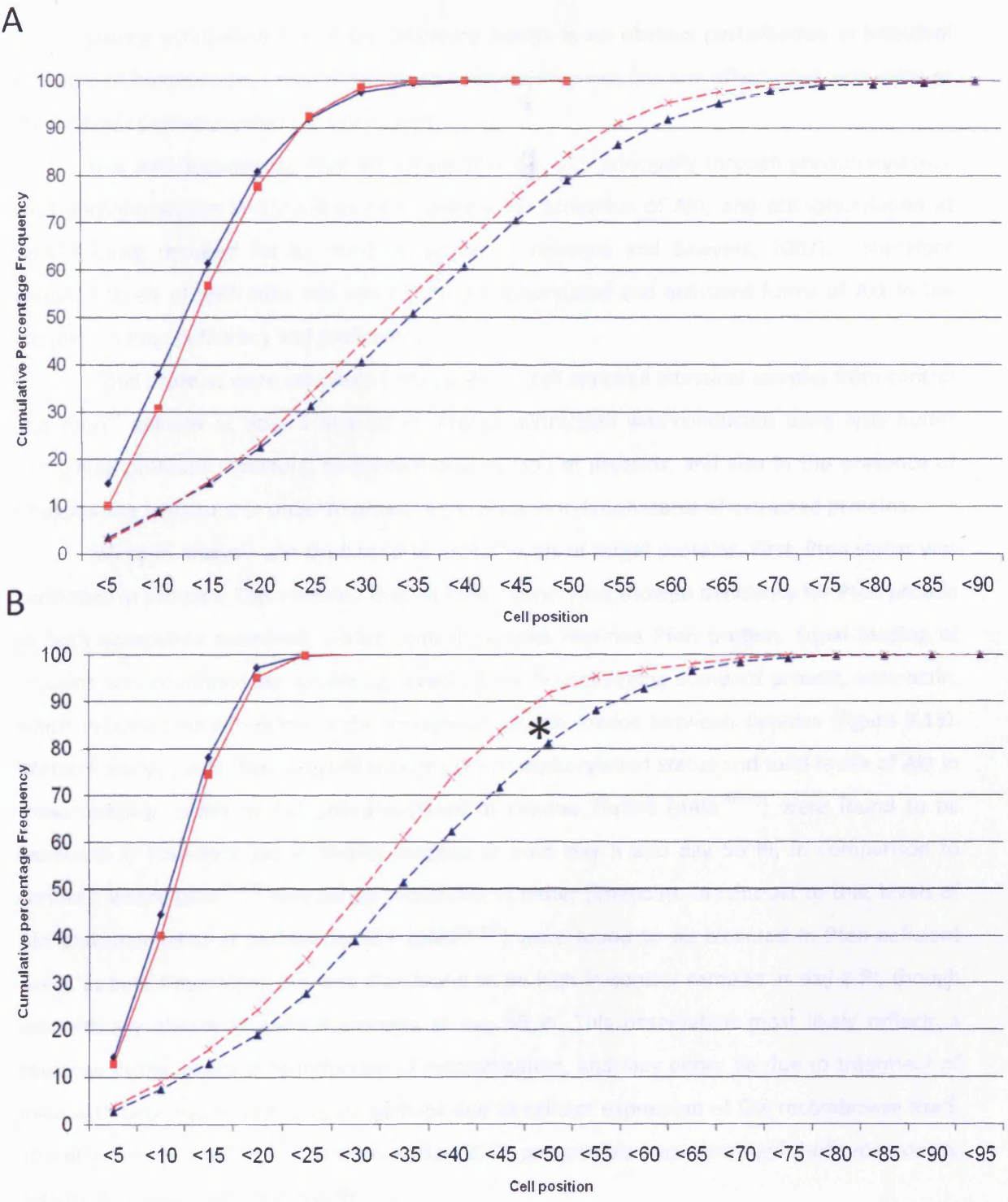

Figure 3.12: ***Quantification of epithelial BrdU-labelled cell migration***
Migration of BrdU-labelled cells in control mice (red lines) compared to $Pten^{f/f}$ mice (blue lines) at days 5 (A) and 50 (B) PI was quantified. Positions of labelled cells were recorded as a cumulative frequency. In both genotypes, labelled cells were shown to move up the crypt villus axis between 2 hours (solid lines) and 24 hours (dashed lines), as indicated by a shift to the right of the cumulative frequency curve. At day 50 PI, a significant difference in migration was observed between control and Pten-deficient cells (Kolmogorov-Smirnov test, 99% confidence interval), with Pten-deficient cells showing a faster rate of migration up the crypt-villus (asterisk).

3.2.8 Akt is activated following epithelial Pten deletion

Having established that Pten deficiency results in no obvious perturbation in intestinal structure of homeostasis, I next determined whether Pten loss has any effect upon activation of the PI3K/Akt pathway within the epithelium.

It is well documented that activation of Akt occurs principally through phosphorylation, with phosphorylation at Thr308 being necessary for activation of Akt, and phosphorylation at Ser473 being required for its maximal activation (Vivanco and Sawyers, 2002). I therefore assessed levels of both total Akt and of the phosphorylated and activated forms of Akt in the contexts of Pten deficiency and proficiency.

Total proteins were extracted from epithelial-cell enriched intestinal samples from control and $Pten^{f/f}$ animals at days 5 and 50 PI. Protein extraction was conducted using lysis buffer containing protease inhibitors, to prevent degradation of proteins, and also in the presence of phosphatase inhibitors, in order to preserve the phosphorylation status of extracted proteins.

Western analysis was then used to assess levels of target proteins. First, Pten status was confirmed in samples. This revealed that all $Pten^{f/f}$ genotypes showed deficiency for Pten protein at both timepoints examined, whilst control samples retained Pten protein. Equal loading of proteins was confirmed by visualising levels of the housekeeping standard protein, beta-actin, which indicated no difference in the amount of protein loaded between samples (Figure 3.13). Western analysis was then directed towards the phosphorylation status and total levels of Akt in these samples. Levels of Akt phosphorylated at residue Thr308 ($pAkt^{Thr308}$) were found to be increased in Pten-deficient epithelial samples at both day 5 and day 50 PI, in comparison to controls, where $pAkt^{Thr308}$ was barely detectable at either timepoint. In contrast to this, levels of Akt phosphorylated at residue Ser473 ($pAkt^{Ser473}$) were found to be elevated in Pten-deficient tissue at both timepoints, but was also found to be high in control samples at day 5 PI, though was virtually absent in control samples at day 50 PI. This observation most likely reflects a response in the intestine to induction of recombination, and may either be due to treatment of mice with beta-naphthoflavone, or perhaps due to cellular expression of Cre recombinase itself. This effect is not apparent in controls at day 50 PI, presumably once beta-naphthoflavone or Cre activity is no longer present in cells.

Levels of total, unphosphorylated Akt were not found to change with respect to genotype or timepoint after induction.

It is therefore clear that, whilst loss of Pten protein does not affect total levels of Akt protein, Akt is phosphorylated at residue Thr308 in response to Pten deficiency, both at day 5 and day 50 PI. Furthermore, levels of $pAkt^{Ser473}$ in Pten-deficient tissue at day 50 PI are elevated

compared to controls, though at day 5 PI no conclusion can be drawn regarding a difference between control and $Pten^{f/f}$ genotypes.

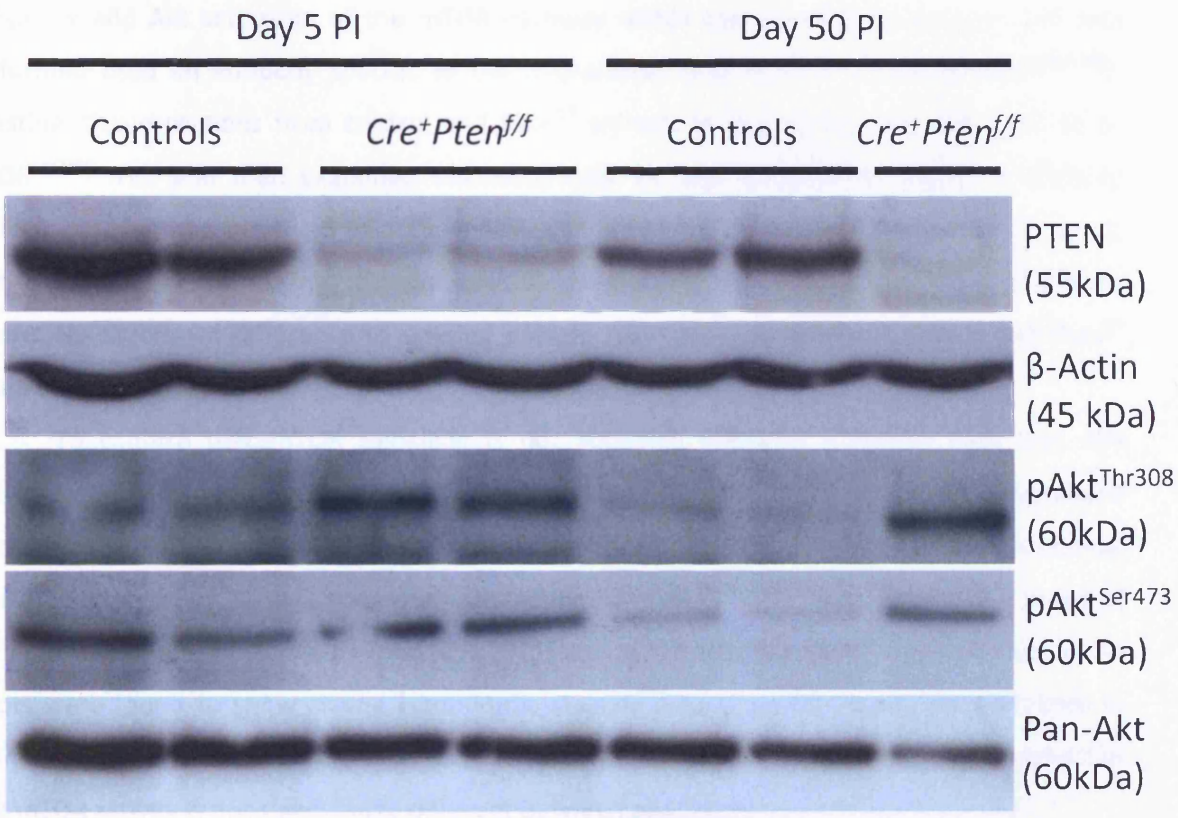

Figure 3.13: ***Deletion of Pten results in activation of Akt***
Western analysis of proteins from epithelial-enriched tissue samples taken from control and $Pten^{f/f}$ animals at days 5 and 50 PI confirmed loss of Pten protein from the epithelium. Beta-actin was used to ensure equal loading of proteins. In samples deficient for Pten, an increase in levels of activated (phospho-) Akt was observed ($pAkt^{Ser473}$ and $pAkt^{Thr308}$). Total levels of Akt were found to be unchanged.

3.2.9 Downstream targets of Akt are not activated following Pten loss

Having found that loss of Pten from the epithelium results in an increase in activation status of Akt, I next examined downstream targets of Akt in order to assess the cellular effect of Akt activation in the epithelium.

Activation of Akt is known to result in activation of the mammalian target of rapamycin (mTOR) pathway (Manning et al., 2002), which is characterised by the phosphorylation of mTOR protein itself at residue Ser2448 (Hay and Sonenberg, 2004). To assess the effect of Pten deficiency and Akt activation of the mTOR pathway within the intestinal epithelium, IHC was performed used an antibody specific to the phospho-Ser2448 form of mTOR (p-mTOR^{Ser2448}). Intestinal tissue sections from control and Pten$^{f/f}$ animals at day 50 PI were subjected to p-mTOR^{Ser2448} IHC, and then examined microscopically for any apparent difference in staining pattern. Staining was observed to occur mainly at the lumenal surface of cells within the crypt, with occasional cells showing strongly positive cytoplasmic staining for p-mTOR^{Ser2448} (Figure 3.14A). No significant difference in staining pattern was observed between control and Pten$^{f/f}$ tissue samples at day 50 PI.

To confirm that mTOR signalling is not activated following epithelial Pten loss, the activation status of a target of mTOR, S6 kinase, was examined. IHC for S6 kinase phosphorylated at residues Thr421 and Ser424 (pS6K$^{Thr421/Ser424}$) was performed on control and Pten$^{f/f}$ intestinal tissue samples at day 50 PI. Strong nuclear staining for pS6K$^{Thr421/Ser424}$ was observed in tissue of both genotypes, and similar to the p-mTOR^{Ser2448} staining pattern observed, occasional cells within crypts were found to show strong cytoplasmic staining (Figure 3.14B). Again, no difference in staining patterns between control and Pten$^{f/f}$ tissue samples was noted, reflecting the observation that mTOR activity is not significantly different between genotypes.

To further assess any changes in the Akt pathway, the expression levels of a number of Akt pathway components was determined using Q-PCR analysis. cDNA was made from RNA extracted from control and Pten$^{f/f}$ epithelial-cell enriched tissue samples at day 50 PI. This was then used to perform Q-PCR with primers directed towards the genes for SH2-containing inositol phosphatase (SHIP), Akt isoforms 1, 2 and 3 (Akt1, Akt2 and Akt3), Tuberous sclerosis genes 1 and 2 (TSC1 and TSC2), mTOR and eukaryotic initiation factor 4E binding protein 1 (eIF4E-BP1).

Expression levels of SHIP were of interest as SHIP is also an inositol phosphatase, and modulation of SHIP levels may provide a possible compensatory mechanism to inactivation of Pten. However, expression levels of SHIP were found to be unaltered in the context of Pten deficiency (Figure 3.15A).

Of the other components of Akt signalling examined, the expression of only one transcript was found to be significantly altered in the context of Pten loss; Akt3. Average cycle time (±

standard deviation) of the product of the Akt3 gene was 10.77±0.10 in controls compared to 13.30±0.51 in $Pten^{f/f}$ samples, which is a significant increase of cycle time in $Pten^{f/f}$ samples compared to controls (Mann-Whitney U Test, n=3, $p<0.0001$). This is equivalent to a 5.78-fold reduction in Akt3 transcript in $Pten^{f/f}$ samples compared to controls. However, the significance of this finding is unclear. All other transcripts examined were found not to show any alteration in expression levels following deletion of Pten (Figure 3.15A). However, this is perhaps not surprising given that activation of the Akt pathway generally occurs through phosphorylation of pathway components, rather than modulation of transcription levels (Cully et al., 2006).

Previous work has suggested a role for activated Akt in mediating activation of the Wnt pathway in the intestine, particularly in intestinal stem cells (He et al., 2004). As I have shown that Akt is activated following loss of Pten, I decided to test the hypothesis proposed by *He et al.*, and investigated the activation status of the Wnt signalling pathway following Pten deletion.

Q-PCR directed towards several well-characterised targets of the Wnt pathway was performed as described above for components of the Akt pathway. Expression levels of Axin2, c-myc and CD44 were found not to be changed in the context of Pten deficiency (Average cycle times ± Standard deviation for control versus $Pten^{f/f}$ samples were Axin-2: 8.23±0.90 Vs 8.57±0.67; CD44: 15.42±0.73 Vs 14.48±0.31; c-myc: 7.46±0.98 Vs 7.64±0.37), whereas cycle time of CyclinD2 in controls was found to be significantly reduced compared to $Pten^{f/f}$ samples (6.37±0.46 Vs 7.57±0.46) (Mann-Whitney U test, n=3, p=0.08), indicating a reduction of CyclinD2 expression in $Pten^{f/f}$ intestines (Figure 3.15B). This therefore indicates that activation of Akt within the epithelium does not result in activation of the Wnt pathway as previously proposed, with no increase in expression of Wnt signalling targets observed in Pten-deficient epithelial cells compared to controls.

A

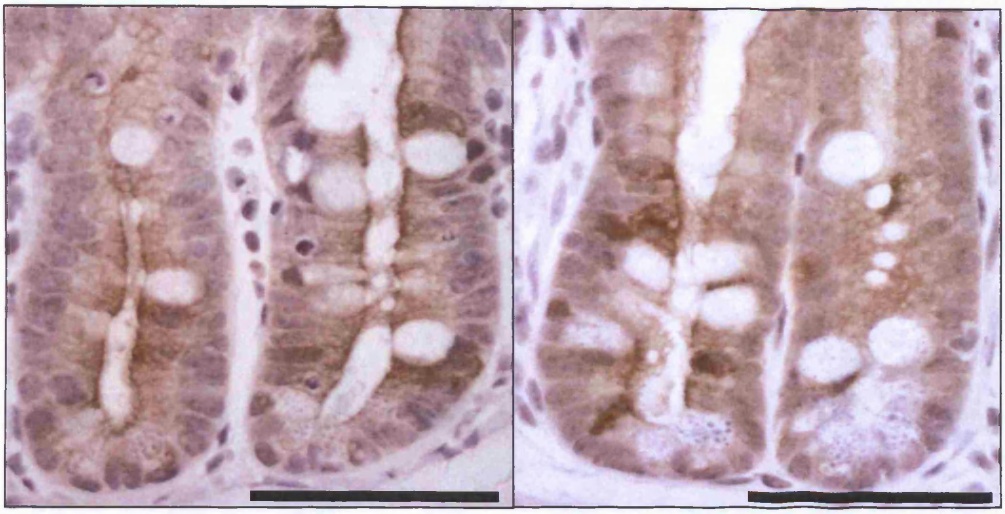

Control $Pten^{f/f}$

B

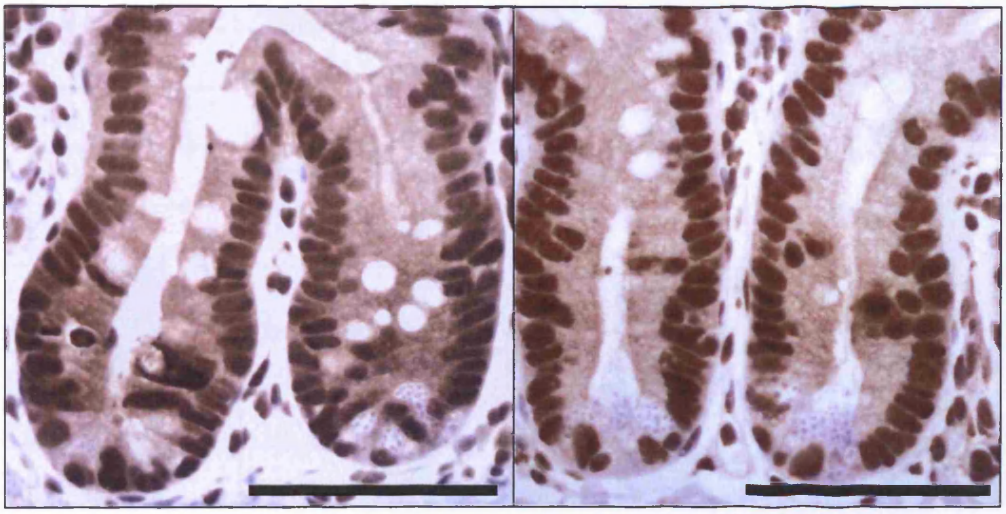

Control $Pten^{f/f}$

Figure 3.14: *Downstream targets of Akt are not activated following Pten deletion*
IHC against known targets of Akt signalling was performed to assess activation of the Akt pathway. Phospho-mTOR^{Ser2448} (A) and phospho-S6 kinase$^{Thr421/Ser424}$ (B) IHC of tissue taken from mice at day 50 PI revealed no difference in staining patterns between control and $Pten^{f/f}$ tissue. Scale bars indicate 100μm.

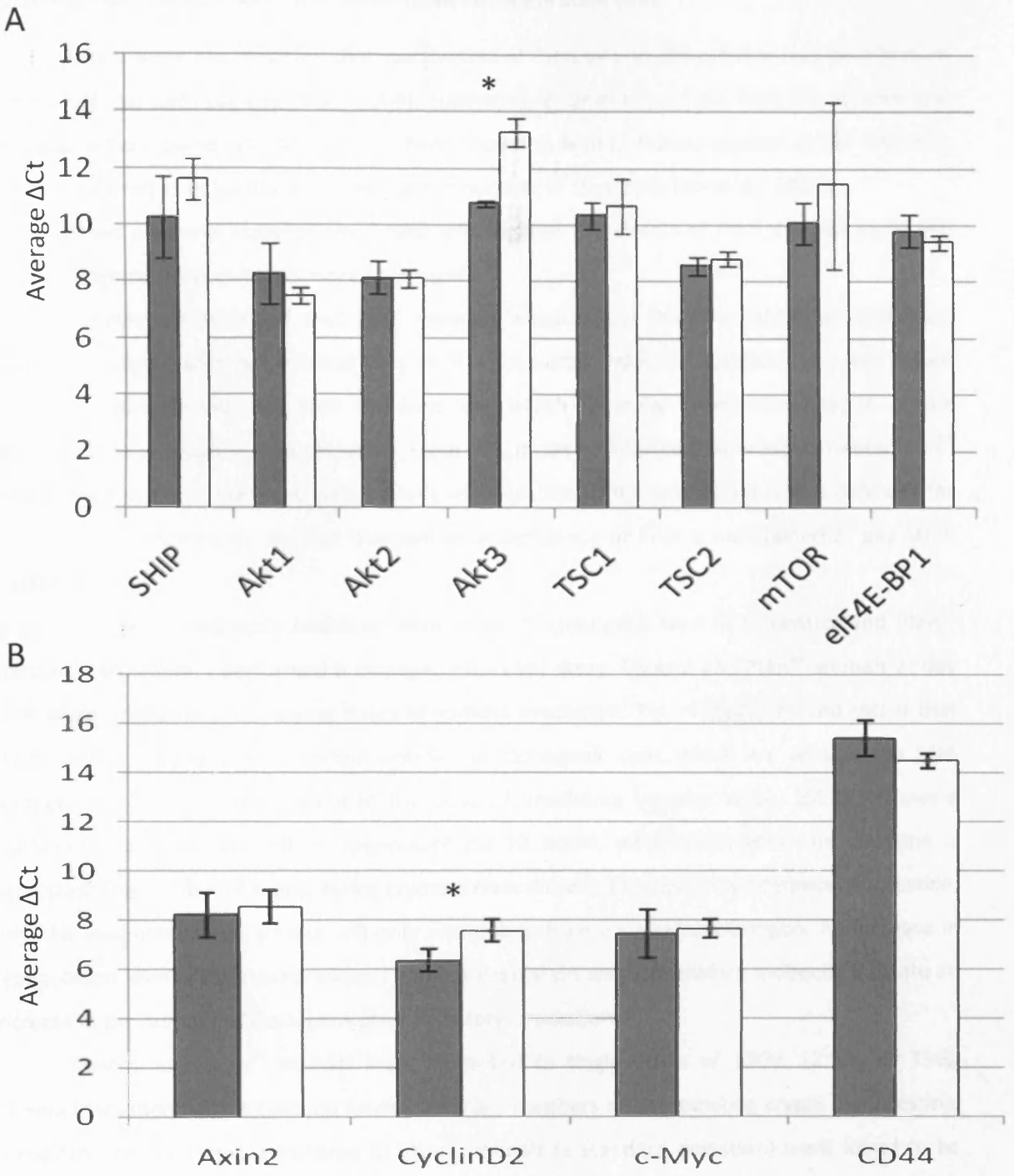

Figure 3.15: ***Q-PCR analysis of PI3K/Akt pathway components and Wnt signalling components in Pten-deficient intestinal epithelium***

Quantitative real-time PCR was used to examine transcriptional activation of the PI3K/Akt pathway (A) and of the Wnt pathway (B) in epithelial-enriched tissue samples of control (grey bars) and $Pten^{f/f}$ (open bars) mice at day 50 PI. Expression PI3K/Akt pathway components (A) was generally found to be unchanged following Pten loss, with the exception of Akt3, which was significantly downregulated in Pten-deficient epithelium compared to controls (Mann-Whitney U test, $p<0.01$). Expression of Wnt target genes Axin2, c-myc and CD44 were found to be unchanged in the context of Pten deficiency (B), whereas CyclinD2 expression was significantly reduced in the context of Pten deficiency (Mann-Whitney U test, $p=0.08$). Asterisks indicate a significant difference in expression between genotypes.

3.2.10 Pten loss has no effect on multiplicity of intestinal stem cells

Recent work has indicated that inactivation of Pten by phosphorylation may be a feature of the intestinal stem cell (He et al., 2004). Furthermore, deletion of Pten from the stromal and epithelial cell compartments has recently been shown to lead to tumourigenesis in the intestine, which is reported as being due to an increase in number of stem cells (He et al., 2007).

Based on these observations, I next investigated the effects of Pten deletion upon the stem/clonogenic cell population more thoroughly.

I previously described that LacZ reporter assays show that the intestinal epithelium remains populated with recombined cells at 100 days after induction (Section 3.3.1 and Figure 3.1). This indirectly indicates that the stem cell which normally drives repopulation of the epithelium has undergone recombination. From this, it can be inferred that in experimental $Pten^{f/f}$ tissues, the functional stem cell which drives repopulation of the epithelium is also deficient for Pten. This is confirmed by the fact that epithelial deficiency of Pten is maintained at day 50 PI (Section 3.3.2).

In order to indirectly examine the number of clonogens present in control and $Pten^{f/f}$ intestinal epithelium, I performed a clonogenic survival assay. Control and $Pten^{f/f}$ animals at day 50 PI were irradiated with varying doses of gamma-irradiation. The rationale behind this is that crypts will be 'cleansed' of a certain number of clonogenic cells, which are sensitive to DNA damage, in a manner proportional to the dose of irradiation (Hendry et al., 1992). Following irradiation, intestines are left to repopulate for 72 hours, after which time the intestine is harvested. The number of repopulating crypts is then scored per radial circumference of intestine, with the assumption that a crypt will only repopulate from a surviving clonogen. An increase in repopulation levels at the same dose of gamma irradiation would therefore indirectly indicate an increase in the number of clonogens present before irradiation.

Control and $Pten^{f/f}$ animals were subjected to single doses of 10Gy, 12.5Gy or 15Gy gamma-irradiation from a caesium source. Average numbers of repopulating crypts per intestinal circumference in controls compared to $Pten^{f/f}$ animals (± standard deviation) were found to be 117.44±10.25 Vs 109.92±1.24 at a dose of 10Gy, 94.41±11.17 Vs 101.06±7.89 at a dose of 12.5Gy and 58.13±14.79 Vs 52.13±7.87 at a dose of 15Gy. At all doses, no significant difference in the numbers of repopulating crypts was observed (Mann-Whitney U test, for all comparisons $n \geq 4$, $p \geq 0.31$) (Figure 3.16). Contrary to previous data, this therefore indicates that the number of clonogenic cells present in Pten-deficient epithelium is not significantly different from that in control epithelium.

To further explore any changes in the intestinal stem cell population following Pten deletion, I then examined the expression of a number of putative stem cell markers.

Nuclear localisation of the Wnt effector beta-catenin has previously been mooted as a marker of the intestinal stem cell. Further, localisation of beta-catenin is thought to be controlled by the Akt pathway, with increased Akt signalling resulting in increased nuclear beta-catenin, which drives stem cell renewal (He et al., 2007). To investigate this in the model presented here, IHC against beta-catenin was used to examine the subcellular localisation of beta-catenin in control and $Pten^{f/f}$ tissue samples at day 50 PI. Staining patterns revealed predominantly cytoplasmic and cell-surface localisation of beta-catenin in epithelial cells of the crypt in both control and $Pten^{f/f}$ tissues (Figure 3.17A). In both genotypes, occasional cells were observed at the very base of the crypt which showed strong nuclear localisation of beta-catenin. These cells may represent clonogenic cells, but may equally be paneth cells. Regardless of this, the staining patterns observed in control and $Pten^{f/f}$ intestines were indistinguishable, indicating that nuclear localisation of beta-catenin is not affected by epithelial-specific deletion of Pten.

Recent data has proposed that DCAMKL-1 is a potential marker of the intestinal stem cell (May et al., 2008). IHC against DCAMKL-1 was performed on intestinal tissue sections of control and Pten-deficient tissue at day 50 PI. In both genotypes, a number of cells stained positively for DCAMKL-1 which were located on the villus, and morphologically appeared to be enteroendocrine cells. However, a small number of cells were also observed to stain within the crypt, at approximately position +4 above paneth cells. Presumably, it is this population of cells which *May et al.* identified as being the intestinal stem cell. DCAMKL-1 staining patterns within the crypt were identical in Pten-deficient intestines compared to controls, again indicating no expansion of the intestinal stem cell population, or at least no expansion in DCAMKL-1-positive cells (Figure 3.17B).

Finally, Q-PCR was used to analyse expression patterns of other recently proposed stem cell markers in Pten proficient compared to Pten deficient tissue. As previously, epithelial-cell enriched tissue samples were used to generate cDNA for analysis. Q-PCR directed at the putative stem cell markers Musashi-1 (Potten et al., 2003), Bmi1 (Sangiorgi and Capecchi, 2008) and Lgr5 (Barker et al., 2007) was performed. Average cycle times needed for amplification of products in control compared to $Pten^{f/f}$ samples (± standard deviation) were: 14.89±1.67 Vs 16.52±0.86 for Musashi-1, 11.13±1.17 Vs 11.23±0.16 for Bmi1 and 14.22±0.50 Vs 15.25±1.23 for Lgr5 (Figure 3.17C). In no instance was a significant difference in expression of any of these markers detected in $Pten^{f/f}$ compared to control tissue (Mann-Whitney U test, n=3, $p \geq 0.38$). Again, this indicates that there is no significant expansion of the stem cell compartment in Pten-deficient tissue compared to controls. These data are therefore at odds with published data, in that I show that deletion of Pten from the epithelial cell compartment (and from the clonogens maintaining the epithelium) does not result in an increase in the number of clonogenic cells or in putative stem cells within the intestine.

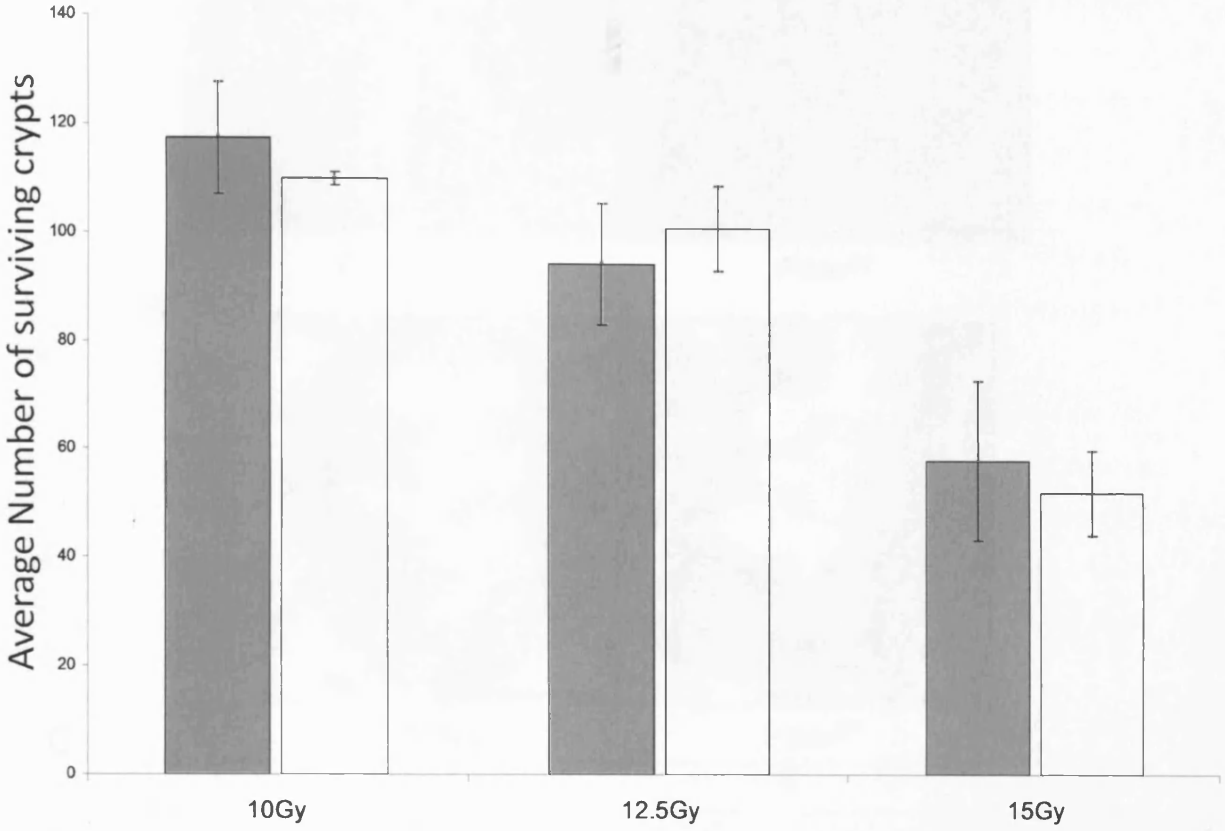

Figure 3.16: ***Clonogenic survival assay reveals no difference in epithelial repopulation following gamma-irradiation in the context of Pten deficiency***

Control (grey bars) and $Pten^{f/f}$ (white bars) animals at day 50 PI were subjected to varying doses of gamma –irradiation (10, 12.5 or 15Gy) in order to ablate clonogenic cells from the intestine. Animals were culled 3 days after exposure, and repopulation of the epithelium assessed by quantification of the numbers of repopulating crypts. No significant difference in numbers of surviving crypts was observed between control and experimental mice across all doses of irradiation (Mann-Whitney U test, $p>0.31$ for all comparisons), indirectly indicating that the number of clonogens in Pten-deficient intestines is the same as that in controls. Error bars indicate standard deviation.

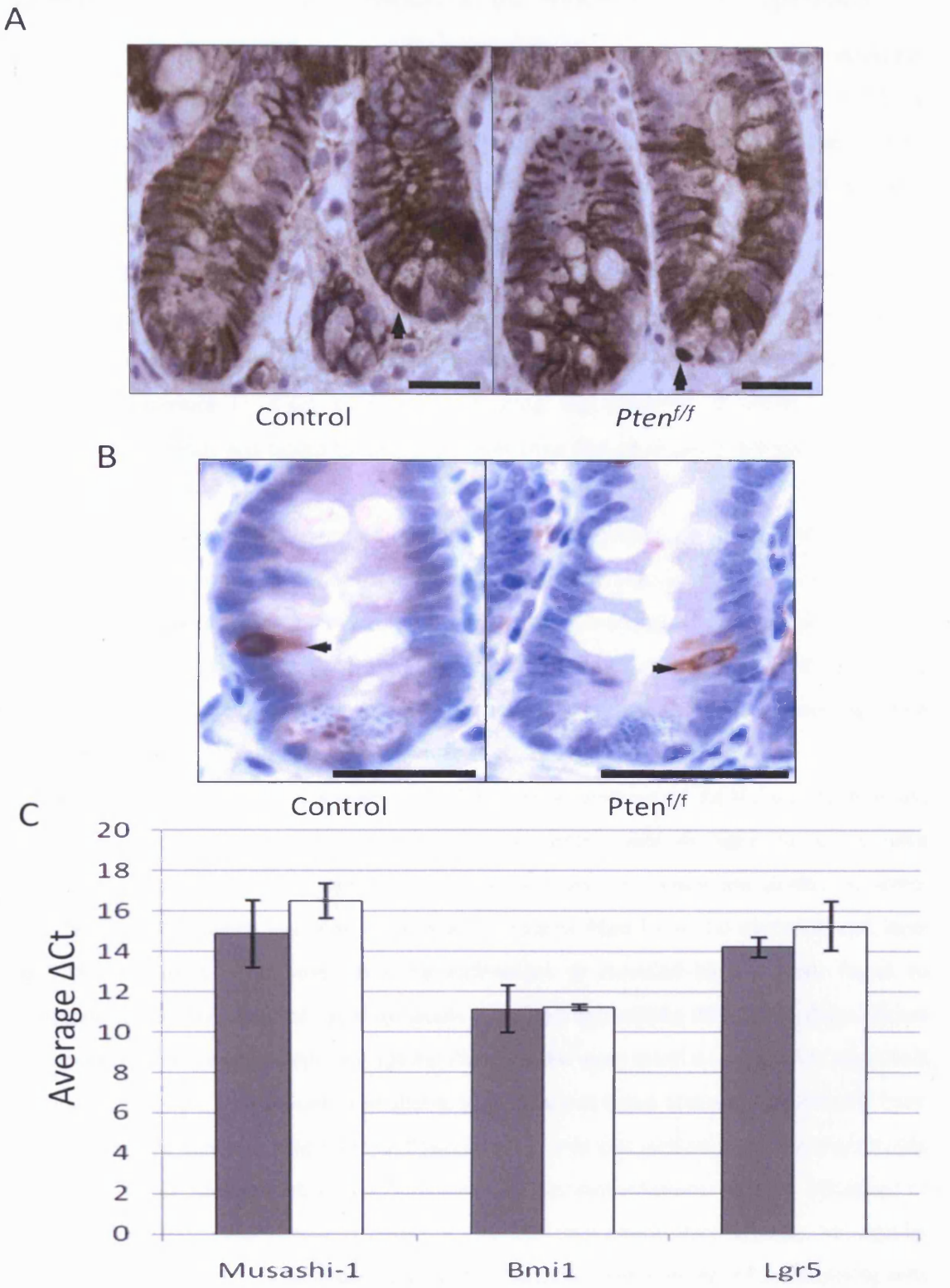

Figure 3.17: ***No difference in expression of putative stem cell markers following Pten loss***
IHC for nuclear beta-catenin (A) and DCAMKL-1 (B) was performed on tissue sections from control and Pten$^{f/f}$ mice at day 50 PI to assess stem cell numbers. No difference in staining patterns between control and Pten$^{f/f}$ tissue was observed. Scale bars indicate 100µm. Quantitative real-time PCR on control (grey bars) and Pten$^{f/f}$ (white bars) epithelial-enriched tissue samples at day 50 PI revealed no significant difference in expression of the putative stem cell markers Musashi-1, Bmi1 or Lgr5 (Mann-Whitney U test, $p>0.38$). Error bars indicate standard deviation.

3.2.11 Pten is not required for normal embryonic development of the intestinal epithelium

In order to assess a potential role for Pten during development of the intestinal epithelium, a number of control and $Pten^{f/f}$ animals were induced *in utero* at day E12.5 by treatment of pregnant females with beta-naphthoflavone. After birth, control and $Pten^{f/f}$ pups were aged to approximately 50 days before being culled and intestines examined. In no cases were any lesions of the intestine apparent macroscopically at dissection.

The LacZ reporter construct was used as previously described in order to confirm that recombination occurred within the intestine of experimental $Pten^{f/f}$ pups when induced *in utero*, and that recombined cells remained present in the adult intestine. Intestines were found to stain blue following exposure to X-gal substrate, indicating the presence of recombined cells. Recombination frequency was noted to be much lower than that observed in animals induced as adults (Figure 3.18A).

Many of the phenotypes observed in $Pten^{f/f}$ animals induced as adults were also found to be present in animals induced during development, including hepatomegaly, susceptibility to lymphoma and behavioural defects. In addition to this, $Pten^{f/f}$ *in utero*-induced animals were also found to have a more shaggy, ruffled appearance to their coat compared to controls (Figure 3.18B). This is again a previously reported phenotype of Pten deficiency, resulting from recombination occurring within the skin (Backman et al., 2004).

IHC against Pten protein was used to confirm that recombination did indeed result in loss of Pten protein from the epithelium. As previously, control animals were found to have widespread staining for Pten in all cell layers of the intestine. In comparison to this, *in utero*-induced $Pten^{f/f}$ animals were found to show specific loss of Pten from the epithelial cell layer (Figure 3.18C). Levels of Pten loss from the epithelium as assessed by IHC were found to approximately reflect the level of recombination identified by staining for LacZ activity. Tissue sections stained immunohistochemically against Pten protein were used to microscopically assess the histological structure of Pten-deficient tissue. Pten deficient tissue was indistinguishable from surrounding tissue which was wild-type for Pten staining, and was indeed also indistinguishable from intestinal tissue samples obtained from controls. No perturbations in gross structure or organisation of the epithelium were apparent in Pten deficient tissue. Furthermore, IHC against the proliferation marker Ki67 was used to examine the location and numbers of proliferating cells in tissue which had lost Pten during development and that which had remained proficient for Pten (Figure 3.18D). The proliferative compartment was found to be correctly localised and of approximately the correct size in tissue deficient for Pten in comparison to controls.

These data therefore indicate that Pten is not needed for normal embryonic development of the intestinal epithelium from day E12.5 of life. Loss of Pten *in utero* does not result in any perturbation in intestinal structure or proliferation status of cells in the adult animal.

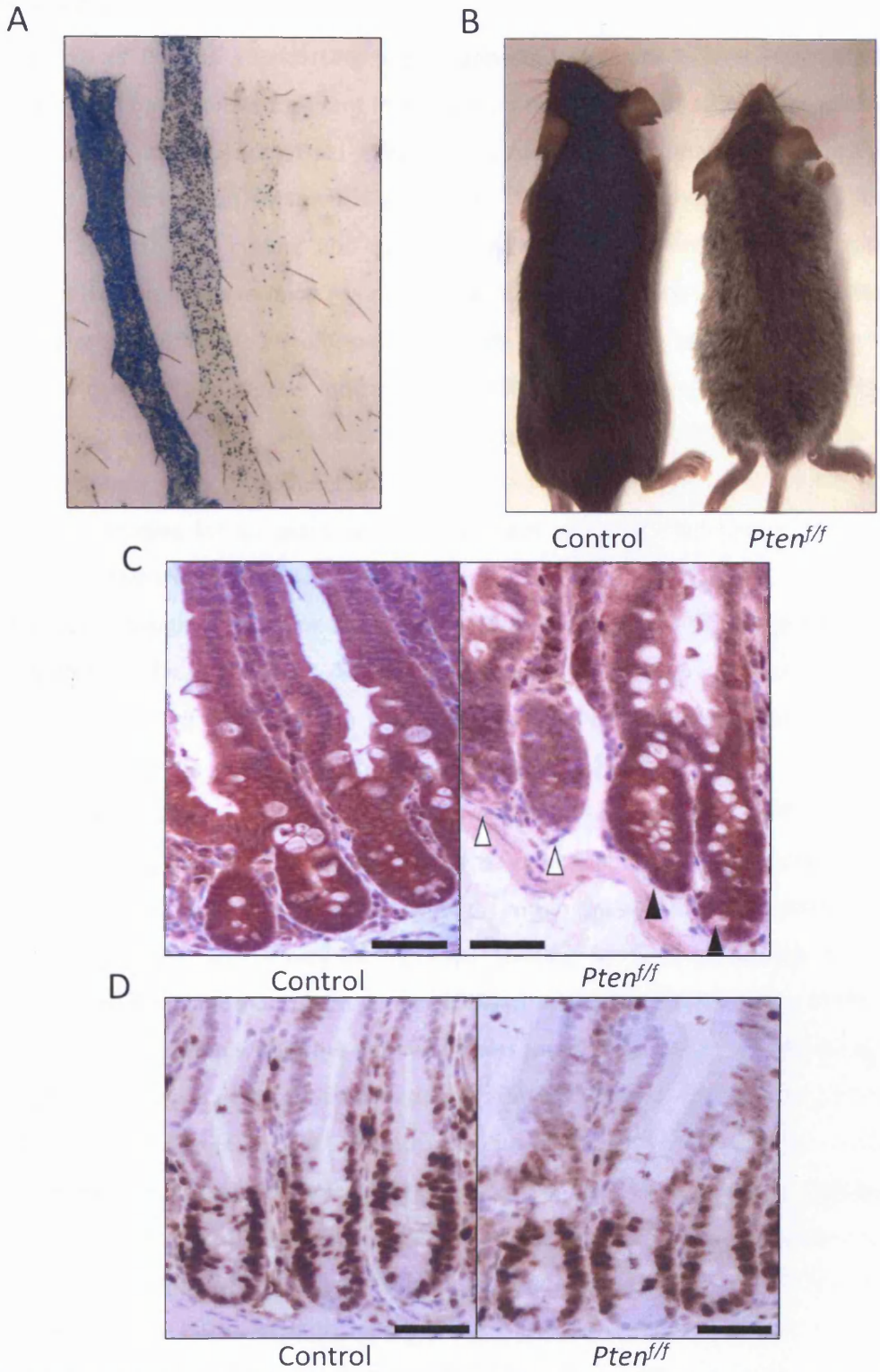

Figure 3.18: ***Loss of Pten during development of the intestine does not perturb epithelial structure***
Induction of Pten loss *in utero* at day E14.5 was used to determine a role for Pten in development of the intestinal epithelium. The LacZ reporter (A) reveals recombination levels much lower than that in mice induced as adults. In addition to the phenotypes outside the intestine previously reported, *in utero* induced Pten$^{f/f}$ mice were also observed to have a shaggy coat compared to controls (B). IHC against Pten was used to confirm loss of Pten protein from the epithelium (C). Staining patterns reflect the lower rate of recombination, with a large number of Pten-proficient (solid arrows) as well as Pten-deficient (open arrows) crypts present in Pten$^{f/f}$ mice. Histology and IHC against Ki67 (D) revealed no changes in the structure of the intestine or organisation of the prolifertive zone in Pten$^{f/f}$ animals. Scale bars indicate 100μm.

3.3 Discussion

The role of Pten in suppressing tumourigenesis in humans is well established, being originally identified based on its frequent mutation in a number of sporadic malignancies (Li and Sun, 1997, Li et al., 1997, Steck et al., 1997). Pten exerts its anti-tumourigenic effect through antagonism of Akt activation (Maehama and Dixon, 1998), the normal effect of which is to promote cell survival, cell cycling and growth (Vivanco and Sawyers, 2002). Heterozygous inactivation of the *Pten* gene in mice has confirmed its role as a tumour suppressor gene *in vivo* (Podsypanina et al., 1999, Di Cristofano et al., 1998, Suzuki et al., 1998). This, together with evidence from other *in vivo* studies indicates that Pten suppresses neoplasia specifically within the intestine (Lu et al., 2007, He et al., 2007). These lines of evidence therefore provide compelling evidence that Pten functions to suppress tumourigenesis within the intestine. However, these studies fail to examine the differential effect of Pten loss from distinct cell compartments within the intestine.

I therefore sought to examine the effects of Pten in the adult murine intestine, specifically from the epithelial cell compartment. To achieve this, a Cre-LoxP-based approach was employed, using LoxP-targeted *Pten* alleles and an inducible form of Cre recombinase which directs high-level recombination to the intestinal epithelium (Ireland et al., 2004).

Following generation of $Pten^{f/f}$ and control animals, I first set about confirming that Pten is deleted from the intestinal epithelium following induction of Cre recombinase activity by treatment with beta-naphthoflavone. Recombination within the intestine was assessed using the ROSA26 reporter allele, and visualised by X-gal staining for beta-lactosidase activity. This confirmed that recombination occurs in almost 100% of epithelial cells regardless of Pten status. Furthermore, recombination within the epithelium was found to be stable, with recombined cells populating the crypt-villus at extended timepoints after induction of Cre activity. This indicates firstly that recombined cells are not deleted from the epithelium, and secondly that the stem cell(s)/clonogens responsible for normal repopulation of the epithelium has undergone the recombination event. Loss of Pten protein in $Pten^{f/f}$ animals following induction of recombination was also confirmed, both by IHC and by western analysis. IHC on tissue sections revealed near-100% loss of Pten from the epithelium, consistent with the level of recombination indicated using the LacZ reporter construct. Western analysis on proteins obtained from tissue samples enriched for epithelial cells further supported the fact that induction results in loss of Pten protein from the epithelium. Finally, Q-PCR analysis of epithelial-enriched samples indicated a significant reduction in levels of Pten expression in the intestine following recombination. This therefore clearly indicates that, following induction, efficient recombination occurs within the intestinal epithelium, which results in rapid loss of both *Pten* transcript and Pten protein.

I also report that, in $Pten^{f/f}$ animals, a number of phenotypes were manifest in tissues outside the intestine. All of the observed phenotypes are previously reported consequences of Pten loss, including hepatic steatosis (Horie et al., 2004, Stiles et al., 2004), predisposition to lymphoma (Lu et al., 2007, Suzuki et al., 1998, Podsypanina et al., 1999, Di Cristofano et al., 1998) and endometrial hyperplasia (Lu et al., 2007, Podsypanina et al., 1999). Whilst these observations are not novel, they serve to confirm that the targeted Pten allele is truly a null allele, and that recombination driven by this system in other tissues results in a clear effect upon phenotype consistent with that previously observed.

3.3.1 Epithelial Pten is not required for normal intestinal homeostasis

Having established that the Pten allele in use here is a true null allele, and that Pten is lost from the intestinal epithelium in $Pten^{f/f}$ animals, I next set out to examine the effect of Pten loss on normal intestinal homeostasis. As Pten is the principal negative regulator of the PI3K/Akt pathway, one could predict that Pten loss would result in activation of this pathway, which would result in increased proliferation and inhibition of apoptosis in the epithelium.

In contrast to this hypothesis, I report here that deletion of Pten from the epithelium has no dramatic effect upon homeostasis up to 50 days after induction. No perturbations in gross histology were identified, and no change in proliferative status was observed, either from anti-Ki67 IHC or from scoring of mitotic index from H&E-stained sections. Levels of apoptosis were unchanged in Pten-deficient tissue, even after irradiation, despite the fact that Pten is implicated in maintaining stability of the pro-apoptotic factor, p53 (Freeman et al., 2003). Qualitative and quantitative analysis of the normal differentiation program of epithelial cells revealed that the presence, location and frequency of mature cell types was unaffected by Pten loss. Finally, analysis of the migratory ability of Pten-deficient epithelial cells revealed no dramatic alteration in migration. Work in cell culture has indicated that Pten functions as a suppressor of cell migration (Gu et al., 1999). In agreement with this, I do report a slight increase in migration of Pten-deficient cells at day 50 PI. However this effect is relatively subtle, and is not observed at day 5 PI despite the fact that I have shown the epithelium to be deficient for Pten at this timepoint. This suggests that the observed increase in migration may be an experimental artefact.

Having observed no dramatic phenotype in Pten-deficient tissues I next investigated the activation status of Akt and its downstream targets. Western analysis revealed that Akt was indeed activated by phosphorylation following Pten loss, as indicated by increased levels of both $pAkt^{Thr308}$ and $pAkt^{Ser473}$ at day 50 PI. However, IHC against the downstream targets of Akt, phospho-mTOR and phospho-S6 Kinase, revealed no increase in activation. Q-PCR analysis was used to examine any effects on expression of PI3K/Akt pathway components, though no

significant changes were observed. Finally, as Pten has previously been proposed to control activity of the Wnt pathway in the intestine through activated Akt (He et al., 2004), I examined activity of the Wnt pathway by analysing expression of a number of well-characterised Wnt target genes. Expression of each of these targets (Axin-2, CyclinD2, c-myc, CD44) was either found to be unchanged or reduced following Pten loss, indicating no activation of the Wnt pathway in the context of Pten deficiency.

Taken together, these data therefore indicate that, despite the fact that deletion of Pten results in a detectable increase in activation of Akt, this does not translate into any cellular effects. This may imply that a 'threshold' effect operates with respect to Akt activation in the intestine. The observed increase in Akt activity following Pten loss is clearly not sufficient for activation of downstream targets of Akt to occur. It may be the case that simple removal of Pten results in a level of activation of Akt which is below the threshold required for it to have a significant effect upon its targets. This notion also fits with the known role of Pten within the PI3K/Akt pathway. Pten is a 'permissive' tumour suppressor, in that it suppresses activation of the pathway (Maehama and Dixon, 1998) but does not directly activate it. Thus, if the pathway itself is not activated upstream of Pten, it can be imagined that removal of Pten will not have a major effect upon Akt activity. Thus, if Akt pathway activity is normally low within the intestinal epithelium (as is likely to be the case based on western analysis of $pAkt^{Thr308}$ and $pAkt^{Ser473}$ levels in control tissue), removal of Pten is unlikely to have any cellular effects. This means that the tumour suppressive function of Pten will only become relevant in a PI3K/Akt pathway-activated environment.

3.3.2 Pten loss in the epithelium does not alter stem cell number or result in immediate tumourigenesis

Evidence from the literature indicates that Pten plays a role in stem cell maintenance in a number of tissues, including the prostate (Wang et al., 2006), lung (Yanagi et al., 2007) and haematopoietic system (Zhang et al., 2006). Recent data has suggested that the intestine is no exception, with Pten reported to control multiplicity of the intestinal stem cell. He et al. (He et al., 2007) report that conditional deletion of Pten from the epithelial and stromal cell compartments of the adult murine intestine results in an increase in stem cell number, which in turn causes polyp formation in the intestine within 3 months following Pten loss. Based on these data, it would therefore be predicted that, in the model I present here, deletion of Pten will cause an expansion of the stem cell population within the crypt, and will result in tumourigenesis.

To address these predictions, I first determined whether any increase in intestinal stem cell number was evident following Pten loss. Firstly, I performed a clonogenic assay in order to

indirectly determine the relative number of clonogenic cells in Pten-deficient tissue compared to control tissue. This showed that there was no alteration in repopulation of the epithelium following irradiation, indicating no change in the number of clonogens in Pten-deficient tissue. The caveat with this experimental approach is that it is not a direct method for examination of stem cell number. Given that recent work has identified a number of good candidate markers of the ISC, I next attempted to examine the effect of Pten deletion upon the stem cell compartment more directly. Nuclear beta-catenin has been proposed as a marker of the ISC, and has been suggested to drive stem cell replication through activity of the Wnt pathway, mediated by inactivation of Pten (He et al., 2004). Based on this data, I would therefore expect to see an increase in nuclear beta-catenin-positive cells following Pten loss. However, in Pten-deficient tissue I observe no change in staining pattern compared to control tissue, indicating that this notion does not hold true in this model. Another recently proposed marker of the intestinal stem cell is DCAMKL-1, which labels occasional cells at position +4 within the crypt (May et al., 2008). IHC against DCAMKL-1 revealed no alteration in distribution or increase in number of positively-labelled cells in the crypts of Pten-deficient tissue compared to controls, again indicating no effect upon the stem cell compartment. Finally, Q-PCR was used to assess the expression of a number of other proposed ISC markers; Musashi-1 (Potten et al., 2003), Bmi1 (Sangiorgi and Capecchi, 2008) and Lgr5 (Barker et al., 2007). This indicated again that no significant increase in expression of these reportedly stem cell-specific genes was observed in Pten-deficient epithelium, confirming no expansion of the stem cell population.

These observations are compelling evidence for the fact that epithelial Pten deletion does not modulate the stem cell compartment in the intestine. However, they are also clearly at odds with the recently published study of *He et al.* (2007). In their study, *He et al.* use the Mx1-Cre construct to drive deletion of Pten from the adult intestine. Although not clearly stated in their paper, previous work has shown that Mx1-Cre drives recombination both in the epithelial and stromal cell populations within the intestine (Schneider et al., 2003). This experimental approach is therefore different to that presented here, as I have used the AhCre construct to drive Pten deletion, the expression of which is tightly restricted to the epithelial cell layer (Ireland et al., 2004). Together, the data published by *He et al.* and the data presented here indicate a differential role for Pten in regulation of the stem cell compartment and suppression of tumourigenesis depending upon the cell type it is lost from. Epithelial-specific deletion of Pten has no immediate effect upon intestinal stem cell homeostasis or susceptibility to tumourigenesis, whereas deletion of Pten from both the epithelium and underlying stroma causes stem cell expansion and rapid tumourigenesis (See Figure 3.19).

What remains unclear from these studies is whether stromal deficiency of Pten alone is sufficient for perturbation of the stem cell niche, or whether the stem cell itself and/or its

surrounding epithelial cells must also be Pten-deficient to allow manifestation of the observed phenotypes. Several lines of evidence have recently indicated that tissue-specific deletion of tumour suppressor genes outside of the epithelial cell population (and indeed, outside of the intestine) can have a profound effect upon homeostasis of intestinal epithelial cells themselves. *Kim et al.* (2006) have previously reported that, whilst deletion of the tumour suppressor SMAD4 from the intestine itself has no effect upon intestinal homeostasis, deletion specifically from T-cells results in rapid intestinal polyposis. This is found to occur in intestinal tissue which is shown to remain wild-type for SMAD4. It is therefore clear that aberrant signalling originating in infiltrating immune cells can have a significant impact upon normal epithelial and/or stromal cells. Furthermore, a very recent paper from Tomi Mäkelä's group has investigated the effects of mesenchymal-specific deletion of the tumour suppressor gene Lkb1/STK11 (Katajisto et al., 2008). They have specifically deleted Lkb1 from intestinal smooth muscle cells, but not from intestinal epithelial cells. Mesenchymal Lkb1 deletion is shown to cause in an increase in SMAD signalling within the stroma, which in turn causes increased proliferation in overlying epithelial cells. This results in polyp formation similar to that observed in constitutive $Lkb1^{+/-}$ mice. This argues for the fact that the loss of heterozygosity (LOH) event which initiates intestinal tumour formation in $Lkb1^{+/-}$ mice may actually occur within a mesenchymal cell, and not necessarily in an epithelial cell.

Parallels between this data and the information available for Pten in intestinal tumourigenesis can be drawn. Intestinal cancer has been shown to be a feature of constitutive $Pten^{+/-}$ mice (Di Cristofano et al., 1998), yet I report here that epithelial-specific deletion of Pten does not perturb the intestine. This suggests that the tumour initiating event in $Pten^{+/-}$ mice may occur within a non-epithelial cell type of the intestine. The data of *He et al.* (2007) would support this being within an underlying stromal cell. Thus, it could be concluded that normal Pten activity (and hence regulated levels of Akt activity) within stromal cells is critically important for both control of intestinal stem cell renewal and also for suppression of intestinal tumourigenesis.

It could also be argued that I did not observe any intestinal tumours here due to a time effect; *He et al.* report tumourigenesis at 3 months following Pten loss, whereas I have only examined mice up to a timepoint of 50 days after induction. In my study, examination of mice older than 50 days was generally not possible due to phenotypes caused by loss of Pten in other tissues. However, in the event that tumourigenesis would have been apparent in my model at extended timepoints after induction, I would expect that perturbation in epithelial homeostasis, early signs of neoplasia and even perhaps even some early lesions would have been evident at day 50 PI. These were never observed, which therefore implies that tumourigenesis is unlikely to occur in this model, even if I was able to age mice up to 3 months after induction.

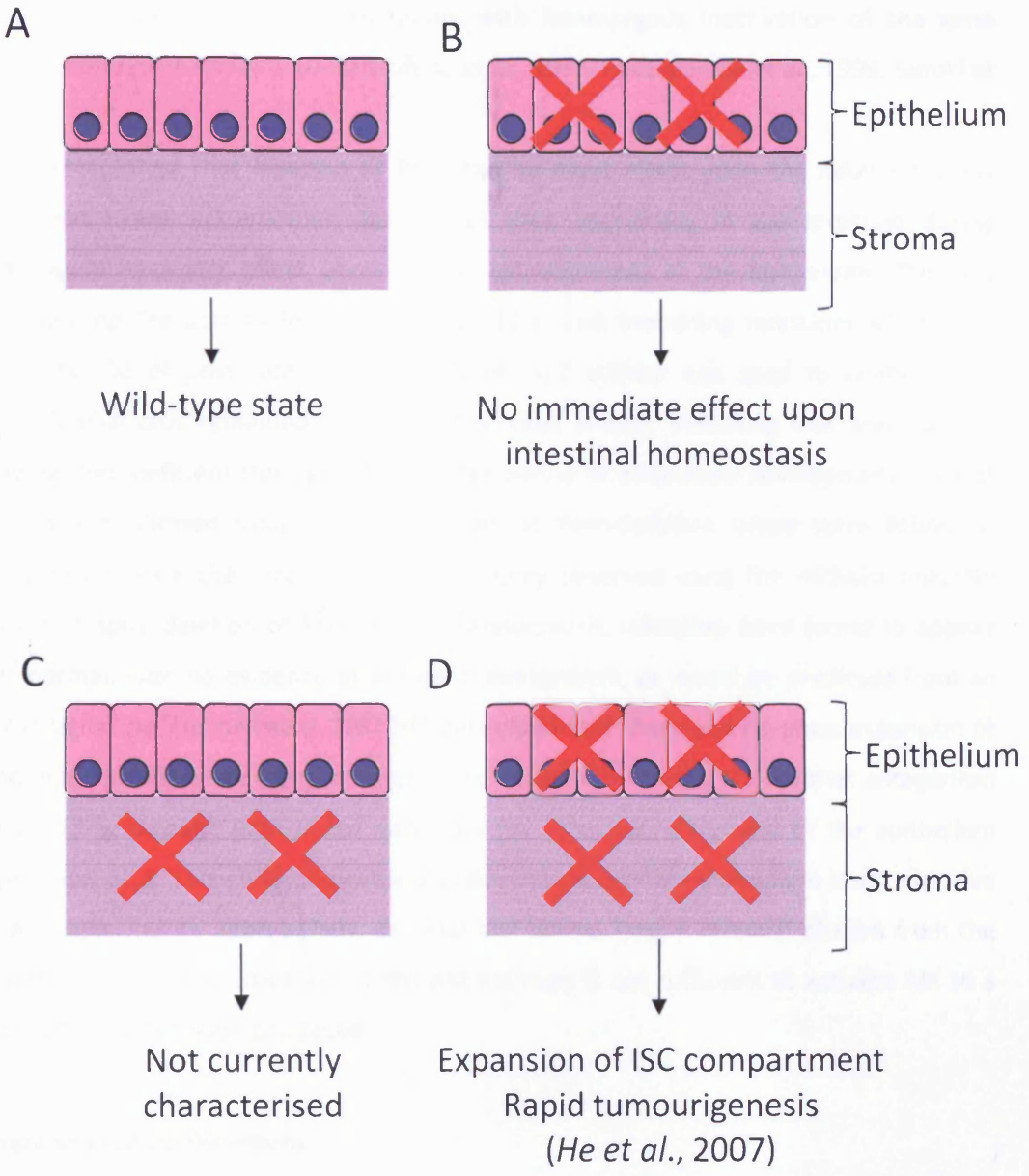

Figure 3.19: ***Epithelial versus Stromal deletion of Pten in the intestine***
Deletion of Pten specifically from the epithelial cell compartment (B) is shown here not to cause a perturbation in intestinal homeostasis compared to the wild-type state (A), and tumourigenesis is not observed up to 50 days after loss of Pten. In contrast to this, *He et al.* (2007) have shown that deletion of Pten from both the epithelial and stromal cell compartments results in an expansion of stem cells within the intestine, which causes rapid tumourigenesis (D). What remains unclear from these studies is whether deletion of Pten from the stroma alone (C) is sufficient to perturb intestinal homeostasis and initiate tumourigenesis.

3.3.3 Pten is not required for *in utero* development of the intestinal epithelium

Many tumour suppressor genes are absolutely required for normal embryonic development, and indeed Pten is no exception, with homozygous inactivation of the gene resulting in early embryonic lethality (Di Cristofano et al., 1998, Podsypanina et al., 1999, Suzuki et al., 1998).

Having established that deletion of Pten has no overt effect upon the adult intestinal epithelium, I next examined whether deletion of Pten specifically in the intestine during development would have any effect upon normal establishment of the epithelium. This was achieved by inducing Cre activity *in utero* at day E12.5, and examining intestines of mice at approximately day 50 of post-natal life. Analysis of LacZ activity was used to confirm that recombined epithelial cells remained present in the adult animal, indicating that areas of the epithelium were Pten-deficient throughout the latter period of embryonic development. Loss of Pten protein was confirmed using IHC, and levels of Pten-deficient tissue were found to approximately recapitulate the recombination frequency observed using the ROSA26 reporter allele. However, despite deletion of Pten during development, intestines were found to appear histologically normal, with no evidence of epithelial overgrowth, as would be predicted from an increase in Akt signalling. Furthermore, Ki67 IHC confirmed that there was no gross expansion or relocalisation in the proliferative compartment of the epithelium. Thus it is clear that antagonism of PI3K/Akt signalling through Pten is not necessary for normal development of the epithelium from embryonic day 12.5. This either indicates that development of the epithelium is not sensitive to levels of Akt signalling, or alternatively, as described above, simple removal of Pten from the epithelium without additional activation of the Akt pathway is not sufficient to activate Akt to a level at which cellular effects are produced.

3.3.4 Summary and Future Directions

In summary, three major conclusions can be drawn from the data I present in this chapter. First, Pten appears to be redundant with respect to epithelial homeostasis and epithelial Pten deficiency does not result in tumourigenesis up to 50 days after induction. Secondly, in contrast to published data, I find that Pten has no overt effect on the intestinal stem cell population. And finally, I find that Pten is not required for normal development of the intestine from day E12.5 of development.

These conclusions raise a number of interesting questions with regard to both Akt signalling in the intestine and regarding the role of Pten in epithelial-stromal interactions and the intestinal stem cell, and provide a number of avenues which warrant further investigation.

My data presented here suggest that a threshold level of Akt signalling must be reached to produce phenotypic consequences within the intestine, and that straightforward removal of Pten is not sufficient for this threshold to be reached. Thus, analysis of the effect of Pten deletion in the context of activated Akt signalling would confirm whether this 'threshold' hypothesis holds true. This could potentially be achieved by activation of the Akt pathway using an exogenous agent, for example insulin or growth factors; however, such agents are likely to have a number of off-target effects. Alternatively, genetic manipulation could be employed to more specifically activate the PI3K/Akt pathway, for instance using constitutively active forms of PI3K itself. Such investigation would reveal whether activation of Akt signalling specifically in the intestinal epithelium will result in any consequences upon normal homeostasis, or whether the intestinal epithelium is refractory to the effects of activated Akt.

Clearly one major caveat of the work I describe here is that I have only analysed the effects of Pten deficiency up to 50 days. Given that tumourigenesis is observed by *He et al.* in their Pten-deficient model at 3 months after Pten loss, examination of intestines at longer timepoints after Pten loss would certainly be warranted in the system I present here. However, as described, this is precluded by the Cre transgene I have used, which also drives recombination in other tissues, causing over-riding phenotypes outside the intestine. In order to circumvent these problems, another transgene expressing Cre recombinase would need to be used, which shows more tightly regulated expression following induction.

The implied phenomenon of stromal loss of Pten initiating stem cell expansion and tumourigenesis in the intestine also needs to be confirmed. This could be unequivocally proven through use of a Cre recombinase which is expressed only within mesenchymal cells of the intestine, such as that used by Katajisto et al. (2008). If this results in tumourigenesis, it would indicate that stromal loss of Pten does indeed provide an initiating event for intestinal cancer. If this does not result in tumourigenesis, then further questions are raised with regard to whether the entire epithelium overlying Pten-deficient stroma also needs to lose Pten for tumourigenesis to ensue, or whether Pten deletion specifically from the intestinal stem cell is sufficient. ISC-specific Pten deletion could potentially be achieved using a transgene expressing Cre driven by the promoter of one of the recently proposed ISC markers, such as Bmi1 (Sangiorgi and Capecchi, 2008) or Lgr5 (Barker et al., 2007).

Finally, the fact that Pten is observed to be mutated in a significant proportion of sporadic cancers, yet apparently plays a less significant role in tumour initiation, suggests that loss of Pten may be a late-stage event in the 'multi-step' model of tumour progression as proposed by Fearon and Vogelstein (Fearon and Vogelstein, 1990). Thus, it would also be pertinent to examine the role of epithelial Pten in an intestinal tumour predisposition model, such as the Apc^{MIN} mouse.

This would allow establishment of Pten as a suppressor of tumour progression rather than tumour initiation within the intestine.

Chapter 4: Analysing the long-term effects of Pten deficiency in the intestine using AhCreER^T

4.1 Introduction

The role of PTEN in suppression of tumourigenesis in the intestine has been well established in a number of transgenic mouse models (Di Cristofano et al., 1998, Lu et al., 2007, He et al., 2007). However, in Chapter 3, I describe work indicating that, surprisingly, loss of Pten from the murine intestinal epithelium does not immediately result in tumourigenesis. I found Pten deletion to have no effect on homeostasis of the epithelium, with respect to gross structure, proliferation, migration and differentiation of cells. Furthermore, I have shown that Pten loss does not alter the epithelial stem cell compartment, as would be predicted from evidence in the literature.

The major caveat in this work was that, due to over-riding phenotypes in tissues other than the intestine, analysis of the effects of very long term Pten loss from the intestinal epithelium was not possible. The most problematic of these phenotypes, forcing premature culling of many AhCre$^+$;Pten$^{f/f}$ animals and precluding analysis of Pten loss past 50 days after induction, was that of behavioural abnormalities and ataxia. This was presumably caused by spontaneous activation of the AhCre transgene and deletion of Pten in the brain during development, as a similar phenotype has previously been reported (Backman et al., 2001).

Background activation of Cre expression is a commonly reported problem with Cre-Lox transgenesis, though has also been exploited as a useful characteristic of the system, delivering low-level recombination to selected tissues, such as the prostate (Pearson et al., 2008). In order to circumvent problems with uninduced expression of transgenes, more tightly regulated forms of Cre recombinase have been developed. One such example of this is the dually-regulated AhCreER^T transgene, the activity of which is controlled both at the transcriptional level and at the post-translational level (Kemp et al., 2004). As with AhCre, transcriptional control is achieved using the inducible CYP1A1 promoter, which is activated in response to exposure to aryl hydrocarbons such as beta-naphthoflavone (Ireland et al., 2004, Campbell et al., 1996). However, in the case of AhCreER^T, this drives expression of a Cre-Estrogen receptor fusion protein. The estrogen receptor domain of the fusion protein, when unbound, sequesters Cre in the cytoplasm, rendering it inactive. The Estrogen receptor is modified such that it binds to the estrogen analog Tamoxifen with high affinity, but does not respond to endogenous estrogens. Exogenous treatment with Tamoxifen is therefore needed to permit entry of Cre into the nucleus and thus allow recombination. As such, problems with uninduced activation of Cre recombinase are avoided.

In this chapter, I aim to make use of this more tightly regulated form of Cre, AhCreER^{T}, in order to examine the effects of Pten loss specifically from the epithelium at timepoints longer than 50 days, the latest timepoint previously examined using AhCre.

4.2 Results

4.2.1 Low-level recombination in the intestinal epithelium following induction of AhCreER^T

Previous reports have indicated that treatment of animals bearing AhCreER^T with both beta-naphthoflavone and Tamoxifen drives expression of cre recombinase within epithelial cells of the intestine (Kemp et al., 2004). In order to ensure that this was the case in the strain of mice I was using, I first generated animals bearing both the AhCreER^T transgene and the ROSA26 LacZ-expressing reporter allele (Soriano, 1999). Animals were induced by treatment with beta-naphthoflavone and Tamoxifen, administered in a combined intraperitoneal injection at a dose of 80mg/kg, which was repeated daily for four consecutive days (Section 2.1.3.3). At day 7 after induction, animals were culled, intestines removed and whole-mounted and subjected to X-gal staining as described (Section 2.2.6). Induced animals bearing both the AhCreER^T transgene and the ROSA26 LacZ reporter allele were found to bear blue-stained epithelial cells within both the crypt and villus of the small intestine, indicating recombination in a proportion of epithelial cells. Animals lacking the AhCreER^T transgene did not show any background blue staining of cells, indicating that recombination had not occured in these tissues (Figure 4.1A). Examination of X-gal stained whole intestines from induced AhCreER^{T+};LacZ$^+$ animals indicated that levels of recombination vary along the longitudinal axis of the intestine. Recombination was observed to occur with the highest frequency at the end of the intestine closest to the stomach, with a gradual decrease in the number of positively-stained epithelial cells along the length of the intestine (Figure 4.1B). At the very distal end of the small intestine and within the colon, recombination within the epithelium was found to be rare, but not absent. Based on these findings, all future analyses performed upon intestines of animals bearing the AhCreER^T transgene were either performed on comparable regions of the small intestine, or else recombination status of the epithelium was first confirmed.

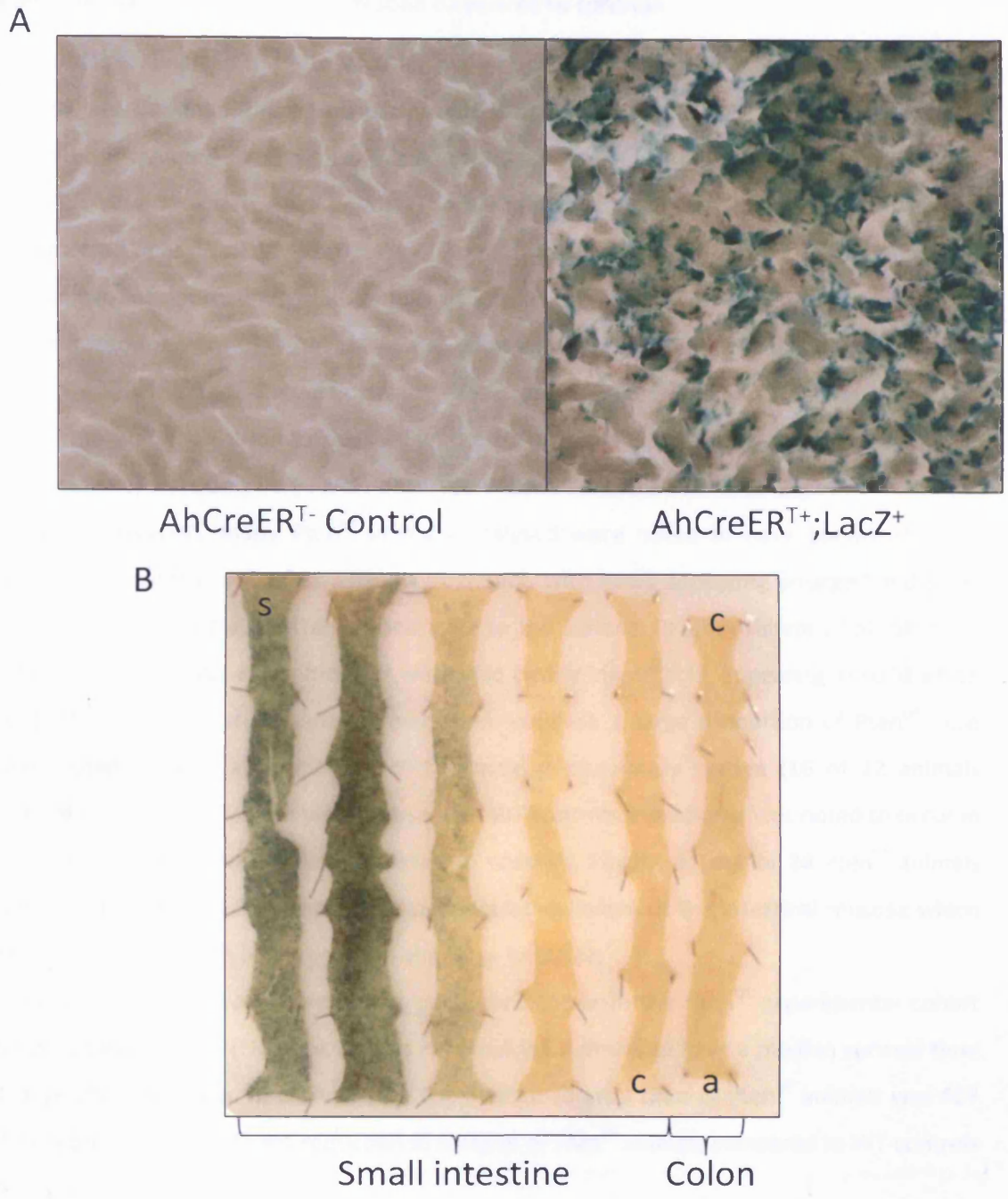

Figure 4.1: ***Analysis of recombination in the intestine driven by AhCreER^{T}***
The ROSA26 LacZ reporter allele was used to confirm that induction of AhCreER^{T} drives recombination within the intestinal epithelium. Animals bearing the AhCreER^{T} and the LacZ reporter transgene were induced by treatment with 4 consecutive daily doses of 80mg/kg beta-naphthoflavone and tamoxifen in one combined intraperitoneal injection. At day 7 PI, recombination was assessed by staining of whole-mounted intestines with X-Gal, which is converted from colourless to blue in recombined cells expressing the LacZ reporter. Levels of recombination were observed to be variable between individual mice, but was typically found to occur in approximately 50% of epithelial cells (A). Mice lacking the AhCreER^{T} transgene did not show any background LacZ activity. Levels of recombination were observed to vary along the intestine of induced mice (B). Recombination was found to be most frequent in the small intestine, in the region proximal to the stomach (S), with levels of recombination decreasing along the length of the small intestine to the end proximal to the caecum (C). Recombination in the colon was noted to be rare, with no change in distribution of recombined regions along the length of the colon from caecum (c) to anus (a).

4.2.2 Pten$^{f/f}$ animals show a reduced lifespan compared to controls

In order to examine the effects of long-term epithelial-specific deletion of Pten, an aging cohort study was designed and performed. Animals bearing the AhCreER^{T} transgene and those bearing the LoxP-targeted Pten alleles (Suzuki et al., 2001) were interbred in order to generate both AhCreER^{T+};Pten$^{f/f}$ experimental animals (herein referred to as 'Pten$^{f/f}$') and AhCreER^{T+};Pten$^{+/+}$ controls (referred to as 'WT'). Large cohorts of Pten$^{f/f}$ (n=30) and WT (n=29) mice were induced as described above, at approximately 10 weeks of age. These mice were then aged, whilst being closely monitored for signs of ill-health. At the point where animals were found to be sick, they were culled and dissected. The majority of Pten$^{f/f}$ animals were found to display abnormal swelling of the abdomen prior to death. Symptoms of intestinal disease (rectal prolapse and bleeding, anaemia) were only very rarely observed in Pten$^{f/f}$ animals before culling.

Upon dissection, many Pten$^{f/f}$ animals analysed were noted to have abnormal livers compared to WT controls (18 of 25 animals analysed), with livers appearing enlarged and pale, and in many cases having a 'spotted' appearance to the surface. In approximately half of these cases, macroscopic lesions within the liver were also clearly identifiable, appearing as solid white masses (9 of 18 animals which showed liver abnormalities). A large proportion of Pten$^{f/f}$ mice were also noted to bear abnormalities of the male genitourinary system (16 of 22 animals analysed), of which similar lesions were not seen in WT controls. Lymphoma was noted to occur in one Pten$^{f/f}$ animal, which was never observed in controls. Finally, 11 out of 24 Pten$^{f/f}$ animals analysed were noted to bear macroscopic, pedunculated lesions of the intestinal mucosa which were found to be present in both the small and large intestine.

Kaplan-Meier survival analysis was performed for both the Pten$^{f/f}$ experimental cohort and the WT control cohort (Figure 4.2). This revealed WT animals to have a median survival time of 801 days after induction. In comparison, the median survival time of Pten$^{f/f}$ animals was 407 days. This represents a significant reduction in lifespan of Pten$^{f/f}$ animals compared to WT controls ($p<0.001$, $\chi^2=54.61$, DF=1).

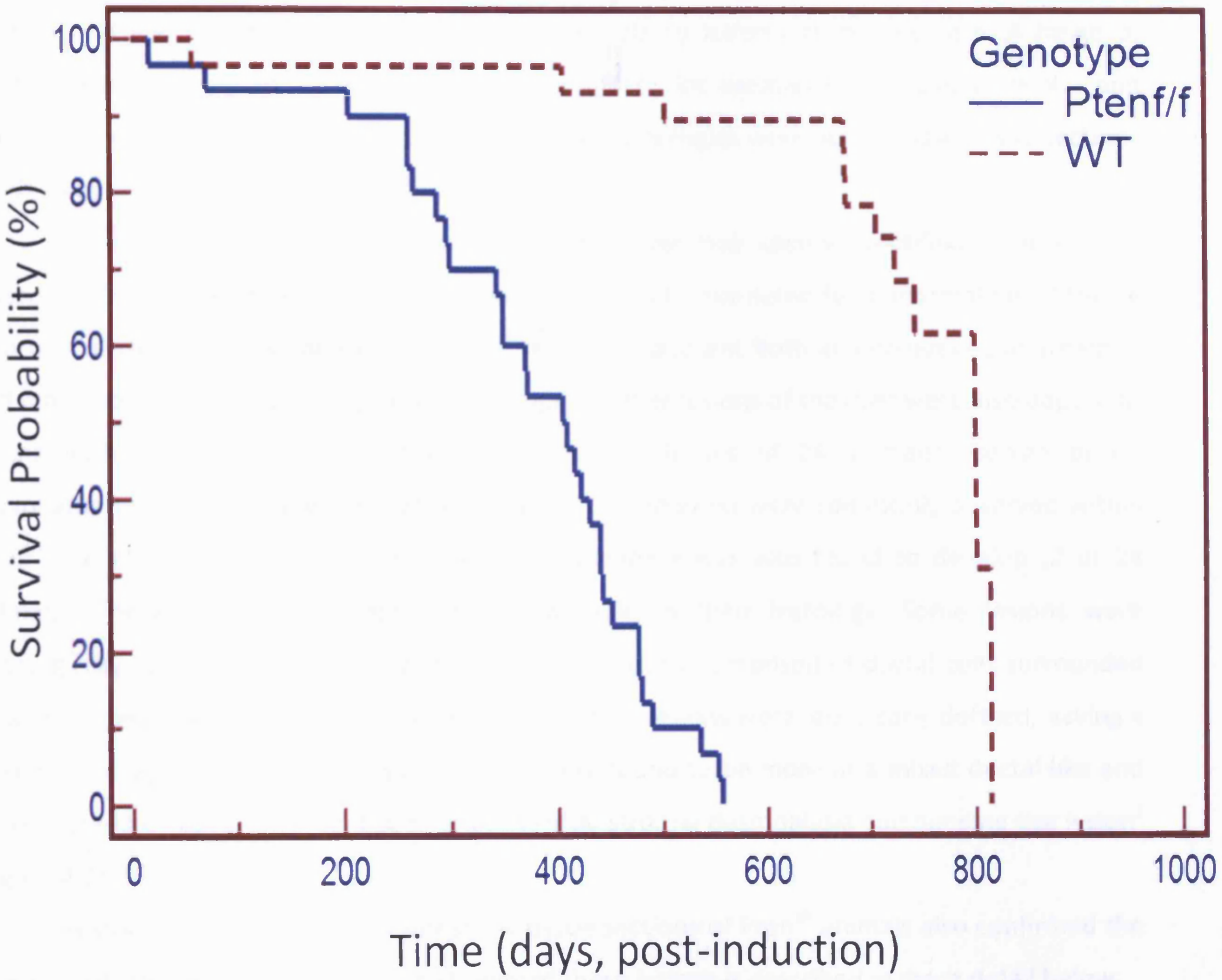

Figure 4.2: ***Reduced survival of Pten$^{f/f}$ animals compared to controls***
Large cohorts of control (WT) and experimental (Pten$^{f/f}$) animals were induced and aged whilst being monitored for signs of disease. Animals were culled when moribund, and Kaplan-Meier survival was performed. Experimental Ptenf/f animals were observed to have a much reduced survival probability compared to controls, and had a reduced median survival time of 407 days compared to that of controls, which was 801 days. Reduction in survival probability in experimental animals compared to controls was found to be highly statistically significant ($p<0.001$, $\chi^2=54.61$, DF=1).

4.2.3 Multiple tissue phenotypes associated with Pten deficiency

Having determined that $Pten^{f/f}$ animals show a reduced lifespan compared to WT controls, and that phenotypes in a number of tissues are present, I next compared tissue sections from control and $Pten^{f/f}$ animals in order to establish the nature of these phenotypes.

Examination of H&E-stained sections of the male genitourinary tract of $Pten^{f/f}$ and WT animals revealed that $Pten^{f/f}$ animals were susceptible to lesions of the prostate. A range of lesions were identified, which included prostate intraepithelial neoplasia (PIN) and adenocarcinoma of the prostate (Figure 4.3). Similar pathologies were not noted in tissue sections of WT mice.

Given that macroscopic assessment of the liver had clearly identified lesions upon dissection, H&E-stained sections of the liver were closely examined for abnormalities. Striking steatosis of the liver was apparent in $Pten^{f/f}$ animals, apparent both as microvesicular steatosis and macrovesicluar steatosis (Figure 4.3). A range of other lesions of the liver were also apparent, arising within epithelial cells of the biliary system (8 out of 24 animals). Benign biliary microhamartoma (also known as Von Meyenberg's complexes) were commonly observed within $Pten^{f/f}$ livers. In a minority of cases, cholangiocarcinoma was also found to develop (2 of 24 animals). These lesions were noted to be variable in their histology. Some lesions were histologically typical of human cholangiocarcinoma, clearly comprised of ductal cells surrounded by a characteristically pale, desmoplastic stroma. Other lesions were less clearly defined, having a mixed histology. Cells comprising such lesions were found to be more of a mixed ductal-like and hepatocyte-like appearance, and bore a less typical stromal desmoplasia surrounding the lesion[2] (Figure 4.3).

Histological examination of intestinal tissue sections of $Pten^{f/f}$ animals also confirmed the presence of intestinal polyposis. The histology of these lesions is described in more detail below.

[2] Characterisation and description of these lesions was kindly provided by Prof Geraint T. Williams, Department of Pathology, University Hospital of Wales, Cardiff University, UK.

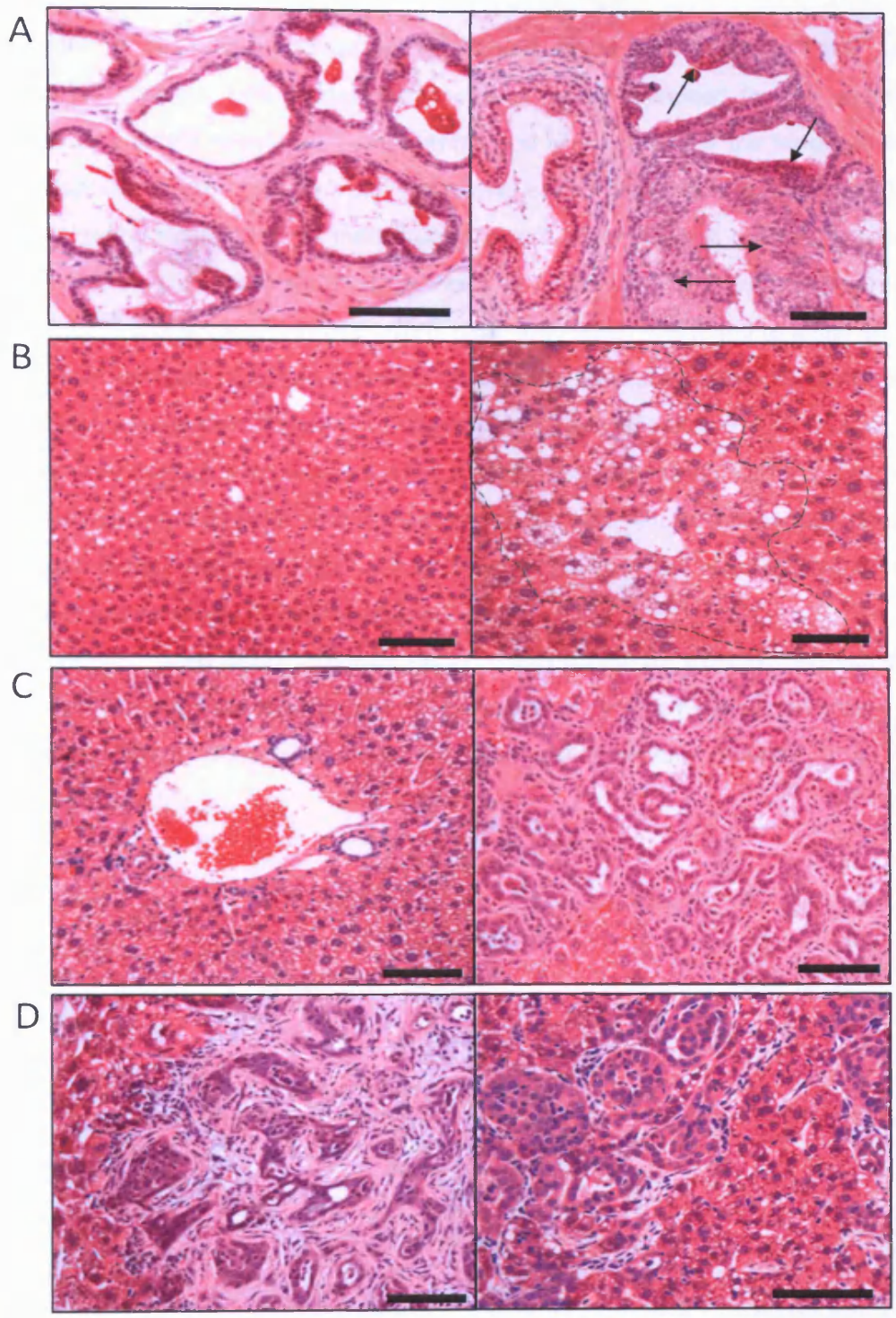

Figure 4.3: ***Aged Pten$^{f/f}$ mice are susceptible to prostate neoplasia, hepatic steatosis and cholangiocarcinoma of varying histology***

In order to assess tissue pathologies outside the intestine in Pten$^{f/f}$ animals, H&E-stained tissue sections of control and experimental animals were compared. Pten$^{f/f}$ animals were found to be susceptible to neoplasia of the prostate (A, Left panel: WT, Right panel: Pten$^{f/f}$, arrows indicate areas of neoplasia), which was not observed in WT controls. Liver steatosis was also common in Pten$^{f/f}$ animals (B, right hand panel, dashed line indicated area of steatosis) compared to controls (B, left hand panel). Lesions of bile duct origins were also noted in Pten$^{f/f}$ livers, which were not noted in control (C, left panel). Types of lesions identified included non-malignant biliary microhamartomas (C, right panel) and cholangiocarcinoma, which presented as two distinct histological forms; cholangiocarcinoma which was histologically typical of that seen in human disease (D, left panel) and that which was atypical of human disease (D, right panel). Scale bars indicate 100μm.

In order to quantify the frequency of various tissue pathologies in $Pten^{f/f}$ animals compared to WT controls, H&E-stained tissue sections were examined for the presence of intestinal lesions, prostate neoplasia, liver steatosis and lymphoma, and the incidence of each lesion type recorded. Microscopically visible intestinal lesions were found to occur in 61.9% of $Pten^{f/f}$ animals, representing 13 of 21 individuals analysed (Figure 4.4). In contrast, just one WT animal was found to have abnormalities of the intestinal epithelium. The most common recorded pathology of $Pten^{f/f}$ animals was that of prostate neoplasia, which was found to affect 90.5% (19 of 20) animals. In contrast, no single incidence of prostate neoplasia was noted in WT controls upon microscopic examination. Steatosis of the liver was also common in $Pten^{f/f}$ animals, 81.0% (17 of 21) showing obvious microscopic evidence of hepatic steatosis. In contrast, just one WT control animal was noted to show limited steatosis of the liver. Finally, microscopic assessment for lymphoma indicated that one $Pten^{f/f}$ animal bore a tumour of this type, and no WT control animals showed any evidence of lymphoma development.

In summary, aged $Pten^{f/f}$ animals show susceptibility to intestinal tumourigenesis, steatosis of the liver accompanied by other liver lesions of varying histology, neoplasia of the prostate and lymphoma. These phenotypes are much less commonly reported in WT control animals of a comparable age.

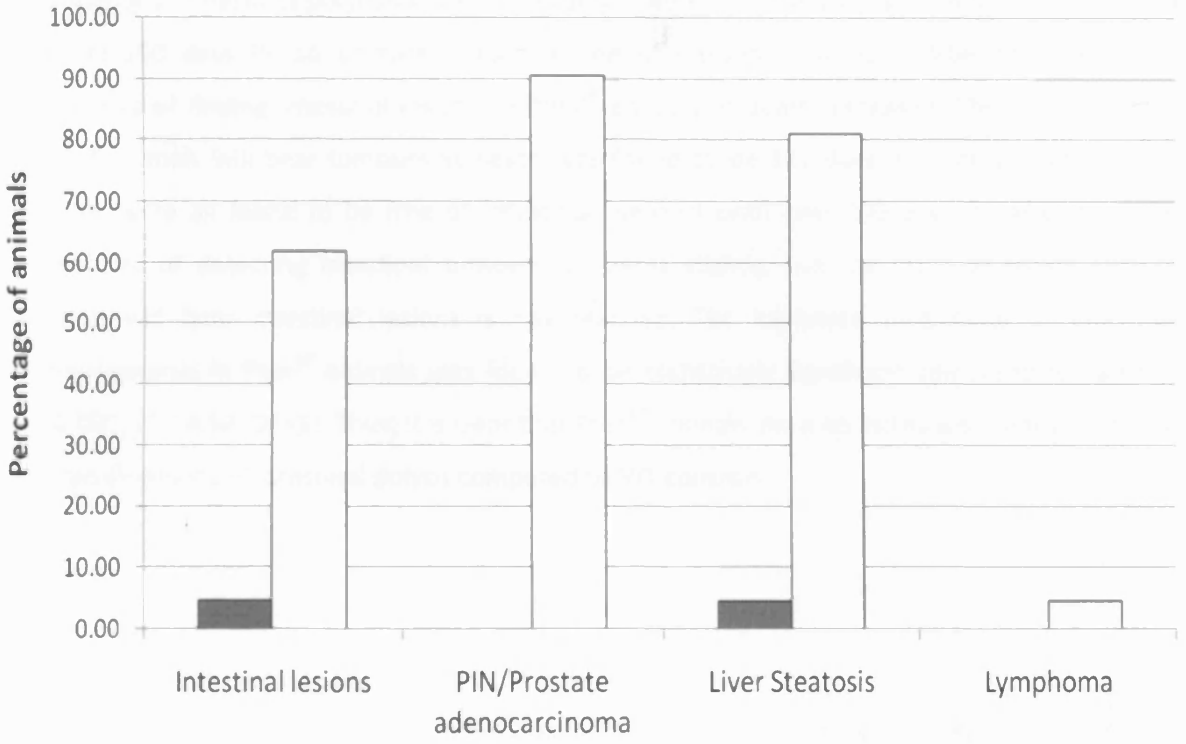

Figure 4.4: ***Pten$^{f/f}$ animals are predisposed to intestinal lesions, prostate neoplasia, liver steatosis and lymphoma***

H&E-stained sections of tissues removed at dissection from aged Pten$^{f/f}$ (white bars) and WT (grey bars) animals were assessed microscopically for any tissue abnormalities. Intestinal lesions, prostate lesions, steatosis of the liver and lymphoma were the most common abnormalities observed. In Pten$^{f/f}$ animals, 61.9% of animals examined (13 out of 21 individuals) were observed to bear intestinal lesions, compared to an incidence of just 4.8% (1 of 21 individuals) in WT controls. Prostate lesions were common in Pten$^{f/f}$ animals, with prostate intraepithelial neoplasia (PIN) being the least severe type of lesion observed. Whilst PIN was not observed in any WT control animals, 19 of 21 Pten$^{f/f}$ animals (90.5%) were observed to show PIN or more severe lesions. Steatosis of the liver was also common in Pten$^{f/f}$ animals, at a frequency of 81.0% (17 of 21 animals), and was much less common in controls (4.6%, 1 out of 22 individuals). Finally, lymphoma was observed in one of 22 Pten$^{f/f}$ animals (4.6%), which was not noted in controls.

4.2.4 Delayed onset of intestinal tumourigenesis following deletion of Pten

As mentioned above, aged $Pten^{f/f}$ animals were noted to bear polyps of the small and large intestine in a number of cases.

I next examined more closely the timescale in which intestinal tumourigenesis ensues in $Pten^{f/f}$ animals compared to WT controls. Kaplan-Meier analysis was employed to determine the probability of intestinal polyposis with increasing time PI of animals (Figure 4.5). This indicated that, at 250 days PI, all animals remained free of intestinal tumours. After this point, the probability of finding intestinal lesions in $Pten^{f/f}$ animals at death increased. The time at which 50% of animals will bear tumours at death was found to be 372 days. In contrast, WT control animals were all found to be free of intestinal tumours until over 700 days PI. After this, the probability of detecting intestinal tumours increases slightly, but the point at which 50% of animals will bear intestinal lesions is not reached. The increased probability of intestinal tumourigenesis in $Pten^{f/f}$ animals was found to be statistically significant compared to controls ($p<0.001$, $\chi^2=34.56$, DF=1). Thus, it is clear that $Pten^{f/f}$ animals show an increased predisposition to the development of intestinal polyps compared to WT controls.

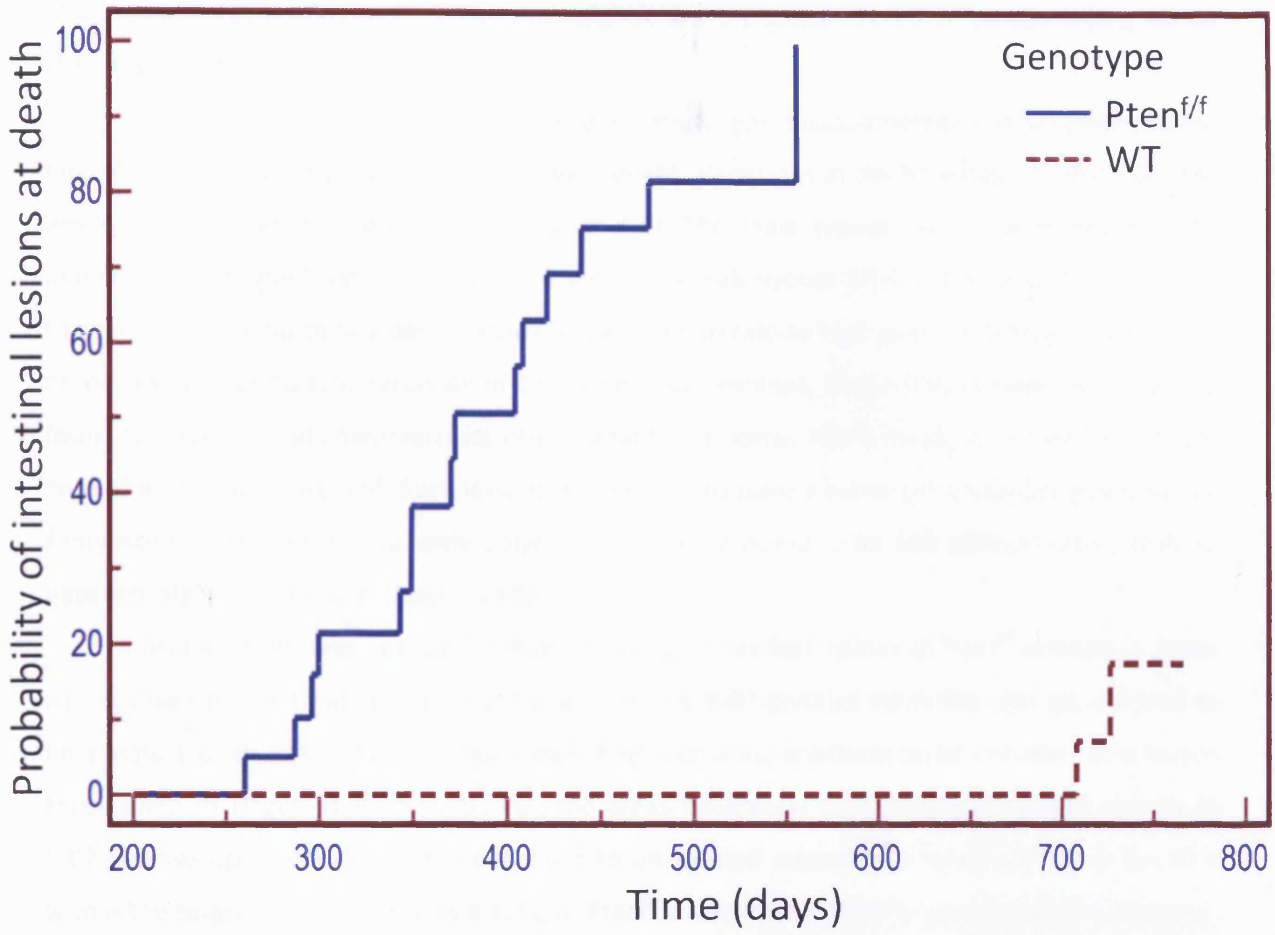

Figure 4.5: ***Probability of Pten$^{f/f}$ and control animals bearing intestinal tumours increases with time***

In order to visualise the timescale with which intestinal tumourigenesis occurs in experimental compared to control animals, Kaplan-Meier analysis was employed to determine the probability of presence of intestinal lesions in animals culled when symptomatic of disease. At less than 250 days, all animals culled and dissected were found to be free of intestinal lesions. After this point, the probability of Pten$^{f/f}$ animals having intestinal lesions increases, with the median time of tumour development being 372 days PI. WT control animals were only observed to bear intestinal lesions when culled at over 700 days, and the point at which half of all control animals were found to bear intestinal lesions (median time) was not reached. The increased probability of the presence of intestinal lesions in experimental animals compared to controls was found to be highly statistically significant ($p<0.001$, $\chi^2=34.56$, DF=1).

4.2.5 Intestinal tumours show varied histology, and are partly comprised of Ki67-positive cells

As described above, a large proportion of $Pten^{f/f}$ animals were noted to bear macroscopic polyposis of the intestine at dissection, which was confirmed microscopically. During this analysis, it was noted that overt polyposis of the colon was much more common and prominent than that of the small intestine. As such, further investigations were concentrated on polyps arising within the large intestine.

In order to further characterise these lesions, expert histopathological descriptions of the typical lesions occurring in these animals was sought. Variations in the histology of colonic lesions arising in $Pten^{f/f}$ animals were noted (Figure 4.6). The most typical lesions were found to be associated with lymphoid follicles present within the submucosa (Figure 4.6A and B). Lesions of this type were found to be Adenomatous, showing moderate to high grade dysplasia. In a number of lesions, a desmoplastic response of the stroma was evident. These lesions were not generally found to show typical characteristics of malignant carcinoma. More rarely, a second histological type of lesion was observed. Such lesions were found to have a hamartomatous tissue pathology reminiscent of that seen in juvenile polyps. Lesions were noted to be well differentiated, with no apparent signs of dysplasia[3] (Figure 4.6C).

Anti-Ki67 IHC was next performed upon large intestinal lesions of $Pten^{f/f}$ animals in order to visualise the proliferative nature of these tumours. Ki67-positive epithelial cells were noted to be a feature of all adenomatous lesions identified, indicating proliferation of epithelial cells within these tumours (Figure 4.7). In particular, the areas apparently containing the highest density of Ki67-positive epithelial cells were observed to be located adjacent to lymphoid tissue present within the tumour. Thus, tumours arising in $Pten^{f/f}$ animals are found to be actively proliferating, with a potential association between high levels of proliferation and close proximity to lymphoid cells.

[3] Histopathological descriptions of the intestinal tumours arising in $Pten^{f/f}$ were provided by both Marnix Jansen, Hubrecht Institute, The Netherlands and by Prof Geraint T. Williams, Department of Pathology, University Hospital of Wales, Cardiff University, UK.

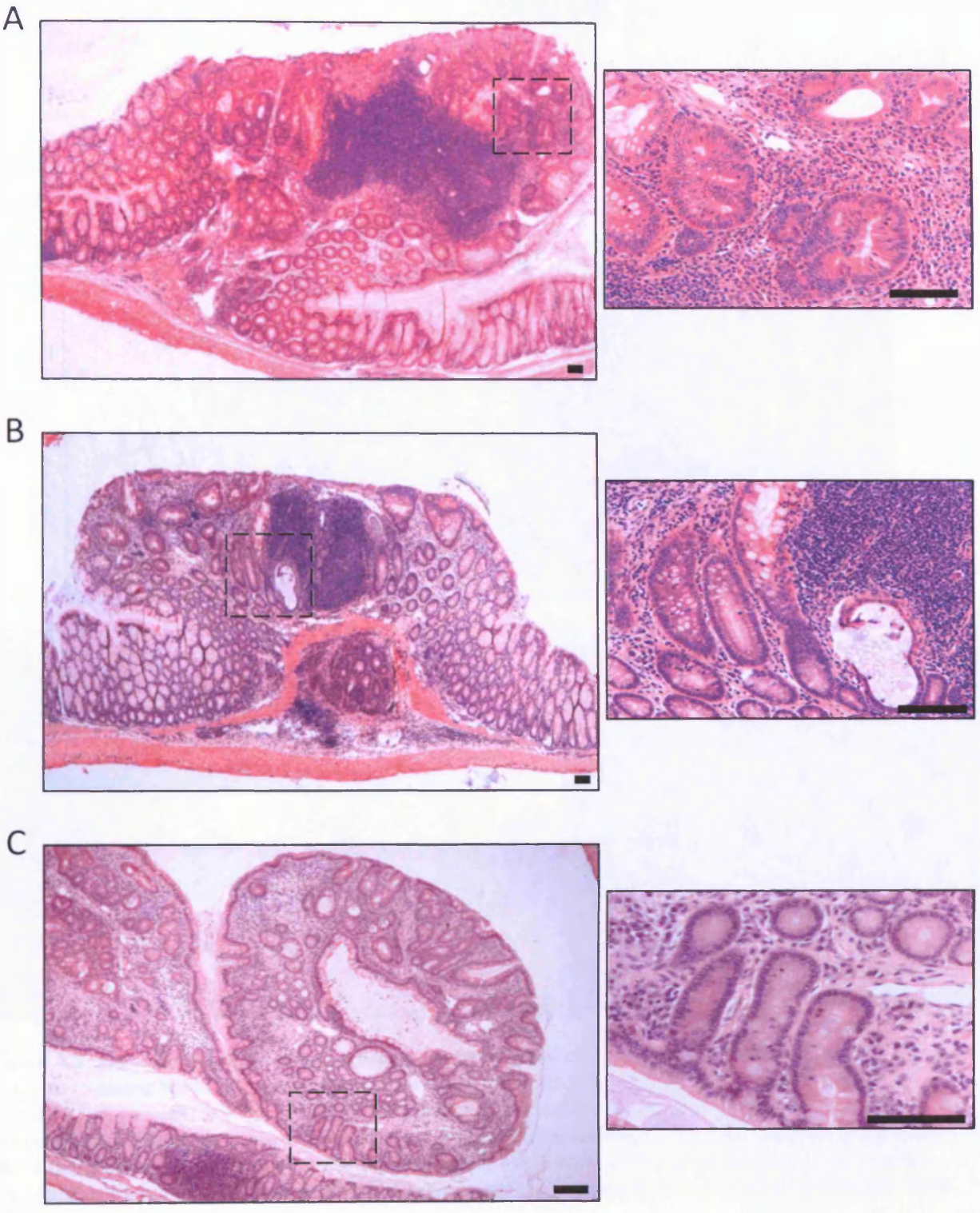

Figure 4.6: ***Intestinal tumours in aged Pten$^{f/f}$ animals show varied histopathology***
H&E-stained intestinal tissue of Pten$^{f/f}$ animals were examined in order to characterise the phenotype of large intestinal lesions arising in these mice. Typical lesions were observed to be adenomatous, and were frequently associated with lymphoid follicles (A and B are typical examples). These lesions showed moderate to high levels of dysplasia. More rarely, lesions of a second histological type were identified (C). These lesions were found to show a hamartomatous pathology reminiscent of juvenile polyposis, with no apparent dysplasia of epithelial cells within the tumour. Scale bars indicate 100μm.

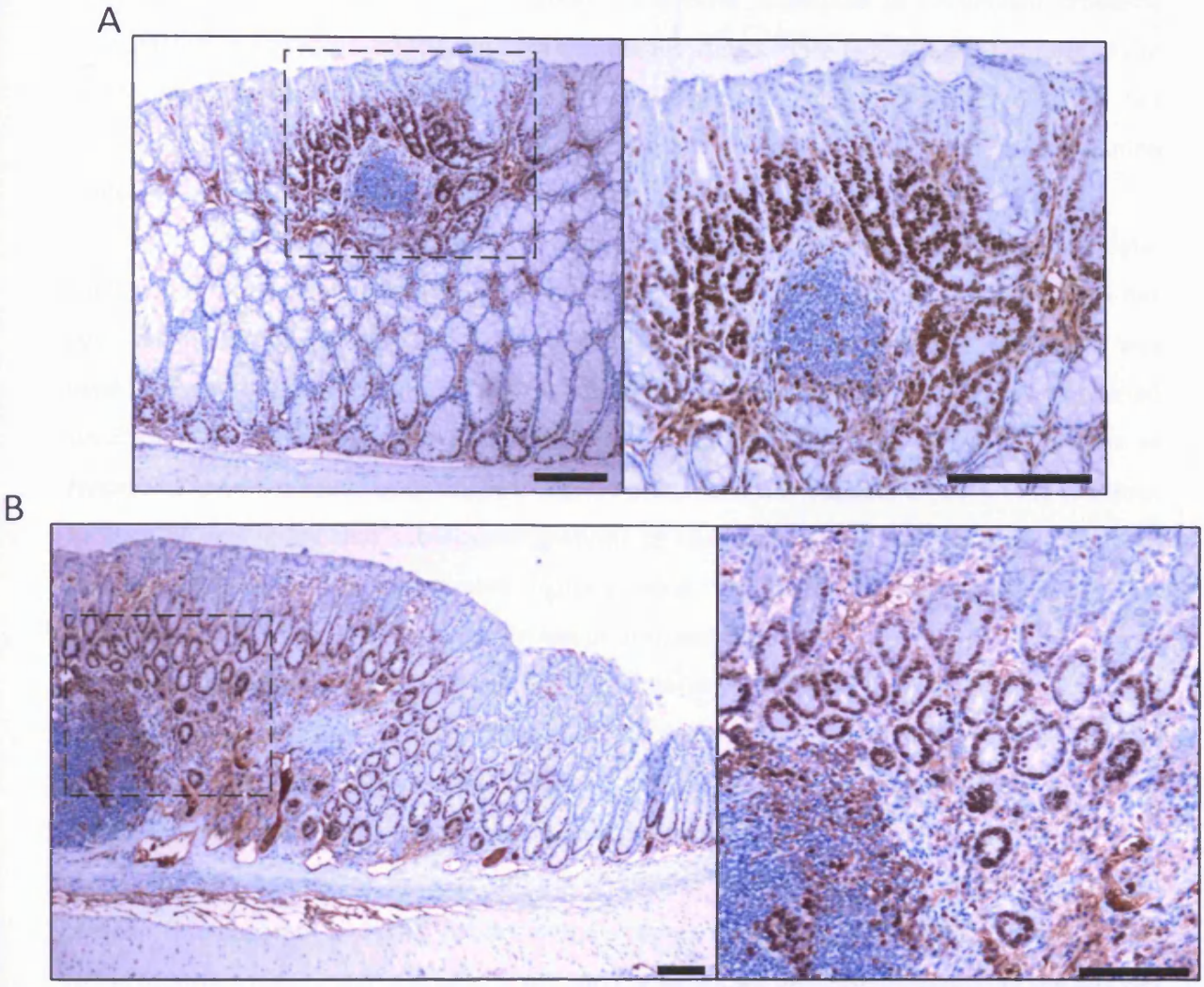

Figure 4.7: *Anti-Ki67-positive cells are present within intestinal lesions of Pten$^{f/f}$ mice*
In order to assess levels of proliferation within large intestinal lesions of Pten$^{f/f}$ experimental animals, anti-Ki67 IHC was performed. All lesions examined revealed that Ki67-positive epithelial cells were present within abnormal areas of tissue (A and B, representative lesions from two individual animals are shown). Proliferating cells appeared to be particularly associated with areas of lymphoid tissue within lesions. For each panel, high-power magnifications (right) of the areas indicated (left) are shown. Scale bars indicate 100μm.

4.3 Discussion

Previously, I have attempted to characterise the effects of Pten in suppressing tumourigenesis of the intestinal epithelium (Chapter 3). However, I was only able to analyse the effects of Pten loss up to 50 days following deletion, due to the presence of over-riding phenotypes in other tissues. In this chapter, I therefore attempted to circumvent problems encountered due to recombination in different tissues using a more tightly-regulated form of Cre recombinase-expressing transgene, AhCreER^{T}. This form of Cre-expressing transgene has previously been reported to show lower levels of uninduced background recombination compared to the AhCre transgene, which was used in Chapter 3 (Kemp et al., 2004).

I first confirmed that induction of animals bearing AhCreER^{T} by treatment with beta-naphthoflavone and Tamoxifen results in recombination within the intestinal epithelium, as has been published (Kemp et al., 2004). The ROSA26 LacZ reporter transgene (Soriano, 1999) was used to visualise recombination within the intestine. This indicated that recombination occurred specifically within the epithelium of the intestine, in both the crypt and villus. Levels of recombination were found to decrease along the proximal-distal longitudinal axis of the intestine. As such, it was noted that subsequent analyses of tissue should be performed on regions of intestine obtained from comparable regions along the length of the intestine, or that recombination in tissues should be confirmed prior to analysis.

Having confirmed that AhCreER^{T} drives recombination within the intestinal epithelium, I next generated AhCreER^{T+};Pten$^{+/+}$ ('WT') and AhCreER^{T+};Pten$^{f/f}$ ('Pten$^{f/f}$') animals in order to determine the phenotype of long-term Pten loss compared to controls. Animals were induced as adults, and aged until culling was necessary due to ill health.

Survival analysis of induced cohorts of animals revealed that a significant reduction in lifespan was apparent in Pten$^{f/f}$ cohort animals compared to WT animals. Pten$^{f/f}$ animals were found to have a median survival time of 407 days, a significant decrease compared to the 801 day median survival time of WT controls. Thus, it is clear that induction of Pten deficiency within transgenic animals results in a significant decrease in survival compared to controls.

4.3.1 Multiple tissue phenotypes associated with deletion of Pten

At dissection, the observed reduction in lifespan and general ill-health observed in Pten$^{f/f}$ animals was found to be attributable to pathologies within the genitourinary tract, liver and intestine.

In the genitourinary tract, Pten$^{f/f}$ animals were noted to be susceptible to development of prostate neoplasia, which was not observed in WT controls. Severity of disease was found to be variable, with lesions varying in histopathology from intraepithelial neoplasia (PIN) to

adenocarcinoma of the prostate in some cases. This phenotype has previously been reported in other models of prostate-specific Pten deletion (Backman et al., 2004). Thus, whilst these findings are not novel, they are useful in that they confirm that recombination in this system drives deletion of the Pten allele.

A number of liver pathologies were observed in $Pten^{f/f}$ animals, which were not noted to be present in aged WT animals. Steatosis of the liver was a common finding, with 81.0% of $Pten^{f/f}$ animals affected, compared to just 4.6% of WT controls. Again, this phenomenon has previously been reported in response to liver-specific deletion of Pten (Stiles et al., 2004). However, in this study I have also observed the occurrence of a number of other liver pathologies, varying in severity from biliary microhamartoma to cholangiocarcinoma of varied histopathology, both typical and less typical of that observed in human disease. These phenotypes are not currently described in the literature as consequences associated with deletion of Pten. However, one study has noted that combined deletion of Pten and of the tumour suppressor and TGF-beta/BMP pathway transducer, SMAD4, results in formation of bile duct abnormalities and eventually cholangiocarcinoma (Xu et al., 2006). Thus, the phenotype observed here and that of *Xu et al.* may together suggest that Pten deficiency alone causes susceptibility to cholangiocarcinoma, but that combined deletion of both Pten and SMAD4 causes a rapid acceleration of this phenotype. However, the cholangiocarcinoma which has been observed here has so far only been preliminarily characterised. Thus, further investigation is needed in order to fully characterise the phenotype observed here, and a comparative study to that of *Xu et al.* is needed to confirm a potential relationship between the phenotypes arising in these mice.

4.3.2 Delayed onset of intestinal tumourigenesis in $Pten^{f/f}$ animals

Previously published data has indicated that conditional deletion of Pten from the intestinal epithelium results in tumourigenesis within 3 months (90 days) following induction (He et al., 2007). In Chapter 3, I reported that epithelial-specific deletion of Pten does not result in tumourigenesis up to day 50 PI. Here, I can expand on these data and report that tumour development does ensue following epithelial-specific deletion of Pten, but that this only occurs at much delayed timepoints. In this study, animals at less than 250 days PI were found to be free of intestinal tumours. After this timepoint, the probability of animals bearing intestinal tumours at death was found to increase, with a 50% probability of tumourigenesis occurring at day 372 PI. Thus, the timescale reported here for development of intestinal tumours following Pten deletion is some 4 times slower than that reported by *He et al.* (2007). WT animals were not noted to develop intestinal tumours until over 700 days PI, and even at this late time point, intestinal tumourigenesis was rare, with only 1 out of 21 individuals affected. The data reported here and

that of He et al therefore indicate that, whilst epithelial-specific deletion of Pten will eventually result in intestinal tumourigenesis, this is apparently substantially accelerated by additional deletion of Pten from the stromal component of the intestine.

In this study, I find that the intestinal tumours which develop in $Pten^{f/f}$ intestines are of varied histology. In most cases, tumours were found to be associated with lymphoid follicles, and were of an Adenomatous histology, with marked dysplastic changes. Rarely, tumours of a second histological type were observed. In these cases, tumours appeared to be of a juvenile-type histopathology, displaying no signs of dysplasia. The variation of tumour histology observed in these animals raises the question of what causes the formation of different histological types of tumour, and whether one tumour type arises within another. It is possible that Adenomatous-type lesions arise within and are a more advanced form of polyps bearing a hamartomatous histology. If this were the case, the low incidence of hamartomatous lesions would suggest rapid progression of tumourigenesis. However, the preliminary data collected here has not allowed determination of whether this is truly the case, and therefore warrants further investigation in the future. In their study, He et al. report the development of lesions of a typically hamartomatous histology in Pten-deficient intestines. These lesions are histologically similar to the lesions observed here. Thus, this further supports the notion that *He et al.* report an acceleration of the same phenotype characterised here, but again further investigation is required in order to fully validate this notion.

Finally, I have examined the proliferative properties of intestinal tumours arising in $Pten^{f/f}$ animals by use of Anti-Ki67 IHC. This revealed that a proportion of epithelial cells comprising each polyp were Ki67-positive, indicating that these cells were actively replicating. In particular, an interesting pattern was noted in that a greater density of proliferative epithelial cells was found to lie adjacent to lymphoid tissue comprising the tumour. This raises the possibility that signals from cells comprising the lymphoid tissue may drive proliferation of epithelial cells within the tumour. However, as this data is again very preliminary, this is currently only speculation and a more detailed investigation of this is needed in order to confirm that this is indeed the case.

4.3.3 Summary and future directions

In summary, the data presented in this chapter indicate that conditional deletion of Pten results in neoplasia of a number of different tissues, including the genitourinary tract, liver and intestine. Cholangiocarcinoma develops within the liver, which is a novel finding not previously reported before following conditional deletion of Pten alone. This phenotype has currently only been preliminarily characterised here, and its novel nature warrants a more in-depth analysis of these tumours in the future.

In the intestine, delayed tumourigenesis is observed to occur at over 250 days following deletion of Pten specifically from the epithelium. Tumours arise of both a hamartomatous and adenomatous histopathology. Given that previous reports have indicated that Pten deletion from both the epithelium and stroma causes tumourigenesis at 90 days PI, this implies that differential deletion of Pten from specific cell compartments results in tumourigenesis at different paces. Deletion of Pten from both the epithelium and underlying stroma causes relatively rapid tumour development (He et al., 2007), whereas epithelial-specific Pten deletion results in tumour development at later timepoints. Additionally, I find that tumours of hamartomatous histology occur less commonly than those of adenomatous histology, whereas *He et al.* (2007) report the exclusive development of hamartomas. The exact reason for this delay tumourigenesis, and change in histopathology of incident tumours, is currently unclear. Indeed, the initiating factor required for tumourigenesis also remains obscure. It could be speculated that another mutation may be needed in order to initiate tumourigenesis, which then progresses rapidly in a Pten-deficient environment. However, this has not been attempted to be characterised in this chapter, and should therefore be investigated in the future.

Chapter 5: Investigating the effects of epithelial Pten loss in the context of activated Wnt signalling

5.1 Introduction

Work described in chapters 3 and 4 indicates that, whilst epithelial-specific Pten loss does not immediately predispose to lesion development, tumours may arise in very aged animals. The reason for such a delay in onset of tumourigenesis in the intestine is unclear, but one plausible explanation is that another genetic mutation must be acquired in order to initiate tumour formation, and that the Pten-deficient environment then permits rapid tumour development once this occurs. In order to address this possibility, and examine the role of Pten as a suppressor of tumour progression rather than initiation, I have investigated the effects of epithelial deletion of Pten in the context of activated Wnt signalling.

Wnt signalling is well documented as a critical regulator of intestinal homeostasis (Clevers, 2006), and is commonly activated in human colorectal cancers. As a critical mediator of the Wnt pathway, the Adenomatous polyposis coli gene product (Apc) is frequently mutated in human cancers, and heritable mutation in Apc leads to the tumour predisposition syndrome, FAP (Kinzler and Vogelstein, 1996). The role of activated Wnt signalling in homeostasis and tumourigenesis of the intestine has been extensively investigated using murine models of Apc mutation (Taketo, 2006). Use of such models has indicated that constitutive homozygous disruption of Apc results in early embryonic lethality (Moser et al., 1995). Studies of heterozygous inactivation of Apc using several different approaches show predisposition to intestinal polyp formation, reminiscent of human FAP (Moser et al., 1990, Shibata et al., 1997). Conditional deletion of both copies of Apc in the adult intestine using the Cre-LoxP approach results in rapid and catastrophic perturbation of epithelial homeostasis, within 5 days of Apc loss. Homeostatic defects observed following Apc deletion include hyperproliferation, blockade of epithelial migration and aberrant cell positioning (Sansom et al., 2004, Andreu et al., 2005).

Recent work investigating the role of Pten mutation in the context of Apc deficiency has indicated that mutation in Pten causes acceleration and progression of disease (Shao et al., 2007). *Shao et al.* report that constitutive heterozygosity for Pten on the Apc^{MIN} background results in an increase in size, number and severity of intestinal lesions compared to those seen on the Apc^{MIN} background with no mutation in Pten. Pten-deficient lesions are observed to be more commonly invasive and show an enhanced stromal response (desmoplasia), and are described by the authors as being characteristic of carcinoma.

However, from data described here (Chapter 3) and elsewhere (He et al., 2007), there appears to be some discrepancy in the function of Pten as a tumour suppressor in the intestine, depending upon which cell compartment it is deleted from. Combined epithelial and stromal loss of Pten results in expansion of stem cell numbers and rapid tumourigenesis (He et al., 2007), whereas epithelial-specific Pten loss has little immediate effect (Chapter 3) but at very extended timepoints results in intestinal tumourigenesis (Chapter 4). As described above, *Shao et al.* employed the use of constitutive Pten deficiency in their studies based on the Apc^{MIN} mouse. What remains unclear from their work is whether it is Pten deficiency within the epithelium itself which drives tumourigenesis, or whether this is the result of Pten loss in a different cell type, for instance in stromal cells.

In this chapter, I therefore aimed to determine the role of epithelial-specific Pten loss in the context of Wnt-initiated tumourigenesis. Activation of Wnt signalling was achieved by conditional deletion of Apc. Conditional inactivation of one allele of Apc has been characterised as a tumour-prone background (Shibata et al., 1997), and has previously been used to test the phenotypic effects of additional mutations (Sansom et al., 2006). Here, co-ordinate homozygous inactivation of Pten and inactivation of one or both alleles of Apc will be used to examine the role of epithelial Pten loss in the context of acute and long-term activation of Wnt signalling.

5.2 Results

5.2.1 Activation and relocalisation of Akt in Pten-deficient, Wnt activated intestinal epithelial cells

In order to examine the immediate, acute effects of combined loss of both Apc and Pten on the intestinal epithelium, mice homozygous for LoxP-targeted alleles of both *Apc* and *Pten* were generated. Experimental animals ($AhCreER^{T+}$;$Apc^{f/f}$;$Pten^{f/f}$, referred to as '$Apc^{f/f}$;$Pten^{f/f}$) and controls ($AhCreER^{T+}$;$Pten^{f/f}$;$Apc^{+/+}$ [$Pten^{f/f}$;$Apc^{+/+}$] $AhCreER^{T+}$;$Pten^{+/+}$;$Apc^{f/f}$ [$Pten^{+/+}$;$Apc^{f/f}$] and $AhCreER^{T+}$;$Pten^{+/+}$;$Apc^{+/+}$ [WT]) were induced and culled at day 5 PI.

IHC on intestinal tissue samples of all genotypes was then performed. As described in Chapter 4, $AhCreER^{T}$ induces recombination at a relatively low level within the intestinal epithelium. In order to confirm that areas of tissues which were truly deficient for Apc and Pten were being examined, IHC was performed on serially-sectioned tissues. Anti-Pten IHC was used to confirm Pten status. Inactivation of Apc was confirmed indirectly by use of anti-beta-catenin IHC, as upregulated expression and strong nuclear localisation of beta-catenin is a previously reported consequence on Wnt pathway activation by Apc loss within the intestine (Sansom et al., 2004).

Examination of small intestinal crypts of stained sections revealed loss of staining for Pten protein in approximately 50% of epithelial cells (depending on the individual animal) in $Apc^{f/f}$;$Pten^{f/f}$ experimental mice and $Pten^{f/f}$;$Apc^{+/+}$ controls (Figure 5.1). Pten staining was not lost from the underlying stroma, indicating that stromal cells were unrecombined and retained Pten expression, even after induction. Controls not bearing the LoxP-targeted Pten alleles ($Pten^{+/+}$;$Apc^{f/f}$ and WT) were found not to show loss of Pten staining, as expected. Similarly, nuclear localisation of beta-catenin was observed at a similar frequency in epithelial cells of $Apc^{f/f}$;$Pten^{f/f}$ experimental tissues and $Pten^{+/+}$;$Apc^{f/f}$ controls (Figure 5.1). Apc-proficient controls ($Pten^{f/f}$;$Apc^{+/+}$ and $Pten^{+/+}$;$Apc^{+/+}$) were not observed to show aberrant staining for nuclear catenin, with the vast majority of cells showing a cytoplasmic and cell-surface staining pattern.

To examine activation of the PI3K/Akt pathway following deletion of Pten or Apc alone, or following deletion both genes, adjacent sections were stained immunohistochemically against activated phospho-Akt^{Ser473} ($pAkt^{Ser473}$). In the crypt, both wild-type and single Apc-deficient tissues showed virtually no staining for $pAkt^{Ser473}$ (Figure 5.1). In Pten-deficient crypts, a very slight increase in staining for $pAkt^{Ser473}$ was evident, compared to directly adjacent epithelial cells which were Pten-proficient. Double-deficient tissue ($Apc^{f/f}$;$Pten^{f/f}$) was observed to show a further increase in levels of $pAkt^{Ser473}$, with staining found to be stronger than that of Pten deficient tissue and clearly stronger than adjacent wild-type tissue on the same section.

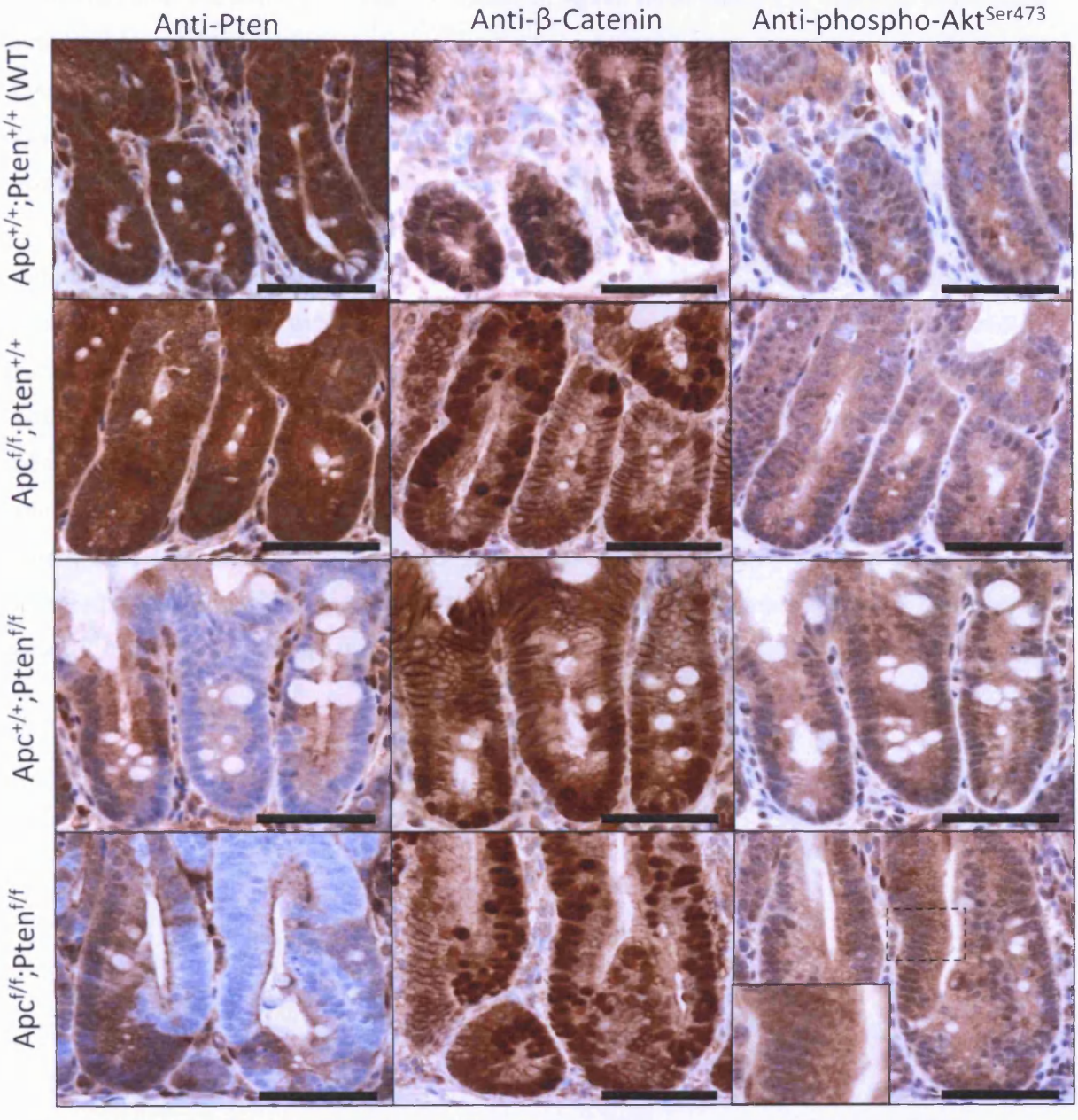

Figure 5.1: ***Increase in activation of Akt within crypts following acute loss of Pten and Apc***
Serial sections of tissue from Apc$^{f/f}$;Pten$^{f/f}$ and Apc$^{f/f}$, Pten$^{f/f}$ and WTcontrol animals ay day 5 PI were generated and subjected to IHC analysis.
Anti-Pten IHC revealed loss of staining for Pten protein in approximately 50% of epithelial cells of Pten$^{f/f}$ genotypes, with no loss of staining of underlying stromal cells. Pten$^{+/+}$ controls were found to retain positivity for Pten protein.
Anti-beta-catenin IHC was used as a surrogate marker of Apc loss, with strong expression and nuclear localisation of beta-catenin indicating activation of the Wnt pathway. Again, approximately 50% of epithelial cells in Apc$^{f/f}$ genotypes show strong nuclear staining for beta-catenin, whereas Apc$^{+/+}$ tissue shows only cytoplasmic and cell-surface localisation of beta-catenin.
Anti-phospho-Akt^{Ser473} IHC was used to assess activation of the PI3K/Akt pathway. Low level staining for pAkt^{Ser473} was evident in WT tissue, with no difference in staining between WT and Apc$^{f/f}$;Pten$^{+/+}$ tissue. Pten-deficient tissue showed a slight increase in pAkt^{Ser473} staining, but staining was clearly stronger in double mutant tissue (digital magnification of image is shown as an inset). Scale bars indicate 100μm.

In contrast to this, staining on the villus of the same tissue sections was found to have a somewhat different pattern of $pAkt^{Ser473}$ positivity. Again, serial sections of intestinal tissue were subjected to anti-Pten and anti-beta-catenin IHC in order to visualise areas of tissue deficient for Pten and Apc respectively (Figure 5.2). As above, anti-phospho-Akt^{Ser473} staining was then used to examine activation of the PI3K/Akt pathway, in this case on the villus, in the presence and absence of Pten and Apc. As previously observed, wild-type tissue was found to show virtually no staining for $pAkt^{Ser473}$. Epithelial cells on the villus of the remaining three genotypes exhibited a different pattern of staining to that observed in the crypt. In $Apc^{f/f}$;$Pten^{+/+}$ tissue, cells on the villus, unlike the crypt, exhibited a clear increase in levels of activated Akt compared to surrounding wild-type tissue. Pten-deficient cells on the villus in $Apc^{+/+}$;$Pten^{f/f}$ tissues were found not to show an appreciable increase in levels of $pAkt^{Ser473}$, which is again in contrast to the pattern observed in the crypt. Finally, the staining pattern for $pAkt^{Ser473}$ observed in epithelial cells of the villus in double deficient tissue ($Apc^{f/f}$;$Pten^{f/f}$) was striking. Not only was $pAkt^{Ser473}$ observed to be clearly upregulated compared to control genotypes, it was additionally found to be more highly localised to the cell surface, an effect which was not evident in any control tissues or in the crypts of $Apc^{f/f}$;$Pten^{f/f}$ tissue samples (Figure 5.2).

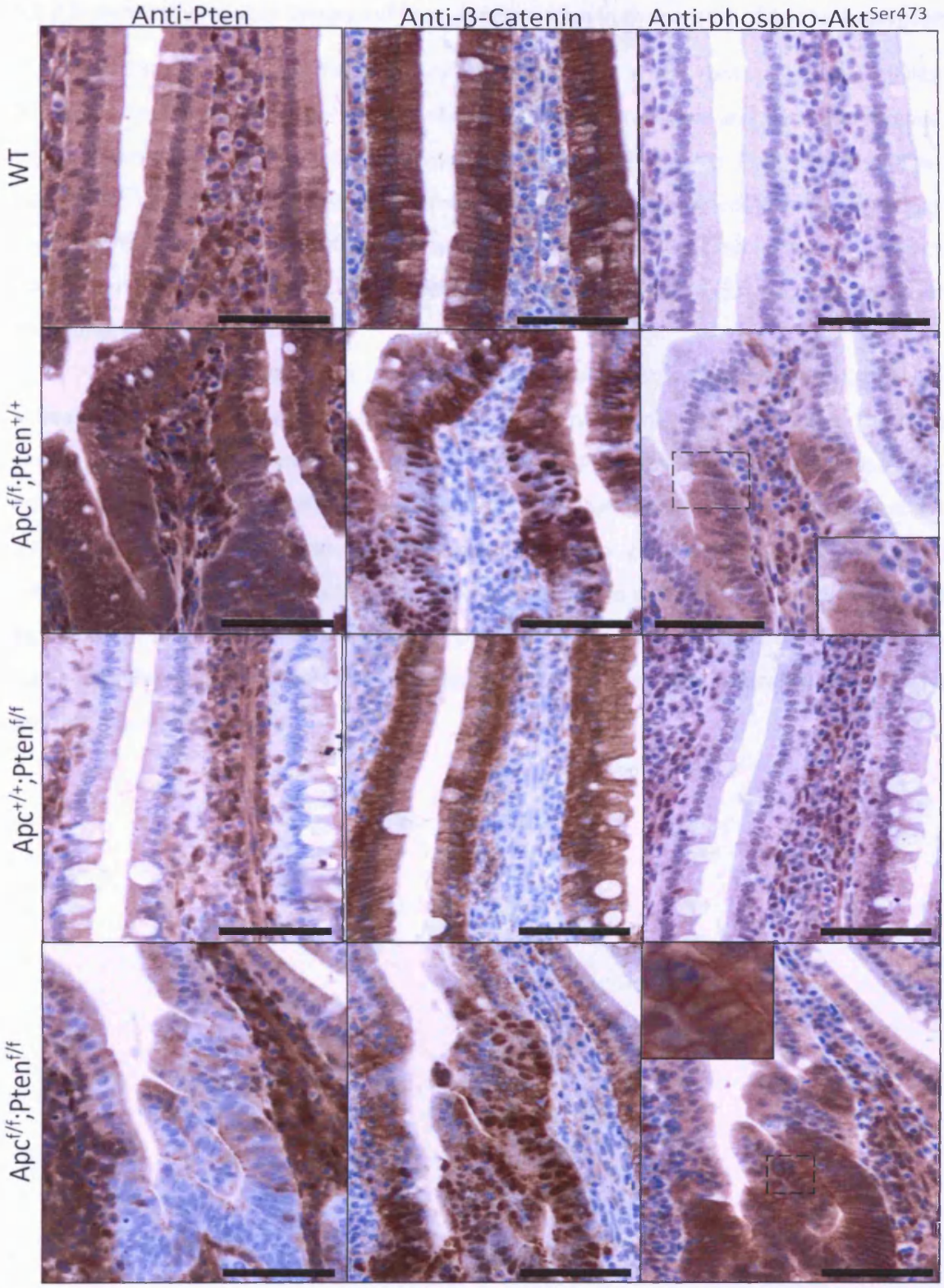

Figure 5.2: ***Increase in activation and relocalisation of Akt in villus epithelium following acute loss of Pten and Apc***

IHC against Pten and beta-catenin was performed on serial sections of intestine in order to identify areas of tissue deficient for Pten and Apc. Anti-phospho-Akt^{Ser473} (pAkt^{Ser473}) IHC was performed on adjacent sections. In tissue wild-type for Pten and Apc, minimal levels of staining for pAkt^{Ser473} was observed. In tissue deficient for Apc, a clear increase in staining against pAkt was observed, which was homogeneously cytoplasmic . No dramatic increase in staining was evident in Pten-deficient tissue. Tissue deficient for both Apc and Pten exhibited a strong increase in staining for pAkt^{Ser473}, which was also coupled with strong membrane localisation, which was not seen in tissue of any control genotype. Insets show digital magnifications of the areas highlighted by dashed boxes. Scale bars indicate 100μm.

5.2.2 Dramatically reduced lifespan of Pten-deficient mice in the context of Apc heterozygosity

In order to examine the effect of Pten deficiency in the context of susceptibility to intestinal tumours, experimental mice bearing the AhCreER^{T} transgene and also heterozygous for the LoxP-targeted Apc allele and homozygous for the LoxP-targeted Pten alleles (AhCreER^{T+} Apc$^{f/+}$;Pten$^{f/f}$) were generated (herein referred to as 'Apc$^{f/+}$;Pten$^{f/f}$') and control mice wild-type for Pten (AhCreER^{T+}Apc$^{f/+}$;Pten$^{+/+}$, referred to as 'Apc$^{f/+}$') were generated. Large cohorts of these mice (n>30) were induced and aged, whilst being monitored for signs of disease, and culled when moribund.

Analysis of survival times using the Kaplan-Meier method revealed that Apc$^{f/+}$;Pten$^{f/f}$ animals had a much reduced lifespan compared to Apc$^{f/+}$ controls (Figure 5.3A). The median survival time of Apc$^{f/+}$ control animals was 490 days PI, which in experimental Apc$^{f/+}$;Pten$^{f/f}$ animals was found to be significantly reduced to just 85 days PI (Kaplan-Meier analysis, $p<0.0001$, $\chi^2=102.71$, DF=1). In comparison to other possible control genotypes (AhCreER^{T+};Apc$^{+/+}$Pten$^{f/f}$, referred to as 'Pten$^{f/f}$' and AhCreER^{T+};Apc$^{+/+}$Pten$^{+/+}$, referred to as 'wild-type'), which are described in Chapter 4, both Apc$^{f/+}$ controls and Apc$^{f/+}$;Pten$^{f/f}$ animals show a reduction in lifespan (Figure 5.3B), with the median survival times of Pten$^{f/f}$ controls and wild-type controls being 407 days PI and 801 days PI respectively.

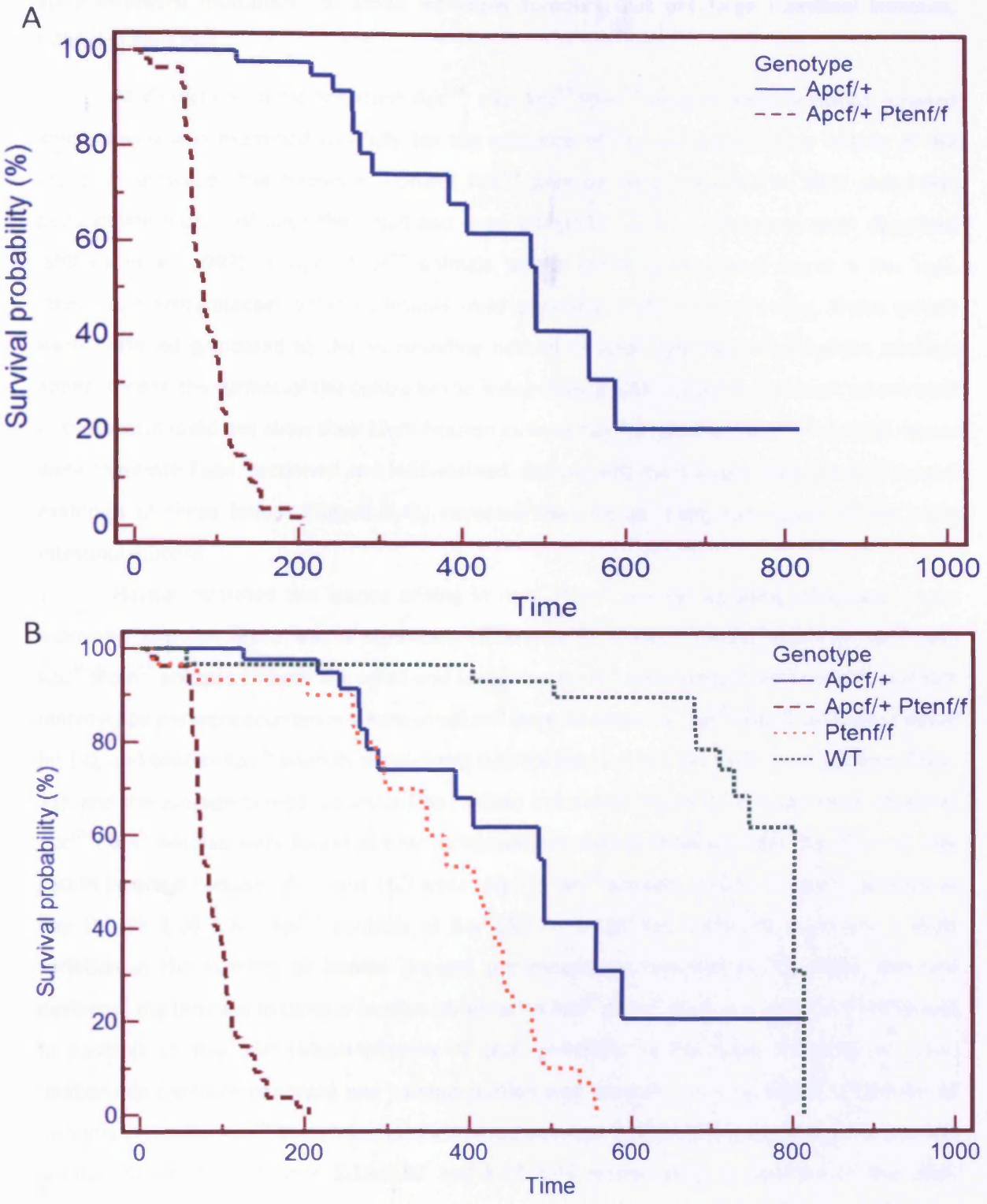

Figure 5.3: ***Pten loss in the context of Apc heterozygosity reduces longevity***
Kaplan-Meier analysis reveals experimental Apcf$^{/+}$;Pten$^{f/f}$ mice (Red dashed line) to have a reduced lifespan, with a median survival time of 85 days, compared to Apcf$^{/+}$ controls (blue line), which have a median survival time of 490 days (A). This reduction in survival is statistically significant ($p<0.0001$, $\chi^2=102.71$, DF=1). In comparison to Pten$^{f/f}$ (Orange dashed line) and Wild-type (WT; Green dashed line) controls, Apcf$^{/+}$;Pten$^{f/f}$ experimental mice also show a reduction in survival time. The median survival time for Pten$^{f/f}$ control mice was 407 days, and for wild-type mice, 801 days.

5.2.3 Increased multiplicity of small intestinal tumours, but not large intestinal tumours, following Pten loss

At dissection, intestines from $Apc^{f/+}$ and $Apc^{f/+};Pten^{f/f}$ animals were removed, opened longitudinally and examined carefully for the presence of any abnormalities or lesions of the mucosal surface of the intestine. Control $Apc^{f/+}$ animals were observed to bear polyp-like, pedunculate lesions of both the small and large intestines, as have previously been described (Shibata et al., 1997). In $Apc^{f/+};Pten^{f/f}$ animals, whilst similar lesions were found in the large intestine, macroscopically different lesions were observed in the small intestine. These lesions were flattened compared to the surrounding normal mucosa, and had an ulcerated, necrotic appearance to the surface of the centre of the lesion (Figure 5.4A). Initial macroscopic assessment of these lesions did not allow their identification as bona fide intestinal tumours. Intestinal tissues were therefore fixed, sectioned and H&E-stained. Subsequent microscopic assessment of typical examples of these lesions (Figure 5.4B) revealed them to be malignant lesions of the small intestinal mucosa.

Having identified the lesions arising in $Apc^{f/+};Pten^{f/f}$ animals as being malignant, I next examined whether there was a significant difference in tumour burden between $Apc^{f/+}$ and $Apc^{f/+};Pten^{f/f}$ animals, in both the small and large intestines. Total numbers of lesions identifiable macroscopically were counted in whole small and large intestines of $Apc^{f/+};Pten^{f/f}$ animals at death (n=14), and control $Apc^{f/+}$ animals which were culled either at 190 days (n=6) or at 250 days PI (n= 11), and the average number of lesions per mouse calculated (Figure 5.5). In the small intestine, $Apc^{f/+};Pten^{f/f}$ animals were found to bear more tumours than controls at either day 190 PI or day 250 PI (average number of lesions ±SD were: $Apc^{f/+};Pten^{f/f}$ animals: 6.93±5.43, $Apc^{f/+}$ controls at day 190 PI: 1.00±1.67, $Apc^{f/+}$ controls at day 250 PI: 1.75±1.96). Although there was a large variation in the number of lesions present per mouse, as indicated by the large standard deviation, the increase in tumour burden observed in $Apc^{f/+};Pten^{f/f}$ mice was significant compared to controls at day 250 (Mann-Whitney U test, p=0.005). In the large intestine, no clear relationship between genotype and tumour burden was apparent. As expected, the number of tumours in control $Apc^{f/+}$ large intestines increased between 190 days PI and 250 days PI (average number of lesions ±SD were 5.33±5.92 and 8.73±8.44 respectively). In contrast to the small intestine, the average number of tumours in the large intestine of $Apc^{f/+};Pten^{f/f}$ animals (average number ±SD was 6.64±5.00) was not significantly different (Mann-Whitney U test, p=0.87) to the number of tumours observed in control $Apc^{f/+}$ mice at day 250 PI. It is therefore clear that in the context of *Apc* heterozygosity, Pten suppresses tumour development in the small intestine, but not in the large intestine.

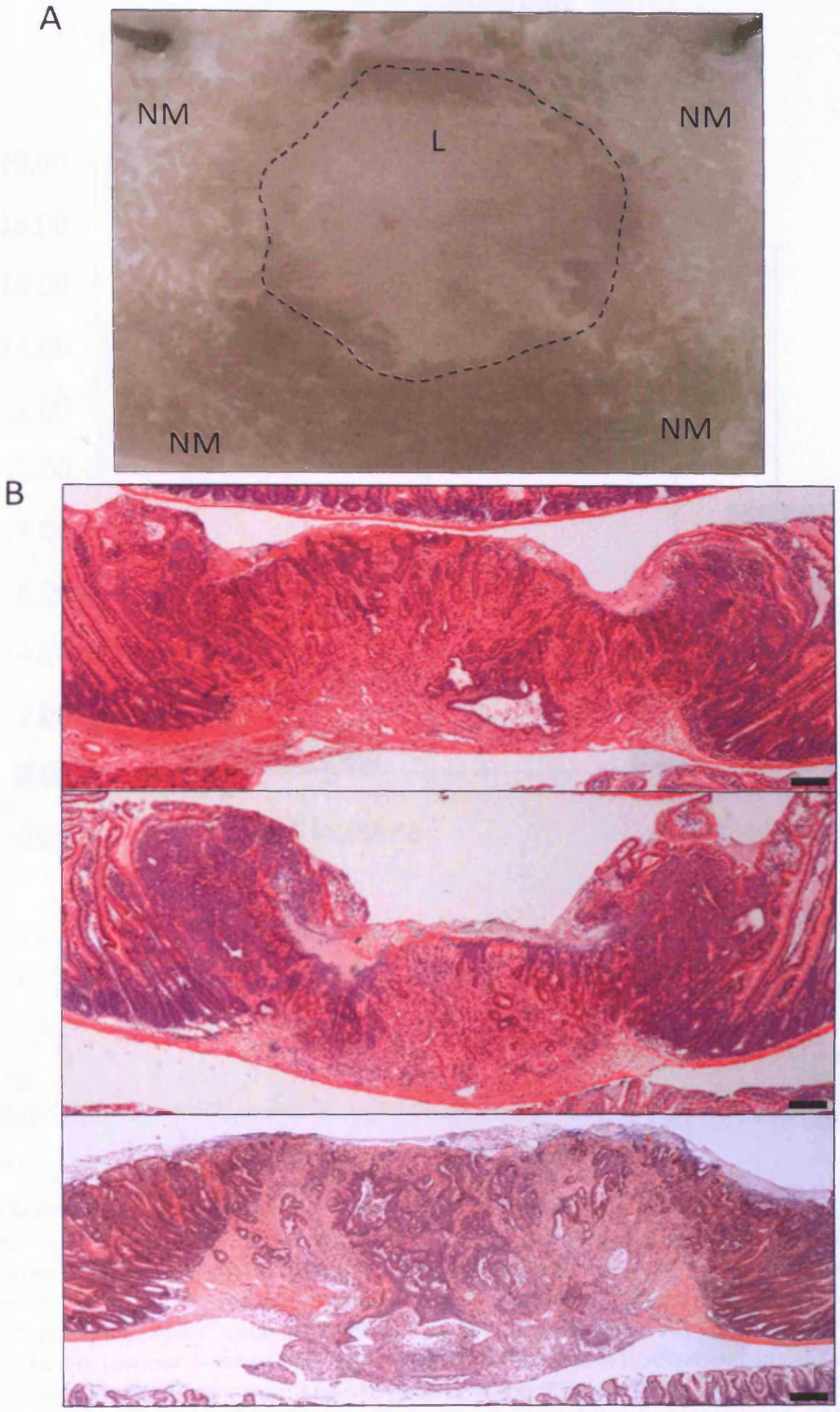

Figure 5.4: ***Gross appearance and histology of tumours arising in Apc$^{f/+}$;Ptenf$^{f/f}$ mice***
At dissection, experimental animals were found to bear numerous lesions in the small intestine. Macroscopic assessment of lesions in wholemounted, unfixed intestine (A, viewed from the lumenal face of the intestine) revealed areas of abnormal appearance (L, approximate boundary outlined) which were flattened compared to the surrounding normal mucosa (NM), with an ulcerated appearance at the centre. Histological assessment of typical examples of these lesions from H&E-stained tissue sections (B) revealed the majority to be invasive adenocarcinomas. Scale bars indicate 100μm.

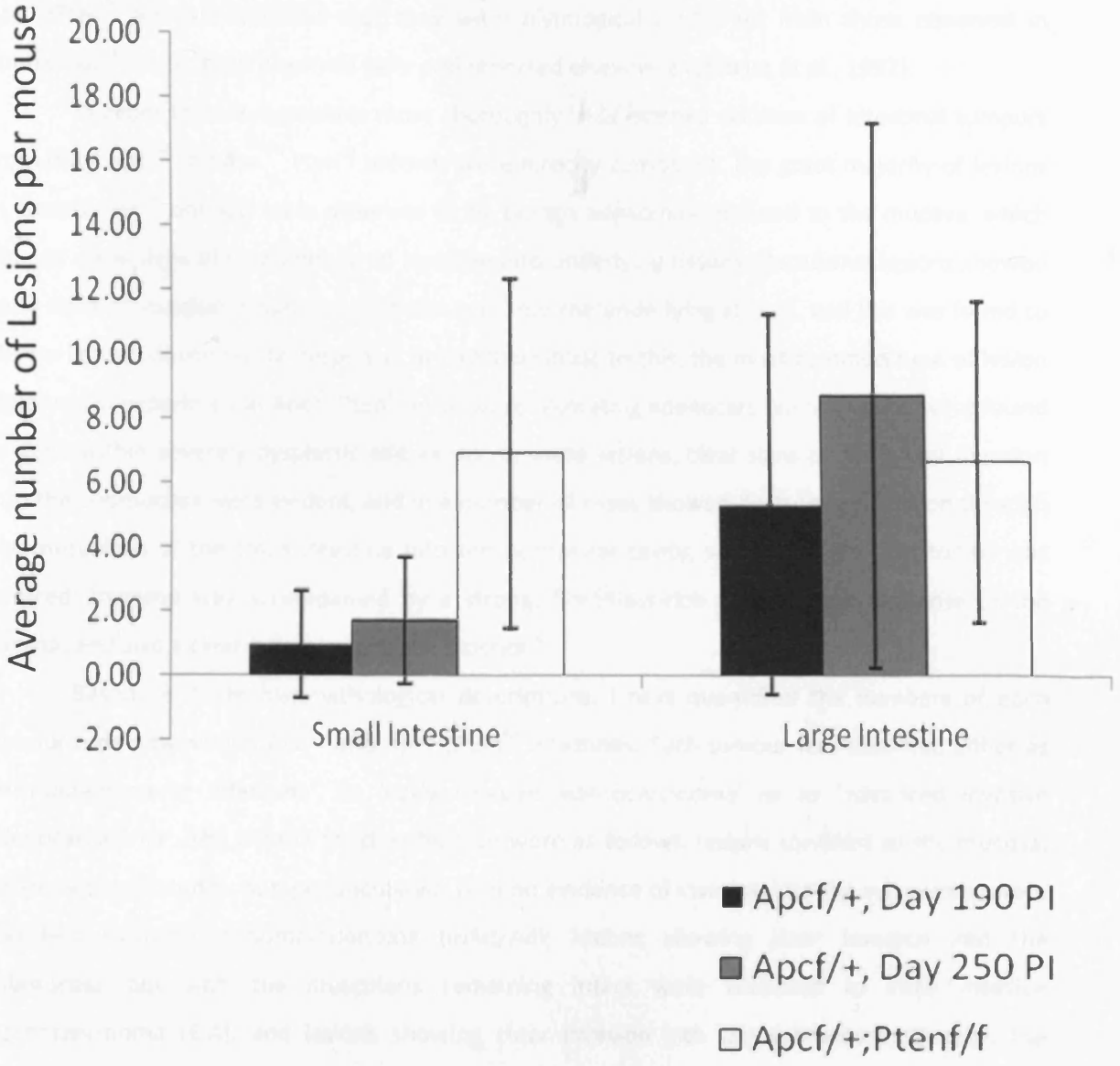

Figure 5.5: ***Increase in small intestinal tumour burden in Apc$^{f/+}$;Pten$^{f/f}$ animals.***
Frequency of tumours evident in Apc$^{f/+}$;Pten$^{f/f}$ and Apc$^{f/+}$ control small and large intestines was scored as total number of lesions per mouse (n>6 for all genotypes and timepoints). Error bars indicate standard deviation. In the small intestine, experimental animals (white bars) had a clear increase in tumour number compared to Apc $^{f/+}$ controls at either day 190 (black bars) or day 250 (grey bars) PI. Despite the large variation in tumour number between mice, the difference in number of tumours in the small intestine in experimental mice compared to control at day 250 is statistically significant (Mann-Whitney U Test, p=0.005). In contrast to this, in the large intestine, no difference in numbers of lesions was observed between experimental animals and controls at either timepoint.

5.2.4 Small intestinal tumours arising in Pten-deficient Apc heterozygotes are more advanced compared to controls

As described above, both macroscopic and microscopic assessment of lesions arising in $Apc^{f/+};Pten^{f/f}$ animals indicated that they were histologically different from those observed in control $Apc^{f/+}$ mice, both observed here and reported elsewhere (Shibata et al., 1997).

In order to investigate this more thoroughly, H&E-stained sections of intestinal tumours from both $Apc^{f/+}$ and $Apc^{f/+};Pten^{f/f}$ animals were directly compared. The great majority of lesions in control $Apc^{f/+}$ animals were observed to be benign adenomas confined to the mucosa, which did not show signs of ulceration or of invasion into underlying tissues. Occasional lesions showed early signs of invasion of tumour epithelial cells into the underlying stroma, and this was found to elicit a limited desmoplastic response. In direct contrast to this, the most common type of lesion observed in experimental $Apc^{f/+};Pten^{f/f}$ mice were ulcerating adenocarcinomas, which were found to arise within severely dysplastic adenomas. In these lesions, clear signs of malignant invasion into the submucosa were evident, and in a number of cases showed destructive invasion through the muscularis of the small intestine into the peritoneal cavity, where localised peritonitis was induced. Invasion was accompanied by a strong, fibroblast-rich desmoplastic response of the stroma, and also a clear inflammatory cell reaction[4].

Based on these histopathological descriptions, I next quantified the numbers of each tumour type observed in $Apc^{f/+}$ and $Apc^{f/+};Pten^{f/f}$ intestines. Each tumour was classified either as 'microadenoma or adenoma', as 'early invasive adenocarcinoma' or as 'advanced invasive adenocarcinoma'. The criteria for classification were as follows: lesions confined to the mucosa, either pedunculated or non-pedunculated, with no evidence of invasion into the submucosa were classified as microadenoma/adenoma (mAd/Ad); lesions showing clear invasion into the submucosa but with the muscularis remaining intact were classified as early invasive adenocarcinoma (EIA); and lesions showing clear invasion into the submucosa, through the muscularis and into the peritoneal cavity were classified as advanced invasive adenocarcinoma (AIA). Tissue sections of intestines from $Apc^{f/+}$ (n=16) and $Apc^{f/+};Pten^{f/f}$ (n=15) mice were examined, and lesions identified and categorised (See Figure 5.6). In control mice, 86% of lesions were found to be mAd/Ad and the remaining 14% of lesions were classed as EIA (numbers of lesions in each category were 12 and 2 respectively, out of a total of 14 lesions). No lesions were observed in control animals which fulfilled the requirements for classification as AIA. In contrast to this, $Apc^{f/+};Pten^{f/f}$ animals showed a reduction in the number of lesions classified as mAd/Ad, at 47% (26 of 56 lesions). An increase in incidence of EIA was observed, with 32% (18 of 56) of

[4] Histopathological descriptions of tumours in control and experimental animals were kindly provided by Prof Geraint T. Williams, Department of Pathology, University Hospital of Wales, Cardiff University, UK.

lesions classified in this category. Finally, 21% (12 of 56) of lesions were found to be sufficiently advanced to be classified as AIA (See Figure 5.7).

From these data, it is therefore clear that in the context of Apc heterozygosity, additional loss of Pten results in rapid progression of tumours, and advancement of disease state, compared to tumours arising in control intestines.

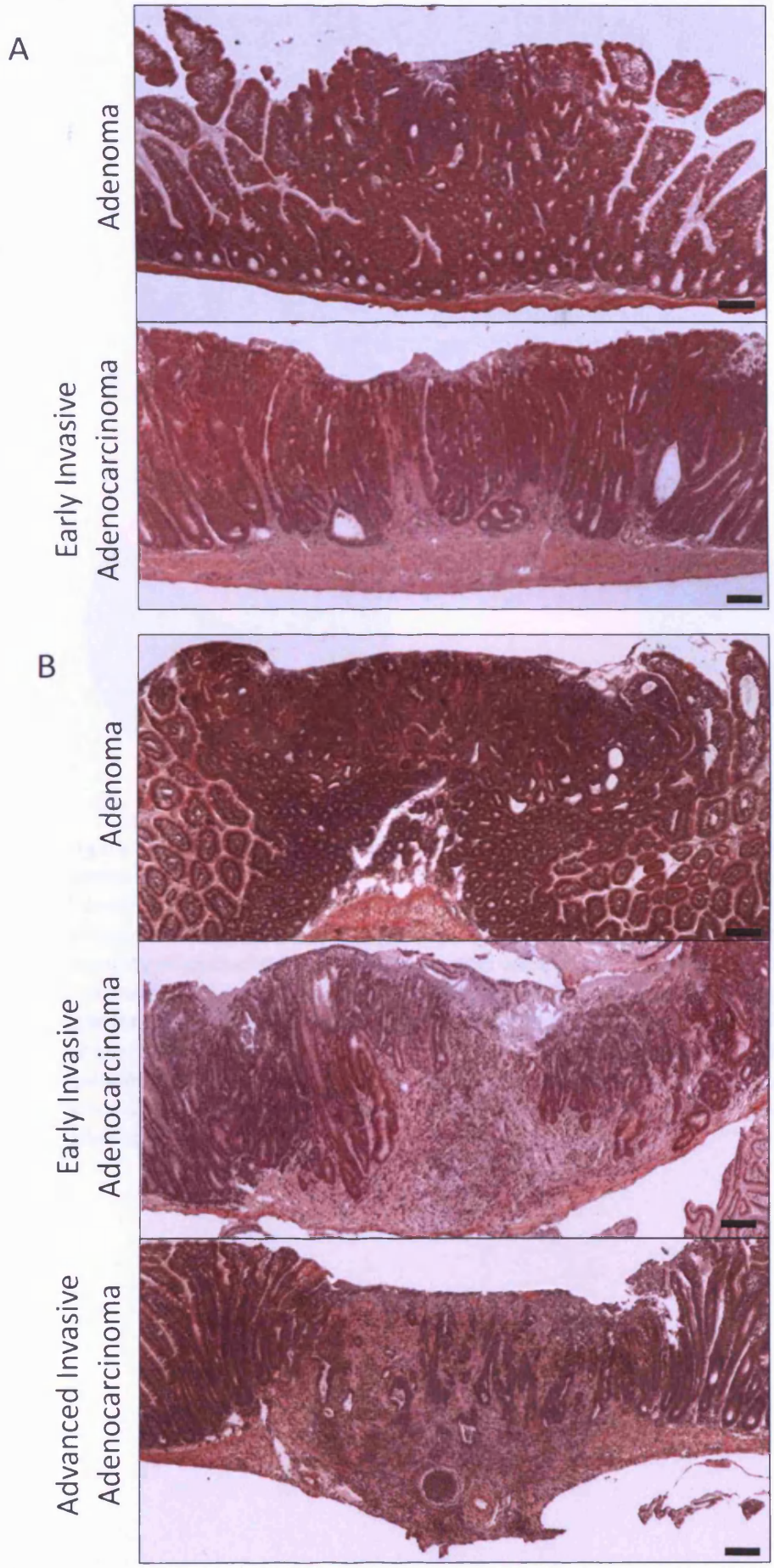

Figure 5.6: ***Histological categorisation of varying grades of tumour severity seen in Apc$^{f/+}$;Pten$^{f/f}$ intestines and Apc$^{f/+}$ controls***
Assessment of H&E-stained sections of small intestinal tumours from Apc$^{f/+}$ and Apc$^{f/+}$;Pten$^{f/f}$ mice revealed varying grades of tumour severity. In Apc$^{f/+}$controls (A), adenomas were identified (top panel), which were confined to the mucosa. In addition, early invasive adenocarcinomas showing invasion into the submucosa were identified (bottom panel). In Apc$^{f/+}$;Pten$^{f/f}$ animals (B), adenomas confined to the mucosa were also evident (top panel), as were early invasive adenocarcinomas (middle panel), though these appeared histologically different to those seen in Apc$^{f/+}$ controls, with a more pronounced desmoplastic response. Apc$^{f/+}$;Pten$^{f/f}$ animals were additionally found to bear advanced invasive adenocarcinomas, characterised by evidence of invasion through the muscularis propria of the intestinal wall into the peritoneal cavity (bottom panel). Scale bars indicate 100μm.

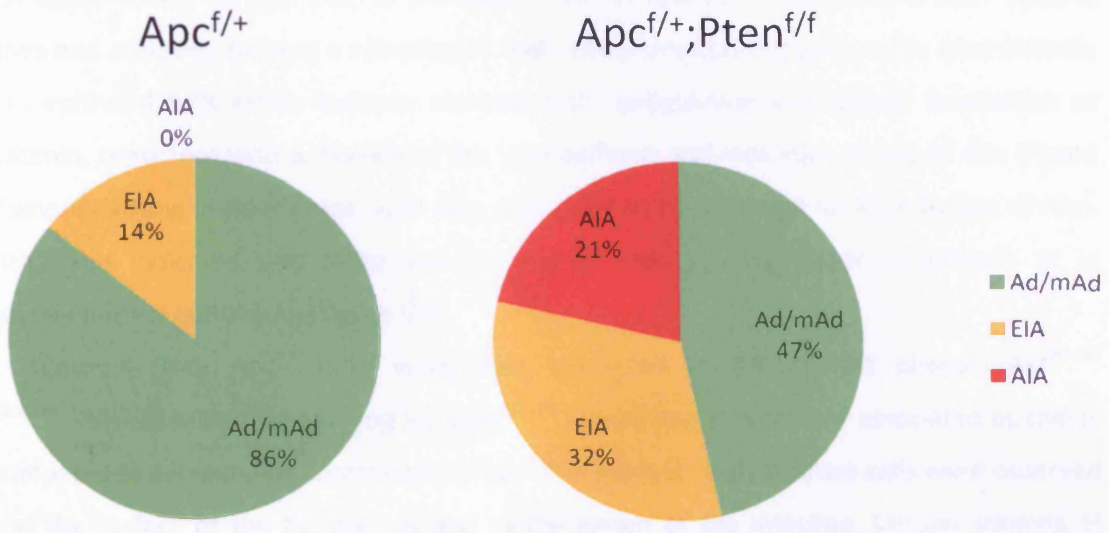

Figure 5.7: ***Increased severity of small intestinal tumours in Apc$^{f/+}$;Pten$^{f/f}$ compared to control mice***

Intestinal tumours arising in control Apc$^{f/+}$ (left) and Apc$^{f/+}$;Pten$^{f/f}$, (right) mice were assessed histologically and categorised according to grade of severity of the tumour. The majority of lesions (86%) in control animals were found to be adenoma or microadenoma (Ad/mAd), with a small number (14%) of lesions showing progression to early invasive adenocarcinoma (EIA). Microadenomas and adenomas were also present in experimental animals, but at a lower frequency (47%). An increased proportion of lesions in experimental animals showed progression to EIA (32%), compared to controls. A subset of lesions (21%) were also found to progress further than EIA, and were categorised as advanced invasive adenocarcinoma (AIA).

5.2.5 Moderate activation of Akt in Pten-proficient tumours arising in Apc heterozygotes

As described above, I previously observed a moderate increase in activation status of Akt, as assessed by IHC staining for phospho-Akt^{Ser473}, following acute loss of both copies of *Apc* alone. This observed increase in activation of Akt was not associated with any change in subcellular localisation. I therefore sought to examine whether the same pattern was apparent in tumours arising in Apc$^{f/+}$ control mice.

I first confirmed that tumours were indeed deficient for Apc using anti-beta-catenin IHC as a surrogate marker for Apc loss, as previously. Non-tumour epithelial tissue in Apc$^{f/+}$ control intestines was observed to have a cytoplasmic and cell-surface staining pattern for beta-catenin, whereas epithelial cells within tumours showed both upregulation and nuclear localisation of beta-catenin, consistent with activation of the Wnt pathway and indicative of loss of Apc (Figure 5.8). Tumours arising in Apc$^{f/+}$ mice were also confirmed to be wild-type for Pten by use of Anti-Pten IHC. This indicated that there was no loss of Pten staining either in tumours or in surrounding normal epithelium (Figure 5.8).

Tumours from Apc$^{f/+}$ mice were then subjected to IHC against phospho-Akt^{Ser473} (pAkt^{Ser473}). This revealed that staining for pAkt^{Ser473} was stronger in tumour-associated epithelial cells compared to surrounding control epithelium. The most strongly positive cells were observed to be at the surface of the tumour, closest to the lumen of the intestine. Cellular staining of pAkt^{Ser473} was noted to be homogeneously cytoplasmic, within no obvious increase in staining at the cell surface. These observations are therefore consistent with the staining patterns described in section 5.2.1, indicating that loss of Apc results in an increase in activation of Akt, but does not alter its subcellular localisation.

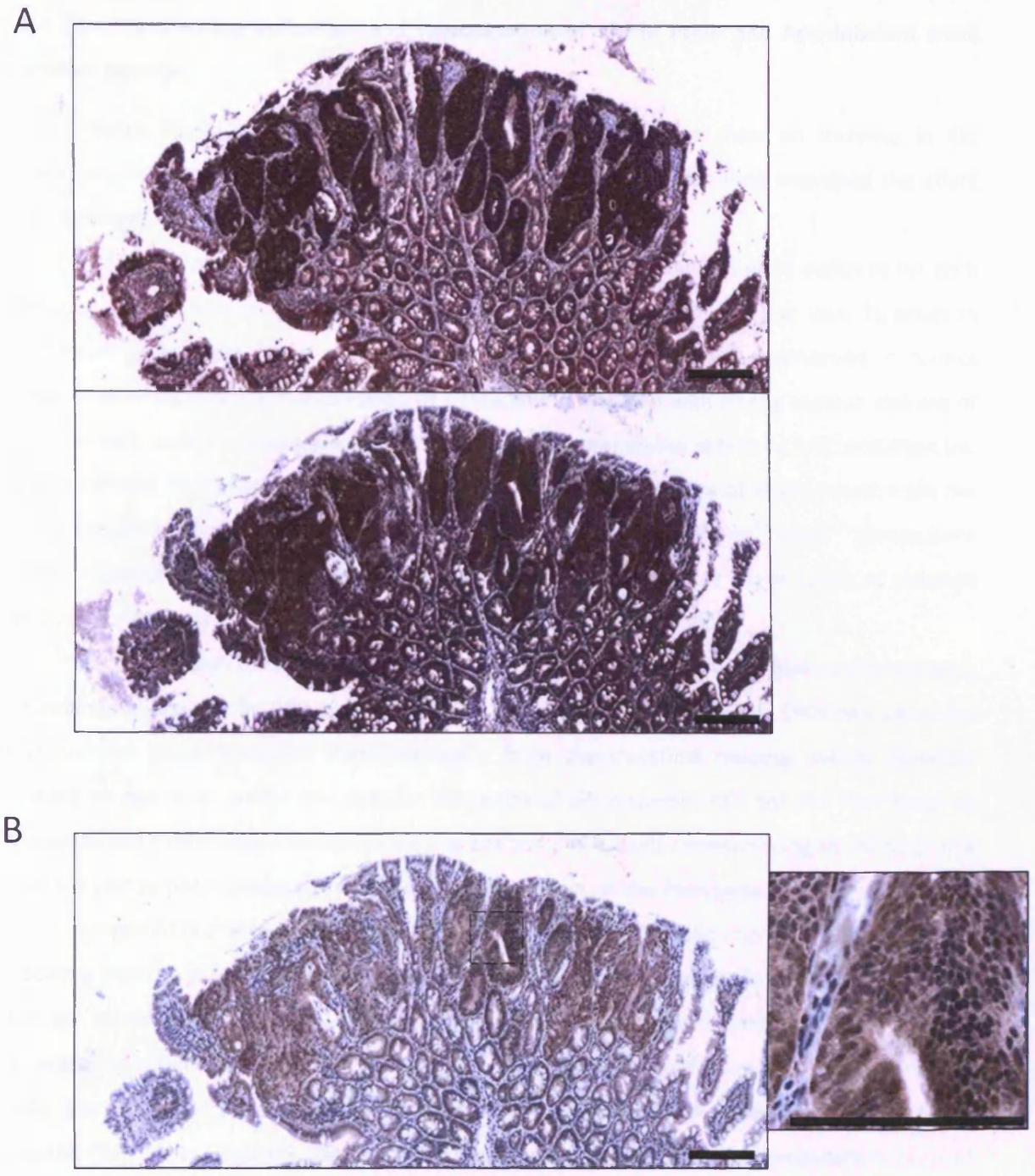

Figure 5.8: ***IHC on tumours arising in Apc$^{f/+}$ control animals confirms loss of Apc and retention of Pten, and indicates a moderate increase in activation of Akt.***
IHC was performed on serial sections of tumours from control Apc$^{f/+}$ mice. Anti-beta-catenin IHC (A, top panel) revealed strong upregulation and nuclear localisation of beta-catenin, indirectly indicating loss of Apc. Anti-Pten IHC (A, bottom panel) confirmed that tumours arising in control mice retained positivity for Pten staining. Anti-pAkt^{Ser473} IHC indicated a moderate upregulation of pAkt levels in control tumours compared to surrounding normal tissue. Staining for pAkt was found to be homogeneously cytoplasmic, as shown in the digital enlargement of the region of the tumour indicated by a dashed box. Scale bars indicate 100μm.

5.2.6 Consistent strong activation and relocalisation of Akt in Pten- and Apc-deficient small intestinal tumours

Having found that tumours arising in control $Apc^{f/+}$ mice show an increase in Akt activation similar to that observed following short-term loss of Apc, I next examined the effect upon Akt signalling in tumours arising in $Apc^{f/+}$;$Pten^{f/f}$ mice.

I first confirmed that the tumours arising in $Apc^{f/+}$;$Pten^{f/f}$ animals were deficient for both Pten and Apc. As above, IHC against beta-catenin was used to indicate Apc loss. Tumours in $Apc^{f/+}$;$Pten^{f/f}$ mice were found to show a similar staining pattern to that observed in control tumours, with an increase in expression of beta-catenin, coupled with strong nuclear staining of epithelial cells within tumours, compared to surrounding normal tissue (Figure 5.9). Anti-Pten IHC was performed on adjacent sections of tumour tissue to examine loss of Pten protein from the epithelium. This indicated that epithelial cells within tumours arising in $Apc^{f/+}$;$Pten^{f/f}$ tissues were indeed negative for Pten staining, whilst the stromal component of these tumours retained positivity for Pten, as expected (Figure 5.9).

Recombination of both the *Apc* and *Pten* alleles within tumours was also confirmed using recombined-allele-specific PCR (see Section 2.6.4 and Figure 2.2). Genomic DNA was extracted from tumour tissue dissected macroscopically from the intestinal mucosa, which therefore contains all cell types within the tumour. Recombined-allele-specific PCR for the *Pten* locus on DNA extracted from tumour samples revealed presence of a band corresponding to 705bp in size in all tumour samples analysed, indicating recombination of the Pten gene. Products generated from the targeted but unrecombined alleles were also present at 514bp and approximately 1.2kb, indicating that the population of cells within the tumour are not all recombined. This is consistent with my observations from IHC analysis of Pten protein expression. Control samples of DNA extracted from tail biopsies of $Apc^{f/+}$;$Pten^{f/f}$ and wild-type mice confirmed that the recombined allele was not detected either in uninduced tissues, or in cells which do not bear the LoxP-targeted Pten alleles (Figure 5.10A). A similar strategy employed to assess recombination status of the Apc allele again confirmed that products corresponding to both the recombined Apc allele (at 258bp in size) and the LoxP-targeted but unrecombined allele (at 314bp in size) were generated from each tumour sample. DNA extracted from tail biopsies of wild-type and uninduced mice bearing the $Apc^{f/f}$ alleles were again used to confirm that the product corresponding to the recombined allele of Apc was not present, but products corresponding to the wild-type Apc allele (at 226bp in size) and the targeted but unrecombined Apc allele (at 314bp) were present respectively in each sample (Figure 5.10B).

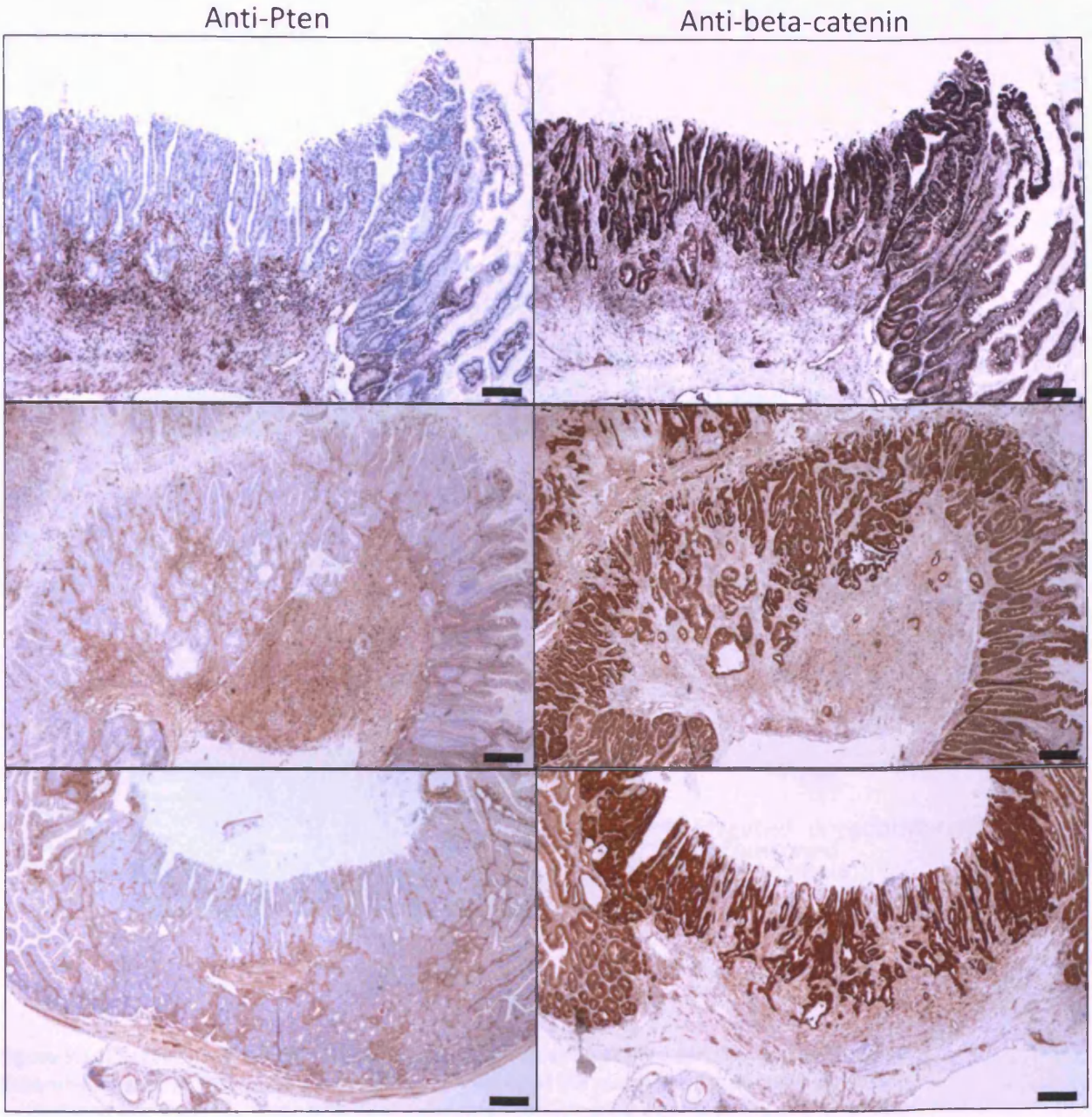

Figure 5.9: ***IHC on tumours arising in Apc$^{f/+}$;Pten$^{f/f}$ animals indicates loss of Pten and Apc in epithelial cells***

Serial sections of tumours arising in Apc$^{f/+}$;Pten$^{f/f}$ animals were subjected to anti-Pten IHC and anti-beta-catenin IHC. Epithelial cells within tumours were found to be consistently negative for anti-Pten staining (Left panel), indicating loss of Pten protein. Staining of adjacent sections revealed epithelial cells of tumours to show upregulation and nuclear localisation of beta-catenin, indirectly confirming loss of Apc and activation of the Wnt pathway in tumours. Three examples of invasive adenocarinomas from individual Apc$^{f/+}$;Pten$^{f/f}$ animals are shown. Scale bars indicate 100μm.

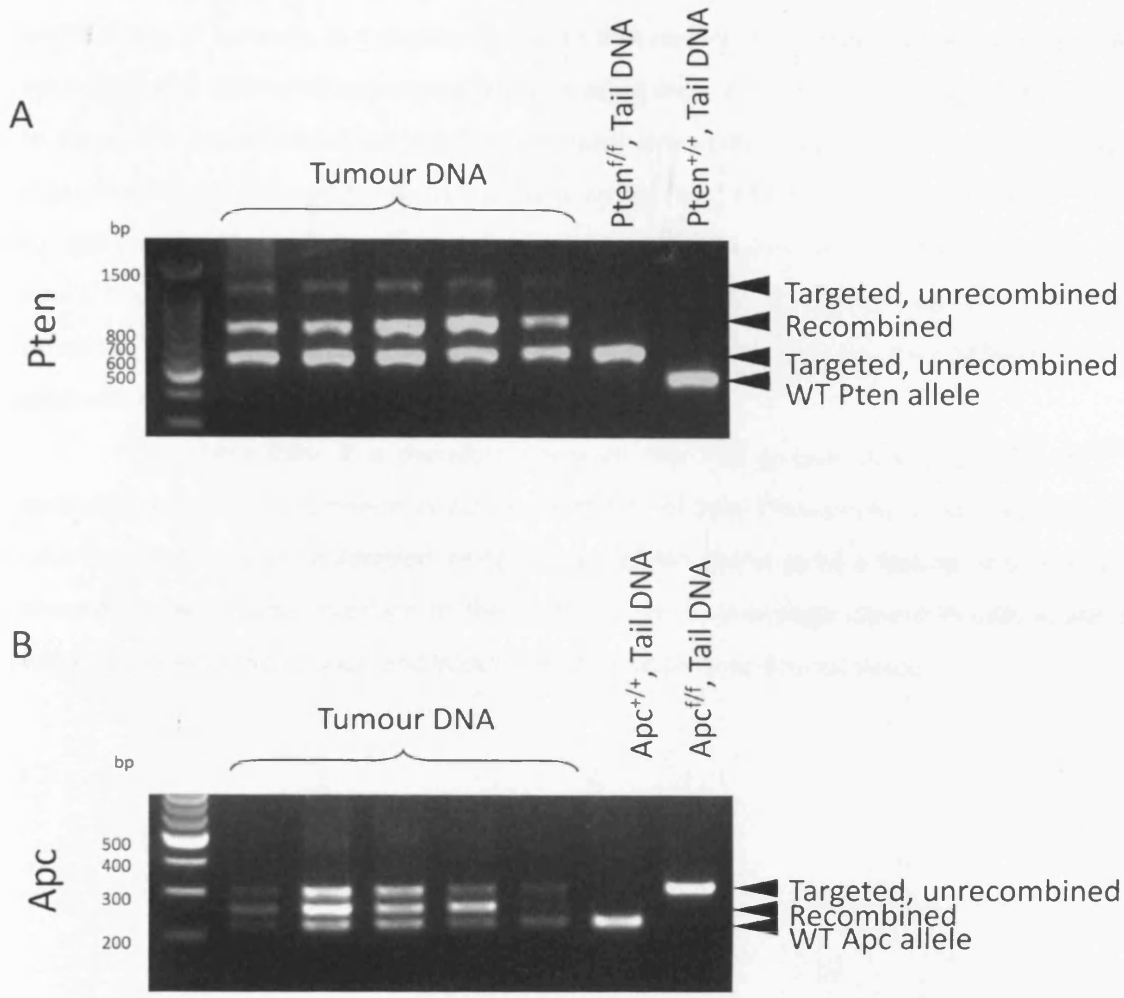

Figure 5.10: ***Recombined-specific PCR indicates recombination at Pten and Apc alleles in tumours***
Recombined-specific PCR was used to confirm presence of the recombined Pten allele (A) or the recombined Apc allele (B) in genomic DNA extracted from intestinal tumours of Apc$^{f/+}$;Pten$^{f/f}$ animals. For Pten recombined PCR, a specific product corresponding to 705bp in size was generated from all tumour samples, indicating presence of the recombined allele. Products corresponding to 514bp and approximately 1.2kbp were also generated, indicating presence of the targeted but unrecombined Pten allele. Control , unrecombined samples did not generate a product corresponding to the 514bp recombined-specific product. In reactions specific for the Apc recombined allele, a product of 258bp indicating recombination at the Apc allele was generated from all tumour samples. Product corresponding to 314bp in size, indicating the targeted but unrecombined allele and 226bp in size, indicating the wild-type Apc allele were also generated (as expected as animals are Apc$^{f/+}$). Control , unrecombined samples did not generate a product corresponding to the 258bp recombined-specific product.

Activation of Akt was then assessed in Apc- and Pten-deficient tumours. Anti-pAkt^{Ser473} IHC revealed an increase in staining of epithelial cells of the tumour compared to surrounding normal epithelial cells in all tumours examined. The strongest staining was observed at the lumenal face of tumours, in a pattern similar to that observed in control tumours arising in Apc$^{f/+}$ mice. Epithelial cells which were apparently invading the submucosa were not generally observed to show an in Akt activation compared to epithelial cells at the surface of the tumour. In addition, areas of epithelial cells were observed to show strong cell surface localisation of pAkt^{Ser473}, similar to that observed in Apc$^{f/f}$;Pten$^{f/f}$ tissues at very early timepoints (as described in Section 5.2.1). Again, the regions of epithelial cells showing this alteration in subcellular localisation of pAkt^{Ser473} tended to be located towards the lumenal surface of the tumour rather than within the invasive epithelial component (Figure 5.11).

From these data, it is therefore apparent that cell surface localisation of pAkt^{Ser473} in epithelial cells is a phenomenon associated with loss of both Pten and Apc, but is not associated with loss of Apc alone. In addition, relocalisation of Akt seems to be a feature of epithelial cells present at the lumenal interface of the tumour, but is surprisingly absent in cells found deep within the bulk of the tumour, and in cells invading underlying stromal tissue.

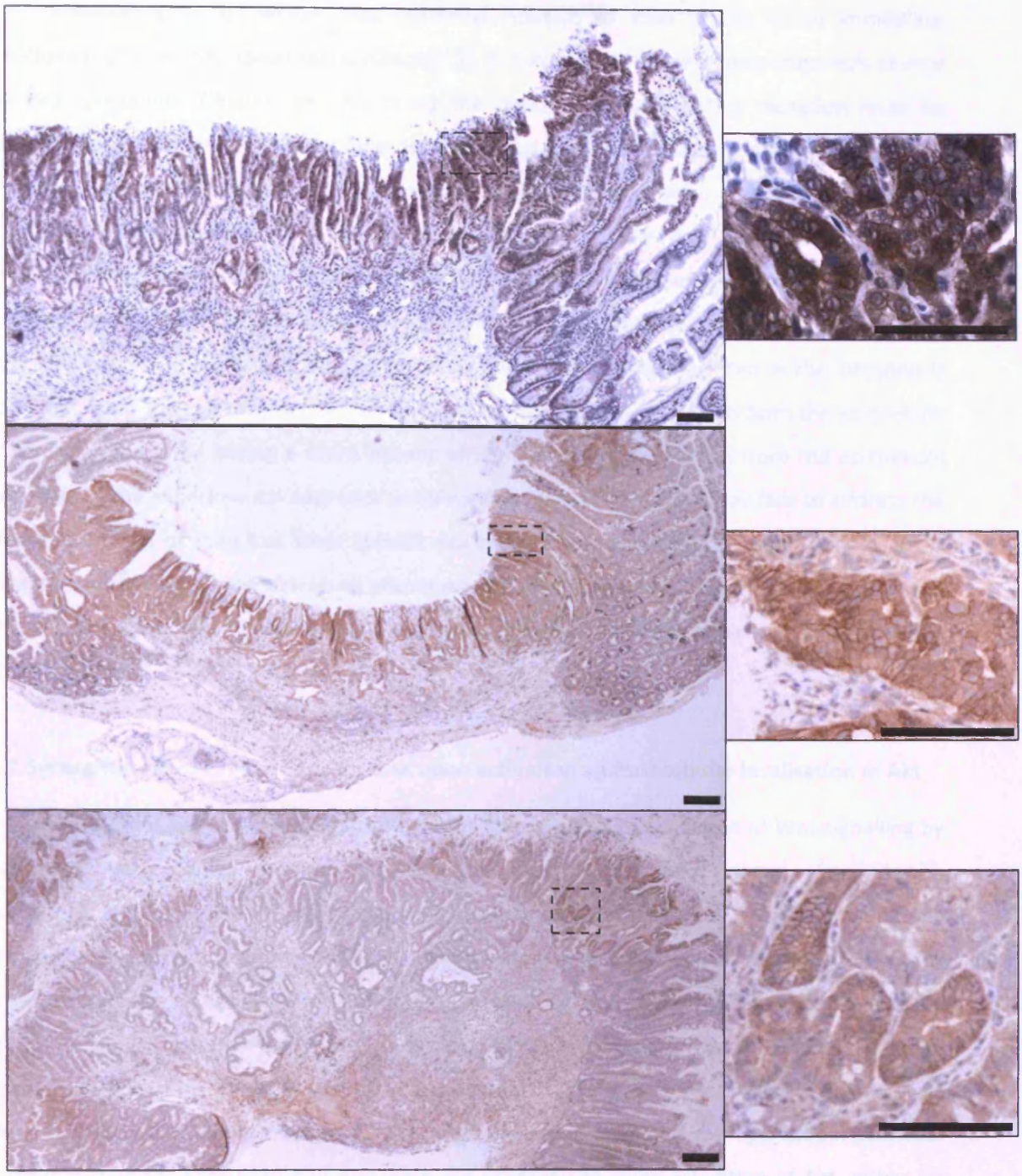

Figure 5.11: ***Activation and cell-surface localisation of Akt in intestinal tumours arising in Apc$^{f/+}$;Pten$^{f/f}$ animals***

Serial sections of tumours from Apc$^{f/+}$;Pten$^{f/f}$ mice, previously confirmed using IHC to be deficient for both Pten and Apc (See Figure 5.9) were subjected to anti-phospho-Akt^{Ser473} (pAkt) IHC. All tumours were found to show upregulated expression of pAkt in subsets of epithelial cells of tumours, compared to surrounding unaffected tissue (Left hand panel). Staining for pAkt was generally found to be most intense at the lumenal surface of the tumour. Regions of all tumours also showed relocalisation of pAkt to the cell surface (digital magnification of areas indicated with dashed boxes shown in right hand panel), which was not seen in surrounding tissue or in tumours arising in control Apc$^{f/+}$ animals (See Figure 5.8). Scale bars indicate 100μm.

5.3 Discussion

Previous work has shown that epithelial deletion of Pten results in no immediate perturbation of intestinal homeostasis (Chapter 3), but eventually permits tumourigenesis at very extended timepoints (Chapter 4). This raises the notion that an initiating mutation must be acquired in order for intestinal tumourigenesis to ensue, and that progression of disease is then facilitated by the Pten-deficient environment. One study examining the role of Pten in suppressing tumourigenesis in a tumour-prone background (the Apc^{MIN} mouse) notes that constitutive heterozygosity for Pten promotes intestinal tumourigenesis (Shao et al., 2007), indicating that this hypothesis may be correct. However, work described here and elsewhere (He et al., 2007) has also indicated that the tumour suppressive function of Pten in the intestine is dependent upon the cell type(s) from which it is lost, with loss of Pten from both the epithelium and stroma apparently having a more potent effect compared to deletion from the epithelium alone. Due to the experimental approach employed by *Shao et al.*, their study fails to address the differential effects of Pten loss from specific cell types in the context of a tumour-prone, Wnt-activated background. I have therefore examined the effects of epithelial-specific Pten loss in the context of activated Wnt signalling, achieved by conditional deletion of either one or both copies of the Apc allele.

5.3.1 Synergistic effect of Pten and Apc loss upon activation and subcellular localisation of Akt

I first examined the effect of Pten deletion following acute activation of Wnt signalling by deletion of both copies of Apc. Experimental ($Apc^{f/f}$;$Pten^{f/f}$) and control ($Apc^{f/f}$;$Pten^{+/+}$, $Apc^{+/+}$;$Pten^{f/f}$ and $Apc^{+/+}$;$Pten^{+/+}$) animals were induced and culled at day 5 PI. Loss of Pten and Apc from the intestine was confirmed by IHC against Pten and against beta-catenin, a surrogate marker for Apc loss, on serial sections of tissue. This allowed visual identification of areas of tissue showing deficiency for Apc, Pten or both. Activation of the PI3K/Akt pathway was then assessed in adjacent tissue sections using IHC against phospho-Akt^{Ser473} ($pAkt^{Ser473}$). This revealed that Akt was differentially activated in the crypt and villus of the intestine depending upon genotype. Epithelial tissues wild-type for both Pten and Apc were not observed to show activation of Akt, either on the crypt or villus. Epithelial cells singly-deficient for Apc alone did not show activation of Akt within the crypt compared to adjacent wild-type tissue, but a clear increase in staining for $pAkt^{Ser473}$ was apparent on the villus. On the villus, staining was observed to occur in a homogeneously cytoplasmic fashion, with no observed alteration in subcellular localisation of activated Akt. In contrast to this, epithelial cells deficient for Pten alone were found to show a slight increase in staining for $pAkt^{Ser473}$ in the crypt, but this was not apparent on the villus. Again, the cellular pattern of staining was observed to be homogeneously cytoplasmic. In tissue deficient

for both Pten and Apc, a clear increase in activation of Akt is observed in the crypt, again with no change in subcellular localisation. On the villus (at the 'leading edge' of Pten- and Apc- deficient tissue), the increase in staining intensity for $pAkt^{Ser473}$ is observed to be much more profound. In addition to this increase in staining, a clear alteration in subcellular localisation of pAkt is also observed, with much stronger staining evident at the cell surface. This is a significant finding, as cell-surface localisation of Akt has previously been associated with an increase in oncogenic potential, both *in vitro* and in a transgenic mouse model (Mende et al., 2001).

The differential staining patterns observed between crypt and villus may be attributed to the age of epithelial cells being examined. The kinetics of cell turnover in the epithelium dictates that the youngest epithelial cells reside in the crypt, with cells increasing in age up the crypt-villus axis towards the villus tip, where the oldest cells will reside (Heath, 1996). Thus, cells at the base of the crypt have arisen from a recombined stem cell, and will have been deficient for Pten and/or Apc for a relatively short period of time in their epithelial lifespan. Cells residing on the villus will have been Pten- and/or Apc-deficient for a more extended amount of time. Taking this into account, it appears that young epithelial cells deficient for Pten alone show an increase in activation of Akt, which then decreases over time as cells migrate up onto the villus. In a reciprocal pattern to this, epithelial cells deficient for Apc alone initially show no increase in activation of Akt, but with time levels of pAkt increase, and cells on the villus show a clear increase in Akt activation. When mutation of both Pten and Apc is combined in the epithelium, it could be hypothesised that these two scenarios combine and become synergistic. Double-deficient epithelial cells show activation of Akt in the crypt, presumably driven by Pten deficiency at this stage. Activation of Akt in double-deficient cells on the villus is maintained, and at this point is presumably driven by activation of Wnt signalling. In older cells on the villus, relocalisation of pAkt to the cell surface is also observed, which is not observed in single mutant controls. This is apparently a synergistic effect of loss of Pten and Apc, with increased expression of pAkt presumably driven by loss of Apc, and its relocalisation to the cell surface permitted by loss of Pten.

These data therefore imply that activation of Wnt signalling and loss of Pten may synergise to cause increased oncogenicity, through increased activation and cell-surface localisation of Akt. However, intestinal deletion of both copies of Apc is catastrophic for intestinal homeostasis, resulting in morbidity within approximately 5-7 days (Sansom et al., 2004). Thus, this model cannot be used to truly test the oncogenic potential of synergy between Wnt and PI3K/Akt signalling. For this reason, I next went on to examine the effect of epithelial Pten loss in the context of a Wnt-driven tumour-prone background, achieved by conditional deletion of one allele of *Apc*.

5.3.2 Rapid progression of Wnt-initiated tumourigenesis in the context of Pten deficiency

Experimental animals ($Apc^{f/+};Pten^{f/f}$) and controls ($Apc^{f/+};Pten^{+/+}$, also referred to as '$Apc^{f/+}$') were generated, induced and aged whilst being monitored for signs of intestinal disease. $Apc^{f/+};Pten^{f/f}$ animals were found to have a significantly reduced lifespan, with a median survival of just 85 days, compared to $Apc^{f/+}$ controls, which had a median survival time of 409 days. Upon dissection, $Apc^{f/+};Pten^{f/f}$ animals were found to contain macroscopically different, flattened lesions within the small intestine and also polyp-like lesions within the large intestine. Histological analysis of small intestinal lesions revealed them to be bona fide malignant lesions of the mucosa. Multiplicity of tumours in the small and large intestines of $Apc^{f/+};Pten^{f/f}$ animals and control $Apc^{f/+}$ animals at timepoints of 190 and 250 days PI was scored. $Apc^{f/+};Pten^{f/f}$ animals were found to have a significant increase in tumour burden within the small intestine. No difference in tumour multiplicity was observed in the large intestine, however it is notable that the tumour burden in the large intestine of $Apc^{f/+};Pten^{f/f}$ animals was comparable to $Apc^{f/+}$ controls at 190 and 250 days PI, given that the median survival time of $Apc^{f/+};Pten^{f/f}$ animals is reduced to 85 days. These data therefore indicate that additional deficiency of Pten increases predisposition to tumour formation in both the small intestine and large intestine in an Apc heterozygous background.

Closer assessment of the small intestinal tumours arising in $Apc^{f/+};Pten^{f/f}$ animals revealed them to be obviously histologically different to the tumours arising in small intestines of $Apc^{f/+}$ controls. Tumours arising in $Apc^{f/+};Pten^{f/f}$ animals were found to be more commonly invasive into both the stroma and the muscularis, showed a stronger desmoplastic response to the lesion and also showed signs of a host immune response to the tumour. These features were generally not observed in lesions of $Apc^{f/+}$ animals, though occasional lesions showed early signs of invasive behaviour. Indeed, quantification of the severity of lesions arising in $Apc^{f/+};Pten^{f/f}$ compared to $Apc^{f/+}$ animals reflected these observations. In $Apc^{f/+}$ animals, the majority of small intestinal lesions were found to be Adenomatous, with a small proportion of lesions found to show invasive characteristics (Early invasive adenocarcinoma; 14%). In contrast, fewer tumours in $Apc^{f/+};Pten^{f/f}$ animals were found to be Adenomatous, with a larger proportion of early invasive adenocarcinomas compared to controls. A further, significant subset of tumours was found to have progressed to the advanced invasive adenocarcinoma stage.

It is therefore clear from these data that in the context of Apc heterozygosity, additional epithelial deletion of Pten drives both an increase in multiplicity of small intestinal lesions and also drives progression of those lesions to a malignant phenotype. The low level of background adenomas present in $Apc^{f/+};Pten^{f/f}$ animals indicates that progression of disease is rapid in the context of Pten loss. In $Apc^{f/+}$ animals, severity of intestinal disease was not observed to equal that of $Apc^{f/+};Pten^{f/f}$ animals, even in very aged animals. This exemplifies the dramatic acceleration of disease progression resulting from epithelial Pten loss in the context of Apc

heterozygosity. This finding is significant, as currently most mouse models of intestinal tumourigenesis model only the very early stages of disease initiation and polyp formation. However, here I have described a robust model of progression of intestinal tumours past the adenoma stage, with frequent development of advanced adenocarcinoma. However, it should be noted that the lesions described here were never observed to be metastatic, and this therefore represents a model of late-stage colorectal cancer, but not metastatic disease.

As described above, in the short-term, loss of both Pten and Apc synergise to cause activation and cell-surface localisation of Akt, which is associated with increased oncogenic potential. I next set about determining whether this phenomenon was associated with advancement of disease in $Apc^{f/+};Pten^{f/f}$ animals compared to $Apc^{f/+}$ controls.

I first confirmed that tumours in $Apc^{f/+}$ small intestines were deficient for Apc but retained staining for Pten protein and that those in $Apc^{f/+};Pten^{f/f}$ small intestines were deficient for both Apc and Pten. Adjacent serial sections were subjected to anti-Pten IHC and anti-beta-catenin IHC. This indicated that epithelial cells of tumours arising in $Apc^{f/+}$ animals had lost Apc and showed increased expression and nuclear localisation of beta-catenin, but remained proficient for Pten protein. Tumours in $Apc^{f/+};Pten^{f/f}$ animals were found to show similar increased expression and nuclear localisation of beta-catenin indicating loss of Apc, and were also found to show deficiency for Pten in epithelial cells, whilst the underlying stromal component retained positivity for Pten protein.

As above, adjacent sections of tumours were then immunohistochemically stained for $pAkt^{Ser473}$. Tumours arising in $Apc^{f/+}$ animals were found to show an increase in staining for pAkt compared to surrounding, unaffected tissue. Similar to single Apc mutant animals at day 5 PI, staining was observed to be homogeneously cytoplasmic, with no differential staining at the subcellular level. The strongest staining for pAkt was observed to be at the surface of the tumour, closest to the lumen of the intestine. Similarly, tumours from $Apc^{f/+};Pten^{f/f}$ animals also showed an increase in staining for pAkt, which was also most apparent at the lumenal surface of the tumour. Additionally, tumours from $Apc^{f/+};Pten^{f/f}$ animals were consistently found to contain regions where staining for pAkt was strongest at the cell surface of epithelial cells, similar to that seen in $Apc^{f/f};Pten^{f/f}$ tissue at day 5 PI. These regions were also generally located at the surface of the tumour, closest to the lumen of the intestine, where pAkt was found to be upregulated. This therefore indicates that upregulation and cell surface localisation of pAkt may play a role in increased severity of disease in $Apc^{f/+};Pten^{f/f}$ intestines. What is surprising, however, is that epithelial cells which are invading into the submucosa in these lesions do not show dramatic activation of Akt, and do not show an increase in cell surface staining for Akt. If cell surface localisation of activated Akt was the main influence driving progression of these lesions, it would be expected that these cells should stain in a similar fashion to those at the tumour surface. Thus,

from these observations, I conclude that whilst the presence of activated Akt at the cell-surface of tumour epithelial cells is characteristic of tumours arising in $Apc^{f/+};Pten^{f/f}$ animals, I cannot confirm that this phenomenon is directly driving progression (or at least invasion) of disease. However, the possibility that cell-surface localisation of pAkt is indirectly driving tumourigenesis remains, and in my opinion warrants further investigation.

5.3.3 Summary and future work

In summary, a number of conclusions can be drawn from the work presented in this chapter. Firstly, loss of Pten and Apc synergise to activate Akt, and also influence its subcellular localisation, resulting in increased association with the cell membrane. However, the implications of this on intestinal tumourigenesis remain unclear. One potential way of clarifying the role of membrane-associated Akt in driving tumourigenesis in $Apc^{f/+}$ mice would be to make use of a conditionally-expressed membrane targeted form of Akt, such as that previously published (Mende et al., 2001). If $Apc^{f/+}$ mice bearing this membrane-targeted form of Akt were found to phenocopy the observed increase in severity of intestinal disease reported here in $Apc^{f/+};Pten^{f/f}$ mice, it would provide compelling evidence for the fact that disease progression is driven by altered subcellular localisation of Akt. Furthermore, it would be interesting to determine whether relocalisation of pAkt to the cell-surface is a feature of advanced human disease, as it may potentially provide a good prognostic marker for colorectal lesions[5].

Secondly, in the context of Apc heterozygosity, it is clear that additional loss of Pten causes a rapid progression of tumourigenesis, resulting in invasive disease. The penetrance of invasive intestinal tumours in these mice is extremely high, meaning that this strain represents a robust model of advanced intestinal cancer, though does not model metastasis of disease. The generation of this model is a significant finding, as few good mouse models of more advanced disease states currently exist. The potential of this model for use both in developing therapies aimed at advanced disease, as well as to allow closer examination into the mechanisms underlying invasion and progression of intestinal lesions, is therefore great. Furthermore, additional mutations could be incorporated into this model in an attempt to generate a model of metastatic colorectal cancer. One good candidate for this would be E-Cadherin, a cell-surface adhesion protein, which is found to be downregulated in more advanced human disease, and has been associated with increased invasiveness and metastasis (Van Aken et al., 1993). If this were achieved, this series of models would then represent all the major stages involved in multi-step

[5] A tissue array based on human colorectal cancer biopsies for presence and subcellular localisation of Akt is currently being carried out in collaboration with Dr Marnix Jansen of Hans Clevers' group, Hubrecht Institute, The Netherlands.

colorectal tumourigenesis, from initiation of disease (in $Apc^{f/+}$ mice), through progression and invasiveness of tumours (in $Apc^{f/+}$;$Pten^{f/f}$ mice) to full-blown metastatic disease (See Figure 5.12).

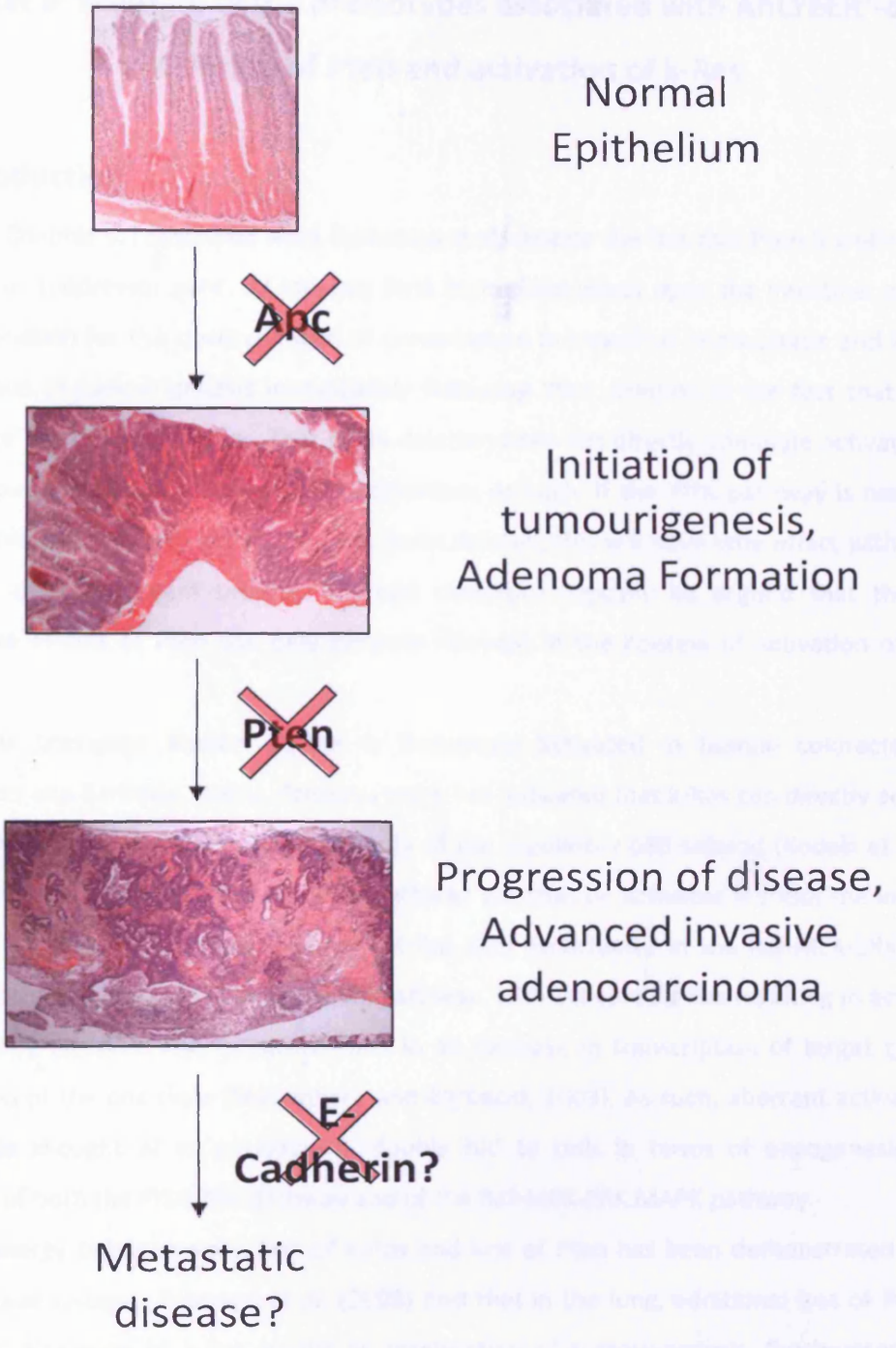

Figure 5.12: ***The potential of Apc and Pten-deficient mice to generate an animal model of step-wise progression of colorectal cancer***

Loss of one copy of Apc alone results in initiation of tumourigenesis and adenoma formation, as described here and elsewhere (Shibata et al., 1997, Moser et al., 1995). Additional loss of Pten results in an increase in severity of tumour phenotype, as indicated by increased dysplasia and invasiveness of epithelial cells and a strong desmoplastic and immune response. However, this does not model metastatic disease. Additional mutations could be incorporated into this model, for instance in the adhesion protein E-Cadherin, in order to promote metastasis of malignant cells.

Chapter 6: Multiple tissue phenotypes associated with AhCreER^{T}-driven deletion of Pten and activation of k-Ras

6.1 Introduction

In Chapter 3, I described work indicating that, despite the fact that Pten is well recognised as a tumour suppressor gene, its loss has little immediate effect upon the intestinal epithelium. One explanation for the observed lack of perturbation in intestinal homeostasis and indeed for the absence of tumourigenesis immediately following Pten deletion is the fact that Pten is a 'permissive' tumour suppressor. That is, its deletion does not directly stimulate activation of the PI3K/Akt pathway; rather it permits its activation. As such, if the PI3K pathway is not normally active within the cell from which Pten has been deleted, this will have little effect with regard to activation of downstream targets. It could therefore logically be argued that the tumour suppressive effects of Pten will only become relevant in the context of activation of the PI3K pathway.

The oncogene Kirsten (k)-Ras is frequently activated in human colorectal cancers (Malumbres and Barbacid, 2003). Previous work has indicated that k-Ras can directly activate the p110 catalytic subunit of PI3K, independently of the regulatory p85 subunit (Kodaki et al., 1994). Through activation of k-Ras, the PI3K/Akt pathway can thus be activated without the influence of upstream signals, such as growth factors. K-Ras also participates in the Raf-MEK-ERK mitogen-activated protein kinase (MAPK) signalling pathway, with activated k-Ras resulting in activation of the signalling cascade. This in turn results in an increase in transcription of target genes, and progression of the cell cycle (Malumbres and Barbacid, 2003). As such, aberrant activation of k-Ras can be thought of as providing a 'double hit' to cells in terms of oncogenesis; causing activation of both the PI3K/Akt pathway and of the Raf-MEK-ERK MAPK pathway.

Synergy between activation of k-Ras and loss of Pten has been demonstrated *in vivo* in several tissue systems. *Iwanaga et al.* (2008) find that in the lung, additional loss of Pten in the context of activation of k-Ras results in acceleration of tumourigenesis. Furthermore, lesions arising in double mutant animals were found to be more advanced than those in k-Ras mutants alone, with an increase in tumour invasion, greater vascularisation of tumours and a marked host immune response. Co-operation between k-Ras and Pten has also been noted in the development of endometrioid ovarian cancer (Dinulescu et al., 2005). This study reports that, whilst mutation of either k-Ras or Pten alone results in the development of pre-neoplastic lesions of the female genitourinary tract, combined mutation of both genes results in rapid development of endometrioid ovarian adenocarcinomas. These cancers were found to be characterised by strong

activation of the PI3K/Akt pathway, as evidenced by detection of high levels of phospho-Akt, phospho-mTOR and phospho-S6 kinase, as well as activation of the Raf-MEK-ERK pathway, as indicated by increased expression of phospho-ERK.

In mouse models such as these, conditional activation of the k-Ras oncogene is accomplished through expression of a constitutively active form of k-Ras, achieved by incorporation of an activating point mutation at codon 12 (Malumbres and Barbacid, 2003). The mutant k-Ras allele is normally kept in a transcriptionally silent state through use of a LoxP-flanked STOP cassette within the transgene. Thus, exposure to Cre recombinase permits the mutant form of k-Ras to be expressed.

In the intestine, studies employing this strategy have indicated that sensitivity exists both with respect to levels of activated k-Ras and with respect to the exact point mutant form of k-Ras which is used. Strong expression of the G12V mutant (glycine to valine substitution at codon 12) of k-Ras has been shown to result in rapid development of intestinal neoplasms (Janssen et al., 2002). In contrast, more moderate expression of the same G12V mutant of k-Ras, driven by its endogenous promoter, results in a less severe spectrum of intestinal phenotypes. One study reports little effect upon intestinal homeostasis following activation of k-Ras (Sansom et al., 2006), whilst a separate study identifies the formation of aberrant crypt foci, but no overt intestinal lesions (Guerra et al., 2003). Furthermore, use of the same endogenous promoter to drive a G12D point mutant for of k-Ras is reported to result in rapid and widespread hyperplasia and dysplasia of the epithelium (Tuveson et al., 2004). Thus it is clear that both levels of expression of k-Ras and the exact mutant form of the oncogene both have a bearing upon intestinal phenotype.

In the intestinal tumour-prone context of activated Wnt signalling, Sansom et al. have further shown that additional aberrant activation of k-Ras (using the endogenously expressed G12V mutation) causes moderate progression of tumour severity, with resulting tumours showing early invasive characteristics (Sansom et al., 2006). However, potential synergy between activation of k-Ras and deletion of Pten specifically within the intestine remains unexplored.

In this chapter, I aimed to investigate the role of Pten as a tumour suppressor in the context of activation of the PI3K pathway. This is achieved by conditional and co-ordinate activation of the endogenous k-Ras^{V12} mutant transgene and deletion of Pten in the intestinal epithelium. This approach was chosen to allow me to address the notion that Pten is a 'permissive' tumour suppressor, and that its loss only becomes significant in the context of activated PI3K signalling. In addition, any potential synergy between Pten loss and k-Ras activation with respect to activation status of the PI3K/Akt and Raf-MEK-ERK pathways will be assessed, and any resulting impact on intestinal homeostasis or tumourigenesis evaluated.

6.2 Results

6.2.1 Mice with induced deficiency of Pten and activation of k-Ras show a dramatic reduction in survival time

Experimental animals, bearing LoxP-targeted Pten alleles ($Pten^{f/f}$) and heterozygous for the LoxP-STOP activated endogenous k-Ras G12V mutant transgene ($kRas^{+/T}$) (Guerra et al., 2003) as well as the double-regulated Cre transgene, $AhCreER^{T}$, were generated ($AhCreER^{T+}$;$Pten^{f/f}$;$kRas^{+/T}$, herein referred to as '$Pten^{f/f}$;$kRas^{+/T}$'). Appropriate controls ($AhCreER^{T+}$;$Pten^{f/f}$;$kRas^{+/+}$, also referred to as '$Pten^{f/f}$', $AhCreER^{T+}$;$Pten^{+/+}$;$kRas^{+/T}$, also referred to as '$kRas^{+/T}$', and $AhCreER^{T+}$;$Pten^{+/+}$;$kRas^{+/+}$, referred to as 'WT') were also generated. Cohorts of all genotypes of mice, each comprised of more than 15 animals, were induced as described (Section 2.1.3.3). Animals were then aged, whilst being monitored for signs of disease, and culled when moribund.

Induced $Pten^{f/f}$;$kRas^{+/T}$ cohort animals were found to rapidly become morbidly underweight, which in the majority of instances forced early culling of the animal. Weight loss was not observed in any control animals.

Kaplan-Meier survival analysis of all cohorts was performed (Figure 6.1). This revealed a prominent reduction in survival time of $Pten^{f/f}$;$kRas^{+/T}$ animals compared to all control genotypes. $Pten^{f/f}$;$kRas^{+/T}$ animals were found to have a median survival time of just 43 days after induction, compared to $Pten^{f/f}$ controls and WT controls which had median survival times of 409 days and 801 days respectively. Median survival time of the $kRas^{+/T}$ control cohort was not determined, as this experiment has not yet reached completion and more than 50% of the animals in the cohort currently remain healthy. The difference in survival times between all control and $Pten^{f/f}$;$kRas^{+/T}$ cohorts was found to be statistically significant (Kaplan-Meier analysis, $p<0.001$, $DF=3$, $\chi^2=125.45$).

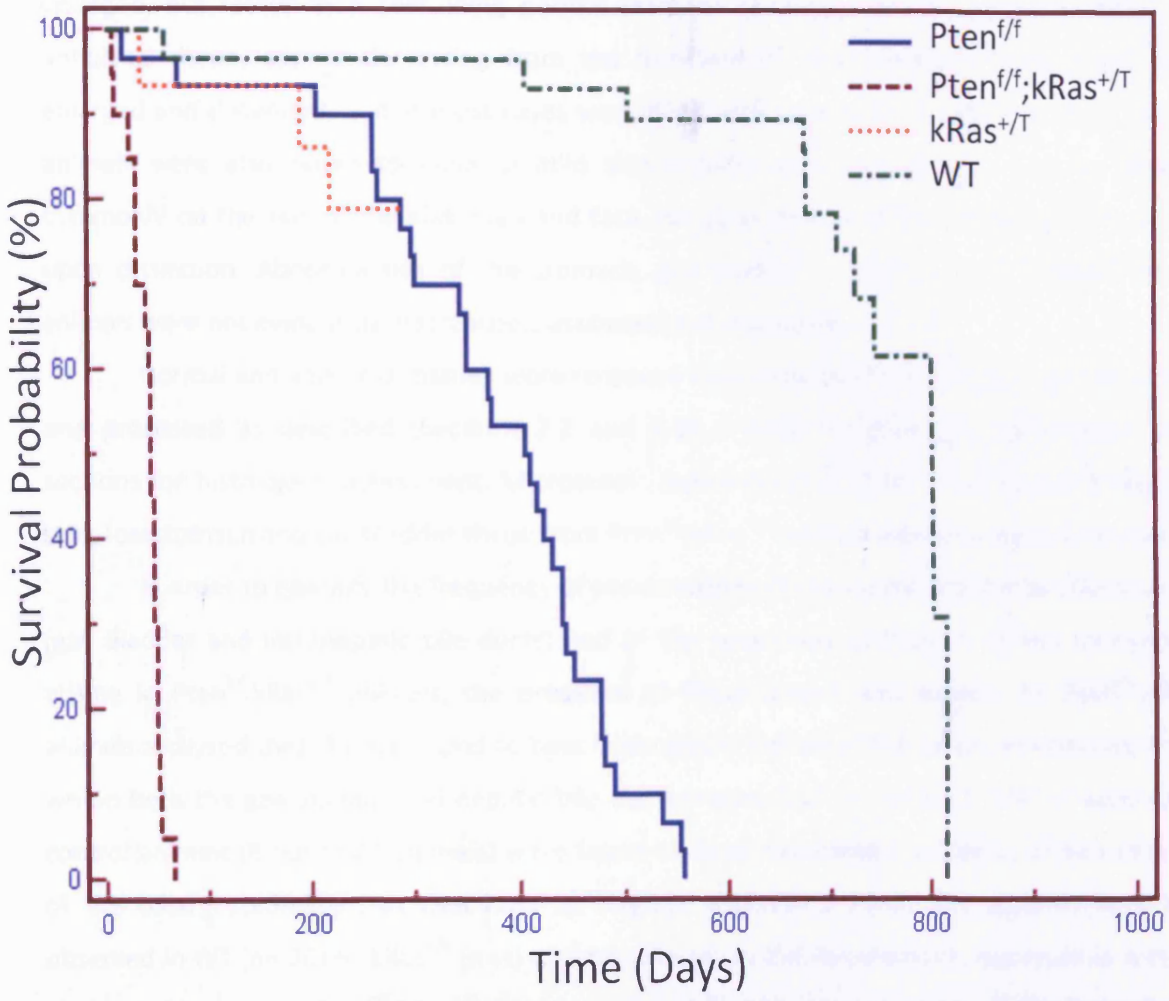

Figure 6.1: ***Kaplan-Meier survival analysis of Pten$^{f/f}$;kRas$^{+/T}$ mice compared to controls***
Pten$^{f/f}$;kRas$^{+/T}$ and controls (Pten$^{f/f}$, kRas$^{+/T}$ and WT) were induced and aged, and culled when symptomatic of disease. Pten$^{f/f}$;kRas$^{+/T}$ animals were found to have a dramatically reduced survival time compared to all controls, with a median survival time of 43 days, compared to 409 days and 801 days of Pten$^{f/f}$ and WT controls respectively. Median survival time of kRas$^{+/T}$ controls was not determined as this experiment has not yet reached completion and more than 50% of the animals in the cohort currently remain healthy. Reduction in survival time of Pten$^{f/f}$;kRas$^{+/T}$ animals was found to be statistically significant (Kaplan-Meier analysis, $p<0.001$, DF=3, $\chi^2=125.45$).

6.2.2 Highly penetrant phenotypes of gall bladder and bile duct lesions, and forestomach squamous hyperplasia in Pten$^{f/f}$;kRas$^{+/T}$ animals

Upon dissection, virtually all Pten$^{f/f}$;kRas$^{+/T}$ animals were found to bear macroscopically visible abnormalities of both the stomach and the gall bladder. Stomachs were found to be grossly enlarged, but rather than containing normal stomach contents were found to be filled with abnormal tissue, apparently arising from the forestomach. Gall bladders were found to be enlarged and distended, and in most cases were filled with clear fluid. A subset of Pten$^{f/f}$;kRas$^{+/T}$ animals were also noted to develop mild skin lesions, which appeared as warty growths, commonly on the skin of the abdomen and face. No gross lesions of the intestine were evident upon dissection. Abnormalities of the stomach, gall bladder or skin of Pten$^{f/f}$, kRas$^{+/T}$ or WT animals were not evident by macroscopic assessment at dissection.

Normal and abnormal tissues were removed from animals of each cohort, and were fixed and processed as described (Sections 2.2 and 2.3) in order to generate H&E-stained tissue sections for histological assessment. Microscopic examination of these sections confirmed that skin, forestomach and gall bladder tissue from Pten$^{f/f}$;kRas$^{+/T}$ animals was histologically abnormal.

In order to quantify the frequency of abnormalities of the epithelium of the biliary system (gall bladder and intrahepatic bile ducts) and of the squamous epithelium of the forestomach arising in Pten$^{f/f}$;kRas$^{+/T}$ animals, the presence of these lesions was scored. All Pten$^{f/f}$;kRas$^{+/T}$ animals analysed (n=15) were found to bear hyperplastic lesions of the biliary epithelium, arising within both the gall bladder and hepatic bile ducts (Figure 6.2). In contrast, 33% of aged Pten$^{f/f}$ control animals (8 out of 24 animals) were found to show microscopic evidence of abnormalities of the biliary epithelium, as described in Chapter 4 (Section 4.2.3). No abnormalities were observed in WT (n= 20) or kRas$^{+/T}$ (n=4) control animals. In the forestomach, hyperplasia was also clearly evident in all Pten$^{f/f}$;kRas$^{+/T}$ tissue examined (n=15). Abnormalities of the forestomach were never observed in WT, Pten$^{f/f}$ or kRas$^{+/T}$ control cohorts (n=20, n=8 and n=4 respectively).

Thus, from this data, it appears that co-ordinate deletion of Pten and activation of k-Ras results in rapid development of epithelial abnormalities of both the biliary system and of the forestomach with complete penetrance.

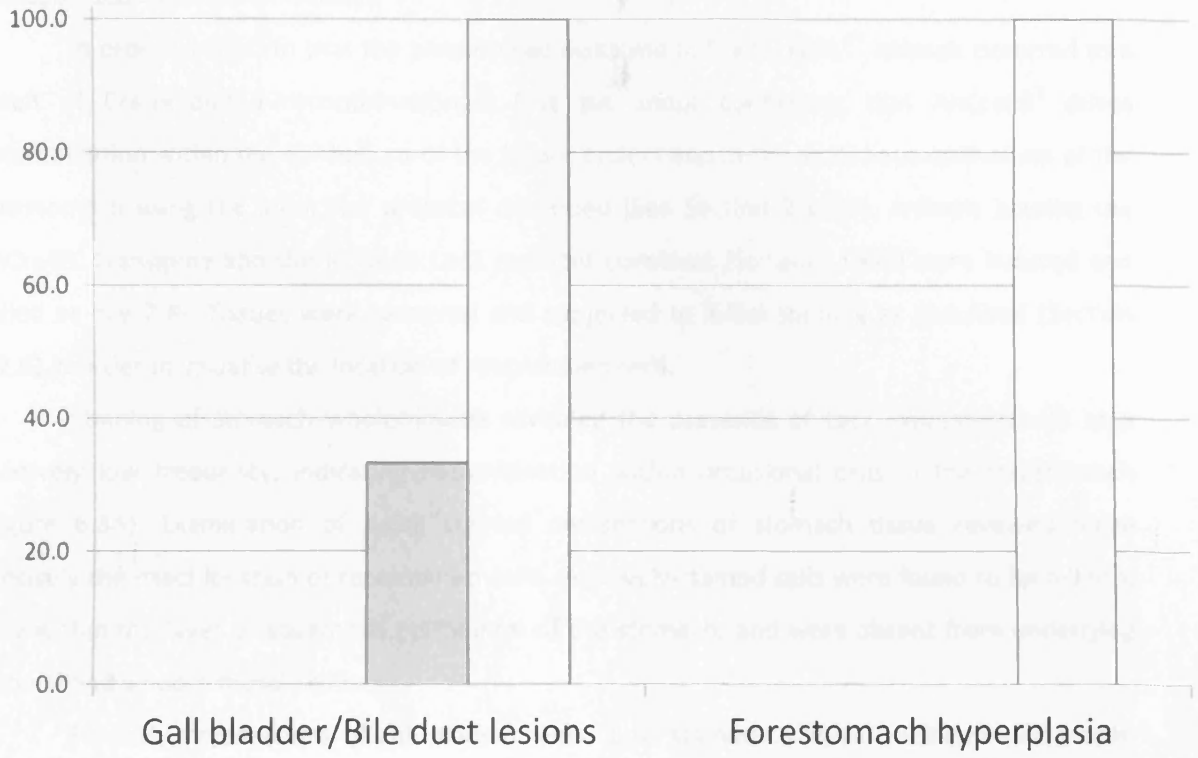

Figure 6.2: ***Scoring of pathologies found in Pten$^{f/f}$;Ras$^{+/T}$ and control animals***
Normal and abnormal tissues were removed from Pten$^{f/f}$, kRas$^{+/T}$ and WT controls and Pten$^{f/f}$;kRas$^{+/T}$ experimental animals , fixed and processed, and H&E-stained tissue sections generated. Tissues were then assessed microscopically for tissue abnormalities. All Pten$^{f/f}$;kRas$^{+/T}$ animals (White bars, 100%, n=15) were found to show evidence of hyperplasia of the epithelial cells of the gall bladder and/or hepatic bile ducts, as well as hyperplasia of the squamous epithelium of the forestomach. In contrast, Pten$^{f/f}$ control animals (grey bars) were found to show histological evidence of gall bladder/bile duct epithelium hyperplasia in 33% of cases (8 out of 24 animals) and did not show evidence of forestomach hyperplasia. WT and kRas$^{+/T}$ control animals were not found to bear either type of lesion in any animal analysed (n=20 and n=4 respectively).

6.2.3 AhCreER^T drives recombination in the gall bladder epithelium and forestomach squamous epithelium

Given that lesions of the forestomach and biliary system were apparently the cause of morbidity in Pten$^{f/f}$;kRas$^{+/T}$ animals, and were present with high penetrance, I more thoroughly characterised these abnormalities.

In order to confirm that the phenotypes observed in Pten$^{f/f}$;kRas$^{+/T}$ animals occurred as a result of Cre-mediated recombination, I first set about confirming that AhCreER^T drives recombination within the epithelium of the biliary system and in the squamous epithelium of the forestomach using the induction protocol described (See Section 2.1.3.3). Animals bearing the AhCreER^T transgene and the ROSA26 LacZ reporter construct (Soriano, 1999) were induced and culled at day 7 PI. Tissues were removed and subjected to X-Gal staining as described (Section 2.2.6) in order to visualise the location of recombined cells.

Staining of stomach wholemounts revealed the presence of LacZ-expressing cells at a relatively low frequency, indicating recombination within occasional cells in the forestomach (Figure 6.3A). Examination of X-Gal stained cryosections of stomach tissue revealed more precisely the exact location of recombined cells. Positively-stained cells were found to be present only within the layer of squamous epithelium of the stomach, and were absent from underlying stromal and smooth muscle cells.

Similarly, cryosections of gall bladder were X-gal stained to reveal LacZ-expressing cells. Positively-stained cells were apparent within the epithelium of the gall bladder, with levels of recombination noted to be higher than that observed in the forestomach (Figure 6.3B). Stained cells were found to be tightly restricted to the gall bladder epithelium, with no staining evident within any other cell types of the tissue.

Thus, it can be concluded that the induction protocol in use here drives low-level activation of Cre recombinase, and hence recombination at the ROSA26 allele within both the forestomach and the gall bladder, and in both cases is restricted to the epithelial cell population.

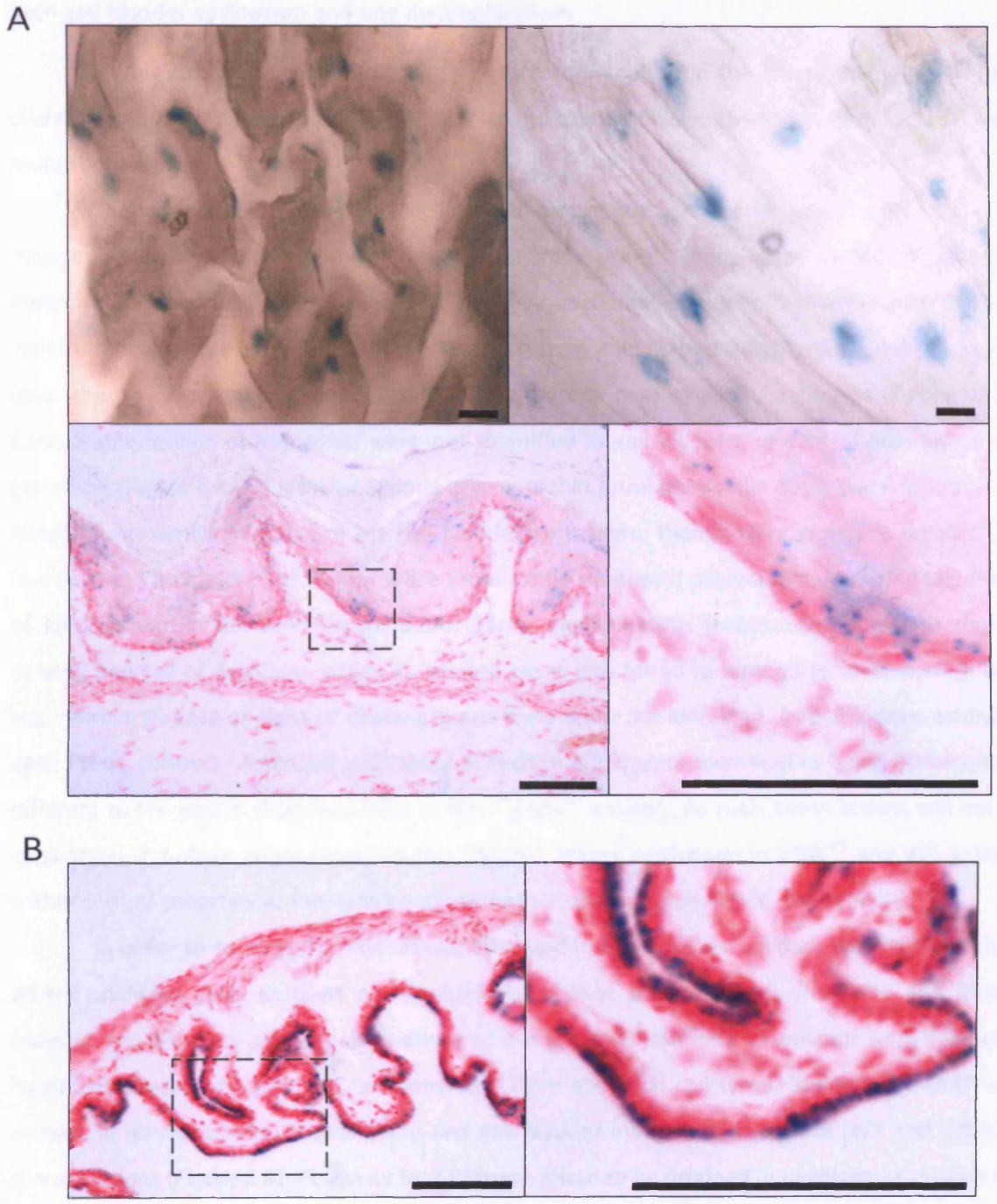

Figure 6.3: ***Low-level recombination in the forestomach and gall bladder epithelium driven by AhCreER^T***

Animals bearing both the AhCreER^T and ROSA26 LacZ reporter transgenes were induced as described, and culled at day 7 PI. Subsequent X-Gal staining allowed visualisation of the location and frequency of recombined cells within the forestomach (A) and gall bladder (B). Wholemount staining of stomachs from two individual animals (A, top panels, as viewed from the lumenal surface of the stomach) revealed occasional cells to be positive for LacZ activity. Staining of cryosections of the forestomach (bottom panels, right hand panel shows a digital enlargement of the indicated area in the left hand panel) revealed positively-stained cells to be solely within the squamous epithelium of the forestomach, with no staining for LacZ activity observed within any other cells types of the tissue. Staining of cryosections of the gall bladder (B, right panel shows a digital enlargement of the region indicated in the left panel) revealed that recombination occurred within epithelial cells lining the gall bladder, but not in other cells types present. Scale bars indicate 100μm.

6.2.4 Co-ordinate loss of Pten and activation of k-Ras results in hyperplasia and papilloma of both gall bladder epithelium and bile duct epithelium

Having established that AhCreER^{T} drives recombination in the biliary epithelium, I next characterised the histopathology of gall bladder and bile duct lesions arising in Pten$^{f/f}$;kRas$^{+/T}$ mice more thoroughly.

The advice of an experienced histopathologist was sought to assist with this[6]. The majority of lesions within the gall bladder of Pten$^{f/f}$;kRas$^{+/T}$ mice were identified as being hyperproliferative papilloma or dysplastic papillary adenomas of the epithelium (Figure 6.4A). A spectrum of lesion severity was identified, varying from mild epithelial hyperplastic foci to, in one case, the development of a moderately differentiated, invasive adenocarcinoma (Figure 6.4B). Comparable lesions of any grade were not identified in gall bladders of control animals of any genotype (Figure 6.4A). Epithelial lesions arising within intrahepatic bile ducts were found to be histologically similar to those of the gall bladder epithelium, though were generally found to be less severe. The majority of lesions were found to be multifocal papillomata, involving bile ducts of all sizes within the liver (Figure 6.5A). These papillomatous lesions were found to display varying degrees of dysplasia, which in isolated cases was found to amount to carcinoma *in situ*, but invasive disease or signs of cholangiocarcinoma were not identified. Ductal lesions arising in aged Pten$^{f/f}$ controls (described in Chapter 4, Section 4.2.3) were identified as being histologically different to the lesions described here in Pten$^{f/f}$;kRas$^{+/T}$ animals. As such, these lesions will not be considered in further analyses within this chapter. Biliary epithelium in kRas$^{+/T}$ and WT animals within control cohorts was found to be of normal histological appearance (Figure 6.5A).

In order to confirm that the lesions observed in Pten$^{f/f}$;kRas$^{+/T}$ animals were derived from biliary epithelial cells, sections of histologically normal control tissues from WT and kRas$^{+/T}$ animals, and lesions arising in gall bladder and bile ducts of Pten$^{f/f}$;kRas$^{+/T}$ animals were subjected to Anti-cytokeratin (CK) 19 IHC, a marker of biliary epithelial cell types. Staining for CK19 was evident in normal bile duct epithelium and gall bladder epithelium of control (WT and k-Ras$^{+/T}$) tissue sections (Figure 6.6). Positivity for CK19 was found to be retained in papillomata of both the bile duct and of the gall bladder epithelium in Pten$^{f/f}$;kRas$^{+/T}$ animals. Thus, this confirms that these lesions are indeed of biliary epithelial cell origin.

To qualitatively examine levels of proliferation within biliary epithelial lesions arising in Pten$^{f/f}$;kRas$^{+/T}$ animals, I next performed Anti-Ki67 IHC upon tissue sections as described in section 2.4. This revealed that lesions arising in the biliary epithelium of Pten$^{f/f}$;kRas$^{+/T}$ animals were highly positive for nuclear Ki67, with the vast majority of epithelial cells comprising the lesion

[6] The histopathological description and comparison of lesions arising in gall bladder and bile duct epithelia of Pten$^{f/f}$;kRas$^{+/T}$ mice and Pten$^{f/f}$ control mice was kindly provided by Prof Geraint T. Williams, Department of Pathology, University Hospital of Wales, Cardiff University, UK.

showing positive staining (Figure 6.7). This staining pattern was in contrast to that of areas of tissue on the same section which were found to be histologically normal. Such normal areas of tissue were found to contain only very occasional epithelial cells which were positively stained for Ki67. These observations therefore confirmed previous histopathological observations, indicating that the lesions arising within the biliary epithelium of $Pten^{f/f}$;$kRas^{+/T}$ animals are highly proliferative and hyperplastic.

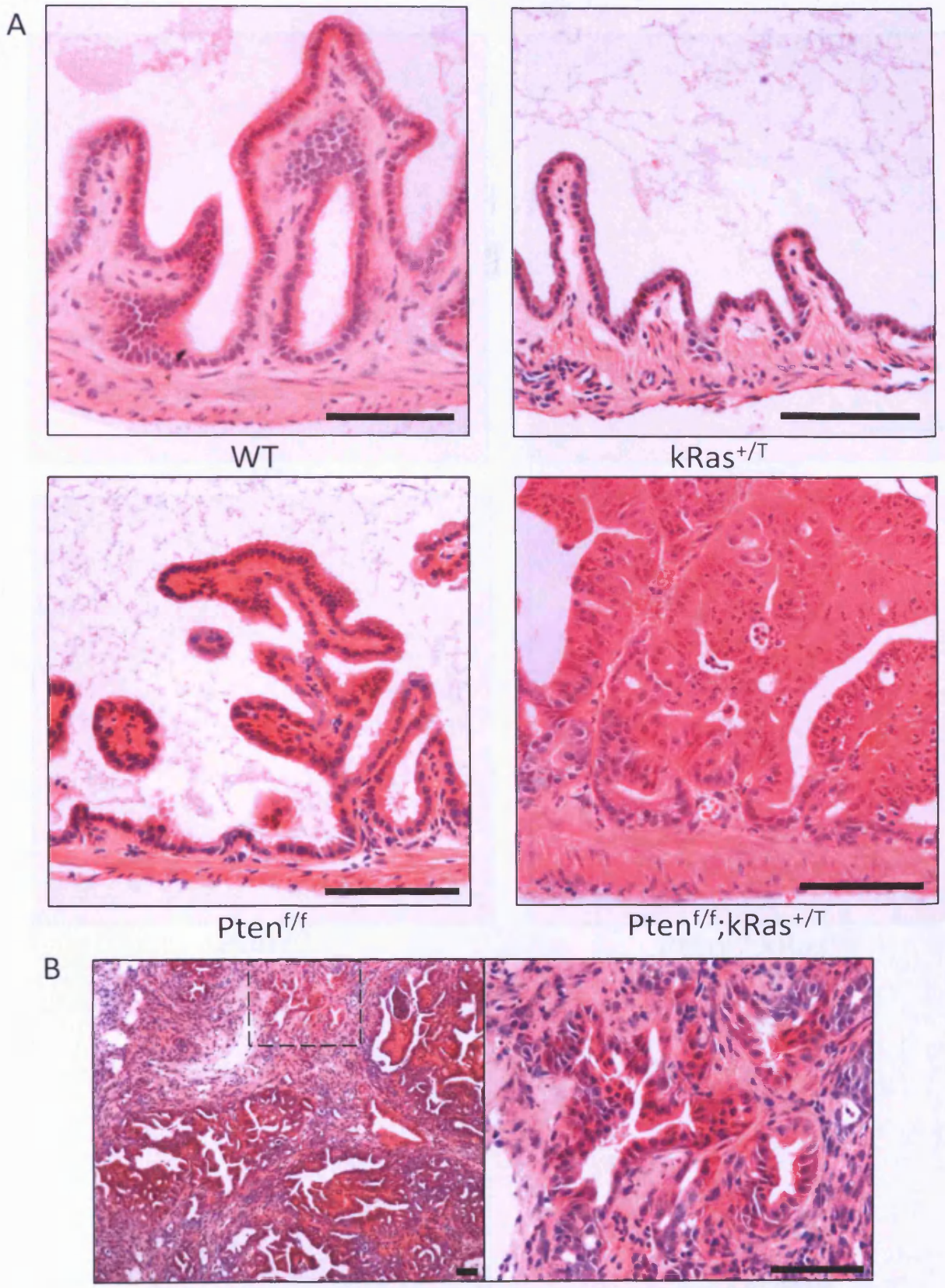

Figure 6.4: *Pten$^{f/f}$;Ras$^{+/T}$ mice are susceptible to hyperproliferative papilloma of the gall bladder epithelium*
Lesions arising within the gall bladder of Pten$^{f/f}$;kRas$^{+/T}$ animals were mostly identified as being hyperproliferative papilloma or dysplastic papillary adenomas of the epithelium (A). Similar lesions were not observed in gall bladder epithelia of control (Pten$^{f/f}$, kRas$^{+/T}$ and WT) animals. Rarely, more severe lesions of the gall bladder were identified, including one moderately differentiated, invasive adenocarcinoma (B, right hand panel shows magnification of the area indicated in the left hand image). Scale bars indicate 100µm.

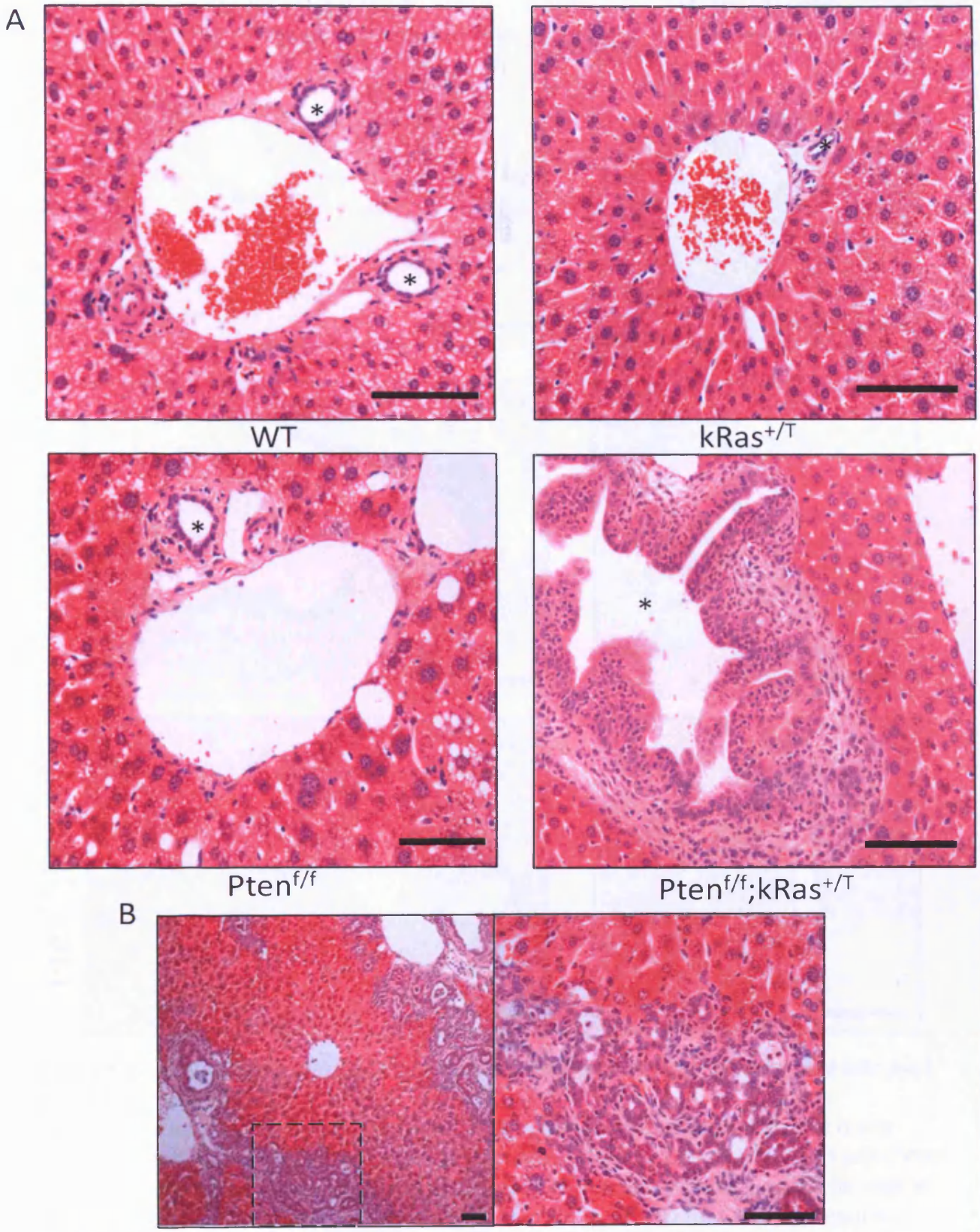

Figure 6.5: ***Pten$^{f/f}$;Ras$^{+/T}$ mice show susceptibility to papilloma of the bile duct***
Papillomatous lesions of the epithelium of intrahepatic bile ducts of all sizes were noted within Pten$^{f/f}$;kRas$^{+/T}$ animals (A). Similar lesions were not observed within bile ducts of control (Pten$^{f/f}$, kRas$^{+/T}$ or WT) animals. Papillomatous lesions arising in experimental animals were found to have varying degrees of dysplasia, which in some cases amounted to carcinoma in situ (B, Right hand panel is an enlargement of the indicated area of the left hand panel). Scale bars indicate 100μm. Asterisks indicate lumen of bile ducts.

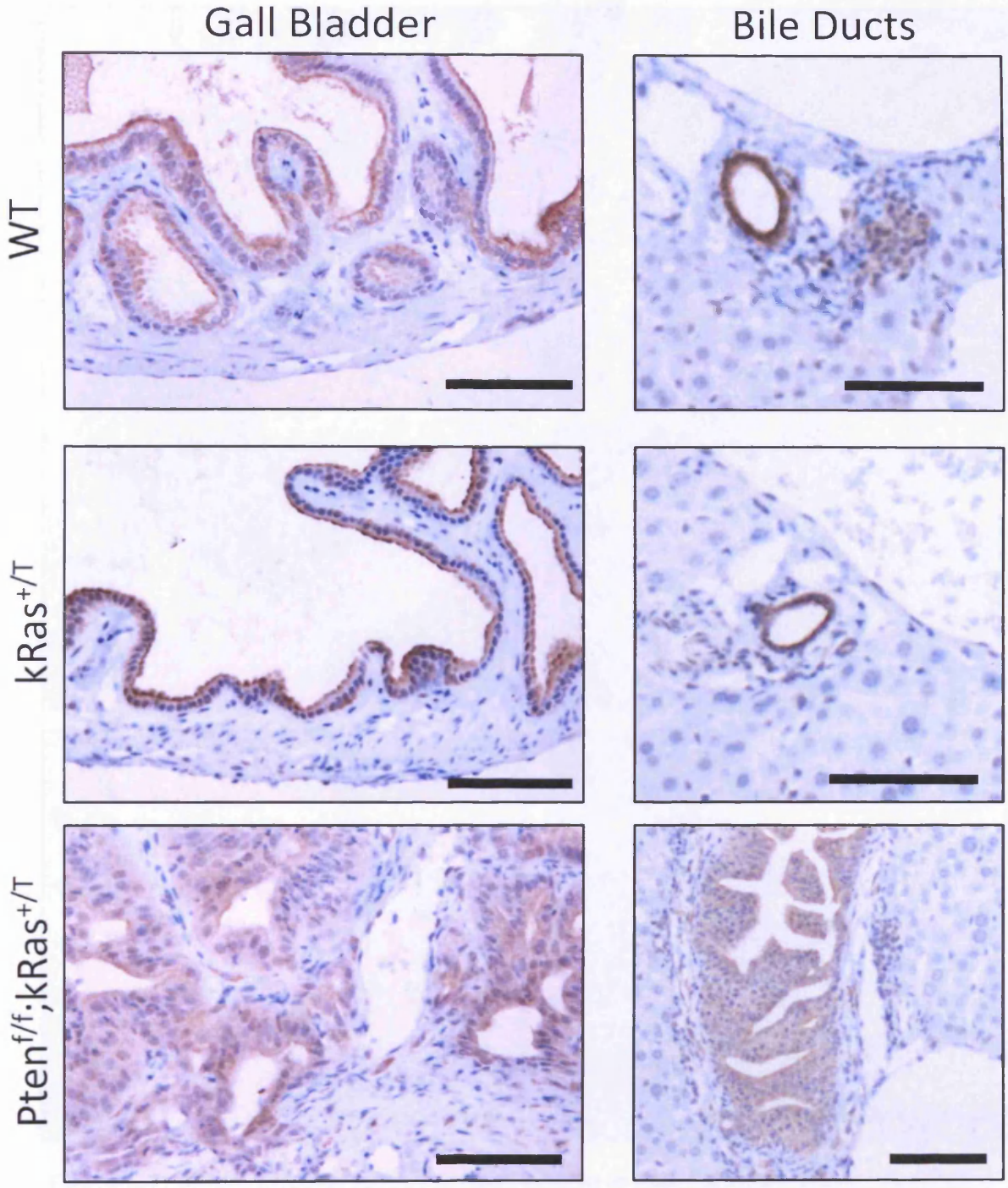

Figure 6.6: ***Anti-Cytokeratin 19 IHC reveals ductal origins of gall bladder and bile duct papillomatous lesions***

Anti-cytokeratin 19 IHC was performed on lesions of the gall bladder and bile ducts arising in $Pten^{f/f};kRas^{+/T}$ animals in order to confirm that the observed lesions arise from epithelial cells of the biliary system. Normal gall bladder and bile duct epithelial cells in WT and $k\text{-}Ras^{+/T}$ control animals were found to stain positively for CK19 expression. Papillomatous lesions within both the gall bladder and bile ducts of $Pten^{f/f};kRas^{+/T}$ animals were also found to show positive staining for CK19, indicating the lesions were indeed derived from biliary epithelial cells. Scale bars indicate 100µm.

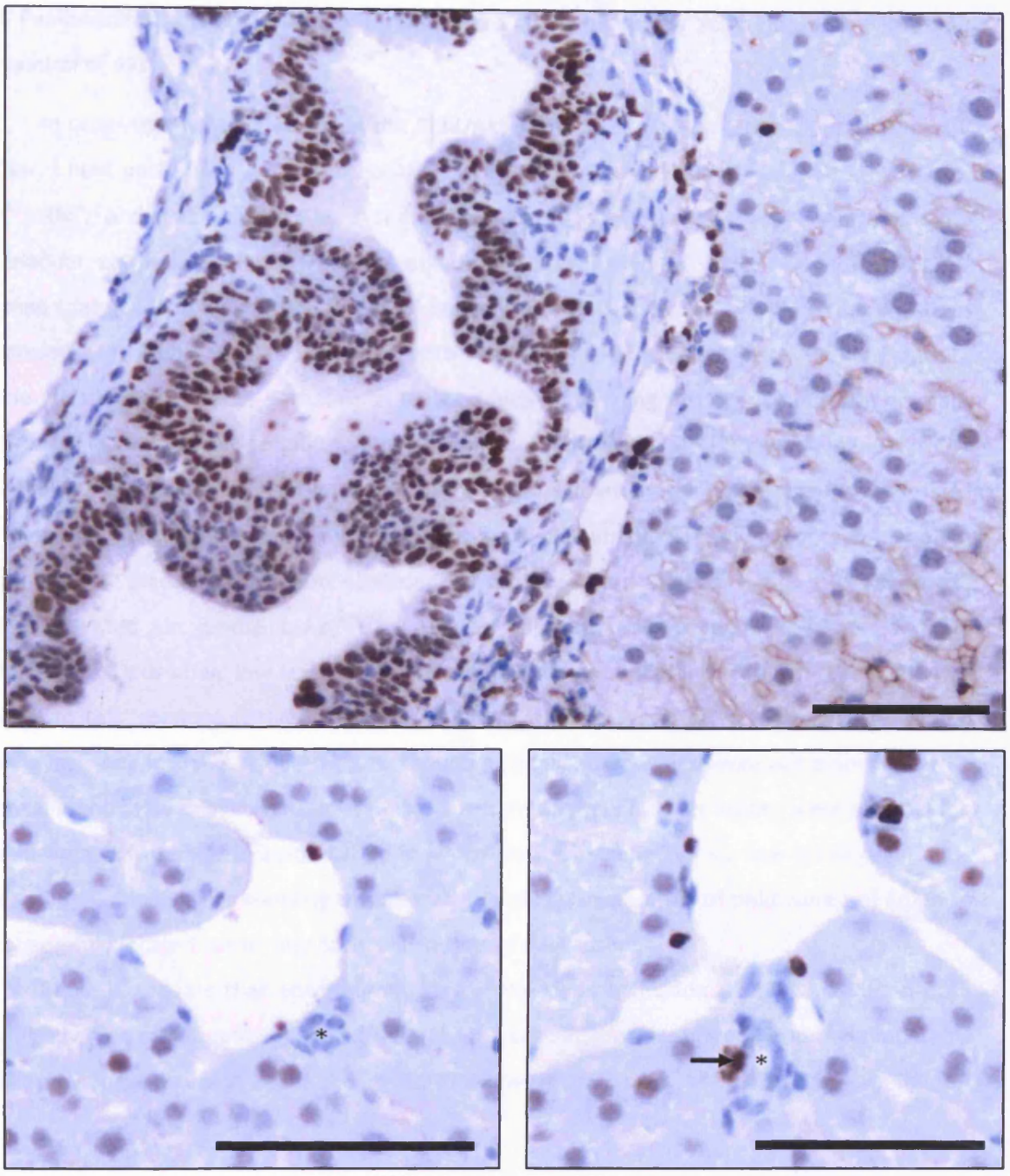

Figure 6.7: ***Biliary papillomatous lesions arising in Pten$^{f/f}$;kRas$^{+/T}$ mice are Ki67 antigen-positive***

In order to assess proliferation within papillomata of the biliary epithelium, IHC against the marker of proliferation, Ki67, was used to identify proliferating cells. Lesions arising in the biliary epithelium of Pten$^{f/f}$;kRas$^{+/T}$ animals were found to be Ki67-positive, with virtually all cells of the lesions showing nuclear staining (Top panel, representative image of a papilloma arising in the bile duct of a Pten$^{f/f}$;kRas$^{+/T}$ animal). In contrast to this, histologically normal bile ducts in the same tissue section were found to contain epithelial cells which were mainly Ki67-negative, indicating a low level of proliferation in normal tissue (Lower panels, Asterisks indicate lumen of unaffected bile ducts. Arrow indicates one example of an occasional ductal epithelial cell found to be Ki67-positive). Scale bars indicate 100μm.

6.2.5 Papillomatous lesions of the gall bladder are characterised by activation and membrane localisation of Akt

In order to assess activation of the PI3K/Akt pathway in papillomatous lesions of the gall bladder, I next performed Anti-phospho-Akt^{Ser473} IHC on serially-sectioned gall bladder tissue of Pten$^{f/f}$;kRas$^{+/T}$ and kRas$^{+/T}$ and WT control animals. First, Pten protein status was confirmed in the gall bladder epithelium of both control and Pten$^{f/f}$;kRas$^{+/T}$ animals using Anti-Pten IHC. This revealed that gall bladder epithelial cells of control mice (WT and kRas$^{+/T}$) stained positively for the presence of Pten protein in all cases, with little staining of underlying stromal and smooth muscle cells (Figure 6.8). In comparison to the levels of staining observed in control animals, Pten$^{f/f}$;kRas$^{+/T}$ animals were found to show a significant reduction in Anti-Pten staining within the epithelial cell layer, although low-level staining was still evident in isolated areas of some lesions and in unaffected epithelial cells. This probably reflects the sub-100% frequency of recombination within the gall bladder epithelium observed by LacZ reporter analysis. I then performed IHC against activated Akt (phospho-Akt^{Ser473}, pAkt) on adjacent tissue sections. In kRas$^{+/T}$ and WT control tissues, extremely low levels of staining for pAkt were apparent within the epithelium. In contrast to this, sections derived from Pten$^{f/f}$;kRas$^{+/T}$ animals were found to have an increased staining intensity for pAkt within lesions, though epithelial cells which were not associated with lesions did not show this increase in staining. Furthermore, gall bladder lesions were observed to contain areas of neoplastic epithelial cells which showed strong cell surface staining for pAkt (Figure 6.8). Epithelial cells showing this altered subcellular localisation of pAkt were not noted to be consistently located within any particular region of each lesion.

Thus, it appears that concomitant loss of Pten and activation of k-Ras results in both strong activation of Akt, and in its localisation to the cell surface. This phenomenon is comparable to that previously observed within the intestine following combined loss of Pten and Apc (Chapter 5).

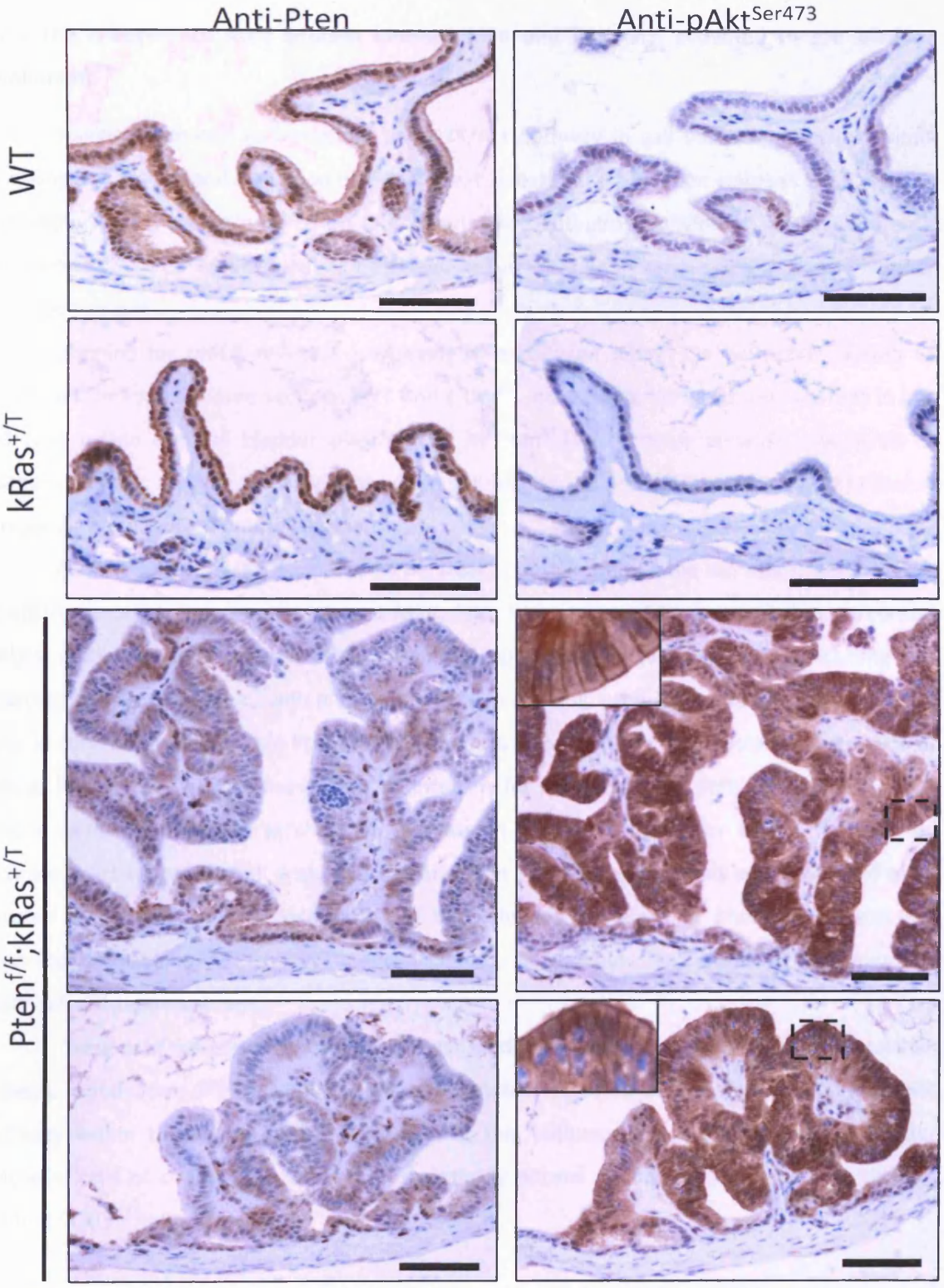

Figure 6.8: ***Upregulation and cell surface localisation of pAkt^{Ser473} in gall bladder lesions of Pten$^{f/f}$;kRas$^{+/T}$ mice***

Anti-Pten IHC confirmed that gall bladder epithelial cells of control genotypes (WT and k-Ras$^{+/T}$) show positivity for Pten, whilst lesions arising in experimental animals (Pten$^{f/f}$;kRas$^{+/T}$, two independent lesions are shown) show a dramatic reduction in Anti-Pten staining. Anti-pAkt^{Ser473} IHC was performed on adjacent serial sections of tissue, which indicated that, whilst tissues from WT and kRas$^{+/T}$ control animals were essentially devoid of staining, upregulation of activated Akt was apparent in lesions of Pten$^{f/f}$;kRas$^{+/T}$ animals. In addition to an increase in activation of Akt, cell surface localisation of pAkt within epithelial lesions was also observed (insets show digital enlargements of the areas indicated in the main image). Scale bars indicate 100µm.

6.2.6 The mitogen-activated protein kinases, MEK and ERK, are activated in gall bladder papillomata

Having confirmed activation of the PI3K/Akt pathway in gall bladder epithelial lesions following loss of Pten and activation of k-Ras, I next assessed the activation status of the Ras-MEK-ERK pathway in these lesions. To do this, I performed anti-phospho-MEK^{Ser221}(pMEK) and anti-phospho-ERK$^{Thr202/Tyr204}$ (pERK) IHC as described in section 2.4, on serial sections of gall bladder from each cohort.

Staining for pMEK revealed low levels of expression within the epithelium across all genotypes. In control tissue sections (WT and kRas$^{+/T}$), no staining for pMEK was evident in any cell type within the gall bladder (Figure 6.9). In Pten$^{f/f}$;kRas$^{+/T}$ tissue sections, low levels of epithelial-specific staining were evident within gall bladder lesions. Staining was not apparent in surrounding, uninvolved epithelial cells.

As staining for pMEK appeared to be weak, I next examined the activation status of the downstream cellular target of activated MEK, ERK. IHC against pERK revealed that, in control tissues, pERK was detected specifically within the epithelial cell layer (Figure 6.9). Staining was observed to be cytoplasmic, with a slight increase in staining intensity at the lumenal surface of cells. In contrast, lesions within Pten$^{f/f}$;kRas$^{+/T}$ animals were found to show increased activation of ERK, as indicated by an increase in staining intensity for pERK. Epithelial cells not associated with lesions were not observed to show an increase in staining intensity for pERK. The detected increase in activation of pERK within lesions arising in Pten$^{f/f}$;kRas$^{+/T}$ animals was also found to be coupled with strong nuclear localisation of the activated protein. This phenomenon was not observed either in kRas$^{+/T}$ or WT control tissues, or in uninvolved areas of epithelium in Pten$^{f/f}$;kRas$^{+/T}$ tissue sections.

These data therefore indicate that, in gall bladder lesions within Pten$^{f/f}$;kRas$^{+/T}$ animals, an increase in activation of both MEK and ERK is detectable, indicating activation of the Raf-MEK-ERK pathway within these neoplasms. Activation of this pathway is not evident in gall bladder epithelial cells of control tissues, or in histologically normal regions of gall bladder epithelium present in Pten$^{f/f}$;kRas$^{+/T}$ animals.

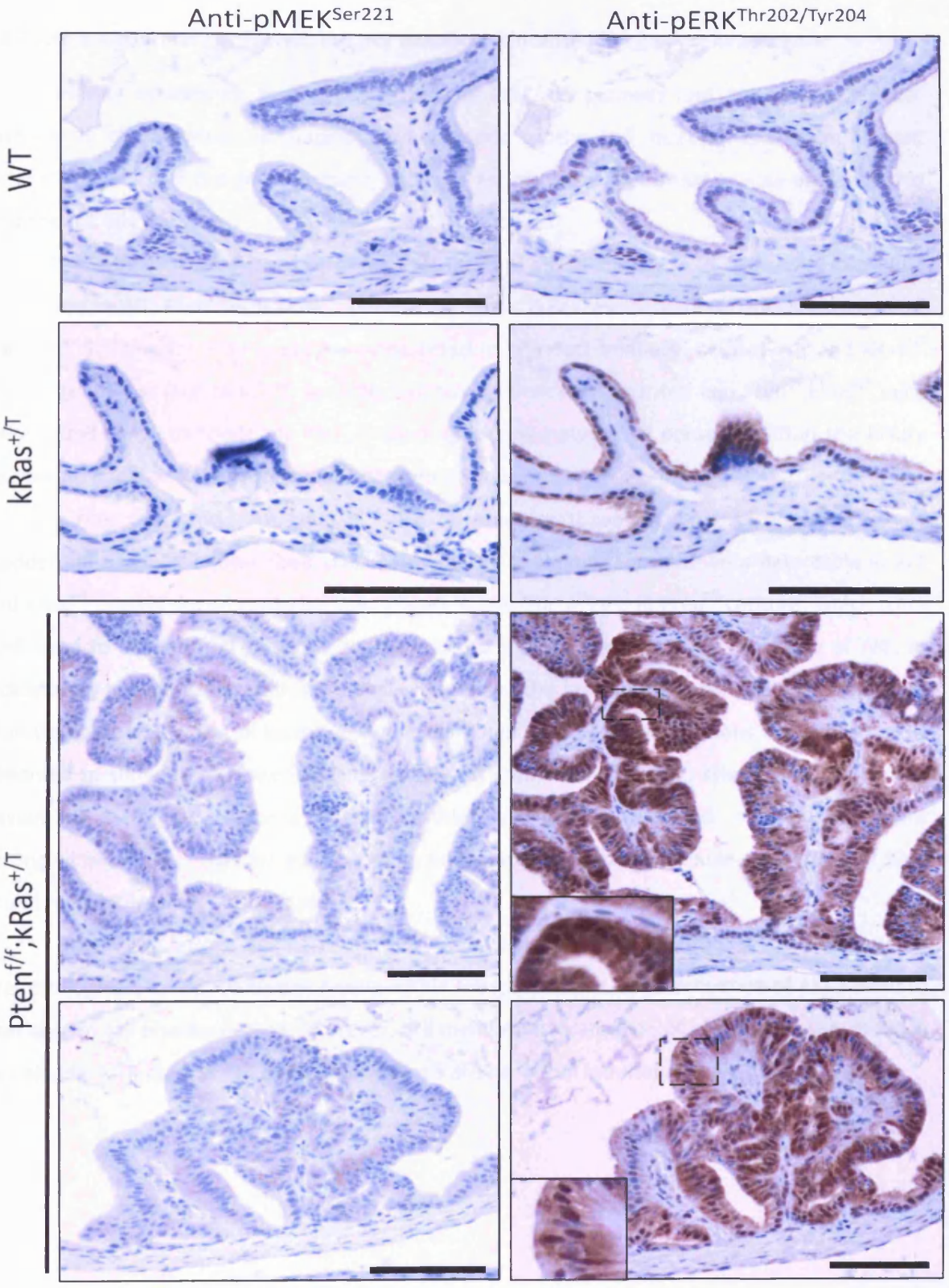

Figure 6.9: ***Upregulation of pMEK^{Ser221} and pERK$^{Thr202/Tyr204}$ in gall bladder lesions of Pten$^{f/f}$;kRas$^{+/T}$ mice.***

Activation of the Raf-MEK-ERK pathway in gall bladder papillomata of Pten$^{f/f}$;kRas$^{+/T}$ mice was assessed using anti-phospho-MEK^{Ser221} and anti-phospho-ERK$^{Thr202/Tyr204}$ IHC. Staining for pMEK was not observed in gall bladder epithelial cells of either control (WT or kRas$^{+/T}$) or Pten$^{f/f}$;kRas$^{+/T}$ animals, though a subtle increase in staining within lesions of Pten$^{f/f}$;kRas$^{+/T}$ animals was apparent. In tissues of WT and kRas$^{+/T}$ control animals, pERK staining was evident in epithelial cells, and was noted to be homogeneously cytoplasmic. In lesions of Pten$^{f/f}$;kRas$^{+/T}$ mice, an increase in staining intensity was observed, together with nuclear localisation of staining (inset images are digital enlargements of the areas indicated on the main image). Scale bars indicate 100µm.

6.2.7 Akt is moderately activated, but not membrane localised in bile duct hyperplasia

Having established that activation of the PI3K/Akt pathway and of the Raf-MEK-ERK pathway is characteristic of papillomatous lesions of the gall bladder epithelium, I next determined whether the same pattern was true for histologically similar lesions arising within intrahepatic bile ducts.

As previously, I first confirmed Pten status within normal and abnormal bile duct epithelium in WT, $Pten^{f/f}$ and $kRas^{+/T}$ control and $Pten^{f/f}$;$kRas^{+/T}$ experimental animals using anti-Pten IHC. Staining for Pten protein was detected in bile duct epithelial cells of WT and $kRas^{+/T}$ control genotypes (Figure 6.10). As expected, tissues from $Pten^{f/f}$ control and $Pten^{f/f}$;$kRas^{+/T}$ mice were found to be deficient for Pten, indicating recombination had occurred within the biliary epithelium and that Pten protein was lost from these cells.

I next performed anti-$pAkt^{Ser473}$ IHC on adjacent tissue sections. As observed in gall bladder epithelial cells (described above), low levels of staining for pAkt were detectable in WT and $kRas^{+/T}$ control ductal epithelial cells (Figure 6.10). Ductal cells in $Pten^{f/f}$ controls, which were confirmed to be deficient for Pten, were found to show a slight increase in activity of Akt, as indicated by an increase in staining intensity. However, this level of Akt activation remained lower than that observed in ductal lesions within $Pten^{f/f}$;$kRas^{+/T}$ animals. These lesions were consistently observed to show an increase in staining for pAkt compared to $Pten^{f/f}$, $kRas^{+/T}$ and WT control tissues and also in comparison to adjacent histologically normal ductal cells. In contrast to lesions arising within the gall bladder epithelium, in no instance was the subcellular localisation of pAkt found to be altered in ductal lesions.

Therefore, lesions arising within intrahepatic bile ducts of $Pten^{f/f}$;$kRas^{+/T}$ animals, which are histologically similar to lesions arising within the gall bladder, show activation of Akt, similar to that seen in gall bladder lesions. However, cell membrane localisation of pAkt, previously noted in gall bladder lesions, was not detected in lesions arising within intrahepatic bile ducts.

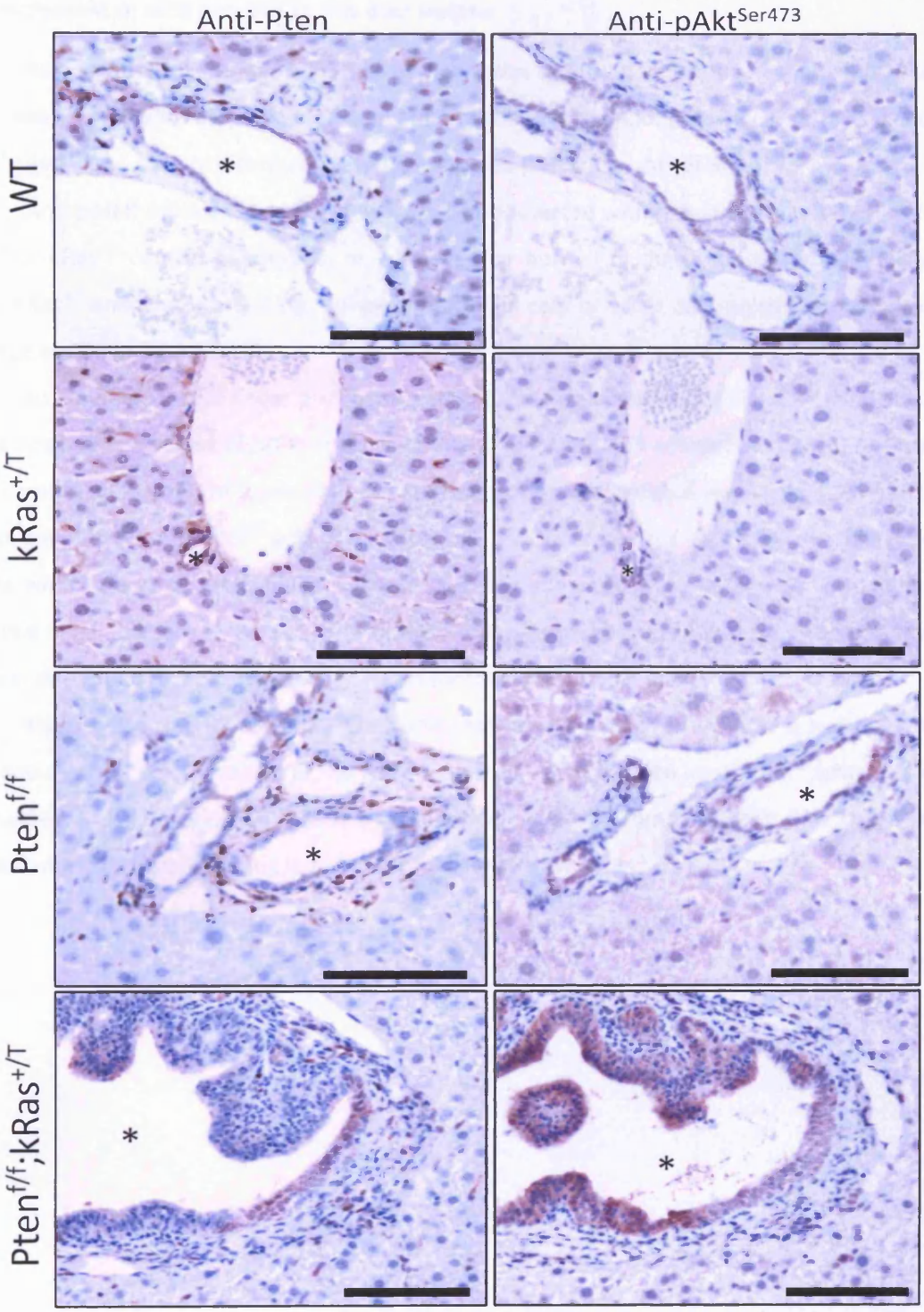

Figure 6.10: *Upregulation of pAkt^{Ser473} in bile duct lesions of Pten$^{f/f}$;kRas$^{+/T}$ mice*
Pten status and activation of Akt was determined in intrahepatic bile duct epithelial cells in WT, kRas$^{+/T}$ and Pten$^{f/f}$ control and Pten$^{f/f}$;kRas$^{+/T}$ experimental tissues. Anti-Pten IHC confirmed Pten expression in epithelial cells of WT and kRas$^{f/+}$ control animals, whilst loss of staining for Pten protein was observed in epithelial cells of Pten$^{f/f}$ controls and in papillomatous lesions arising in Pten$^{f/f}$;kRas$^{+/T}$ animals. Activation of Akt was not observed in Pten-proficient ductal epithelia in WT and kRas$^{+/T}$ control animals. A slight increase in staining for pAkt was observed in Pten$^{f/f}$ bile ducts, but the strongest staining was observed in lesions arising in Pten$^{f/f}$;kRas$^{+/T}$ animals. This increase in activation of Akt was not found to be associated with any change in subcellular localisation of the protein. Scale bars indicate 100μm. Asterisks indicate lumen of bile ducts.

6.2.8 Activation of MEK and ERK in bile duct lesions

As activation of the Raf-MEK-ERK pathway was observed in lesions of the gall bladder in $Pten^{f/f};kRas^{+/T}$ animals, I next assessed activation of the Raf-MEK-ERK pathway in serially-sectioned $Pten^{f/f};kRas^{+/T}$ and control bile duct epithelia using anti-pMEK and anti-pERK IHC.

Anti-pMEK IHC indicated that pMEK was not detected within ductal epithelial cells of WT, $Pten^{f/f}$ or $kRas^{+/T}$ control genotypes, or within either normal or abnormal ductal epithelium of $Pten^{f/f};kRas^{+/T}$ animals. No staining, either of epithelial cells or other cells types was noted across all tissue sections (Figure 6.11).

As staining for pMEK was previously noted to be weak, I examined the activation status of ERK, a downstream target of MEK, regardless of the fact that MEK activation was not detected in ductal lesions. Low levels of expression of pERK were observed in ductal epithelial cells of all three control genotypes (WT, $kRas^{+/T}$ and $Pten^{f/f}$). Despite the fact that MEK activation was not noted in lesions within ducts of $Pten^{f/f};kRas^{+/T}$ animals, strong staining for activated ERK was noted. As observed in gall bladder lesions in $Pten^{f/f};kRas^{+/T}$ animals, this increase in expression of activated ERK was also found to be associated with nuclear localisation of the protein (Figure 6.11).

From these data, I therefore conclude that, whilst activation of MEK is not detected, a clear activation of ERK in lesions of the intrahepatic bile duct epithelium of $Pten^{f/f};kRas^{+/T}$ animals is observed. This activation and nuclear localisation of ERK is comparable to that noted in gall bladder epithelial lesions arising in animals of the same genotype.

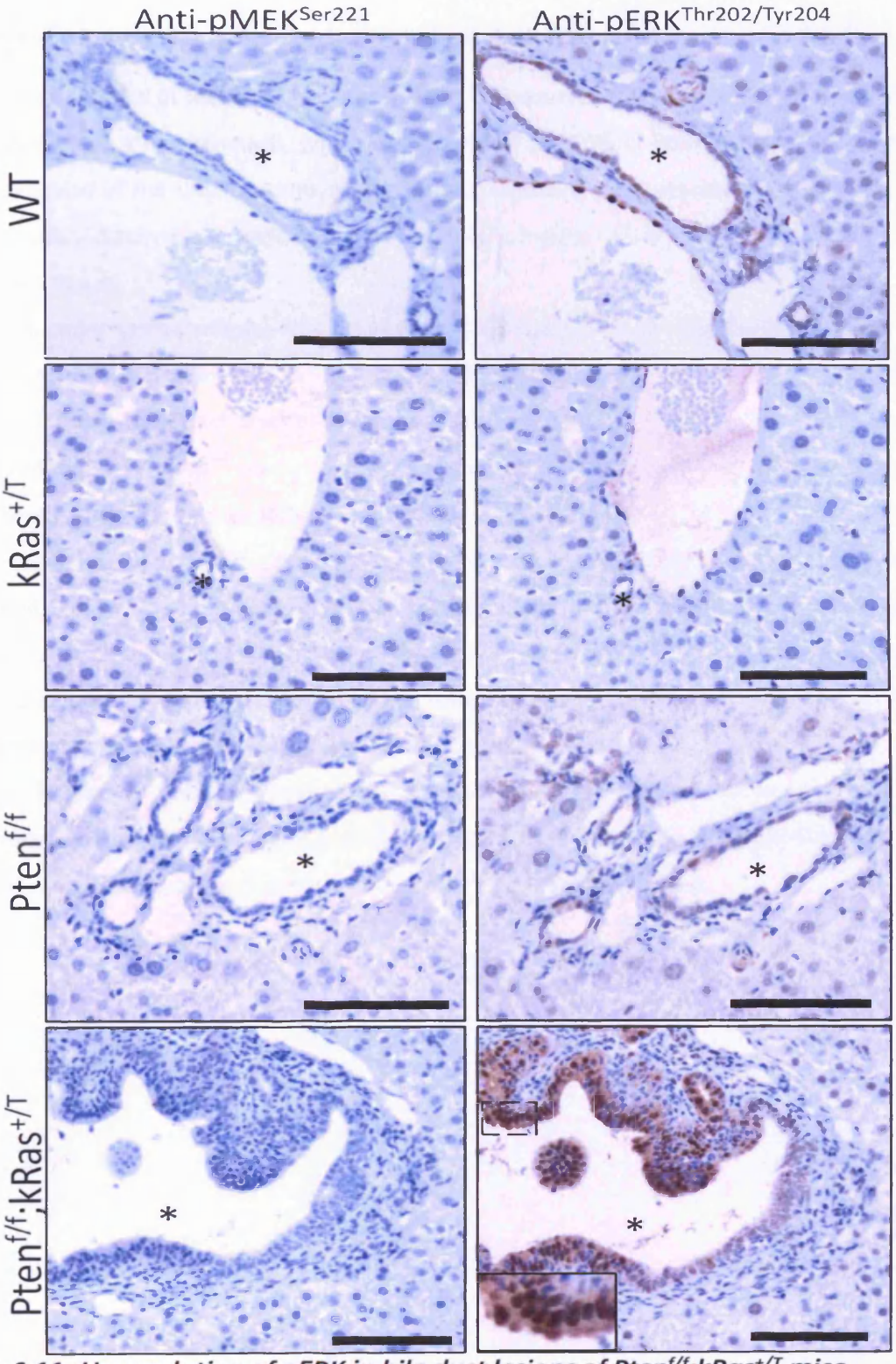

Figure 6.11: *Upregulation of pERK in bile duct lesions of Pten$^{f/f}$;kRas$^{+/T}$ mice*
IHC against pMEK and pERK was used to determine activation status of the Raf-MEK-ERK pathway in lesions arising within intrahepatic bile ducts in Pten$^{f/f}$;kRas$^{+/T}$ animals. Expression of activated MEK (pMEK) was not detected within lesions of Pten$^{f/f}$;kRas$^{+/T}$ mice, or in normal tissues from WT, kRas$^{+/T}$ or Pten$^{f/f}$ control animals. Despite this, mild activation of ERK (pERK) was observed in WT, kRas$^{+/T}$ and Pten$^{f/f}$ control tissues. Lesions within Pten$^{f/f}$;kRas$^{+/T}$ animals were found to show an increase in staining intensity for pERK, together with nuclear localisation of the activated protein (Inset images show digital enlargement of the area indicated in the main image). Scale bars indicate 100μm. Asterisks indicate lumen of bile ducts.

6.2.9 Pten$^{f/f}$;kRas$^{+/T}$ animals develop hyperplasia of the forestomach squamous epithelium

As described in section 6.2.2, Pten$^{f/f}$;kRas$^{+/T}$ mice were also noted to be highly susceptible to abnormalities of the stomach, which was observed in 100% of Pten$^{f/f}$;kRas$^{+/T}$ mice analysed. Recombination of the LacZ reporter allele was also detected in squamous epithelial cells of the forestomach (Section 6.2.3), indicating that AhCreER^{T} is indeed induced and drives recombination, within this tissue.

In order to characterise this phenotype, H&E-stained tissue sections of WT, kRas$^{+/T}$ and Pten$^{f/f}$ control animals and Pten$^{f/f}$;kRas$^{+/T}$ experimental animals were examined (Figure 6.12), and a detailed histopathological description of the lesions found in Pten$^{f/f}$;kRas$^{+/T}$ mice was obtained[7]. Lesions within Pten$^{f/f}$;kRas$^{+/T}$ animals were always found to arise from the forestomach. They were consistently characterised as diffuse papillomatous hyperplasias of the squamous epithelium, which were found to affect the vast majority of the tissue present on each tissue section examined. Florid hyperkeratosis was also noted on the lumenal surface of the forestomach. Occasional incidences of atypical features of basal cells were observed, but in no instance was this found to amount to squamous carcinoma. No evidence of invasive disease was observed. Lesions of this histological nature were not observed in any control animals.

Thus, loss of Pten and activation of k-Ras synergise within the squamous epithelium of the forestomach, resulting in dramatic and widespread hyperproliferation and hyperkeratosis of the squamous epithelium, but this is not found to result in malignant disease.

[7] Histopathological descriptions of forestomach lesions arising in experimental mice was provided by Prof Geraint T. Williams, Department of Pathology, University Hospital of Wales, Cardiff University, UK.

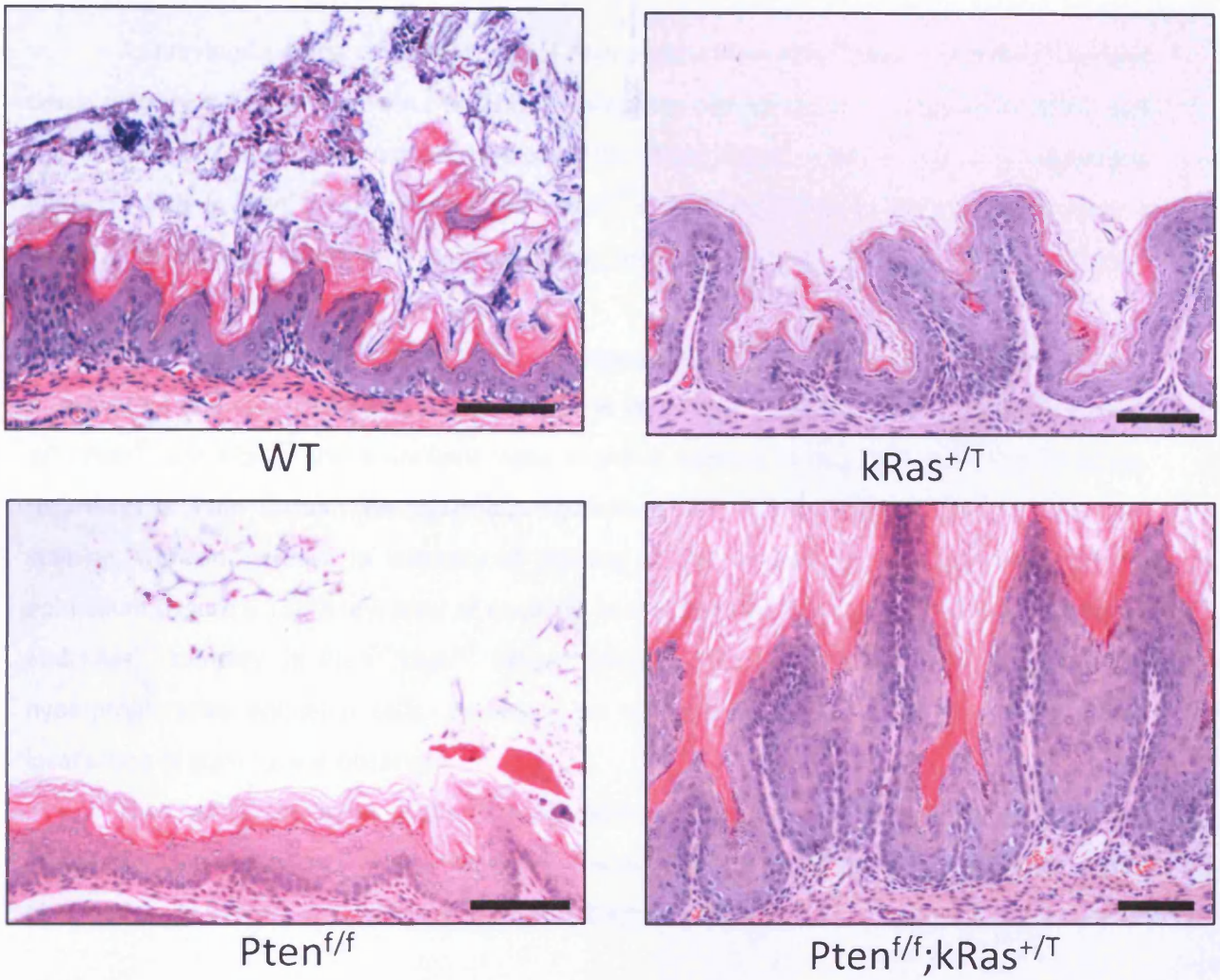

Figure 6.12: ***Susceptibility of Pten$^{f/f}$;kRas$^{+/T}$ animals to papillomatous hyperplasia of the forestomach squamous epithelium***

H&E-stained tissue sections of forestomach from WT, Pten$^{f/f}$, kRas$^{+/T}$ and Pten$^{f/f}$;kRas$^{+/T}$ animals were examined in order to determine the histopathological nature of forestomach lesions arising in Pten$^{f/f}$;kRas$^{+/T}$ animals. Lesions within Pten$^{f/f}$;kRas$^{+/T}$ tissues were found to be diffuse hyperplastic papillomatous lesions of the squamous epithelium, accompanied by florid hyperkeratosis. Lesions were not noted to be malignant. Lesions of a similar histopathology were not noted in animals of any control genotype (WT, kRas$^{+/T}$ or Pten$^{f/f}$). Scale bars indicate 100μm.

6.2.10 Activated Akt is present, but its levels are not increased in hyperplastic forestomach epithelium

Given that activation of the PI3K/Akt pathway and Raf-MEK-ERK pathway is observed in epithelial lesions of the biliary tree, I next determined whether activation of these pathways was also driving hyperplasia within the forestomach.

As previously, I first confirmed loss of Pten protein from $Pten^{f/f}$;$kRas^{+/T}$ and $Pten^{f/f}$ control tissue sections by use of anti-Pten IHC. This revealed that normal squamous epithelium of WT and $kRas^{+/T}$ control tissues were positively stained for Pten (Figure 6.13). In contrast, squamous epithelial cells in $Pten^{f/f}$ control and $Pten^{f/f}$;$kRas^{+/T}$ experimental tissues were found to show a reduction in staining intensity for Pten, indicating loss of Pten protein within this cell layer (Figure 6.13).

I next performed anti-$pAkt^{Ser473}$ IHC on adjacent tissue sections in order to visualise levels of activation and subcellular localisation of Akt in WT, $Pten^{f/f}$, $kRas^{+/T}$ and $Pten^{f/f}$;$kRas^{+/T}$ tissues. WT, $Pten^{f/f}$ and $kRas^{+/T}$ tissue sections were found to show a comparable pattern of staining, regardless of Pten status. The squamous epithelium was noted to be positive for anti-pAkt staining, with an increase in intensity of staining at the lumenal, keratinised surface of the epithelium (Figure 6.13). A low level of nuclear staining for pAkt was also apparent in WT, $Pten^{f/f}$ and $kRas^{+/T}$ samples. In $Pten^{f/f}$;$kRas^{+/T}$ tissues, staining for pAkt was noted to be retained in hyperproliferative epithelial cells. However, no increase in levels or change in subcellular localisation of staining was observed.

Thus, whilst activation of the PI3K/Akt pathway is observed in the context of combined loss of Pten and activation of k-Ras, the level of activation of the pathway is not different to that observed in control tissue samples, at least as detected by IHC.

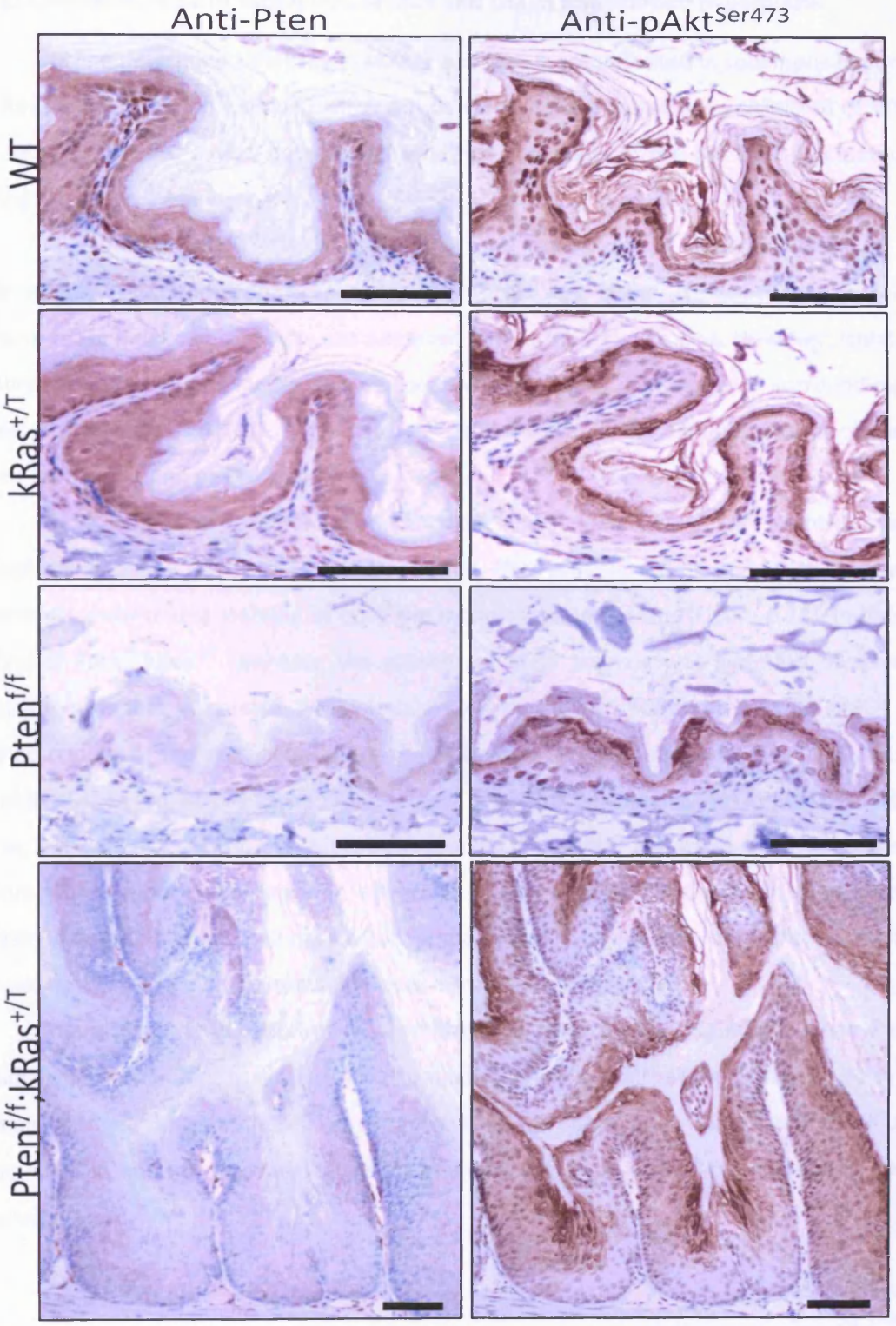

Figure 6.13: ***Hyperplastic cells of forestomach squamous epithelium in Pten$^{f/f}$;kRas$^{+/T}$ mice express normal levels of pAkt^{Ser473}***

Anti-Pten IHC was used to confirm loss of Pten from the squamous epithelium of the forestomach. WT and kRas$^{+/T}$ control tissues were found to retain positivity for Pten, as expected. Pten$^{f/f}$ control and Pten$^{f/f}$;kRas$^{+/T}$ experimental tissues were found to have a significant reduction in staining for Pten, indicating loss of the protein. Anti-pAkt^{Ser473} IHC was performed on adjacent tissue sections in order to examine activation of the PI3K/Akt pathway. Staining for activated Akt was found to be present in WT, Pten$^{f/f}$ and kRas$^{+/T}$ tissues, with an increase in staining intensity at the lumenal, keratinised surface of the epithelium. In Pten$^{f/f}$;kRas$^{+/T}$ tissues, whilst staining for pAkt was retained, no change in intensity or localisation of staining was observed. Scale bars indicate 100µm.

6.2.11 Limited increase in expression of MEK and ERK in forestomach hyperplasia

Having determined that the PI3K/Akt pathway is not activated in squamous hyperplasia of the forestomach in $Pten^{f/f};kRas^{+/T}$ mice compared to normal squamous epithelium of WT, $Pten^{f/f}$ and $kRas^{+/T}$ controls, I next determined whether activation of the Raf-MEK-ERK pathway was driving the observed phenotype.

Anti-phospho-MEK^{Ser221} IHC revealed that expression of activated MEK is virtually undetectable in squamous epithelial cells of WT, $Pten^{f/f}$ and $kRas^{+/T}$ control tissues. In general, an increase in staining for pMEK was not apparent in $Pten^{f/f};kRas^{+/T}$ tissues. However, isolated areas of abnormal tissue were found to stain positively for pMEK compared to surrounding tissues. These positively-stained areas tended to be located towards the lumenal surface of the lesions rather than within the basal region (Figure 6.14).

Despite no detectable activation of MEK in WT, $Pten^{f/f}$ and $kRas^{+/T}$ control tissues, IHC against the activated downstream target of MEK, ERK, on adjacent tissue sections indicated that all controls show strong staining of both the cytoplasm and nucleus (Figure 6.14). In hyperplastic lesions of $Pten^{f/f};kRas^{+/T}$ animals, the pattern of pERK staining was generally observed to be comparable to that in control, normal squamous epithelium. However, as with pMEK staining, defined regions of the epithelium were found to show a strong increase in cytoplasmic staining for pERK. Similar to pMEK, these regions were found to be towards the lumenal surface of the lesion, and when adjacent tissue sections stained for pMEK and pERK were compared, these regions were found to overlap. The subcellular staining pattern for pERK in these regions was notable in that no nuclear staining was observed, in contrast to surrounding areas of tissue which showed both a nuclear and cytoplasmic staining pattern (Figure 6.14).

In summary, it is apparent that activation of Raf-MEK-ERK signalling is not widespread within hyperplastic lesions of the forestomach squamous epithelium arising in $Pten^{f/f};kRas^{+/T}$ animals. Defined areas of lesions are apparent which show activation of both MEK and ERK, however it is unclear whether these areas are sufficient to drive the neoplastic phenotype observed.

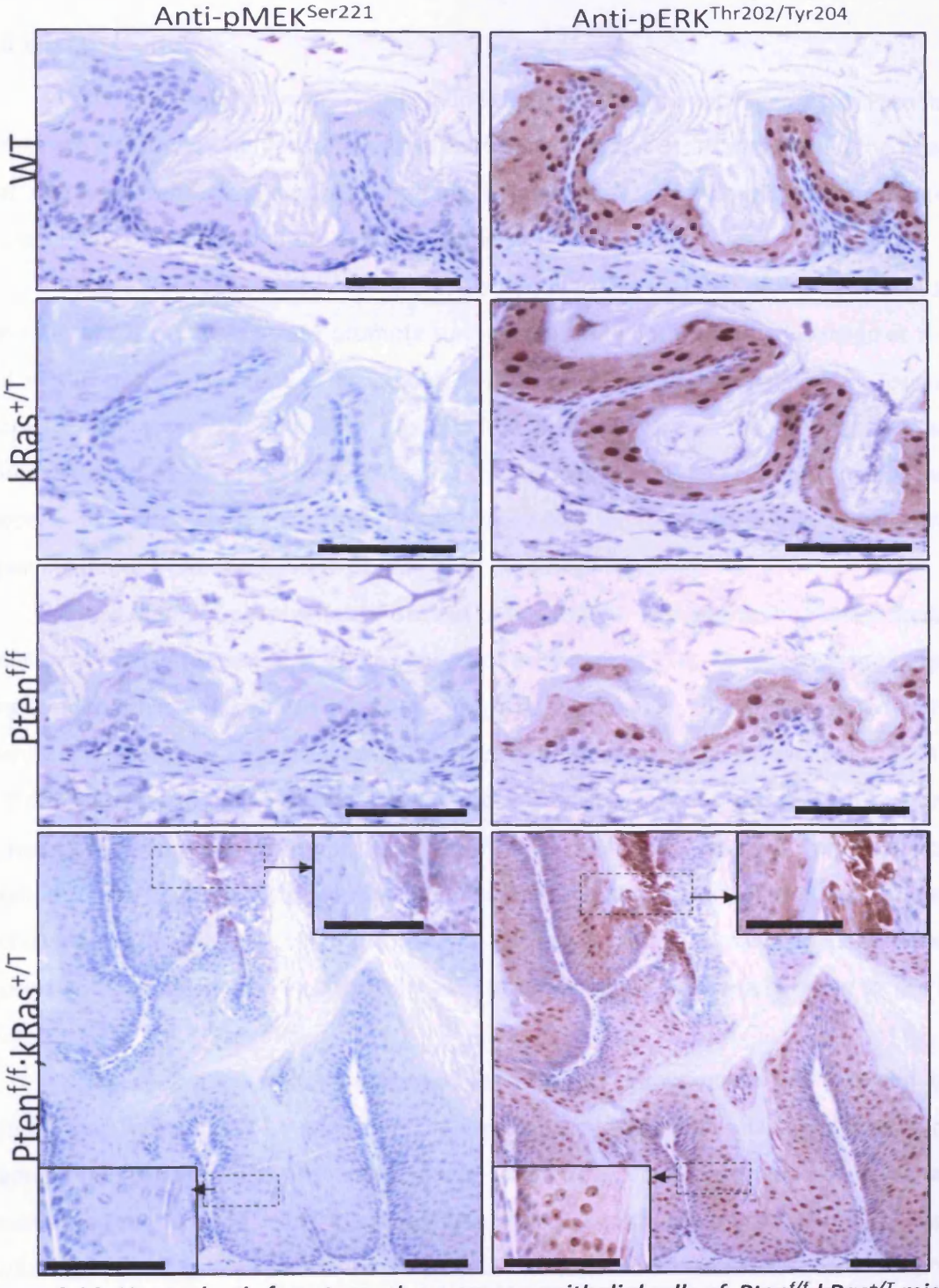

Figure 6.14: ***Hyperplastic forestomach squamous epithelial cells of Pten$^{f/f}$;kRas$^{+/T}$ mice show a limited increase in expression of pMEK and pERK***

pMEK and pERK IHC was used to assess activation of the Raf-MEK-ERK pathway in forestomach lesions of Pten$^{f/f}$;kRas$^{+/T}$ animals. Anti-pMEK staining reveals virtually undetectable levels of MEK activation within WT, Pten$^{f/f}$ and kRas$^{+/T}$ control tissues. In general, lesions in Pten$^{f/f}$;kRas$^{+/T}$ tissues show no increase in activation of MEK, except for isolated areas located towards the lumenal surface of the lesions which showed an increase in staining intensity. Staining of adjacent sections for activation of ERK revealed presence of pERK staining in WT, Pten$^{f/f}$ and kRas$^{+/T}$ control sections, despite no detection of activated MEK. In Pten$^{f/f}$;kRas$^{+/T}$ tissues, staining levels and localisation of pERK was generally observed to be comparable to control tissues, except for defined areas which showed an increase in levels of cytoplasmic staining. These areas were noted to be overlapping with regions showing strong expression of pMEK. Inset images show digital enlargements of the indicated areas of main images. Scale bars indicate 100µm.

6.3 Discussion

In the intestine, I have previously found that loss of the tumour suppressor Pten has little immediate effect upon homeostasis of the epithelium (Chapter 3). This has raised the hypothesis that, due to its 'permissive' nature as a tumour suppressor, loss of Pten will only become relevant in the context of activation of the PI3K/Akt pathway.

Recent work published in the literature has indicated that loss of Pten and activation of the k-Ras oncogene synergise to promote tumourigenesis in both the lung (Iwanaga et al., 2008) and in the ovary (Dinulescu et al., 2005). In the latter case, tumourigenesis is found to be characterised by activation of both the PI3K/Akt pathway, and of the Raf-MEK-ERK pathway (Dinulescu et al., 2005). The observed activation of PI3K/Akt signalling in this model therefore supports evidence which indicates that activated Ras family proteins can activate PI3K/Akt signalling through direct activation of PI3K itself (Kodaki et al., 1994).

Based on these observations, I set out in this chapter to examine the tumour suppressive function of Pten in the intestine in the context of activation of PI3K. The experimental approach I employed to achieve this was to generate transgenic mice bearing both LoxP-targeted *Pten* alleles (Suzuki et al., 2001), as well as a LoxP-STOP-*k-Ras*^{V12} mutant transgene (Guerra et al., 2003). Thus, in these animals, expression of Cre recombinase will result in loss of both alleles of the *Pten* gene as well as permitting expression of the constitutively active *k-Ras*^{V12} mutant from its endogenous promoter. Having previously determined that the AhCreER^{T} transgene drives efficient cre recombinase expression within the intestinal epithelium with minimal uninduced background expression (Chapter 4), this was the form of Cre recombinase transgene I chose to use for this study.

Upon generation and induction of Pten$^{f/f}$;kRas$^{+/T}$ experimental animals and controls (Pten$^{f/f}$, kRas$^{+/T}$ and WT), it was immediately obvious that Pten$^{f/f}$;kRas$^{+/T}$ animals showed a dramatic reduction in survival time compared to controls. Upon dissection and examination of tissue from Pten$^{f/f}$;kRas$^{+/T}$ mice, it was apparent that ill-health in the vast majority of cases was attributable to dramatic papillomatous hyperplasia of both the forestomach squamous epithelium and of the epithelium lining the biliary system. At dissection, lesions of the intestinal epithelium were not apparent. This may simply reflect a difference in the timescale of development of lesions of different histological origins in Pten$^{f/f}$;kRas$^{+/T}$ mice. It is possible that hyperplasia development within the forestomach and biliary system is a much more rapid process than in other tissues, such the intestinal epithelium.

Scoring of the tissue pathologies present in Pten$^{f/f}$;kRas$^{+/T}$ animals compared to controls revealed that hyperplasia of the forestomach and of the biliary tree occurred with complete penetrance in Pten$^{f/f}$;kRas$^{+/T}$ animals. A proportion of Pten$^{f/f}$ controls were noted to bear biliary lesions within the liver, but there were noted to be histologically different to the lesions observed

in $Pten^{f/f}$;$kRas^{+/T}$ mice. $Pten^{f/f}$ controls were not found to show abnormalities of the forestomach, and neither forestomach nor biliary system lesions were observed in $kRas^{+/T}$ and WT controls. Given that these phenotypes were considered to cause morbidity in $Pten^{f/f}$;$kRas^{+/T}$ animals, and were so highly penetrant, I focused my subsequent analyses on these tissues.

I first confirmed that induction of $AhCreER^T$ as described here does indeed result in recombination within the gall bladder and the forestomach. Use of the LacZ reporter allele confirmed the previously reported observation that activity of $AhCreER^T$ is induced in epithelial cells of the gall bladder (Kemp et al., 2004). I was also able to detect LacZ activity (and therefore recombination) within the squamous epithelium of the forestomach. These observations therefore indicate that Cre activity does indeed drive recombination within epithelial cells of these tissues.

Previous work has described synergy between k-Ras activation and Pten loss in a mouse model of ovarian carcinoma, which is driven by activation of the PI3K/Akt and Raf-MEK-ERK pathways (Dinulescu et al., 2005). I next set about characterising both the histological severity of lesions arising in $Pten^{f/f}$;$kRas^{+/T}$ mice, and determining whether, as in ovarian carcinoma, activation of the PI3K/Akt and/or Raf-MEK-ERK pathways could be attributed to the observed phenotypes.

6.3.1 Activation of PI3K/Akt signalling and the Raf-MEK-ERK pathway drives papillomatous hyperplasia of the biliary epithelium

Histopathological assessment of the lesions arising in the gall bladder and in intrahepatic bile ducts of $Pten^{f/f}$;$kRas^{+/T}$ animals revealed that a spectrum of lesions was present. Lesions of the biliary tree were most commonly identified as epithelial papillomata, but a range of lesions from hyperproliferative foci to invasive papillary adenocarcinoma were observed. The most severe lesions were only ever identified within the epithelium of the gall bladder, and not within intrahepatic bile ducts. This observation may reflect a difference in environmental constraints affecting proliferation of epithelial cells in each location. Epithelial cells within intrahepatic bile ducts are fewer in number, and their proliferation may be physically constrained by surrounding connective tissue cells and hepatocytes. In contrast to this, the gall bladder environment is much more dynamic, with the gall bladder itself being capable of expanding in size, normally allowing storage of bile produced by the liver. Thus, the physical environment of the gall bladder may be more permissive for hyperplasia than the intrahepatic bile ducts. This may also permit the rapid development and progression of lesions arising within the gall bladder.

In order to examine whether PI3K/Akt and/or Raf-MEK-ERK signalling was driving development of the lesions present in the biliary epithelium, I next examined the activation status

of these pathways in control and Pten$^{f/f}$;kRas$^{+/T}$ tissues using IHC. Loss of Pten was confirmed in tissues from animals bearing the Pten$^{f/f}$ alleles, which confirmed that lesions in Pten$^{f/f}$;kRas$^{+/T}$ animals arose from recombined cells. Anti-pAkt IHC indicated that low levels of activated Akt were detectable in epithelial cells of WT, kRas$^{+/T}$ and Pten$^{f/f}$ control tissues. In contrast, strong activation of Akt was detected in lesions of Pten$^{f/f}$;kRas$^{+/T}$ animals arising in both intrahepatic bile ducts and in the gall bladder. In addition, cell surface localisation of pAkt was observed, but this was only found to be present in lesions of the gall bladder. As described in Chapter 5, cell surface localisation of Akt has previously been associated with an increase in oncogenic potential of the protein (Mende et al., 2001). The observations here appear to support this observation; lesions in the gall bladder which were previously identified as generally being histologically more severe show localisation of pAkt to the cell surface, whereas less severe lesions arising within intrahepatic bile ducts do not show this staining pattern. Thus, it appears that more severe lesions are characterised by cell surface expression of activated Akt.

Activation of the Raf-MEK-ERK pathway was also assessed in WT, kRas$^{+/T}$ and Pten$^{f/f}$ control and Pten$^{f/f}$;kRas$^{+/T}$ tissues by IHC against activated MEK and activated ERK. In control tissues, low background activity of MEK and ERK were detected, indicating that the pathway is normally relatively dormant within the biliary epithelium. In gall bladder lesions, a slight elevation in MEK activity was detected, which was not apparent in small lesions of the bile ducts. However, despite these observations, the reported downstream target of MEK, ERK, was found to be strongly activated in all lesions of the gall bladder and bile duct epithelia in Pten$^{f/f}$;kRas$^{+/T}$ mice. This may potentially indicate that, in these lesions, ERK is activated by a MEK-independent mechanism. Alternatively, the very low levels of MEK activation detected may be sufficient in order for ERK to become activated. In either scenario, it is clear that strong activation and nuclear localisation of ERK is characteristic of all types of lesions arising in the biliary epithelium of Pten$^{f/f}$;kRas$^{+/T}$ animals, but is not observed in normal epithelial cells in Pten$^{f/f}$;kRas$^{+/T}$ and WT, kRas$^{+/T}$ and Pten$^{f/f}$ control animals.

6.3.2 Hyperplasia of the forestomach squamous epithelium is not characterised by increased activation of PI3K/Akt signalling, and shows only limited increase in activation of the Raf-MEK-ERK pathway

Extensive hyperplasia of the forestomach was also observed to occur with high penetrance in Pten$^{f/f}$;kRas$^{+/T}$ animals but not in WT, kRas$^{+/T}$ and Pten$^{f/f}$ controls. Histopathological examination of lesions arising within the forestomach revealed them all to be histologically similar. Lesions were identified as being diffuse hyperplastic papillomata of the squamous

epithelium, typified by florid hyperkeratosis of the lumenal surface. In no instance were these lesions found to be malignant.

Given that activation of both the PI3K/Akt pathway and the Raf-MEK-ERK pathway are both characteristic of the development of lesions of the biliary tract, I next determined whether activation of these pathways is responsible for driving development of the lesions observed in this tissue. As previously, loss of Pten and hence recombination in lesions was confirmed. Examination of pAkt staining patterns immediately indicated that the PI3K/Akt pathway is normally active within the squamous epithelium of the forestomach, as indicated by strong staining of normal tissues from WT, $kRas^{+/T}$ and $Pten^{f/f}$ controls. As such, no increase in staining for pAkt was observed within hyperproliferative lesions of $Pten^{f/f}$;$kRas^{+/T}$ animals, though pAkt was found to remain present. No change in localisation of pAkt was observed in forestomach lesions, in contrast to lesions arising in the gall bladder epithelium which showed relocalisation of Akt to the cell surface. Staining for pMEK and pERK in control animals indicated that, whilst levels of MEK were virtually undetectable in all genotypes, strong staining for activated ERK was evident in epithelial cells of all genotypes, indicating activation of MAPK signalling in normal cells. In hyperproliferative lesions of the forestomach arising in $Pten^{f/f}$;$kRas^{+/T}$ animals, no difference in staining intensity was generally observed compared to control tissues. However, distinct areas were found to show a co-ordinate increase in staining intensity for both pMEK and pERK. These areas of tissue were generally found to be located at the lumenal surface of lesions. The relevance of strong activation of Raf-MEK-ERK signalling in these small and infrequent areas of tissue with respect to the overall hyperplastic phenotype remains unclear. Given that, in general, the hyperproliferative cells of the squamous epithelium do not show increased activation of Raf-MEK-ERK or PI3K/Akt signalling compared to control tissues, it seems unlikely that these pathways are driving the hyperproliferative phenotype. This therefore suggests that loss of Pten and activation of k-Ras may co-operate to drive hyperproliferation within the forestomach through an alternative pathway. Further investigation needs to be carried out in order to ascertain the exact mechanism which is driving this phenotype.

6.3.3 Summary and future directions

In summary, data presented in this chapter indicates for the first time that synergy between Pten loss and activation of k-Ras exists within epithelial cells of both the biliary tract and the forestomach.

These data also indicate that tissue-specific sensitivity exists within epithelial cells with respect to activation of the PI3K/Akt and Raf-MEK-ERK pathways and the subsequent tumourigenesis which ensues. In the biliary epithelium, loss of Pten and activation of k-Ras drive

both activation and membrane localisation of pAkt, and also activation of MEK and ERK in epithelial lesions. These phenomena in turn appear to drive rapid tumour development and progression.

In contrast, the squamous epithelium of the forestomach is found to have a higher basal level of both PI3K/Akt and Raf-MEK-ERK pathway activity in its normal state. As such, activation of k-Ras and deletion of Pten does not appear to have a dramatic effect on these signalling pathways, despite the fact that a synergistic effect upon tissue phenotype is evident. This implies that hyperproliferation may be driven by another pathway, which currently remains elusive and warrants further investigation in the future.

In the intestine, tumourigenesis is not apparently initiated in this model. However, the very rapid development of hyperplastic disease in other tissues may eclipse the timescale required for tumourigenesis in the intestinal epithelium. Thus, it has not been possible to examine synergy between Pten loss and k-Ras activation in intestinal tumourigenesis in this model. Given the short timescales involved in this study (the average survival time of $Pten^{f/f};kRas^{+/T}$ animals was just 43 days), it seems likely that disease within the intestine might be observed if animals were to be aged longer than was possible here. As such, further investigation of the combined role of Pten loss and k-Ras activation in the intestinal epithelium is warranted, but a system which does not permit recombination either in the biliary epithelium or the squamous epithelium of the forestomach must be utilised.

Chapter 7: Analysis of the short- and long-term consequences of Vil-CreER^T-mediated activation of k-Ras and loss of Pten in the intestine

7.1 Introduction

Previous work, described both in this thesis and elsewhere, has indicated that combined loss of Pten and activation of k-Ras has a synergistic effect upon neoplastic transformation of epithelial cells of the lung (Iwanaga et al., 2008), ovary (Dinulescu et al., 2005), biliary system and forestomach (Chapter 6). In each of these systems, loss of Pten and activation of k-Ras has been found to result in hyperproliferation of epithelial cells. In the ovary (Dinulescu et al., 2005) and biliary epithelium (Chapter 6), neoplasia is characterised by an increase in both PI3K/Akt signalling and Raf-MEK-ERK pathway activation.

In the intestinal epithelium, the existence of any co-operative effect between Pten loss and k-Ras activation remains unconfirmed. In Chapter 6, I attempted to characterise the effects upon the intestinal epithelium following conditional loss of Pten and activation of k-Ras driven by the AhCreER^T transgene. However, due to the rapid and catastrophic phenotypes occurring within epithelial cells of the biliary tree and of the forestomach, it was not possible to analyse any synergistic effects in tumourigenesis of the intestinal epithelium.

Thus, in order to examine the effects of combined loss of Pten and activation of k-Ras in the intestinal epithelium using this system, recombination within both the epithelium of the biliary system and the squamous epithelium of the forestomach must be avoided. One method of achieving this is to use an inducible Cre-expressing transgene which drives cre expression more specifically within the intestine. An example of such as transgene is Vil-CreER^T (el Marjou et al., 2004). This transgene makes use of the Cre recombinase-estrogen receptor fusion protein as described for AhCreER^T, which must be exposed to Tamoxifen in order to gain access to the nucleus and act on its targets. In the Vil-CreER^T transgene, expression of the fusion protein is driven by the *Villin* gene promoter, rather than by the inducible CYP1A1 promoter as was described for the AhCreER^T transgene (Kemp et al., 2004). The Villin gene is endogenously expressed in an intestine- and kidney-specific manner. In the intestine, its expression is noted to be further restricted to the epithelial cell population, within no expression in other cell types (Pinto et al., 1999). Reporter analysis of induced Vil-CreER^T expression indicates that Cre is activated with high efficiency specifically within the epithelial cell population, reflecting the endogenous expression pattern of the Villin gene (el Marjou et al., 2004).

In this chapter, I aimed to make use of this Vil-CreER^T transgene in order to achieve efficient and specific inducible recombination in the intestinal epithelium in order to drive both

deletion of Pten and activation of the endogenous k-Ras^{V12} (G12V mutant) transgene. As Vil-CreER^{T} is not expressed within the epithelium of the biliary system or in the forestomach, this should circumvent previous problems of confounding phenotypes within these tissues, allowing analysis of any resulting intestinal phenotypes[8].

[8] Data presented in this chapter was collected with the assistance of Emma J. Davies. Breeding of animals to generate experimental genotypes was conducted by me. Induction, dissection and analysis of experimental animals were performed together with Emma, under my direction and supervision.

7.2 Results

7.2.1 Induction of Vil-CreER^{T} causes recombination in epithelial cells at the LoxP-targeted Pten locus and the k-Ras^{V12} transgene

Animals bearing the Vil-CreER^{T} transgene (el Marjou et al., 2004), the LoxP-targeted Pten alleles (Suzuki et al., 2001) and the k-Ras^{V12} mutant transgene (Guerra et al., 2003) were interbred. This generated experimental animals, of the genotype Vil-CreER^{T+};Pten$^{f/f}$;kRas$^{+/T}$ (herein referred to as 'Pten$^{f/f}$;kRas$^{+/T}$'), and controls of genotypes Vil-CreER^{T+}; Pten$^{f/f}$;kRas$^{+/+}$ ('Pten$^{f/f}$'), Vil-CreER^{T+};Pten$^{+/+}$;kRas$^{+/T}$ ('kRas$^{+/T}$') and Vil-CreER^{T+};Pten$^{+/+}$;kRas$^{+/+}$ ('WT'). Animals were induced as described (Section 2.1.3.2) and were culled at day 14 post-induction (PI).

I first confirmed that recombination occurred within the intestinal epithelium using this system and induction protocol. To do this, samples of tissue were obtained from WT, Pten$^{f/f}$ and kRas$^{+/T}$ controls and Pten$^{f/f}$;kRas$^{+/T}$ experimental animals by scraping of the mucosal surface of the intestine as described (Section 2.2.7.5). This allowed crude enrichment of tissue samples for epithelial cells, which is the cell type in which recombination is induced in this system (el Marjou et al., 2004). Total genomic DNA was extracted from these epithelial-enriched samples and was used for multiplex PCR amplification of products specific to the wild-type, LoxP-targeted and recombined forms of the *Pten* allele and *k-Ras* transgene (See Section 2.6.4 and Figure 2.2). DNA samples from animals WT for the Pten locus (Pten$^{+/+}$;kRas$^{+/+}$ [WT] and Pten$^{+/+}$;kRas$^{+/T}$) were found to amplify products of a size corresponding only to the wild-type Pten allele (428bp) (Figure 7.1). Samples from induced animals bearing the LoxP-targeted *Pten* alleles (Pten$^{f/f}$;kRas$^{+/+}$ and Pten$^{f/f}$;kRas$^{+/T}$) were found to generate products corresponding to both the LoxP-targeted but unrecombined allele (514bp) and to the recombined allele (705bp). As all animals bear at least one copy of the wild-type *k-Ras* allele, a product corresponding to the wild-type *k-Ras* allele (403bp) was detected in tissue samples from all genotypes. In addition to this, samples from animals bearing the *k-Ras* transgene (Pten$^{+/+}$;kRas$^{+/T}$ and Pten$^{f/f}$;kRas$^{+/T}$) were found to generate products corresponding to the LoxP-targeted, unrecombined *k-Ras* transgene (621bp) and to the recombined form of the transgene (669bp) (Figure 7.1). This therefore confirms that, using this system, induction results in recombination at both the *Pten* allele and the *k-Ras* transgene within the intestinal epithelium.

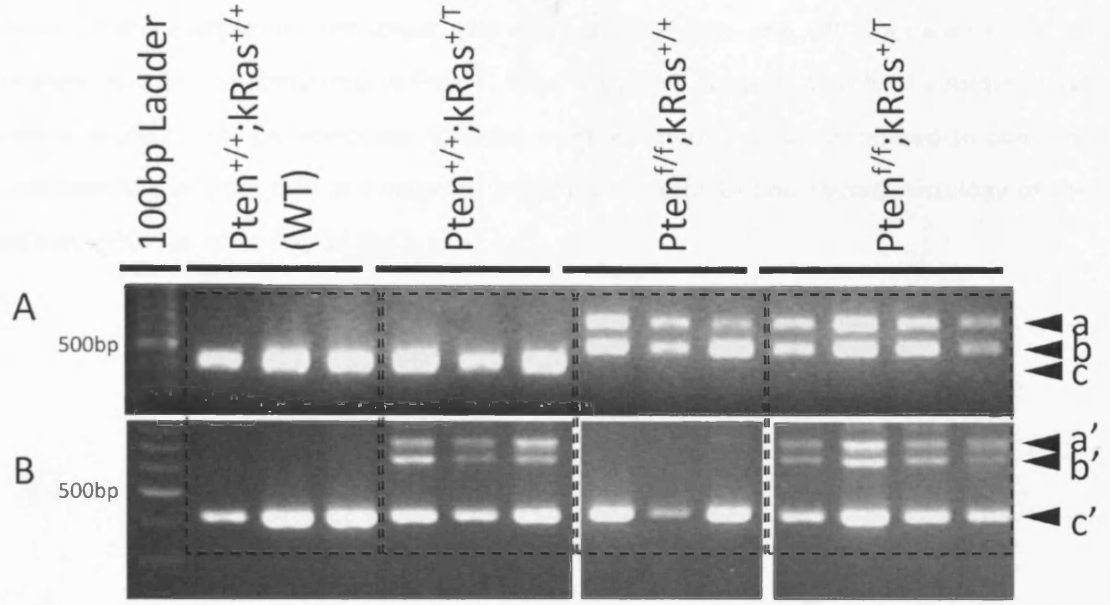

Figure 7.1: ***Recombined-specific PCR confirms recombination at the Pten locus and the kRas^{V12} transgene in the intestinal epithelium of experimental animals***

PCR reactions designed to specifically detect the wild-type, LoxP-targeted and recombined alleles of the *Pten* (A) and *k-Ras* (B) genes were performed on genomic DNA extracted from epithelial-enriched intestinal tissue samples. Samples from induced animals wild-type for the *Pten* gene (Pten$^{+/+}$;kRas$^{+/+}$ and Pten$^{+/+}$;kRas$^{+/T}$) were found to generate only the wild-type allele-specific product (c, 428bp). Samples from induced animals bearing the LoxP-Targeted *Pten* alleles (Pten$^{f/f}$;kRas$^{+/+}$ and Pten$^{f/f}$;kRas$^{+/T}$) were found to generate products specific to both the LoxP-Targeted unrecombined allele (b, 514bp) and to the recombined allele (a, 705bp), indicating the presence of both recombined and unrecombined cells. As all animals bear at lest one copy of the wild-type k-Ras allele, samples from all animals were found to produce the wild-type alelle-specific product (c', 403bp), as expected. Samples from induced *k-Ras* transgenic animals (Pten$^{+/+}$;kRas$^{+/T}$ and Pten$^{f/f}$;kRas$^{+/T}$) additionally generated products corresponding to the LoxP-targeted but unrecombined allele (b', 621bp) and to the recombined allele (a', 669bp).

7.2.2 No change in gross intestinal structure associated with Pten loss and k-Ras activation at day 14 PI

Experimental $Pten^{f/f}$;$kRas^{+/T}$ and control ($Pten^{f/f}$, $kRas^{+/T}$ and WT) animals were induced and culled at day 14 PI. Intestines were removed, fixed and sectioned before being stained with H&E for histological assessment (Sections 2.2 and 2.3). Microscopic examination of tissue sections revealed no difference in gross histology between $Pten^{f/f}$;$kRas^{+/T}$ experimental intestines and controls (Figure 7.2). Tissues from $Pten^{f/f}$;$kRas^{+/T}$ animals were found to have normal structural organisation of the epithelium into crypt and villus units. Crypts and villi appeared to be of approximately normal size compared to $Pten^{f/f}$, $kRas^{+/T}$ and WT controls. Levels of apoptosis and mitosis were noted to not be obviously different in $Pten^{f/f}$;$kRas^{+/T}$ tissue compared to controls. Thus, combined loss of Pten and activation of k-Ras has no effect upon normal histology of the intestinal epithelium at up to day 14 PI.

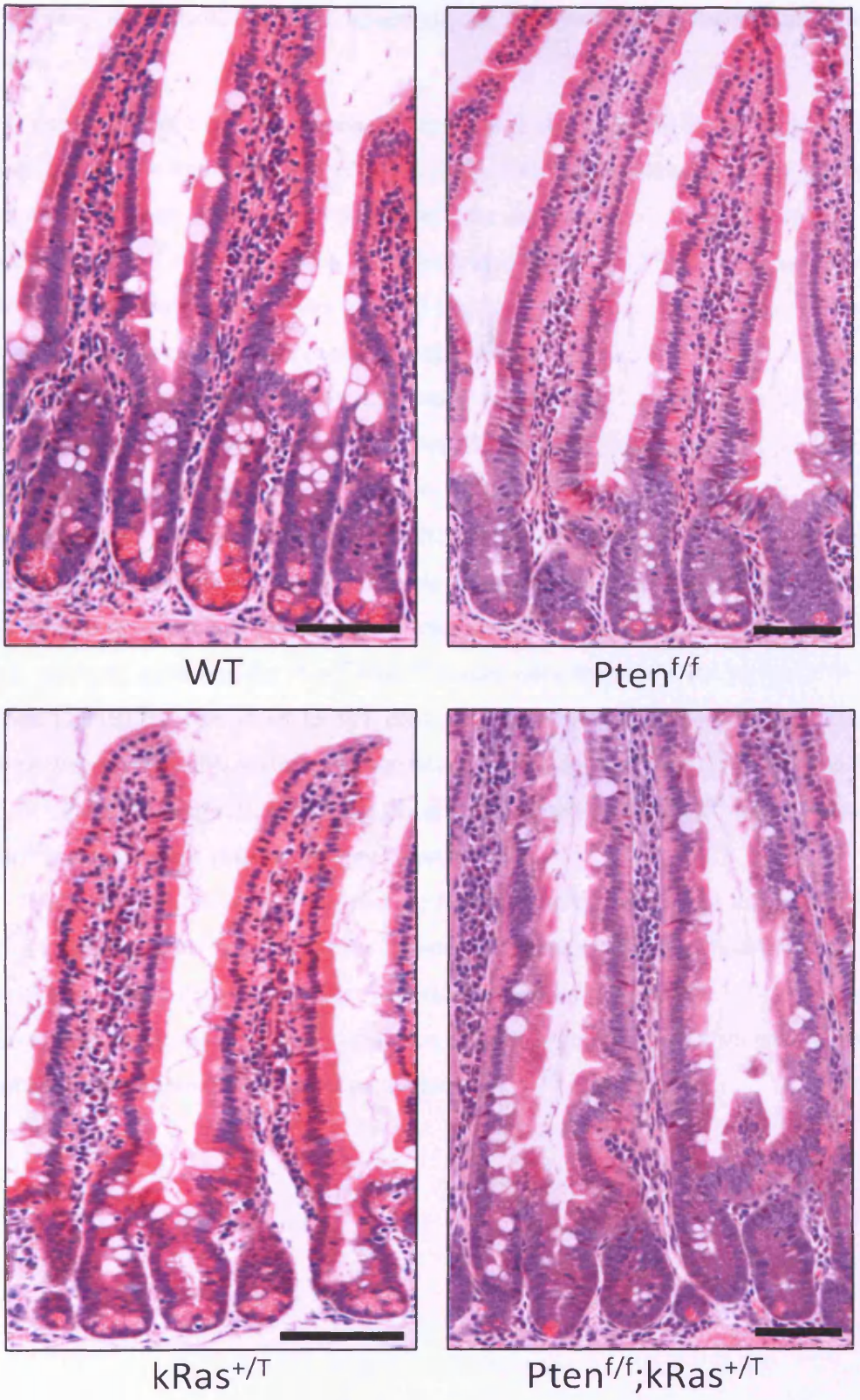

Figure 7.2: ***No perturbation of gross intestinal histology at 14 days following intestine-specific loss of Pten and activation of k-Ras***

Control (WT, Pten$^{f/f}$ and kRas$^{+/T}$) and experimental (Pten$^{f/f}$;kRas$^{+/T}$) animals were induced and culled at 14 days PI. Intestines were then removed, fixed and processed before being sectioned and H&E stained. Histological examination of intestinal tissues from experimental animals revealed no obvious perturbation in gross structure or histology of the intestine at this timepoint compared to control genotypes. Scale bar indicates 100μm.

7.2.3 Increase in mitosis, but not apoptosis, in Pten-deficient k-Ras-activated intestinal epithelium

In order to more closely investigate more subtle perturbations of intestinal homeostasis following loss of Pten and activation of k-Ras, I quantitatively examined levels of apoptosis and mitosis in H&E-stained sections of $Pten^{f/f};kRas^{+/T}$ tissues compared to $Pten^{f/f}$, $kRas^{+/T}$ and WT controls. Mitoses and apoptoses were identified based on their morphological appearance, and the number of figures per crypt was counted (Figure 7.3). Scoring for apoptosis revealed that there was no significant difference in the average frequency of apoptosis scored in $Pten^{f/f};kRas^{+/T}$ experimental tissues (Average number ±Standard deviation of 0.22±0.06) compared to $Pten^{f/f}$ (0.23±0.16), $kRas^{+/T}$ (0.26±0.04) or WT 0.29±0.11) controls (Mann-Whitney U test for the comparison $Pten^{f/f};kRas^{+/T}$ Vs. WT, $p=0.63$). In contrast, levels of mitosis were found to vary between genotypes. Whilst no difference in mitotic index was observed between WT (1.02±0.15) and $Pten^{f/f}$ (1.26±0.20) controls, $kRas^{+/T}$ controls were found to have a significant increase in the number of mitoses per crypt (at 1.46±0.19) compared to WT controls (Mann-Whitney U test, $p<0.001$). Similarly, experimental $Pten^{f/f};kRas^{+/T}$ tissues were found to show an elevation in levels of mitosis (1.33±0.23) compared to WT controls (Mann-Whitney U test, $p<0.1$), though this difference was not as highly statistically significant as that between WT and $kRas^{+/T}$ controls. No significant difference in mitotic index was observed between $Pten^{f/f};kRas^{+/T}$ experimental tissues and $kRas^{+/T}$ control tissues (Mann-Whitney U test, $p=0.63$).

These data therefore indicate that activation of k-Ras within the intestinal epithelium results in a significant increase in mitosis compared to tissues lacking activated k-Ras, however additional loss of Pten does not further modulate this phenotype. Neither activation of k-Ras or deletion of Pten alone, nor combined activation of k-Ras and deletion of Pten has an effect upon levels of apoptosis within the intestinal epithelium.

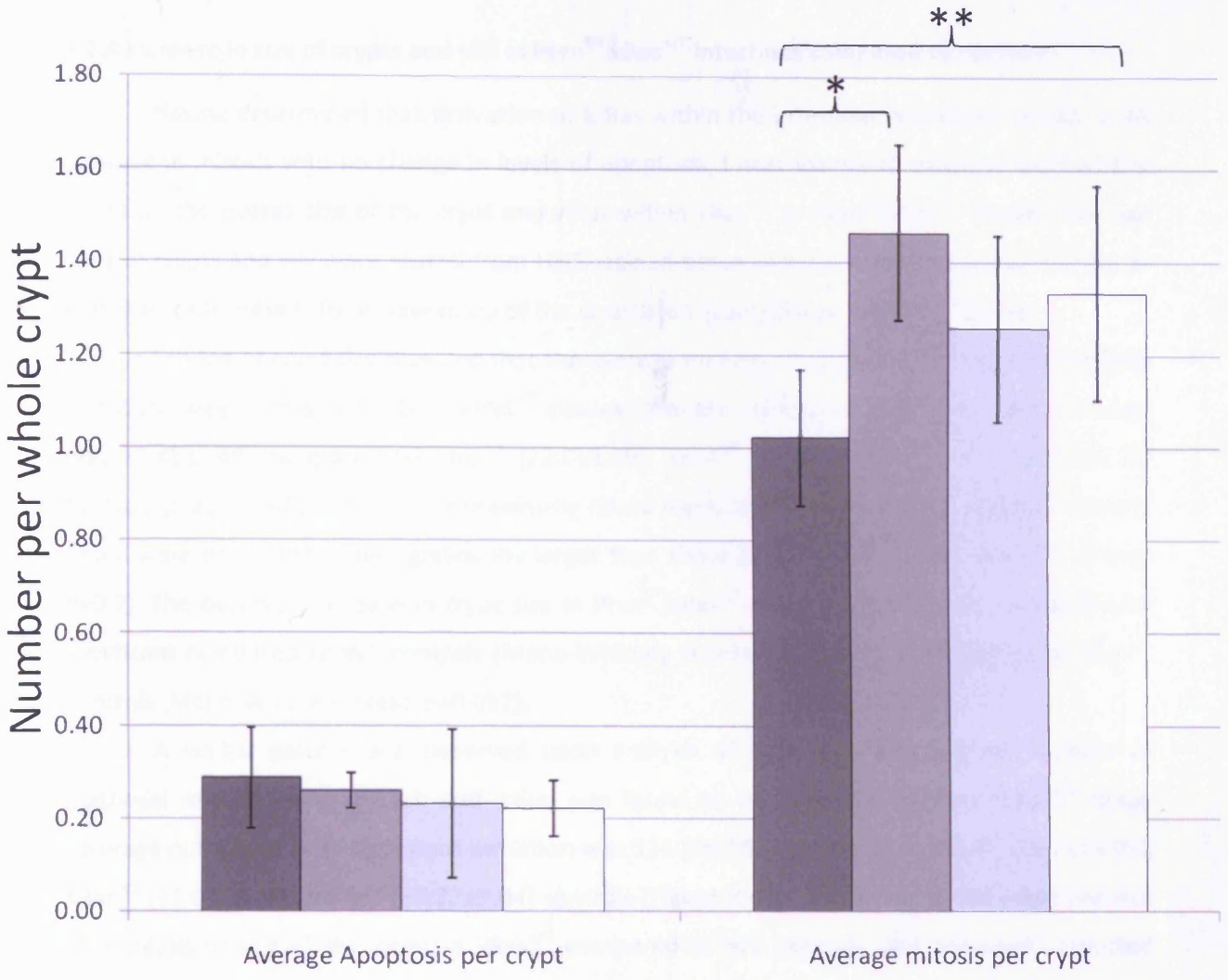

Figure 7.3: ***Increase in mitosis with no change in apoptosis following loss of Pten and activation of kRas***

Apoptoses and mitoses within intestinal crypts was scored from H&E-stained tissue sections based on morphological appearance. Scoring of apoptosis revealed no difference in number of apoptotic cells per crypt between WT (dark grey bar), $kRas^{+/T}$ (medium grey bar) and $Pten^{f/f}$ (light grey bar) controls and experimental ($Pten^{f/f}$;$kRas^{+/T}$ - white bar) tissues samples. In contrast, scoring of the number of mitoses per crypt revealed a significant alteration in the number of mitotic figures present. $kRas^{+/T}$ controls (medium grey bar) were found to have a significant increase in levels of mitosis compared to WT controls (dark grey bar) (*, Mann-Whitney U test, significant at $p<0.01$), and also apparently showed an increase in mitosis compared to $Pten^{f/f}$ controls (light grey bar), though this was not statistically significant. In addition, experimental tissues (white bar) showed a significant increase in number of mitoses per crypt compared to WT controls (**, Mann-Whitney test, significant at $p<0.1$), though this difference was not significant compared to $Pten^{f/f}$ controls. Error bars indicate standard deviation.

7.2.4 Increase in size of crypts and villi in $Pten^{f/f};kRas^{+/T}$ intestines compared to controls

Having determined that activation of k-Ras within the intestinal epithelium results in an increase in mitosis with no change in levels of apoptosis, I next examined whether this had any effect on the overall size of the crypt and villus within $kRas^{+/T}$ or $Pten^{f/f};kRas^{+/T}$ tissues. Average sizes of crypts and villi were scored from H&E-stained tissue sections by counting the number of epithelial cells present from base to tip of the structure in comparable regions of tissue.

Scoring of crypt size revealed that the average number of epithelial cells comprising each half crypt was increased in $Pten^{f/f};kRas^{+/T}$ tissues (average number of cells ±Standard deviation was 30.48±3.49) compared to $Pten^{f/f}$ (22.0±1.19), $kRas^{+/T}$ (25.47±2.91) and WT (24.26±3.38) controls (Figure 7.4A). Despite the previously noted increase in mitosis, crypts of $kRas^{+/T}$ control tissue were not found to be significantly larger than those in WT tissues (Mann-Whitney U test, P=0.7). The observed increase in crypt size in $Pten^{f/f};kRas^{+/T}$ experimental tissue was statistically significant compared to WT controls (Mann-Whitney U test, p=0.057) and compared to $kRas^{+/T}$ controls (Mann-Whitney U test, p=0.057).

A similar pattern was observed upon analysis of villus size. The average number of epithelial cells comprising each half villus was found to be increased in $Pten^{f/f};kRas^{+/T}$ tissue (average number of cells ±Standard deviation was 114.19±7.97) compared to $Pten^{f/f}$ (79.72±9.05), $kRas^{+/T}$ (93.63±8.16) and WT (65.27±9.04) controls (Figure 7.4B). In contrast to the observed lack of increase in size of the crypt in $kRas^{+/T}$ compared to WT controls, the previously reported increase in mitotic index was found to be translated into a significant increase in villus size (Mann-Whitney U test, $p<0.001$) in this control group. However, villus size in $Pten^{f/f};kRas^{+/T}$ tissues was further found to be significantly increased compared to both $kRas^{+/T}$ controls, as well as compared to WT controls (Mann-Whitney U test, $p<0.001$ for both comparisons).

In summary, combined loss of Pten and activation of kRas within the intestinal epithelium causes an increase in size of both the crypt and villus compared to $Pten^{f/f}$, $kRas^{+/T}$ or WT controls, whereas activation of k-Ras alone causes an increase in villus size, but not in crypt size, compared to WT controls.

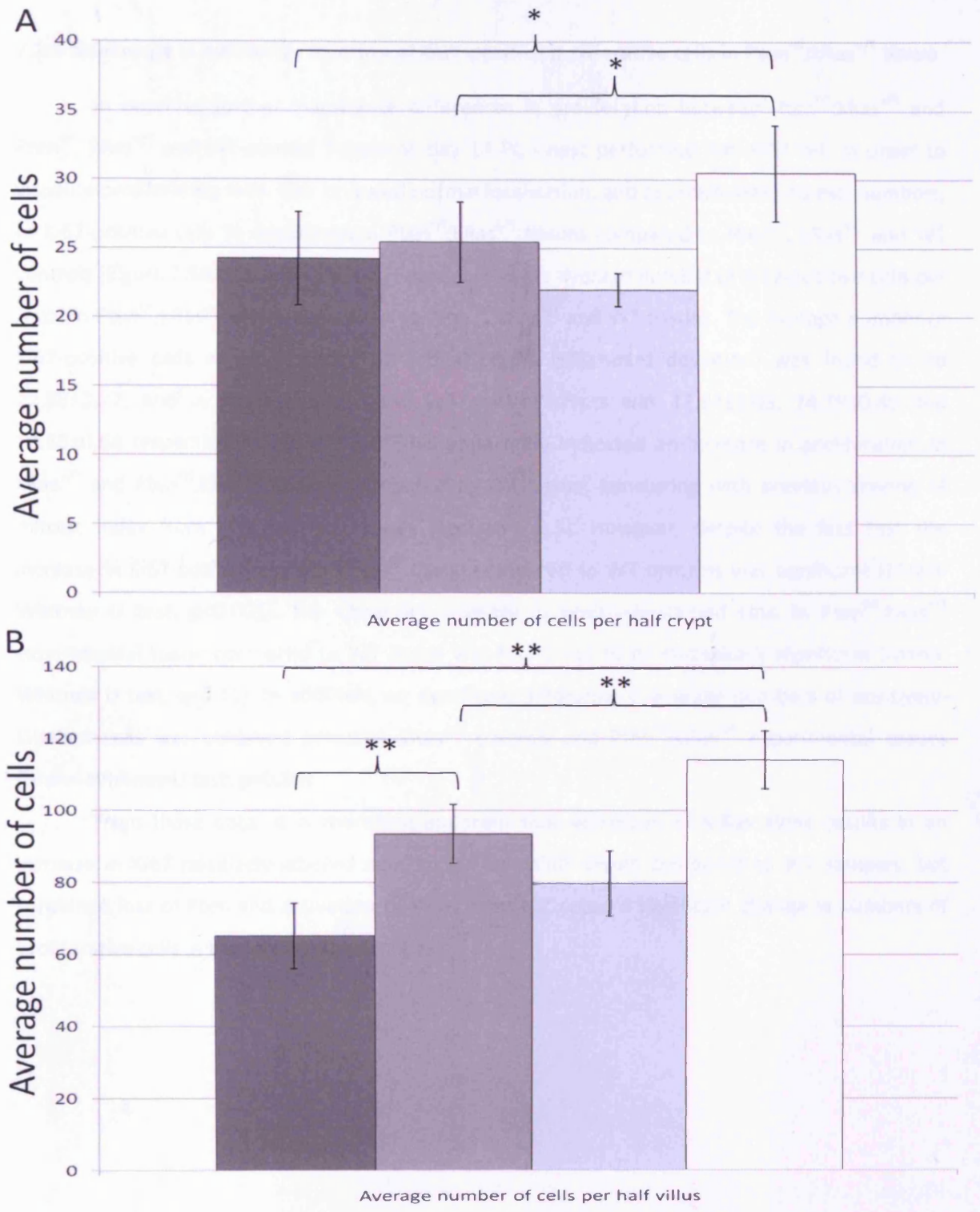

Figure 7.4: ***Significant increase in size of crypts and villi in Pten$^{f/f}$;kRas$^{+/T}$ intestines at day 14 PI***
Size of both crypts (A) and villi (B) in WT, kRas$^{+/T}$ and Pten$^{f/f}$ control and Pten$^{f/f}$;kRas$^{+/T}$ experimental tissue samples was scored by counting the number of epithelial cells present from base to top of the structure in comparable areas of tissue sections. A significant increase in the number of cells within the crypt (A) was observed in Pten$^{f/f}$;kRas$^{+/T}$ animals (white bar) compared to all controls (WT: dark grey bar, kRas$^{+/T}$: medium grey bar, Pten$^{f/f}$: light grey bar) (*, Mann-Whitney U test, significant at $p<0.1$). A similar pattern of villus size was observed (B), with Pten$^{f/f}$;kRas$^{+/T}$ animals (white bar) showing a significant increase in the number of epithelial cells comprising the villus compared to controls (WT: dark grey bar, kRas$^{+/T}$: medium grey bar, Pten$^{f/f}$: light grey bar) . Additionally, kRas$^{+/T}$ controls were noted to show a significant increase in villus size compared to WT controls. (**, Mann-Whitney U test, significant at $p<0.001$). Error bars indicate standard deviation.

7.2.5 No change in number or location of Ki67-positive proliferative cells in Pten$^{f/f}$;kRas$^{+/T}$ tissue

In order to further investigate differences in proliferation between Pten$^{f/f}$;kRas$^{+/T}$ and Pten$^{f/f}$, kRas$^{+/T}$ and WT control tissues at day 14 PI, I next performed anti-Ki67 IHC in order to visualise proliferating cells. This revealed normal localisation, and approximately normal numbers, of Ki67-positive cells in experimental Pten$^{f/f}$;kRas$^{+/T}$ tissues compared to Pten$^{f/f}$, kRas$^{+/T}$ and WT controls (Figure 7.5A). To quantify this, I next scored the average number of Ki67-positive cells per crypt in Pten$^{f/f}$;kRas$^{+/T}$ tissue compared to Pten$^{f/f}$, kRas$^{+/T}$ and WT tissues. The average number of Ki67-positive cells in Pten$^{f/f}$;kRas$^{+/T}$ intestinal crypts (±Standard deviation) was found to be 22.88±3.77, and in Pten$^{f/f}$, kRas$^{+/T}$ and WT control crypts was 17.84±2.05, 24.79±0.85 and 18.53±0.64 respectively (Figure 7.5B). This apparently indicated an increase in proliferation in kRas$^{+/T}$ and Pten$^{f/f}$;kRas$^{+/T}$ tissues compared to WT tissue, concurring with previous scoring of mitotic index from H&E-stained tissues (Section 7.2.3). However, despite the fact that the increase in Ki67-positive cells in kRas$^{+/T}$ tissue compared to WT controls was significant (Mann-Whitney U test, $p<0.001$), the observed increase in positively-stained cells in Pten$^{f/f}$;kRas$^{+/T}$ experimental tissue compared to WT tissue was found not to be statistically significant (Mann-Whitney U test, $p=0.11$). In addition, no significant difference in average numbers of positively-labelled cells was observed between kRas$^{+/T}$ controls and Pten$^{f/f}$;kRas$^{+/T}$ experimental tissues (Mann-Whitney U test, $p=0.86$).

From these data, it is therefore apparent that activation of k-Ras alone results in an increase in Ki67 positively-labelled cells within intestinal crypts compared to WT samples, but combined loss of Pten and activation of k-Ras does not cause a significant change in numbers of proliferative cells in the intestinal epithelium.

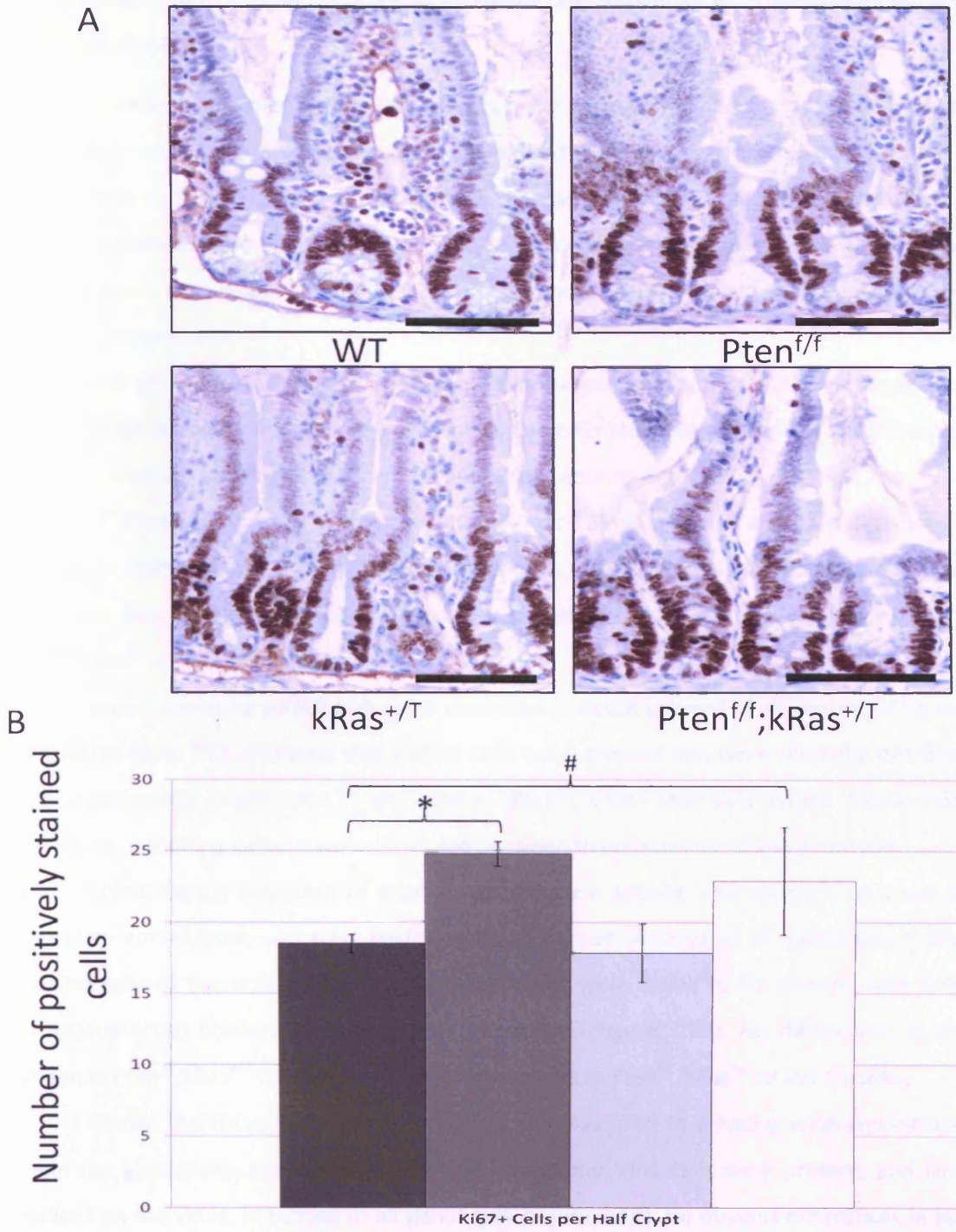

Figure 7.5: ***No significant alteration in number of Ki67 antigen-positive cells in Pten$^{f/f}$;kRas$^{+/T}$ intestines at day 14 PI***

In order to visualise proliferative cells and the proliferative zone in control and experimetnal tissues, anti-Ki67 IHC was performed (A). This revealed that the proliferation compartment is normally localised in experimental tissues compared to controls, and that there is no obvious change in numbers of Ki67-positive cells. Scale bars indicate 100μm. In order to quantify this observation, the number of Ki67-positively stained cells was scored from these sections in control and experimental tissues (B). A significant increase in the number of positively labelled cells was observed in kRas$^{+/T}$ controls (medium grey bar) compared to WT controls (dark grey bar) (*, Mann-Whitney U test, $p<0.001$). No difference was observed between WT controls and Pten$^{f/f}$ controls (light grey bar). Despite an average increase in the number of Ki-67-positive cells present in Pten$^{f/f}$;kRas$^{+/T}$ tissues (white bar) compared to WT tissues, this change was not statistically significant (#,Mann-Whitney U test, $p=0.11$). Error bars indicate standard deviation.

7.2.6 No impairment in differentiation of epithelial cells associated with combined Pten loss and activation of k-Ras

In order to examine any further effects upon intestinal homeostasis caused by combined loss of Pten and activation of k-Ras, I next examined the differentiation program of epithelial cell types in this context. Tissue sections of experimental $Pten^{f/f}$;$kRas^{+/T}$ and $Pten^{f/f}$, $kRas^{+/T}$ and WT control intestines at day 14 PI were subjected to IHC or special stains in order to visualise the four differentiated cell types of the epithelium; Paneth cells, goblet cells, enterocytes and enteroendocrine cells.

IHC against lysozyme was used to identify paneth cells within intestinal tissue samples. This revealed that paneth cells were present at approximately the expected frequency and were correctly localised at the base of the crypt in tissue sections of all genotypes (WT, $Pten^{f/f}$, $kRas^{+/T}$ and $Pten^{f/f}$;$kRas^{+/T}$) (Figure 7.6A). In experimental $Pten^{f/f}$;$kRas^{+/T}$ tissues, some weak anti-lysozyme staining of epithelial cells in both the crypt and villus, which were histologically similar to goblet cells, was also apparent. This phenomenon was not observed in intestinal tissue sections of $Pten^{f/f}$, $kRas^{+/T}$ or WT genotypes.

Mucin-secreting goblet cells were identified in tissue sections of all genotypes by staining with Alcian blue. This indicated that goblet cells were present and were normally distributed in both experimental ($Pten^{f/f}$;$kRas^{+/T}$) and control ($Pten^{f/f}$, $kRas^{+/T}$ and WT) tissues (Figure 7.6B). No alterations in staining pattern were observed between tissue samples of any genotype.

Colourimetric detection of alkaline phosphatase activity, characteristic of brush border absorptive enterocytes, was next performed upon tissue sections of all genotypes in order to visualise cells of the enteroctye lineage. Enterocytes were found to be present, and formed a continuous brush border, in tissues of all genotypes (Figure 7.7A). No differences in staining pattern in $Pten^{f/f}$;$kRas^{+/T}$ tissue was observed compared to $Pten^{f/f}$, $kRas^{+/T}$ or WT tissues.

Finally, the Grimelius silver staining method was used to visualise enteroendocrine cells within the epithelium. Staining revealed that enteroendocrine cells were present, and correctly localised on the villus, in tissues of all genotypes (Figure 7.7B). No obvious differences in staining patterns were apparent in $Pten^{f/f}$;$kRas^{+/T}$ tissue compared to $Pten^{f/f}$, $kRas^{+/T}$ or WT controls.

In summary, combined activation of k-Ras and deletion of Pten has no apparent effect upon the presence or localisation of mature, differentiated cell types within the intestinal epithelium at day 14 PI. A mild perturbation in differentiation is observed in that $Pten^{f/f}$;$kRas^{+/T}$ goblet cells seem to express low levels of lysozyme, which is normally only characteristic of paneth cells, however this does not seem to have any effect upon the number or location of normal, mucin-secreting goblet cells.

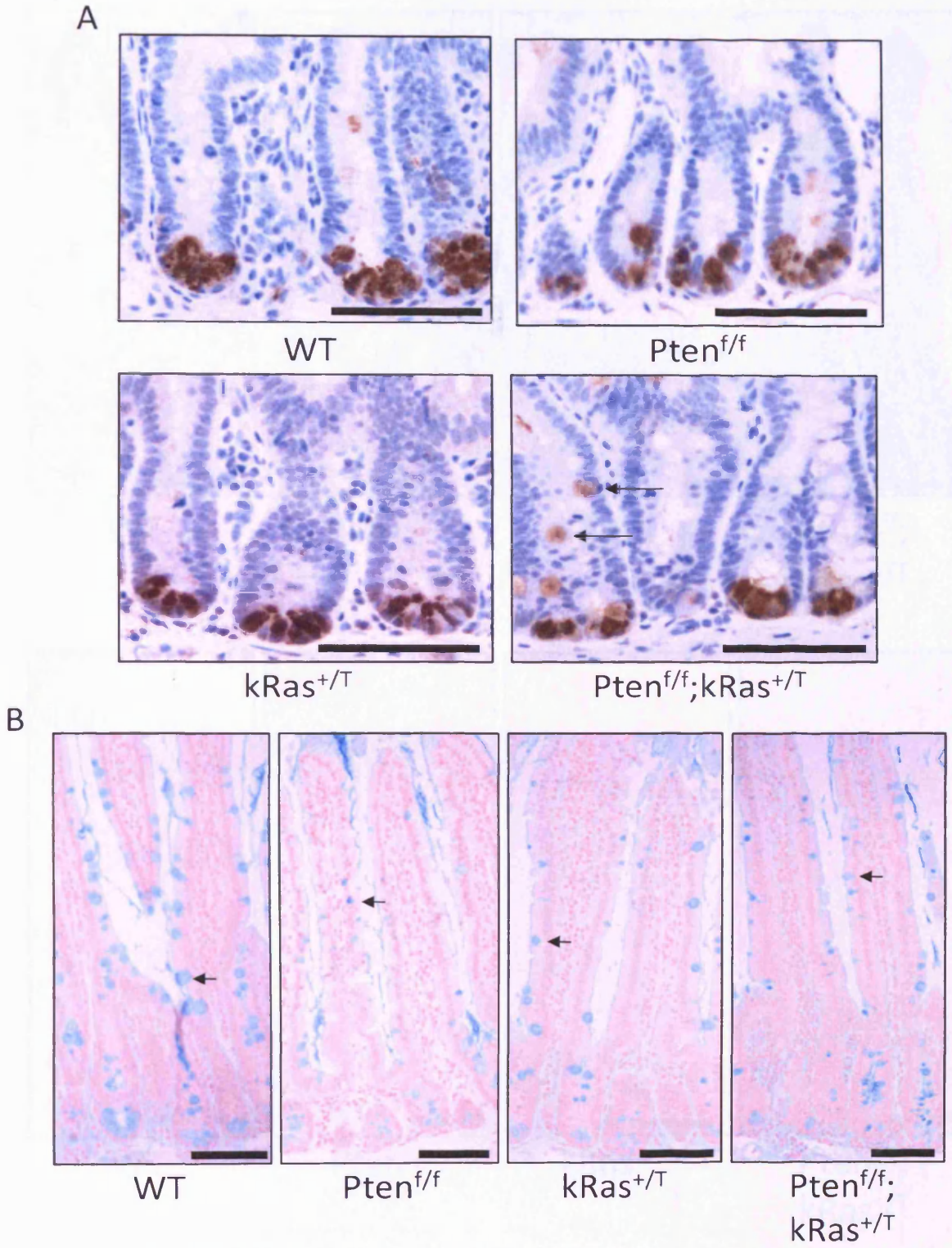

Figure 7.6: ***No alteration in presence or localisation of Paneth cells and Goblet cells in Pten$^{f/f}$;kRas$^{+/T}$ intestines at day 14 PI***

Anti-Lysozyme IHC (A) and Alcian blue staining (B) were used to visualise mature paneth cells and goblet cells respectively within WT, Pten$^{f/f}$ and kRas$^{+/T}$ control and Pten$^{f/f}$;kRas$^{+/T}$ tissues at day 14 PI. Anti-Lysozyme IHC revealed presence and normal localisation of paneth cells in experimental (Pten$^{f/f}$;kRas$^{+/T}$) and control (WT, Pten$^{f/f}$ and kRas$^{+/T}$) tissues. A number of epithelial cells in Pten$^{f/f}$;kRas$^{+/T}$ tissues, which appeared morphologically to resemble goblet cells, were noted to stain positively for anti-lysozyme (Arrows). Alcian blue staining revealed presence and normal distribution of mucin-secreting goblet cells in Pten$^{f/f}$;kRas$^{+/T}$ tissues compared to controls (arrows indicate examples of positively-labelled cells). Scale bars indicate 100μm.

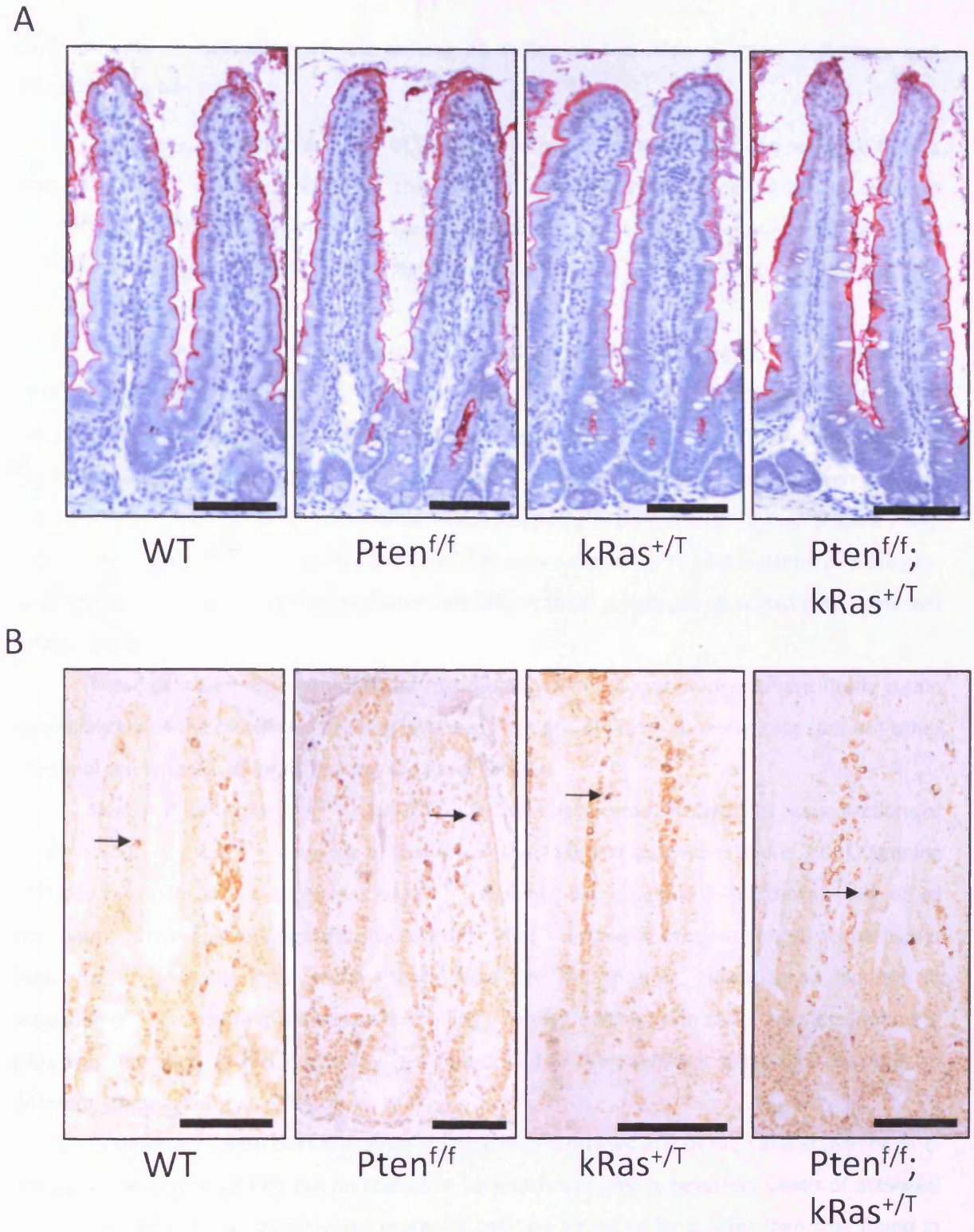

Figure 7.7: ***No alteration in differentiation or localisation of Enterocytes and Enteroendocrine cells in Pten$^{f/f}$;kRas$^{+/T}$ intestines at day 14 PI***

Alkaline phosphatase staining (A) and the grimelius method (B) were used to visualise enterocytes and enteroendocrine cells (B) in WT, Pten$^{f/f}$ and kRas$^{+/T}$ control and Pten$^{f/f}$;kRas$^{+/T}$ tissues. No obvious difference in the location or differentiation of enterocytes was apparent in experimental Pten$^{f/f}$;kRas$^{+/T}$ tissues compared to control (WT, Pten$^{f/f}$ and kRas$^{+/T}$) tissues (A). Enteroendocrine cells were also found to be present and normally localised in Pten$^{f/f}$;kRas$^{+/T}$ tissues compared to controls (Arrows indicate examples of positively-stained cells). Scale bars indicate 100μm.

7.2.7 Increase in activation of Akt at day 14 following induction of Pten deficiency and activation of k-Ras

Previously, combined deletion of Pten and activation of k-Ras has been noted to have a synergistic effect upon activation of the PI3K/Akt pathway in tissues outside the intestine (Chapter 6). In order to determine if Pten loss and k-Ras activation synergise in the intestinal epithelium to activate PI3K/Akt signalling, I next examined the activation status of this pathway using anti-phospho-Akt^{Ser473} IHC.

I first confirmed that the intestinal epithelium of induced animals bearing the LoxP-targeted Pten alleles was indeed deficient for Pten protein at day 14 PI. To do this, anti-Pten IHC was performed on intestinal tissue samples of all genotypes. This revealed that almost 100% of the epithelium of induced Pten$^{f/f}$ and Pten$^{f/f}$;kRas$^{+/T}$ animals was negative for anti-Pten staining, whist underlying stromal cells and smooth muscle cells retained expression of Pten (Figure 7.8A). In comparison, epithelial cells of WT and kRas$^{+/T}$ tissues were found to retain strong positivity for anti-Pten staining, indicating that epithelial cells within these genotypes remained Pten proficient following induction.

These data therefore confirm that recombination in this system occurs specifically within epithelial cells of the intestine, resulting in loss of Pten protein from epithelial cells (but not other intestinal cell types) in animals bearing the Pten$^{f/f}$ alleles.

Next, Anti-phospho-Akt^{Ser473} (pAkt^{Ser473}) IHC was performed on intestinal tissue sections of all genotypes in order to visualise activation of the PI3K/Akt pathway (Figure 7.8B). Staining patterns revealed that cytoplasmic pAkt^{Ser473} staining was detected in epithelial cells of all genotypes. However, staining intensity of Pten$^{f/f}$;kRas$^{+/T}$ epithelial cells was noted to be higher than that of epithelial cells within Pten$^{f/f}$, kRas$^{f/+}$ or WT controls, indicating an increase in activation of Akt. Despite this increase in staining intensity, no change in subcellular localisation of pAkt was detected, as has previously been described in Pten-deficient k-Ras-activated cells of different epithelial origins (Chapter 6).

In summary, these data therefore indicate that combined loss of Pten and activation of k-Ras causes activation of Akt, but no change in localisation of pAkt is reported. Levels of activated Akt in Pten-deficient, k-Ras activated epithelial cells are found to be greater than that found in wild-type epithelial cells, or in epithelial cells in which deletion of Pten or activation of k-Ras alone has been induced.

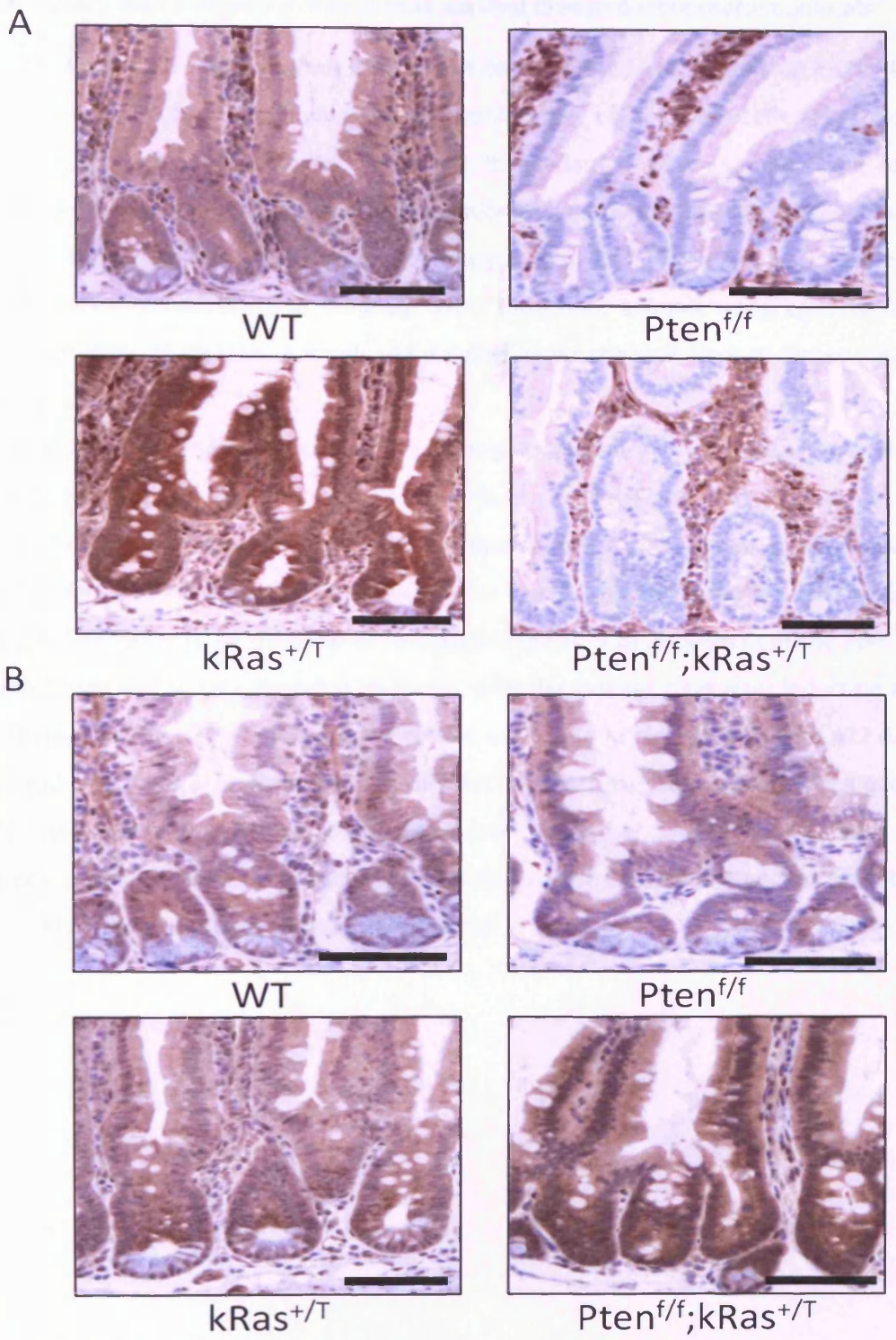

Figure 7.8: ***IHC analysis of Akt activation in Pten$^{f/f}$;kRas$^{+/T}$ intestines***

Anti-Pten IHC (A) was used to confirm recombination in epithelial cells at day 14 following induction of the Villin-CreER^{T} transgene. Animals wild-type for the Pten gene (WT and kRas$^{+/T}$ controls) were found to retain expression of Pten protein in the epithelium, as indicated by strong staining of epithelial cells. Pten$^{f/f}$ controls and Pten$^{f/f}$;kRas$^{+/T}$ experimental tissues were found to show epithelial-specific loss of Pten protein in virtually 100% of all cells but not from stromal cells, indicating high-frequency recombination within the epithelium. To examine activation of the PI3K/Akt pathway in Pten$^{f/f}$;kRas$^{+/T}$ compared to WT, Pten$^{f/f}$ and kRas$^{+/T}$ control tissues, anti-phospho-Akt^{Ser473} IHC was performed. This revealed an increase in staining intensity in Pten$^{f/f}$;kRas$^{+/T}$ tissue compared to all controls. The staining pattern in Pten$^{f/f}$;kRas$^{+/T}$ tissue was observed to be homogeneously cytoplasmic, indicating no alteration in subcellular localisation of pAkt. Scale bars indicate 100μm.

7.2.8 Preliminary data indicates a reduction in survival time in double-mutant animals

The above data establish that, in the short-term (at day 14 PI), combined loss of Pten and activation of k-Ras results in an increase in proliferation of epithelial cells characterised by activation of the PI3K/Akt pathway. Based on these data, I next examined the long-term consequences of combined loss of Pten and activation of k-Ras within the intestinal epithelium.

In order to do this, cohorts of experimental $Pten^{f/f};kRas^{+/T}$ (n=20) and control $kRas^{+/T}$ (n=10) mice were generated and induced. After induction, animals were aged whilst being monitored for signs of disease. Animals were culled when showing signs of illness, and tissues removed for analysis.

Whilst this experiment is currently on-going, preliminary Kaplan-Meier survival analysis has been performed on early survival data from these cohorts (Figure 7.9). The current trend in survival of the two cohorts of animals indicates that $Pten^{f/f};kRas^{+/T}$ animals show a reduction in survival compared to $kRas^{+/T}$ controls, however this trend is not currently statistically significant ($p=0.14$, $\chi^2= 2.13$, DF = 1). At the time of writing this thesis, 9 of 20 animals in the $Pten^{f/f};kRas^{+/T}$ cohort (45%) had had to be culled due to illness, with the average time after induction at culling being 148 days PI. The oldest animal in the cohort was found to remain healthy at 422 days PI. In contrast, just one of 10 animals in the control $kRas^{+/T}$ cohort had been culled, which occurred at day 7 PI. The oldest animal in this cohort also remained alive and healthy at 422 days PI. Thus, these preliminary data and observations indicate that combined loss of Pten and activation of k-Ras in the intestinal epithelium results in a reduction in lifespan.

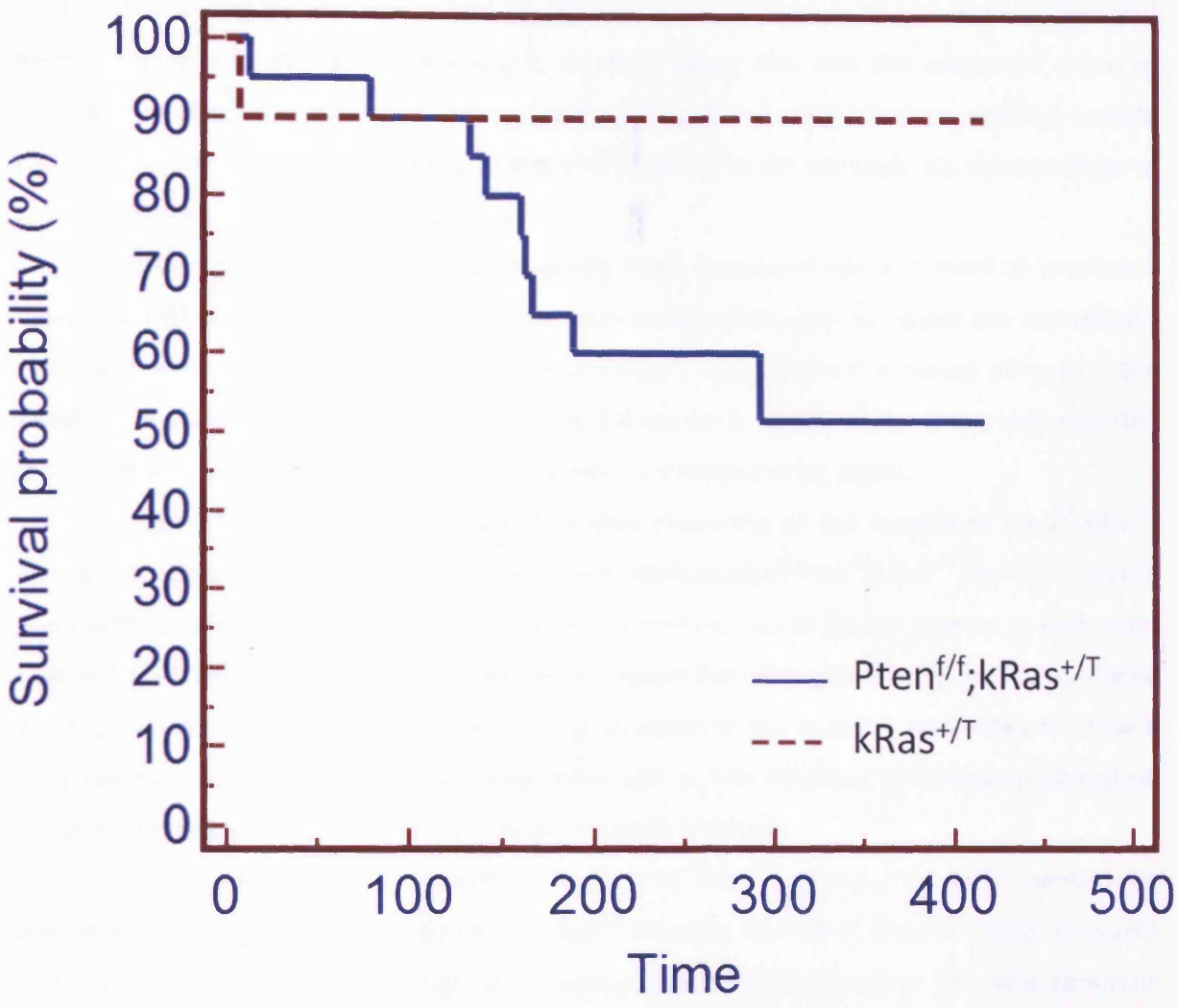

Figure 7.9: ***Survival of Pten$^{f/f}$;kRas$^{+/T}$ mice compared to kRas$^{+/T}$ controls***
Cohorts of experimental animals (Pten$^{f/f}$;kRas$^{+/T}$) and controls (kRas$^{+/T}$) were induced and aged whilst being monitored for signs of disease. Animals were culled when symptomatic of disease, and Kaplan-Meier survival analysis performed. This indicates a reduction in survival time of experimental animals compared to controls, however this difference is not statistically significant ($p=0.14$, $\chi^2= 2.13$, DF = 1). Median survival times of each cohort were not calculated, as this experiment is not currently complete, and more than 50% of each cohort currently remain healthy. However, the current trend of these data indicates that experimental animals are likely to show a significant reduction in median survival time compared to controls.

7.2.9 Decrease in survival of Pten$^{f/f}$;kRas$^{+/T}$ animals is caused by intestinal pathologies

Pten$^{f/f}$;kRas$^{+/T}$ animals were culled when symptomatic of disease and dissected. At dissection, a number of animals were found to bear intussusception of the large bowel (longitudinal folding of the bowel into itself), which had caused blockage of the colon and haemorrhaging into the lumen of the gut. In these cases, this was the presumed cause of morbidity. In all animals dissected, removal and opening of the small intestine revealed notable thickening of the mucosa, particularly at the end proximal to the stomach. No abnormalities of any other tissues were noted at dissection.

Organs and intestines were subsequently fixed, processed and sectioned as previously described. H&E-stained sections of all tissues were examined in order to detect any microscopic histological abnormalities. No microscopic abnormalities were detected in tissues other than the intestine. In particular, no abnormalities of the kidney were noted, which is the only reported location of Vil-CreER^{T} activity outside of the intestine (el Marjou et al., 2004).

In the intestine, the macroscopically visible thickening of the mucosa of Pten$^{f/f}$;kRas$^{+/T}$ animals was clearly evident microscopically. The epithelium of all Pten$^{f/f}$;kRas$^{+/T}$ animals analysed was found to be hyperproliferative, with numerous obvious mitotic figures present in each crypt (Figure 7.10A). Levels of mitosis were noted to be greater than that observed in tissue of the same genotype at day 14 PI. The hyperproliferative phenotype of the intestine was noted to show a clear decrease in severity along the longitudinal axis of the intestine, with hyperproliferation being most pronounced at the stomach end of the small intestine.

Along the length of the intestine in aged Pten$^{f/f}$;kRas$^{+/T}$ animals, villi were noted to be abnormal in structure compared to Pten$^{f/f}$;kRas$^{+/T}$ tissue at day 14 PI (Figure 7.10B). Frequent branching of the villus tip was noted, which was not observed in tissues of the same genotype harvested at day 14 PI. Gross invaginations of the epithelium along the crypt-villus axis were also noted to be very common, giving the epithelium of the villus a 'crinkled' appearance. Again, such abnormalities of the gross appearance of the epithelium were not observed in Pten$^{f/f}$;kRas$^{+/T}$ intestines at day 14 PI.

In one case, an aged Pten$^{f/f}$;kRas$^{+/T}$ animal (which was culled at day 166 PI) was noted to have developed a large tumour of the small intestine, proximal to the stomach. Microscopic assessment of this lesion revealed it to be an aggressive adenocarcinoma, which displayed clear invasion of epithelial cells into the underlying submucosa, and generated an obvious desmoplastic response. However, this preliminarily remains the only example of overt malignant disease observed in this cohort.

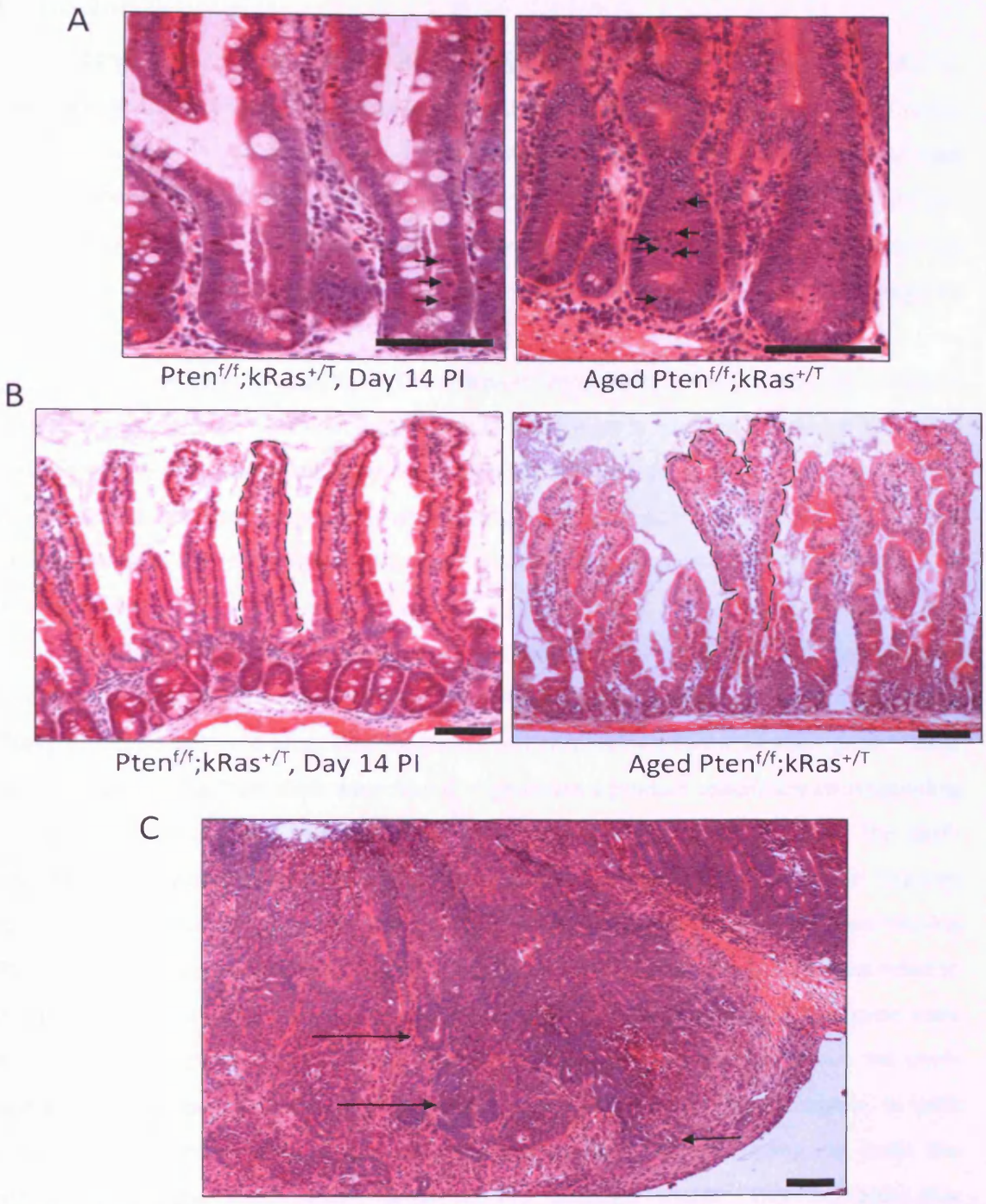

Figure 7.10: ***Intestinal histology of aged Pten$^{f/f}$;kRas$^{+/T}$ mice reveals hyperproliferation of epithelial cells, abnormal villus structure and adenocarcinoma.***
H&E-stained tissue sections of intestines from aged Pten$^{f/f}$;kRas$^{+/T}$ animals were examined for the presence of any histological abnormalities. An increase in proliferation within crypts of aged Pten$^{f/f}$;kRas$^{+/T}$ animals was apparent (A, Right hand panel, arrows indicate mitoses) compared to tissue of the same genotype at day 14 PI (Left panel), particularly at the end of the small intestine proximal to the stomach. Levels of mitosis appeared further elevated in aged Pten$^{f/f}$;kRas$^{+/T}$ animals in comparison to the previously characterised increase in mitosis at day 14 PI in animals of the same genotype. Along the length of the intestine, gross abnormalities in villus structure were apparent in aged Pten$^{f/f}$;kRas$^{+/T}$ animals, including branching of villi (B, right hand panel, dashed lines indicate outline of a single villus). Such abnormalities were not noted in tissue of the same genotype at day 14 PI (left hand panel). In one instance a Pten$^{f/f}$;kRas$^{+/T}$ animal, culled at day 166 PI, was found to have developed invasive adenocarcinoma of the proximal small intestine (C, arrows indicate epithelial cells invading into the submucosa). Scale bars indicate 100μm.

7.3 Discussion

In Chapter 6, I described work indicating that loss of Pten and activation of k-Ras is strongly synergistic in promoting neoplasia in the epithelial lining of the biliary system and in the squamous epithelium of the forestomach. Data published in the literature also indicates that synergy exists between Pten loss and k-Ras activation in promoting tumourigenesis both of the lung (Iwanaga et al., 2008) and of the ovary (Dinulescu et al., 2005). However, the combined effect of deletion of Pten and activation of k-Ras upon the intestinal epithelium remains uncharacterised.

In this chapter, I aimed to examine the effects of co-ordinate loss of Pten and activation of the k-Ras^{V12} transgene in the intestinal epithelium. In order to circumvent previous problems, this required expression of Cre in a highly intestinal-specific manner. To do this, I made use of the Villin-CreER^{T} Cre-expressing transgene, which drives recombination specifically within the intestinal epithelium and the kidney following induction by administration of Tamoxifen (el Marjou et al., 2004).

I first confirmed that cre activity is induced in experimental mice, and that recombination occurs at the LoxP-targeted *Pten* allele and/or the *k-Ras* transgene, using PCR reactions designed specifically to detect the wild-type, LoxP-targeted and recombined forms of each gene. Tissue samples wild-type for the Pten allele were found to generate a product specifically corresponding to the wild-type product only. In contrast, samples from induced animals bearing the LoxP-targeted Pten alleles were found to generate products corresponding to both the LoxP-targeted unrecombined allele and to the recombined allele. Similarly, samples from animals not bearing the kRas^{V12} transgene were found to generate a single product, the size of which corresponded to the wild-type-specific product. Samples from induced animals bearing the k-Ras transgene were found to generate all three types of product, corresponding to the wild-type allele, the LoxP-targeted but unrecombined transgene and to the recombined form of the transgene. In both cases, transgenic animals were found to generate products corresponding to both the unrecombined and the recombined forms of the targeted alleles. This indicates that recombination has not occurred in all copes of genomic DNA present in the sample. This can be explained by two possible scenarios. Recombination may not have occurred with 100% efficiency in all epithelial cell types. Alternatively, or indeed additionally, non-epithelial cell types would almost certainly have been present in tissue samples. Thus, cell types in which Cre activity is not induced, such as stromal cells, would not have recombined, explaining detection of the non-recombined allele.

7.3.1 Combined loss of Pten and activation of k-Ras results in an increase in proliferation and expansion in crypt and villus size in the intestinal epithelium at day 14 PI

Having established that treatment with Tamoxifen results in recombination at both the Pten allele and the k-Ras transgene, I next examined the effect of Pten loss and k-Ras activation upon homeostasis of the intestinal epithelium. Scoring for apoptosis in $Pten^{f/f};kRas^{+/T}$ tissue at day 14 PI revealed that there was no difference compared to $Pten^{f/f}$, $kRas^{+/T}$ and WT controls, indicating that combined loss of Pten and activation of k-Ras has no effect upon cell death within the crypt. In contrast to this, scoring for mitosis revealed an increase in proliferation in both $Pten^{f/f};kRas^{+/T}$ and $kRas^{+/T}$ tissues compared to WT tissues. These data therefore indicate that the observed increase in mitosis in these tissues is driven by activation of k-Ras, and occurs independently of Pten status. To examine the effect of this increase in cell division upon homeostasis of the epithelium, average sizes of crypts and villi were scored in tissue of all genoytpes. A significant increase in crypt size (as scored by numbers of cells per crypt) was observed in $Pten^{f/f};kRas^{+/T}$ tissues compared to WT, $Pten^{f/f}$ and $kRas^{+/T}$ tissues. This is probably reflective of the observed increase in levels of mitosis in the crypt, which is presumably driving an increase in the number of cells comprising the crypt. However, despite the fact that a similar increase in mitosis was observed in $kRas^{+/T}$ tissues, this was not found to be translated into an increase in crypt size compared to wild-type tissue. These data therefore suggest that whilst activation of k-Ras drives proliferation within the crypt, additional loss of Pten is required in order for this perturbation in cell division to become manifest as an increase in crypt size.

In contrast to this, scoring of villus size revealed a significant increase in the number of cells comprising the villus in both $Pten^{f/f};kRas^{+/T}$ and $kRas^{+/T}$ tissues compared to WT and Ptenf/f controls. Villi from $Pten^{f/f};kRas^{+/T}$ tissues were also noted to be significantly larger than those in $kRas^{+/T}$ tissues. Thus, these data indicate that whilst activation of k-Ras alone results in a significant increase in villus size, additional inactivation of Pten causes exacerbation of this phenotype. This indicates that the observed increase in mitosis has a moderate impact upon villus size in $kRas^{+/T}$ tissue, but similar to the situation in the crypt, additional loss of Pten is required for this to become fully manifest.

In order to further investigate the phenotype of increased proliferation in the crypt following activation of k-Ras, analysis of Ki67-positive cells in tissues of all genotypes was next performed. Anti-Ki67 IHC revealed that the approximate size and location of the proliferative zone was constant between WT, $Pten^{f/f}$, $kRas^{+/T}$ and $Pten^{f/f};kRas^{+/T}$ tissues. Scoring of the number of Ki67-positive cells within the epithelium confirmed previous observations indicating an increase in proliferative cells in response to activation of k-Ras. The number of Ki67-positive cells present in $kRas^{+/T}$ tissues was found to be significantly increased compared to WT controls. However, a similar increase in $Pten^{f/f};kRas^{+/T}$ tissues was found not to be statistically significant. This is

probably due to high variability between samples, as indicated by a large standard deviation of the data. Future scoring of a larger sample size may allow determination as to whether this change is truly significant or not.

I next investigated the effect of combined loss of Pten and activation of k-Ras upon intestinal homeostasis by examining the presence and localisation of differentiated epithelial cell types. Special stains or IHC to detect specific markers of each cell type revealed the presence and normal localisation of Paneth cells, goblet cells, enterocytes and enteroendocrine cells in $Pten^{f/f};kRas^{+/T}$ tissues compared to $Pten^{f/f}$, $kRas^{+/T}$ and WT controls. This indicates that combined loss of Pten and activation of k-Ras has no dramatic effect upon the differentiation program of mature cells types, or on their location within the epithelium. One subtle phenotype was observed in $Pten^{f/f};kRas^{+/T}$ tissues however, which was that a number of cells which appeared morphologically to be goblet cells were noted to stain weakly positively for anti-lysozyme, which is normally only expressed by paneth cells. This may imply that the differentiation program of secretory cell lineages may be perturbed in the context of Pten loss and k-Ras activation. However, these data are currently only preliminary observations, and further characterisation of the phenotype is necessary in order to confirm this notion.

7.3.2 Increase in activation of Akt following co-ordinate loss of Pten and activation of k-Ras

Combined loss of Pten and activation of k-Ras has previously been noted to have varying effects upon activation of Akt, depending upon the exact tissue type. In the gall bladder epithelium Pten loss and k-Ras activation has been found to result in strong activation of Akt together with its membrane localisation. In bile duct epithelium, activation of Akt was noted, but its subcellular localisation was not changed. In the forestomach, no increase in activation of Akt compared to controls was noted (Chapter 6). Given that tissue-specific differences exist with respect to activation of PI3K/Akt signalling following loss of Pten and activation of k-Ras, I next examined the effects of these mutations upon Akt activation within the intestinal epithelium.

As in previous chapters, anti-Pten IHC was first used to confirm that induced animals bearing the $Pten^{f/f}$ alleles were deficient for Pten protein. This revealed that Pten was lost from the epithelium in $Pten^{f/f}$ and $Pten^{f/f};kRas^{+/T}$ animals with high efficiency. No loss of Pten staining was observed from the underlying stroma or from smooth muscle cells. In contrast, WT and $kRas^{+/T}$ animals (both of which are $Pten^{+/+}$) were shown to retain Pten positivity in the epithelial cell layer.

Anti-phospho-Akt^{Ser473} (pAkt) IHC was then performed upon intestinal tissue sections of all genotypes. In tissues sections of WT, $Pten^{f/f}$ and $kRas^{+/T}$ animals, staining for pAkt was detected, but was fairly low and was consistent between all three genotypes. In contrast, pAkt staining of

$Pten^{f/f}$;$kRas^{+/T}$ tissues showed an increase in staining intensity, indicating an increase in activation of Akt. However, no change in localisation of pAkt was observed, with staining found to be uniform across the cytoplasm of epithelial cells. Thus, from these data I conclude that a synergistic effect of activation of k-Ras and loss of Pten results in activation of Akt, which is not seen in WT or single-mutant tissues. Whilst synergistic activation of Akt is observed however, in this tissue, change in subcellular localisation of the activated protein is not.

7.3.3 Hyperplasia of the intestinal epithelium following prolonged loss of Pten and activation of k-Ras

At day 14 PI, it was apparent that a phenotype of increased proliferation, in turn resulting in an increase in epithelial cell number in the crypt and villus, was driven by combined loss of Pten and activation of k-Ras in the short term. In order to investigate the consequences of this phenotype upon intestinal homeostasis over the longer term, I next conducted an aging study of induced $Pten^{f/f}$;$kRas^{+/T}$ mice. Whilst preliminary data has been collected from this experiment and is reported here, full analysis of this study falls outside the scope of this thesis.

Survival analysis of induced $Pten^{f/f}$;$kRas^{+/T}$ animals indicated a reduction in survival time compared to $kRas^{+/T}$ controls. This trend is currently not significant, however the fact that at the time of analysis, almost half of all $Pten^{f/f}$;$kRas^{+/T}$ animals had been culled due to sickness whereas the vast majority of $kRas^{+/T}$ animals remained healthy, suggests that this trend is likely to continue. This therefore indicates that synergy within the intestinal epithelium between loss of Pten and activation of k-Ras may cause a reduction in lifespan.

Histopathological assessment of tissues from aged $Pten^{f/f}$;$kRas^{+/T}$ animals was then performed in order to confirm that intestinal pathologies were the cause of death of these animals, rather than phenotypes occurring on tissues outside of the intestine. The discovery that no abnormalities of any tissues other than the intestine were found indicated that this was indeed the case. Examination of intestinal tissues revealed that gross abnormalities were apparent. Extensive hyperproliferation of the epithelium was noted, which was found to be much more marked than that observed at day 14 PI. An obvious variation in severity of the hyperproliferative phenotype was noted along the longitudinal axis of the small intestine, with hyperproliferation most obvious at the end of the intestine proximal to the stomach. This variation in phenotype can potentially be explained in two ways; firstly, levels of Cre expression (and thus levels of recombination) may vary along the length of the intestine. This has previously reported as a characteristic of other Cre-expressing transgenes such as AhCre (Ireland et al., 2004), but has not been noted for the Villin-$CreER^T$ transgene in use here (el Marjou et al., 2004), and therefore seems unlikely. Alternatively, differences in biology of the intestine along its length may mean

that some regions are more susceptible to stimulation of proliferation by combined loss of Pten and activation of k-Ras. This however, has not been proven here, and requires further investigation in order to fully characterise the observed effects. Another obvious abnormality of the intestinal epithelium in aged $Pten^{f/f};kRas^{+/T}$ mice was that of perturbation of villus structure. Along the entire length of the intestine, villi were observed to show an unusual arrangement of the epithelial cells of which they were comprised. Epithelial cells were observed to form frequent invaginations into the underlying stromal core of the villus, giving the epithelium a 'wrinkled' appearance. Furthermore, branching of villi was also frequently observed, which occurred both at the tip of the villus and lower down on the structure. These phenotypes were not observed in $Pten^{f/f};kRas^{+/T}$ animals at day 14 PI. Thus, it is clear that long-term combined activation of k-Ras and deletion of Pten causes alteration in the normal structure of villi. This phenotype could possibly be explained by a failure of cells at the villus tip to undergo apoptosis and/or be shed into the intestinal lumen, as would normally occur. It is conceivable that a block in shedding of cells from the villus tip combined with increased proliferation and crypt-villus migration of epithelial cells could result in abnormal patterning of the epithelium, as seen here. However, as these data remain preliminary, this is pure speculation. Further investigation of the kinetics of cell migration and shedding within the epithelium in the future may allow confirmation of this hypothesis.

Finally, the most severe intestinal pathology observed in an aged $Pten^{f/f};kRas^{+/T}$ animal was that of the development of adenocarcinoma, which has so far only been noted in one individual, at day 166 PI. This lesion was noted to be large and aggressive, and occurred proximal to the stomach. Clear invasiveness of epithelial cells into the underlying stroma was noted in this lesion. This therefore indicates that, in the context of combined loss of Pten and activation of k-Ras, tumour initiation and rapid tumour progression is possible. However, the penetrance of this phenotype, and determination of whether it is truly driven by Pten-deficient, k-Ras activated cells, remains to be fully determined.

7.3.4 Summary and future directions

In summary, the data presented in this chapter indicate that in the short term, k-Ras activation and Pten loss within the intestinal epithelium results in an increase in proliferation and a consequent increase in crypt and villus size within the intestine. Pten deletion and activation of k-Ras have been found to synergise with respect to activation of the PI3K/Akt pathway, but change in subcellular localisation of activated Akt is not observed. In the longer term, double-mutant animals show a reduction of lifespan, with morbidity being directly caused by intestinal pathologies. Dramatic hyperplasia, abnormalities of villus structure and the development of

adenocarcinoma have all been observed in the intestine following long-term activation of k-Ras and deletion of Pten.

The data presented here represent only the preliminary findings of this study, and there is therefore scope for this investigation to continue. Firstly, I described in Chapter 6 that biliary tract lesions in tissues with combined loss of Pten and activation of k-Ras are driven by activation of both PI3K/Akt signalling and the Raf-MEK-ERK pathway. Contribution of activation of the Raf-MEK-ERK pathway in the phenotypes observed here in the intestinal epithelium have not yet been characterised, and this should be addressed. Furthermore, the observed increase in number of cells present in both the crypt and villus implies that there may be some form of block in migration of epithelial cells occurring following combined loss of Pten and activation of k-Ras. This therefore warrants further characterisation.

The data reported here analysing the long-term effects of Pten loss and k-Ras activation on the intestinal epithelium are currently poorly characterised. This needs to be addressed in order to confirm that the phenotypes reported here are truly synergistic consequences of loss of Pten and activation of k-Ras. The fact that the development of adenocarcinoma has been reported here represents the first evidence that Pten and k-Ras synergise to initiate and drive intestinal tumourigenesis. However, as this has currently only been described in one cohort animal, the penetrance of this phenotype remains undetermined. One potential reason explaining why malignancy has developed in so few cases is that the widespread hyperproliferative phenotype of the epithelium observed may be causing morbidity of animals before tumourigenesis ensues. Thus, it would be worthwhile in future experiments to aim to achieve lower levels of recombination directed towards the intestinal epithelium. This should generate a more restricted hyperproliferative phenotype within the intestine, which may then allow longer survival of animals, providing a longer time-frame for bona fide intestinal tumours to develop.

Chapter 8: General Discussion

Colorectal cancer (CRC) is a significant cause of human mortality in the UK, being the third most common form of cancer (Cancer Research UK, 2007). Despite an increasing incidence of CRC, mortality rates for colorectal disease are actually steadily falling (Cancer Research UK, 2007); this is probably due to improved awareness of the disease and better detection methods, as well as significantly improved treatment methods (NICE Guidelines, 2004).

The step-wise model of colorectal cancer initiation and progression hypothesises that a series of genetic mutations must be acquired in order for malignant disease to become manifest (Fearon and Vogelstein, 1990). These mutations include both inactivation of tumour suppressor genes, such as Apc and p53, and activation of oncogenes, such as k-Ras.

Up to 40% of sporadic human colorectal cancers are reported to bear mutations within components of the PI3K/Akt signalling pathway, resulting in its activation (Parsons et al., 2005). The tumour suppressor PTEN is one of the principal antagonists of this pathway, functioning as a lipid phosphatase, which dephosphorylates phosphatidylinositol-3, 4, 5-trisphosphate (PIP3) at the 3 position of the inositol ring (Maehama and Dixon, 1998). As such, mutational inactivation of Pten results in activation of the Akt signalling cascade.

PTEN is well characterised as a suppressor of tumourigenesis, and in humans is commonly reported to be mutated in cancers of the breast (Saal et al., 2008), prostate (Cairns et al., 1997), endometrium (Tashiro et al., 1997), cervix (Kurose et al., 2000) and skin (Birck et al., 2000). Furthermore, Germline mutation of Pten leads to a spectrum of hamartoma predisposition syndromes (PTEN Hamartoma Tumour Syndromes; PHTS), the most common form of which is Cowden's disease (Nelen et al., 1999). Lesions of the gastrointestinal mucosa are thought to occur in between 35-75% of individuals with Cowden's disease (Carlson et al., 1984, Merg and Howe, 2004).

Evidence from mouse-based studies has further indicated that PTEN plays an important role in suppressing neoplasia of the intestine. Mice constitutively heterozygous for Pten have been noted to develop neoplasia of multiple tissues, including the intestine (Di Cristofano et al., 1998, Podsypanina et al., 1999, Suzuki et al., 1998). Widespread conditional deletion of Pten in the mouse has also been shown to result in susceptibility to intestinal cancer (Lu et al., 2007). More restricted conditional deletion of both copies of Pten within both stromal and epithelial cells of the intestine is reported to result in rapid tumourigenesis, which is attributed to an expansion of the stem cell compartment (He et al., 2007). Previous data from the same laboratory has also indicated that inactivation of Pten by phosphorylation is a characteristic of the intestinal stem cell, playing a role in modulating interaction of the Wnt and BMP signalling pathways (He et

al., 2004). Together, these data provide compelling evidence indicating a role for Pten in regulation of the intestinal stem cell, and in suppressing intestinal tumourigenesis.

In this thesis, I set about investigating the effects of homozygous deletion of Pten specifically from the epithelial cell compartment of the intestine using a Cre-LoxP-based approach. I aimed to examine the effects of Pten deletion upon normal homeostasis of the intestine, with particular emphasis on the stem cell. Further, I wished to examine the effects of Pten deletion upon tumourigenesis of the intestine, both in otherwise normal intestinal epithelium, and also in the context of genetic activation of signalling pathways known to play a role in homeostasis of the intestine.

8.1 Pten, the intestinal stem cell and epithelial-stromal interactions

In Chapter 3, I describe work investigating the short-term effects of epithelial-specific deletion of Pten from the murine small intestine. My investigations revealed that up to 50 days following Pten loss, no perturbations in intestinal homeostasis occur. No changes to the gross histology or structure of the intestine were observed, and no effects upon proliferation, apoptosis, migration or differentiation of epithelial cells were noted in the context of Pten deficiency. These findings were surprising considering that loss of Pten was confirmed, and that increased levels of activated Akt were detected in the intestinal epithelium. This therefore indicated that Pten is redundant with respect to normal homeostasis of the intestine, at least at short timepoints following its loss.

Given that recent data in the literature has indicated that Pten loss may play a role in regulation of the ISC (He et al., 2007), I set about examining any changes to the stem cell compartment in the Pten-deficient model I was using. Indirect examination of the clonogen content of the intestine indicated no increase in putative stem cells in Pten-deficient intestines. Furthermore, I examined the expression of previously proposed markers of the intestinal stem cell, DCAMKL-1 (May et al., 2008), Musashi-1 (Potten et al., 2003), Bmi1 (Sangiorgi and Capecchi, 2008) and Lgr5 (Barker et al., 2007). This analysis indicated no increase in expression of any of these markers in Pten deficient tissues, as would be expected if the number of stem cells had increased following Pten deletion. Thus, from my data, I conclude that epithelial-specific deletion of Pten does not affect multiplicity of intestinal stem cells up to day 50 following Pten loss.

Clearly, there is some discrepancy between the data I report here, and that of the recently published data of *He et al.* (2007). In their study, *He et al.* used an inducible form of Cre transgene which has previously been described as being expressed in both the epithelial and stromal cell compartments of the intestine following induction (Schneider et al., 2003). Here, I have used a form of Cre recombinase which shows a pattern of expression which is tightly restricted to the epithelial cell layer (Ireland et al., 2004). Thus, the difference in phenotype

observed between these studies may be attributed to differing patterns of recombination in each system used. My data indicate that epithelial-specific deletion has little effect upon intestinal homeostasis, whereas *He et al.* (2007) report that combined epithelial and stromal deletion of Pten causes rapid expansion of stem cell multiplicity, which in turn results in tumourigenesis. This therefore suggests that Pten and PI3K/Akt signalling may play an important role in epithelial-stromal interactions within the stem cell niche in order to control stem cell multiplicity.

Thorough analysis of this hypothesis is currently precluded by the present failure to definitively characterise the intestinal stem cell, and consequently the lack of specific markers allowing identification and visualisation of ISCs. Until this information is available, direct analysis of the role of Pten and PI3K/Akt signalling and interaction within the intestinal stem cell niche will not be possible.

Additionally, these studies do not address the question of whether stromal Pten deficiency alone is sufficient for expansion of the stem cell compartment, or whether the stem cell itself (and/or its surrounding epithelial cells) also has to be Pten-deficient in order for this to occur. One experiment which could potentially resolve this issue would be to examine the effects of deleting Pten specifically from the stromal cell compartment. A potential method for achieving this would be to use a form of Cre recombinase transgene which is expressed specifically within fibroblasts of the stromal cell population, such as that driven by the pro-alpha2-collagen (*Col1a2*) gene promoter, which has been described by *Zheng et al.* (2002). This line of analysis is currently being pursued within our laboratory, and currently mice bearing both the Col1a2-Cre transgene and LoxP-targeted Pten alleles have been generated, but not yet analysed.

The major caveat of the work I first described analysing the role of Pten in the intestinal epithelium was that only short-term analysis of the effects of Pten deletion were possible. This was due to the presence of over-riding phenotypes within other tissues, which precluded analysis of Pten deficiency in the intestine at more extended timepoints. In order to circumvent these problems, I next crossed animals bearing LoxP-targeted *Pten* alleles to animals bearing a more tightly regulated inducible form of Cre recombinase, AhCreER^{T}. This transgene has previously been reported to drive recombination within the intestinal epithelium after induction, but minimises levels of background recombination previously found to be problematic with AhCre (Kemp et al., 2004). Indeed, analysis of Pten deletion at greatly extended timepoints after induction was possible in this study. Notably, these animals were found to develop intestinal hamartomas at a low frequency, and may therefore provide a useful model of intestinal lesions of a similar histopathology to that observed in human Cowden's syndrome. Additionally, intestinal lesions of a more severe, adenomatous histology were noted to be present in these animals. However, evidence of these types of lesions being a progression of hamartomatous lesions was

not detected. Thus, further analysis of the timecourse of development of intestinal lesions is warranted in order to ascertain whether this is truly the case.

Based on the data of *He et al.* (2007), it could be predicted that the development of intestinal lesions may be initiated by an increase in stem cell number following Pten loss. This hypothesis has not yet been addressed here, but further analysis may allow confirmation of this proposed mechanism of tumour initiation. Alternatively, the delay in onset of tumourigenesis in these mice may suggest that an initiating mutation must be acquired in order for tumour formation to ensue. Again, this has not been analysed here, but mutational analysis of DNA extracted from tumour samples would allow confirmation of this notion.

8.2 Pten suppresses tumour progression

8.2.1 In the context of activated Wnt signalling

Having established that deletion of Pten alone from the intestinal epithelium has no immediate effect upon intestinal homeostasis, but results in delayed intestinal tumourigenesis, I next investigated the role of Pten as a suppressor of tumour progression in the context of activation of other regulatory pathways.

As the Wnt signalling pathway is known to be critical for intestinal homeostasis and has a well characterised role in intestinal tumourigenesis (Reviewed by Clevers, 2006), I first chose to examine the effects of Pten deletion in the context of activated Wnt signalling. This was achieved by additional conditional deletion of one copy of the Apc gene within the intestinal epithelium, which has previously been reported as an intestinal tumour-prone model (Shibata et al., 1997).

My data indicated that deletion of Pten in the context of activated Wnt signalling causes a rapid progression of disease, with resulting formation of adenocarcinomas. This is significant for two reasons. Firstly, there is a paucity of mouse models which show robust development of more advanced intestinal disease. Secondly, it places Pten among the few tumour suppressor genes which have been found to have a clear role in progression, rather than initiation, of intestinal tumourigenesis.

Advanced tumours arising in $Apc^{f/+};Pten^{f/f}$ animals were also noted to show a characteristic pattern of increased activation of Akt, which was coupled with relocalisation of the protein to the cell surface. This phenomenon was also observed following both acute activation of Wnt signalling and deletion of Pten (in $Apc^{f/f};Pten^{f/f}$ animals). This finding was significant given that experiments targeting Akt isoforms to the cell membrane have previously been performed, which was found to result in an increase in oncogenic potential both in cell lines and in vivo

(Mende et al., 2001). The potential implications of this observation are discussed in more detail below.

8.2.2 In the context of k-Ras activation

Pten is well characterised as a suppressor of tumourigenesis in multiple tissues, functioning as a negative regulator of Akt activation (For review, see Dahia, 2000). However, my observations described in Chapter 3 indicate that Pten has little tumour suppressive effect in the intestinal epithelium, at least in the short term following its deletion, despite an observed increase in levels of activated Akt. Additionally, data described in Chapter 5 indicate that hyper-activation of Akt, following combined loss of Pten and activation of the Wnt pathway, results in rapid intestinal tumourigenesis. These observations therefore raise two hypotheses. First, the notion that Pten is a 'permissive' tumour suppressor gene (in that its deletion passively permits, rather than actively stimulates, the PI3K/Akt pathway) is raised; suggesting that loss of Pten will only become relevant in the context of activated PI3K/Akt signalling. Second, these data allude to the possibility of a 'threshold' of Akt activation in the intestine, with low levels of Akt having little effect upon intestinal homeostasis, whereas increased activation of Akt is associated with tumourigenesis.

To examine these notions, I next investigated the effects of Pten deletion in the context of activation of both the PI3K/Akt pathway and of the Raf-MEK-ERK MAPK pathway. This was achieved using a conditionally inducible form of activated Kirsten-Ras. Previous studies have indicated that deletion of Pten and activation of k-Ras co-operate to promote tumourigenesis of both the lung (Iwanaga et al., 2008) and the ovary (Dinulescu et al., 2005). In the ovary, this was found to be driven by activation of both the PI3K/Akt pathway and of the Raf-MEK-ERK signalling pathway (Dinulescu et al., 2005).

When driven by AhCreER^{T}, I found combined deletion of Pten and activation of k-Ras to have a synergistic effect in promoting rapid neoplasia of both the epithelium of the biliary system and hyperplasia of the squamous epithelium of the forestomach. Lesions were found to be most advanced within the gall bladder of Pten$^{f/f}$;kRas$^{+/T}$ mice. These lesions were noted to show strong activation of both Akt, and of MEK and ERK. Furthermore, the phenomenon of membrane association of Akt was observed once again. In bile ducts, lesions were found to generally be smaller and less severe. They too exhibited an increase in activated Akt and ERK expression, but did not show the strong cell surface localisation of phospho-Akt which was noted in lesions of the gall bladder. Finally, hyperplasia of the forestomach was not noted to show increased activation of Akt compared to normal control tissues, and only showed limited activation of MEK and ERK.

These data therefore represent the first evidence indicating that Pten loss and activation of k-Ras act synergistically to promote neoplasia of the biliary epithelium and hyperplasia of the squamous forestomach epithelium. These data also indicate that the mechanism by which this is achieved is highly tissue-dependent. In the biliary epithelium, the resultant phenotype is apparently driven by strong activation of both PI3K/Akt signalling and Raf-MEK-ERK signalling, whereas in the forestomach the observed phenotype is apparently largely PI3K/Akt- and Raf-MEK-ERK-independent. Similar phenotypes to those reported here have also been noted following combined deletion of both Pten and the transducer of TGF-beta/BMP signalling, SMAD4. Separate studies have indicated that combined deletion of both these tumour suppressor genes results in squamous forestomach carcinoma (Teng et al., 2006) and cholangiocellular carcinoma (Xu et al., 2006). In these studies, similar phenotypes to those reported here following combined deletion of Pten and activation of k-Ras were observed, though in both cases the phenotypes reported were more severe than those described here. The similarity between these phenotypes may suggest that, despite perturbations of different pathways at a molecular level, the effects of these mutations may converge on a cellular level to drive tumourigenesis. However, this is purely speculative, and further investigation is needed in order to examine this hypothesis.

In the intestine, combined deletion of Pten and activation of k-Ras driven by the Villin-CreER^{T} transgene has further indicated a co-operative effect of these mutations (Chapter 7). Despite the fact that the results of this study are preliminary, current data indicates that combined loss of Pten and activation of k-Ras within the intestinal epithelium results in a marked hyperproliferative phenotype. In the short term, this is characterised by an increase in mitosis and increase in crypt and villus size compared to controls. This is found to also be associated with an increase in activation of Akt. Over longer periods of time, the hyperproliferative phenotype becomes more marked, with gross defects in villus structure apparent. The development of adenocarcinoma has also been noted. Thus, although analysis of this data is not yet complete, the current indication is that Pten loss and k-Ras activation act synergistically to promote hyperplasia and tumourigenesis in the intestinal epithelium. Again, this is significant as it represents the first evidence of synergy between these two mutations in this tissue type.

8.3 Potential significance of membrane-localised activated Akt

It has been noted throughout this thesis that cell-surface localisation of phospho-Akt^{Ser473} is a recurring phenomenon in Pten-deficient tissues showing strong activation of Akt. This phenomenon also appears to be more commonly associated with advanced states of disease. Based on these observations, it would seem reasonable to suggest that cell-surface localisation of activated Akt may not simply be a passing observation, but could actually be closely linked to progression of disease.

There is currently no evidence in the literature to suggest that membrane localisation of phospho-Akt is a particular feature of human cancer, or that it is associated with increased severity of disease. Thus, before this phenomenon is investigated further, it must first be confirmed that it is indeed relevant to tumourigenesis in humans. To this end, a tissue microarray study of biopsies taken from human colorectal cancers is currently being pursued[9] in order to ascertain whether membrane localisation of Akt can be detected, and whether it is associated with advancement of disease or clinical outcome. The detection of cell surface activated Akt in human cancers would potentially have two significant applications; first, it could be used as a prognostic marker of disease, and second, it could be an appropriate target for therapy. However, each of these potential applications requires further investigation before potentially being implemented.

The use of membranous Akt as a prognostic marker in human disease would first require examination of a large number of human cancers of different tissue origins in order to ascertain a clear relationship between subcellular localisation of Akt and stage of disease.

If membrane-localised Akt were to be explored as a potential target for therapy, a mechanistic link between location of Akt at the cell surface and progression of disease would need to be established. This could involve expressing membrane-targeted forms of Akt in the context of activation of Wnt signalling or PI3K/Akt and Raf-MEK-ERK signalling, and examining whether the resulting phenotypes are comparable to that achieved following deletion of Pten. This would provide convincing evidence that tumourigenesis resulting from Pten deletion is driven principally through cell surface localisation of Akt. If this notion were to be proven, then activated and membrane-localised Akt may provide a good potential therapeutic target for the malignancies described here. Indeed, inhibitors of Akt are already in use as chemotherapeutics, but often show problems with off-target effects. One such inhibitor of Akt, Perifosine, is a synthetic phospholipid analog known to elicit its anti-tumourigenic effects by decreasing association of Akt to the membrane (Kondapaka et al., 2003). Thus, agents such as this would probably be highly effective if specifically selected to treat lesions which show strong membrane localisation of activated Akt. However, as with many cancer therapies, the challenge of specifically targeting therapeutic agents to cancer cells whilst sparing normal cells remains.

8.4 Developing a faithful mouse model of step-wise colorectal cancer progression

A secondary aim of the work described here was to generate a good, faithful mouse model of step-wise colorectal cancer progression.

[9] The tissue microarray study is currently being performed in collaboration with Dr Marnix Jansen, Hubrecht Institute, The Netherlands.

Mouse models of human disease have undoubtedly been massively beneficial in the field of cancer research. They provide a mammalian model of disease, which is easy to use and relatively easy to genetically manipulate, which has allowed basic research into the biology of disease. Furthermore, they provide an excellent platform in which to test novel and potential therapeutic agents *in vivo*. However, particularly with respect in intestinal tumourigenesis, the current mouse models available do leave some scope for improvement. For instance, one of the most commonly used mouse models of intestinal disease is the Apc^{MIN} mouse (Moser et al., 1990). The Apc^{MIN} mouse tends to develop a large number of polyps of both the small and large intestine, the vast majority of which are adenomatous polyps. Morbidity is usually caused by tumour burden, rather than by advancement of disease. In contrast to this, most humans with sporadic CRC will develop a single lesion, usually located within the lower colon or rectum. In humans, disease is currently often much more advanced before it is detected and treated (NICE Guidelines, 2004). Thus, there are three clear discrepancies between the Apc^{MIN} model and the actual human disease situation. First, lesion development in the Apc^{MIN} mouse is too prolific compared to the usual situation in humans. Second, those lesions generally develop along the entire length of the small and large intestine, and do not show preferential development in the distal colon, as is commonly the case in humans. Finally, the polyps which develop in Apc^{MIN} mice do not show advancement of disease. Invasiveness and metastasis of tumours arising in Apc^{MIN} mice is not reported.

Here, I have addressed the final point of these discrepancies in that I have developed a robust model of disease progression in the $Apc^{f/+};Pten^{f/f}$ mouse. Thus, between the $Apc^{f/+}$ and $Apc^{f/+};Pten^{f/f}$ models, the first few stages of intestinal cancer initiation and progression have been modelled. In order for mouse models of CRC to completely come to fruition, future work must focus on targeting tumour development to the colon, on reducing the numbers of tumours which develop in these models, and on generating a model of metastatic disease.

Reference List

ABREMSKI, K. & HOESS, R. (1984) Bacteriophage P1 site-specific recombination. Purification and properties of the Cre recombinase protein. *J Biol Chem,* 259**,** 1509-14.

ANDREU, P., COLNOT, S., GODARD, C., GAD, S., CHAFEY, P., NIWA-KAWAKITA, M., LAURENT-PUIG, P., KAHN, A., ROBINE, S., PERRET, C. & ROMAGNOLO, B. (2005) Crypt-restricted proliferation and commitment to the Paneth cell lineage following Apc loss in the mouse intestine. *Development,* 132**,** 1443-51.

ANDREYEV, H. J., NORMAN, A. R., CUNNINGHAM, D., OATES, J., DIX, B. R., IACOPETTA, B. J., YOUNG, J., WALSH, T., WARD, R., HAWKINS, N., BERANEK, M., JANDIK, P., BENAMOUZIG, R., JULLIAN, E., LAURENT-PUIG, P., OLSCHWANG, S., MULLER, O., HOFFMANN, I., RABES, H. M., ZIETZ, C., TROUNGOS, C., VALAVANIS, C., YUEN, S. T., HO, J. W., CROKE, C. T., O'DONOGHUE, D. P., GIARETTI, W., RAPALLO, A., RUSSO, A., BAZAN, V., TANAKA, M., OMURA, K., AZUMA, T., OHKUSA, T., FUJIMORI, T., ONO, Y., PAULY, M., FABER, C., GLAESENER, R., DE GOEIJ, A. F., ARENDS, J. W., ANDERSEN, S. N., LOVIG, T., BREIVIK, J., GAUDERNACK, G., CLAUSEN, O. P., DE ANGELIS, P. D., MELING, G. I., ROGNUM, T. O., SMITH, R., GOH, H. S., FONT, A., ROSELL, R., SUN, X. F., ZHANG, H., BENHATTAR, J., LOSI, L., LEE, J. Q., WANG, S. T., CLARKE, P. A., BELL, S., QUIRKE, P., BUBB, V. J., PIRIS, J., CRUICKSHANK, N. R., MORTON, D., FOX, J. C., AL-MULLA, F., LEES, N., HALL, C. N., SNARY, D., WILKINSON, K., DILLON, D., COSTA, J., PRICOLO, V. E., FINKELSTEIN, S. D., THEBO, J. S., SENAGORE, A. J., HALTER, S. A., WADLER, S., MALIK, S., KRTOLICA, K. & UROSEVIC, N. (2001) Kirsten ras mutations in patients with colorectal cancer: the 'RASCAL II' study. *Br J Cancer,* 85**,** 692-6.

ANDREYEV, H. J., TILSED, J. V., CUNNINGHAM, D., SAMPSON, S. A., NORMAN, A. R., SCHNEIDER, H. J. & CLARKE, P. A. (1997) K-ras mutations in patients with early colorectal cancers. *Gut,* 41**,** 323-9.

BACKMAN, S. A., GHAZARIAN, D., SO, K., SANCHEZ, O., WAGNER, K.-U., HENNIGHAUSEN, L., SUZUKI, A., TSAO, M.-S., CHAMPMAN, W. B., STAMBOLIC, V. & MAK, T. W. (2004) Early onset of neoplasia in the prostate and skin of mice with tissue-specific deletion of Pten. *Proceedings of the National Academy of Sciences of the United States of America,* 101**,** 1725-1730.

BACKMAN, S. A., STAMBOLIC, V., SUZUKI, A., HAIGHT, J., ELIA, A., PRETORIUS, J., TSAO, M. S., SHANNON, P., BOLON, B., IVY, G. O. & MAK, T. W. (2001) Deletion of Pten in mouse brain causes seizures, ataxia and defects in soma size resembling Lhermitte-Duclos disease. *Nature Genetics,* 29**,** 396-403.

BARDOU, M., MONTEMBAULT, S., GIRAUD, V., BALIAN, A., BOROTTO, E., HOUDAYER, C., CAPRON, F., CHAPUT, J. C. & NAVEAU, S. (2002) Excessive alcohol consumption favours high risk polyp or colorectal cancer occurrence among patients with adenomas: a case control study. *Gut,* 50**,** 38-42.

BARKER, N., VAN ES, J. H., KUIPERS, J., KUJALA, P., VAN DEN BORN, M., COZIJNSEN, M., HAEGEBARTH, A., KORVING, J., BEGTHEL, H., PETERS, P. J. & CLEVERS, H. (2007) Identification of stem cells in small intestine and colon by marker gene Lgr5. *Nature,* 449**,** 1003-1007.

BATLLE, E. (2008) A new identity for the elusive intestinal stem cell. *Nat Genet,* 40**,** 818-9.

BATLLE, E., HENDERSON, J. T., BEGHTEL, H., VAN DEN BORN, M. M., SANCHO, E., HULS, G., MEELDIJK, J., ROBERTSON, J., VAN DE WETERING, M., PAWSON, T. & CLEVERS, H. (2002) Beta-catenin and TCF mediate cell positioning in the intestinal epithelium by controlling the expression of EphB/ephrinB. *Cell,* 111**,** 251-63.

BATTS, L. E., POLK, D. B., DUBOIS, R. N. & KULESSA, H. (2006) Bmp signaling is required for intestinal growth and morphogenesis. *Dev Dyn,* 235, 1563-70.

BECK, P. L., ROSENBERG, I. M., XAVIER, R. J., KOH, T., WONG, J. F. & PODOLSKY, D. K. (2003) Transforming growth factor-beta mediates intestinal healing and susceptibility to injury in vitro and in vivo through epithelial cells. *Am J Pathol,* 162, 597-608.

BERGSTROM, A., PISANI, P., TENET, V., WOLK, A. & ADAMI, H. O. (2001) Overweight as an avoidable cause of cancer in Europe. *Int J Cancer,* 91, 421-30.

BIRCK, A., AHRENKIEL, V., ZEUTHEN, J., HOU-JENSEN, K. & GULDBERG, P. (2000) Mutation and allelic loss of the PTEN/MMAC1 gene in primary and metastatic melanoma biopsies. *J Invest Dermatol,* 114, 277-80.

BJERKNES, M. & CHENG, H. (1981) Methods for the isolation of intact epithelium from the mouse intestine. *Anatomical Record,* 199, 565-74.

BJERKNES, M. & CHENG, H. (2005a) Gastrointestinal stem cells. II. Intestinal stem cells. *Am J Physiol Gastrointest Liver Physiol,* 289, G381-7.

BJERKNES, M. & CHENG, H. (2005b) Re-examination of P-PTEN staining patterns in the intestinal crypt. *Nat Genet,* 37, 1016-7; author reply 1017-8.

BOIVIN, G. P., WASHINGTON, K., YANG, K., WARD, J. M., PRETLOW, T. P., RUSSELL, R., BESSELSEN, D. G., GODFREY, V. L., DOETSCHMAN, T., DOVE, W. F., PITOT, H. C., HALBERG, R. B., ITZKOWITZ, S. H., GRODEN, J. & COFFEY, R. J. (2003) Pathology of mouse models of intestinal cancer: consensus report and recommendations. *Gastroenterology,* 124, 762-77.

BONNET, D. & DICK, J. E. (1997) Human acute myeloid leukemia is organized as a hierarchy that originates from a primitive hematopoietic cell. *Nat Med,* 3, 730-7.

BOOLBOL, S. K., DANNENBERG, A. J., CHADBURN, A., MARTUCCI, C., GUO, X. J., RAMONETTI, J. T., ABREU-GORIS, M., NEWMARK, H. L., LIPKIN, M. L., DECOSSE, J. J. & BERTAGNOLLI, M. M. (1996) Cyclooxygenase-2 overexpression and tumor formation are blocked by sulindac in a murine model of familial adenomatous polyposis. *Cancer Res,* 56, 2556-60.

BOS, J. L. (1989) ras oncogenes in human cancer: a review. *Cancer Res,* 49, 4682-9.

BOURDON, J. C. (2007) p53 Family isoforms. *Curr Pharm Biotechnol,* 8, 332-6.

BRADFORD, M. M. (1976) A rapid and sensitive method for the quantitation of microgram quantities of protein utilizing the principle of protein-dye binding. *Analytical Biochemistry,* 72, 248-54.

BRITTAN, M. & WRIGHT, N. A. (2002) Gastrointestinal stem cells. *J Pathol,* 197, 492-509.

CAIRNS, P., OKAMI, K., HALACHMI, S., HALACHMI, N., ESTELLER, M., HERMAN, J. G., JEN, J., ISAACS, W. B., BOVA, G. S. & SIDRANSKY, D. (1997) Frequent inactivation of PTEN/MMAC1 in primary prostate cancer. *Cancer Res,* 57, 4997-5000.

CAMPBELL, S. J., CARLOTTI, F., HALL, P. A., CLARK, A. J. & WOLF, C. R. (1996) Regulation of the CYP1A1 promoter in transgenic mice: an exquisitely sensitive on-off system for cell specific gene regulation. *J Cell Sci,* 109 (Pt 11), 2619-25.

CANCER RESEARCH UK (2007) Cancer Research UK. *CancerStats.* Cancer Research UK.

CARLSON, G. J., NIVATVONGS, S. & SNOVER, D. C. (1984) Colorectal polyps in Cowden's disease (multiple hamartoma syndrome). *American Journal of Surgical Pathology,* 8, 763-70.

CHAO, A., THUN, M. J., JACOBS, E. J., HENLEY, S. J., RODRIGUEZ, C. & CALLE, E. E. (2000) Cigarette smoking and colorectal cancer mortality in the cancer prevention study II. *J Natl Cancer Inst,* 92, 1888-96.

CHENG, H. (1974a) Origin, differentiation and renewal of the four main epithelial cell types in the mouse small intestine. II. Mucous cells. *Am J Anat,* 141, 481-501.

CHENG, H. (1974b) Origin, differentiation and renewal of the four main epithelial cell types in the mouse small intestine. IV. Paneth cells. *Am J Anat,* 141, 521-35.

CHENG, H. & LEBLOND, C. P. (1974a) Origin, differentiation and renewal of the four main epithelial cell types in the mouse small intestine. I. Columnar cell. *Am J Anat,* 141, 461-79.

CHENG, H. & LEBLOND, C. P. (1974b) Origin, differentiation and renewal of the four main epithelial cell types in the mouse small intestine. III. Entero-endocrine cells. *Am J Anat,* 141, 503-19.

CHENG, H. & LEBLOND, C. P. (1974c) Origin, differentiation and renewal of the four main epithelial cell types in the mouse small intestine. V. Unitarian Theory of the origin of the four epithelial cell types. *Am J Anat,* 141, 537-61.

CHU, E. C. & TARNAWSKI, A. S. (2004) PTEN regulatory functions in tumour suppression and cell biology. *Medical Science Monitor,* 10, RA235-241.

CLARKE, A. R., CUMMINGS, M. C. & HARRISON, D. J. (1995) Interaction between murine germline mutations in p53 and APC predisposes to pancreatic neoplasia but not to increased intestinal malignancy. *Oncogene,* 11, 1913-20.

CLEVERS, H. (2006) Wnt/beta-catenin signaling in development and disease. *Cell,* 127, 469-80.

CLEVERS, H. & BATLLE, E. (2006) EphB/EphrinB receptors and Wnt signaling in colorectal cancer. *Cancer Res,* 66, 2-5.

CONLIN, A., SMITH, G., CAREY, F. A., WOLF, C. R. & STEELE, R. J. (2005) The prognostic significance of K-ras, p53, and APC mutations in colorectal carcinoma. *Gut,* 54, 1283-6.

CRANE, R. (1968) Digestive-absorptive surface of the small bowel mucosa. *Annu Rev Med,* 19, 57-68.

CULLY, M., YOU, H., LEVINE, A. J. & MAK, T. W. (2006) Beyond PTEN mutations: the PI3K pathway as an integrator of multiple inputs during tumorigenesis. *Nat Rev Cancer,* 6, 184-92.

DAHIA, P. L. (2000) PTEN, a unique tumor suppressor gene. *Endocrine-related Cancer,* 7, 115-29.

DALERBA, P., DYLLA, S. J., PARK, I. K., LIU, R., WANG, X., CHO, R. W., HOEY, T., GURNEY, A., HUANG, E. H., SIMEONE, D. M., SHELTON, A. A., PARMIANI, G., CASTELLI, C. & CLARKE, M. F. (2007) Phenotypic characterization of human colorectal cancer stem cells. *Proceedings of the National Academy of Sciences of the United States of America,* 104, 10158-10163.

DE LA CHAPELLE, A. (2004) Genetic predisposition to colorectal cancer. *Nat Rev Cancer,* 4, 769-80.

DI CRISTOFANO, A., PESCE, B., CORDON-CARDO, C. & PANDOLFI, P. P. (1998) Pten is essential for embryonic development and tumour suppression. *Nature Genetics,* 19, 348-55.

DINULESCU, D. M., INCE, T. A., QUADE, B. J., SHAFER, S. A., CROWLEY, D. & JACKS, T. (2005) Role of K-ras and Pten in the development of mouse models of endometriosis and endometrioid ovarian cancer. *Nat Med,* 11, 63-70.

EL MARJOU, F., JANSSEN, K. P., CHANG, B. H., LI, M., HINDIE, V., CHAN, L., LOUVARD, D., CHAMBON, P., METZGER, D. & ROBINE, S. (2004) Tissue-specific and inducible Cre-mediated recombination in the gut epithelium. *Genesis,* 39, 186-93.

ENG, C. (2003) PTEN: one gene, many syndromes. *Hum Mutat,* 22, 183-98.

FAZELI, A., DICKINSON, S. L., HERMISTON, M. L., TIGHE, R. V., STEEN, R. G., SMALL, C. G., STOECKLI, E. T., KEINO-MASU, K., MASU, M., RAYBURN, H., SIMONS, J., BRONSON, R. T., GORDON, J. I., TESSIER-LAVIGNE, M. & WEINBERG, R. A. (1997) Phenotype of mice lacking functional Deleted in colorectal cancer (Dcc) gene. *Nature,* 386, 796-804.

FEARON, E. R., CHO, K. R., NIGRO, J. M., KERN, S. E., SIMONS, J. W., RUPPERT, J. M., HAMILTON, S. R., PREISINGER, A. C., THOMAS, G., KINZLER, K. W. & ET AL. (1990) Identification of a chromosome 18q gene that is altered in colorectal cancers. *Science,* 247, 49-56.

FEARON, E. R. & VOGELSTEIN, B. (1990) A genetic model for colorectal tumorigenesis. *Cell,* 61, 759-767.

FEIL, R., BROCARD, J., MASCREZ, B., LEMEUR, M., METZGER, D. & CHAMBON, P. (1996) Ligand-activated site-specific recombination in mice. *Proc Natl Acad Sci U S A,* 93, 10887-90.

FEIL, R., WAGNER, J., METZGER, D. & CHAMBON, P. (1997) Regulation of Cre recombinase activity by mutated estrogen receptor ligand-binding domains. *Biochem Biophys Res Commun,* 237, 752-7.

FEVR, T., ROBINE, S., LOUVARD, D. & HUELSKEN, J. (2007) Wnt/beta-catenin is essential for intestinal homeostasis and maintenance of intestinal stem cells. *Mol Cell Biol,* 27, 7551-9.

FINGAR, D. C., RICHARDSON, C. J., TEE, A. R., CHEATHAM, L., TSOU, C. & BLENIS, J. (2004) mTOR controls cell cycle progression through its cell growth effectors S6K1 and 4E-BP1/eukaryotic translation initiation factor 4E. *Mol Cell Biol,* 24, 200-16.

FRE, S., HUYGHE, M., MOURIKIS, P., ROBINE, S., LOUVARD, D. & ARTAVANIS-TSAKONAS, S. (2005) Notch signals control the fate of immature progenitor cells in the intestine. *Nature,* 435, 964-8.

FREEMAN, D. J., LI, A. G., WEI, G., LI, H. H., KERTESZ, N., LESCHE, R., WHALE, A. D., MARTINEZ-DIAZ, H., ROZENGURT, N., CARDIFF, R. D., LIU, X. & WU, H. (2003) PTEN tumor suppressor regulates p53 protein levels and activity through phosphatase-dependent and -independent mechanisms. *Cancer Cell,* 3, 117-30.

FRIEDL, W., UHLHAAS, S., SCHULMANN, K., STOLTE, M., LOFF, S., BACK, W., MANGOLD, E., STERN, M., KNAEBEL, H. P., SUTTER, C., WEBER, R. G., PISTORIUS, S., BURGER, B. & PROPPING, P. (2002) Juvenile polyposis: massive gastric polyposis is more common in MADH4 mutation carriers than in BMPR1A mutation carriers. *Hum Genet,* 111, 108-11.

GIARDIELLO, F. M., YANG, V. W., HYLIND, L. M., KRUSH, A. J., PETERSEN, G. M., TRIMBATH, J. D., PIANTADOSI, S., GARRETT, E., GEIMAN, D. E., HUBBARD, W., OFFERHAUS, G. J. & HAMILTON, S. R. (2002) Primary chemoprevention of familial adenomatous polyposis with sulindac. *N Engl J Med,* 346, 1054-9.

GIOVANNUCCI, E., RIMM, E. B., STAMPFER, M. J., COLDITZ, G. A., ASCHERIO, A., KEARNEY, J. & WILLETT, W. C. (1994) A prospective study of cigarette smoking and risk of colorectal adenoma and colorectal cancer in U.S. men. *J Natl Cancer Inst,* 86, 183-91.

GOSSEN, M. & BUJARD, H. (1992) Tight control of gene expression in mammalian cells by tetracycline-responsive promoters. *Proc Natl Acad Sci U S A,* 89, 5547-51.

GREGORIEFF, A., PINTO, D., BEGTHEL, H., DESTREE, O., KIELMAN, M. & CLEVERS, H. (2005) Expression pattern of Wnt signaling components in the adult intestine. *Gastroenterology,* 129, 626-38.

GU, J., TAMURA, M., PANKOV, R., DANEN, E. H., TAKINO, T., MATSUMOTO, K. & YAMADA, K. M. (1999) Shc and FAK differentially regulate cell motility and directionality modulated by PTEN. *The Journal of Cell Biology,* 146, 389-403.

GUERRA, C., MIJIMOLLE, N., DHAWAHIR, A., DUBUS, P., BARRADAS, M., SERRANO, M., CAMPUZANO, V. & BARBACID, M. (2003) Tumor induction by an endogenous K-ras oncogene is highly dependent on cellular context. *Cancer Cell,* 4, 111-20.

HAHM, K. B., LEE, K. M., KIM, Y. B., HONG, W. S., LEE, W. H., HAN, S. U., KIM, M. W., AHN, B. O., OH, T. Y., LEE, M. H., GREEN, J. & KIM, S. J. (2002) Conditional loss of TGF-beta signalling

leads to increased susceptibility to gastrointestinal carcinogenesis in mice. *Aliment Pharmacol Ther,* 16 Suppl 2, 115-27.

HALBERG, R. B., KATZUNG, D. S., HOFF, P. D., MOSER, A. R., COLE, C. E., LUBET, R. A., DONEHOWER, L. A., JACOBY, R. F. & DOVE, W. F. (2000) Tumorigenesis in the multiple intestinal neoplasia mouse: redundancy of negative regulators and specificity of modifiers. *Proc Natl Acad Sci U S A,* 97, 3461-6.

HARAMIS, A. P. G., BEGTHEL, H., VAN DEN BORN, M., VAN ES, J., JONKHEER, S., OFFERHAUS, G. J. A. & CLEVERS, H. (2004) De Novo Crypt Formation and Juvenile Polyposis on BMP Inhibition in Mouse Intestine. *Science,* 303, 1684-1686.

HAY, N. & SONENBERG, N. (2004) Upstream and downstream of mTOR. *Genes Dev,* 18, 1926-45.

HE, X. C., YIN, T., GRINDLEY, J. C., TIAN, Q., SATO, T., TAO, W. A., DIRISINA, R., PORTER-WESTPFAHL, K. S., HEMBREE, M., JOHNSON, T., WIEDEMANN, L. M., BARRETT, T. A., HOOD, L., WU, H. & LI, L. (2007) PTEN-deficient intestinal stem cells initiate intestinal polyposis. *Nature Genetics,* 39, 189-198.

HE, X. C., ZHANG, J., TONG, W. G., TAWFIK, O., ROSS, J., SCOVILLE, D. H., TIAN, Q., ZENG, X., HE, X., WIEDEMANN, L. M., MISHINA, Y. & LI, L. (2004) BMP signaling inhibits intestinal stem cell self-renewal through suppression of Wnt-beta-catenin signaling. *Nature Genetics,* 36, 1117-1121.

HEATH, J. P. (1996) Epithelial cell migration in the intestine. *Cell Biol Int,* 20, 139-46.

HEDRICK, L., CHO, K. R., FEARON, E. R., WU, T. C., KINZLER, K. W. & VOGELSTEIN, B. (1994) The DCC gene product in cellular differentiation and colorectal tumorigenesis. *Genes Dev,* 8, 1174-83.

HELTON, E. S. & CHEN, X. (2007) p53 modulation of the DNA damage response. *J Cell Biochem,* 100, 883-96.

HENDRY, J. H., ROBERTS, S. A. & POTTEN, C. S. (1992) The clonogen content of murine intestinal crypts: dependence on radiation dose used in its determination. *Radiat Res,* 132, 115-9.

HOESS, R. H., ZIESE, M. & STERNBERG, N. (1982) P1 site-specific recombination: nucleotide sequence of the recombining sites. *Proc Natl Acad Sci U S A,* 79, 3398-402.

HORIE, Y., SUZUKI, A., KATAOKA, E., SASAKI, T., HAMADA, K., SASAKI, J., MIZUNO, K., HASEGAWA, G., KISHIMOTO, H., IIZUKA, M., NAITO, M., ENOMOTO, K., WATANABE, S., MAK, T. W. & NAKANO, T. (2004) Hepatocyte-specific Pten deficiency results in steatohepatitis and hepatocellular carcinomas. *Journal of Clinical Investigation,* 113, 1774-1783.

HOWE, J. R., SAYED, M. G., AHMED, A. F., RINGOLD, J., LARSEN-HAIDLE, J., MERG, A., MITROS, F. A., VACCARO, C. A., PETERSEN, G. M., GIARDIELLO, F. M., TINLEY, S. T., AALTONEN, L. A. & LYNCH, H. T. (2004) The prevalence of MADH4 and BMPR1A mutations in juvenile polyposis and absence of BMPR2, BMPR1B, and ACVR1 mutations. *J Med Genet,* 41, 484-91.

HU, M. C. & DAVIDSON, N. (1990) A combination of derepression of the lac operator-repressor system with positive induction by glucocorticoid and metal ions provides a high-level-inducible gene expression system based on the human metallothionein-IIA promoter. *Mol Cell Biol,* 10, 6141-51.

IACOPETTA, B. (2003) TP53 mutation in colorectal cancer. *Hum Mutat,* 21, 271-6.

ILYAS, M., STRAUB, J., TOMLINSON, I. P. & BODMER, W. F. (1999) Genetic pathways in colorectal and other cancers. *Eur J Cancer,* 35, 335-51.

INOKI, K., CORRADETTI, M. N. & GUAN, K. L. (2005) Dysregulation of the TSC-mTOR pathway in human disease. *Nature Genetics,* 37, 19-24.

IRELAND, H., KEMP, R., HOUGHTON, C., HOWARD, L., CLARKE, A. R., SANSOM, O. J. & WINTON, D. J. (2004) Inducible Cre-mediated control of gene expression in the murine gastrointestinal tract: Effect of loss of beta-catenin. *Gastroenterology,* 126, 1236-1246.

ISHIZUYA-OKA, A. (2005) Epithelial-connective tissue cross-talk is essential for regeneration of intestinal epithelium. *J Nippon Med Sch,* 72, 13-8.

IWANAGA, K., YANG, Y., RASO, M. G., MA, L., HANNA, A. E., THILAGANATHAN, N., MOGHADDAM, S., EVANS, C. M., LI, H., CAI, W. W., SATO, M., MINNA, J. D., WU, H., CREIGHTON, C. J., DEMAYO, F. J., WISTUBA, II & KURIE, J. M. (2008) Pten inactivation accelerates oncogenic K-ras-initiated tumorigenesis in a mouse model of lung cancer. *Cancer Res,* 68, 1119-27.

JANSSEN, K. P., EL-MARJOU, F., PINTO, D., SASTRE, X., ROUILLARD, D., FOUQUET, C., SOUSSI, T., LOUVARD, D. & ROBINE, S. (2002) Targeted expression of oncogenic K-ras in intestinal epithelium causes spontaneous tumorigenesis in mice. *Gastroenterology,* 123, 492-504.

JASS, J. R., WHITEHALL, V. L., YOUNG, J. & LEGGETT, B. A. (2002a) Emerging concepts in colorectal neoplasia. *Gastroenterology,* 123, 862-76.

JASS, J. R., YOUNG, J. & LEGGETT, B. A. (2002b) Evolution of colorectal cancer: change of pace and change of direction. *J Gastroenterol Hepatol,* 17, 17-26.

JOHNS, L. E. & HOULSTON, R. S. (2001) A systematic review and meta-analysis of familial colorectal cancer risk. *Am J Gastroenterol,* 96, 2992-3003.

JONES, D. L. & WAGERS, A. J. (2008) No place like home: anatomy and function of the stem cell niche. *Nat Rev Mol Cell Biol,* 9, 11-21.

KAESTNER, K. H., SILBERG, D. G., TRABER, P. G. & SCHUTZ, G. (1997) The mesenchymal winged helix transcription factor Fkh6 is required for the control of gastrointestinal proliferation and differentiation. *Genes Dev,* 11, 1583-95.

KATAJISTO, P., VAAHTOMERI, K., EKMAN, N., VENTELA, E., RISTIMAKI, A., BARDEESY, N., FEIL, R., DEPINHO, R. A. & MAKELA, T. P. (2008) LKB1 signaling in mesenchymal cells required for suppression of gastrointestinal polyposis. *Nat Genet,* 40, 455-9.

KATOH, Y. & KATOH, M. (2006) Hedgehog signaling pathway and gastrointestinal stem cell signaling network (review). *Int J Mol Med,* 18, 1019-23.

KEINO-MASU, K., MASU, M., HINCK, L., LEONARDO, E. D., CHAN, S. S., CULOTTI, J. G. & TESSIER-LAVIGNE, M. (1996) Deleted in Colorectal Cancer (DCC) encodes a netrin receptor. *Cell,* 87, 175-85.

KEMP, R., IRELAND, H., CLAYTON, E., HOUGHTON, C., HOWARD, L. & WINTON, D. J. (2004) Elimination of background recombination: somatic induction of Cre by combined transcriptional regulation and hormone binding affinity. *Nucleic Acids Res,* 32, e92.

KIM, B. G., LI, C., QIAO, W., MAMURA, M., KASPRZAK, B., ANVER, M., WOLFRAIM, L., HONG, S., MUSHINSKI, E., POTTER, M., KIM, S. J., FU, X. Y., DENG, C. & LETTERIO, J. J. (2006) Smad4 signalling in T cells is required for suppression of gastrointestinal cancer. *Nature,* 441, 1015-9.

KINZLER, K. W. & VOGELSTEIN, B. (1996) Lessons from hereditary colorectal cancer. *Cell,* 87, 159-70.

KODACH, L. L., BLEUMING, S. A., MUSLER, A. R., PEPPELENBOSCH, M. P., HOMMES, D. W., VAN DEN BRINK, G. R., VAN NOESEL, C. J., OFFERHAUS, G. J. & HARDWICK, J. C. (2008a) The bone morphogenetic protein pathway is active in human colon adenomas and inactivated in colorectal cancer. *Cancer,* 112, 300-6.

KODACH, L. L., WIERCINSKA, E., DE MIRANDA, N. F., BLEUMING, S. A., MUSLER, A. R., PEPPELENBOSCH, M. P., DEKKER, E., VAN DEN BRINK, G. R., VAN NOESEL, C. J., MORREAU,

H., HOMMES, D. W., TEN DIJKE, P., OFFERHAUS, G. J. & HARDWICK, J. C. (2008b) The bone morphogenetic protein pathway is inactivated in the majority of sporadic colorectal cancers. *Gastroenterology,* 134, 1332-41.

KODAKI, T., WOSCHOLSKI, R., HALLBERG, B., RODRIGUEZ-VICIANA, P., DOWNWARD, J. & PARKER, P. J. (1994) The activation of phosphatidylinositol 3-kinase by Ras. *Curr Biol,* 4, 798-806.

KONDAPAKA, S. B., SINGH, S. S., DASMAHAPATRA, G. P., SAUSVILLE, E. A. & ROY, K. K. (2003) Perifosine, a novel alkylphospholipid, inhibits protein kinase B activation. *Mol Cancer Ther,* 2, 1093-103.

KORINEK, V., BARKER, N., MOERER, P., VAN DONSELAAR, E., HULS, G., PETERS, P. J. & CLEVERS, H. (1998) Depletion of epithelial stem-cell compartments in the small intestine of mice lacking Tcf-4. *Nat Genet,* 19, 379-83.

KUEHN, M. R., BRADLEY, A., ROBERTSON, E. J. & EVANS, M. J. (1987) A potential animal model for Lesch-Nyhan syndrome through introduction of HPRT mutations into mice. *Nature,* 326, 295-8.

KUHN, R., SCHWENK, F., AGUET, M. & RAJEWSKY, K. (1995) Inducible gene targeting in mice. *Science,* 269, 1427-9.

KUHNERT, F., DAVIS, C. R., WANG, H. T., CHU, P., LEE, M., YUAN, J., NUSSE, R. & KUO, C. J. (2004) Essential requirement for Wnt signaling in proliferation of adult small intestine and colon revealed by adenoviral expression of Dickkopf-1. *Proc Natl Acad Sci U S A,* 101, 266-71.

KUROSE, K., ZHOU, X. P., ARAKI, T. & ENG, C. (2000) Biallelic inactivating mutations and an occult germline mutation of PTEN in primary cervical carcinomas. *Genes Chromosomes Cancer,* 29, 166-72.

LAURENT-PUIG, P., BLONS, H. & CUGNENC, P. H. (1999) Sequence of molecular genetic events in colorectal tumorigenesis. *Eur J Cancer Prev,* 8 Suppl 1, S39-47.

LEE, J. O., YANG, H., GEORGESCU, M. M., DI CRISTOFANO, A., MAEHAMA, T., SHI, Y., DIXON, J. E., PANDOLFI, P. & PAVLETICH, N. P. (1999) Crystal structure of the PTEN tumor suppressor: implications for its phosphoinositide phosphatase activity and membrane association. *Cell,* 99, 323-34.

LEES, C., HOWIE, S., SARTOR, R. B. & SATSANGI, J. (2005) The hedgehog signalling pathway in the gastrointestinal tract: implications for development, homeostasis, and disease. *Gastroenterology,* 129, 1696-710.

LI, D. M. & SUN, H. (1997) TEP1, encoded by a candidate tumor suppressor locus, is a novel protein tyrosine phosphatase regulated by transforming growth factor beta. *Cancer Research,* 57, 2124-9.

LI, F. P., FRAUMENI, J. F., JR., MULVIHILL, J. J., BLATTNER, W. A., DREYFUS, M. G., TUCKER, M. A. & MILLER, R. W. (1988) A cancer family syndrome in twenty-four kindreds. *Cancer Res,* 48, 5358-62.

LI, G., ROBINSON, G. W., LESCHE, R., MARTINEZ-DIAZ, H., JIANG, Z., ROZENGURT, N., WAGNER, K. U., WU, D. C., LANE, T. F., LIU, X., HENNIGHAUSEN, L. & WU, H. (2002) Conditional loss of PTEN leads to precocious development and neoplasia in the mammary gland. *Development,* 129, 4159-70.

LI, J., YEN, C., LIAW, D., PODSYPANINA, K., BOSE, S., WANG, S. I., PUC, J., MILIARESIS, C., RODGERS, L., MCCOMBIE, R., BIGNER, S. H., GIOVANELLA, B. C., ITTMANN, M., TYCKO, B., HIBSHOOSH, H., WIGLER, M. H. & PARSONS, R. (1997) PTEN, a putative protein tyrosine phosphatase gene mutated in human brain, breast, and prostate cancer. *Science,* 275, 1943-7.

LIU, W., DONG, X., MAI, M., SEELAN, R. S., TANIGUCHI, K., KRISHNADATH, K. K., HALLING, K. C., CUNNINGHAM, J. M., BOARDMAN, L. A., QIAN, C., CHRISTENSEN, E., SCHMIDT, S. S., ROCHE, P. C., SMITH, D. I. & THIBODEAU, S. N. (2000) Mutations in AXIN2 cause colorectal cancer with defective mismatch repair by activating beta-catenin/TCF signalling. *Nat Genet,* 26, 146-7.

LIVAK, K. J. & SCHMITTGEN, T. D. (2001) Analysis of relative gene expression data using real-time quantitative PCR and the 2(-Delta Delta C(T)) Method. *Methods,* 25, 402-8.

LLOYD, K. M., 2ND & DENNIS, M. (1963) Cowden's disease. A possible new symptom complex with multiple system involvement. *Ann Intern Med,* 58, 136-42.

LU, T. L., CHANG, J. L., LIANG, C. C., YOU, L. R. & CHEN, C. M. (2007) Tumor spectrum, tumor latency and tumor incidence of the Pten-deficient mice. *PLoS ONE,* 2, e1237.

MACDONALD, T. T. (2003) The mucosal immune system. *Parasite Immunol,* 25, 235-46.

MADISON, B. B., BRAUNSTEIN, K., KUIZON, E., PORTMAN, K., QIAO, X. T. & GUMUCIO, D. L. (2005) Epithelial hedgehog signals pattern the intestinal crypt-villus axis. *Development,* 132, 279-89.

MADISON, B. B., DUNBAR, L., QIAO, X. T., BRAUNSTEIN, K., BRAUNSTEIN, E. & GUMUCIO, D. L. (2002) Cis elements of the villin gene control expression in restricted domains of the vertical (crypt) and horizontal (duodenum, cecum) axes of the intestine. *J Biol Chem,* 277, 33275-83.

MAEHAMA, T. & DIXON, J. E. (1998) The tumor suppressor, PTEN/MMAC1, dephosphorylates the lipid second messenger, phosphatidylinositol 3,4,5-trisphosphate. *The Journal of Biological Chemistry,* 273, 13375-8.

MALUMBRES, M. & BARBACID, M. (2003) RAS oncogenes: the first 30 years. *Nat Rev Cancer,* 3, 459-65.

MANNING, B. D., TEE, A. R., LOGSDON, M. N., BLENIS, J. & CANTLEY, L. C. (2002) Identification of the tuberous sclerosis complex-2 tumor suppressor gene product tuberin as a target of the phosphoinositide 3-kinase/akt pathway. *Molecular Cell,* 10, 151-62.

MARSH, D. J., COULON, V., LUNETTA, K. L., ROCCA-SERRA, P., DAHIA, P. L., ZHENG, Z., LIAW, D., CARON, S., DUBOUE, B., LIN, A. Y., RICHARDSON, A. L., BONNETBLANC, J. M., BRESSIEUX, J. M., CABARROT-MOREAU, A., CHOMPRET, A., DEMANGE, L., EELES, R. A., YAHANDA, A. M., FEARON, E. R., FRICKER, J. P., GORLIN, R. J., HODGSON, S. V., HUSON, S., LACOMBE, D., ENG, C. & ET AL. (1998) Mutation spectrum and genotype-phenotype analyses in Cowden disease and Bannayan-Zonana syndrome, two hamartoma syndromes with germline PTEN mutation. *Hum Mol Genet,* 7, 507-15.

MAY, R., RIEHL, T. E., HUNT, C., SUREBAN, S. M., ANANT, S. & HOUCHEN, C. W. (2008) Identification of a novel putative gastrointestinal stem cell and adenoma stem cell marker, doublecortin and CaM kinase-like-1, following radiation injury and in adenomatous polyposis coli/multiple intestinal neoplasia mice. *Stem Cells,* 26, 630-7.

MAZELIN, L., BERNET, A., BONOD-BIDAUD, C., PAYS, L., ARNAUD, S., GESPACH, C., BREDESEN, D. E., SCOAZEC, J. Y. & MEHLEN, P. (2004) Netrin-1 controls colorectal tumorigenesis by regulating apoptosis. *Nature,* 431, 80-4.

MEHLEN, P. & FEARON, E. R. (2004) Role of the dependence receptor DCC in colorectal cancer pathogenesis. *J Clin Oncol,* 22, 3420-8.

MEHLEN, P. & FURNE, C. (2005) Netrin-1: when a neuronal guidance cue turns out to be a regulator of tumorigenesis. *Cell Mol Life Sci,* 62, 2599-616.

MENDE, I., MALSTROM, S., TSICHLIS, P. N., VOGT, P. K. & AOKI, M. (2001) Oncogenic transformation induced by membrane-targeted Akt2 and Akt3. *Oncogene,* 20, 4419-23.

MERG, A. & HOWE, J. R. (2004) Genetic conditions associated with intestinal juvenile polyps. *American Journal of Medical Genetics. Part C, Seminars in Medical Genetics,* 129, 44-55.

MERRITT, A. J., ALLEN, T. D., POTTEN, C. S. & HICKMAN, J. A. (1997) Apoptosis in small intestinal epithelial from p53-null mice: evidence for a delayed, p53-independent G2/M-associated cell death after gamma-irradiation. *Oncogene,* 14, 2759-66.

METZGER, D., CLIFFORD, J., CHIBA, H. & CHAMBON, P. (1995) Conditional site-specific recombination in mammalian cells using a ligand-dependent chimeric Cre recombinase. *Proc Natl Acad Sci U S A,* 92, 6991-5.

MINAMOTO, T., YAMASHITA, N., OCHIAI, A., MAI, M., SUGIMURA, T., RONAI, Z. & ESUMI, H. (1995) Mutant K-ras in apparently normal mucosa of colorectal cancer patients. Its potential as a biomarker of colorectal tumorigenesis. *Cancer,* 75, 1520-6.

MOLOFSKY, A. V., PARDAL, R., IWASHITA, T., PARK, I. K., CLARKE, M. F. & MORRISON, S. J. (2003) Bmi-1 dependence distinguishes neural stem cell self-renewal from progenitor proliferation. *Nature,* 425, 962-7.

MORIN, P. J., SPARKS, A. B., KORINEK, V., BARKER, N., CLEVERS, H., VOGELSTEIN, B. & KINZLER, K. W. (1997) Activation of beta-catenin-Tcf signaling in colon cancer by mutations in beta-catenin or APC. *Science,* 275, 1787-90.

MOSER, A. R., PITOT, H. C. & DOVE, W. F. (1990) A dominant mutation that predisposes to multiple intestinal neoplasia in the mouse. *Science,* 247, 322-4.

MOSER, A. R., SHOEMAKER, A. R., CONNELLY, C. S., CLIPSON, L., GOULD, K. A., LUONGO, C., DOVE, W. F., SIGGERS, P. H. & GARDNER, R. L. (1995) Homozygosity for the Min allele of Apc results in disruption of mouse development prior to gastrulation. *Dev Dyn,* 203, 422-33.

MUNCAN, V., SANSOM, O. J., TERTOOLEN, L., PHESSE, T. J., BEGTHEL, H., SANCHO, E., COLE, A. M., GREGORIEFF, A., DE ALBORAN, I. M., CLEVERS, H. & CLARKE, A. R. (2006) Rapid loss of intestinal crypts upon conditional deletion of the Wnt/Tcf-4 target gene c-Myc. *Mol Cell Biol,* 26, 8418-26.

MURPHY, T. K., CALLE, E. E., RODRIGUEZ, C., KAHN, H. S. & THUN, M. J. (2000) Body mass index and colon cancer mortality in a large prospective study. *Am J Epidemiol,* 152, 847-54.

NAF, D., KRUPKE, D. M., SUNDBERG, J. P., EPPIG, J. T. & BULT, C. J. (2002) The Mouse Tumor Biology Database: a public resource for cancer genetics and pathology of the mouse. *Cancer Res,* 62, 1235-40.

NAGY, A. (2008) Nagy Laboratory. *Cre-X-Mice: A Database of Cre Transgenic Mice* <http://www.mshri.on.ca/nagy/>.

NAKAMURA, M., OKANO, H., BLENDY, J. A. & MONTELL, C. (1994) Musashi, a neural RNA-binding protein required for Drosophila adult external sensory organ development. *Neuron,* 13, 67-81.

NELEN, M. R., KREMER, H., KONINGS, I. B., SCHOUTE, F., VAN ESSEN, A. J., KOCH, R., WOODS, C. G., FRYNS, J. P., HAMEL, B., HOEFSLOOT, L. H., PEETERS, E. A. & PADBERG, G. W. (1999) Novel PTEN mutations in patients with Cowden disease: absence of clear genotype-phenotype correlations. *Eur J Hum Genet,* 7, 267-73.

NICE GUIDELINES (2004) *Improving Outcomes in Colorectal Cancers,* National Institute for Clinical Excellence.

NORAT, T., BINGHAM, S., FERRARI, P., SLIMANI, N., JENAB, M., MAZUIR, M., OVERVAD, K., OLSEN, A., TJONNELAND, A., CLAVEL, F., BOUTRON-RUAULT, M. C., KESSE, E., BOEING, H., BERGMANN, M. M., NIETERS, A., LINSEISEN, J., TRICHOPOULOU, A., TRICHOPOULOS, D., TOUNTAS, Y., BERRINO, F., PALLI, D., PANICO, S., TUMINO, R., VINEIS, P., BUENO-DE-MESQUITA, H. B., PEETERS, P. H., ENGESET, D., LUND, E., SKEIE, G., ARDANAZ, E.,

GONZALEZ, C., NAVARRO, C., QUIROS, J. R., SANCHEZ, M. J., BERGLUND, G., MATTISSON, I., HALLMANS, G., PALMQVIST, R., DAY, N. E., KHAW, K. T., KEY, T. J., SAN JOAQUIN, M., HEMON, B., SARACCI, R., KAAKS, R. & RIBOLI, E. (2005) Meat, fish, and colorectal cancer risk: the European Prospective Investigation into cancer and nutrition. *J Natl Cancer Inst,* 97, 906-16.

O'BRIEN, C. A., POLLETT, A., GALLINGER, S. & DICK, J. E. (2007) A human colon cancer cell capable of initiating tumour growth in immunodeficient mice. *Nature,* 445, 106-110.

ODRIOZOLA, L., SINGH, G., HOANG, T. & CHAN, A. M. (2007) Regulation of PTEN activity by its carboxyl-terminal autoinhibitory domain. *J Biol Chem,* 282, 23306-15.

OHLSTEIN, B. & SPRADLING, A. (2007) Multipotent Drosophila intestinal stem cells specify daughter cell fates by differential notch signaling. *Science,* 315, 988-92.

OHMAE, S., TAKEMOTO-KIMURA, S., OKAMURA, M., ADACHI-MORISHIMA, A., NONAKA, M., FUSE, T., KIDA, S., TANJI, M., FURUYASHIKI, T., ARAKAWA, Y., NARUMIYA, S., OKUNO, H. & BITO, H. (2006) Molecular identification and characterization of a family of kinases with homology to Ca2+/calmodulin-dependent protein kinases I/IV. *J Biol Chem,* 281, 20427-39.

OKANO, H., KAWAHARA, H., TORIYA, M., NAKAO, K., SHIBATA, S. & IMAI, T. (2005) Function of RNA-binding protein Musashi-1 in stem cells. *Exp Cell Res,* 306, 349-56.

OMIM (2008) Online Mendelian Inheritance in Man, OMIM (TM). McKusick-Nathans Institute of Genetic Medicine, Johns Hopkins University (Baltimore, MD) and National Center for Biotechnology Information, National Library of Medicine (Bethesda, MD).

OWEN, R. L. & JONES, A. L. (1974) Epithelial cell specialization within human Peyer's patches: an ultrastructural study of intestinal lymphoid follicles. *Gastroenterology,* 66, 189-203.

PARK, I. K., QIAN, D., KIEL, M., BECKER, M. W., PIHALJA, M., WEISSMAN, I. L., MORRISON, S. J. & CLARKE, M. F. (2003) Bmi-1 is required for maintenance of adult self-renewing haematopoietic stem cells. *Nature,* 423, 302-5.

PARSONS, D. W., WANG, T. L., SAMUELS, Y., BARDELLI, A., CUMMINS, J. M., DELONG, L., SILLIMAN, N., PTAK, J., SZABO, S., WILLSON, J. K., MARKOWITZ, S., KINZLER, K. W., VOGELSTEIN, B., LENGAUER, C. & VELCULESCU, V. E. (2005) Colorectal cancer: mutations in a signalling pathway. *Nature,* 436, 792.

PEARSON, H. B., MCCARTHY, A., COLLINS, C. M., ASHWORTH, A. & CLARKE, A. R. (2008) Lkb1 deficiency causes prostate neoplasia in the mouse. *Cancer Res,* 68, 2223-32.

PIETERSEN, A. M., EVERS, B., PRASAD, A. A., TANGER, E., CORNELISSEN-STEIJGER, P., JONKERS, J. & VAN LOHUIZEN, M. (2008) Bmi1 regulates stem cells and proliferation and differentiation of committed cells in mammary epithelium. *Curr Biol,* 18, 1094-9.

PINTO, D., GREGORIEFF, A., BEGTHEL, H. & CLEVERS, H. (2003) Canonical Wnt signals are essential for homeostasis of the intestinal epithelium. *Genes Dev,* 17, 1709-13.

PINTO, D., ROBINE, S., JAISSER, F., EL MARJOU, F. E. & LOUVARD, D. (1999) Regulatory sequences of the mouse villin gene that efficiently drive transgenic expression in immature and differentiated epithelial cells of small and large intestines. *J Biol Chem,* 274, 6476-82.

PODSYPANINA, K., ELLENSON, L. H., NEMES, A., GU, J., TAMURA, M., YAMADA, K. M., CORDON-CARDO, C., CATORETTI, G., FISHER, P. E. & PARSONS, R. (1999) Mutation of Pten/Mmac1 in mice causes neoplasia in multiple organ systems. *Proceedings of the National Academy of Sciences of the United States of America,* 96, 1563-1568.

POTTEN, C. S. (1998) Stem cells in gastrointestinal epithelium: numbers, characteristics and death. *Philos Trans R Soc Lond B Biol Sci,* 353, 821-30.

POTTEN, C. S., BOOTH, C., TUDOR, G. L., BOOTH, D., BRADY, G., HURLEY, P., ASHTON, G., CLARKE, R., SAKAKIBARA, S. & OKANO, H. (2003) Identification of a putative intestinal stem cell and early lineage marker; musashi-1. *Differentiation,* 71, 28-41.

POTTEN, C. S., KELLETT, M., ROBERTS, S. A., REW, D. A. & WILSON, G. D. (1992) Measurement of in vivo proliferation in human colorectal mucosa using bromodeoxyuridine. *Gut,* 33, 71-8.

POTTEN, C. S. & LOEFFLER, M. (1990) Stem cells: attributes, cycles, spirals, pitfalls and uncertainties. Lessons for and from the crypt. *Development,* 110, 1001-20.

POTTEN, C. S., OWEN, G. & ROBERTS, S. A. (1990) The temporal and spatial changes in cell proliferation within the irradiated crypts of the murine small intestine. *Int J Radiat Biol,* 57, 185-99.

PURDIE, C. A., O'GRADY, J., PIRIS, J., WYLLIE, A. H. & BIRD, C. C. (1991) p53 expression in colorectal tumors. *Am J Pathol,* 138, 807-13.

RAMALHO-SANTOS, M., MELTON, D. A. & MCMAHON, A. P. (2000) Hedgehog signals regulate multiple aspects of gastrointestinal development. *Development,* 127, 2763-72.

REED, K. R., MENIEL, V. S., MARSH, V., COLE, A., SANSOM, O. J. & CLARKE, A. R. (2008) A limited role for p53 in modulating the immediate phenotype of Apc loss in the intestine. *BMC Cancer,* 8, 162.

RICCI-VITIANI, L., LOMBARDI, D. G., PILOZZI, E., BIFFONI, M., TODARO, M., PESCHLE, C. & DE MARIA, R. (2007) Identification and expansion of human colon-cancer-initiating cells. *Nature,* 445, 111-115.

RIVERA, F., VEGA-VILLEGAS, M. E. & LOPEZ-BREA, M. F. (2008) Cetuximab, its clinical use and future perspectives. *Anticancer Drugs,* 19, 99-113.

ROSNER, A. J. & KEREN, D. F. (1984) Demonstration of M cells in the specialized follicle-associated epithelium overlying isolated lymphoid follicles in the gut. *J Leukoc Biol,* 35, 397-404.

SAAL, L. H., GRUVBERGER-SAAL, S. K., PERSSON, C., LOVGREN, K., JUMPPANEN, M., STAAF, J., JONSSON, G., PIRES, M. M., MAURER, M., HOLM, K., KOUJAK, S., SUBRAMANIYAM, S., VALLON-CHRISTERSSON, J., OLSSON, H., SU, T., MEMEO, L., LUDWIG, T., ETHIER, S. P., KROGH, M., SZABOLCS, M., MURTY, V. V., ISOLA, J., HIBSHOOSH, H., PARSONS, R. & BORG, A. (2008) Recurrent gross mutations of the PTEN tumor suppressor gene in breast cancers with deficient DSB repair. *Nat Genet,* 40, 102-7.

SAAM, J. R. & GORDON, J. I. (1999) Inducible gene knockouts in the small intestinal and colonic epithelium. *J Biol Chem,* 274, 38071-82.

SANCHO, E., BATLLE, E. & CLEVERS, H. (2003) Live and let die in the intestinal epithelium. *Curr Opin Cell Biol,* 15, 763-70.

SANCHO, E., BATLLE, E. & CLEVERS, H. (2004) Signaling pathways in intestinal development and cancer. *Annu Rev Cell Dev Biol,* 20, 695-723.

SANGIORGI, E. & CAPECCHI, M. R. (2008) Bmi1 is expressed in vivo in intestinal stem cells. *Nat Genet,* 40, 915-20.

SANSOM, O. J., MENIEL, V., WILKINS, J. A., COLE, A. M., OIEN, K. A., MARSH, V., JAMIESON, T. J., GUERRA, C., ASHTON, G. H., BARBACID, M. & CLARKE, A. R. (2006) Loss of Apc allows phenotypic manifestation of the transforming properties of an endogenous K-ras oncogene in vivo. *Proc Natl Acad Sci U S A,* 103, 14122-7.

SANSOM, O. J., REED, K. R., HAYES, A. J., IRELAND, H., BRINKMANN, H., NEWTON, I. P., BATLLE, E., SIMON-ASSMANN, P., CLEVERS, H., NATHKE, I. S., CLARKE, A. R. & WINTON, D. J. (2004) Loss of Apc in vivo immediately perturbs Wnt signaling, differentiation, and migration. *Genes Dev,* 18, 1385-90.

SANSOM, O. J., STARK, L. A., DUNLOP, M. G. & CLARKE, A. R. (2001) Suppression of intestinal and mammary neoplasia by lifetime administration of aspirin in Apc(Min/+) and Apc(Min/+), Msh2(-/-) mice. *Cancer Res,* 61, 7060-4.

SCHNEIDER, A., ZHANG, Y., GUAN, Y., DAVIS, L. S. & BREYER, M. D. (2003) Differential, inducible gene targeting in renal epithelia, vascular endothelium, and viscera of Mx1Cre mice. *Am J Physiol Renal Physiol,* 284, F411-7.

SCHOFIELD, R. (1978) The relationship between the spleen colony-forming cell and the haemopoietic stem cell. *Blood Cells,* 4, 7-25.

SCHWEINFEST, C. W., JORCYK, C. L., FUJIWARA, S. & PAPAS, T. S. (1988) A heat-shock-inducible eukaryotic expression vector. *Gene,* 71, 207-10.

SCOVILLE, D. H., SATO, T., HE, X. C. & LI, L. (2008) Current view: intestinal stem cells and signaling. *Gastroenterology,* 134, 849-64.

SHAO, J., WASHINGTON, M. K., SAXENA, R. & SHENG, H. (2007) Heterozygous disruption of the PTEN promotes intestinal neoplasia in APCmin/+ mouse: roles of osteopontin. *Carcinogenesis,* 28, 2476-83.

SHENG, H., SHAO, J., TOWNSEND, C. M., JR. & EVERS, B. M. (2003) Phosphatidylinositol 3-kinase mediates proliferative signals in intestinal epithelial cells. *Gut,* 52, 1472-8.

SHI, Y. & MASSAGUE, J. (2003) Mechanisms of TGF-beta signaling from cell membrane to the nucleus. *Cell,* 113, 685-700.

SHIBATA, H., TOYAMA, K., SHIOYA, H., ITO, M., HIROTA, M., HASEGAWA, S., MATSUMOTO, H., TAKANO, H., AKIYAMA, T., TOYOSHIMA, K., KANAMARU, R., KANEGAE, Y., SAITO, I., NAKAMURA, Y., SHIBA, K. & NODA, T. (1997) Rapid colorectal adenoma formation initiated by conditional targeting of the Apc gene. *Science,* 278, 120-3.

SHMELKOV, S. V., BUTLER, J. M., HOOPER, A. T., HORMIGO, A., KUSHNER, J., MILDE, T., ST CLAIR, R., BALJEVIC, M., WHITE, I., JIN, D. K., CHADBURN, A., MURPHY, A. J., VALENZUELA, D. M., GALE, N. W., THURSTON, G., YANCOPOULOS, G. D., D'ANGELICA, M., KEMENY, N., LYDEN, D. & RAFII, S. (2008) CD133 expression is not restricted to stem cells, and both CD133+ and CD133- metastatic colon cancer cells initiate tumors. *J Clin Invest,* 118, 2111-20.

SHOEMAKER, A. R., GOULD, K. A., LUONGO, C., MOSER, A. R. & DOVE, W. F. (1997) Studies of neoplasia in the Min mouse. *Biochim Biophys Acta,* 1332, F25-48.

SIMPSON, L. & PARSONS, R. (2001) PTEN: life as a tumor suppressor. *Experimental Cell Research,* 264, 29-41.

SLATTERY, M. L., EDWARDS, S., CURTIN, K., MA, K., EDWARDS, R., HOLUBKOV, R. & SCHAFFER, D. (2003) Physical activity and colorectal cancer. *Am J Epidemiol,* 158, 214-24.

SOKAL, R. R., ROHLF, F. J. (1981) *Biometry: The Principles and Practise of Statistics in Biological Research*, W. H. Freeman and Company.

SORIANO, P. (1999) Generalized lacZ expression with the ROSA26 Cre reporter strain. *Nature Genetics,* 21, 70-1.

SPARKS, A. B., MORIN, P. J., VOGELSTEIN, B. & KINZLER, K. W. (1998) Mutational analysis of the APC/beta-catenin/Tcf pathway in colorectal cancer. *Cancer Res,* 58, 1130-4.

STECK, P. A., PERSHOUSE, M. A., JASSER, S. A., YUNG, W. K., LIN, H., LIGON, A. H., LANGFORD, L. A., BAUMGARD, M. L., HATTIER, T., DAVIS, T., FRYE, C., HU, R., SWEDLUND, B., TENG, D. H. & TAVTIGIAN, S. V. (1997) Identification of a candidate tumour suppressor gene, MMAC1, at chromosome 10q23.3 that is mutated in multiple advanced cancers. *Nature Genetics,* 15, 356-62.

STERNBERG, N. & HAMILTON, D. (1981) Bacteriophage P1 site-specific recombination. I. Recombination between loxP sites. *J Mol Biol,* 150, 467-86.

STILES, B., WANG, Y., STAHL, A., BASSILIAN, S., LEE, W. P., KIM, Y.-J., SHERWIN, R., DEVASKAR, S., LESCHE, R., MAGNUSON, M. A. & WU, H. (2004) Liver-specific deletion of negative regulator Pten results in fatty liver and insulin hypersensitivity. *Proceedings of the National Academy of Sciences of the United States of America,* 101, 2082-2087.

SU, L. K., KINZLER, K. W., VOGELSTEIN, B., PREISINGER, A. C., MOSER, A. R., LUONGO, C., GOULD, K. A. & DOVE, W. F. (1992) Multiple intestinal neoplasia caused by a mutation in the murine homolog of the APC gene. *Science,* 256, 668-70.

SUBAUSTE, M. C., NALBANT, P., ADAMSON, E. D. & HAHN, K. M. (2005) Vinculin controls PTEN protein level by maintaining the interaction of the adherens junction protein beta-catenin with the scaffolding protein MAGI-2. *J Biol Chem,* 280, 5676-81.

SUZUKI, A., LUIS DE LA POMPA, J., STAMBOLIC, V., ELIA, A. J., SASAKI, T., DEL BARCO BARRANTES, I., HO, A., WAKEHEM, A., ITIE, A., KHOO, W., FUKUMOTO, M. & MAK, T. W. (1998) High cancer susceptibility and embryonic lethality associated with mutation of the PTEN tumor suppressor gene in mice. *Current Biology,* 8, 1169-1178.

SUZUKI, A., YAMAGUCHI, M. T., OHTEKI, T., SASAKI, T., KAISHO, T., KIMURA, Y., YOSHIDA, R., WAKEHAM, A., HIGUCHI, T., FUKUMOTO, M., TSUBATA, T., OHASHI, P. S., KOYASU, S., PENNINGER, J. M., NAKANO, T. & MAK, T. W. (2001) T cell-specific loss of Pten leads to defects in central and peripheral tolerance. *Immunity,* 14, 523-34.

TAKAKU, K., MIYOSHI, H., MATSUNAGA, A., OSHIMA, M., SASAKI, N. & TAKETO, M. M. (1999) Gastric and duodenal polyps in Smad4 (Dpc4) knockout mice. *Cancer Res,* 59, 6113-7.

TAKETO, M. M. (2006) Mouse models of gastrointestinal tumors. *Cancer Sci,* 97, 355-61.

TAMGUNEY, T. & STOKOE, D. (2007) New insights into PTEN. *J Cell Sci,* 120, 4071-9.

TASHIRO, H., BLAZES, M. S., WU, R., CHO, K. R., BOSE, S., WANG, S. I., LI, J., PARSONS, R. & ELLENSON, L. H. (1997) Mutations in PTEN are frequent in endometrial carcinoma but rare in other common gynecological malignancies. *Cancer Res,* 57, 3935-40.

TEE, A. R. & BLENIS, J. (2005) mTOR, translational control and human disease. *Seminars in Cell and Developmental Biology,* 16, 29-37.

TENG, Y., SUN, A. N., PAN, X. C., YANG, G., YANG, L. L., WANG, M. R. & YANG, X. (2006) Synergistic function of Smad4 and PTEN in suppressing forestomach squamous cell carcinoma in the mouse. *Cancer Res,* 66, 6972-81.

THIAGALINGAM, S., LENGAUER, C., LEACH, F. S., SCHUTTE, M., HAHN, S. A., OVERHAUSER, J., WILLSON, J. K., MARKOWITZ, S., HAMILTON, S. R., KERN, S. E., KINZLER, K. W. & VOGELSTEIN, B. (1996) Evaluation of candidate tumour suppressor genes on chromosome 18 in colorectal cancers. *Nat Genet,* 13, 343-6.

THYAGARAJAN, B., GUIMARAES, M. J., GROTH, A. C. & CALOS, M. P. (2000) Mammalian genomes contain active recombinase recognition sites. *Gene,* 244, 47-54.

TORRES, J. & PULIDO, R. (2001) The tumor suppressor PTEN is phosphorylated by the protein kinase CK2 at its C terminus. Implications for PTEN stability to proteasome-mediated degradation. *The Journal of Biological Chemistry,* 276, 993-8.

TUVESON, D. A., SHAW, A. T., WILLIS, N. A., SILVER, D. P., JACKSON, E. L., CHANG, S., MERCER, K. L., GROCHOW, R., HOCK, H., CROWLEY, D., HINGORANI, S. R., ZAKS, T., KING, C., JACOBETZ, M. A., WANG, L., BRONSON, R. T., ORKIN, S. H., DEPINHO, R. A. & JACKS, T. (2004) Endogenous oncogenic K-ras(G12D) stimulates proliferation and widespread neoplastic and developmental defects. *Cancer Cell,* 5, 375-87.

VAN AKEN, J., CUVELIER, C. A., DE WEVER, N., ROELS, J., GAO, Y. & MAREEL, M. M. (1993) Immunohistochemical analysis of E-cadherin expression in human colorectal tumours. *Pathol Res Pract,* 189, 975-8.

VAN CUTSEM, E. & GEBOES, K. (2007) The multidisciplinary management of gastrointestinal cancer. The integration of cytotoxics and biologicals in the treatment of metastatic colorectal cancer. *Best Pract Res Clin Gastroenterol,* 21, 1089-108.

VAN DEN BRINK, G. R. (2007) Hedgehog signaling in development and homeostasis of the gastrointestinal tract. *Physiol Rev,* 87, 1343-75.

VAN ENGELAND, M., ROEMEN, G. M., BRINK, M., PACHEN, M. M., WEIJENBERG, M. P., DE BRUINE, A. P., ARENDS, J. W., VAN DEN BRANDT, P. A., DE GOEIJ, A. F. & HERMAN, J. G. (2002) K-ras mutations and RASSF1A promoter methylation in colorectal cancer. *Oncogene,* 21, 3792-5.

VAN ES, J. H., JAY, P., GREGORIEFF, A., VAN GIJN, M. E., JONKHEER, S., HATZIS, P., THIELE, A., VAN DEN BORN, M., BEGTHEL, H., BRABLETZ, T., TAKETO, M. M. & CLEVERS, H. (2005a) Wnt signalling induces maturation of Paneth cells in intestinal crypts. *Nat Cell Biol,* 7, 381-6.

VAN ES, J. H., VAN GIJN, M. E., RICCIO, O., VAN DEN BORN, M., VOOIJS, M., BEGTHEL, H., COZIJNSEN, M., ROBINE, S., WINTON, D. J., RADTKE, F. & CLEVERS, H. (2005b) Notch/gamma-secretase inhibition turns proliferative cells in intestinal crypts and adenomas into goblet cells. *Nature,* 435, 959-63.

VIVANCO, I. & SAWYERS, C. L. (2002) The phosphatidylinositol 3-kinase-AKT pathway in human cancer. *Nature Reviews Cancer,* 2, 489-501.

VOGELSTEIN, B., LANE, D. & LEVINE, A. J. (2000) Surfing the p53 network. *Nature,* 408, 307-10.

VOUSDEN, K. H. & LANE, D. P. (2007) p53 in health and disease. *Nat Rev Mol Cell Biol,* 8, 275-83.

WAITE, K. A. & ENG, C. (2002) Protean PTEN: form and function. *American Journal of Human Genetics,* 70, 829-44.

WANG, S., GARCIA, A. J., WU, M., LAWSON, D. A., WITTE, O. N. & WU, H. (2006) Pten deletion leads to the expansion of a prostatic stem/progenitor cell subpopulation and tumor initiation. *Proc Natl Acad Sci U S A,* 103, 1480-5.

WILSON, A. & RADTKE, F. (2006) Multiple functions of Notch signaling in self-renewing organs and cancer. *FEBS Lett,* 580, 2860-8.

XU, X., KOBAYASHI, S., QIAO, W., LI, C., XIAO, C., RADAEVA, S., STILES, B., WANG, R. H., OHARA, N., YOSHINO, T., LEROITH, D., TORBENSON, M. S., GORES, G. J., WU, H., GAO, B. & DENG, C. X. (2006) Induction of intrahepatic cholangiocellular carcinoma by liver-specific disruption of Smad4 and Pten in mice. *J Clin Invest,* 116, 1843-52.

YAMADA, S., YASHIRO, M., MAEDA, K., NISHIGUCHI, Y. & HIRAKAWA, K. (2005) A novel high-specificity approach for colorectal neoplasia: Detection of K-ras2 oncogene mutation in normal mucosa. *Int J Cancer,* 113, 1015-21.

YANAGI, S., KISHIMOTO, H., KAWAHARA, K., SASAKI, T., SASAKI, M., NISHIO, M., YAJIMA, N., HAMADA, K., HORIE, Y., KUBO, H., WHITSETT, J. A., MAK, T. W., NAKANO, T., NAKAZATO, M. & SUZUKI, A. (2007) Pten controls lung morphogenesis, bronchioalveolar stem cells, and onset of lung adenocarcinomas in mice. *J Clin Invest,* 117, 2929-40.

ZECCHINI, V., DOMASCHENZ, R., WINTON, D. & JONES, P. (2005) Notch signaling regulates the differentiation of post-mitotic intestinal epithelial cells. *Genes Dev,* 19, 1686-91.

ZHANG, J., GRINDLEY, J. C., YIN, T., JAYASINGHE, S., HE, X. C., ROSS, J. T., HAUG, J. S., RUPP, D., PORTER-WESTPFAHL, K. S., WIEDEMANN, L. M., WU, H. & LI, L. (2006) PTEN maintains

haematopoietic stem cells and acts in lineage choice and leukaemia prevention. *Nature,* 441, 518-22.

ZHENG, B., ZHANG, Z., BLACK, C. M., DE CROMBRUGGHE, B. & DENTON, C. P. (2002) Ligand-dependent genetic recombination in fibroblasts : a potentially powerful technique for investigating gene function in fibrosis. *Am J Pathol,* 160, 1609-17.

ZHU, D., KEOHAVONG, P., FINKELSTEIN, S. D., SWALSKY, P., BAKKER, A., WEISSFELD, J., SRIVASTAVA, S. & WHITESIDE, T. L. (1997) K-ras gene mutations in normal colorectal tissues from K-ras mutation-positive colorectal cancer patients. *Cancer Res,* 57, 2485-92.

Appendix 1: Publication List

Marsh, V., Winton, D.J., Williams, G.T., Sansom, O.J., Clarke, A.R.; Epithelial Pten is dispensable for intestinal homeostasis, but suppresses adenoma development and progression following Apc mutation; 2008; Nature Genetics 40 (12); 1436-44.

Reed, K.R., Meniel, V.S., Marsh, V., Cole, A. M., Sansom, O.J., Clarke, A.R.; A Limited role for p53 in modulating the immediate phenotype of Apc loss in the intestine; 2008; BMC Cancer; 8; 162.

Marsh, V. & Clarke, A.; Intestinal homeostasis and neoplasia studied using conditional transgenesis; 2007; Expert Review of Anticancer Therapy; 7(4); 519-31. (Review).

Sansom, O.J., Meniel, V., Wilkins, J.A., Cole, A.M., Oien, K.A., Marsh, V., Jamieson, T.J., Guerra, C., Ashton, G.H., Barbacid, M., Clarke, A.R.; Loss of Apc allows phenotypic manifestation of the transforming properties of an endogenous K-ras oncogene in vivo; 2006; Proceedings of the National Academy of Sciences USA; 103 (38); 14122-7.

nature genetics

Epithelial Pten is dispensable for intestinal homeostasis but suppresses adenoma development and progression after *Apc* mutation

Victoria Marsh[1], Douglas J Winton[2], Geraint T Williams[3], Nicole Dubois[4,6], Andreas Trumpp[4,6], Owen J Sansom[5] & Alan R Clarke[1]

PTEN acts as a tumor suppressor in a range of tissue types and has been implicated in the regulation of intestinal stem cells. To study Pten function in the intestine, we used various conditional transgenic strategies to specifically delete *Pten* from the mouse intestinal epithelium. We show that Pten loss specifically within the adult or embryonic epithelial cell population does not affect the normal architecture or homeostasis of the epithelium. However, loss of Pten in the context of Apc deficiency accelerates tumorigenesis through increased activation of Akt, leading to rapid development of adenocarcinoma. We conclude that Pten is redundant in otherwise normal intestinal epithelium and epithelial stem cells but, in the context of activated Wnt signaling, suppresses progression to adenocarcinoma through modulation of activated Akt levels.

Phosphatase and tensin homolog mutated on chromosome 10 (PTEN) acts as a potent tumor suppressor in a range of tissue types and is commonly mutated in sporadic cancers of multiple origins[1–3]. PTEN elicits its antitumorigenic effects through antagonism of the phosphatidylinositol 3-kinase (PI3K)/Akt pathway[4], which normally promotes proliferation and cell survival and stimulates progression of the cell cycle (reviewed extensively, including in ref. 5). Activating mutations of PI3K pathway components have been reported in almost 40% of all human colorectal cancers[6]. Germline mutation of *PTEN* in humans leads to multiple hamartoma syndromes, of which Cowden's syndrome is the most common. Individuals with Cowden's syndrome show susceptibility to hamartoma development in various organ systems, including the gastrointestinal tract[7,8]. Mouse studies have shown that, whereas constitutive *Pten* deletion causes embryonic lethality, heterozygous inactivation of *Pten* predisposes to neoplasia in a range of tissues, including skin, thyroid and genitourinary and gastrointestinal tracts[9–11]. *Pten* heterozygotes have been reported to develop dysplasia of the colonic epithelium accompanied by invasion into the lamina propria, described as being consistent with adenocarcinoma[9].

Inactive, phosphorylated Pten has been identified as a potential marker of intestinal stem cells (ISCs)[12], although there has been some debate over this interpretation[13]. Previous studies also showed that inactivation of Pten and increased activation of Akt correlate with accumulation of nuclear β-catenin[14]. This suggests that Pten inactivation confers stem-like properties to cells within the intestinal epithelium. Recently, a conditional transgenic approach was used to delete *Pten* from a number of intestinal cell types, resulting in rapid tumorigenesis that was attributed to an expansion of the ISC population[15].

To determine the role of Pten in homeostasis and tumorigenesis, specifically within the epithelial cell compartment of the adult small intestine, we used a conditional strategy to delete *Pten* in a temporally and spatially controlled manner.

RESULTS

AhCre-mediated deletion of *Pten*

We achieved conditional deletion of *Pten* in the mouse small intestine by crossing mice carrying *loxP*-flanked *Pten* alleles[16] with mice carrying Cre recombinase under control of the *Cyp1a1* aryl hydrocarbon–responsive promoter (*Tg(Cyp1a1-cre)1Dwi* transgene, abbreviated here as *AhCre*)[17]. We induced Cre-mediated excision of exons 4 and 5 of the *Pten* allele by intraperitoneal injection of β-naphthoflavone, which induces Cre expression within the small intestinal crypt[17,18]. After maximal recombination (achieved by daily injection of 80 mg/kg for four consecutive days), nearly 100% recombination is achieved in Cre^+ mice[17], as scored using the *Gt(ROSA)26Sor* marker allele (referred to here as *Rosa26R*) for recombination[19].

To determine the consequences of deletion of *Pten* from the intestinal epithelium, we induced adult experimental (cre^+;$Pten^{f/f}$) and control (cre^-; $Pten^{f/f}$, cre^+; $Pten^{+/+}$, cre^+; $Pten^{f/+}$ or cre^-; $Pten^{f/+}$) mice and killed them at defined time points after induction. Total

[1]Cardiff School of Biosciences, Cardiff University, CF10 3US, UK. [2]Cambridge Research Institute, Li Ka Shing Centre, Cambridge CB2 0RE, UK. [3]Wales College of Medicine, Cardiff University, CF14 4XN, UK. [4]Ecole Polytechnique Fédérale de Lausanne, Swiss Institute for Experimental Cancer Research, School of Life Science, CH-1066 Epalinges, Switzerland. [5]The Beatson Institute, Garscube Estate, Glasgow G61 1BD, UK. [6]Present addresses: McEwen Centre for Regenerative Medicine, University Health Network, Toronto, Ontario M5G 1L7, Canada (N.D.) and Division of Cell Biology, Deutsches Krebsforschungszentrum (DKFZ) DKFZ-ZMBH Alliance, Im Neuenheimer Feld 280, D-69120 Heidelberg, Germany (A.T.). Correspondence should be addressed to O.J.S. (o.sansom@beatson.gla.ac.uk).

Received 23 May; accepted 27 August; published online 16 November 2008; doi:10.1038/ng.256

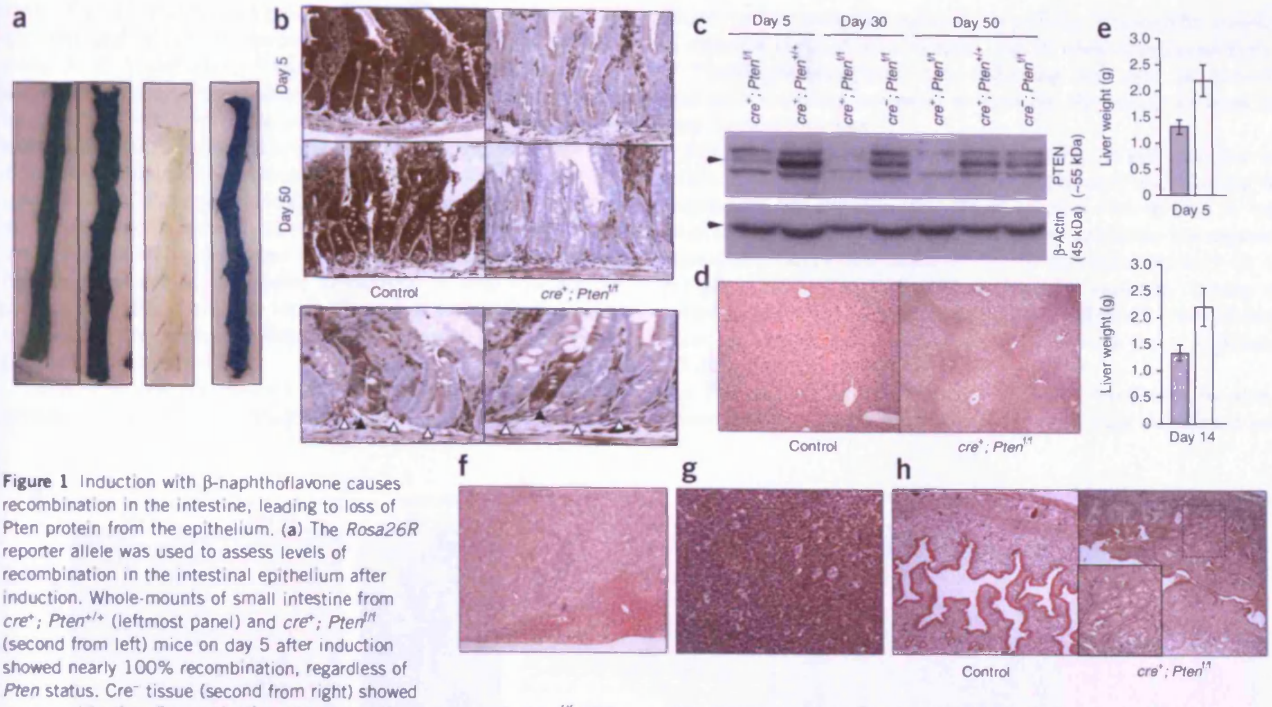

Figure 1 Induction with β-naphthoflavone causes recombination in the intestine, leading to loss of Pten protein from the epithelium. (**a**) The *Rosa26R* reporter allele was used to assess levels of recombination in the intestinal epithelium after induction. Whole-mounts of small intestine from *cre*$^+$; *Pten*$^{+/+}$ (leftmost panel) and *cre*$^+$; *Pten*$^{f/f}$ (second from left) mice on day 5 after induction showed nearly 100% recombination, regardless of *Pten* status. Cre$^-$ tissue (second from right) showed no recombination. Recombination was seen in tissue from *cre*$^+$; *Pten*$^{f/f}$ mice more than 100 d after induction (right panel), indicating that recombination in the intestine was stable. (**b**) Loss of Pten protein from the intestinal epithelium was shown by immunohistochemistry. On days 5, 30 and 50 after induction, levels of Pten protein in the epithelial layer were much lower in *cre*$^+$; *Pten*$^{f/f}$ tissue than in controls (top panel). *cre*$^+$; *Pten*$^{f/f}$ tissue on day 50 after induction (bottom panel) revealed occasional crypts that retained Pten (filled arrows), surrounded by crypts deficient for Pten (open arrows), reflecting the sub-100% recombination efficiency delivered by this system. (**c**) Pten protein loss from the intestinal epithelium was confirmed by western blot analysis of epithelium-enriched tissue samples. Samples from *cre*$^+$; *Pten*$^{f/f}$ mice on days 5, 30 and 50 after induction had markedly lower Pten protein than did controls. Western blot membranes were reprobed with antibody to β-actin to confirm equal loading of protein samples. (**d–h**) Recombination in tissues outside the intestine led to additional phenotypes, which were previously reported. (**d**) In the liver, areas of steatosis were observed in experimental mice, but not in controls. (**e**) Development of hepatomegaly in experimental mice (open bars) compared to control mice (gray bars) was evident on days 5 and 14 after induction. Error bars indicate s.d. (**f**) A single *cre*$^+$; *Pten*$^{f/f}$ mouse also developed hepatocellular carcinoma. (**g**) Experimental mice were highly susceptible to lymphoma. (**h**) Female experimental mice commonly developed complex atypical hyperplasia of the endometrium, which was never observed in control mice. Inset shows boxed area, magnified ×2.

numbers of control versus experimental mice, respectively, analyzed in this study were 38 versus 22 on day 5 after induction, 3 versus 5 on day 30 and 33 versus 35 on day 50. Not all analyses were conducted on every sample. No mice were observed to develop hamartomatous lesions of the intestine over the course of the study.

On day 5 after induction, we stained intestines for activity of the LacZ recombination reporter transgene, which showed nearly 100% recombination in Cre$^+$ mice regardless of *Pten* status; this level of recombination remained stable for over 100 d after induction (**Fig. 1a**). To examine the kinetics of Pten loss from the epithelium after recombination, we analyzed Pten by immunohistochemistry and western blotting. Immunohistochemistry revealed that Pten levels were greatly reduced in experimental mice compared to control mice (**Fig. 1b**). Occasional crypts retaining Pten were detected in experimental mice (**Fig. 1b**), consistent with recombination occurring at less than 100% efficiency. Western blot analysis of epithelium-enriched tissue samples supported our immunohistochemistry results, showing very little Pten on day 5 after induction (**Fig. 1c**) and no appreciable Pten on days 30 and 50. Quantitative real-time PCR on RNA extracted from epithelial-enriched tissue samples showed that experimental mice had a 99.8% and 99.95% reduction in *Pten* expression on days 5 and 50, respectively.

The *AhCre* transgene drives low-level recombination in a number of other tissues[17,18]. This allowed us to confirm Cre-mediated inactivation of *Pten* in our model, as we recapitulated multiple phenotypes of Pten deficiency outside the intestine. In the liver, Pten deficiency led to steatosis (**Fig. 1d**) and hepatomegaly (**Fig. 1e**), which in one case progressed to hepatocellular carcinoma (**Fig. 1f**). Recombination in the midbrain caused behavioral defects of varying severity, which in many cases forced us to kill the mouse prematurely. Other phenotypes observed included predisposition to lymphoma (**Fig. 1g**) and complex atypical hyperplasia of the endometrium (**Fig. 1h**). These phenotypes have all been reported as consequences of Pten deficiency[20–22].

We next characterized the consequences of Pten loss in the small intestine. Histological analysis revealed no major alterations in crypt-villus architecture after Pten loss (**Fig. 2a**). Crypt size, mitotic index and levels of apoptosis were scored from these sections and did not vary significantly between experimental and control tissue on days 5 or 50 after induction (for all comparisons, $n \geq 3$ and Mann-Whitney *U*-test $P \geq 0.39$). Immunohistochemical analysis of the proliferation marker Ki67 showed that Pten-deficient cells were permissive for cell division and that the location and size of the proliferative compartment in the crypt were comparable to controls (**Fig. 2a**). We confirmed the presence and correct localization of all differentiated intestinal cell lineages in Pten-deficient tissue using specific stains or immunohistochemical analysis of markers of the differentiated cell

types (**Fig. 2b**). Numbers of goblet cells and enteroendocrine cells in the crypt and villus were comparable with controls (for all comparisons, $n \geq 3$ and Mann-Whitney U-test $P \geq 0.19$). Finally, we determined whether Pten-deficient epithelial cells are able to migrate normally up the crypt-villus axis. On day 5 after induction, we injected mice with bromodeoxyuridine (BrdU) and killed them after 2 or 24 h. Immunohistochemical analysis of BrdU (**Fig. 2c**) and quantification of the position of labeled cells (**Fig. 2d**) revealed that Pten-deficient cells showed a normal migration pattern between 2 and 24 h after labeling compared to controls (Kolmogorov-Smirnov test for difference in cumulative distribution of data was not significant at a 99% confidence level). These data are therefore in stark contrast to the prediction that Pten loss should lead to a crypt progenitor cell phenotype.

As Pten is well documented to elicit its tumor suppressive properties through negative regulation of the PI3K/Akt pathway, we determined the activation status of this pathway. Western blot analysis of epithelial-enriched tissue samples (**Fig. 3**) revealed increased levels of Thr308-phosphorylated Akt—indicating activation of Akt—in Pten-deficient tissue compared to controls. No change in levels of total Akt was observed.

PTEN has been shown to promote stability of p53, and loss of PTEN has been shown to lead to p53 degradation and blocking of apoptosis[23]. We therefore determined whether loss of Pten in the intestine protects cells against p53-mediated apoptosis. We exposed experimental and control mice on day 50 after induction to 5 Gy of gamma irradiation and killed them 6 h after exposure. Scoring of apoptosis revealed no impairment in the ability of Pten-deficient tissue to engage apoptosis compared to controls ($n = 3$, Mann-Whitney U-test $P = 1.00$).

It has recently been postulated that Pten is inactivated by phosphorylation specifically in dividing ISCs[12], and Pten inactivation has

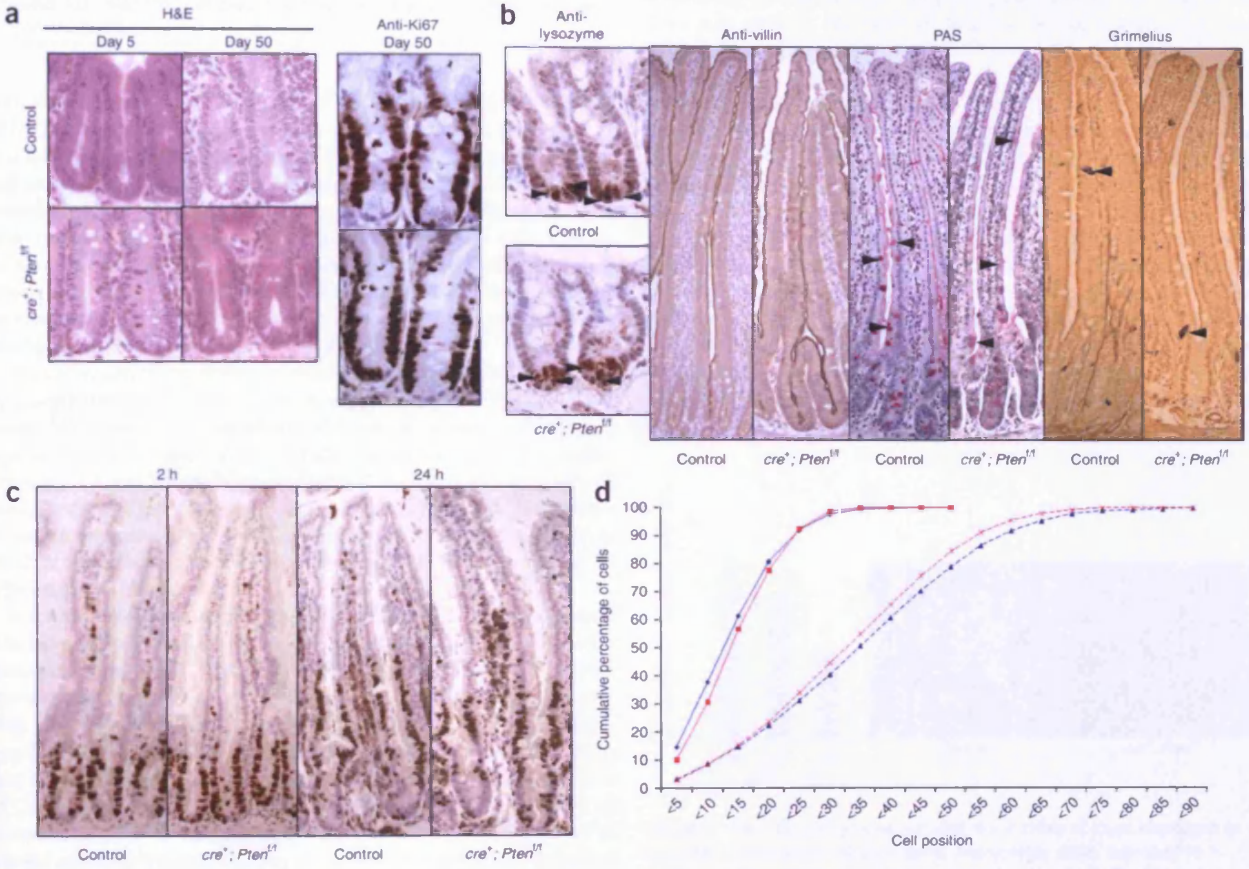

Figure 2 Loss of Pten does not cause gross phenotypic changes in the small intestine. (**a**) Left, H&E-stained intestinal tissue from control and experimental mice on days 5 or 50 after induction revealed no alterations to the architecture of the crypt-villus axis or to levels of apoptosis and mitosis. Right, immunohistochemical analysis of Ki67 in control and experimental mice 50 d after induction showed that Pten-deficient cells were capable of division and that the location of the proliferative compartment was unchanged. (**b**) Visualization of the four differentiated cell types of the epithelium. Immunohistochemical analysis of lysozyme and villin and staining with periodic acid–Schiff stain (PAS) and Grimelius stain revealed Paneth cells, enterocytes, goblet cells and enteroendocrine cells, respectively (examples of positively stained cells are indicated with arrowheads). All cell types were present at the expected frequency and location in Pten-deficient tissue, compared to control tissue on day 50 after induction. (**c**) Cell migration was assessed by labeling cells on day 5 after induction with BrdU and killing mice 2 or 24 h after labeling. Immunohistochemical analysis of BrdU revealed that control and Pten-deficient cells at 2 h incorporated the label at similar frequencies and positions and by 24 h had migrated to similar positions on the crypt-villus axis. (**d**) Migration of BrdU-labeled cells was quantified, and a cumulative frequency plot was generated. Control (red lines) and experimental (blue lines) tissues had distributions of labeled cells at both 2 h (solid lines) and 24 h (dashed lines) that were not significantly different from each other (Kolmogorov-Smirnov, not significant at a 99% confidence level).

Figure 3 Pten deletion results in increased levels of activated Akt. Activation status of Akt in response to Pten deficiency was assessed by western blot analysis of protein samples extracted from a population of epithelial-enriched intestinal cells from both control and experimental mice on days 5 and 50 after induction. Membranes were probed with antibody to Pten to ensure that Pten protein was lost from the samples and with antibody to β-actin to ensure equal protein loading. Replicate membranes were probed with antibody to Thr308-phosphorylated Akt ($pAkt^{Thr308}$) and pan-Akt, revealing that Pten-deficient tissue showed increased levels of activated Akt ($pAkt^{Thr308}$) at days 5 and 50 after induction, with no change in total Akt levels.

been shown to lead to accumulation of nuclear β-catenin through Akt activation in cell lines[14]. Given these observations, one prediction is that inactivation of Pten confers stem-like properties on intestinal cells and may increase the number of clonogens in the intestinal crypt. To investigate this, we scored clonogenic survival in the intestine 72 h after exposure to various doses of gamma irradiation (10, 12.5 or 15 Gy), as previously described[24]. No significant difference (for all comparisons, $n \geq 4$ and Mann-Whitney U-test $P \geq 0.31$) in crypt survival was observed in the absence of Pten, indicating no increase in clonogen numbers in the crypt (**Fig. 4a**).

We also analyzed expression of recently proposed stem cell markers by quantitative real-time PCR in Pten-proficient and Pten-deficient tissue. We observed no significant differences between control and experimental genotypes on day 50 after induction (for all comparisons, $n = 3$ and Mann-Whitney U-test $P > 0.05$) in expression of *Msi1*, *Bmi1* or *Lgr5* (adjusted average cycle times ± s.d. for control versus experimental samples were as follows: *Msi1*, 14.89 ± 1.69 versus 16.52 ± 0.86; *Bmi1*, 11.13 ± 1.17 versus 11.29 ± 0.16; *Lgr5*, 14.22 ± 0.50 versus 15.25 ± 1.23).

A second prediction is that Pten loss results in increased numbers of cells with nuclear-localized β-catenin and that these cells should have a stem-like phenotype[14], as has been observed after deletion of *Apc*. However, we observed no such differences by immunohistochemistry (**Fig. 4b**). We also used quantitative real-time PCR on epithelial-enriched control and experimental tissue samples to examine expression of well-characterized Wnt signaling pathway targets. Expression of *Cd44*, *Tcf4*, *Axin2* and *Myc* was not significantly different (for all comparisons, $n = 3$ and Mann-Whitney U-test $P > 0.05$) between control and experimental samples on day 50 after induction (adjusted average cycle times ± s.d. for control versus experimental samples were as follows: *Cd44*, 15.42 ± 0.73 versus 14.48 ± 0.31; *Tcf4*, 9.57 ± 0.02 versus 9.48 ± 0.38; *Axin2*, 8.23 ± 0.90 versus 8.57 ± 0.67; *Myc*, 7.46 ± 0.98 versus 7.64 ± 0.37). Thus, Pten inactivation does not activate Wnt signaling or confer stem-like properties on intestinal epithelial cells.

Villin-CreER^{T2}–mediated *Pten* deletion

To validate our observations from *AhCre*-mediated loss of Pten from the adult intestinal epithelium, we used a different genetic system to achieve epithelial Pten loss. In this case, we used tamoxifen-inducible Cre under the control of the villin 1 (*Vil1*) promoter (*Tg(Vil-cre/ESR1)23Syr*, abbreviated here as *Villin-CreER*^{T2}) to direct recombination specifically to the intestinal epithelium[25]. We induced 6- to 8-week-old adult mice with tamoxifen (five consecutive daily doses at 50 mg/kg), killed them 12 weeks after induction, and assessed their intestines for any gross changes in architecture or homeostasis using histology and immunohistochemistry. No hamartomas were observed in any genotype. Loss of Pten from the intestine was confirmed by Southern blot analysis (**Supplementary Fig. 1a** online) and immunohistochemical analysis (**Supplementary Fig. 1b**). Assessment of hematoxylin and eosin (H&E)-stained intestinal sections revealed no changes in crypt-villus architecture and no obvious perturbation in apoptotic or mitotic levels after Pten loss (**Supplementary Fig. 1c**). Specific stains or immunohistochemical analyses for differentiated cell types in the epithelium revealed that all were present and correctly localized after Pten loss (**Supplementary Fig. 1c**). The proliferation zone within the crypt was visualized by immunohistochemistry against the proliferation marker Ki67 and by labeling of replicating cells using BrdU. Both methods revealed that loss of Pten does not perturb the size or location of the proliferation zone (**Supplementary Fig. 1d**).

In utero deletion of *Pten*

Pten deletion in embryonic intestinal epithelium allowed us to assess the role of Pten during development. We induced experimental and control mice *in utero* on embryonic day 12.5. Mice treated in this way were viable and were obtained at the expected Mendelian ratio. This procedure delivered ~50% recombination at the proximal end of the small intestine, as assessed by LacZ expression in mice transgenic for the *Rosa26R* allele (**Fig. 5a**). When allowed to age, *in utero*–induced *cre*$^{+}$; *Pten*$^{f/f}$ mice developed many of the symptoms previously described in uninduced and induced *cre*$^{+}$; *Pten*$^{f/f}$ mice. *In utero*–induced *cre*$^{+}$; *Pten*$^{f/f}$ mice also showed recombination in the skin, resulting in an abnormally shaggy coat (**Fig. 5b**), which is again consistent with previous reports[26]. Examination of Pten loss in the

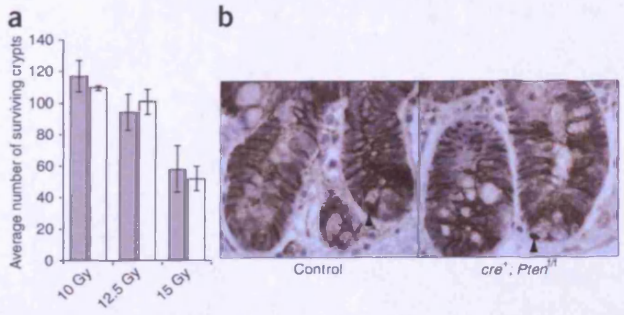

Figure 4 Pten deficiency does not alter the number of crypt clonogens or β-catenin localization. (**a**) Clonogenic microcolony assay was used to determine the number of clonogens present in the crypt. Control and experimental mice were exposed to 15 Gy of gamma irradiation and killed after 72 h. The number of surviving crypts per circumference of the intestine was then scored from H&E-stained sections. There was no significant difference in the number of surviving crypts in *Pten*$^{f/f}$ tissue (open bars) compared to control tissue (gray bars; $n = 5$; Mann-Whitney U-test, $P = 0.63$). Error bars indicate s.d. (**b**) Immunohistochemical analysis of β-catenin was done on control and experimental tissue on day 5 after induction. Pten-deficient tissue showed a β-catenin distribution pattern comparable to control tissue—that is, predominantly membrane associated in cells of the crypt, with occasional nuclear staining (examples indicated by arrowheads) of long-lived cells in the base of the crypt, presumably Paneth cells and stem cells.

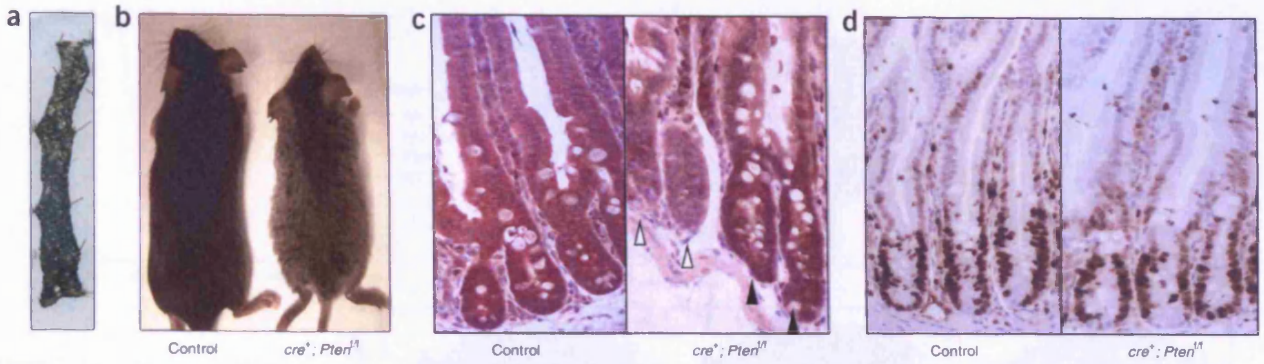

Figure 5 Loss of Pten *in utero* does not affect the normal development of the mouse small intestine. (**a**) Induction of recombination *in utero* at embryonic day 12.5 resulted in ~50% recombination in experimental and control mice in the proximal region of the intestine, as assessed by LacZ staining. (**b**) *In utero*–induced *cre*$^{+}$; *Pten*$^{f/f}$ mice showed recombination in the skin, resulting in a ruffled coat compared to that of control mice, consistent with previous reports. (**c**) Pten deficiency in the intestine of *in utero*–induced mice was assessed by immunohistochemistry. Control mice showed strong Pten staining in the epithelium, whereas ~50% of crypts in *cre*$^{+}$; *Pten*$^{f/f}$ mice retained Pten protein (indicated by filled arrowheads) and the remaining crypts were deficient for Pten (open arrowheads). (**d**) Ki67 immunohistochemistry revealed no difference in the ability of Pten-deficient cells to proliferate or in the size and location of the proliferative compartment compared to controls.

proximal small intestine by immunohistochemistry revealed that ~50% of intestinal crypts lacked Pten, consistent with the estimate of recombination derived from the *Rosa26R* allele (**Fig. 5c**). Histological analysis revealed no gross differences in crypt size, apoptosis or differentiation status in the absence of Pten. Immunohistochemical analysis of Ki67 showed no differences in staining (**Fig. 5d**). Our data therefore indicate that Pten is not required for normal development of the small intestinal epithelium, and its deficiency does not result in overgrowth as might be predicted from its proposed role in ISCs.

Combined deletion of *Apc* and *Pten*

Despite the above observations, PTEN loss remains implicated in intestinal neoplasia, raising the hypothesis that its status only becomes relevant in the context of activated Wnt signaling. To test this hypothesis, we crossed the *loxP*-flanked *Pten* allele onto a conditional *Apc* background[27]. We circumvented problems caused by recombination of the *AhCre* transgene in tissues other than the intestine by use of the *Tg(Cyp1a1-cre/ESR1)1Dwi* transgene (abbreviated here as *AhCreER*^{T}), a more tightly regulated form of aryl hydrocarbon–responsive Cre that requires binding of tamoxifen for activity[28].

We induced Cre recombinase activity in experimental mice (*AhCreER*$^{T+}$; *Pten*$^{f/f}$; *Apc*$^{f/f}$) and control mice (*AhCreER*$^{T+}$; *Pten*$^{f/f}$; *Apc*$^{+/+}$, *AhCreER*$^{T+}$; *Pten*$^{+/+}$; *Apc*$^{f/f}$ and *AhCreER*$^{T+}$; *Pten*$^{+/+}$; *Apc*$^{+/+}$) using both β-naphthoflavone and tamoxifen. After induction, we

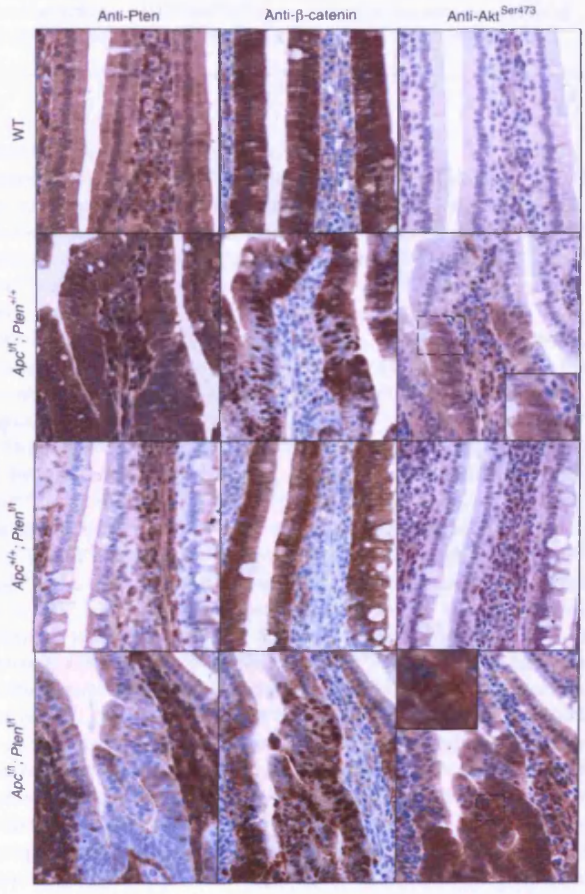

Figure 6 Deficiency of both Pten and Apc leads to activation of Akt. Serial sections of tissue from WT (*AhCreER*$^{T+}$; *Apc*$^{+/+}$; *Pten*$^{+/+}$), *Apc*$^{f/f}$; *Pten*$^{+/+}$ (*AhCreER*$^{T+}$; *Apc*$^{f/f}$; *Pten*$^{+/+}$), *Apc*$^{+/+}$; *Pten*$^{f/f}$ (*AhCreER*$^{T+}$; *Apc*$^{+/+}$; *Pten*$^{f/f}$) and *Apc*$^{f/f}$; *Pten*$^{f/f}$ (*AhCreER*$^{T+}$; *Apc*$^{f/f}$; *Pten*$^{f/f}$) mice killed 7 d after induction were assessed for loss of Apc and Pten protein and activation of Akt by immunohistochemistry. Pten was lost from ~50% of epithelial cells in *Pten*$^{f/f}$ genotypes, with *Pten*$^{+/+}$ genotypes retaining 100% staining for Pten. β-catenin was used as a surrogate marker of Apc loss, and nuclear localization of β-catenin was seen in the majority of epithelial cells in *Apc*$^{f/f}$ genotypes. To assess differences between recombined and nonrecombined tissue, areas of tissue showing a lower than usual level of recombination were selectively photographed. Nuclear localization of β-catenin was not seen in *Apc*$^{+/+}$ genotypes. Activation of Akt was assessed by immunohistochemical analysis of Ser473-phosphorylated Akt (pAkt^{Ser473}). Wild-type tissue had no detectable activation of Akt within the epithelium. Tissue deficient for either Pten or Apc alone had slightly elevated levels of activated Akt, which was distributed evenly within the cytoplasm. Tissue deficient for both Pten and Apc had a large increase in activation of Akt; areas of tissue with high activation of Akt also showed increased association of activated Akt within the plasma membrane (insets magnified ×3).

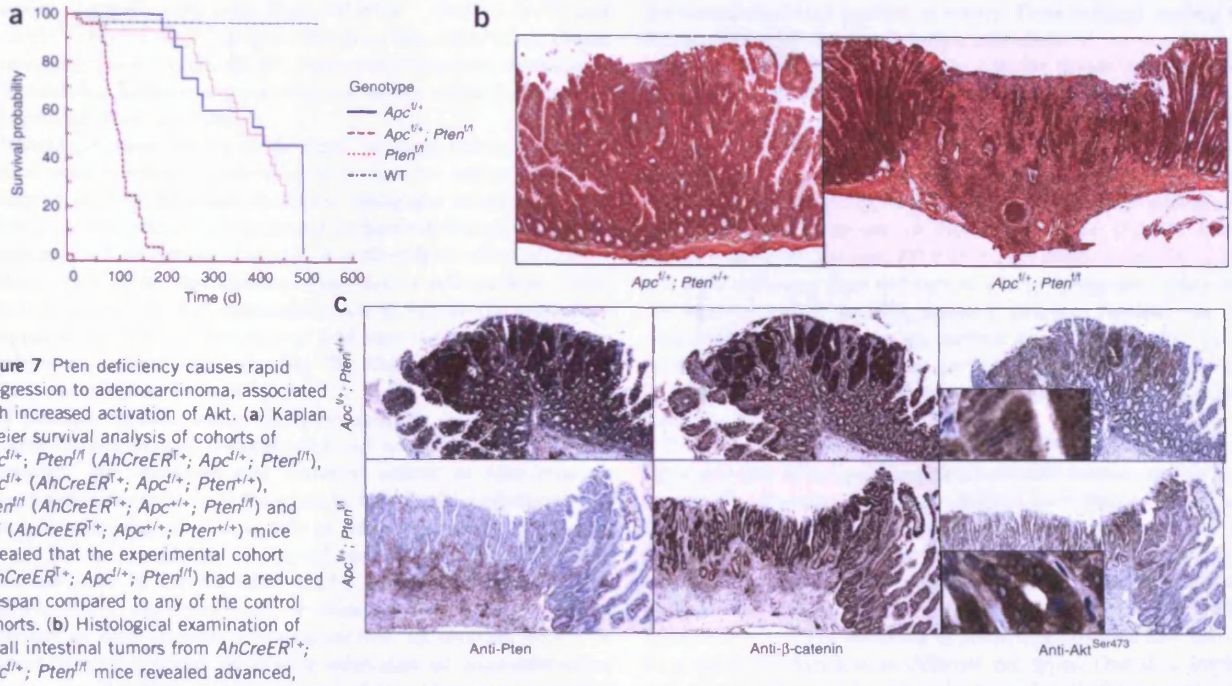

Figure 7 Pten deficiency causes rapid progression to adenocarcinoma, associated with increased activation of Akt. (**a**) Kaplan-Meier survival analysis of cohorts of *Apc*$^{f/+}$; *Pten*$^{f/f}$ (*AhCreER*$^{T+}$; *Apc*$^{f/+}$; *Pten*$^{f/f}$), *Apc*$^{f/+}$ (*AhCreER*$^{T+}$; *Apc*$^{f/+}$; *Pten*$^{+/+}$), *Pten*$^{f/f}$ (*AhCreER*$^{T+}$; *Apc*$^{+/+}$; *Pten*$^{f/f}$) and WT (*AhCreER*$^{T+}$; *Apc*$^{+/+}$; *Pten*$^{+/+}$) mice revealed that the experimental cohort (*AhCreER*$^{T+}$; *Apc*$^{f/+}$; *Pten*$^{f/f}$) had a reduced lifespan compared to any of the control cohorts. (**b**) Histological examination of small intestinal tumors from *AhCreER*$^{T+}$; *Apc*$^{f/+}$; *Pten*$^{f/f}$ mice revealed advanced, ulcerating, invasive adenocarcinomas that penetrated the full thickness of the small intestinal wall, destroying the muscularis propria and leading to a localized peritonitis (right). Tumors in *AhCreER*$^{T+}$; *Apc*$^{f/+}$; *Pten*$^{+/+}$ mice, by contrast, were mostly nonulcerated, noninvasive, benign intramucosal adenomas (left). (**c**) Immunohistochemistry of small intestinal tumors confirmed that they were deficient for Pten and showed strong nuclear localization of β-catenin, indicating loss of Apc. Apc and Pten double-deficient adenocarcinomas also had elevated activated Akt (pAkt^{Ser473}), particularly at the lumenal surface of the tumor. As seen previously, areas with strong expression of activated Akt also showed association of activated Akt within the cell membrane (insets magnified ×8).

observed recombination in ~50% of intestinal epithelial cells. On day 7 after induction, we identified tissue deficient for Pten and Apc by immunohistochemical analysis of Pten and β-catenin (β-catenin served as a surrogate marker of Apc loss, as specific nuclear localization of β-catenin is a well-recognized immediate effect of dysregulated Wnt signaling[29]). Immunohistochemical analysis of serial sections of intestine from experimental and control mice (**Fig. 6**) revealed that ~50% of epithelial cells were deficient for Pten in *Pten*$^{f/f}$ mice compared to *Pten*$^{+/+}$ mice, where the entire epithelium retained positivity for Pten. The majority of epithelial cells in *Apc*$^{f/f}$ mice showed strong nuclear localization of β-catenin, indicating loss of Apc protein, compared to *Apc*$^{+/+}$ control mice, where β-catenin was predominantly cytoplasmic or membrane associated.

To examine the effect of Apc and Pten loss on pathways downstream of Pten, we carried out immunohistochemical analysis of activated (Ser473-phosphorylated) Akt on adjacent tissue sections (**Fig. 6**). Consistent with previous western blot analysis of Thr308-phosphorylated Akt, there was a small increase in levels of activated Akt in tissues deficient for Pten or Apc alone. This level was lower than that seen in tissue deficient for both Apc and Pten. In addition, activated Akt was membrane associated in cells deficient for both Pten and Apc, but not in tissue deficient for Apc or Pten alone. These phenomena were generally observed in epithelial cells of the villus, not within the crypt (**Supplementary Fig. 2** online). Previous work has shown that targeting of Akt isoforms to the cell membrane both *in vitro* and *in vivo* increases its oncogenic potential[30]. Here we showed that loss of both Pten and Apc synergistically increases overall levels of activated Akt and increases its membrane association.

Pten loss in the context of Apc deficiency

To investigate whether the activation and change in localization of Akt we observed at this early stage could lead to a change in intestinal tumor phenotype, we generated *AhCreER*$^{T+}$; *Pten*$^{f/f}$; *Apc*$^{f/+}$ mice. We induced cohorts of more than 25 experimental (*AhCreER*$^{T+}$; *Pten*$^{f/f}$; *Apc*$^{f/+}$) and control (*AhCreER*$^{T+}$; *Pten*$^{+/+}$; *Apc*$^{f/+}$, *AhCreER*$^{T+}$; *Pten*$^{f/f}$; *Apc*$^{+/+}$ and *AhCreER*$^{T+}$; *Pten*$^{+/+}$; *Apc*$^{+/+}$) mice, allowed them to age and monitored them for signs of intestinal tumors (rectal bleeding, prolapse and anemia) or other illness. We killed the mice when they became symptomatic of disease and retained their tissue for histological analysis.

Experimental *AhCreER*$^{T+}$; *Pten*$^{f/f}$; *Apc*$^{f/+}$ mice had a median survival of 99 d, a significant reduction compared to *AhCreER*$^{T+}$; *Pten*$^{+/+}$; *Apc*$^{f/+}$ and *AhCreER*$^{T+}$; *Pten*$^{f/f}$; *Apc*$^{+/+}$ control mice, which had a median survival of 405 and 409 d, respectively ($\chi^2 = 45.16$, d.f. = 1, $P \leq 0.0001$ for *AhCreER*$^{T+}$; *Pten*$^{f/f}$; *Apc*$^{f/+}$ versus *AhCreER*$^{T+}$; *Pten*$^{+/+}$; *Apc*$^{f/+}$; **Fig. 7a**). Ninety-five percent of experimental mice analyzed ($n = 19$) had large, flattened, ulcerated lesions within the small intestine, with an average of 6.9 lesions per mouse ($n = 14$). By contrast, a cohort of 30 *AhCreER*$^{T+}$; *Pten*$^{+/+}$; *Apc*$^{f/+}$ mice remained healthy up to 200 d after induction. We killed groups of control *AhCreER*$^{T+}$; *Pten*$^{+/+}$; *Apc*$^{f/+}$ mice 180 or 250 d after induction (±10%) to assess intestinal tumor burden. At 180 d after induction, 33% of control mice analyzed bore polyp-like lesions within the small intestine, with an average of 1.0 lesions per mouse ($n = 6$). At 250 d after induction, 58% of control mice had small intestinal polyps, and the average number of lesions increased to 1.8 per mouse ($n = 12$). Despite these increases, the frequency of lesions remained less than

that seen in experimental mice. Both *AhCreER*$^{T+}$; *Pten*$^{+/+}$; *Apc*$^{+/+}$ and *AhCreER*$^{T+}$; *Pten*$^{f/f}$; *Apc*$^{+/+}$ control cohorts remained free of symptoms of intestinal disease more than 200 d after induction, with no evidence of hamartoma formation, supporting our earlier conclusions regarding epithelial Pten redundancy.

Histological examination of the small intestinal lesions of experimental mice revealed the majority to be invasive adenocarcinomas arising in severely dysplastic adenomas. Malignant invasion into the submucosa was evident, accompanied by luminal ulceration and the presence of a desmoplastic stroma rich in fibroblasts, often associated with a mixed acute and chronic inflammatory cell reaction. Many adenocarcinomas showed destructive invasion through the muscularis propria of the small intestinal wall and into the peritoneal serosa, resulting in localized peritonitis (**Fig. 7b**). This is in direct contrast to lesions observed in *AhCreER*$^{T+}$; *Pten*$^{+/+}$; *Apc*$^{f/+}$ control mice in this and previous studies, where the great majority of small intestinal neoplasms were benign, nonulcerating and noninvasive intramucosal adenomas. We examined and classified lesions as adenomas or microadenomas confined to the mucosa, early invasive adenocarcinomas infiltrating the submucosa only or advanced invasive adenocarcinomas that infiltrated into or through the muscularis propria of the intestinal wall. In control mice, 85.7% of tumors identified were characterized as microadenomas or adenomas and 14.3% were characterized as early invasive adenocarcinomas. In contrast, 46.4% of tumors in experimental mice were adenomas or microadenomas, 32.1% were classified as early invasive adenocarcinomas and 21.5% were advanced adenocarcinomas showing invasion through the muscularis propria, which were never found in control mice.

We analyzed small intestinal tumors of control *AhCreER*$^{T+}$; *Pten*$^{+/+}$; *Apc*$^{f/+}$ and experimental *AhCreER*$^{T+}$; *Pten*$^{f/f}$; *Apc*$^{f/+}$ mice using immunohistochemistry. Analysis of Pten β-catenin (**Fig. 7c**) confirmed Pten and Apc status. Analysis of Ser473-phosphorylated Akt (**Fig. 7c**) revealed that tumors arising in *AhCreER*$^{T+}$; *Pten*$^{f/f}$; *Apc*$^{f/+}$ and *AhCreER*$^{T+}$; *Pten*$^{+/+}$; *Apc*$^{f/+}$ mice showed activation of Akt, particularly at the lumenal surface of the tumor. Activated Akt was also commonly localized to the cell membrane in tumor cells from *AhCreER*$^{T+}$; *Pten*$^{f/f}$; *Apc*$^{f/+}$ mice, although this was not seen in tumors from *AhCreER*$^{T+}$; *Pten*$^{+/+}$; *Apc*$^{f/+}$ mice. These observations are consistent with our observations after immediate loss of Apc and/or Pten, where membrane localization of activated Akt was only observed after loss of both Apc and Pten. This suggests that activation and relocalization of Akt to the membrane, which arises through deficiency of both Pten and Apc but not Pten or Apc alone, allows the progression of a tumor from adenoma to adenocarcinoma.

DISCUSSION

It has been repeatedly shown through mutational analysis that PTEN functions as a tumor suppressor and is lost or mutated in a variety of different tumor types in humans (reviewed in ref. 31). Inherited mutation in one copy of *PTEN* causes Cowden's syndrome, which is characterized by the development of hamartomatous tumors of various origins, including the gastrointestinal tract[7,8].

Extensive mouse studies have shown that constitutive *Pten* deficiency is incompatible with life[9–11]. However, *Pten* heterozygotes model some features of Cowden's disease, including predisposition to papillary thyroid carcinoma and skin hyperkeratosis[9], endometrial neoplasia[10] and intestinal polyposis[11]. In addition, studies using conditional deletion strategies have shown that Pten loss in tissues as diverse as the liver[20,21], skin[26], prostate[26] and breast[32] leads to neoplasia or carcinoma, or both. Here we report recapitulation of several of these phenotypes as a consequence of low-level expression of Cre recombinase in a number of tissues. These findings confirm that the recombined *Pten* allele is truly a null allele.

It is clear that Pten functions as a major tumor suppressor, and evidence in the literature suggests that *Pten* deletion in the intestine leads to deregulation of growth control and the subsequent development of hamartomatous polyps. In direct contrast to these predictions, however, we found in two independent genetic models that deletion of *Pten* specifically within the epithelium has no adverse effect on intestinal development or homeostasis, nor does it lead to hamartoma formation over 200 d after *Pten* deletion. We also showed that Pten deficiency does not impose a 'crypt progenitor' phenotype, nor does it perturb the Wnt signaling pathway. Furthermore, Pten deficiency does not confer an increase in clonogens after gamma irradiation, as might have been predicted from the literature. Taken together, our data argue that Pten is normally redundant in the mouse small intestinal epithelium.

These conclusions contrast with the findings of He *et al.*, who reported rapid tumorigenesis after conditional deletion of *Pten* in the intestine[15]. However, that strategy differed from the one used here in that the former used an inducible *cre* construct driven by the *Mx1* promoter to drive Pten deficiency in epithelial and stromal cells of the small intestine[33]. Here, we drove Pten deletion using either *AhCre* or *Villin-CreER*^{T2}, both of which are restricted to the epithelium within the intestine[25,28]. The difference in phenotype observed may therefore be a result of Pten loss in different cell types. Our data implying redundancy of Pten within normal intestinal epithelium, together with the data of He *et al.*, suggest that tumor formation is initiated by loss of Pten in another cell compartment within the intestine, probably within the underlying stroma. The findings of He *et al.* are also consistent with the increased predisposition to intestinal tumors of humans with Cowden's syndrome and mice with a constitutive *Pten* deletion, where all cell types of the tissue are effectively heterozygous for *Pten*. Tumor formation in this case may actually be initiated by loss of Pten within a stromal cell, rather than in the epithelial compartment. These data highlight the importance of interaction between epithelial cells and other cell types in their neighboring environment in the development and progression of intestinal tumors. Indeed, the importance of this interaction for suppression of tumorigenesis has very recently been shown in two studies. First, deletion of the bone morphogenetic protein type II receptor specifically in the stroma was shown to have a marked effect on epithelial homeostasis, ultimately resulting in hamartoma development[34]. Second, mesenchymal-specific deletion of the tumor suppressor *Stk11* (also known as *Lkb1*) was shown to result in polyposis, which recapitulates that seen in constitutive *Stk11*-heterozygous animals[35]. These data, together with those of He *et al.*[15] and the observations we report here, provide evidence supporting the notion that the initiating event for hamartoma formation occurs outside of the epithelial cell population[36].

To further investigate the role of Pten within the intestinal epithelium, we characterized the effects of Pten loss in the context of activated Wnt signaling, achieved by combined deletion of both *Pten* and *Apc*. In epithelium deficient for *Pten* or *Apc* alone, we observed a small increase in activated Akt levels. In tissues deficient for both genes, we observed higher levels of activated Akt in the epithelium coupled with strong membrane localization, a phenomenon previously associated with increased oncogenic potential[30]. Pten-deficient tumors arising in *Apc*-heterozygous mice also showed increased levels of activated Akt, which was again localized to the cell periphery. In these mice, the majority of lesions showed clear evidence of progression to adenocarcinoma, in direct contrast to *Apc*-heterozygous mice, which only develop adenomas. These data

therefore show that Pten loss increases the levels of activated Akt and alters its cellular localization, the consequences of which are increased adenoma predisposition and progression. Within the prostate, neoplasia driven by Pten loss has been found to be absolutely dependent upon functional Akt[37]. Our data support the notion that activation of Akt is the key tumor-promoting event after Pten loss. When Akt activation is weak, as in the context of Pten loss alone, no tumor suppressor function is seen. However, when Akt activation is high, such as when both *Pten* and *Apc* are deleted, rapid tumor onset and progression ensue. Our data therefore add *Pten* to the relatively short list of genes that have been directly implicated in adenoma progression. This, along with the observation that the PI3K pathway is activated in a large percentage of colorectal cancers[6], argues for the therapeutic targeting of Akt in intestinal adenomas and adenocarcinomas.

METHODS

Mice. All procedures were conducted in accordance with local and national regulations as appropriate. Mice were maintained on an outbred background, and all mice were genotyped as previously described for the targeted *Pten* allele[16], the targeted *Apc* allele[27], the *Rosa26R* allele[19] and the *cre* transgene[29]. Control mice were derived from the same colony as the experimental mice, but they were not always littermates. Cre activity was induced in control and experimental *AhCre* mice by intraperitoneal injection with 80 mg/kg β-naphthoflavone (Sigma) dissolved in corn oil for four consecutive days[29]. Mice bearing the *AhCreER*^{T} transgene received a combined intraperitoneal injection of 80 mg/kg β-naphthoflavone and tamoxifen (Sigma), dissolved together in corn oil, for four consecutive days. Mice bearing the *Villin-CreER*^{T2} transgene[25] were induced by intraperitoneal injection of tamoxifen at a dose of 50 mg/kg for five consecutive days.

To examine S-phase labeling *in vivo*, selected mice were injected with 100 μg of BrdU (Sigma) and killed at indicated time points after labeling. For the clonogenic microcolony assay, control and experimental mice were exposed to 15 Gy of gamma irradiation and killed 72 h later. Kaplan-Meier survival analysis was done using MedCalc software (version 8.2.1.0; available at http://www.medcalc.be).

Whole intestines were removed and flushed well with water. As recombination levels decrease along the proximal-distal axis of the intestine[17], small intestinal tissue was consistently collected from defined points along the intestine. The first 5 cm of the intestine was fixed in methacarn (4:2:1 ratio of methanol:chloroform:acetic acid) for histological analysis. The next 3 cm was bundled using surgical tape and fixed in ice-cold 10% neutral buffered formalin overnight to be used for immunohistochemistry. The following 10 cm was used fresh for enrichment of epithelial cells (see below).

β-galactosidase analysis. Assessment of β-galactosidase activity was used to examine the efficiency of recombination at the *Rosa26R* reporter allele after induction of Cre activity. Intestinal whole-mounts were prepared, fixed and exposed to X-gal substrate using a method previously reported[29].

Histology and immunohistochemistry. Intestinal tissue was fixed in ice-cold 10% neutral buffered formalin (Sigma) for no longer than 24 h before being processed into paraffin blocks according to standard procedures. Tissue sections (5 μm) were either stained with H&E for histological analysis or used for immunohistochemistry. The following primary antibodies were used for immunohistochemistry: Ab-2 rabbit antibody to Pten (1:25; Lab Vision), rabbit antibody to Pten (1:100, Cell Signaling Technology), mouse antibody to Ki67 (1:100; Novacastra), rabbit antibody to lysozyme (1:100; Neomarkers), rabbit antibody to villin (1:100; Santa Cruz), mouse antibody to BrdU (1:100; Becton Dickinson), mouse antibody to β-catenin (1:200; Transduction Labs) and rabbit antibody to Ser473-phosphorylated Akt (1:50; Cell Signaling Technology). Periodic acid–Schiff (PAS) staining and Grimelius staining were done according to standard protocols[29].

Enrichment for epithelial cells. To obtain a population of cells enriched for epithelial cells, we used an epithelial extraction protocol based on one previously described[38] on freshly collected intestine. Briefly, a 10-cm section of small intestine was flushed well with water before being tied off at one end and inverted over a 4-mm glass rod. Vibration was then applied to the glass rod, and the intestine was placed in 10 mM EDTA in Hank's balanced salt solution (Gibco) at 37 °C for 15 min. The intestine was then moved into a clean tube of 10 mM EDTA in Hank's balanced salt solution and incubated in the same fashion for a further 15 min. Centrifugation (2,700 *g*, 4 °C, 15 min) yielded a pellet containing predominantly epithelial cells.

Quantitative real-time PCR. RNA was isolated from cells obtained by epithelial extraction using a standard phenol-chloroform protocol. RNA was purified using the RNeasy kit (Qiagen) and treated with RQ1 RNase-free DNase (Promega) according to the manufacturer's instructions to remove genomic DNA. Reverse transcription was done using the SuperScriptII reverse transcriptase kit (Invitrogen) and random hexamers (Invitrogen) according to the manufacturer's instructions. Quantitative real-time PCR was done to assess expression of *Pten*, *CD44*, *Tcf4*, *Axin2*, *Myc*, *Msi1*, *Bmi1* and *Lgr5*. Primer sequences are provided in **Supplementary Table 1** online.

DyNAmo HS SYBR Green (Finnzymes) was added to appropriate cDNA samples and primers. β-actin was used as a loading control. Reactions were run on a PTC-200 thermal cycler and a Chromo4 continuous fluorescence detector (both from MJ Research), which were used in conjunction with Opticon Monitor analysis software (version 2.03, MJ Research) to calibrate and run the reaction. Data were analyzed using the $2^{-\Delta\Delta Ct}$ method[39].

Western blot analysis. Protein was extracted from epithelial-enriched samples by standard methods using lysis buffer (20 mM Tris-HCl (pH 8.0), 2 mM EDTA (pH 8.0) and 0.5% (vol/vol) NP-40) containing protease inhibitors (Complete, Mini protease inhibitor tablets, Roche) and phosphatase inhibitors (25 mM sodium β-glycerophosphate, 100 mM sodium fluoride, 20 nM calyculin A and 10 mM sodium pyrophosphate). Solubilized proteins (30 μg) were separated by standard SDS-PAGE on a 10% polyacrylamide separating gel with 5% stacking gel and then transferred to polyvinylidene fluoride membrane (Hybond-P, Amersham Biosciences) by standard methods.

The following primary antibodies were used to probe blots: Ab-2 rabbit antibody to Pten (1:500; Lab Vision), rabbit antibody to Akt (1:1,000; Cell Signaling), rabbit antibody to Thr308-phosphorylated Akt (1:300; Cell Signaling) and mouse antibody to β-actin (1:5,000; Sigma). Appropriate horseradish peroxidase–conjugated secondary antibodies were used (Amersham Biosciences). Blots were developed using ECL, ECL Plus or ECL Advance reagents (Amersham Biosciences) according to the manufacturer's instructions.

Note: Supplementary information is available on the Nature Genetics website.

ACKNOWLEDGMENTS

We thank M. Bishop, L. Pietzka and D. Scarborough for technical assistance and R. Kemp for assistance with the epithelial extraction protocol. Villin-CreER^{T2} mice were provided by S. Robine (Center National de la Recherche Scientifique/Institut Curie). This work was supported by Cancer Research UK and the Wales Gene Park and by grants to A.T. from the Swiss National Science Foundation, the Swiss Cancer League, the EU FP6 INTACT program and the EU FP7 program 'Eurosystem'.

AUTHOR CONTRIBUTIONS

V.M., O.J.S., A.T. and A.R.C. designed this study; V.M., O.J.S., G.T.W. and N.D. did the phenotype assessment; and V.M., D.J.W., O.J.S. and A.R.C. contributed to the writing of this paper.

Published online at http://www.nature.com/naturegenetics/
Reprints and permissions information is available online at http://npg.nature.com/reprintsandpermissions/

1. Steck, P.A. *et al.* Identification of a candidate tumor suppressor gene, *MMAC1*, at chromosome 10q23.3 that is mutated in multiple advanced cancers. *Nat. Genet.* **15**, 356–362 (1997).
2. Li, D.M. & Sun, H. TEP1, encoded by a candidate tumor suppressor locus, is a novel protein tyrosine phosphatase regulated by transforming growth factor beta. *Cancer Res.* **57**, 2124–2129 (1997).
3. Li, J. *et al. PTEN*, a putative protein tyrosine phosphatase gene mutated in human brain, breast, and prostate cancer. *Science* **275**, 1943–1947 (1997).
4. Stambolic, V. *et al.* Negative regulation of PKB/Akt-dependent cell survival by the tumor suppressor PTEN. *Cell* **95**, 29–39 (1998).

5. Vivanco, I. & Sawyers, C.L. The phosphatidylinositol 3-kinase-AKT pathway in human cancer. *Nat. Rev. Cancer* **2**, 489–501 (2002).
6. Parsons, D.W. *et al.* Colorectal cancer: mutations in a signalling pathway. *Nature* **436**, 792 (2005).
7. Carlson, G.J., Nivatvongs, S. & Snover, D.C. Colorectal polyps in Cowden's disease (multiple hamartoma syndrome). *Am. J. Surg. Pathol.* **8**, 763–770 (1984).
8. Merg, A. & Howe, J.R. Genetic conditions associated with intestinal juvenile polyps. *Am. J. Med. Genet. C. Semin. Med. Genet.* **129**, 44–55 (2004).
9. Di Cristofano, A., Pesce, B., Cordon-Cardo, C. & Pandolfi, P.P. Pten is essential for embryonic development and tumor suppression. *Nat. Genet.* **19**, 348–355 (1998).
10. Podsypanina, K. *et al.* Mutation of *Pten/Mmac1* in mice causes neoplasia in multiple organ systems. *Proc. Natl. Acad. Sci. USA* **96**, 1563–1568 (1999).
11. Suzuki, A. *et al.* High cancer susceptibility and embryonic lethality associated with mutation of the *PTEN* tumor suppressor gene in mice. *Curr. Biol.* **8**, 1169–1178 (1998).
12. He, X.C. *et al.* BMP signaling inhibits intestinal stem cell self-renewal through suppression of Wnt-β-catenin signaling. *Nat. Genet.* **36**, 1117–1121 (2004).
13. Bjerknes, M. & Cheng, H. Re-examination of P-PTEN staining patterns in the intestinal crypt. *Nat. Genet.* **37**, 1016–1017 (2005); reply **37**, 1017–1018 (2005).
14. Persad, S., Troussard, A.A., McPhee, T.R., Mulholland, D.J. & Dedhar, S. Tumor suppressor PTEN inhibits nuclear accumulation of β-catenin and T cell/lymphoid enhancer factor 1-mediated transcriptional activation. *J. Cell Biol.* **153**, 1161–1174 (2001).
15. He, X.C. *et al.* PTEN-deficient intestinal stem cells initiate intestinal polyposis. *Nat. Genet.* **39**, 189–198 (2007).
16. Suzuki, A. *et al.* T cell-specific loss of Pten leads to defects in central and peripheral tolerance. *Immunity* **14**, 523–534 (2001).
17. Ireland, H. *et al.* Inducible Cre-mediated control of gene expression in the murine gastrointestinal tract: Effect of loss of β-catenin. *Gastroenterology* **126**, 1236–1246 (2004).
18. Sansom, O.J., Griffiths, D.F., Reed, K.R., Winton, D.J. & Clarke, A.R. Apc deficiency predisposes to renal carcinoma in the mouse. *Oncogene* **24**, 8205–8210 (2005).
19. Soriano, P. Generalized lacZ expression with the ROSA26 Cre reporter strain. *Nat. Genet.* **21**, 70–71 (1999).
20. Horie, Y. *et al.* Hepatocyte-specific Pten deficiency results in steatohepatitis and hepatocellular carcinomas. *J. Clin. Invest.* **113**, 1774–1783 (2004).
21. Stiles, B. *et al.* Liver-specific deletion of negative regulator Pten results in fatty liver and insulin hypersensitivity. *Proc. Natl. Acad. Sci. USA* **101**, 2082–2087 (2004).
22. Backman, S.A. *et al.* Deletion of Pten in mouse brain causes seizures, ataxia and defects in soma size resembling Lhermitte-Duclos disease. *Nat. Genet.* **29**, 396–403 (2001).
23. Freeman, D.J. *et al.* PTEN tumor suppressor regulates p53 protein levels and activity through phosphatase-dependent and -independent mechanisms. *Cancer Cell* **3**, 117–130 (2003).
24. Sansom, O.J. *et al.* MBD4 deficiency reduces the apoptotic response to DNA-damaging agents in the murine small intestine. *Oncogene* **22**, 7130–7136 (2003).
25. El Marjou, F. *et al.* Tissue-specific and inducible Cre-mediated recombination in the gut epithelium. *Genesis* **39**, 186–193 (2004).
26. Backman, S.A. *et al.* Early onset of neoplasia in the prostate and skin of mice with tissue-specific deletion of Pten. *Proc. Natl. Acad. Sci. USA* **101**, 1725–1730 (2004).
27. Shibata, H. *et al.* Rapid colorectal adenoma formation initiated by conditional targeting of the *Apc* gene. *Science* **278**, 120–123 (1997).
28. Kemp, R. *et al.* Elimination of background recombination: somatic induction of Cre by combined transcriptional regulation and hormone binding affinity. *Nucleic Acids Res.* **32**, e92 (2004).
29. Sansom, O.J. *et al.* Loss of Apc *in vivo* immediately perturbs Wnt signaling, differentiation and migration. *Genes Dev.* **18**, 1385–1390 (2004).
30. Mende, I., Malstrom, S., Tsichlis, P.N., Vogt, P.K. & Aoki, M. Oncogenic transformation induced by membrane-targeted Akt2 and Akt3. *Oncogene* **20**, 4419–4423 (2001).
31. Dahia, P.L. PTEN, a unique tumor suppressor gene. *Endocr. Relat. Cancer* **7**, 115–129 (2000).
32. Li, G. *et al.* Conditional loss of PTEN leads to precocious development and neoplasia in the mammary gland. *Development* **129**, 4159–4170 (2002).
33. Schneider, A., Zhang, Y., Guan, Y., Davis, L.S. & Breyer, M.D. Differential, inducible gene targeting in renal epithelia, vascular endothelium, and viscera of Mx1Cre mice. *Am. J. Physiol. Renal Physiol.* **284**, F411–F417 (2003).
34. Beppu, H. *et al.* Stromal inactivation of BMPRII leads to colorectal epithelial overgrowth and polyp formation. *Oncogene* **27**, 1063–1070 (2008).
35. Katajisto, P. *et al.* LKB1 signaling in mesenchymal cells required for suppression of gastrointestinal polyposis. *Nat. Genet.* **40**, 455–459 (2008).
36. Jansen, M. *et al.* Mucosal prolapse in the pathogenesis of Peutz-Jeghers polyposis. *Gut* **55**, 1–5 (2006).
37. Chen, M.L. *et al.* The deficiency of Akt1 is sufficient to suppress tumor development in Pten+/- mice. *Genes Dev.* **20**, 1569–1574 (2006).
38. Bjerknes, M. & Cheng, H. Methods for the isolation of intact epithelium from the mouse intestine. *Anat. Rec.* **199**, 565–574 (1981).
39. Livak, K.J. & Schmittgen, T.D. Analysis of relative gene expression data using real-time quantitative PCR and the 2(-delta delta C(T)) method. *Methods* **25**, 402–408 (2001).

Intestinal homeostasis and neoplasia studied using conditional transgenesis

Victoria Marsh and Alan Clarke[†]

Constitutive mouse models of intestinal neoplasia, such as the $Apc^{min/+}$ (multiple intestinal neoplasia) mouse have proven valuable tools both for furthering our understanding of tumorigenesis and for the development of therapeutic strategies. However, the *in vivo* study of a number of genes has been precluded by their absolute requirement during embryonic development. This has led to the development of conditional strategies that allow gene regulation *in vivo*. This review describes the principal techniques used to achieve conditional transgenesis within the mouse intestine, with a particular focus upon the Cre–Lox and Tet-regulable systems. Further, we discuss how these techniques are being used to dissect the mechanisms governing both normal homeostasis and neoplastic development within the intestine.

Expert Rev. Anticancer Ther. 7(4), 519–531 (2007)

CONTENTS

Conditional transgenic technology
Wnt signaling
Apc
β-catenin
c-Myc
Oct-4
Notch pathway
Transforming growth factor-β & bone morphogenic protein signaling
Other pathways
Expert commentary
Five-year view
Key issues
References
Affiliations

[†]*Author for correspondence*
Cardiff University, Cardiff School of Biosciences, Cardiff, CF10 3US, UK
Tel.: +44 292 087 4609
Fax: +44 292 087 4116
clarkear@cardiff.ac.uk

KEYWORDS:
bone morphogenic protein, conditional, Cre–Lox, intestine, mouse, neoplasia, Notch, Wnt

The ability to model intestinal neoplasia in the mouse has proven a crucial factor in increasing our understanding of the complex processes that underlie neoplasia. Modeling has also facilitated the identification of novel potential therapeutic targets, as well as providing an *in vivo* setting for testing existing and novel therapeutic agents. The models currently available to us have been developed through the constitutive overexpression of known oncogenes, as randomly generated mutants or as specific knockouts of known tumor-suppressor genes. One of the best characterized and most extensively used models of intestinal tumor development is the $Apc^{min/+}$ (multiple intestinal neoplasia) mouse. The $Apc^{min/+}$ strain was generated by random mutagenesis following exposure to ethylnitrosourea, creating a line that spontaneously developed polyps within both the large and small intestine [1]. Subsequent sequencing of this mutant revealed a point mutation within the *Apc* gene at codon 850 [2]. Since its development and characterization, the $Apc^{min/+}$ mouse has been used as an accurate model of the human disease familial adenomatous polyposis (FAP), although it should be noted that some differences do exist between the $Apc^{min/+}$ model and human FAP patients: FAP patients tend to develop tumors within the colon and rectum, whereas $Apc^{min/+}$ mice predominantly develop small intestinal tumors. This model has been particularly valuable for expanding our knowledge of the neoplastic process in the intestine [3] and has also been a useful tool for the screening and development of chemotherapeutic and chemopreventative agents. For example, the efficacy of nonsteroidal anti-inflammatory drugs in the prevention and treatment of intestinal tumors has been widely tested in the $Apc^{min/+}$ model. Examples of specific studies include Sansom and colleagues, who showed that treatment of $Apc^{min/+}$ mice with aspirin from conception onwards results in dramatic suppression of intestinal adenoma development [4], and Boolbol and colleagues who showed that the administration of sulindac to $Apc^{min/+}$ mice results in reduced tumor incidence [5]. Encouragingly, the findings of the latter study have been recapitulated in human FAP patients treated with the same agent [6].

Constitutive knockout models have also been used to provide insight into factors contributing to neoplasia within the intestine. One example of this is deletion of the tumor-suppressor gene *p53*, which has been widely studied in a range

10.1586/14737140.7.4.519

ISSN 1473-7140

of tissues in the mouse. We have previously examined the role of *p53* in the DNA damage response of the intestine [7]. This study found that deficiency of *p53* allowed cells bearing radiation-induced DNA damage to evade apoptosis. At the time, this supported the notion that *p53* deficiency may contribute to tumorigenesis by allowing mutant cells to persist. This notion has now been directly tested using a mouse model in which *p53* status can be reversibly switched *in vivo* between functional and inactive states, to demonstrate that that the *p53*-mediated pathological response to whole-body irradiation is actually irrelevant, at least for the suppression of radiation-induced lymphoma [8]. Whether this remains true for all tissues, including the intestine, remains unclear.

Despite their obvious successes, the extensive use of constitutive knockouts has been hampered by the fact that many oncogenes and tumor-suppressor genes are required for embryonic development. Furthermore, analysis of gene function within a given tissue has often been precluded or compromised by overriding phenotypes within other tissues. It has also been argued that constitutive knockout models may not faithfully represent the normal process of neoplasia, as this is normally characterized by sequential mutations occurring within a subset of cells (usually) within an adult organism in the context of genetically normal neighboring cells. This situation contrasts with that in constitutive models in two significant ways:

- The cells in a constitutively mutant animal all possess the mutation of interest
- Constitutive mutants provide an opportunity for compensation by other genes to occur during the process of development

In order to circumvent these issues, conditional transgenic strategies have been developed that allow a gene to be deleted specifically within a single cell type or at a particular stage of development. This review aims to deal with how conditional transgenesis can be achieved within the murine intestine and also to examine recent studies that have used conditional technology to investigate the contribution of various regulatory pathways to intestinal neoplasia.

Conditional transgenic technology

Systems that permit switching of gene expression are designed such that transgenesis occurs only once defined conditions are met. Such conditions may include cell or tissue specificity, developmental stage, exposure to xenobiotics or indeed a combination of these factors. Here, we briefly review the methods of achieving conditional transgenesis in the intestine, although it should be noted that more extensive reviews can be found elsewhere [9–12]. In its very simplest form, conditional transgenesis involves the use of a tissue-specific promoter, which drives expression of a chosen transgene. For instance, the promoter of the *Villin* gene has been used to drive transgene expression specifically and efficiently in the small and large intestinal epithelium [13].

Early attempts to develop truly switchable systems used exogenous agents, such as steroids, heat-shock or heavy metals, to induce promoters that would directly drive transgene expression in a temporally controlled manner [14,15]. However, such approaches were found to be somewhat problematic, with inducing agents often being toxic to cells and with poor levels of gene expression being achieved. More sophisticated conditional systems have now been developed, many of which are bipartite in mechanism, involving both an 'effector' and a 'targeted' transgene, upon which the effector acts to switch the gene on or off. Such binary approaches include the causes recombination (Cre)–locus of crossover (Lox), Flp–Flp recognition target (Frt) and tetracycline (Tet)-regulable sysms.

Probably the most popular method of achieving conditional transgenesis within the intestine is the Cre–Lox approach. The effector, Cre recombinase, was initially isolated from the bacteriophage P1 [16] and catalyzes recombination between pairs of recognition sequences, termed LoxP (locus of crossover P1) sites [17,18]. If a target gene or one or more of its essential coding regions, is placed between a pair of LoxP sites and exposed to Cre recombinase, the region of DNA between the two LoxP sites is completely excised (or 'floxed' out), resulting in inactivation of the gene. It is also possible to activate transgenes using this system, by engineering the transgene so that it contains a 'STOP' cassette flanked by a pair of LoxP sites. When Cre is expressed, the STOP cassette is then removed, permitting expression of the transgene [19].

Control of the Cre–LoxP system is achieved principally through careful selection of the promoter to drive expression of Cre recombinase. Examples of promoter-Cre constructs commonly used to drive recombination within the intestine include Villin–Cre [20,21], Fabp–Cre [22], Mx1–Cre [23] and Ah–Cre [24]. Both the Villin- and fatty acid-binding protein promoters are active specifically in the intestine by embryonic day (E) 12.5 [21] and E13.5 [22], respectively, and Cre recombinase is therefore constitutively but specifically expressed within the intestine throughout development and into adulthood. Mx1–Cre requires exposure to interferon or polyinosinic–polycytidylic acid (pI–pC; which stimulates host interferon production) in order for Cre to be expressed [23]. The promoter of the cytochrome P450 1A1 subfamily is used to drive Cre expression in the Ah–Cre transgene, thus exposure to aryl hydrocarbons, such as β-naphthoflavone, is required to induce activity [24,25]. Each of these constructs show differences in the patterns of recombination within the intestine, with Villin–Cre and Ah–Cre showing recombination restricted to epithelial cells [20,21,24], whereas Mx1–Cre also drives recombination more widely [26]. Furthermore, recombination patterns can differ even within a single cell type. For example, although Villin–Cre and Ah–Cre both drive recombination within the epithelial compartment, there are differences in the exact location of their activity. Villin–Cre is expressed in epithelial cells along the entirety of the crypt–villus axis, driving recombination in both mature differentiated cells and immature precursor cells [13]. This is in contrast to Ah–Cre, which is principally expressed within the stem and precursor cell compartment located towards the base of the crypt [24].

Systems that employ post-translational control over Cre recombinase activity through dependence on ligand binding have also been developed. For instance, fusion proteins of Cre recombinase and a modified estrogen receptor (ER) have been generated (e.g., $CreER^{T}$, $CreER^{T2}$ and $CreER^{TM}$) [21,27–29]. Once translated, the ER domain of the protein sequesters the recombinase in the cytoplasm, preventing it from acting on its target sequences contained within the nucleus. On binding of the estrogen analog tamoxifen, the nuclear localization signal of the receptor is exposed and the fusion protein is able to translocate to the nucleus, where it can act on its target. Such fusion proteins can also be placed under the control of the promoters described previously, which provides much tighter control of Cre expression. One example of this is the Ah–$CreER^{T}$ construct, which requires both exposure to an aryl hydrocarbon to induce transcription of the transgene, plus additional binding of tamoxifen to allow activation of the recombinase (FIGURE 1) [30].

One of the main advantages of the Cre–Lox approach is its popularity: this has meant that a large number of both the targeted transgenes and Cre-expressing transgenes have been developed [101]. However, this approach also has several disadvantages. These include aberrant Cre expression or 'leakiness' in other tissues, although it has been argued that this is a benefit of some systems. Also, the discovery of pseudo-LoxP recognition sites within mammalian genomes, which can be acted upon by Cre recombinase [31], has prompted the suggestion that Cre expression in mammalian cells may cause double-stranded DNA breaks and perhaps promote genomic instability. Finally, with respect to genetic manipulation one of the major drawbacks of this system is that it is irreversible: once the targeted region has been excised there is no way of restoring it.

Flp–Frt systems work on very similar principles to those of Cre–LoxP systems. Flp recombinase, isolated from the yeast *Saccharomyces cerevisiae*, is another site-specific recombinase that acts to cause recombination between pairs of Flp recombination target (Frt) sites [32]. However, Flp–Frt is not commonly used within the intestine, therefore its use is not dealt with in detail here. The final binary system of conditional transgenesis that will be discussed here, and which has been used in the intestine to some extent, is the Tet-regulable approach. Tet-dependent systems were originally adapted from their *Escherichia coli* origins and modified for use in mammalian systems by Gossen and Bujard [33]. They differ from the recombination-based Cre–LoxP and Flp–Frt systems described previously in that the effector transgene acts to transactivate the target transgene. The effector transgene typically consists of a tissue-specific promoter that drives the expression of a fusion protein consisting of the *E. coli* tetracycline-resistance (TetR) DNA-binding domain and the VP16 transactivation domain derived from the herpes simplex virus. This product can then act on the second component of the system. The target construct consists of the human cytomegalovirus promoter under the control of the *E. coli* Tet operator (TetO), which together drive the expression of the gene of interest. In the case of the tetracycline-controlled transactivator (tTA), or 'Tet-off' system, when doxycycline is present, it is bound by the TetR domain of the fusion protein, inactivating it and preventing expression of the target gene [34]. An adaptation of this system, known as the reverse-tTA (rtTA), or 'Tet-on' system, employs use of a mutant TetR protein, which is only active when bound to doxycycline, and therefore is required for target gene expression [35]. The main advantage of the Tet-regulable systems over the systems described previously, which require recombination, is undoubtedly that it is completely reversible and allows gene expression to be turned on and off at will. However, the system also has several drawbacks, including a lack of responsiveness to doxycycline in certain tissues and 'leaky' expression of transgenes [12].

Conditional transgenesis has undoubtedly revolutionized the way in which gene function can be studied in the mouse. Examples of uses of the technology, employed specifically to investigate homeostasis and neoplasia within the intestine, are described later and are grouped according to regulatory pathway. The examples described here are summarized in TABLE 1.

Wnt signaling

By virtue of its frequent association with intestinal cancer in humans, the Wnt signaling pathway is probably the best studied of the regulatory pathways in the mouse intestine (further Wnt pathway reviews can also be found [36,37]). A number of Wnt pathway components have been conditionally modified within the intestine and these studies are described below.

Apc

Often referred to as the 'gatekeeper' of intestinal tumorigenesis, the adenomatous polyposis coli gene product, or *Apc*, is central to the Wnt signaling pathway, forming part of the β-catenin destruction complex along with glycogen synthase kinase (GSK)-3β and Axin. Study of complete inactivation of *Apc in vivo* has previously been precluded by the fact that biallelic mutation causes embryonic lethality [38]. *Apc* was first deleted from the adult intestinal epithelium by Sansom and colleagues in 2004 [39]. In this study, a Cre–Lox approach was employed, with Cre expressed from the Ah–Cre transgene following induction using β-naphthoflavone and both copies of the *Apc* gene targeted for recombination with LoxP sites. This approach allowed characterization of the very early effects of *Apc* loss *in vivo* prior to adenoma formation, which had not previously been achieved using any other model system. Loss of *Apc* was found to rapidly lead to overexpression and nuclear localization of β-catenin, which was coincident with perturbation of the normal crypt–villus architecture of the epithelium. The proliferative compartment of the epithelium was found to dramatically expand following *Apc* deletion, resulting in abnormally large, aberrant crypt-like structures and a greatly increased number of cells in S-phase. Differentiation of epithelial precursor cells into the four mature cell types of the epithelium was found to be perturbed, with failure of *Apc*-deficient cells to express Villin (a marker of the brush border), and a lack of goblet cells and enteroendocrine cells. Paneth cells were found to be present, although their localization was grossly

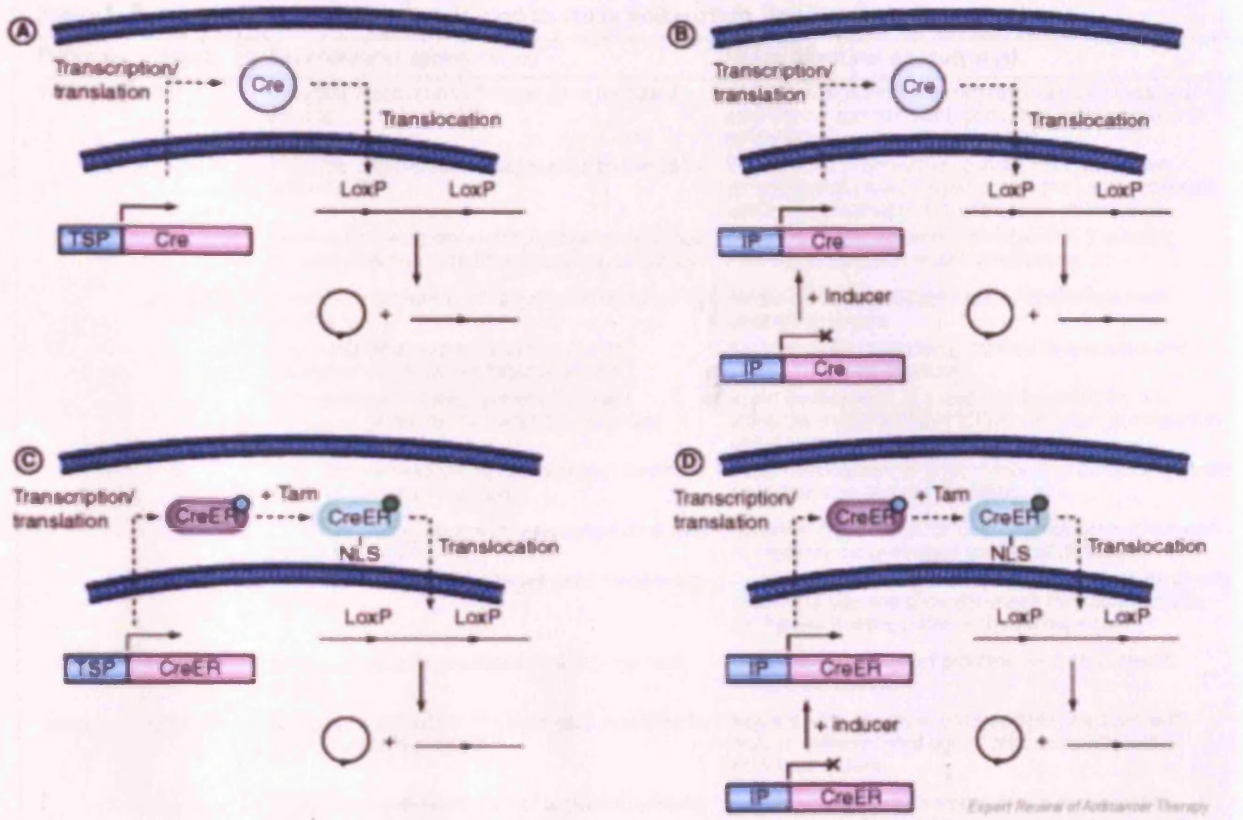

Figure 1. Overview of conditional Cre–Lox-based experimental strategies. (A) Cre expression can be targeted to selected cell types by use of a tissue-specific promoter. Activation of the tissue-specific promoter drives expression of the Cre transgene, which is translated in the cytosol. Cre recombinase can then translocate to the nucleus, where it catalyzes recombination between pairs of LoxP sites. Examples of this type of regulation in the intestine include Villin–Cre, fatty acid-binding protein (liver)–Cre and Ck19–Cre. **(B)** Transcriptional control of Cre expression can be achieved through the use of inducible promoters. The Cre transgene is transcriptionally silent in the absence of an appropriate inducer. On administration of the inducer, the inducible promoter is activated and the Cre transgene expressed. Cre is translated in the cytosol and translocates to the nucleus as described for **(A)**. Inducible expression of Cre in the intestine can be achieved through use of constructs such as Ah–Cre (which requires induction using β-naphthoflavone) and Mx1–Cre (which requires induction using interferon or poly(I) poly(C) motifs). **(C)** Cre activity can be modulated in a post-translational manner through use of a fusion protein composed of Cre recombinase and a modified ER. The CreER fusion protein is usually expressed from a tissue-specific promoter as described for **(A)**. However, as a consequence of heat-shock protein–ER domain interaction, the fusion protein is sequestered in the cytosol until administration of Tam. This synthetic estrogen binds to the ER domain of the fusion protein and allows exposure of the nuclear localization signal. The fusion protein is then able to translocate to the nucleus, where Cre can act on target sequences as described in **(A)**. **(D)** Both transcriptional and post-translational control of Cre activity can be achieved through use of inducible promoters coupled with CreER fusion proteins. Transcription of the CreER fusion protein is regulated as described for **(B)**. Post-translational control of the fusion protein is achieved as described in **(C)**. An example of use of this tightly regulated Cre in the intestine is the Ah–CreER construct, which requires both β-naphthoflavone administration to stimulate CreER expression and Tam binding to allow Cre to access the nucleus.
Cre: Causes recombination; ER: Estrogen receptor; IP: Inducible promoter; LoxP: Locus of crossover in P1; NLS: Nuclear localization signal; Tam: Tamoxifen; TSP: Tissue-specific promoter.

abnormal, and this was attributed to disruption of the erythropoietin-producing hepatocellular (Eph)B gradient on the crypt–villus axis, which would normally provide positional cues for differentiated cells.

In 2005, Andreu and colleagues conducted a separate study to address the same question as Sansom and coworkers, again using a Cre–Lox approach to inactivate *Apc* [40]. In this case however, Cre was expressed under the control of the Villin promoter in the form of a $CreER^{T2}$ fusion protein, requiring exposure to tamoxifen for Cre to become active. This study largely recapitulated the results of Sansom and colleagues, with the description of similar phenotypes of gross expansion of the crypt compartment, migration failure and perturbed differentiation. By using the Villin promoter to drive Cre expression, Andreu and colleagues were additionally able to address the role of *Apc* in mature, differentiated cells of the villus, which was not possible in the Sansom and colleagues study due to the fact that Ah–Cre induces principally within the proliferative compartment. Andreu and colleagues found that differentiated cells were not susceptible to the effects of increased β-catenin signaling, with no change in morphology and failure to re-enter the cell cycle. The authors concluded that their observations (and

Table 1. Summary of conditional models used to study homeostasis and neoplasia in the intestine.

Pathway	Target	Experimental approach(es)	Major intestinal phenotype(s)	Ref.
Wnt	*Apc*	Inducible inactivation of target gene mediated by Ah-Cre	Disruption of normal intestinal architecture; expansion of proliferative compartment; perturbed differentiation of epithelial cell types; failed migration	[39]
		Inducible inactivation of target gene mediated by Villin-CreER^{T2}	Expansion of proliferative compartment; perturbed differentiation; failed migration; no phenotype observed within the postmitotic cell population of the villus	[40]
		Conditional inactivation of target gene mediated by local infection with Cre-encoding adenovirus	Colorectal adenoma development within 3 months; eventual progression to adenocarcinoma	[42]
	β-catenin	Inducible inactivation of target gene mediated by Ah-Cre	Ablation of crypts; detachment of epithelium from underlying stroma	[24]
		Expression of a stable truncation mutant transgene driven by the Fabpl promoter	Abnormal villus branching; increase in apoptosis and mitosis; impaired migration	[46]
		Expression of a stable truncation mutant transgene driven by the Calbindin promoter	Rapid development of numerous dysplastic lesions along the length of the intestine; increased proliferation and apoptosis	[47]
		Inducible stabilization by exon deletion mediated by Ck19-Cre and Fabpl-Cre	Rapid development of large numbers of polyps within the small intestine, but not the colon	[48]
	c-Myc	Conditional inactivation of target gene mediated by Villin-CreER^{T2}	Defective crypt formation during development followed by recovery; no phenotype seen in adult tissue	[50]
		Inducible inactivation of target gene mediated by Ah-Cre	Deletion not tolerated in the adult crypt; crypts are greatly reduced in size and show decreased metabolic activity; epithelium is repopulated with wild-type cells	[51]
	Oct-4	Ectopic expression mediated by a Tet-regulable system	Dysplasia; expansion of proliferative compartment; failed differentiation	[57]
Notch	CSL/RBP-J	Inducible inactivation of target gene mediated by Ah-Cre and Villin-CreER^{T2}	Replacement of cells in transit amplifying zone with mature, differentiated goblet cells; complete loss of proliferative zone	[59]
	Notch-1 receptor	Conditional overexpression of active intracellular domain mediated by Villin-Cre	Lack of secretory cell lineages within the mucosa; expansion of proliferative zone; increased apoptosis; defects in apical surface of enterocytes	[60]
		Inducible overexpression of active intracellular domain mediated by Ah-Cre	Increase in numbers of goblet cells present on villus; increased apoptosis	[61]
TGFβ/BMP	TGF-β type II receptor	Overexpression of dominant negative mutant driven by ITF promoter	Increased susceptibility to colon tumours in response to carcinogen treatment	[63]
	BMPR1a	Inducible inactivation of target gene mediated by Mx1-Cre	Increase in proliferative cells, development of intestinal polyps	[66]
	Noggin	Overexpression of transgene driven by Villin promoter	Abnormal villus structure; development of mislocalised crypt–villus structures; formation of polyps histologically similar to those seen in human JPS	[69]
		Overexpression of transgene driven by Fabpl promoter	Formation of polyps histologically similar to those seen in human JPS	[70]
	SMAD4	Conditional inactivation mediated by mmtv)-Cre and ttr-Cre in epithelia and Lck-Cre and CD4-Cre in T cells	No phenotype when deleted from epithelial cells. T-cell specific deletion leads to formation of polyps histologically similar to those seen in human JPS	[71]
PI3K/Akt	PTEN	Inducible inactivation of target gene mediated by Mx1-Cre	Development of polyps in small intestine; altered Wnt signaling in stem cells, leading to an increase in proliferative intestinal stem cells	[72]
Ras	k-Ras	Overexpression of activated mutant driven by Villin promoter	Rapid development of neoplastic lesions	[74]
		Conditional expression of activated mutant from endogenous promoter mediated by Fabpl-Cre	Hyperplasia and dysplasia; increased proliferation	[75]
		Inducible expression of activated mutant from endogenous promoter mediated by Ah-Cre	No phenotype in adult tissue	[76]

BMP: Bone morphogenic protein; BMPR: Bone morphogenic protein receptor; Cre: Causes recombination; ER: Estrogen receptor; Fabpl: Fatty acid-binding protein, liver; ITF: Intestinal trefoil factor; JPS: Juvenile polyposis syndrome; Lck: Src family protein tyrosine kinase; mmtv: Murine mammary tumor virus; PTEN: Phosphatase and Tensin homolog mutated on chromosome 10; RBP-J: Recombination signal binding protein for immunoglobulin κJ region; SMAD: Mothers against decapentaplegic; Tet: Tetracycline; TGF: Transforming growth factor; ttr: Transthyretin.

indeed those of Sansom and colleagues) support the 'bottom-up' hypothesis of intestinal tumorigenesis, which proposes that early adenoma initiation occurs within the crypt, with spreading of the adenoma in an upwards manner [41].

In order to address the fact that most mouse models of *Apc* deficiency predominantly develop small intestinal tumors rather than the colorectal lesions more commonly seen in humans, attempts have been made to generate models that more accurately recapitulate the human tumor distribution. Shibata and colleagues used a Cre–Lox approach to delete exon 14 of the *Apc* gene specifically from the colon and rectum by local infection with a recombinant adenovirus encoding the Cre recombinase [42]. Although the incidence of adenoma formation was somewhat low using this approach, this strategy modeled the tumor distribution observed in human colorectal FAP more accurately, with recombination leading to colorectal adenoma formation within 3 months and progression to adenocarcinoma at later time points. The findings of this study have also been recapitulated more recently using a similar model [43].

β-catenin

β-catenin is a multifunctional protein, playing multiple cellular roles. It is involved in cell adhesion through interaction with α-catenin and the cadherins [44]. Importantly for intestinal homeostasis, it is also one of the major effectors of the Wnt pathway, acting in a complex with Tcf-4 to promote transcription of Wnt target genes [45].

A number of conditional strategies have been used to study the role of β-catenin in the intestine. Ireland and colleagues conditionally deleted β-catenin from the epithelium using the Ah–Cre–Lox approach described previously [24]. This study demonstrated that deficiency in β-catenin results in a loss of crypt structures and detachment of enterocytes from the villus. This confirms an absolute requirement of β-catenin for maintenance of the crypt proliferative compartment and shows that it is also required for adequate cell adhesion within the intestinal epithelium.

In other earlier studies, β-catenin was stabilized by either truncation of the protein [46,47] or exon deletion [48], both resulting in loss of phosphorylation sites that would normally target the protein for degradation, allowing the protein to accumulate in the cytoplasm and translocate to the nucleus. Wong and coworkers generated a line expressing an N-terminal truncation mutant of β-catenin (ΔN89) as a transgene from the rat fatty-acid binding protein, liver (Fabpl) promoter, allowing intestinal-specific expression [46]. Expression of β-cateninΔN89 had previously been shown to simulate Wnt pathway activation in both *Drosophila* and *Xenopus*. This truncated form of β-catenin lacks a number of residues that are normally phosphorylated by GSK-3β to target the protein for ubiquitination and subsequent proteasomal degradation. As the mutant protein cannot be phosphorylated by GSK-3β, it is not degraded and accumulates within the cell. The intestinal phenotype of expression of this construct was found to be rather subtle. Intestinal defects included abnormal branching of villus structures, along with an increase in both mitotic index and apoptosis within the mucosa. Although no changes in the differentiation program of precursor cells were observed, the migration of epithelial cells was found to be impaired in areas of transgene expression, a phenotype similar to that seen in conditional *Apc*-deficient adult tissue [39,40]. Surprisingly, neoplastic development within the epithelium was not observed in the course of this study. The authors suggest that this may be attributed to the fact that epithelial cells retain normal levels of *Apc* expression.

A further study by Romagnolo and colleagues used a strain expressing a similar N-terminal truncated form of β-catenin (ΔN131); however, in this case expression was driven from the promoter of the calbindin gene, with additional enhancer elements derived from the aldolase B promoter sequence [47]. The mutant form of β-catenin was found to be strongly expressed along the length of the small and large intestine, and also in the cecum and kidney. Mice were sacrificed at 4 weeks of age owing to morbidity and, in dramatic contrast to the previous study, necropsy revealed numerous dysplastic lesions in the small intestine. The distribution and histological appearance of lesions within the small intestine were described as being reminiscent of early intestinal lesions found in *Apc* heterozygous mice and were found to display increased proliferation and increased apoptosis, again similar to *Apc*-deficient lesions. It was concluded that the contrasting phenotypes observed between this study and that of Wong and colleagues may be attributed to a number of differences in experimental approach, including different expression patterns of the relative transgenes within the intestine, as well as differences in the exact forms of truncated β-catenin used.

In one further study, Harada and colleagues generated a novel β-catenin allele that bears LoxP sites flanking exon 3 of the endogenous gene [48]. Recombination between LoxP sites causes deletion of exon 3, leading to the generation of messenger (m)RNA in which exon 4 directly follows exon 2, although the reading frame of the transcript is maintained. Translation of this mRNA produces a mutant form of β-catenin protein lacking 76 amino acids, four of which are phosphorylation target sites of GSK-3β. Mouse lines bearing the mutant form of β-catenin were generated and crossed to lines expressing Cre constitutively in the intestine either under the control of the cytokeratin (Ck)19 or Fabpl promoters. Both types of compound mutants were found to develop large numbers of small intestinal polyps at a young age, with polyp density being highest at the proximal (stomach) end, gradually decreasing along the length of the small intestine. In both strains, virtually no lesions were found in the colon, concurring with previous observations [47]. Polyps were found to strongly express the mutant form of β-catenin, whereas adjacent normal tissue did not, suggesting that polyp formation occurred in virtually every location where the mutant protein was expressed in the small intestine. This was in contrast to the large intestine where, even though mutant β-catenin expression was detected, essentially no lesions were found. Polyps from Fabpl–Cre-mediated mutants were further analyzed and again found to be histologically similar to polyps observed previously in *Apc* mutant mice. Immunohistochemistry against cyclooxygenase

(COX)-2 also revealed stromal staining patterns comparable with those seen in *Apc*-deficient adenomas. The authors compare their contrasting phenotype with that of Wong and colleagues, and explain that the differences in phenotype observed are probably due to lower expression levels of mutant β-catenin in the Wong and colleagues' study compared with this study, which allows mutant β-catenin to be expressed from its endogenous promoter.

The similarities in phenotype observed among the studies of stable mutants of β-catenin and those of conditional deletion of *Apc* clearly imply that β-catenin is one of, if not the only, key downstream effector of *Apc*-mediated tumor suppression. It could be argued that loss of *Apc* and stabilization of β-catenin are equivalent in the intestine, with both resulting in nuclear accumulation of β-catenin and increased transcription of Wnt target genes. However, we see from the aforementioned examples that some differences in phenotype do exist. It remains to be clarified whether these differences observed are due to non-equivalence of *Apc* deletion and β-catenin stabilization or whether the differences are due to non-Wnt-related roles played by each protein in tumorigenesis.

c-Myc

c-Myc has been shown to be an *in vivo* target of the Wnt signaling pathway through analysis of both normal crypts [49] and of *Apc*-deficient tissue [39]. Studies in colorectal cancer cell lines have shown that *c-Myc* plays a vital role in maintenance of proliferative precursor cells [49]. Based on these observations, it could be predicted that *c-Myc* might play a critical role in maintenance of the intestinal epithelium. Two recent studies have aimed to address this hypothesis through conditional deletion of *c-Myc* using a Cre–Lox approach.

Bettess and colleagues conditionally deleted *c-Myc* from both the developing and the adult intestinal epithelium using a Villin–CreER^{T2} system, where treatment with tamoxifen allows Cre activation and excision of exons 2 and 3 of targeted *c-Myc* alleles [50]. Loss of *c-Myc* was induced before complete intestinal architecture had developed, at postnatal day (P) 7. Histological analysis of intestines from these animals culled at day 6 after induction revealed areas showing widespread defects in crypt structure formation compared with controls, suggesting that *c-Myc* is absolutely required for crypt invagination. However, this effect was found to be transient and mice were able to recover and showed normal intestinal histology by day 10 after induction. Adult mice with induced *c-Myc* deficiency were also assessed. In stark contrast to its predicted role in the intestine, it was found that *c-Myc* deficiency does not affect proliferation, differentiation or the apoptotic response of the epithelium. It was therefore argued that there may be a compensatory mechanism involving other *Myc* family members that operates following *c-Myc* deletion or that a *c-Myc*-independent homeostatic program must exist within the intestine.

The requirement for *c-Myc* has been further studied by Muncan and colleagues, who used the Ah–Cre system to delete *c-Myc* with high efficiency within adult crypts [51]. In marked contrast to the study of Bettess and colleagues, this study found that deletion of *c-Myc* in the adult crypt was not tolerated, resulting in replacement of mutant crypts with wild-type crypts by day 28 post induction. Early analysis of *c-Myc*-deficient crypts (before replacement of mutant crypts) revealed them to be much smaller than their wild-type counterparts, with a fourfold reduction in cell number per crypt. The size of *c-Myc*-deficient cells was also found to be smaller and cells showed reduced metabolic activity compared with controls. No changes in apoptotic levels were found following *c-Myc* deletion. Finally, although loss of *c-Myc* was not found to alter the proliferation state of cells within the crypt, the cell-cycle rate was slower, leading to slowed migration of cells out of the crypt compartment. These findings clearly contrast those of Bettess and colleagues, suggesting that *c-Myc* is indeed required for the maintenance of proliferative cells within the crypt. The most likely explanation offered by the authors for this contrast in phenotype is that the differences relate to the efficiency with which *c-Myc* is deleted from the epithelium, which is a direct result of the contrasting expression patterns of the Cre transgenes used.

A recent study has addressed the role of *c-Myc* in tumorigenesis within the *Apc*$^{min/+}$ mouse [52]. This study constitutively deleted *c-Myc* from the intestinal epithelium of *Apc*$^{min/+}$ mice through use of Fabpl–Cre. The finding that *c-Myc*-deficient intestines were morphologically normal in this study corroborates the data of Bettess and colleagues; however, this study also found an increase in apoptosis in *c-Myc*-deficient regions, which is in contrast to both previous studies. Small intestinal tumorigenesis of *Apc*$^{min/+}$ mice was found to be significantly reduced in mice additionally deficient for *c-Myc* compared with controls. This observation most likely concurs with those of Muncan and colleagues, and suggests that *c-Myc*-deficient cells have a reduced proliferative capacity compared with wild-type controls. Finally, Sansom and colleagues have used the Ah–Cre system to simultaneously delete both *Apc* and *c-Myc* from the epithelium [53]. This study confirms an absolutely critical role for *c-Myc* in Wnt-mediated tumorignenesis, as the immediate phenotype of *Apc* deficiency is completely repressed in the absence of *c-Myc*.

These studies confirm *c-Myc* as a key player in intestinal tumorigenesis. However, its role in normal intestinal homeostasis is less clear, with conflicting data emerging from the different models used. Such differences in phenotype may well reflect differences in the experimental systems used, an issue that clearly now needs to be addressed within the field.

Oct-4

The Pit-1, Oct-1/2 and Unc-86 domain transcription factor Octamer (Oct)-4 has previously been shown to be necessary for the maintenance of stem cell pluripotency [54]. Given the importance of the Wnt pathway in maintenance of the stem cell compartment, it seems likely that the effects of Oct-4 and the Wnt pathway may be linked. Evidence in both zebrafish [55] and mouse and human embryonic stem cells [56] has further suggested that Oct-4 may be a regulatory factor upstream of the Wnt pathway.

In the intestine, recent work has suggested support for this hypothesis in mammalian systems. Hochedlinger and colleagues have generated a Tet-regulable system to ectopically express Oct-4 in epithelial cells upon administration of doxycycline [57]. This resulted in a phenotype of striking similarity to that observed by Sansom and colleagues following deletion of *Apc* [39]. Areas of dysplasia were found to contain abnormal crypts with a greatly expanded proliferative cell compartment coupled with failure of progenitor cells to differentiate normally. Oct-4 expression was also strongly associated with nuclear localization of β-catenin. The observed phenotypes were found to be completely reversible following withdrawal of doxycycline treatment, indicating dependence of these phenotypes on continued Oct-4 expression. The authors therefore tentatively hypothesize that in adult proliferative progenitor cells, Oct-4 acts to maintain the immature progenitor state through upregulation of β-catenin. Ectopic expression of Oct-4 or activation of the Wnt pathway would therefore lead to both the crypt progenitor phenotype described here and previously [39].

Notch pathway

The Notch pathway has been shown to play an important role in both embryonic development and the adult homeostasis of a number of different organ systems. It has been implicated in the regulation of processes such as proliferation, stem cell maintenance, cell fate specification and differentiation programs, and therefore plays a particularly pertinent role in self-renewing tissues [58].

One of the first studies that demonstrated an absolute requirement of Notch signaling for *in vivo* intestinal homeostasis was that of van Es and colleagues [59]. The critical Notch pathway transcription factor CSL/recombination signal binding protein for immunoglobulin κ J region was targeted with LoxP sites and deleted in adult intestinal epithelium using both Ah–Cre and Villin–CreER^{T2}. Deletion mediated by either Cre-expressing transgene resulted in identical, highly penetrant phenotypes of the replacement of transit amplifying cells with mature, fully differentiated goblet cells. Loss of the transit amplifying compartment was confirmed by Ki-67 staining and bromodeoxyuridine incorporation, which both revealed a marked deficiency in replicating cells. Paneth cell and enteroendocrine cell frequency was found to be unchanged, suggesting a skew in the differentiation program towards the secretory cell lineages of the epithelium. Therefore, these observations indicate that Notch signaling is required for both maintenance of the transit amplifying compartment in an undifferentiated state, and also for maturation of the absorptive cell lineage. This study also went on to treat adenomas arising in *Apc*$^{min/+}$ mice with a γ-secretase inhibitor, dibenzazepine, which blocks Notch pathway signaling. Dibenzazepine treatment led to goblet cell conversion of a subset of cells within the adenoma, forcing them into a postmitotic state. However, similar changes were also observed within surrounding normal intestinal epithelium, which limited treatment studies. Therefore, if Notch inhibition were to be pursued as a potential therapeutic strategy, a method of targeting it specifically to tumors and not normal epithelium would need to be devised.

In a reverse approach, Fre and colleagues examined the effect of increased Notch signaling by overexpression of a constitutively active intracellular domain of the Notch-1 receptor (n1ic) specifically in the intestine, by use of Villin–Cre and a Rosa26–n1ic construct [60]. The Rosa26 promoter is strongly expressed in all tissues of the mouse; however, in this case a LoxP-flanked STOP cassette was present in the transgene, preventing expression of n1ic in tissues lacking active Cre recombinase. As would be expected, this study essentially observed a reciprocal phenotype to that seen by van Es and colleagues; transgenic mice became moribund at the very early stage of day 3 post Cre induction. Examination of intestines for differentiated cell types revealed a complete lack of secretory cell lineages, with no staining for markers of goblet cells or enteroendocrine cells, and no expression of Paneth cell markers. The proliferative compartment of the epithelium was also found to expand significantly and an increase in apoptosis within the villus was observed. In addition, this study observed defects in the apical surface of absorptive cells, with poor organization and lower frequency of microvilli comprising the brush border. In summary, the results reported in this study support those of van Es and colleagues, with opposing genetic manipulation of the Notch pathway resulting in an almost exact reversal of phenotype.

One further study used a similar Rosa26 promoter construct to conditionally overexpress a form of activated Notch-1 receptor, again consisting of only the intracellular domain of the protein [61]. In this case, recombination and expression of the transgene was achieved by induction of Ah–Cre. Surprisingly, the phenotype observed more closely resembled that of van Es and colleagues, and not Fre and colleagues as would be expected. A dramatic increase in the numbers of goblet cells was observed; however, in this case the location of these cells was within the postmitotic cells of the villus, as opposed to the transit amplifying cells of the crypt, as seen in the previous study. Some aspects of the phenotype did resemble that observed by Fre and colleagues, such as an increase in levels of apoptosis following Notch-1 overexpression. In contrast to both previous studies, no changes in the frequency of enteroendocrine cells or Paneth cells, or in the size or location of the proliferative zone within the crypt were reported. The differences between this study and that of Fre and colleagues were most probably due to two differences in experimental approach; first, in this study recombination (and therefore overexpression of mutant Notch-1) was achieved in a much more efficient manner than that of Fre and colleagues, and second, this study overexpressed Notch-1 in adult, fully developed epithelium, compared with the previous study where expression was induced at very early stages of intestinal development.

This study, combined with the findings of van Es and colleagues, suggests a dose dependency of Notch signaling for normal differentiation patterns within the adult intestine, with both too much and too little Notch signaling resulting in a default differentiation program of precursor cells into goblet cells.

Transforming growth factor-β & bone morphogenic protein signaling

Transforming growth factor (TGF)-β signaling is involved in the regulation of a number of diverse processes, including proliferation and cell differentiation. Disruption of TGF-β signaling has been implicated in human colorectal cancers, particularly in the progression of tumors from benign growths to invasive cancers [62]. One study has examined the effect of loss of TGF-β signaling on carcinogenesis in the mouse intestine. Hahm and colleagues achieved this by generating a dominant negative mutant of the TGF-β Type II receptor [63]. This was then expressed specifically in the intestine under the control of the intestinal trefoil factor promoter, which constitutively expresses within the epithelial compartment. As TGF-β signaling is implicated in tumor progression rather than initiation, mice were treated with a low dose of the carcinogen azoxymethane in order to promote intestinal tumor formation. It was found that mice lacking TGF-β signaling were much more susceptible to colon tumor formation compared with control littermates, showing an increase in both the formation of aberrant crypt foci as well as colon carcinoma. These data therefore demonstrate the clear role of TGF-β signaling in cancer progression and suggest that this pathway must be maintained in order to prevent carcinogenesis.

Bone morphogenic proteins (BMPs) are members of the TGF-β family of proteins and BMP signaling is thought to play a role in maintenance of the intestinal epithelium through interaction with the underlying mesenchyme [64]. The role of this pathway in the regulation of intestinal homeostasis is exemplified by the human disease juvenile polyposis syndrome (JPS), characterized by the development of numerous intestinal polyps at a very young age, which has in many cases been associated with mutation of BMP receptor (Bmpr)1A subtype or of a downstream transcription factor of the pathway, SMAD4 [65].

Conditional disruption of the BMP pathway in adult mice has gone some way to modeling human JPS. He and colleagues generated a LoxP-targeted *Bmpr1a* allele, which was inactivated specifically in the intestine following pI–pC administration causing induction of Mx1–Cre [66]. Disruption of BMP signaling was found to cause an increase in the number of proliferative cells within the epithelium, and all mutant mice subsequently developed intestinal polyps, which showed similar histology to human JPS polyps. An increased number of cells expressing stem cell markers were also found in *Bmpr1a* mutant crypts. Further analysis of mutant intestinal epithelium led the authors to hypothesize that BMP signaling plays a role in suppressing intestinal stem cell replication and that attenuation of BMP signaling is necessary for full activation of Wnt signaling and thus renewal of the stem cell. This hypothesis has, however, been the subject of some debate [67,68].

A further study investigating the effect of BMP signal abrogation on the intestinal epithelium made use of a gut-specific transgene constitutively expressing the BMP inhibitor, noggin [69]. A transgene consisting of the *Xenopus* noggin complementary DNA under the control of the mouse Villin promoter was generated. Mice bearing the transgene were found to have marked abnormalities of the intestinal epithelium at a young age. At 4 weeks of age, transgenic intestines were found to contain villi that were abnormally broad at the base of the structure and had abnormal invaginations of proliferative epithelial cells. At 12 weeks after birth, these abnormal invaginations had developed into complete crypt–villus units, which had grown perpendicular to the original crypt–villus axis and contained a proliferative zone and differentiated cell types, comparable with that of normal crypt structures. When allowed to age to 6–8 months, transgenic mice developed polyps that were characterized by a complex arrangement of branched epithelium interspersed with dilated cystic structures. The authors describe the histological appearance of these polyps as being typical of that observed in human JPS lesions. Based on the observation that epithelium lacking BMP signaling develops normally but ectopically, it is proposed that BMP signaling mediates interaction between the epithelium and underlying mesenchyme to ensure that crypt–villus structures only develop within the correct context. A separate study, in this case of *Xenopus* noggin under the control of the Fabpl promoter, has supported these findings [70].

The BMP pathway downstream transcription factor SMAD4 is also implicated in human JPS. A recent study has detailed the consequences of Cre-mediated inactivation of *Smad4* in both the gastrointestinal (GI) tract epithelium and in T cells [71]. *Smad4* deletion was achieved in a broad range of epithelia by use of Cre under the control of either the murine mammary tumor virus promoter (Mmtv)–Cre) or the transthyretin promoter (Ttr–Cre). Although loss of *Smad4* was confirmed in both systems, neither showed evidence of epithelial tumorigenesis in the course of the study. However, in dramatic contrast to this, T-cell-specific deletion of *Smad4* (mediated by Lck–Cre or CD4–Cre) resulted in a number of abnormalities in GI epithelia. In the small and large intestine, a phenotype highly reminiscent of that seen by Haramis and colleagues and Batts and colleagues was seen, with epithelial cells growing into the stroma and the presence of numerous cystic structures. Tumors were found to progress to invasive carcinomas, which also gave rise to distant metastases, again described as consistent with phenotypes observed in human hereditary JPS. The findings of this study therefore imply that although *Smad4* appears to be redundant within epithelial cells, normal BMP signaling within T cells is required for suppression of GI epithelial tumors.

Other pathways

Numerous other signaling pathways have been implicated in human colorectal tumorigenesis. This has prompted the investigation of a number of pathways that are not classically considered a vital for normal intestinal homeostasis, but clearly play a role in tumor suppression within the intestine.

The phosphoinositide 3-kinase (PI3K)–Akt pathway has previously been proposed as a mediator between the Wnt and BMP pathways in the intestine [66]. Indeed, a recent paper has examined the consequences of increased PI3K–Akt signaling on intestinal homeostasis through deletion of the pathway antagonist

and tumor suppressor PTEN (Phosphatase and Tensin homolog mutated on chromosome 10). He and colleagues deleted PTEN specifically in the epithelial and stromal cells of the adult intestine through use of conditional *PTEN* alleles and Mx1–Cre [72]. Mice were found to quickly develop multiple polyps within the small intestine following induction of PTEN loss. Further analysis went on to suggest a role for PTEN, through modulation of the PI3K–Akt pathway, in regulating activation of Wnt signaling in the intestinal stem cell, and therefore modulating the replicative capacity of the intestinal stem cell. Thus, *PTEN* loss was shown to result in an excess of proliferative intestinal stem cells within the crypt.

However, recent findings in our own laboratory have indicated that *PTEN* deletion specifically within the epithelial cell population of the intestine does not result in an overt phenotype [MARSH ET AL., SUBMITTED]. This is in contrast to the phenotype observed in this study, which arises following PTEN deletion in both the stromal and epithelial compartments. These observations raise the tantalizing hypothesis that the tumor-suppressor function of PTEN within the intestine is cell-type specific and also emphasize the importance of stromal–epithelial interactions in maintaining homeostasis.

The Ras pathway, which also plays a role in modulation of the PI3K–Akt signaling cascade, is implicated in colorectal tumorigenesis, with up to 50% of human colorectal cancers showing oncogenic activation of kirsten–Ras (k-Ras) [73]. Overexpression of an activated mutant of k-Ras specifically within the intestine under the control of the Villin promoter has previously been shown to lead to rapid formation of neoplastic intestinal lesions [74]. However, it has been argued that this is not an accurate model of human tumorigenesis, owing to the fact that human tumors rarely show overexpression of k-Ras but more often display normal expression levels of mutant proteins. This has led to studies in which mutant k-Ras is expressed under the control of its endogenous promoter. Tuveson and colleagues have generated mice harboring a floxed-STOP form of mutant k-Ras, which is conditionally expressed from its endogenous promoter following Cre-mediated excision of the STOP cassette [75]. When crossed with cytomegalovirus–Cre, which is mosaically expressed throughout development, mice were not viable, indicating that activated k-Ras is not tolerated during development. Expression of the activated k-Ras allele was also induced specifically in the developing and adult GI tract through use of the Fabp–Cre construct. This was shown to lead to intestinal hyperplasia in all mutant mice analyzed, with a marked increase in proliferation in hyperplastic and dysplastic areas. In contrast to this, another study has shown that activation of k-Ras within the adult epithelium specifically does not result in disruption of normal intestinal homeostasis [76]. However, when combined with *Apc* mutation, this study shows that active k-Ras significantly accelerates intestinal tumorigenesis and drives progression to adenocarcinoma. These data therefore suggest that k-Ras is important both for the developing intestinal epithelium and in intestinal tumors, but is perhaps redundant in the fully developed adult epithelium.

Since the development of the first transgenic strains of mice, there has been a revolution in our capacity to manipulate the genome of the mouse and so begin to understand the true *in vivo* consequences of gene function. Approaches based upon addition transgenics and constitutive knockouts have proven extremely valuable in reaching these goals but are limited in certain respects, for example, owing to embryonic lethality. The development of conditional strategies has given researchers the ability to delete genes in a more controlled manner, both spatially and temporally. In this review, we have summarized the major strategies currently in use in the intestine and have illustrated their use with respect to several major pathways. These approaches have given startling new insights into both normal and disease physiology and have established the intestine as a paradigm system for the analysis of genotype–phenotype relationships.

Expert commentary

Recent technical advances have now made it possible to genetically manipulate the intestine. First, there is an ever increasing battery of conventional transgenics that over- or misexpress a given gene. Although this now represents a fairly unsophisticated approach, with no true control over the level of transgene expression, such models are still capable of revealing important insights, for example in establishing the role of individual genes in crypt development. The more refined use of knockout mice has greatly extended our analytical power, allowing *in vivo* analysis of loss of function. Although knockout technology is currently dominant within the field, it still suffers from a number of caveats that have precluded the study of many genes within the intestine. The more recent advent of conditional strategies has given the field new impetus, extending both the genes that can be analyzed and the range of questions that can now be addressed. Taken together, these strategies are building a comprehensive genetic understanding of the intestine, one that is principally focused upon the crypt–villus axis of the small intestine.

Five-year view

This review highlights a range of techniques used to modify the mouse genome in a spatially and/or temporally controlled manner. This means that we are now theoretically capable of introducing any mutation of choice into any cell of choice at any desired time. However, the theoretical capacity to achieve this does not yet equate to the practical situation. To gain such fine control over gene expression *in vivo* remains remarkably technically challenging, and indeed the current state of the art remains limited to a number of systems within the intestine. However, these have proved remarkably powerful in revealing true phenotype–genotype relationships and disease mechanisms, as well as identifying novel therapeutic targets. The way forward has to be through increased refinement of these systems to generate increasingly accurate models of normal and diseased physiology. For example, we now need to develop models in which the genetics of adjacent cells can be independently controlled and so allow a determination of the

importance of cell–cell interactions. We also need to develop the capacity to specifically target gene manipulation to tumors in order to model therapeutic treatment. Finally, models need to be generated in which we control not only the genome, but where we begin to control the kinome, methylome, proteome and glycome. Such modeling will be challenging to achieve, but remains the only true way of understanding both normal and diseased physiology.

Key issues

- Modeling in the mouse using constitutive overexpression and knockout approaches has proven very powerful, but can be limited due to lack of spatial and temporal control over gene expression.
- The development of conditional strategies, based upon causes recombination-locus of crossover (Cre-Lox), Flp-Frt and use of tetracycline- and estrogen-dependent systems, has largely obviated these difficulties.
- Conditional strategies have been used to show that activation of the Wnt pathway through loss of *Apc* confers a dramatic phenotype upon the intestine, revealing the key cellular consequences of Wnt activation.
- Conditional deletion of the Wnt pathway components β-catenin and c-*Myc* shows them to play key roles in both tumorigenesis and normal intestinal homeostasis.
- Different experimental approaches can however yield slightly different results, for example, following c-*Myc* deficiency.
- Conditional deregulation of the Notch pathway changes cell fate in the small intestine, specifically in relation to secretary cells.
- Conditional activation of the Ras pathway through mutation of kirsten-Ras accelerates intestinal tumorigenesis, although again different experimental systems show somewhat different effects.
- Conditional activation of the phosphoinositide 3-kinase–Akt pathway also predisposes to intestinal neoplasia, but again different experimental approaches are identifying subtleties in this association.

References

Papers of special note have been highlighted as:
• of interest
•• of considerable interest

1 Moser AR, Pitot HC, Dove WF. A dominant mutation that predisposes to multiple intestinal neoplasia in the mouse. *Science* 247(4940), 322–324 (1990).

• **First characterisation of the *Apc*$^{min/+}$ mouse, which carries a point mutation in the *Apc* gene and is predisposed to intestinal polyp formation.**

2 Su LK, Kinzler KW, Vogelstein B *et al.* Multiple intestinal neoplasia caused by a mutation in the murine homolog of the *APC* gene. *Science* 256(5057), 668–670 (1992).

3 Shoemaker AR, Gould KA, Luongo C, Moser AR, Dove WF. Studies of neoplasia in the Min mouse. *Biochim. Biophys. Acta* 1332(2), F25–F48 (1997).

4 Sansom OJ, Stark LA, Dunlop MG, Clarke AR. Suppression of intestinal and mammary neoplasia by lifetime administration of aspirin in *Apc*(Min/+) and *Apc*(Min/+), Msh2(-/-) mice. *Cancer Res.* 61(19), 7060–7064 (2001).

5 Boolbol SK, Dannenberg AJ, Chadburn A *et al.* Cyclooxygenase-2 overexpression and tumor formation are blocked by sulindac in a murine model of familial adenomatous polyposis. *Cancer Res.* 56(11), 2556–2560 (1996).

6 Giardiello FM, Yang VW, Hylind LM *et al.* Primary chemoprevention of familial adenomatous polyposis with sulindac. *N. Engl. J. Med.* 346(14), 1054–1059 (2002).

7 Clarke AR, Gledhill S, Hooper ML, Bird CC, Wyllie AH. p53 dependence of early apoptotic and proliferative responses within the mouse intestinal epithelium following γ-irradiation. *Oncogene* 9(6), 1767–1773 (1994).

8 Christophorou MA, Ringshausen I, Finch AJ, Swigart LB, Evan GI. The pathological response to DNA damage does not contribute to p53-mediated tumour suppression. *Nature* 443(7108), 214–217 (2006).

9 Lewandoski M. Conditional control of gene expression in the mouse. *Nat. Rev. Genet.* 2(10), 743–755 (2001).

10 Bullard DC, Weaver CT. Cutting-edge technology: IV. Genomic engineering for studies of the gastrointestinal tract in mice. *Am. J. Physiol. Gastrointest. Liver Physiol.* 283(6), G1232–G1237 (2002).

11 Garcia EL, Mills AA. Getting around lethality with inducible Cre-mediated excision. *Semin. Cell Dev. Biol.* 13(2), 151–158 (2002).

12 Ryding AD, Sharp MG, Mullins JJ. Conditional transgenic technologies. *J Endocrinol.* 171(1), 1–14 (2001).

13 Pinto D, Robine S, Jaisser F, El Marjou FE, Louvard D. Regulatory sequences of the mouse Villin gene that efficiently drive transgenic expression in immature and differentiated epithelial cells of small and large intestines. *J. Biol. Chem.* 274(10), 6476–6482 (1999).

14 Schweinfest CW, Jorcyk CL, Fujiwara S, Papas TS. A heat-shock-inducible eukaryotic expression vector. *Gene* 71(1), 207–210 (1988).

15 Hu MC, Davidson N. A combination of derepression of the lac operator-repressor system with positive induction by glucocorticoid and metal ions provides a high-evel-inducible gene expression system based on the human metallothionein-IIA promoter. *Mol. Cell Biol.* 10(12), 6141–6151 (1990).

16 Abremski K, Hoess R. Bacteriophage P1 site-specific recombination. Purification and properties of the Cre recombinase protein. *J. Biol. Chem.* 259(3), 1509–1514 (1984).

17 Hoess RH, Ziese M, Sternberg N. P1 site-specific recombination: nucleotide sequence of the recombining sites. *Proc. Natl Acad. Sci. USA* 79(11), 3398–3402 (1982).

18 Sternberg N, Hamilton D. Bacteriophage P1 site-specific recombination. I. Recombination between loxP sites. *J. Mol. Biol.* 150(4), 467–486 (1981).

19 Lakso M, Sauer B, Mosinger B Jr *et al.* Targeted oncogene activation by site-specific recombination in transgenic mice. *Proc. Natl Acad. Sci. USA* 89(14), 6232–6236 (1992).

20 Madison BB, Dunbar L, Qiao XT, Braunstein K, Braunstein E, Gumucio DL. Cis elements of the Villin gene control expression in restricted domains of the vertical (crypt) and horizontal (duodenum, cecum) axes of the intestine. *J. Biol. Chem.* 277(36), 33275–33283 (2002).

21 el Marjou F, Janssen KP, Chang BH *et al.* Tissue-specific and inducible Cre-mediated recombination in the gut epithelium. *Genesis* 39(3), 186–193 (2004).

22 Saam JR, Gordon JI. Inducible gene knockouts in the small intestinal and colonic epithelium. *J. Biol. Chem.* 274(53), 38071–38082 (1999).

23 Kuhn R, Schwenk F, Aguet M, Rajewsky K. Inducible gene targeting in mice. *Science* 269(5229), 1427–1429 (1995).

24 Ireland H, Kemp R, Houghton C *et al.* Inducible Cre-mediated control of gene expression in the murine gastrointestinal tract: effect of loss of β-catenin. *Gastroenterology* 126(5), 1236–1246 (2004).

25 Campbell SJ, Carlotti F, Hall PA, Clark AJ, Wolf CR. Regulation of the CYP1A1 promoter in transgenic mice: an exquisitely sensitive on-off system for cell specific gene regulation. *J. Cell Sci.* 109 (Pt 11), 2619–2625 (1996).

26 Schneider A, Zhang Y, Guan Y, Davis LS, Breyer MD. Differential, inducible gene targeting in renal epithelia, vascular endothelium, and viscera of Mx1Cre mice. *Am. J. Physiol. Renal Physiol.* 284(2), F411–F417 (2003).

27 Metzger D, Clifford J, Chiba H, Chambon P. Conditional site-specific recombination in mammalian cells using a ligand-dependent chimeric Cre recombinase. *Proc. Natl Acad. Sci. USA* 92(15), 6991–6995 (1995).

28 Feil R, Brocard J, Mascrez B, LeMeur M, Metzger D, Chambon P. Ligand-activated site-specific recombination in mice. *Proc. Natl Acad. Sci. USA* 93(20), 10887–10890 (1996).

29 Feil R, Wagner J, Metzger D, Chambon P. Regulation of Cre recombinase activity by mutated estrogen receptor ligand-binding domains. *Biochem. Biophys. Res. Commun.* 237(3), 752–757 (1997).

30 Kemp R, Ireland H, Clayton E, Houghton C, Howard L, Winton DJ. Elimination of background recombination: somatic induction of Cre by combined transcriptional regulation and hormone binding affinity. *Nucleic Acids Res.* 32(11), E92 (2004).

31 Thyagarajan B, Guimaraes MJ, Groth AC, Calos MP. Mammalian genomes contain active recombinase recognition sites. *Gene* 244(1–2), 47–54 (2000).

32 Senecoff JF, Bruckner RC, Cox MM. The FLP recombinase of the yeast 2-micron plasmid: characterization of its recombination site. *Proc. Natl Acad. Sci. USA* 82(21), 7270–7274 (1985).

33 Gossen M, Bonin AL, Bujard H. Control of gene activity in higher eukaryotic cells by prokaryotic regulatory elements. *Trends Biochem. Sci.* 18(12), 471–475 (1993).

34 Gossen M, Bujard H. Tight control of gene expression in mammalian cells by tetracycline-responsive promoters. *Proc. Natl Acad. Sci. USA* 89(12), 5547–5551 (1992).

35 Gossen M, Freundlieb S, Bender G, Muller G, Hillen W, Bujard H. Transcriptional activation by tetracyclines in mammalian cells. *Science* 268(5218), 1766–1769 (1995).

36 Clarke AR. Wnt signalling in the mouse intestine. *Oncogene* 25(57), 7512–7521 (2006).

37 Clevers H. Wnt/β-catenin signaling in development and disease. *Cell* 127(3), 469–480 (2006).

38 Moser AR, Shoemaker AR, Connelly CS *et al.* Homozygosity for the Min allele of *Apc* results in disruption of mouse development prior to gastrulation. *Dev. Dyn.* 203(4), 422–433 (1995).

39 Sansom OJ, Reed KR, Hayes AJ *et al.* Loss of *Apc in vivo* immediately perturbs Wnt signaling, differentiation, and migration. *Genes Dev.* 18(12), 1385–1390 (2004).

•• **Description of the immediate consequences of *Apc* loss using an inducible Cre–Lox approach.**

40 Andreu P, Colnot S, Godard C *et al.* Crypt-restricted proliferation and commitment to the Paneth cell lineage following *Apc* loss in the mouse intestine. *Development* 132(6), 1443–1451 (2005).

•• **A second paper addressing the immediate consequences of *Apc* loss.**

41 Preston SL, Wong WM, Chan AO *et al.* Bottom-up histogenesis of colorectal adenomas: origin in the monocryptal adenoma and initial expansion by crypt fission. *Cancer Res.* 63(13), 3819–3825 (2003).

42 Shibata H, Toyama K, Shioya H *et al.* Rapid colorectal adenoma formation initiated by conditional targeting of the *Apc* gene. *Science* 278(5335), 120–123 (1997).

43 Colnot S, Niwa-Kawakita M, Hamard G *et al.* Colorectal cancers in a new mouse model of familial adenomatous polyposis: influence of genetic and environmental modifiers. *Lab. Invest.* 84(12), 1619–1630 (2004).

44 Lilien J, Balsamo J. The regulation of cadherin-mediated adhesion by tyrosine phosphorylation/dephosphorylation of β-catenin. *Curr. Opin. Cell Biol.* 17(5), 459–465 (2005).

45 Wong NA, Pignatelli M. β-catenin-a linchpin in colorectal carcinogenesis? *Am. J. Pathol.* 160(2), 389–401 (2002).

46 Wong MH, Rubinfeld B, Gordon JI. Effects of forced expression of an NH_2-terminal truncated β-catenin on mouse intestinal epithelial homeostasis. *J. Cell Biol.* 141(3), 765–777 (1998).

47 Romagnolo B, Berrebi D, Saadi-Keddoucci S *et al.* Intestinal dysplasia and adenoma in transgenic mice after overexpression of an activated β-catenin. *Cancer Res.* 59(16), 3875–3879 (1999).

48 Harada N, Tamai Y, Ishikawa T *et al.* Intestinal polyposis in mice with a dominant stable mutation of the β-catenin gene. *EMBO J.* 18(21), 5931–5942 (1999).

49 van de Wetering M, Sancho E, Verweij C *et al.* The β–catenin/TCF-4 complex imposes a crypt progenitor phenotype on colorectal cancer cells. *Cell* 111(2), 241–250 (2002).

50 Bettess MD, Dubois N, Murphy MJ *et al.* *c-Myc* is required for the formation of intestinal crypts but dispensable for homeostasis of the adult intestinal epithelium. *Mol. Cell Biol.* 25(17), 7868–7878 (2005).

51 Muncan V, Sansom OJ, Tertoolen L *et al.* Rapid loss of intestinal crypts upon conditional deletion of the Wnt/Tcf–4 target gene *c-Myc*. *Mol. Cell Biol.* 26(22), 8418–8426 (2006).

52 Ignatenko NA, Holubec H, Besselsen DG *et al.* Role of *c–Myc* in intestinal tumorigenesis of the $Apc^{Min/+}$ mouse(1). *Cancer Biol. Ther.* 5(12) 1658-1664 (2006).

53 Sansom OJ, Meniel VS, Muncan V *et al.* Myc deletion rescues Apc deficiency in the small intestine. *Nature* DOI:10.1038/nature05674 (2007) (Epub ahead of print).

54 Saito S, Liu B, Yokoyama K. Animal embryonic stem (ES) cells: self-renewal, pluripotency, transgenesis and nuclear transfer. *Hum. Cell* 17(3), 107–115 (2004).

55 Burgess S, Reim G, Chen W, Hopkins N, Brand M. The zebrafish spiel-ohne-grenzen (*spg*) gene encodes the POU domain protein Pou2 related to mammalian Oct4 and is essential for formation of the midbrain and hindbrain, and for pre-gastrula morphogenesis. *Development* 129(4), 905–916 (2002).

56 Sato N, Meijer L, Skaltsounis L, Greengard P, Brivanlou AH. Maintenance of pluripotency in human and mouse embryonic stem cells through activation of Wnt signaling by a pharmacological GSK-3-specific inhibitor. *Nat. Med.* 10(1), 55–63 (2004).

57 Hochedlinger K, Yamada Y, Beard C, Jaenisch R. Ectopic expression of Oct-4 blocks progenitor-cell differentiation and causes dysplasia in epithelial tissues. *Cell* 121(3), 465–477 (2005).

• **Demonstration of the strong 'crypt progenitor' phenotype imposed by the embryonic stem cell marker Oct-4.**

58 Wilson A, Radtke F. Multiple functions of Notch signaling in self-renewing organs and cancer. *FEBS Lett.* 580(12), 2860–2868 (2006).

59 van Es JH, van Gijn ME, Riccio O *et al.* Notch/γ-secretase inhibition turns proliferative cells in intestinal crypts and adenomas into goblet cells. *Nature* 435(7044), 959–963 (2005).

•• **Demonstration of the strong phenotype of Notch suppression in switching differentiation to goblet cells.**

60 Fre S, Huyghe M, Mourikis P, Robine S, Louvard D, Artavanis-Tsakonas S. Notch signals control the fate of immature progenitor cells in the intestine. *Nature* 435(7044), 964–968 (2005).

• **Modulation of intestinal cell fate through Notch.**

61 Zecchini V, Domaschenz R, Winton D, Jones P. Notch signaling regulates the differentiation of post-mitotic intestinal epithelial cells. *Genes Dev.* 19(14), 1686–1691 (2005).

• **Paper looking at the effects of Notch deregulation within the crypt.**

62 Sancho E, Batlle E, Clevers H. Signaling pathways in intestinal development and cancer. *Annu. Rev. Cell Dev. Biol.* 20, 695–723 (2004).

63 Hahm KB, Lee KM, Kim YB *et al.* Conditional loss of TGF-β signalling leads to increased susceptibility to gastrointestinal carcinogenesis in mice. *Aliment. Pharmacol. Ther.* 16(Suppl 2), 115–127 (2002).

64 Ishizuya-Oka A. Epithelial-connective tissue cross-talk is essential for regeneration of intestinal epithelium. *J. Nippon Med. Sch.* 72(1), 13–18 (2005).

65 Chow E, Macrae F. A review of juvenile polyposis syndrome. *J. Gastroenterol. Hepatol.* 20(11), 1634–1640 (2005).

66 He XC, Zhang J, Tong WG *et al.* BMP signaling inhibits intestinal stem cell self-renewal through suppression of Wnt–β–catenin signaling. *Nat. Gen.* 36(10), 1117–1121 (2004).

67 Bjerknes M, Cheng H. Re-examination of P-PTEN staining patterns in the intestinal crypt. *Nat. Genet.* 37(10), 1016–1017; author reply 1017–1018 (2005).

68 He XC, Li L. Reply to Re-examination of P-PTEN staining patterns in the intestinal crypt. *Nat. Genet.* 37, 1017–1018 (2005).

69 Haramis AP, Begthel H, van den Born M *et al. De novo* crypt formation and juvenile polyposis on BMP inhibition in mouse intestine. *Science* 303(5664), 1684–1686 (2004).

•• **Generation of a good murine model of juvenile polyposis.**

70 Batts LE, Polk DB, Dubois RN, Kulessa H. BMP signaling is required for intestinal growth and morphogenesis. *Dev. Dyn.* 235(6), 1563–1570 (2006).

71 Kim BG, Li C, Qiao W *et al.* Smad4 signalling in T cells is required for suppression of gastrointestinal cancer. *Nature* 441(7096), 1015–1019 (2006).

72 He XC, Yin T, Grindley JC *et al.* PTEN-deficient intestinal stem cells initiate intestinal polyposis. *Nat. Genet.* 39(2), 189–198 (2007).

73 Malumbres M, Barbacid M. RAS oncogenes: the first 30 years. *Nat. Rev. Cancer* 3(6), 459–465 (2003).

74 Janssen KP, El-Marjou F, Pinto D *et al.* Targeted expression of oncogenic K-Ras in intestinal epithelium causes spontaneous tumorigenesis in mice. *Gastroenterology* 123(2), 492–504 (2002).

75 Tuveson DA, Shaw AT, Willis NA *et al.* Endogenous oncogenic K-Ras(G12D) stimulates proliferation and widespread neoplastic and developmental defects. *Cancer Cell* 5(4), 375–387 (2004).

76 Sansom OJ, Meniel V, Wilkins JA *et al.* Loss of *Apc* allows phenotypic manifestation of the transforming properties of an endogenous K-Ras oncogene *in vivo*. *Proc. Natl Acad. Sci. USA* 103(38), 14122–14127 (2006).

Website

101 Nagy Lab
www.mshri.on.ca/nagy/default.htm

Affiliations

- *Victoria Marsh*
Cardiff University, Cardiff School of Biosciences, Cardiff, CF10 3US, UK
Tel.: +44 292 087 9115
Fax: +44 292 087 4116
marshv@cardiff.ac.uk
- *Alan Clarke*
Cardiff University, Cardiff School of Biosciences, Cardiff, CF10 3US, UK
Tel.: +44 292 087 4609
Fax: +44 292 087 4116
clarkear@cardiff.ac.uk